

DE GRUYTER

GRADUATE

*Giancarlo Cravotto,  
Diego Carnaroglio (Eds.)*

# MICROWAVE CHEMISTRY

Copyright 2017. De Gruyter. All rights reserved. May not be reproduced in any form without permission from the publisher except fair use as permitted under U.S. or applicable copyright law.

Cravotto, Carnaroglio (Eds.)

**Microwave Chemistry**

De Gruyter Graduate

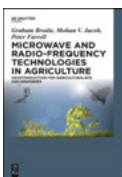
## Also of Interest



*Sustainable Green Chemistry.*

Benvenuto (Ed.); 2017

ISBN 978-3-11-044189-5, e-ISBN 978-3-11-043585-6



*Microwave and Radio-Frequency Technologies in Agriculture.*

*An Introduction for Agriculturalists and Engineers*

Brodie, Jacob, Farrell; 2016

ISBN 978-3-11-045539-7, e-ISBN 978-3-11-045540-3



*Flow Chemistry.*

*Vol. 1: Fundamentals; Vol. 2: Applications*

Darvas, Hessel, Dorman (Eds.); 2014

ISBN 978-3-11-028915-2, e-ISBN 978-3-11-028916-9



*Inorganic Micro- and Nanomaterials.*

*Synthesis and Characterization*

Dibeneditto, Aresta (Eds.); 2013

ISBN 978-3-11-030666-8, e-ISBN 978-3-11-030687-3



*Green Processing and Synthesis.*

Hessel (Editor-in-Chief)

ISSN 2191-9542, e-ISSN 2191-9550

# Microwave Chemistry

---

Edited by  
Giancarlo Cravotto, Diego Carnaroglio



**MILESTONE**  
H E L P I N G  
C H E M I S T S

**DE GRUYTER**

**Editors**

Professor Giancarlo Cravotto  
University of Turin  
Dip. di Scienza e Tecnologia  
del Farmaco  
Via Petro Giuria 9  
10125 Turin  
Italy

Dr. Diego Carnaroglio  
Milestone Srl  
Via Fatebenefratelli 1/5  
24010 Sorisole (BG)  
Italy

ISBN 978-3-11-047992-8  
e-ISBN (PDF) 978-3-11-047993-5  
e-ISBN (EPUB) 978-3-11-048002-3

**Library of Congress Cataloging-in-Publication Data**

A CIP catalog record for this book has been applied for at the Library of Congress.

**Bibliographic information published by the Deutsche Nationalbibliothek**

The Deutsche Nationalbibliothek lists this publication in the Deutsche Nationalbibliografie; detailed bibliographic data are available on the Internet at <http://dnb.dnb.de>.

© 2017 Walter de Gruyter GmbH, Berlin/Boston  
Cover image: Milestone Srl  
Typesetting: le-tex publishing services GmbH, Leipzig  
Printing and binding: CPI Books GmbH, Leck  
☉ Printed on acid-free paper  
Printed in Germany

[www.degruyter.com](http://www.degruyter.com)

---

This book is dedicated to my entire research group, a fantastic team of researchers, post-docs, and PhD students from different countries who share the same passion and enthusiasm.

Giancarlo Cravotto

To my parents Giovanna and Ludovico,  
to whom I am grateful for teaching me an effective working model that combines professionalism and competence in innovation and global business.

And to Giancarlo for his high-quality advice, support, direction, and pastoral responsibility during my PhD period and beyond.

Diego Carnaroglio

## Preface

The 1940s brought with them the discovery of the heating effects of microwaves which, ten to 15 years later, became an innovation that was pride of place in many American kitchens. At the same time, microwave (MW) pioneers carried out chemical experiments on polymers and glasses, and generated little more than curiosity. In the mid-1980s, however, the MW heating technique was used widely in chemical experimentation as a new energy source and its salient advantages over conventional heating were well documented. In the initial absence of dedicated MW ovens during the 1990s, kitchen MW ovens were frequently used by chemists to provide the activation energy; in this way Prof. Rajender Varma explored a wide variety of oxidation, reduction, cleavage, condensation, multicomponent reactions, combinatorial chemistry and synthesis of heterocycles in less than three minutes under solvent-free conditions<sup>1</sup>. Despite the inadequate measurement of temperatures inside the reaction vessels during irradiation, often erroneously described as a ‘magic effect’, the gradual diffusion of professional mono- and multimode reactors finally shed light on the spectacular reaction rate enhancements that the technique can generate. MW-assisted organic synthesis conducted in dedicated MW equipment has now grown into a mature field that has been widely adapted in drug discovery, particularly due to the rapid synthesis of a large number of ‘lead’ compounds, high yields, improved purity and, frequently, greener reaction conditions<sup>2</sup>. Although readers are most familiar with the great potential of dielectric heating, the advantages and disadvantages of a particular device or the conditions needed for maximizing efficiency and functionality may perhaps be less clear. Since the publication of Van Noorden’s 2008 report entitled *Microwaving myths*<sup>3</sup>, in which several experts described the current status of MW-assisted chemistry, new technological advances have been made that have broadened both the chemical applications and scientific interest; J. Moseley (Astra Zeneca) quipped “virtually all new compounds now have their first synthesis in a microwave” and this fact has acquired even more relevance years later. The latest generation of lab-scale reactors<sup>4</sup> are extremely versatile and can accommodate a wide range of reaction conditions. Rapid technological advances have enabled faster heating and cooling, accurate parameter measurement and control, and a wider range of operative pressures and temperatures, and these coupled with the availability of gas inlets and pressurization mean that the technique can now be used in a much broader

---

1 Varma RS. Green chemistry, 1999, 1 (1), 43–55.

2 Varma RS. Advances in green chemistry: chemical synthesis using microwave irradiation (2002), Astra Zeneca Research Foundation, Bangalore, India, ISBN: 81-901238-5-8.

3 Van Noorden R. Microwaving myths, Chem. World, 2008, 5, 40.

4 Rinaldi L, Carnaroglio D, Rotolo L, Cravotto G. J A Microwave-Based Chemical Factory in the Lab: From Milligram to Multigram Preparations of Chemistry 2015, ID 879531, 8 pp.

array of fields: organic and inorganic (nanomaterial) synthesis, plant extraction, biomass depolymerisation and pollutant degradation are some of the beneficiaries.<sup>5</sup> The rapid cooling off on completion of reactions can minimize degradation and side reactions. Furthermore, recent advances have been achieved on the 'kilolab' scale using a continuous flow MW system, as described by Morschhauser et al.<sup>6</sup> that involves a transmission line short-circuited waveguide reactor, which combines the benefits of the existing mono- and multimode technologies.

A number of research fields have taken advantage of the fast, molecularly selective and volumetric heating that is created by the direct coupling of MW energy and the bulk mixture; a condition that often cannot be reproduced by classical conductive heating. Several articles published in the *Journal of Chemical Education*<sup>7</sup> convinced a number of institutions to use this heating tool to reduce the time of experiments in undergraduate organic chemistry laboratories. The initial reports of explosions caused by scientifically misplaced use of pressurised containers and Teflon<sup>®</sup> bombs with solvents in domestic MW ovens evoked general concern over student safety, which reflected adversely on the technology itself. The use of domestic MW ovens in chemical laboratories is now not advisable.

Among other benefits, the efficient heat transfer and shorter reaction times of MW technology renders it a valuable asset to green chemistry concepts. MW technology allows the reactions to be performed on small scales: in milligrams rather than grams to be used in teaching laboratories, thus reducing the cost of reagents and chemicals and the associated waste disposal, while also multiplying the creativity of more efficient students. Although MW technologies are now used in every facet of chemistry, from the dissolution of samples for laboratory analysis to large-scale preparations of high-value fine chemicals and even larger-scale processing of ceramic products, it is quite difficult to find dedicated undergraduate courses on the subject, with some relief during advanced PhD research activities.

Despite the publication of a number of excellent books on MW chemistry and processing, there is a lack of suitable textbooks that address the needs of MS and PhD students, who need ready access to the relevant knowledge to help them appropriately design and carry out new experiments under dielectric heating. Although numerous other activation methods and technologies are accessible for conducting a chemical

---

5 Tagliapietra S, Cravotto G, Calcio Gaudino E, Visentin S, Mussi V, Functionalization of single-walled Carbon Nanotubes via the 1,3-Cycloaddition of Carbonyl ylides under Microwave Irradiation, *Synlett*, 2012, 1459–1462.

6 Morschhauser R, Krull M, Kayser C, Boberski C, Bierbaum R, Puschner PA, Glasnov TN, Kappe CO. Microwave-assisted continuous flow synthesis on industrial scale, *Green Process Synth.* 1, 2012, 281–290.

7 Parquet E, Lin Q, Microwave Assisted Wolff-Kischner-Reduction Reaction, *J. Chem. Educ.*, 1997, 74 (10), 1225 ; Cresswell SL, Haswell SJ, Microwave ovens – out of the kitchen, *J. Chem. Educ.*, 2001, 78 (7), 900; Coleman WF, Microwave-assisted heterocyclic chemistry, *J. Chem. Educ.*, 2006, 83 (4), 621.



reaction, it is hard to imagine a chemical research laboratory without a MW reactor like a typical household kitchen.

We sincerely hope that this textbook will contribute to encouraging a new generation of chemists to exploit the MW heating technique as a common tool in their research endeavours. All the eminent authors of the chapters in this textbook are steadfast MW users that deserve my heartfelt thanks for being willing to take the time and energy to contribute their wealth of knowledge in writing their chapters.

After several years of fascinating investigations into the use of MW-assisted chemical processes and beyond, I would like to highlight my own personal pleasure in coediting this book with an expert that was once one of my most successful ever PhD students. We would also like to acknowledge three entrepreneurs that have made a remarkable contribution to the success of MW chemistry by garnering excellent reputations worldwide for their respective companies; I had the honour of personally meeting Werner Lautenschläger, Franco Visinoni and Mike Collins.

Prof. Giancarlo Cravotto  
Director of the *Department of  
Drug Science and Technology*  
(University of Turin – Italy)

# Contents

## Preface — VI

Giancarlo Cravotto and Pedro Cintas

- 1 Microwave chemistry: history, development and legacy — 1**
- 1.1 Introduction — 1
- 1.2 How it all began — 1
- 1.3 From cooking to chemistry — 3
- 1.4 The thermal conundrum — 5
- 1.4.1 The search for specific effects: a long journey — 6
- 1.5 Efficient and fine-tuned heating: the role of outliers — 11
- 1.5.1 Conveying MW energy: susceptors — 11
- 1.5.2 A peculiar device: cooling while heating — 12
- 1.6 Efficient by design: tailor-made reactors — 13
- 1.7 Conclusions — 14

Paolo Veronesi

- 2 An Introduction to dielectric heating — 18**
- 2.1 The electromagnetic spectrum and the industrial, scientific, and medical frequencies — 18
- 2.2 Basis of dielectric heating — 19
- 2.2.1 Selectivity — 24
- 2.2.2 Self-regulating reactions — 26
- 2.2.3 Volumetric heating — 26
- 2.2.4 Inversion of temperature profile — 27
- 2.2.5 Rapid heating — 28
- 2.2.6 Thermal runaway — 28

Cristina Leonelli

- 3 Microwave generators, transmission, and interaction with different materials — 31**
- 3.1 Introduction — 31
- 3.2 Microwave generators — 33
- 3.2.1 Magnetron — 33
- 3.2.2 Solid-state generators — 34
- 3.2.3 Other microwave sources — 35
- 3.3 Wave Propagation — 36
- 3.3.1 Waveguide modes — 36
- 3.4 Antennas — 38

3.5	Microwave chambers —	<b>39</b>
3.5.1	Single-mode cavities —	<b>39</b>
3.5.2	Multimode applicators —	<b>40</b>
3.5.3	Leakage suppression —	<b>42</b>
3.6	Radiant microwave applicators —	<b>43</b>
3.7	Monitoring and control of microwave applicators —	<b>45</b>
3.7.1	Temperature measurement —	<b>45</b>
3.7.2	Pressure measurement —	<b>47</b>
3.7.3	Power control —	<b>48</b>
3.8	Maintenance —	<b>49</b>
3.9	Safety —	<b>49</b>
3.10	Conclusions —	<b>50</b>

György Keglevich and Zoltán Mucsi

<b>4</b>	<b>Interpretation of the rate enhancing effect of microwaves —</b>	<b>53</b>
4.1	Introduction —	<b>53</b>
4.2	Thermal versus nonthermal effects for rate enhancement —	<b>53</b>
4.3	Reaction energetics versus MW assistance —	<b>54</b>
4.4	Modeling the rate-enhancing effect of MWs —	<b>57</b>

Marilena Radoiu

<b>5</b>	<b>Industrial microwave reactors: components and set up —</b>	<b>65</b>
5.1	MW heating and process scale-up —	<b>65</b>
5.2	MW equipment —	<b>66</b>
5.2.1	The MW generator —	<b>67</b>
5.2.2	The MW power transmission line —	<b>73</b>
5.2.3	MW applicators —	<b>75</b>
5.3	Good engineering practice —	<b>76</b>
5.3.1	Quick estimation of theoretical power $P_a$ —	<b>76</b>
5.3.2	Simple calorimetry to assess available MW power of equipment —	<b>78</b>
5.4	Economics and process scale-up —	<b>79</b>
5.4.1	Power requirements for heating a product —	<b>79</b>
5.4.2	Choice of MW frequency —	<b>80</b>
5.5	What can be improved – good engineering practice, good manufacturing practice —	<b>81</b>
5.6	Industrial applications —	<b>81</b>
5.6.1	Food processing —	<b>81</b>
5.6.2	Drying at atmospheric or vacuum pressure —	<b>83</b>
5.6.3	Plasma processing —	<b>84</b>
5.6.4	Chemistry —	<b>85</b>
5.7	Conclusions —	<b>86</b>

- 5.8 A two-page definition guide to MW energy for beginners — 87
- 5.8.1 What is MW energy? — 87
- 5.8.2 How are MWs generated? — 87
- 5.8.3 What are dielectric properties? — 87
- 5.8.4 What happens to other materials? — 88
- 5.8.5 Ionizing and nonionizing radiation — 88

Antonio de la Hoz and Pilar Prieto

## **6 The impact of microwaves in organic synthesis — 91**

- 6.1 Introduction — 91
- 6.2 Acceleration effects — 92
- 6.3 Multistep synthesis — 94
- 6.4 Natural products — 95
- 6.5 Homogeneous and heterogeneous catalysis — 97
- 6.6 Biocatalysis — 101
- 6.7 Reactions involving radicals — 102
- 6.8 Selectivity under microwave irradiation — 104
- 6.9 Computational calculations in MAOS — 106

Yuji Wada, Dai Mochizuki, Taishi Ano, Masato M. Maitani, Shuntaro Tsubaki, and Naoto Haneishi

## **7 Chemical reactions on the interfaces of solids under microwaves — 113**

- 7.1 Introduction — 113
- 7.2 In situ observation of selective heating of inorganic particles dispersed in solution — 115
- 7.3 Accelerated chemical reactions by nonequilibrium local heating of solid interfaces — 120
- 7.4 Strategic design of zeolite filled with carbon at its core — 122
- 7.5 Summary — 125

Satoshi Horikoshi and Nick Serpone

## **8 Some aspects of catalysis with microwaves — 127**

- 8.1 Historical aspects of catalyzed reactions under microwave radiation — 127
- 8.2 Heterogeneously catalyzed reactions — 129
  - 8.2.1 Advantages of MW-assisted heterogeneous catalytic method — 129
  - 8.2.2 Microwave heterogeneous gas-phase catalytic systems — 131
  - 8.2.3 Microwave heterogeneous liquid-phase catalytic systems — 137
- 8.3 Problems with the MW catalytic method and possible solutions — 140
- 8.4 Conclusions — 144

Frédéric Delbecq, Rafael Luque, and Christophe Len

**9      Microwaves in flow chemistry — 149**

- 9.1      Introduction — **149**
- 9.2      Different flow reactors for microwave applications — **152**
  - 9.2.1      Microfluidic systems for chemistry — **152**
  - 9.2.2      Mesofluidic system for chemistry — **153**
- 9.3      Applications of microwaves in flow chemistry — **155**
  - 9.3.1      Production of nanoparticles — **155**
  - 9.3.2      Organic synthesis — **160**

Ángel Díaz-Ortiz and José R. Carrillo

**10     Microwaves in green and sustainable chemistry — 167**

- 10.1     Microwaves and the 12 principles of green chemistry. Energy Efficiency — **167**
  - 10.1.1     Dielectric properties (solvents and polar compounds) — **168**
  - 10.1.2     Use of susceptors — **169**
  - 10.1.3     Thermal effects — **170**
- 10.2     Reactions in green solvents — **171**
  - 10.2.1     Solvent-free reactions — **171**
  - 10.2.2     Reactions in water — **172**
  - 10.2.3     Reactions in ionic liquids — **173**
  - 10.2.4     Fluorous chemistry — **174**
- 10.3     Reactions with solid supports — **175**
- 10.4     Synergy with other sustainable technologies — **176**
  - 10.4.1     Ultrasound — **176**
  - 10.4.2     Electrochemistry — **177**
  - 10.4.3     Photochemistry — **178**
  - 10.4.4     Flow chemistry — **179**
- 10.5     Conclusions — **180**

Abhishek Sharma and Erik Van der Eycken

**11     Synthesis of medium-sized heterocycles under microwave irradiation — 184**

- 11.1     Introduction — **184**
- 11.2     Microwave-assisted synthesis of seven-membered heterocycles — **185**
  - 11.2.1     Benzazepine and benzoxazepine derivatives — **185**
  - 11.2.2     Diazepines and their analogs — **188**
  - 11.2.3     Thiazepine and thiadiazepine derivatives — **191**
  - 11.2.4     Oxacycles — **193**
- 11.3     Microwave-assisted synthesis of eight-membered heterocycles — **194**

- 11.4 Microwave-assisted synthesis of nine-membered heterocycles and beyond — 199
- 11.5 Conclusion — 202

Jacek Wojnarowicz, Tadeusz Chudoba, Andrzej Majcher, and Witold Łojkowski

- 12 Microwaves applied to hydrothermal synthesis of nanoparticles — 205**
  - 12.1 Introduction — 205
  - 12.2 Benefits of microwave synthesis in a Teflon<sup>®</sup> reaction chamber — 205
  - 12.3 Reactions initiated by microwaves in a liquid environment — 210
  - 12.4 Obtaining nanometric ZnO in hydrothermal processes — 213
  - 12.5 Obtaining ZnO nanopowders in microwave reactors — 214
  - 12.6 Solvothermal production of ZnO nanopowders in microwave reactors — 217
  - 12.7 Comparison of different methods of obtaining ZnO NPs — 219
  - 12.8 Summary — 220

Rodrigo González-Prieto, Santiago Herrero, Reyes Jiménez-Aparicio, Emilio Morán, Jesús Prado-Gonjal, José Luis Priego, and Rainer Schmidt

- 13 Microwave-assisted solvothermal synthesis of inorganic compounds (molecular and non molecular) — 225**
  - 13.1 Introduction — 225
  - 13.2 Influence of parameters and reaction conditions — 227
    - 13.2.1 Solvent — 227
    - 13.2.2 Reaction time — 228
    - 13.2.3 Temperature — 229
    - 13.2.4 Reactant ratio — 230
    - 13.2.5 Other variables — 231
  - 13.3 Molecular solids — 231
    - 13.3.1 Discrete species — 231
    - 13.3.2 Polymeric species — 234
  - 13.4 Nonmolecular solids — 236
    - 13.4.1 Binary metallic oxides — 238
    - 13.4.2 Oxides also containing hydrogen — 240
    - 13.4.3 Ternary oxides — 240
    - 13.4.4 Other materials — 242

Satoshi Horikoshi and Nick Serpone

- 14 Microwave-assisted synthesis of nanoparticles — 248**
  - 14.1 Introduction — 248
  - 14.2 Nanoparticle: definition — 248

- 14.3 Homogeneous and heterogeneous nucleation — **249**
- 14.4 Microwave nanoparticle synthesis — **251**
- 14.5 Advantage(s) of the microwave method — **252**
  - 14.5.1 Uniform nucleating particle size — **252**
  - 14.5.2 Synthesis of nanoparticles of uniform sizes: mechanism — **254**
  - 14.5.3 Efficient synthesis of metal nanoparticles at different microwave frequencies — **257**
  - 14.5.4 Advantage(s) of shape control — **259**
  - 14.5.5 Microwave local heating effects — **259**
  - 14.5.6 Microwave synthesis of core-shell nanoparticles — **260**
- 14.6 Microwave desktop system of nanoparticle synthesis in continuous-flow reactors — **262**
- 14.7 Synthesis of core-shell metal chalcogenide nanoparticles — **266**
- 14.8 Epilog — **267**

Dariusz Bogdal

- 15 Microwaves in polymer chemistry — 270**
  - 15.1 Free-radical polymerization — **271**
  - 15.2 Controlled radical polymerization — **273**
    - 15.2.1 Atom transfer radical polymerization — **273**
    - 15.2.2 Nitroxide-mediated polymerization — **275**
    - 15.2.3 Reversible addition-fragmentation chain transfer — **276**
  - 15.3 Ring-opening polymerization — **276**
  - 15.4 Ring-opening metathesis polymerization — **279**
  - 15.5 Microwave-assisted acyclic diene metathesis (ADMET) — **281**
  - 15.6 Step growth polymerization and preparation of composite/hybrid materials — **282**

Sandrine Perino, Emmanuel Petitcolas, and Farid Chemat

- 16 Microwave extraction of natural products in the teaching laboratory: fundamentals of essential oils green extraction — 293**
  - 16.1 Introduction — **293**
  - 16.2 Microwave versus conventional heating — **294**
  - 16.3 Experimental setup — **294**
    - 16.3.1 Portable microwave-assisted extraction — **294**
    - 16.3.2 Solvent-free microwave extraction — **295**
    - 16.3.3 Microwave hydrodiffusion and gravity — **296**
  - 16.4 Advantages — **299**
    - 16.4.1 Green production rapidity — **299**
    - 16.4.2 Green production efficiency — **299**
    - 16.4.3 Green production messages — **300**
  - 16.5 Future prospects — **300**

Cláudia P. Passos and Manuel A. Coimbra

- 17 Microwave extraction of bioactive compounds from industrial by-products — 302**
- 17.1 Industrial waste, byproducts, or coproducts? — **303**
  - 17.2 Availability and opportunities for industrial byproduct recycling — **305**
  - 17.3 Microwave extraction — **306**
    - 17.3.1 Essential oils — **320**
    - 17.3.2 Phenolics — **322**
    - 17.3.3 Polysaccharides — **324**
    - 17.3.4 Other MAE applications — **326**
  - 17.4 From laboratory to pilot – perspectives on the industrial scale — **326**
  - 17.5 Conclusion — **326**

Simona Collina and Serena Della Volpe

- 18 The Use of microwaves in drug discovery — 334**
- 18.1 Introduction — **334**
  - 18.2 MAOS in drug discovery: synthesis of small molecules — **335**
  - 18.3 MAOS in drug development: synthesis of radioligands for PET — **343**
  - 18.4 MAE: drug discovery based on natural products — **346**
  - 18.5 MAOS and biotechnology — **348**
  - 18.6 Conclusions — **351**

Karin Engen, Jonas Sävmarker, Luke R. Odell, and Mats Larhed

- 19 Microwave heating in medicinal chemistry — 358**
- 19.1 Introduction — **358**
  - 19.2 Lead identification — **360**
  - 19.3 Lead optimization — **364**
  - 19.4 MW-assisted synthesis of active pharmaceutical ingredients — **366**
    - 19.4.1 Imatinib — **366**
    - 19.4.2 Sildenafil — **367**
    - 19.4.3 Fluoxetine — **368**

Silvia Tabasso

- 20 Microwave-assisted biomass conversion — 370**
- 20.1 Introduction — **370**
  - 20.2 Composition of biomass — **371**
  - 20.3 Microwave interactions with biomass — **373**
    - 20.3.1 Hydrothermal conversion of cellulose — **374**
    - 20.3.2 Microwave-assisted pyrolysis of biomass — **376**



- 20.4 Case studies — **378**
- 20.4.1 Application of microwave heating in lignocellulosic biomass pretreatment for bioethanol production — **378**
- 20.4.2 MW-assisted valorization of postharvest tomato plant wastes (PHTP) — **379**
- 20.5 Conclusion — **381**

Zhilin Wu and Giancarlo Cravotto

**21 Microwave technology for environmental remediation — 383**

- 21.1 Microwave-induced plasmas — **383**
- 21.1.1 Dissociation of hydrogen sulfide — **385**
- 21.1.2 Desulfurization and denitrification of flue gas — **386**
- 21.1.3 Abatement of greenhouse gas: PFCs — **386**
- 21.1.4 Destruction of VOCs — **387**
- 21.2 MW-assisted evaporation and desorption — **388**
- 21.2.1 Ammonia evaporation from wastewater — **388**
- 21.2.2 Desorption of organic pollutants on granulated activated carbon — **388**
- 21.2.3 Dehydration of sludge, solid waste and biomass — **389**
- 21.2.4 Desorption of organics from contaminated soil — **390**
- 21.2.5 Stripping of oil from drill cuttings — **391**
- 21.2.6 Regeneration of adsorbents — **391**
- 21.3 Microwave-driven pyrolysis — **394**
- 21.3.1 Organic waste and biomass — **395**
- 21.3.2 Sewage sludge — **397**
- 21.3.3 Municipal solid waste — **401**
- 21.3.4 Polymeric materials — **401**
- 21.3.5 Waste oil — **404**
- 21.4 Microwave-enhanced decomposition — **405**
- 21.4.1 Decomposition of gaseous pollutants — **405**
- 21.4.2 Organic wastewater treatment — **407**
- 21.4.3 Soil remediation — **415**

María M. Delgado-Povedano and María D. Luque de Castro

**22 Microwaves in the omics field — 429**

- 22.1 Introduction — **429**
- 22.1.1 Steps in the analytical process — **430**
- 22.1.2 Omics definitions — **431**
- 22.1.3 Common aspects of MW-assisted steps in omics — **432**
- 22.2 MW assistance in genomics and transcriptomics — **434**
- 22.2.1 MW assistance in sample preparation in genomics and transcriptomics — **434**

- 22.2.2 MW-assisted detection in genomics and transcriptomics — 437
- 22.3 MW assistance in proteomics — 438
- 22.3.1 MW assistance in sample preparation in proteomics — 438
- 22.3.2 MW assistance in identification/quantitation in proteomics — 441
- 22.4 MW assistance in metabolomics — 441
- 22.4.1 MW-assisted drying in metabolomics — 442
- 22.4.2 MW-assisted solid–liquid extraction in metabolomics — 442
- 22.4.3 MW-assisted digestion in metabolomics — 444
- 22.4.4 MW-assisted liquid–liquid extraction in metabolomics — 445
- 22.4.5 MW-assisted steam distillation in metabolomics — 445
- 22.4.6 MW-assisted derivatization in metabolomics — 445
- 22.5 Trends in MW assistance in omics — 446

Cezar Augusto Bizzi, Erico Marlon de Moraes Flores, and Marcia Foster Mesko

- 23     Microwaves in sample preparation for elemental determination — 452**
- 23.1 Introduction to microwave-assisted sample preparation — 452
- 23.2 Microwave-assisted wet digestion/dissolution — 454
- 23.2.1 Microwave-assisted wet digestion of organic matrices — 454
- 23.2.2 Microwave-assisted wet decomposition/dissolution of inorganic matrices — 465
- 23.3 Microwave-assisted extraction — 466
- 23.3.1 Microwave-assisted extraction for speciation studies — 467
- 23.4 Microwave-assisted sample combustion — 468
- 23.4.1 Dry ashing — 469
- 23.4.2 Microwave-induced combustion — 470
- 23.5 Safety aspects, quality control, and quality assurance — 474
- 23.5.1 General aspects of safety — 474
- 23.5.2 Analytical quality assurance — 477
- 23.6 Conclusions — 480

Juliano Smanioto Barin, Fábio Andrei Duarte, Paola de Azevedo Mello, and Éder Lisandro de Moraes Flores

- 24     Microwave-assisted sample preparation for organic analysis — 488**
- 24.1 Introduction — 488
- 24.2 General aspects of microwave-assisted extraction — 489
- 24.3 Applications of MAE to the analysis of organic compounds — 497

Richard Morrison

- 25     Microwave chemistry in the organic instructional laboratory — 505**
- 25.1 Introduction — 505
- 25.2 Advantages of microwave promotion — 506
- 25.2.1 Safety — 506

- 25.2.2 Yields and product purity — **507**
- 25.2.3 Reduced heating times — **507**
- 25.2.4 Reactant and reagent unknowns — **508**
- 25.3 Examples of instructional laboratory experiments that utilize microwave promotion — **508**
- 25.4 Conclusions — **520**

**A snapshot of more common commercial microwave reactors — 523**

# List of contributors

## Chapter 1

**Giancarlo Cravotto**

University of Turin,  
Dip. di Scienza e Tecnologia del Farmaco,  
Via Petro Giuria 9,  
10125 Turin, Italy

**Pedro Cintas**

## Chapter 2

**Paolo Veronesi**

## Chapter 3

**Cristina Leonelli**

## Chapter 4

**György Keglevich**

**Zoltán Mucsi**

## Chapter 5

**Marilena Radoiu**

## Chapter 6

**Antonio de la Hoz**

**Pilar Prieto**

## Chapter 7

**Yuji Wada**

**Dai Mochizuki**

**Taishi Ano**

**Masato M. Maitani**

**Shuntaro Tsubaki**

**Naoto Haneishi**

## Chapter 8

**Satoshi Horikoshi**

Department of Materials and Life Sciences,  
Faculty of Science and Technology,  
Sophia University,  
7-1 Kioicho, Chiyodaku,  
Tokyo 102-8554, Japan.  
Email: horikosi@sophia.ac.jp

**Nick Serpone**

PhotoGreen Laboratory,  
Dipartimento di Chimica,  
Universita di Pavia,  
Via Taramelli 10,  
Pavia 27100, Italy.  
Email: nick.serpone@unipv.it

## Chapter 9

**Frédéric Delbecq**

Ecole Supérieure de Chimie Organique et  
Minérale,  
1 rue du Réseau Jean-Marie Buckmaster,  
60200 Compiègne, France.  
Email: f.delbecq@escom.fr

**Rafael Luque**

Departamento de Química Organica,  
Universidad de Cordoba, Campus de Rabales,  
Edificio Marie Curie (C-3), Ctra Nnal IV-A,  
Km 396, E14014, Cordoba, Spain.  
Email: q62alsor@uco.es

**Christophe Len**

Sorbonne Universités,  
Université de Technologie Compiègne,  
Centre de Recherche Royallieu,  
CS 60309, F-60203 Compiègne, France.  
Email: christophe.len@utc.fr

**Chapter 10**

**Ángel Díaz-Ortiz**

**José R. Carrillo**

**Chapter 11**

**Abhishek Sharma**

Department of Biomedical Engineering,  
Chemistry and Biological Sciences,  
Stevens Institute of Technology,  
Hoboken, NJ, 07030, United States

**Erik Van der Eycken**

Laboratory for Organic & Microwave-Assisted  
Chemistry (LOMAC),  
Department of Chemistry,  
University of Leuven (KU Leuven),  
Celestijnenlaan 200F, B-3001, Leuven, Belgium

**Chapter 12**

**Jacek Wojnarowicz**

Institute of High Pressure Physics,  
Polish Academy of Science (IHPP PAS),  
Warsaw, Poland

**Tadeusz Chudoba**

Institute of High Pressure Physics,  
Polish Academy of Science (IHPP PAS),  
Warsaw, Poland

**Andrzej Majcher**

Institute for Sustainable Technologies (NRI)  
Control Systems Department,  
Radom, Poland

**Witold Łojkowski**

Institute of High Pressure Physics,  
Polish Academy of Science (IHPP PAS),  
Warsaw, Poland

**Chapter 13**

**Rodrigo González-Prieto**

Departamento de Química Inorgánica,  
Facultad de Ciencias Químicas,  
Universidad Complutense de Madrid

**Santiago Herrero**

Departamento de Química Inorgánica,  
Facultad de Ciencias Químicas,  
Universidad Complutense de Madrid

**Reyes Jiménez-Aparicio**

Departamento de Química Inorgánica,  
Facultad de Ciencias Químicas,  
Universidad Complutense de Madrid

**Emilio Morán**

Departamento de Química Inorgánica,  
Facultad de Ciencias Químicas,  
Universidad Complutense de Madrid

**Jesús Prado-Gonjal**

Departamento de Química Inorgánica,  
Facultad de Ciencias Químicas,  
Universidad Complutense de Madrid

**José Luis Priego**

Departamento de Química Inorgánica,  
Facultad de Ciencias Químicas,  
Universidad Complutense de Madrid

**Rainer Schmidt**

Departamento de Física de Materiales,  
Facultad de Ciencias Físicas,  
Universidad Complutense de Madrid

**Chapter 14**

**Satoshi Horikoshi**

Department of Materials and Life Sciences,  
Faculty of Science and Technology,  
Sophia University,  
7-1 Kioicho, Chiyodaku,  
Tokyo 102-8554, Japan.  
Email: horikosi@sophia.ac.jp

**Nick Serpone**

PhotoGreen Laboratory,  
Dipartimento di Chimica,  
Universita di Pavia,  
Via Taramelli 10,  
Pavia 27100, Italy.  
Email: nick.serpone@unipv.it

**Chapter 15****Dariusz Bogdal**

Cracow University of Technology,  
Krakow, Warszawska 24, Poland

**Chapter 16****Sandrine Perino**

Avignon University,  
INRA, Green Extraction Team, UMR408,  
F-84000 Avignon, France.

**Emmanuel Petitcolas**

Avignon University,  
INRA, Green Extraction Team, UMR408,  
F-84000 Avignon, France.

**Farid Chemat**

Avignon University,  
INRA, Green Extraction Team, UMR408,  
F-84000 Avignon, France.

**Chapter 17****Cláudia P. Passos****Manuel A. Coimbra****Chapter 18****Simona Collina**

Department of Drug Sciences,  
University of Pavia,  
Viale Taramelli, 12,  
27100 Pavia, Italy  
E-mail: simona.collina@unipv.it

**Serena Della Volpe****Chapter 19****Karin Engen**

Department of Medicinal Chemistry,  
Division of Organic Pharmaceutical Chemistry,  
Uppsala Biomedical Center, Uppsala University,  
P.O. Box 574,  
SE-751 23 Uppsala, Sweden

**Jonas Sävmarker**

The Beijer Laboratory for Drug Discovery,  
Department of Medicinal Chemistry,  
Uppsala Biomedical Center,  
Uppsala University,  
P. O. Box 574,  
SE-751 23 Uppsala, Sweden

**Luke R. Odell**

Department of Medicinal Chemistry,  
Division of Organic Pharmaceutical Chemistry,  
Uppsala Biomedical Center, Uppsala University,  
P.O. Box 574,  
SE-751 23 Uppsala, Sweden

**Mats Larhed**

Department of Medicinal Chemistry,  
Science for Life Laboratory,  
Uppsala Biomedical Center,  
Uppsala University,  
P. O. Box 574,  
SE-751 23 Uppsala, Sweden  
E-mail: mats@orgfarm.uu.se

**Chapter 20****Silvia Tabasso**

Dipartimento di Chimica,  
University of Turin,  
Via Pietro Giuria, 7  
10125 Turin, Italy

**Chapter 21****Zhilin Wu****Giancarlo Cravotto**

University of Turin,  
Dip. di Scienza e Tecnologia del Farmaco,  
Via Petro Giuria 9,  
10125 Turin, Italy

## Chapter 22

**María M. Delgado-Povedano**

Department of Analytical Chemistry,  
Annex C-3, Campus of Rabanales,  
University of Córdoba,  
E-14071, Córdoba, Spain.

**María D. Luque de Castro**

Maimónides Institute of Biomedical Research  
(IMIBIC),  
Reina Sofía Hospital,  
University of Córdoba,  
E-14014, Córdoba, Spain.

## Chapter 23

**Cezar Augusto Bizzi**

Departamento de Química,  
Universidade Federal de Santa Maria,  
Santa Maria, RS, Brazil

**Erico Marlon de Moraes Flores**

Departamento de Química,  
Universidade Federal de Santa Maria,  
Santa Maria, RS, Brazil

**Marcia Foster Mesko**

Centro de Ciências Químicas,  
Farmacêuticas e de Alimentos,  
Universidade Federal de Pelotas,  
Pelotas, PR, Brazil

## Chapter 24

**Juliano Smanioto Barin**

Departamento de Tecnologia e Ciência dos  
Alimentos,  
Universidade Federal de Santa Maria,  
Santa Maria, RS, 97105-900, Brazil

**Fábio Andrei Duarte**

Departamento de Química,  
Universidade Federal de Santa Maria,  
Santa Maria, RS, 97105-900, Brazil

**Paola de Azevedo Mello**

Departamento de Química,  
Universidade Federal de Santa Maria,  
Santa Maria, RS, 97105-900, Brazil

**Éder Lisandro de Moraes Flores**

Departamento de Química,  
Universidade Federal Tecnológica do Paraná,  
Medianeira, PR, 85884-000, Brazil

## Chapter 25

**Richard Morrison**

## Appendix

**Giancarlo Cravotto**

University of Turin,  
Dip. di Scienza e Tecnologia del Farmaco,  
Via Petro Giuria 9,  
10125 Turin, Italy

**Diego Carnaroglio**

Milstone Srl  
Via Fatebenefratelli 1/5  
24010 Sorisole (BG), Italy

Giancarlo Cravotto and Pedro Cintas

# 1 Microwave chemistry: history, development and legacy

## 1.1 Introduction

The reader may be surprised to see an introductory chapter on the history of microwaves (MW) in this textbook on MW chemistry; after all, MWs are hardly ancient history! In fact, MW chemistry is very much an active research field and one for which a definitive model of chemical reactivity has yet to be established, despite the fact that the discipline has grown exponentially since the now-distant, late 1980s. The exact nature of the thermal, and any potential nonthermal effects of MWs remain the subject of intense debate, and particular mechanisms that account for specific or anomalous cases are proposed from time to time. Despite all this, we still had the strange feeling that writing this sort of memoir should be undertaken by the field's pioneers, who have since retired from science, as they take us through the developments they experienced and contributed to. However, you have us – authors who are currently engaged in MW chemistry and can therefore view this growing subject from up close.

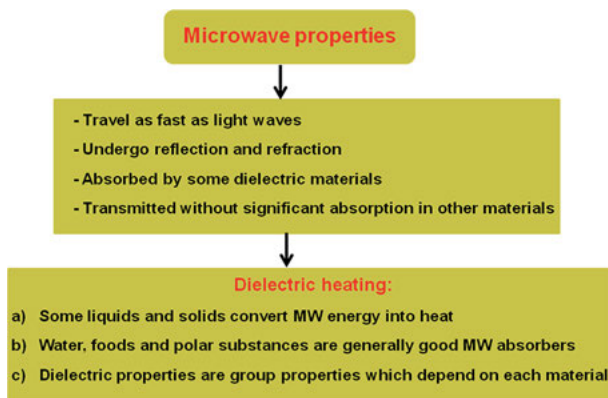
However, far from being solely a comprehensive historical survey, this chapter's purpose is twofold: (1) to describe the historical breakthroughs that originally launched MW-based science and (2) to highlight a series of instrumental developments in MW chemistry. In doing so, there will be inevitable omissions, especially in the applied domain, which will be covered by other contributors throughout this book. Emphasis is placed on seminal findings and conceptual toeholds whose significance was often only unveiled in retrospect. We feel that these subjects should be of interest to younger readers and experienced MW practitioners alike. As is often the case in science, we will see that while many breakthroughs in MW science and technology came about thanks to chance, all have been invariably driven by curiosity.

## 1.2 How it all began

MW radiation does not lie in the most energetic zone of the electromagnetic spectrum. It falls between radio frequencies and infrared (IR) radiation, at frequencies of between around 300 MHz (0.3 GHz) and 300 GHz, while most commercial devices operate at a standard 2.45 GHz. The corresponding wavelengths (between 1 m and 1 cm), clearly indicate that MWs and matter do not interact at either the atomic or molecular levels. The existence of electromagnetic waves was a prediction forged

<https://doi.org/10.1515/9783110479935-001>





**Fig. 1.1:** Physical properties of MW radiation.

from Maxwell's equations, formulated in 1873, although experimental verification was not accomplished until much later, in the 1880s, by Heinrich Hertz, who was able to produce and detect MWs (*ca.* 1 GHz) using a rudimentary generator [1]. For a few decades, up until the invention of radio transmitters, these so-called shortwaves were little more than an academic curiosity, even if their salient properties, such as heating, were immediately noticeable [2]. Figure 1.1 summarizes these physical properties.

The use of high-frequency radio waves to heat substances, and particularly for cooking, dates back to the 1920s and can be traced to the invention of vacuum tube radio transmitters. However, a curious note appeared in an American magazine for radio experimenters entitled "Cooking by ultra short waves" as early as 1933 [3]. The single-column note contained the following statement:

"Food can be cooked by means of the ultra short wave radio transmitter. The food is heated by internally passing high frequency current through it. This is probably the only basic advance in the art of preparing food for human consumption since cavemen, thousands of years ago, first burned meat over a fire and heated vegetables in crude vessels of boiling water.

For cooking, the ultra high frequency current is made to pass from one pan-shaped electrode to another. The uncooked food is placed between two electrodes, directly in the path of the radio transmitter's power.

Bread is toasted in a half dozen seconds or so, steaks, potatoes, and other solid meats and vegetables require several minutes, as does the boiling of water for making coffee or cooking vegetables."

Both Westinghouse and Bell Laboratories released patent applications in the late 1930s, demonstrating the cooking of foods between metal plates attached to a short-wave device working at *ca.* 60 MHz [4].

Although the heating effect of electromagnetic fields at both radio and MW frequencies is caused by dielectric heating, *i.e.*, by the reorientation of polarized molecules in a rapidly alternating electric field, the use of an MW power genera-

tor inside a cavity (*the magnetron*, as in modern domestic ovens) was not originally intended for cooking. The different versions of magnetrons that were developed between 1920 and 1940 were designed for radar transmitters and radar devices for air defense, which, of course, became instrumental during World War II [2]. There is a widespread consensus that Percy L. Spencer should be credited with the invention of MW cooking. Spencer, a self-taught man, became an expert on radio technology and was contracted by Raytheon to develop radar equipment for military purposes. One day, while Spencer was standing in front of an MW source, he noticed that a candy bar had melted in his pocket. Inspired by this serendipitous finding, Spencer and his colleagues attempted to heat other food, such as the world's first microwaved popcorn. Whether or not these and other eureka moments actually occurred as they are described in popular science narratives may now be irrelevant. The observation marked the beginning of MW cooking, and Raytheon filed the first related patent in 1945, and subsequent improvements followed [5]. The first commercially available oven was an MW chamber weighing around 750 pounds (ca. 340 kg) and was about 6 feet (ca. 180 cm) tall, sold at the prohibitive price of US\$ 5000 a unit. Affordable kitchen ovens (less than US\$ 500) did not become available until 1967. At this point, food processing became the first industrial application of MW technology and ranged from cooking itself to sterilization and drying [6].

### 1.3 From cooking to chemistry

If you consider the fact that that MW cooking is essentially the conversion of electromagnetic energy into heat, you would be forgiven for thinking that MW-activated chemical reactions emerged soon after the application of MWs to food preparation. After all, thermal stimulation is the oldest means of inducing chemical transformations. However, this transition was lengthier than one might expect. Unlike conventional conductive heating, dielectric heating is a complex issue based on physical properties that require microscopic interpretation and in-depth mathematical formalism, incomprehensible jargon to most chemical practitioners. For many years, the use of MW ovens was a lab trick. The late 1980s saw in the chemical literature descriptions of numerous examples of activated reactions that overlooked accurate temperature estimations and other technical details. As a consequence, the systematic abuse and misuse of domestic ovens often led to irreproducible results that varied from lab to lab.

Take, for example, a talk in the mid-1990s at a meeting of organic chemists given by Jack Hamelin, one of the pioneers of synthetic MW chemistry, which was received with both interest and skepticism. Even scientists familiar with other forms of radiation found it difficult to understand how thermal effects arose from the action of electromagnetic waves. In the year 2000, however, at the biannual meeting of the European Society of Sonochemistry, the inaugural lecture by MW expert D. M. P. Mingos


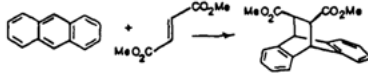
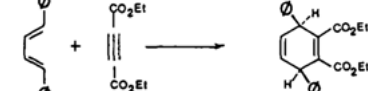
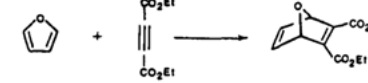
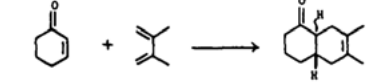

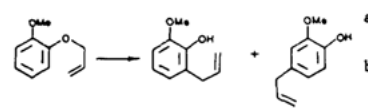
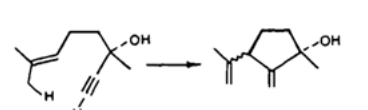
was greeted by applause and relatively few questions about the mechanism of action. Change had come.

In a broad sense, the first chemical applications of MW heating lay in sample pretreatment, such as digestion and ashing [7–10]. The technique has now become routine and provides fast and simplified protocols. One of the earliest, if not the first, application of MW frequencies to synthetic chemistry was a 1969 Dow Chemical Co. patent that reported MW-induced emulsion polymerization of vinyl monomers using pulsed radiation (from the radio frequency to MW range) [11]. However, this application still used a two-electrode device, not characteristic magnetron power. In 1973, a paper coauthored by Ponomarev and Tarasenko, dealt with the activation of chemical processes by MW irradiation [12]. These authors described both rubber vulcanization and the polymerizations of methyl methacrylate and styrene in benzene. Reactions were either conducted in glass vessels or directly inside the metal MW resonator; twofold acceleration was observed at the beginning of polymerization. The paper, published in Russian in a journal not readily accessible to the international scientific community, was largely ignored, even if it paved the way for future developments.

It is usually accepted that two papers published in *Tetrahedron Letters* in 1986 represented the real birth of synthetic MW chemistry and launched the routine exploration of chemical reactions using cheap domestic ovens that could boast of no more than manual time and power controls. The first, by Gedye et al. [13], reported significant increases in the reaction rates of four typical organic reactions: the acid hydrolysis of benzamide, the oxidation of toluene with  $\text{KMnO}_4$ , the esterifications of benzoic acid with alcohols and the  $\text{S}_{\text{N}}2$  reaction of sodium 4-cyanophenoxide and benzyl chloride (up to thousand-fold rate enhancements were observed for this last reaction). All reactions were carried out in sealed Teflon vessels under reflux conditions, and the authors took note of the direct relationship between rate and vessel pressure. In fact, a violent explosion took place when the oxidation of toluene was conducted for prolonged reaction times; unfortunately, no temperature measurements were given.

The second 1986 paper, by Giguere et al. [14], focused mainly on cycloaddition reactions. These authors addressed safety concerns in connection with MW oven use and temperature measurements (which may differ by  $\pm 5$  °C inside and outside vessels) for the first time. The relationship between thermal efficiency and solvent dielectric constants and, remarkably, the superheating effect of dielectric heating were noticeable points as well. Clearly, as remarked by Giguere et al., the excellent yields and enhanced rates had more to do with thermal effects, in view of the high temperatures attained, than the influence of pressure (Figure 1.2).

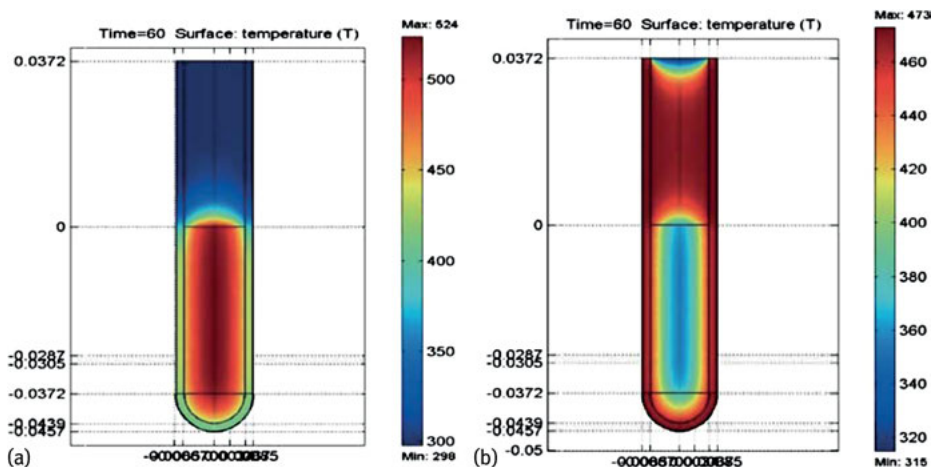
Worth mentioning are the seminal papers by Rajender Varma that, starting in 1993 [15], introduced several smart applications of MWs in organic synthesis, highlighting their relevant role in green chemistry [16].

REACTION	MICROWAVE	LITERATURE	CONTROL
1. 	3 min <sup>4a</sup> p-xylene, 92% 160°<187°C	10 min <sup>17</sup> p-xylene, 90% 138°C	10 min p-xylene, 90% 138°C
2. 	10 min <sup>4a,b</sup> p-xylene, 87% 325°<361°C	72 h <sup>18</sup> dioxane, 90% 101°C	4 h p-xylene, 67% 138°C
3. 	12 min <sup>4b</sup> NEAT, 55% 325°<361°C	5 h <sup>19</sup> NEAT, 67% 150°C	5 h NEAT, 81% 150°C
4. 	10 min <sup>4b</sup> NEAT, 66% 325°<361°C	4 h <sup>20</sup> NEAT, 95% 100°C	4 h NEAT, 68% 100°C
5. 	15 min <sup>4b</sup> NEAT, 25% 400°<425°C	72 h <sup>21</sup> NEAT, 20% 200°C	a) 3 days, NEAT <sup>22</sup> 89%, 195°C b) 2 h, NEAT <sup>22</sup> 75%, 195°C
6. 	a) 10 min, <sup>4b</sup> NEAT 21%, 325°<361°C b) 6 min, DMF 92%, 325°<361°C	6 h <sup>23</sup> NEAT, 85% 220°C	6 min NEAT, 17% 320°C
7. 	a) 12 min, <sup>4b</sup> NEAT 71%, 370°<400°C b) 5 min, <sup>4b</sup> DMF 72%, 300°<315°C c) 90 sec, <sup>4b</sup> N-methylformamide 87%, 276°<300°C	85 min <sup>23</sup> NEAT, 85% 240°C	a) 45 min NEAT, 71% 265°C b) 12 min NEAT, 92% 320°C
8. 	15 min NEAT, 62% 400°<425°C	12 h <sup>24</sup> NEAT, 85% 180°C	12 h NEAT, 60% 180°C

**Fig. 1.2:** Dramatic accelerations for some cycloadditions, -ene reactions, and Claisen rearrangements under MW irradiation in sealed vessels surrounded by vermiculite to absorb MW energy and avoid explosions. Note the salient temperature differences between irradiated and conventional conditions. Reproduced directly from the original source (Ref. [14]) with permission. Copyright 1986 Pergamon Journals Ltd.

## 1.4 The thermal conundrum

Common wisdom would have it that conventional and MW heating are different processes. The former hinges on the thermal conductivity of a vessel that attains a temperature higher than that of the reaction mixture inside. MW heating, however, is not directly dependent on the thermal conductivity of the container, but rather on the ability of reactants and solvent molecules to absorb MW energy via two basic mechanisms, dipole rotation and ionic conduction [17]. As a result, the thermal gradient in MW-assisted processes exhibits a pattern different from that of conductive heating, as localized superheating of anything inside the vessel will occur via the action of MWs,



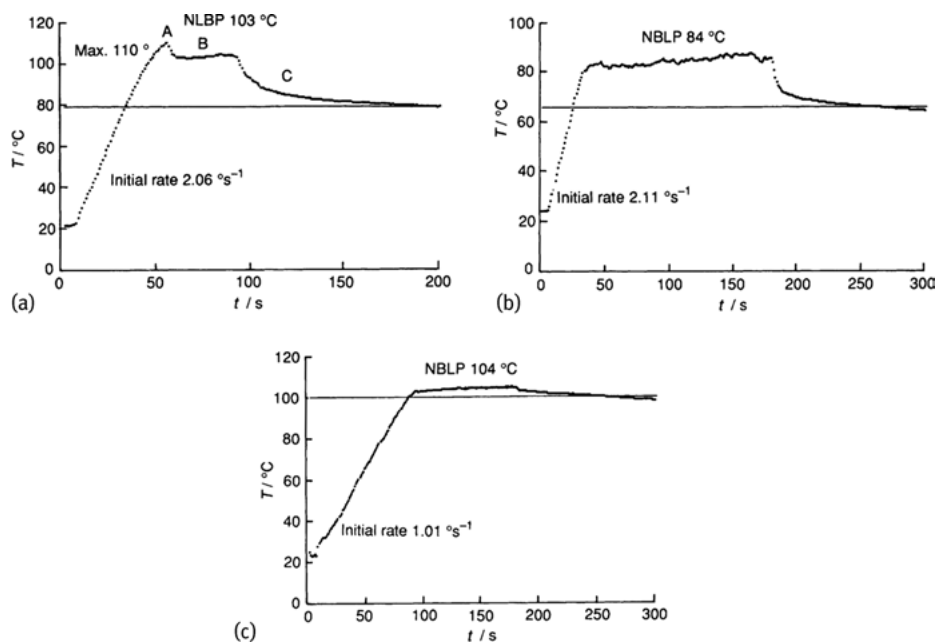
**Fig. 1.3:** Images, taken using IR thermography, of temperature gradients across an unstirred reaction heated for 60 s under MW irradiation (a) and conventional heating in an oil bath (b). The temperature scale is given in Kelvin; zero on the vertical axis indicates the position of the meniscus. Reproduced with permission from Ref. [18]. Copyright 2003 Kluwer Academic Publishers.

and the numerous materials employed for vessels are transparent to MW energy. Figure 1.3 has become an eye-catching and iconic representation of MW heating *versus* heating in oil baths (*vide infra*) [18].

Early synthetic studies of MW-assisted reactions often invoked the aforementioned mechanisms of energy transfer, based on the presence of polar molecules or ionic species in the substance being heated to justify the observed reactivity. Unfortunately, such mechanisms are insufficient to accurately explain how dielectric heating takes place, especially in the absence of quantitative data, and hence how MWs increase reaction rates. Concepts such as *dielectric loss*, *dielectric permittivity*, and relaxation times for dipole orientations at different temperatures may better account for the dielectric performance of a given material. A series of theoretical models, generally based on the classical Debye model, were introduced in the 1950s to rationalize dielectric properties [2, 19–22]. This theory lies beyond the scope of this chapter, although it is worth mentioning for its historical significance. Suffice it to say that chemists now think of MW activation in terms of parameters such as *loss tangent* or loss factor ( $\tan \delta$ ), i.e., the dissipation factor of the sample, which expresses how efficiently MW energy is converted into thermal energy [23].

#### 1.4.1 The search for specific effects: a long journey

It is now well established that MW heating causes some thermal abnormalities that may be responsible for high rate enhancements that would only be possible at high



**Fig. 1.4:** Heating curve for ethanol (a), methanol (b), and water (c) under MW irradiation. (NBLP: nucleation-limited boiling point.) Reproduced with permission from Ref. [25]. Copyright 1992 Royal Society of Chemistry.

pressures under conventional heating. Kinetic studies suggest that reactions occur at *virtually the same rate under MW and conventional heating at the same temperature*, which appears to be a useful and predictive corollary. Accordingly, acceleration may be due to, among other factors, local and general superheating of the solvent; inaccurate temperature measurements; nonhomogeneous distribution of temperature (*hot spots*), which may lead to more marked MW effects in solids and viscous media as radiation is absorbed directly by the reagents; solvent evaporation in open vessels, thereby increasing solute concentrations; and finally the existence of putative non-thermal effects [24].

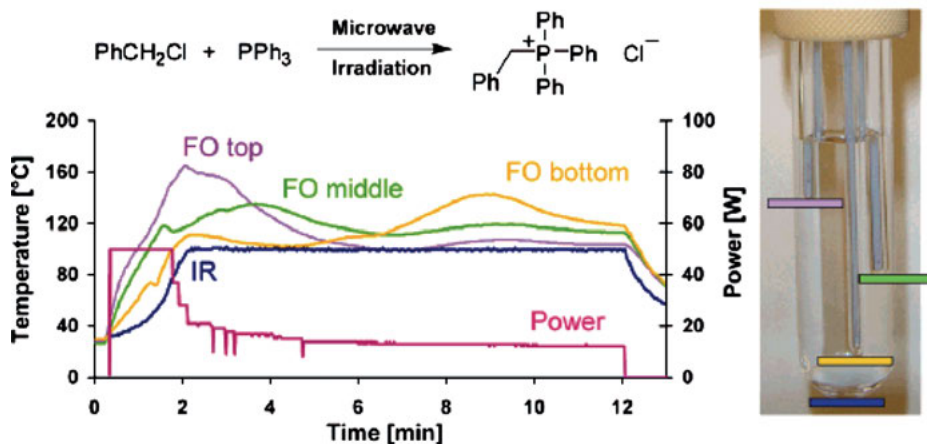
Overheating is probably one of the most significant of the known abnormalities, although it can be greatly attenuated under stirring or via the addition of nucleation modifiers. The first study on MW heating boiling phenomena appeared in 1992, written by Baghurst and Mingos, and proved that MW-heated organic solvents can boil above their typical boiling point at atmospheric pressure, with  $\Delta T$  from 13 to nearly 26 °C (Figure 1.4) [25]. This effect was attributed to the existence of boiling nuclei at the free liquid surface, a fact further corroborated by the fact that irradiation boiling begins in the liquid surface under MW, while there are no boiling nuclei in the bulk of the solvent [26].

If any single aspect of MW heating has become a controversial issue, it is surely the existence, or absence, of nonthermal effects. By definition, nonthermal, or athermal, effects are those that do not correlate with a macroscopic change in temperature. As we shall see later, the term has also become confusing from a conceptual (even semantic, *vide infra*) viewpoint because some researchers assume that specific effects, such as hot spots, are nonthermal abnormalities because the uneven distribution of the electric field will lead to local zones with temperatures much greater than the macroscopic temperature. Conversely, others suggest that most experimental observations result from *specific thermal effects* rather than *specific nonthermal effects*, ruling out an artificial dichotomy.

In a strict sense, nonthermal effects could be rationalized in terms of a highly polarizing field that might affect molecular mobility and diffusion, among other factors, thereby influencing terms, such as the preexponential factor of the Arrhenius equation and activation energy. These considerations would then account for the acceleration or selectivity in MW-heated reactions. It is fair to mention the impressive detective work carried out by Loupy and associates on this subject. They have collected a vast amount of experimental evidence and theoretical studies that support the idea of electromagnetic field dependence. Importantly, Loupy et al. have suggested suitable conditions for observing specific effects and have cautioned the community over conditions that may be detrimental. High temperatures, for instance, may produce good yields in short reaction times under conventional heating. If it is true that MW effects do actually exist, these will occur at lower temperatures where classical heating gives rise to fairly poor yields. Otherwise, the MW effect will be masked at higher temperatures. A comprehensive review published in 2001 by Loupy and Perreux compiled previous literature and a tentative rationalization of nonthermal effects [27] and was subsequently updated in 2006 and 2012 [28].

Specific effects, and hence enhanced rates, seem to be especially relevant in some reactions that follow polar mechanisms, where the polarity increases from the ground state to the transition state. In these cases, the MW-based transition structure and its position along the reaction coordinate are different from those in conventional conditions [24, 28]. As claimed in a recent study on the transformations of simple molecules, such as NO and H<sub>2</sub>S, over solid catalysts under MW irradiation, the electromagnetic field appears to considerably reduce activation energies [29].

Although it should be admitted that there may not be a simple explanation for all the cases gathered in the literature, any mechanism will invariably require accurate temperature control in MW-assisted reactions. Kappe and his group in particular, although other leading experts in the field share similar views, have emphasized that specific MW effects are caused by the uniqueness of the dielectric heating mechanisms discussed earlier and not by effects that are largely independent of the bulk reaction temperature [30, 31]. An illustrative study that exemplifies the effect of temperature inhomogeneity along the MW field was reported by this group in 2008. They made use of a setup that allowed accurate internal temperature measurements to be performed



**Fig. 1.5:** Temperature profiles as measured for the MW-assisted solventless alkylation of triphenylphosphine with benzyl chloride using a fiber-optic sensor and an external IR pyrometer. A picture of the reaction vial also shows different temperatures (fiber-optic probe) at the bottom, middle, and upper areas of the mixture. Reproduced with permission from Ref. [32]. Copyright 2008 American Chemical Society.

using a fiber-optic probe for four reactions run in both MW and conventionally heated reactors [32]. The temperature measurements made using a multiple-fiber-optic sensor at different positions in a 10 mL vial containing 5 mL of the organic solvent, *N*-methylpyrrolidone, clearly highlighted a thermal gradient that showed differences of up to 30 °C between the bottom and middle of the vessel. This gradient can, however, be minimized by the efficient stirring of the reaction mixture. The issue is particularly problematic in solvent-free protocols, where agitation may not be efficient and the measured temperature may not be an accurate representation of the true temperature inside the MW reactor. In fact, the solvent-free alkylation of triphenylphosphine by benzyl chloride was apparently conducted at 100 °C (standard external IR sensor), while the fiber-optic device gave a much higher temperature (165 °C), which also varied according to the position of the internal sensor (Figure 1.5).

This example and others all highlight the importance of controlling experimental conditions to minimize temperature gradients, which are invariably present in heated single-mode MW reactors, especially where solid or heterogeneous solid-liquid mixtures are involved. Efficient stirring is key to this end. The use of external IR pyrometers, which have seen widespread use over the years, is strongly discouraged, while internal fiber-optic sensors provide not only faster responses but also give accurate temperatures at single locations in the reaction mixture. Moreover, simultaneous external and internal temperature measurements provide a much more complete picture of thermal gradients [33].



Of particular relevance is the increasing use of spectroscopic techniques, including both *ex situ* and *in situ* monitoring, to measure thermal profiles across reaction mixtures. IR thermography, in situ Raman spectroscopy, and more sophisticated techniques, such as neutron and X-ray scattering, have been introduced and are suitable for testing the action of MW radiation on materials of different textures and compositions [34].

At this point, one may wonder whether purely thermal effects can actually be disentangled from other properties of the electromagnetic field. The answer is complex, and every case requires careful assessment. Since MW heating is largely associated with the electric vector of electromagnetic radiation, as dipoles are subjected to an alternating electric field of high frequency, the higher the field strength, the more pronounced the effect. Thus, dielectric heating can, *a priori*, be independent of macroscopic temperature. Frequency effects have been observed in MW-assisted transformations and can be instrumental in certain applications, such as the generation of nanoparticles, or in flow reactors because wave penetrability depends on frequency. At 5.8 GHz, MW radiation shows lower penetration into solvents than at the standard 2.45 GHz, but it shows greater energy conversion. Dielectric constants and, hence, dissipation factors ( $\tan \delta$ ) are also dependent on the frequency of the MW beam [35, 36]. Unfortunately, MW reactors that operate at frequencies other than 2.45 GHz are not readily available from commercial suppliers, and in general, specific applications will require *ad hoc* designs.

While on the subject of nonthermal effects, one cannot forget that magnetic fields can affect reaction outcomes as well. Even more remarkably, magnetic losses in the MW band will occur in certain materials, such as iron oxides and ferroelectrics. Accordingly, magnetic permeabilities need to be checked, even if these species are only present as impurities [2].

Despite all of the controversy, effects that do not show bulk temperature dependence, at least to a significant extent, may well be genuine. This appears to be the case with heterogeneous reactions that involve the formation of organometallic reagents, such as Grignard reagents, which are significantly accelerated by the electrostatic etching of the metal surface caused by MW irradiation in a multimode instrument [37]. The interaction between MWs and Mg turnings produced, as expected, visible electrostatic discharges (*arcing*), thus causing their activation thanks to the cleansing effect (i.e., removing the passivating layer) and the concomitant formation of smaller and more reactive spherical Mg particles. The process has been investigated in conventional conditions (bottom flask fitted with a reflux condenser and stirring under an inert Ar atmosphere) and MW heating in a variety of instruments. The poorly reactive 2-chloropyridine was selected as it would enable any rate enhancements under MW irradiation to be detected. Remarkably, both experiments were conducted at an identical macroscopic bulk temperature of 65 °C [38]. While multimode instruments lead to successful Mg insertion into C-Cl bonds, the use of single-mode reactors, which provide higher electric field strength, also causes more intense electrostatic discharges to

occur on the metal surface, together with the pyrolytic decomposition of the volatile solvent, tetrahydrofuran (THF). This pyrolysis leads to the formation of carbonaceous particles that passivate the Mg metal and suppresses the formation of the Grignard reagent.

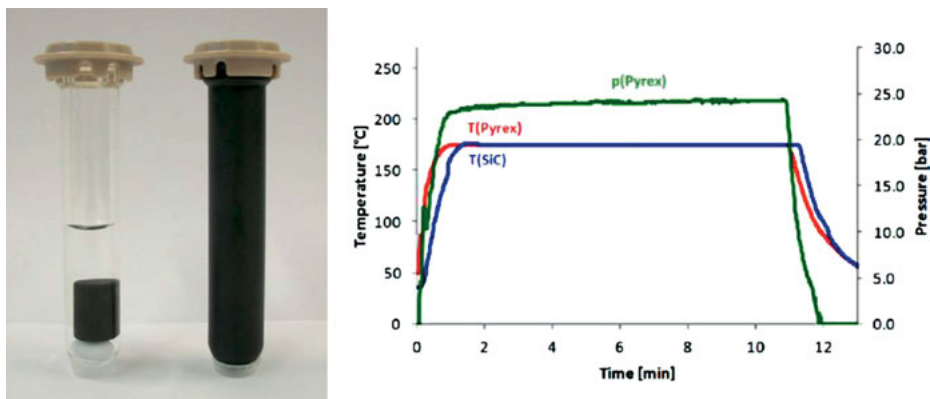
The debate on MW phenomena and specific effects on the rates of organic reactions is still open owing to conflicting data and to the fundamental challenges associated with reproducibility and accurate temperature measurement. The discussion moved from the so-called nonthermal effects of the early literature to superheating and superboiling phenomena, carefully investigated by several authors [39–41].

## 1.5 Efficient and fine-tuned heating: the role of outliers

So far, we have concentrated our discussion of MW effects on the electromagnetic field, which is inherently the origin of thermal activation and dictates its fate. The development of MW activation as a mature discipline, boosted in addition by the advent of green chemistry, has benefited from numerous improvements in the control and performance of radiation, yet in relatively low-cost operations. The first home-made control mechanism at the dawn of MW-assisted synthesis in domestic ovens was perhaps simply the routine addition of porous and polar adsorbents (e.g., alumina, clays) that are capable of absorbing MW radiation, thereby preventing hazards and allowing reactions to be carried out in open vessels fitted to reflux condensers. In fact, the combined use of MW and supported reagents is truly a major advance in organic synthesis [42].

### 1.5.1 Conveying MW energy: susceptors

A few recent improvements certainly warrant further attention here. Traditional absorbers have, over time, been replaced by energy *susceptors* or *sensitizers*, which convey MW energy to chemical substrates and catalysts inside the flask. Some materials, in particular amorphous carbon, graphite, and silicon carbide (SiC), strongly interact with MWs and are rapidly heated at high temperatures at the standard 2.45 GHz frequency. Their use has been documented by numerous organic synthesis and catalysis research groups [43]. The applications of graphite, which exhibits high thermal conductivity, are generally twofold: (1) in reactions that require high temperatures and (2) in reactions involving either MW-transparent materials or substrates with low dielectric loss, which will be poorly heated by MW irradiation. Moreover, graphite can also be used as a solid support catalyst for MW or conventionally heated reactions. The idea of using an invasive polar or MW-absorbing material to convey MW energy can be extrapolated to neoteric solvents, such as ionic liquids, which are strong MW absorbers. Small volumes often suffice to perform MW-activated reactions conducted with nonpolar solvents or reagents [44, 45].



**Fig. 1.6:** Comparative image of MW vials (10 mL each) made of pyrex containing a magnetic bar and a cylindrical SiC passive element. The graph shows a comparison of temperature profiles (internal fiber-optic sensor) for the heating of methanol ( $\tan \delta = 0.659$ ) to 175 °C carried out in the aforementioned pyrex and SiC vials for 10 min, with very similar heating and cooling profiles. The pressure profile ( $p$ ) for the pyrex experiment is also shown. Reproduced with permission from Ref. [46]. Copyright 2013 American Chemical Society.

Heating with commercially available MW-absorbing polymers, such as Weflon<sup>®</sup> and Carboflon<sup>®</sup>, has become popular, although heating is limited to ca. 240 °C. The introduction, in 2006, of a new generation of sintered SiC-based ceramics has enabled high-temperature applications to be performed thanks to the material's high melting point (~2700 °C) [43, 46]. Furthermore, it can be used as a support material and employed as an MW sensitizer in the form of powders, granules or cylinders. In addition, vessels made of SiC take advantage of high thermal conductivity as well as enhanced mechanical and chemical resistance (Figure 1.6). MW-transparent solvents (e.g., hydrocarbons) can be heated in SiC vials at approximately the same rate as polar alcohols (strong MW-absorbing solvents). SiC technology is therefore suitable for dissecting specific and nonthermal effects because it effectively prevents MW radiation from penetrating to the reaction medium, which will mostly be activated by conventional rather than dielectric heating [46, 47].

### 1.5.2 A peculiar device: cooling while heating

As perplexing as it may seem, significant improvements (yields and selectivity) can sometimes be attained by the simultaneous and paradoxical combination of cooling and MW heating, as documented in recent reviews [24, 48]. Cooling allows for higher levels of MW energy to be applied to the reaction mixture, while maintaining the system at a relatively low bulk temperature. Positive effects include a greater selectivity,

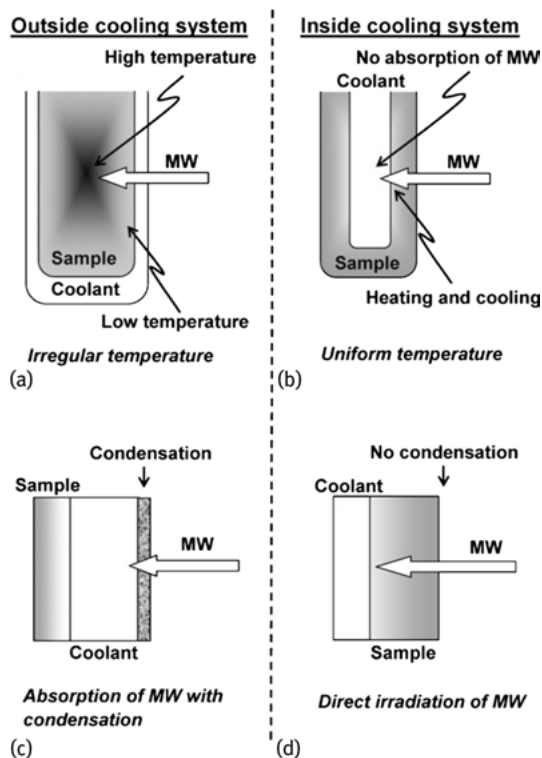


Fig. 1.7: Schematic representation of MW reactors with inside and outside cooling systems. Reproduced with permission from Ref. [49]. Copyright 2008 Royal Society of Chemistry.

by avoiding the formation of thermal decomposition side products, and a higher tolerance to sensitive functional groups or unstable substrates.

External cooling is usually provided by a stream of compressed air or an MW-transparent cooling liquid. This may, however, result in condensation on the reactor surface, thus attenuating the power input. Horikoshi and associates designed a cylindrical MW reactor that included both internal cooling and temperature monitoring, using a fiber-optic sensor, to prevent condensation, as shown in Figure 1.7 [49].

## 1.6 Efficient by design: tailor-made reactors

The development of modern MW chemistry would have been impossible without the parallel and progressive development of MW reactors that may now be designed to accomplish a variety of processes and transformations. The inherent drawbacks of domestic ovens were soon overcome by the introduction of professional multimode and single-mode reactors. Scaling-up is likewise feasible, although it faces problems

of energy efficiency, uniform thermal distribution and safety. Moreover, MW reactors have also been adapted to both batch and flow conditions [50, 51].

The interdisciplinary subject of MW reactor design lies beyond the scope of this chapter, and the reader is referred to a recent and detailed review [52], as well as subsequent chapters. Hybrid reactors, which combine MW radiation with other physical fields and technologies, are certainly worth mentioning as they could well provide synergistic effects and novel reaction mechanisms. In some cases, they have evolved from home-made devices, for specific purposes, to more efficient and robust designs, in collaboration with industrial partners. Thus, the combined use of MW heating with *electrochemical* techniques [53], *photochemistry* [54], and *sonochemistry* [55, 56] is especially worthy of note.

## 1.7 Conclusions

This chapter has summarized a number of historical points and concepts that have driven the use of MW technology in chemistry forwards and upwards. Although rooted in the interaction between electromagnetic radiation and matter, which dates back to the late nineteenth century, MW chemistry actually is a young subdiscipline that needed 30 years before sound background knowledge on MW effects was developed. It is widely recognized that MW heating is a particular form of energy transfer, one that uses safe and innocuous radiation, under standard lab precautions, capable of inducing enormous reaction acceleration and other efficiency and processing advantages. As noted in the introductory remarks, the chapter did not aim to be comprehensive, but it did attempt to give readers a glimpse of the key steps and moments of progress. Leading protagonists were cited and others can be found in the bibliographic section, which is chiefly made up of review articles and chapters. Accordingly, the references contain a veritable plethora of works by scientists who have contributed to the development of MW-assisted chemistry. Needless to say, we apologize for any unintentional omissions or oversight in the chapter, *which should be read as a collection of stories from MW history*. Subsequent chapters will doubtless describe the most up-to-date points of an engaging and interdisciplinary area for both education and research.

## Bibliography

- [1] Lee TH. Planar engineering. Cambridge, UK, Cambridge University Press, 2004.
- [2] Stuerger D. Microwave-materials interactions and dielectric properties: from molecules and macromolecules to solids and colloidal suspensions. In: De la Hoz A, Loupy A, eds. *Microwaves in organic synthesis*. 3rd ed. Weinheim, Germany, Wiley-VCH, 2012, 3–56.
- [3] Gensback H, ed. *Cooking by ultra short waves*. Short wave craft-the radio experimenter's magazine, November issue, 1933, pp 394, 429.

- [4] Microwave oven. Wikimedia Foundation, Accessed 21 Aug. 2016. Available from: [en.wikipedia.org/wiki/Microwave\\_oven](http://en.wikipedia.org/wiki/Microwave_oven).
- [5] Spencer PL. Method of treating foodstuffs. US Patent 2495429A, 1950.
- [6] Decareau RV. *Microwaves in the food processing industry*. New York, NY, USA, Academic Press, 1985.
- [7] Heseck JA, Wilson RC. Practical analysis of high-purity chemicals. X. Use of a microwave oven in in-process control. *Anal Chem* 1974, 46, 1160.
- [8] Abu-Samra A, Morris JS, Koirtiyohann SR. Wet ashing of some biological samples in a microwave oven. *Anal Chem* 1975, 47, 1475–1477.
- [9] Barrett P, Davidowski Jr LJ, Penaro KW, Copeland TR. Microwave oven-based wet digestion technique. *Anal Chem* 1978, 50, 1021–1023.
- [10] Nadkarni RA. Applications of microwave oven sample dissolution in analysis. *Anal Chem* 1984, 56, 2233–2237.
- [11] Vanderhoff JW. Method for carrying out chemical reactions using microwave energy. US Patent 3432413, 1969.
- [12] Ponomarev AN, Tarasenko VA. Application of microwave frequency irradiation for stimulation of chemical processes. *Zh Vses Khim Ob-va Im DI Mendeleeva* 1973, 18, 34–42.
- [13] Gedye R, Smith F, Westaway K, Ali H, Baldisera L, Laberge L, Rousell J. The use of microwave ovens for rapid organic synthesis. *Tetrahedron Lett* 1986, 27, 279–282.
- [14] Giguere RJ, Bray TL, Duncan SM, Majetich G. Application of commercial microwave ovens to organic synthesis. *Tetrahedron Lett* 1986, 27, 4945–4948.
- [15] Varma RS, Chatterjee AK, Varma M. Alumina-mediated deacetylation of benzaldehyde diacetates. A simple deprotection method. *Tetrahedron Lett*, 1993, 34, 3207–3210.
- [16] Polshettiwar V, Varma RS. Aqueous microwave chemistry: a clean and green synthetic tool for rapid drug discovery. *Chem Soc Rev*, 2008, 37, 1546–1557.
- [17] Collins MJ. Introduction to microwave chemistry. In: Hayes BL, ed. *Microwave synthesis. Chemistry at the speed of light*. Matthews, NC, USA, CEM Publishing, 2002, 11–27.
- [18] Schanche JS. Microwave synthesis solutions from Personal chemistry. *Mol Divers* 2003, 7, 293–300.
- [19] Cole KS, Cole RH. Dispersion and absorption in dielectrics I. Alternating current characteristics. *J Chem Phys* 1949, 9, 341–345.
- [20] Davidson DW, Cole RH. Dielectric relaxation in glycerine. *J Chem Phys* 1951, 18, 1417.
- [21] Glarum SH. Dielectric relaxation of polar liquids. *J Chem Phys* 1960, 33, 1371–1375.
- [22] Anderson JE, Ullman R. Molecular relaxation in a fluctuating environment. *J Chem Phys* 1967, 47, 2178–2184.
- [23] Kappe CO. Controlled microwave heating in modern organic synthesis. *Angew Chem Int Ed* 2004, 43, 6250–6284.
- [24] De la Hoz A, Díaz-Ortiz A, Gómez MV, Prieto P, Sánchez-Migallón A. Elucidation of microwave effects: methods, theories, and predictive models. In: De la Hoz A, Loupy A, eds. *Microwaves in organic synthesis*. 3rd. ed. Weinheim, Germany, Wiley-VCH, 2012, 245–295.
- [25] Baghurst DR, Mingos DMP. Superheating effects associated with microwave dielectric heating. *J Chem Soc Chem Commun* 1992, 674–677.
- [26] Chemat F, Esveld E. Microwave super-heated boiling of organic liquids: origin, effect and application. *Chem Eng Technol* 2001, 24, 735–744.
- [27] Perreux L, Loupy A. A tentative rationalization of microwave effects in organic synthesis according to the reaction medium, and mechanistic considerations. *Tetrahedron* 2001, 57, 9199–9223.

- [28] Perreux L, Loupy A, Petit A. Nonthermal effects of microwaves in organic synthesis. In: De la Hoz A, Loupy A, eds. *Microwaves in organic synthesis*. 3rd. ed. Weinheim, Germany, Wiley-VCH, 2012, 127–207.
- [29] Zhou J, Xu W, You Z, Wang Z, Luo Y, Gao L, Yin C, Peng R, Lan L. A new type of power energy accelerating chemical reactions: the nature of a microwave-driving force for accelerating chemical reactions. *Sci Rep* 2016, 6, 25149.
- [30] Kappe CO, Stadler A, Dallinger D. *Microwaves in organic and medicinal chemistry*. 2nd ed. Weinheim, Germany, Wiley-VCH, 2012, 9–39.
- [31] Kappe CO, Pieber B, Dallinger D. Microwave effects in organic synthesis: myth or reality? *Angew Chem Int Ed* 2013, 52, 1088–1094.
- [32] Herrero MA, Kremsner JM, Kappe CO. Nonthermal microwave effects revisited: on the importance of internal temperature monitoring and agitation in microwave chemistry. *J Org Chem* 2008, 73, 36–47.
- [33] Kappe CO. How to measure reaction temperature in microwave-heated transformations. *Chem Soc Rev* 2013, 42, 4977–4990.
- [34] Leadbeater NE, Schmink JR, Hamlin TA. Tools for monitoring reactions performed using microwave heating. In: De la Hoz A, Loupy A, eds. *Microwaves in organic synthesis*. 3rd. ed. Weinheim, Germany, Wiley-VCH, 2012, 347–376.
- [35] Horikoshi S, Serpone N, eds. *Microwaves in nanoparticle synthesis*. New York, NY, USA, Wiley-VCH, 2013.
- [36] Horikoshi S, Serpone N. Microwave frequency effects in organic synthesis. In: De la Hoz A, Loupy A, eds. *Microwaves in organic synthesis*. 3rd. ed. Weinheim, Germany, Wiley-VCH, 2012, 377–423.
- [37] Dressen MHCL, van de Kruijs BHP, Meuldijk J, Vekemans JAJM, Hulshof LA. Vanishing microwave effects: influence of heterogeneity. *Org Process Res Dev* 2007, 11, 865–869.
- [38] Gutmann B, Schwan AM, Reichart B, Gspan C, Hofer F, Kappe CO. Activation and deactivation of a chemical transformation by an electromagnetic field: evidence for specific microwave effects in the formation of Grignard reagents. *Angew Chem Int Ed* 2011, 50, 7636–7640.
- [39] Hayden S, Studentschnig AFH, Schober S, Kappe, CO, Critical Investigation on the Occurrence of Microwave Effects in Emulsion Polymerizations. *Macromol Chem Phys* 2014, 215(23), 2318–2326.
- [40] Ferrari A, Hunt J, Stiegman A, Dudley GB, Microwave-Assisted Superheating and/or Microwave-Specific Superboiling (Nucleation-Limited Boiling) of Liquids Occurs under Certain Conditions but is Mitigated by Stirring. *Molecules* 2015, 20(12), 21672–21680.
- [41] Wu Y, Gagnier J, Dudley GB, Stiegman AE, Chem. The “chaperone” effect in microwave-driven reactions, *Chem Commun* 2016, 52, 11281–11283.
- [42] Varma RS, Nasir Baig RB. Organic synthesis using microwaves and supported reagents. In: De la Hoz A, Loupy A, eds. *Microwaves in organic synthesis*. 3rd. ed. Weinheim, Germany, Wiley-VCH, 2012, 427–486.
- [43] Besson T, Kappe CO. Microwave susceptors. In: De la Hoz A, Loupy A, eds. *Microwaves in organic synthesis*. 3rd. ed. Weinheim, Germany, Wiley-VCH, 2012, 297–346.
- [44] Baxendale IR, Lee AL, Ley SV. A concise synthesis of the natural product carpanone using solid-supported reagents and scavengers. *Synlett* 2001, 1482–1484.
- [45] Hoffmann J, Nüchter M, Ondruschka B, Wasserscheid P. Ionic liquids and their behavior during microwave irradiation—a state of the art report. *Green Chem* 2003, 5, 296–299.
- [46] Kappe CO. Unraveling the mysteries of microwave chemistry using silicon carbide reactor technology. *Acc Chem Res* 2013, 46, 1579–1587.

- [47] Gutmann B, Obermayer D, Reichart B, Prekodravac B, Irfan M, Kremsner JM, Kappe CO. Sintered silicon carbide: a new ceramic vessel material for microwave chemistry in single-mode reactors. *Chem Eur J* 2010, 16, 12182–12194.
- [48] O'Brien M, Denton R, Ley SV. Lesser-known enabling technologies for organic synthesis. *Synthesis* 2011, 1157–1192.
- [49] Horikoshi S, Tsuzuki J, Kajitani M, Abe M, Serpone N. Microwave-enhanced radical reactions at ambient pressure. Part 3: highly selective radical synthesis of 3-cyclohexyl-1-phenyl-1-butanone in a microwave double cylindrical cooled reactor. *New J Chem* 2008, 32, 2257–2262.
- [50] Baxendale IR, Hayward JJ, Ley SV. Microwave reactions under continuous flow conditions. *Comb Chem High Throughput Screening* 2008, 10, 802–836.
- [51] Morschhäuser R, Krull M, Kayser C, Boberski C, Bierbaum R, Püschner PA, Glasnov TN, Kappe CO. Microwave-assisted continuous flow synthesis on industrial scale. *Green Process Synthesis* 2012, 1, 281–290.
- [52] Ondruschka B, Bonrath W, Stuerge D. Development and design of reactors in microwave-assisted chemistry. In: De la Hoz A, Loupy A, eds. *Microwaves in organic synthesis*. 3rd. ed. Weinheim, Germany, Wiley-VCH, 2012, 57–103.
- [53] Dale SEC, Compton RG, Marken F. Microwaves and electrochemistry. In: De la Hoz A, Loupy A, eds. *Microwaves in organic synthesis*. 3rd. ed. Weinheim, Germany, Wiley-VCH, 2012, 525–539.
- [54] Církva V. Microwaves in photochemistry and photocatalysis. In: De la Hoz A, Loupy A, eds. *Microwaves in organic synthesis*. 3rd. ed. Weinheim, Germany, Wiley-VCH, 2012, 563–605.
- [55] Cravotto G, Cintas P. The combined use of microwaves and ultrasound: methods and practice. In: De la Hoz A, Loupy A, eds. *Microwaves in organic synthesis*. 3rd. ed. Weinheim, Germany, Wiley-VCH, 2012, 541–562.
- [56] Cintas P, Cravotto G, Canals A. Combined ultrasound-microwave technologies. In: Chen D, Sharma SK, Mudhoo A, eds. *Handbook on applications of ultrasound. Sonochemistry for sustainability*. Boca Raton, FL, USA, CRC Press, 2012, 659–673.



Paolo Veronesi

## 2 An Introduction to dielectric heating

Dielectric heating is usually indicated as the rapid and uniform heating throughout a nonconducting material by means of a high-frequency electromagnetic field. However, this basic definition can be extended considering also cases in which heating is not necessarily uniform (i.e., selective heating) or heating involves semiconductors or even conducting metallic or nonmetallic materials. How this can be accomplished using electromagnetic fields at radio or microwave (MW) frequencies is addressed in this chapter. Basic equations describing dielectric heating are introduced and used to deduce the unique characteristics of dielectric heating.

### 2.1 The electromagnetic spectrum and the industrial, scientific, and medical frequencies

Dielectric heating usually refers to the use of high-frequency electromagnetic fields to generate heat in a given load. Electromagnetic waves ranging from 3 kHz to 300 GHz are generally called radio frequency (RF), and those over 300 MHz are called specifically MW. In this framework, the term RF can be referred to the frequencies between 3 kHz and 300 MHz, as shown in Figure 2.1.

It is evident that RF and MWs are nonionizing radiations, i.e., their energy is not enough to ionize atoms or molecules. Nevertheless, dielectric heating applied to chemical reactions, usually called *MW chemistry*, has a large number of benefits in terms of yields, selectivity, and greener processing, most of them attributable to MW-related thermal effects.

Radio and MW frequencies are also widely used by radio communication systems; hence, to avoid possible interference, the competent authorities have allocated some bands (range of frequencies) for industrial, scientific, and medical (ISM) use. The worldwide allowed frequencies of industrial relevance for dielectric heating ap-

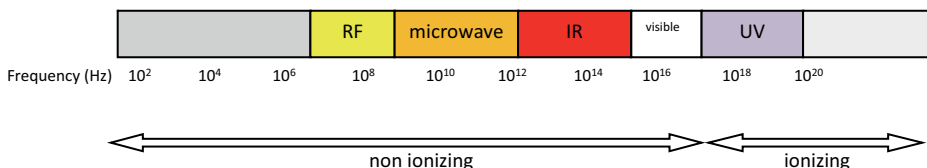


Fig. 2.1: The electromagnetic spectrum.

<https://doi.org/10.1515/9783110479935-002>

**Tab. 2.1:** ISM frequencies (<sup>n</sup> allocated in region *n* only, with some exceptions)

Frequency range		Center frequency
6.765 MHz	6.795 MHz	6.780 MHz
13.553 MHz	13.567 MHz	13.56 MHz
26.957 MHz	27.283 MHz	27.12 MHz
40.66 MHz	40.7 MHz	40.68 MHz
433.050 MHz	434.790 MHz	433.920 MHz <sup>1</sup>
902 MHz	928 MHz	915 MHz <sup>2</sup>
2.4 GHz	2.5 GHz	2.45 GHz
5.725 GHz	5.875 GHz	5.8 GHz
24 GHz	24.25 GHz	24.125 GHz

plications are listed in Table 2.1, and an updated version of the European allocated frequencies can be found at <http://www.efis.dk>:

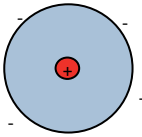
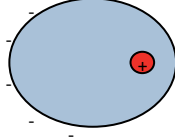
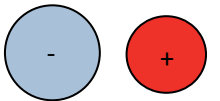
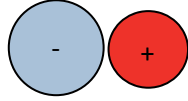
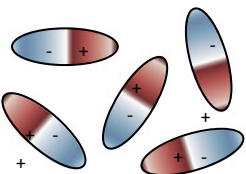
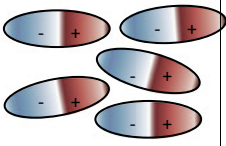
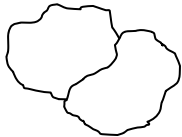
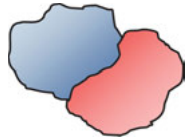
Within the ISM frequencies, radio communication systems using these bands must accept possible interference from ISM equipment.

## 2.2 Basis of dielectric heating

Both MW and RF heating, also called dielectric heating, are techniques that make it possible to volumetrically heat a portion of matter, referred to as *load* due to the heat generated inside such a load as a result of the electromagnetic field–matter interactions. Such techniques are usually (but not exclusively) applied to heating dielectric materials, which have low thermal conductivity and hence benefit from the possibility to internally generate heat. However, the extent of the region affected by direct heat generation is strictly dependent on the nature of the load and of the electromagnetic wave used, and it can constitute a limiting factor when applying such heating technologies. It is therefore necessary to understand which mechanisms are involved in electromagnetic field–matter interactions. Interaction with an alternating electric field is usually expressed in terms of a redistribution of charges or polarization in the material. These interactions are dissipative, leading to heat generation, and include electronic polarization, dipolar polarization, ionic polarization and interfacial polarization. Magnetic losses can be present as well, especially in conductive materials, like metals, and include hysteresis, eddy currents, domain wall and electron spin resonance.

Figure 2.2 provides a simplified illustration of the polarization mechanisms.

Electronic polarization occurs when electrons are shifted, under the effect of an electric field, with respect to the positive nuclei, leading to a nonzero dipole moment. In covalent solids, the electrons in the covalent bond are easily moved from their orig-

Polarization	$E=0$	$E \neq 0$ $\rightarrow$
Electronic		
Ionic		
Dipolar		
Interfacial		

**Fig. 2.2:** Polarization mechanisms.

inal position. Electrons have a small inertia and can easily follow the alternating field up to the frequencies of the visible light.

Dipolar polarization occurs when an external electric field tends to align the existing dipoles of the material (polar molecules, like water, for instance) parallel to the field. If the electric field is alternating at a high frequency, as in typical dielectric heating applications, a phase difference exists between the orientation of the field and the orientation of the dipoles, which is responsible for the dissipative interactions (heat generation). Molecules with permanent dipoles can have a rather high mass, so their polarization requires more time and takes place near radio or MW frequencies.

Ionic polarization involves the relative shift of the barycenter of the positively and negatively charged ions, as in alkali halides, from their equilibrium position in the lattice, leading to a net dipole moment different from zero. The vibration of atoms or ions depends on the thermal energy, and their vibrations roughly correspond to the infrared region of the electromagnetic spectrum. This means that their polarization occurs practically in phase with the alternating field, and this does not affect MW heating.

Interfacial polarization occurs when free charges accumulate at the interfaces located within a material, like grain boundaries or interfaces among different phases. The application of the electric field displaces the more mobile charges, which are then accumulated where discontinuities occur, like the free surface or phase boundaries. The movement and build-up of charges requires longer times compared to electronic polarization, so this type of polarization occurs at much lower frequencies, which can fall under the MW or RF region of the electromagnetic spectrum.

In dielectric heating applications, it is necessary to quantify such a degree of interaction, which is macroscopically described by the complex relative permittivity. The complex relative permittivity is a measure of how an electric field affects – and is affected by – a dielectric medium. Different polarization mechanisms (electronic, atomic, orientation or dipolar, and ionic) are involved, at different frequencies, in determining the material permittivity, which is a frequency-dependent quantity, affected also by the dielectric material temperature and chemical composition. The complex relative permittivity can be expressed as

$$\varepsilon_d^* = \varepsilon' - j\varepsilon_d'' = \varepsilon_0(\varepsilon_r' - j\varepsilon_r'' d), \quad (2.1)$$

where

$$j = \sqrt{-1};$$

$\varepsilon_0 = 8.86 \times 10^{-12}$  F/m, empty space permittivity;

$\varepsilon_r'$ : relative dielectric constant;

$\varepsilon_r''$ : loss factor for dipolar loss mechanism.

The subscript “d” is used to address the fact that only dipolar losses are accounted for. However, practically separating the contribution of each loss mechanism (like ionic polarization and atomic polarization, but also conductive losses) when measuring permittivity of a given load is not practical, so an effective loss factor,  $\varepsilon_{\text{eff}}''$ , is introduced:

$$\varepsilon^* = \varepsilon' - j\varepsilon_{\text{eff}}'' = \varepsilon' - j \left( \varepsilon_d'' + \frac{\sigma}{\omega\varepsilon_0} \right), \quad (2.2)$$

where  $\sigma$  is the electrical conductivity and  $\omega = 2\pi f$ , with  $f$  being the frequency of the electromagnetic field.

Table 2.2 shows an example of some measured permittivity values involving solvents.

Similarly, the dipolar losses could be included in equivalent conductivity losses, thereby expressing the dielectric properties in terms of  $\varepsilon'$  and conductivity  $\sigma_{\text{eff}}$ . An example of this way of expressing dielectric properties is given in Table 2.3, which relates to body tissues. Strong variations occur as a consequence of the different water content in living tissues, showing that an incident electromagnetic field can be absorbed to a different extent by each tissue.

Alternatively, the dielectric properties of matter can also be expressed in terms of  $\varepsilon'$  and of a further parameter,  $\tan \delta$ , the loss tangent, which is the ratio of the imagi-

**Tab. 2.2:** Permittivity of some solvents at 2.45 GHz at room temperature (after data from [1])

Solvent	Dielectric constant ( $\epsilon'$ )	Loss tangent ( $\tan \delta$ )	Loss factor ( $\epsilon''$ )
Water	80.4	9.889	12.3
Ethylene Glycol	37.0	1.35	49.950
Methanol	32.6	0.856	21.483
Ethanol	24.3	0.941	22.866
Chloroform	4.8	0.091	0.437
Toluene	2.4	0.040	0.096
Hexane	1.9	0.020	0.038

nary to the real part of the complex dielectric constant:

$$\tan \delta = \epsilon''_{\text{eff}} / \epsilon' \quad (2.3)$$

Another important piece of information to quantify the effects of electromagnetic field–matter interactions, strictly related to the dielectric properties, is the power density (Pd). It is defined as the power per unit volume that is dissipated in a load exposed to MWs, according to the simplified equation

$$P_d(x, y, z) = \omega \epsilon_0 \epsilon''_{\text{eff}} E_{\text{rms}}^2 + \omega \mu_0 \mu''_{\text{eff}} H_{\text{rms}}, \quad (2.4)$$

where:

$P_d$ : power density in material ( $\text{W}/\text{m}^3$ ) at position  $(x, y, z)$ ;

$\epsilon''_{\text{eff}}$ : effective loss factor, including conductivity losses;

$\mu''_{\text{eff}}$ : imaginary part of effective magnetic permeability;

$E_{\text{rms}}$ : local  $(x, y, z)$  electric field strength ( $\text{V}/\text{m}$ );

$H_{\text{rms}}$ : local  $(x, y, z)$  magnetic field strength ( $\text{A}/\text{m}$ ).

The second term in Equation (2.4) takes into account magnetic losses, but this term is usually neglected for most dielectrics, like polymeric and ceramic materials, unless they possess relevant magnetic properties (i.e., ferrites). This usually applies also to most of the chemical compounds, which tend to interact with the electric field through the polarization mechanisms discussed earlier.

However, the effective values of the E and H fields strictly depend on the power output of the electromagnetic source (generator) and on the shape and dimension of the space – usually an enclosure – where electromagnetic field-matter interactions occur (Chapter 3). Hence, Equation (2.4) also shows the importance of a properly designed applicator since it determines, together with the generator, the load nature, position and geometry, the fields' strength and distribution [2].

The power penetration depth is used to quantify how deep the power from an external electromagnetic field can penetrate in a material, until a given attenuation is achieved, typically  $1/e$  (0.368) of the power density value at the load surface. For

**Tab. 2.3:** Permittivity of body tissues at 2.45 GHz (data computed according to 4-Cole–Cole Model and implemented in FCC Body Tissue Dielectric Parameters tool: <https://www.fcc.gov/general/body-tissue-dielectric-parameters>)

Tissue	$\epsilon'$	$\sigma$
Bladder	18.000759	0.685294
Blood	58.263756	2.544997
Bone_Cancellous	18.548979	0.805112
Bone_Cortical	11.381223	0.394277
Bone_Marrow_Infiltrated	10.308158	0.458822
Bone_Marrow_Not_Infiltr	5.296872	0.095031
Breast_Fat	5.146670	0.137039
Cartilage	38.771160	1.755682
Cerebellum	44.803696	2.101270
Cerebro_Spinal_Fluid	66.243279	3.457850
Colon(Large_Intestine)	53.878193	2.038204
Cornea	51.614494	2.295194
Dura	42.035004	1.668706
Eye_Tissue(Sclera)	52.627628	2.033048
Fat	5.280096	0.104517
Fat(Mean)	10.820482	0.267954
Gall_Bladder	57.633728	2.059032
Gall_Blad_Bile	68.360931	2.800733
Grey_Matter	48.911255	1.807664
Heart	54.814018	2.256186
Kidney	52.742668	2.429709
Lens_Cortex	44.625317	1.504036
Lens_Nucleus	33.973507	1.086901
Liver	43.034443	1.686411
Lung(Inflated)	20.476801	0.804128
Lung(Deflated)	48.380974	1.682395
Muscle(Parallel_Fiber)	54.417614	1.882011
Muscle(Transverse_Fibr)	52.729469	1.738781
Nerve(Spinal_chord)	30.145145	1.088474
Ovary	44.699692	2.263874
Skin(Dry)	38.006660	1.464073
Skin(Wet)	42.852562	1.591928
Small_Intestine	54.424351	3.172779
Spleen	52.449310	2.238070
Stomach_Esop_Duodenum	62.158325	2.210518
Tendon	43.121975	1.684531
Testis_Prostate	57.550518	2.167421
Thyroid_Thymus	57.200367	1.967798
Tongue	52.627628	1.802514
Trachea	39.732574	1.448737
Uterus	57.813835	2.246464
Vitreous_Humour	68.208023	2.478094
White_Matter	36.166599	1.215008

dielectric materials, a simplified equation describing the power penetration depth in a semi-infinite slab is

$$D_p = \frac{\lambda_0}{2\pi} \sqrt{\frac{1}{2\mu\epsilon_0\epsilon'}} \left[ \sqrt{1 + \left(\frac{\epsilon''_{\text{eff}}}{\epsilon'}\right)^2} - 1 \right]^{-\frac{1}{2}}, \quad (2.5a)$$

which, in the case of  $\epsilon'' \ll \epsilon'$ , becomes the commonly used

$$D_p = \frac{\lambda_0 \sqrt{\epsilon'_r}}{2\pi\epsilon''_r} \quad (2.5b)$$

where  $\lambda_0$  is the wavelength of the incident MWs.

Noticeably, Equations (2.5) do not imply that no heating beyond the power penetration depth is achievable, but that around 63% of the incident power is dissipated within the penetration depth, the remaining being dissipated in the deeper regions of the load. The power penetration depth quantifies neither how the temperature profile is generated within the load, because Equations (2.5) do not take into account the heat transfer, nor the thermal properties of the load. Nevertheless, Equations (2.4) and (2.5) make it possible to gain better insight into some of the relevant aspects of dielectric heating.

#### *Power penetration depth at work*

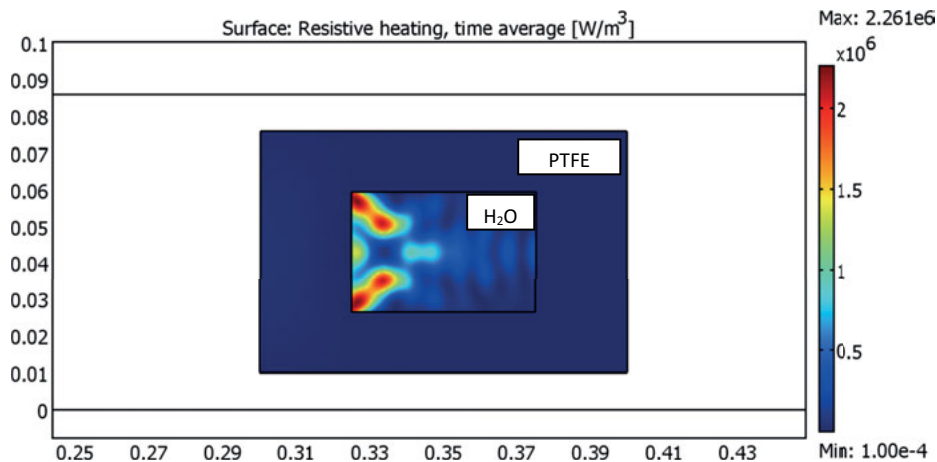
Consider a load made of a substance whose permittivity changes with temperature (see table). How large can the material be to be effectively processed by MW heating at 2450 MHz?

Temperature (°C)	Frequency (MHz)	$\epsilon'$	$\epsilon''$
-20	2450	5	1
+25	2450	53	20

The calculated power penetration depth, according to Equation (2.5b), is 43.59 mm at -20 °C and 7.09 mm at 25 °C. Considering that in a real multimode applicator MWs can enter from both sides of the load (i.e., the real load is not a semi-infinite plane), it can be assumed that a maximum thickness of the load of approximately 15 mm is suitable to remain within the power penetration depth of MWs at 25 °C throughout the entire heating process. Using larger loads would mean achieving a rather good penetration at low temperature but a tendency to overheat the outer regions as the temperature increases.

### 2.2.1 Selectivity

According to Equation (2.4), if a heterogeneous (in terms of chemical composition, phases, or even density) load is subjected to dielectric heating, by exposure to the



**Fig. 2.3:** Power density distribution showing selective MW heating of water in a closed PTFE container enclosed in a metallic applicator (outer region, not shown) where MWs propagate from the left side.

same  $E$ -field strength, the resulting power density, and thus heating rate, will be higher for material with a higher loss factor. This is depicted in Figure 2.3, where MW heating at 2.45 GHz of a region of water inside a polytetrafluoroethylene (PTFE) block positioned in a rectangular applicator is simulated and expressed in terms of power density or resistive heating, averaged over time. This means that heat is generated more into the part of the material that presents a higher loss factor, which is selectively heated.

As an example, in the case of materials presenting a nonhomogeneous moisture distribution, heating occurs more rapidly in regions containing more water, which are dried faster than the remaining parts of the material, leading to moisture leveling. This highly unique feature of dielectric heating, usually exploited more at RFs, is known as *selective heating*, and it is currently applied to level the moisture of snack foods, wooden products, leather products, and many more.

Heating selectivity is also the basis of many MW-assisted synthesis-related papers, which assumed that it was possible to selectively excite functional groups or even single molecules, thereby resulting in completely new and different reaction paths and product yields. However, heat transfer on such a small scale is extremely rapid, much faster than a period of an MW (whose typical frequency is 2.45 GHz), so selectivity at this scale should be unlikely to occur unless the resulting heat transfer is particularly difficult, as in solid-state reactions or when using heterogeneous catalysts. Instead, it is more likely that different temperature distributions and high heating rates, achievable by dielectric heating, will be the basis of the observed increased yields, product selectivity and the opening of entirely new reaction pathways not experienced at lower temperatures [3]. However, when addressing temperature, it must be considered that



when using dielectric heating, differential heating or localized hot spots with slightly higher temperatures at reaction sites can occur, which cannot be measured by normal sensors, which give information on much wider areas. Hence, a comparison of temperatures between a dielectric-heating-assisted reaction and a conventionally heated one requires great care.

### 2.2.2 Self-regulating reactions

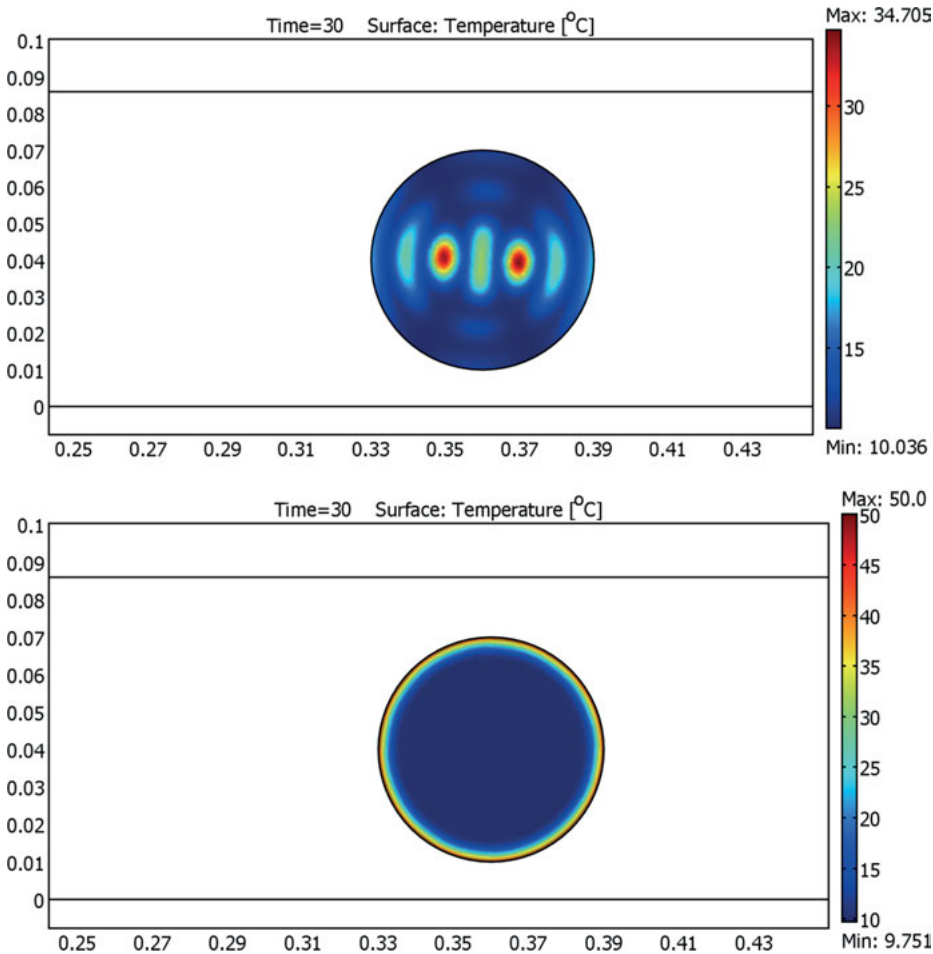
According to Equation (2.4), if products have different dielectric properties compared to the starting reactants, then self-regulation of a reaction can occur, as opposed to thermal runaway. If products have a much lower loss factor than reactants, then conversion of the electromagnetic field energy into heat decreases as the reaction approaches completion, and a reduction of the heating rate or even a temperature drop can be observed in much the same way as moisture leveling. This is particularly interesting as it avoids overheating of products, especially when the reaction is started nonhomogeneously in the reactant mixture. On the other hand, possible transformations (even phase transformations) can hinder the capability of the dielectric heating to continue to provide energy to the reaction as it proceeds, as in the case of low-loss reaction intermediates or when reaching the Curie temperature of ferromagnetic reactants [4].

### 2.2.3 Volumetric heating

According to Equation (2.5), dielectric heating can penetrate deep into a material, depending on the frequency of the electromagnetic field and of the material properties. This makes it possible to generate heat inside the load, possibly involving the whole volume. Figure 2.4 shows an example of a comparison between the first seconds of conventional heating (load has boundary conditions set at 50 °C on its walls) and 2.45 GHz MW heating of a cylinder of butter starting at 10 °C ( $43 - j0.42$ ) at 1 kW power.

For this reason, dielectric heating can be considered volumetric. It must be pointed out that, owing to the attenuation of the electromagnetic field as its energy is converted into heat in the load, the dielectric heating of a homogeneous semi-infinite slab results in higher power density generation at its surface, exponentially decreasing as the electromagnetic field enters the load. For this reason, when using extremely high frequencies to process high loss materials, such a volumetric heating effect can turn out to be negligible, in agreement with Equation (2.5b).

Last but not least, because permittivity is a function of temperature, the power penetration depth is therefore temperature-dependent as well. This practically means that the amount of load directly exposed to dielectric heating can vary as heating proceeds and that a load initially considered too large for processing can become more



**Fig. 2.4:** Volumetric MW heating (top) compared to surface conventional heating (bottom) of a block of butter. The  $x$ -axis shows the dimensions in meters.

suitable when a certain temperature level is reached. Again, as in the case of self-regulation reactions, this is how permittivity changes with temperature (i.e., as an increasing or decreasing temperature function), which determines the behavior.

#### 2.2.4 Inversion of temperature profile

Selective and volumetric heating of materials usually presenting low thermal conductivity or exposed to cold environments during processing can evidence the phenomenon of temperature profile inversion. This phenomenon is erroneously explained as being based on the fact that microwaves *heat from the inside*. In conven-

tional heating processes, the outer surface of the load is hotter (because it is exposed to the furnace environment, where resistance heating elements, hot air generators or IR lamps are installed) and temperature progressively decreases toward the inside as a consequence of heat transfer. In dielectric heating, temperature can be higher in the inner parts of the load, while the surface remains colder. This is a combination of two peculiarities of dielectric heating: selectivity, which implies that the air in the furnace (applicator) is not heated, and volumetric heating, which implies that heat is generated also below the load surface. Thus, the surface of the workload is exposed to *cold* air, which lowers its temperature, while the inside is *thermally insulated* by the outer layers of the load itself, while heat generation occurs in such layers.

Such inversion of temperature profiles can be used proficiently when combining conventional and dielectric heating techniques (hybrid systems): the resulting profile, obtained by the superimposition of the two, can be particularly flat, allowing high heating rates to be applied without any distortion or residual stress arising in the load because its temperature is kept almost constant throughout its volume [5].

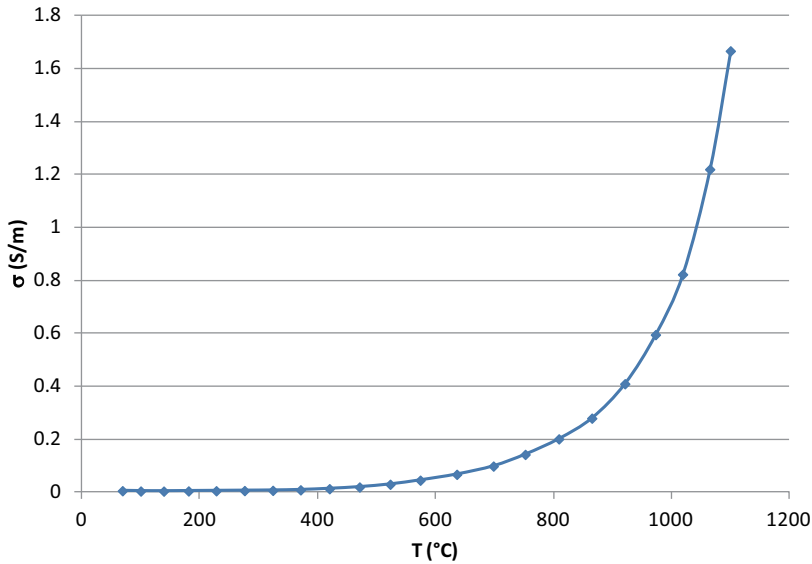
### 2.2.5 Rapid heating

Provided the electric field strength remains below the dielectric strength of the material composing the load and that of the surrounding medium, high power densities can be achieved in the load itself, making dielectric heating more rapid than conventional heating that relies on heat transfer [6]. In these scenarios, the heating rate could turn out to be a direct and highly controllable function of energy input. Rapid heating, faster than in conventional heating, is easily experienced when processing materials having low thermal conductivity. However, it should be pointed out that for such materials a rather homogeneous heating must be achieved in order to avoid deformations or cracks induced by thermal expansion. Heating homogeneity is always an issue, even in large dielectric heating applicators, so care must be taken when applying extremely rapid heating schedules. Too high a heating rate, moreover, is likely to induce thermal runaway in the load, as described in the next section.

Cooling can be an issue as well, as the load is rapidly exposed to the environmental temperature (usually much lower) when the electromagnetic field generator is turned off, and this can lead to extremely rapid temperature drops, localized at the surface, where radiation and convection losses predominate.

### 2.2.6 Thermal runaway

*Thermal runaway* is the term used to address the rapid and uncontrollable overheating of parts of a load under processing. It usually happens with materials having a low thermal conductivity (or subjected to extremely high heating rates) and whose



**Fig. 2.5:** Loss factor expressed in terms of equivalent conductivity of zirconia, at 2.45 GHz; data compiled after [7].

loss factor increases as the temperature increases. In this case, the heat transfer cannot compensate for possible lack of heating homogeneity, with the result that the hotter parts of the load become lossier and thus are heated more than the colder zones. According to Equation (2.4), the power density at a given electric field strength is dependent on the loss factor, meaning that more heat is generated in the lossier regions of the load. However, as these zones are heated, their loss factor increases and more and more heat is generated in the same region, until the process becomes extremely fast and uncontrollable, a classic example being in defrosting, as described earlier.

Strong variations of the loss factor as a function of temperature are typical in most ceramics and glasses. For example, zirconia's loss factor is plotted in Figure 2.5, where the values of electric conductivity  $\sigma$  appear as calculated from corresponding data for  $\epsilon''$  at 2.45 GHz.

## Bibliography

- [1] Metaxas AC. *Foundations of Electroheat: A Unified Approach*. John Wiley & Sons, 1996
- [2] Poli G, Sola R, Veronesi P. Microwave-assisted combustion synthesis of NiAl intermetallics in a single mode applicator: Modeling and optimisation. *Materials Science and Engineering A*. 2006, 441(1-2):149–156.
- [3] Kappe CO, Pieber B, Dallinger D. Microwave Effects in Organic Synthesis: Myth or Reality?. *Angew. Chem. Int. Ed.*, 2313, 52:1088–1094.

- [4] Rosa R, Veronesi P, Casagrande A, Leonelli C. Microwave ignition of the combustion synthesis of aluminides and field-related effects. *Journal of Alloys and Compounds*, 2016, 657:59–67.
- [5] Rosa R, Veronesi P, Leonelli C. A review on combustion synthesis intensification by means of microwave energy. *Chemical Engineering and Processing: Process Intensification*, 2013, 71:2–18.
- [6] Veronesi P, Leonelli C, Poli G, Casagrande A. 'Enhanced reactive NiAl coatings by microwave-assisted SHS'. *COMPEL – The international journal for computation and mathematics in electrical and electronic engineering*, 2008, 27(2):491–499
- [7] Vadim Yakovlev V, Shawn Allan M, Morgana Fall L, Holly Shulman S. Computational Study of Microwave Processing of Zirconia: Effects of Frequency and Temperature-Dependent Material Parameters. In: *Proc of 13th Seminar Computer Modeling in Microwave Engineering & Applications*, Thun, Switzerland, March 7–8, 2011

Cristina Leonelli

### **3 Microwave generators, transmission, and interaction with different materials**

The purpose of this chapter is to provide chemists with some basic elements of the construction of a microwave applicator to enable better use of commercial apparatuses and, eventually, their modifications. The equations underlying the choice of the dimensions of the applicator operating at the most used microwave frequency of 2.45 GHz are not even presented. The most common geometries adopted for commercial microwave applicators used in the chemical lab are reported, while specific pieces of machinery are treated in other chapters and in several dedicated books [1–4].

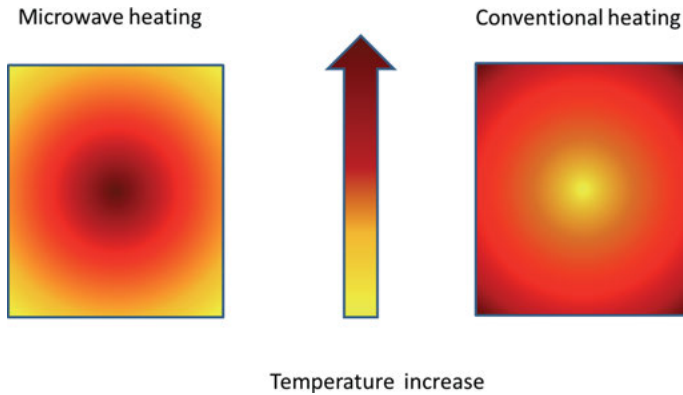
Some of the simplification adopted to write this chapter are addressed to those chemists who still see the so-called magic in microwave heating of reactants. The physical understanding of a microwave applicator as well as the interaction of the electromagnetic field with matter (Chapter 2) should help the reader to fully understand what is happening when chemicals are heated with microwaves. As with many instruments, if a system is very complicated to operate, it generally becomes either a glorified shelf to store things on or a headache to those having to operate it. The easier a microwave system is to use and understand, the better off one will be.

Readers are strongly advised to enrich their basic knowledge of the subject matter covered in this chapter [5–7].

#### **3.1 Introduction**

In a high-frequency heating process, the high-frequency waves heat the lossy dielectric or magnetic materials in the complete volume by penetrating into the material, depending on the penetration depth of the waves. Provided the material is not too thick, the high-frequency waves transfer more or less the same amount of energy to every volume element of the material, resulting in a homogeneous temperature increase. Theoretically this would give every volume element the same temperature. In a practical situation when the material to heat is positioned within an empty microwave applicator, the surface of the material would lose heat to the ambient atmosphere, which is not heated by high-frequency waves. Therefore, the surface temperature is reduced, resulting in a temperature profile where the highest temperature is inside, while the lowest temperature is on the surface of the material (Figure 3.1). This temperature profile is the inverse of conventional or radiative heating processes such as those adopted in resistance muffle furnaces or oil baths.

<https://doi.org/10.1515/9783110479935-003>



**Fig. 3.1:** Temperature distribution for conventional and dielectric heating.

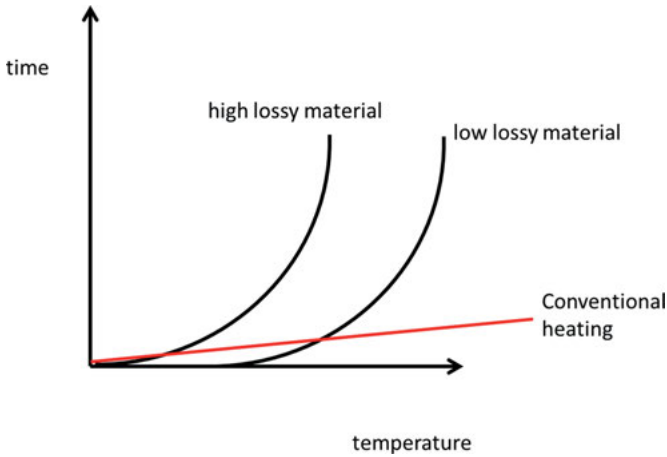
This peculiar temperature profile creates problems when deciding on the position of a temperature sensor. If the temperature sensor is positioned on the surface of the sample being heated by microwaves, then the warmest surface will be monitored and the hottest will not be. In these conditions there will be another problem, explained as follows.

High-frequency heating is governed by the dielectric and/or magnetic properties of the material. These properties depend on the frequency and the temperature.

The dielectric properties of most chemical compounds dependent mainly on temperature, whereby the coupling is increased as the temperature increases. These materials are prone to a thermal runaway effect that is initially caused by low temperature differences in the material. Those areas with a slightly higher temperature than the surrounding material take up more energy because of better coupling to the high-frequency waves. This results in a faster temperature increase, which in turn leads to even better coupling and increased energy uptake, and so on (Figure 3.2). This thermal runaway can result in local destruction or even melting of the material and its container.

Besides volumetric heating, microwave heating offers a number of advantages, as follows [8–11]:

- Selective material heating;
- Rapid heating;
- Noncontact heating;
- Quick startup and stopping of microwave irradiation so that the heating process can be precisely controlled;
- Portability of equipment and processes;
- High heating efficiency (efficiency of 80% or higher can be achieved);
- It is silent and generates no exhaust gas.



**Fig. 3.2:** Temperature profile during thermal runaway phenomenon for two different materials: the more lossy one starts increasing the temperature sometime before the less lossy one. Conventional heating is reported as reference.

It also has the following disadvantages:

- The capacity of its power generator is limited to about 100 kW or less;
- Electrical discharge easily occurs with an object material containing solid or powder metal.

To come up with a proper heating process using microwave irradiation, an applicator or a microwave processing system must be built, which includes generator, applicator, and control systems. While the basic components are simple, the interaction of materials with microwave fields and changes in fundamental material properties during processing make the design and development of microwave processes very complex. This complexity may be dealt with using an integrated approach with a process design team consisting of the materials and process engineer, the microwave equipment manufacturer, and an electromagnetic specialist.

This chapter identifies basic but key considerations in generator, applicator, and control systems, leaving equipment selection and design and numerical process simulation to engineers.

## 3.2 Microwave generators

### 3.2.1 Magnetron

The type of microwave generator most frequently used is the magnetron vacuum tube, or simply magnetron. Magnetrons were developed in the 1950s for radar applications



and have been used for microwave heating since the discovery of this application for high-frequency waves.

Magnetrons are produced with an output power ranging from 200 W to 60 kW or even higher. The majority of the magnetrons are produced with an output power between 800 and 3000 W for laboratory microwave ovens. Unlike the magnetrons used for domestic ovens, in the case of laboratory equipment, the microwave power is continuously erogated to better control the heating cycles.

Owing to the mass production of magnetrons with a power of about 800 to 1200 W, the price of these magnetrons is comparatively low. Therefore, these magnetrons are often preferred also when the total output power reaches 3000–3600 W, cases where the combination of two or more magnetrons is a more economically affordable solution.

During operation magnetrons must be cooled to prevent overheating. Magnetrons with a power of up to about 2 kW are usually air cooled, while those with a higher power are usually water cooled, requiring water recirculation units. Those magnetrons also require the use of special protection equipment against reflected power that could overheat and destroy the magnetron. Low-power magnetrons are more robust and can be operated without protection equipment.

### 3.2.2 Solid-state generators

In the 1970s another technology was proposed for the construction of microwave generators, solid-state microwave generators [12]. Only recently has the potential market value of solid-state microwave heating systems, in particular for domestic microwave ovens, prompted several companies to develop, patent, and market this technology [13]. Solid-state microwave heating (S<sup>2</sup>MH) technology offers several advantages over magnetrons in various microwave heating applications:

- Frequency and phase variability and control,
- Low input-voltage requirements,
- Compactness and rigidity,
- Reliability,
- Better compatibility with other electronic circuitry (and with the future Internet-of-Things).

On the other hand, S<sup>2</sup>MH generators are more sensitive to power reflections (unless they are protected by expensive ferrite isolators), and yet their efficiency is lower than that of magnetrons. The full utilization of the S<sup>2</sup>MH advantages (e.g., the frequency variation during the process) requires higher levels of system design and process control (note that sometimes resonance tracking may couple to hot spots and cause damage).

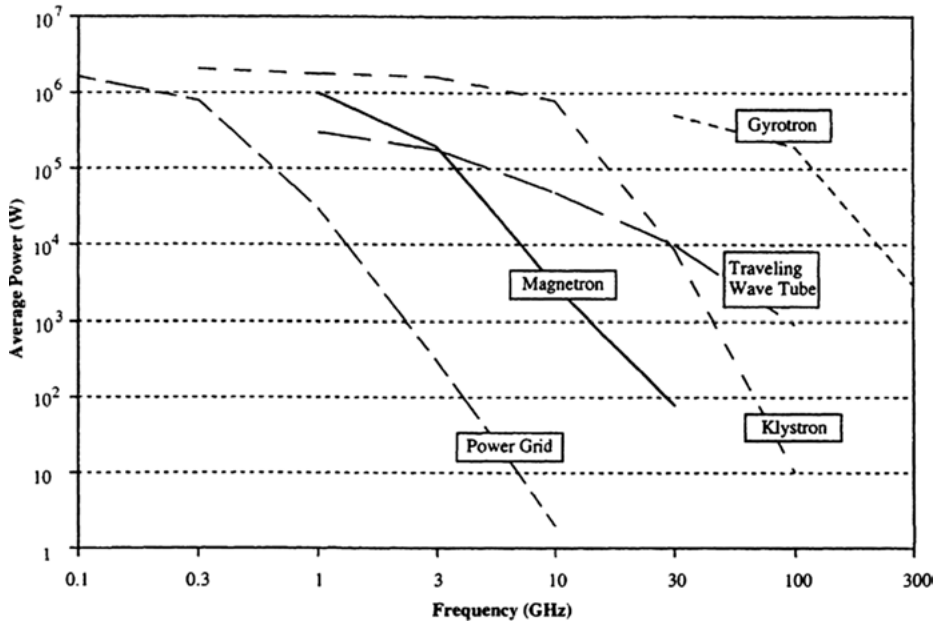


Fig. 3.3: Power vs. frequency limits of microwave generators.

Though technology-wise the  $S^2MH$  solution might be preferable in certain applications, the main question remains the expected price gap. The cost predictions are yet subject to uncertainties, such as the market response to the new technology and the level of mass demand for the  $S^2MH$  products.

### 3.2.3 Other microwave sources

There are many other types of microwave generators, like power grid tubes, klystrons, klystrodes (a combination of a tetrode power grid tube and klystron), magnetrons, crossed-field amplifiers, traveling wave tubes, and gyrotrons. None of these generator types are used for industrial microwave heating because the costs are too high compared to magnetrons.

It is instructive to show the device performance range on a power vs. frequency plot, as in Figure 3.3, for a number of different microwave generators.

In addition to power and frequency, other performance factors are important to specific applications. Gain, linearity, noise, phase and amplitude stability, coherence, size, weight, and cost must also be considered [6]. Concerning the cost, reader should know that it is usually given as device cost and cost per watt of power generated. These costs, as well as the cost of ancillary equipment such as power conditioning, control circuitry, transmission line, and applicator, must be added.

### 3.3 Wave Propagation

Once microwaves are generated, they should be transported to the chamber where interaction with the sample/reactants leads to the proper heating process. Microwave propagation in air or in materials depends on the dielectric and the magnetic properties of the medium. Many complex equations describe the propagation of electromagnetic waves at the microwave frequency, but they are outside the scope of this chapter.

One thing should be clear in the reader's mind: to propagate microwaves, the medium should not interact with the electromagnetic field; otherwise the amplitude of the wave will decrease exponentially as it propagates, that is, wave energy is dissipated during propagation. For an isotropic medium, one remarkable property of the wave is that it carries an equal amount of energy in the electric and magnetic fields.

In connection with what was said in Chapter 2, the transmission line should be made from metal to assure almost perfect reflection and zero adsorption.

The transmission lines are built in such a way that waves carry an equal amount of electric and magnetic energy and that wave impedance remains constant in the propagation direction. These are intrinsic properties of transmission lines and are true as long as the forward and backward traveling waves are separate. However, these conditions no longer hold when both forward and backward traveling waves exist simultaneously. It is the responsibility of the constructor to choose the proper geometry for the transmission line and the proper medium to minimize power dissipation along the transmission path.

#### 3.3.1 Waveguide modes

Metallic waveguides can be divided into three types (Figure 3.4). For transverse electromagnetic (TEM) waves, all fields are transverse. These are an approximation of radiation waves in free space. They are also the kinds of waves that propagate between two parallel wires, two parallel plates, or in a coaxial line.

Parallel wires or, more precisely, twisted pairs and coaxial lines are used in the telephone industry. Transverse electric (TE or H) waves and transverse magnetic (TM or E) waves are the kind that are in waveguides and that are typically hollow conducting pipes having either a rectangular or a circular cross section. In TE waves, the  $z$  component of the electric field is missing, and in TM waves, the  $z$  component of the magnetic field is missing. Complicating the matter further, each TE and TM wave in a waveguide can have different field configurations. Each field configuration is called a mode and is identified by the indexes  $m$  and  $n$ . In mathematics, those indexes are the eigenvalues of the wave solution.

Field distributions for various modes of propagation in rectangular and cylindrical waveguides are reported in Figures 3.5 and 3.6 [5]. In the figures, electric fields are represented by solid lines and magnetic fields by dashed lines, and wave propaga-

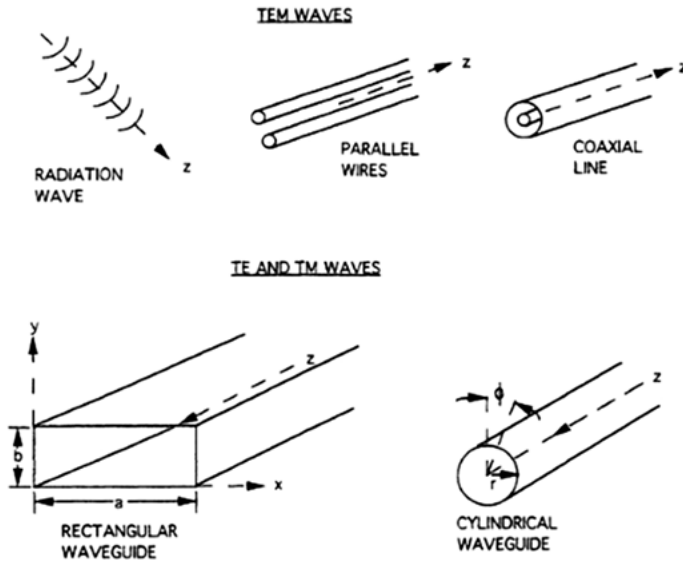


Fig. 3.4: Waveguides – TEM, TE, and TM waves.

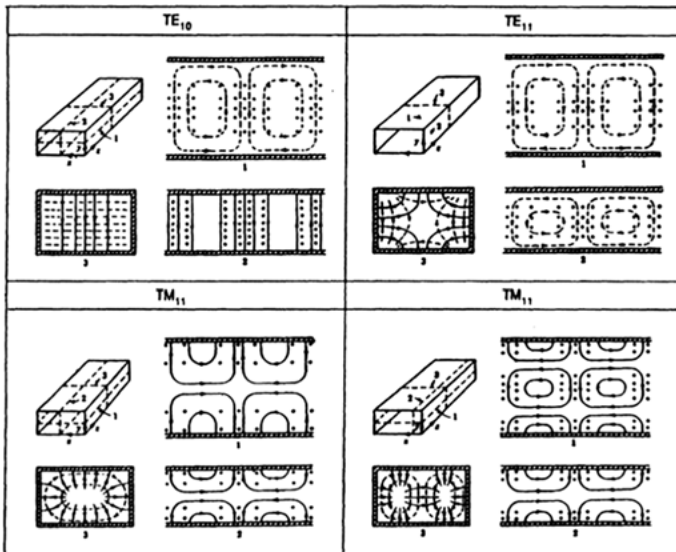


Fig. 3.5: Field distributions and key expressions of calculation for modes in rectangular waveguides.

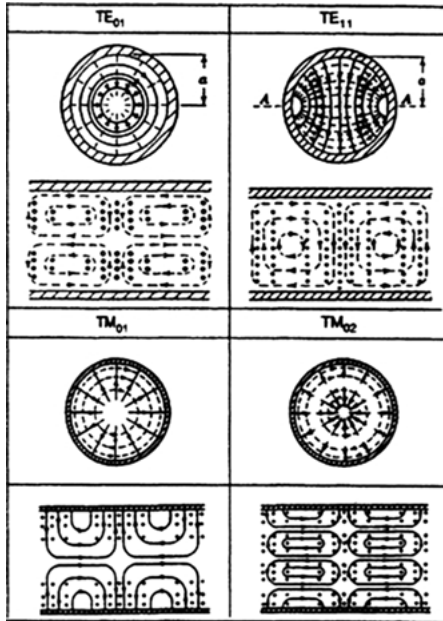


Fig. 3.6: Field distributions and key expressions of calculation for modes in cylindrical waveguides.

tion is always in the  $z$ -direction.  $TE_{mn}$  and  $TM_{mn}$  modes are considered in rectangular waveguides, and  $TE_{n1}$  and  $TM_{n1}$  modes are considered in cylindrical waveguides, where the indices  $m$ ,  $n$ , and 1 are the order of the modes. The field distributions in Figures 3.5 and 3.6 are quite complex. In general, at a conducting surface, electric field lines are normal to the surface, and magnetic field lines are parallel to it. Away from the surface, all field lines follow continuity.

Waveguides propagate microwaves of different frequencies, and each constructor will optimize the geometry of the waveguide to transport microwave energy, limiting its dissipation. As an example, to propagate a 2.45 GHz wave, a rectangular waveguide, indicated also by WR 340 with dimensions 3.4 inch [86.36 mm]  $\times$  1.7 inch [43.18 mm], is needed.

### 3.4 Antennas

Microwave antennas can replace waveguides to transfer the electromagnetic field energy from one point to another. These devices are designed for telecommunication microwave systems in all common frequency ranges from 4 to 60 GHz. When used to transfer energy with the main goal of providing localized heating, their geometry is more simplified since the signal does not need to be perfectly reproduced as in telecommunications [14].

Microwave antennas can be directly inserted into the reaction vessel, as will be explained in Section 3.6, Radiant microwave applicators.

## 3.5 Microwave chambers

Simply stated, microwave chambers or cavities are the part of an applicator that are designed to heat a material by exposing it to a microwave field in a controlled environment. The objective is to cause a controlled interaction between the microwave energy and the material under safe, reliable, repeatable, and economical operating conditions. The electromagnetic wave is transferred from the generator to the cavity by the waveguide, so each cavity should have at least one entrance, often protected by a microwave-transparent material, hence referred to as a *window*, for the microwave.

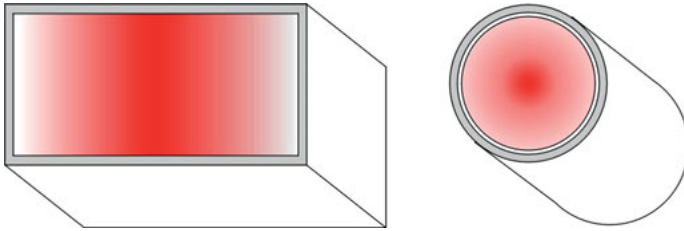
To keep the microwave radiation inside, the microwave cavity is built from massive amounts of metal often covered by a microwave-transparent polymer for cleaning purposes only.

Microwave energy may also be combined inside a cavity with other energy sources, such as hot air, infrared radiation, and steam, to achieve special results. Microwave cavities may also be designed to permit controlled interactions under a variety of ambient conditions, ranging from vacuum to high pressure and humidity. These latter features could also be used in reactors rather than in cavities. Reactors, which are usually made of glass or Pyrex<sup>®</sup> vessels, are located inside a microwave cavity, can be of various shapes and sizes, and can bear temperature and pressure probes. In the cavities of microwave ovens for chemical uses, vacuum or high pressure and humidity are kept within the reactor to avoid the contamination and degradation of the chamber.

In general, two different types of microwave chambers or cavities can be distinguished: single-mode and multimode cavities. In single-mode cavities, a single standing wave pattern is generated, while in multimode cavities a large number of resonant modes is supported.

### 3.5.1 Single-mode cavities

The standing wave that is supported by a single-mode cavity depends on the frequency and dimensions of the cavity. Various wave patterns exist and are differentiated by the number and position of the maxima of the electric and magnetic fields. The technically most important wave patterns are the TE<sub>10</sub> and TM<sub>01</sub> modes (Figure 3.7). The TE<sub>10</sub> mode is supported in a rectangular cavity, having its maximum of field intensity in the middle of the cavity. In a cylindrical cavity, the TM<sub>01</sub> mode is supported, having its maximum of field intensity in the axis of the cavity.



**Fig. 3.7:** Wave pattern in different single-mode cavities (left side:  $TE_{10}$  mode, right side:  $TM_{01}$  mode).

In their simplest form, single-mode applicators consist of a section of waveguide operating at a frequency near cutoff. They usually have had holes or slots cut in them to let product in or out. In more demanding applications, they may consist of resonant, high Q cavities. Some advantages of single-mode applicators follow:

- High fields are possible.
- The applicators can operate in standing or traveling wave configurations.
- Fields are well defined.
- Fields can be matched to product geometry.
- The applicators are useful for heating both low-loss and high-loss materials.
- The applicators are compatible with continuous product flow.
- High efficiency is possible.

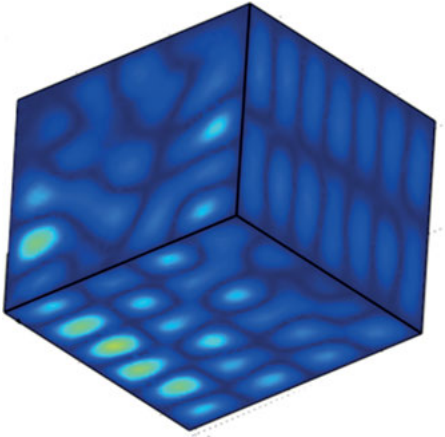
Taking advantage of the fact that very high electric field strengths can be achieved and calculated, knowledge of the electromagnetic field configuration enables the material under treatment to be placed in the position of the maximum electric/magnetic field. This results in a high absorption of the incident wave.

Despite these advantages, the use of single-mode cavities in technical applications is limited owing to size restrictions of the cavities. The cross section of the cavities for a specific wave pattern depends on the frequency. For a certain frequency, the cross section is fixed and may not be altered without changing the wave pattern. Therefore, single-mode cavities are mainly used for comparatively small products.

In a multimode cavity the superposition of the large number of resonant modes that are supported by the cavity is used to generate a comparatively even microwave field in the useful volume of the cavity. Therefore, it is advantageous to generate as many different resonant modes as possible to improve the homogeneity of the electromagnetic field.

### 3.5.2 Multimode applicators

Multimode cavities are not limited in their dimensions, and therefore very large heating chambers can be used. The advantage of a multimode chamber is the even microwave field (either electric or magnetic), which enables the heating of large or



**Fig. 3.8:** Wave pattern in multimode cubic cavity.

complex shaped products. In comparison to single-mode cavities, multimode systems have higher output power combined with a relatively low electric field strength or density, resulting in lower heating rates.

Key features of multimode ovens include the following:

- Suitability for bulk processing applications;
- Oven dimensions that are often determined by product dimensions;
- Moderate to high efficiency;
- Adaptability to batch or continuous product flow;
- Performance that is less sensitive to product position or geometry;
- Good uniformity that may require motion of product or hybrid heating.

Multimode applicators are often used for processing bulk materials or arrays of discrete materials whose overall dimensions are too large (larger than the wavelength of the operating frequency) to permit consideration for use in a single-mode oven. These applicators, in their simplest configuration, take the form of a metal box that is excited (driven) at a frequency well above its fundamental cutoff frequency. For example, the common home microwave oven typically has internal dimensions on the order of 12 inch [30.48 cm] to 16 inch [40.64 cm], while the wavelength is 4.8 inch [12.192 cm]. The larger dimension corresponds to a cutoff frequency of about 400 MHz as compared with an operating frequency of 2.450 GHz.

Because the dimensions of the enclosure are very large when expressed in terms of the free-space wavelength of the operating frequency, a large number of standing-wave modes can exist at or very near the operating frequency inside the cavity (Figure 3.8). To establish a reasonably uniform electric field strength throughout the cavity, it is desirable to excite as many of these modes as possible. When multiple modes are excited, heating nonuniformity is minimized even when field perturbing effects of the materials being processed are present.



A peculiar application of multimode cavities for sample preparation and for synthetic applications is the *single reaction chamber technology* [15]. Microwave irradiation is performed inside a pressurized stainless steel vessel where different geometries of vials placed in a rack allow for multipurpose synthesis (for details, see commercial products Ultraclave, Ultrawave, and Synthwave from MLS-Milestone). Multimode applicator design involves a number of basic design parameters. They include uniformity of heating, required microwave power, applicator size, leakage suppression, and required performance characteristics.

### 3.5.2.1 Heating uniformity

Uniform heating is difficult to achieve in a multimode oven. This difficulty arises from the unpredictable way in which the parameters affecting uniformity change with time. As a result, a number of techniques, in addition to excitation of multiple standing-wave modes, are used to promote uniform heating. They include metallic mode stirrers to ensure that all possible modes are excited; surface scanning to direct the energy at regions of interest; product motion; and, in some cases, hybrid heating using conventional heating to replace surface losses.

In a typical chemical lab microwave oven, that is to say a batch applicator, product motion may be introduced in a variety of ways that include rotation, orbital motion, and linear (vertical or horizontal) translation.

Since many chemical reactions modify the dielectric and magnetic properties of a batch as they proceed, it is also important to manage the microwave-power-handling capability under no-load conditions. Such no-load conditions, interpreted as the conditions in which the microwave cavity is empty or contains a small amount (below that indicated by the producer) of sample, are critical when the output microwave power is high as in multimode cavities.

It is essential that an applicator be capable of operating under no-load conditions without electric field breakdown and without leakage for at least a sufficient amount of time to allow equipment and personnel safety devices to shut the system down. Each constructor implements special precautions, one being the *lossy* (high-lossy) walls to suppress leakage. Under no-load conditions, the lossy walls act as parasitic loads that help reduce field strength in the cavity, thereby reducing the risk of destructive arcing.

### 3.5.3 Leakage suppression

The suppression of microwave leakage from microwave oven doors and product openings is required for personnel safety and to reduce electromagnetic interference. Although these are two very different issues, they must be dealt with simultaneously by a choke or suppression tunnel design. The current safety standard for microwave ovens is an emission specification that limits emissions at a distance of 5 cm from the surface

of an oven to a maximum of  $5 \text{ mW/cm}^2$ . Safety standards are discussed in more detail in a later section of this chapter.

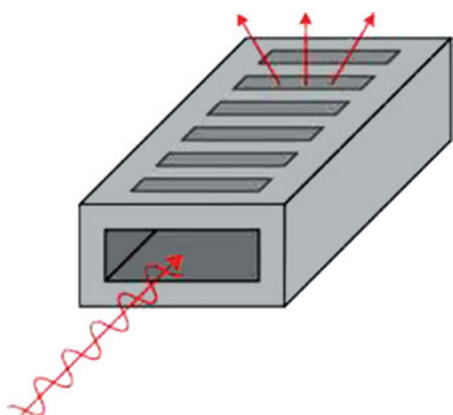
Leakage can usually be suppressed by means of reactive chokes, provided that the other dimension of the opening is less than approximately half a wavelength. Good examples of these types of openings are the door seals for industrial and conventional home microwave ovens and slot openings to permit ingress and egress of thin web belt materials processed in industrial microwave ovens.

### 3.6 Radiant microwave applicators

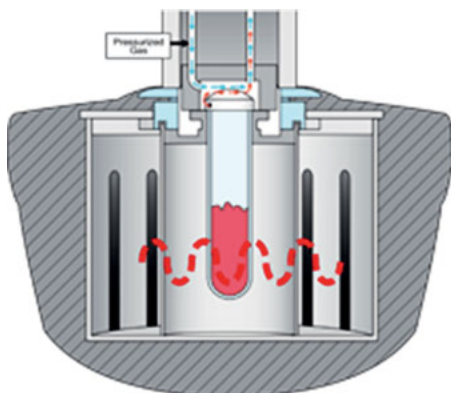
When rectangular waveguides are opened in a sequence of properly designed slots on a side, they are known as *slotted waveguides*. This peculiar geometry of the waveguide is capable of emitting microwaves all along its length with a final effect where the irradiation is similar to a shower (Figure 3.9).

Slotted waveguides have been commonly used to feed microwaves within large multimode cavities, but they are also used in chemical reactors. In particular, when the slots are cut so that irradiation is radial toward a center, as reported in Figure 3.10, the reacting vial can be uniformly heated.

Aside from these most common slotted waveguides, a movable and easy-to-use radiant structure in the shape of an antenna inserted into a long tube of protective and microwave-transparent material has been patented for chemical preparations (Figure 3.11) [14]. The antenna can be inserted inside the reacting material contained in a common glass vessel. This device can be used for activating chemical reactions in a homogeneous or heterogeneous phase, in either continuous or pulsed mode. Additionally, if the reactor is properly designed, the device can also be used in high pressure conditions.

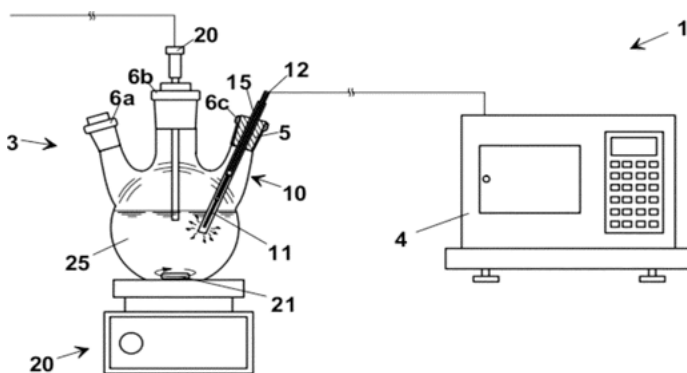


**Fig. 3.9:** Slotted waveguide indicating entrance of microwave radiation and direction of emission from one slot as an example. All slots irradiate microwaves.



**Fig. 3.10:** Slotted waveguide bend around a reacting vial in a microwave applicator dedicated to chemical synthesis (Courtesy CEM, DISCOVER & EXPLORER SP FEATURES at <http://it.cem.com/e107/discover-sp-features.html>).

The arrangement of the antenna in the reacting material provides quick and effective heating, but unfortunately low power microwave irradiation should be used. Furthermore, it is possible to significantly increase the control and efficiency of physicochemical processes to which the previously described heating technique is applied. This also allows for significant energy savings with respect to the apparatus, which consists of a vessel within a multimode cavity. A homogeneity of the vessel's temperature profile can be obtained using a magnetic stirrer.



**Fig. 3.11:** Microwave heating apparatus with (4) microwave source, operatively connected to (10) an end of an antenna at a connector (12). The end of the antenna (11) is inserted into (3) a reaction container with apertures (6a, 6b, and 6c) and reacting material (25). The antenna was coated with a sheath (15) that prevents direct contact with the reacting material. To optimize mixing, a magnetic bar (21) and a stirrer (20) can be used.

## 3.7 Monitoring and control of microwave applicators

Microwave applicators are places where electromagnetic fields interact with materials: the various responses that may take place were already listed in Chapter 2. The overall heating process requires, if possible, continuous monitoring and control.

Nowadays, the best-performing equipment used in chemical labs is fully monitored and perfectly controlled, but unfortunately this is not the case with adjusted domestic ovens or self-assembled units.

In what follows, the temperature, pressure, and power monitor and control are discussed.

### 3.7.1 Temperature measurement

The most important parameter to be measured in thermal processing units is the temperature. While it is usually sufficient for the control of a conventional process to know the furnace temperature, for dielectric heating the product temperature is usually much higher than the furnace temperature. Therefore, it is usually necessary to measure the product temperature to regulate dielectric heating units. Either contact or noncontact measurement techniques may be used to measure the product temperature.

The temperature of a body is its thermal state and is regarded as a measure of its ability to transfer heat to other bodies. The indication of how a numerical value may be associated with temperature requires a review of the laws of thermodynamics, which is certainly beyond the scope of this chapter. To establish procedures for accurate temperature measurement, temperature may be defined as a quantity that takes the same value in two systems that are brought into thermal contact with one another and are allowed to come to thermal equilibrium. Based on this definition, it may be suggested that for accurate temperature measurements, both the body and the measuring device should make good thermal contact, and both bodies should be in thermal equilibrium. These conditions are difficult to establish during microwave heating because of its intrinsic rapidity. Nevertheless, an effort in the direction of monitoring the temperature and, based on this measurement, control the output power of microwave irradiation to regulate the entire heating process should be made.

Figure 3.12 identifies various temperature-measuring instruments and their ranges.

Probably the most common contact temperature measurement method uses a thermocouple. Unfortunately, the use of thermocouples in dielectric heating is limited because the electric field of the units may interfere with measurement. It is possible to shield the thermocouple to mitigate the problem, but for certain applications with high electric field strengths, a shielded thermocouple may still be unsuitable (Figure 3.13).

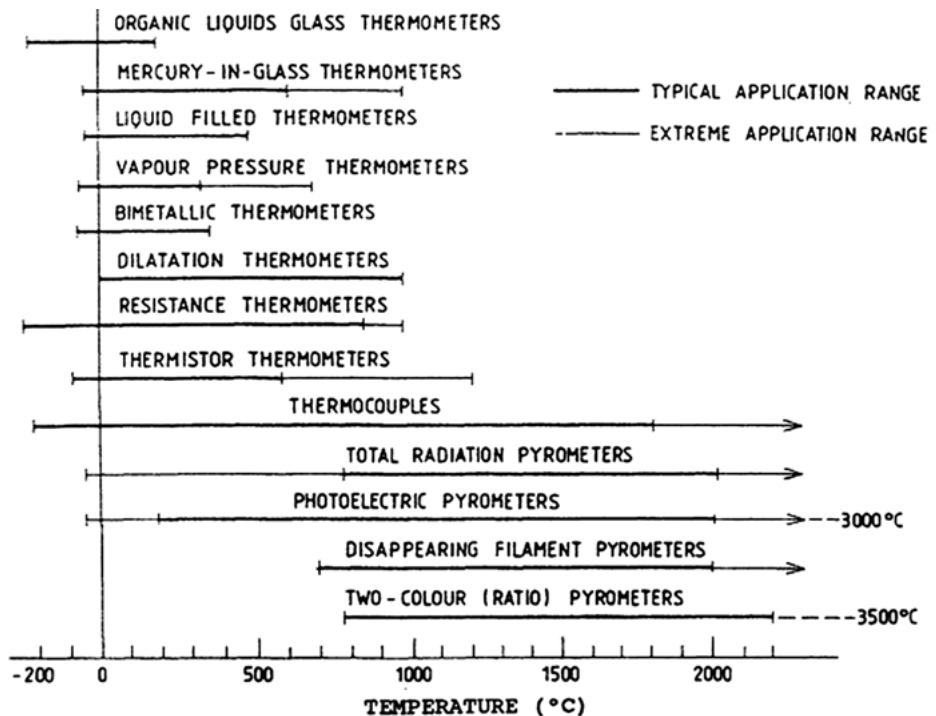


Fig. 3.12: Classification of temperature-measuring instruments.

A contact temperature measurement device that was specially developed for dielectric heating and similar applications is the so-called optical fiber thermometer. This technology is based on a special sensor material that emits or reflects light depending on its temperature. The sensor material is placed on the tip of a glass fiber that transmits the emitted or reflected light to a control unit that calculates the tem-

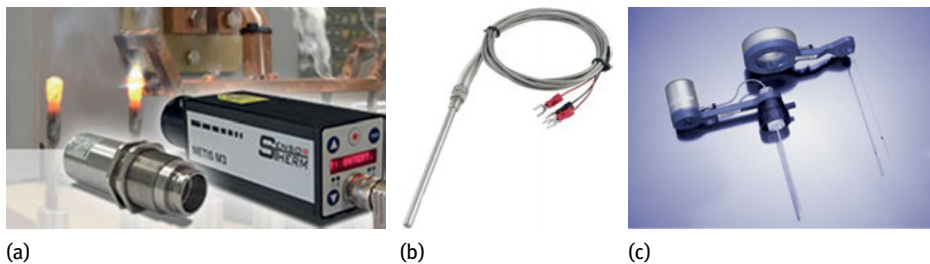


Fig. 3.13: Images of sensors frequently adopted in microwave-irradiated environments: (a) infrared pyrometer (Courtesy Sensortherm GmbH); (b) Pt shielded thermocouple; (c) pressure sensors (Courtesy Anton-Paar GmbH).

perature of the sensor. Owing to the optical measuring principle, the measurement is not affected by the electromagnetic field of dielectric heating.

The most common noncontact temperature measurement device is the pyrometer. These units detect infrared light emitted by a material and calculate the surface temperature based on the adjusted emission factor. Unlike contact measurement devices, pyrometers can only measure the surface temperature.

When comparing temperature measurements of conventional and dielectric heating processes, the inverse temperature profile of dielectric heating must be considered for correct interpretation of the results.

### 3.7.2 Pressure measurement

The suitability of microwaves for heating liquids in sealed reactors was soon employed for various chemical processes [16]. Microwave digestion of samples has become a fundamental technique of dissolution of samples prepared for analysis in liquid form. Sealed vessels resistant to strong acids, the availability of temperatures up to 300 °C (equilibrium pressure to 100 bar), and the very high rate of microwave heating have enabled shortening the cycle of sample preparation for analytical tests, sometimes from many days to several minutes [17]. Similarly, in the organic synthesis reactions occurring under such conditions a surprising increase was observed in the reaction yield and rate, often combined with a marked improvement in the product purity due to the specific catalytic effect [18]. The most important factor here is the ability to quickly obtain a high temperature as a result of microwave heating, as has been described for nanopowder production in hydrothermal and solvothermal processes [16]. Basically, the high pressure autogenously produced in these conditions can play a positive role only if some substrates are in gaseous form, although it is a rare case in laboratory practice. Therefore, if only high boiling point solvents can be used, safety considerations favor their use. However, other factors should also be taken into account, such as, for instance, the difficulty in dissolving many valuable reagents in some solvents or the difficulty in removing the remaining high boiling point solvents from products. Therefore, water – and, optionally, its solutions with different mineral or organic additives – is the preferred reaction medium, even if equipment fit for high pressures must then be used as a consequence.

Since in many reactions, digestion for example, pressure may rise due to the discharge of gaseous products, for security reasons microwave reactor designs have preferred devices with sealed vessels (Figure 3.13). Actually, microwave applicators able to withstand pressures above 100 bar are rare, mainly due to the lack of suitable materials for the reactors. The most commonly used polytetrafluoroethylene (PTFE) (a synthetic fluoropolymer of tetrafluoroethylene, IUPAC name: poly(1,1,2,2-tetrafluoroethylene, commercially known as Teflon®) provides a high purity of the reaction medium but has a limited thermal stability (ca. 300 °C, and less in an alkaline environment).

Devices in stainless steel able to withstand up to 200 bar are offered by single reaction chamber technology, MILESTONE, Italy. Moreover, several publications have shown useful applications of this specific technology under gas pressure thanks to multiple gas inlets. Previous technologies did not operate safely at high pressures and with different gas mixtures (e.g., CO<sub>2</sub>, CO + N<sub>2</sub>, H<sub>2</sub> + N<sub>2</sub> or Ar).

In any case, the end user should strictly follow the instructions of the microwave device manufacturer, especially when pressurized reactions are involved.

### 3.7.2.1 Expanding the range of parameters achieved by microwave reactors

Typical designs of microwave devices pose certain limitations for their users. In particular, it is difficult to seal them so as to make them suitable for use at higher pressures. Because the course of many reactions, especially those related to the digestion (decomposition) of laboratory samples or solvothermal syntheses, depends on increased temperature (and the corresponding pressure), appropriate reactor design solutions have been developed [19]. The main limitations are still the properties of the materials from which reaction containers can be made. Containers made of PTFE can withstand up to 270 °C and 100 bar and, when used as inner liners for steel vessels, can reach up to 200 bar [15]. Containers made of quartz can be used at higher temperatures (even up to 700 °C), but their low mechanical strength limits the pressure range down to 100 bar. In special cases, again when inserted into larger pressurized chambers, as in the aforementioned single reaction chamber technology, these limitations can be overwhelmed and pressure as high as 200 bar can be reached [15]. In rare cases manufacturers specify higher performance parameters. This is possible when the entire reactor is made of steel, which, unfortunately, is not recommended in clean chemical processes and additionally requires the use of nonstandard sealed microwave power supply systems.

### 3.7.3 Power control

Depending on the application, microwave heating units may have pulse-, phase-, or noncontrolled magnetrons. For pulse-controlled magnetrons, the microwave power is constantly switched on and off to achieve an average power of the desired value. Phase-controlled magnetrons can be adjusted continuously between typically 15 and 100% of its maximum power. Noncontrolled magnetrons are either switched on at full power or off.

The decision to choose a given type of control depends on the application. For applications that require good control of the incident power, like laboratory applications or those with fast changing throughputs, either pulse or phase control is used. For industrial applications with constant throughputs, it is usually sufficient to use noncontrolled magnetrons. The number of activated magnetrons is set during process

development and saved in the programmable logic controller or programmable controller program.

### 3.8 Maintenance

Microwave applicators for chemical labs are complex and sensitive pieces of equipment. To cool themselves, they will typically draw in outside air. As a result, keeping acidic or corrosive materials in the same area as the microwave (such as in a fume hood) will be detrimental to the functioning of the microwave device.

Keep microwaves out of fume hoods and away from corrosives to ensure smooth functioning of the electronics.

If this cannot be avoided, some vendors may have a solution to pull cooling air from another source, to help protect the microwave electronics.

Regularly inspecting vessels for wear and tear is also important; most manufacturers provide specific guidelines for what to look for when inspecting their vessels. It is also important to make sure the vessel is assembled correctly and that excessive amounts of sample are not used.

### 3.9 Safety

At radio and microwave frequencies, electric and magnetic fields are considered together as the two components of an electromagnetic wave. Power density, measured in watts per square meter ( $W/m^2$ ), describes the intensity of these fields. Low frequency and high frequency electromagnetic waves affect the human body in different ways. The main effect of radio frequency electromagnetic fields is the heating of body tissues.

There is no doubt that short-term exposure to very high levels of electromagnetic fields can be harmful to health. Current public concern focuses on possible long-term health effects caused by exposure to electromagnetic fields at levels below those required to trigger acute biological responses.

Laboratory-scale microwave ovens operate at very high power levels, similar to those of domestic ovens. However, effective shielding reduces leakage outside the ovens to almost nondetectable levels, and all manufacturers nowadays meet current regulations and labeling requirements for user safety. Furthermore microwave leakage falls very rapidly with increasing distance from the oven. Many countries have manufacturing standards that specify maximum leakage levels for new ovens; an oven that meets the manufacturing standards presents no hazard to consumers.

The World Health Organization's International EMF Project was launched to provide scientifically sound and objective answers to public concerns about the possible hazards of low-level electromagnetic fields [20]. Despite extensive research, to date



there is no evidence suggesting that exposure to low-level electromagnetic fields is harmful to human health.

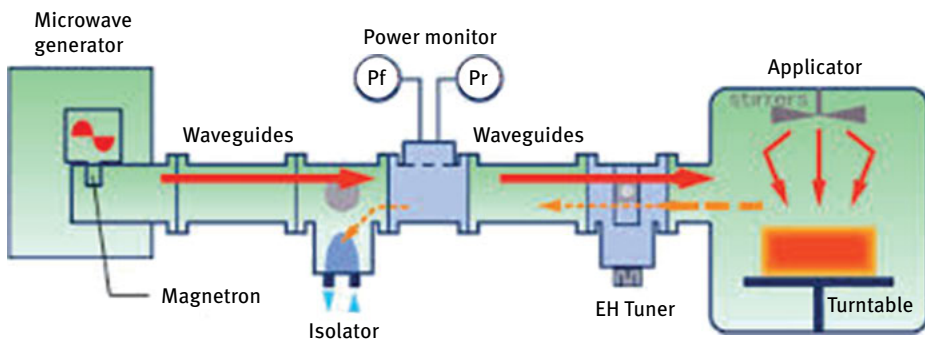
### 3.10 Conclusions

Microwave applicators are very complex pieces of equipment, but their daily use in chemical labs requires a knowledge of their construction, as does the material/microwave interaction physics. A schematic of a complete microwave applicator is presented in Figure 3.14.

In conclusion, some general features that characterize modern microwave applicators designed for chemical synthesis, digestion, extraction, and so on can be simplified as follows:

- High durability,
- Low maintenance,
- Intuitive controls and software,
- Speed of heating,
- Large capacity in terms of volume and weight,
- Short cool-down time.

Some parameters for decision makers to pay attention to when acquiring new laboratory equipment are those relating to the commercialization of microwave ovens for chemical labs:



**Fig. 3.14:** Complete microwave applicator. From left: magnetron (microwave source); metallic waveguide (transmission line for high-power microwave radiation); insulator (device to prevent radiation from returning to magnetron); power monitor device (device to measure forward power (Pf) and reflected power (Pr), as well as the power absorbed by part of the sample as the difference between Pf and Pr); tuner (device to optimize the position of the electric field (E) and the magnetic field (H) on the sample); and applicator (in this case, a multimode cavity).

- Price,
- Vendor reputation,
- Service and support.

Besides equipment cost, supplier reputation, and service support, the choice of equipment should of course be made in accordance with the user's needs, for example, reaction volume, pressure range, use of gas, or need to work with special glassware.

## Bibliography

- [1] Loupy A. *Microwaves in Organic Synthesis*. 2nd edn., Wiley-VCH, November 2006.
- [2] Kappe CO, Dallinger D, Murphree SS. *Practical Microwave Synthesis for Organic Chemists*. Wiley-VCH, November 2008.
- [3] Horikoshi S, Serpone N. *Microwaves in Catalysis: Methodology and Applications*. John Wiley & Sons, September 2015.
- [4] Horikoshi S, Serpone N. *Microwaves in Nanoparticle Synthesis: Fundamentals and Applications*. John Wiley & Sons, May 2013.
- [5] Metaxas AC. *Foundations of Electroheat: A Unified Approach*. John Wiley & Sons, 1996.
- [6] National Research Council (U.S.) Committee on Microwave Processing of Materials: An Emerging Industrial Technology.; National Research Council (U.S.). National Materials Advisory Board.; National Research Council (U.S.). Commission on Engineering and Technical Systems. *Microwave Processing of Materials*, National Academies Press, February 1994, ISBN: 9780309050272. doi:10.17226/2266. x. Open Source: <https://www.nap.edu/read/2266/chapter/1>.
- [7] Chen LF, Ong CK, Neo CP, Varadan VV, Varadan VK. *Microwave Electronics: Measurement and Materials Characterization*. John Wiley & Sons, 2004.
- [8] Stuerga D. Microwave–Material Interactions and Dielectric Properties, Key Ingredients for Mastery of Chemical Microwave Processes. In: Loupy A, ed. *Microwaves in Organic Synthesis*. Second edn. Wiley-VCH Verlag GmbH & Co. KGaA, Weinheim, 2006.
- [9] Menéndez JA, Arenillas A, Fidalgo B, Fernández Y, Zubizarreta L, Calvo EG, Bermúdez JM. Microwave heating processes involving carbon materials. *Fuel Process. Technol.*, 2010, 91, 1–8.
- [10] Haque KE. Microwave energy for mineral treatment processes – A brief review. *Int. J. Miner. Process.* 1999, 57, 1–24.
- [11] Umeysu K, Tomizawa Y. Designing of Microwave Applicators by Electromagnetic Wave Analysis, NIPPON STEEL Technical Report No. 89. January 2004, 74.
- [12] McAvoy BR. Solid-state microwave oven. US Patent 3557333, 1971.
- [13] Schwartz E. Historical Notes on Solid-State Microwave Heating. *AMPERE Newsletter*, 2016, 89, 4–7, Available from: <https://drive.google.com/file/d/0B6QoiA18sYDVGptdkKZK2F0ZKE/view>.
- [14] Longo I. Microwave Chemical Reactor. US Patent 20120103978, 2012.
- [15] Lautenschlager W. High Pressure Vessel. US Patent 9132406B2, 2015.
- [16] Leonelli C, Łojkowski W. Main development directions in the application of microwave irradiation to the synthesis of nanopowders. *Chemistry Today*, 2007, 25(3):34–38.
- [17] Smith FE, Arsenault EA. Microwave-assisted sample preparation in analytical chemistry. *Talanta*, 1996, 43(8):1207–1268.
- [18] Hoz A, Díaz-Ortiz A, Moreno A. Review on non-thermal effects of microwave irradiation in organic synthesis. *Journal of Microwave Power & Electromagnetic Energy*, 2007, 41(1):45–66.

- [19] Łojkowski W, Chudoba T, Reszke E, Majcher A, Mazurkiewicz A, Sibera D, Opalinska A, Leonelli C. Synthesis of nanoparticles and doped nanoparticles using novel microwave reactors. Proceeding of EuroNanoForum 2009. Nanotechnology for Sustainable Economy. European and International Forum on Nanotechnology. Prague July 2009, 181.
- [20] WHO – World Health Organization. What are electromagnetic fields? Available from: [www.who.int/peh-emf/about/WhatisEMF/en/](http://www.who.int/peh-emf/about/WhatisEMF/en/), accessed on 16 July 2017.

György Keglevich and Zoltán Mucsi

## 4 Interpretation of the rate enhancing effect of microwaves

Regarding the explanation for the rate-enhancing effect of microwaves, most chemists agree that thermal effects may cause the phenomenon. In this chapter, the theories on nonthermal versus thermal effects are summarized, then the scope and limitation of the use of the MW technique is outlined considering the typical energetical backgrounds for organic chemical reactions. The distribution of the local overheatings may be modeled in different ways, and the effect may be predicted by the Arrhenius equation considering the elemental segments.

### 4.1 Introduction

The spread of the use of the microwave (MW) technique in organic syntheses has led to a real breakthrough [1–3]. In most cases, the reactions became more efficient, meaning shorter reaction times, higher conversions and yields, and more selective transformations [4–7]. Also, reactions that fail to occur under conventional heating may be accomplished with MW irradiation [8]. Another possibility is to replace catalysts by MW irradiation [9, 10] or to simplify catalytic systems under MW conditions [11]. Further advantageous applications of MWs should be explored.

### 4.2 Thermal versus nonthermal effects for rate enhancement

Initially, nonthermal effects were assumed for polar transition states in apolar aprotic solvents or under solvent-free conditions [12]. Other nonthermal explanations include a supposition of change in thermodynamic parameters [13] or that of increase in the preexponential factor [14, 15]. By now, nonthermal theories have largely been rejected [16, 17], and thermal effects are considered. According to a major approach, local overheatings occurring statistically in the bulk of mixtures are responsible for the beneficial effects of MWs [4, 18]. The ultimately distributed so-called nano-size overheatings cannot be measured individually. Modest thermal differences may have a significant impact on reaction time [19]. A newer theory suggests that MW-absorbing solutes in MW-transparent solvents may be responsible for the special rate-enhancing effect [20–22].

<https://doi.org/10.1515/9783110479935-004>

### 4.3 Reaction energetics versus MW assistance

Each reaction has its own thermodynamics. Enthalpy change ( $\Delta H^0$ ) is a basic characteristic. Exothermic reactions can be performed easily, and, especially on a larger scale, care should be taken for cooling. Thermoneutral reactions may lead to equilibrium, while endothermic transformations may remain incomplete. The other energetic feature, the enthalpy of activation ( $\Delta H^\ddagger$ ), is connected to kinetics, that is, it is decisive from the point of view of the rate of reaction. Transformations with lower  $\Delta H^\ddagger$  values are usually fast, while those with higher  $\Delta H^\ddagger$  barriers may require elevated temperatures to overcome. It is also possible that a higher  $\Delta H^\ddagger$  will prevent a reaction. To be able to predict the usefulness of MW irradiation for a particular reaction, let us consider a few cases with typical energetics, as shown in Figure 4.1. In general, and on the basis of experimental results (to be discussed in the second part of this subchapter), the following considerations should be made. In cases where  $H^\ddagger$  is not too high and there is a significant enthalpy gain, as in reactions with carboxylic acid chlorides, for example, esterifications, amidations, and Friedel–Crafts reactions (Figure 4.1a/1), or the reaction is practically without an enthalpy change, as in esterification and amidation reactions of carboxylic acids (Figure 4.1b/1), common heating should be the tool used to conduct the chemical transformations. For variations with a higher  $\Delta H^\ddagger$  (Figure 4.1a/2 and Figure 4.1b/2), the reactions may be expected to be enhanced well by MWs. Moreover, thermoneutral transformations with a higher  $\Delta H^\ddagger$  (as shown by Figure 4.1b/2) may be the ideal subjects for MW activation. This may be exemplified by the esterification of phosphinic acids (see subsequent discussion). At the same time, endothermic transformations featured by Figure 4.1c/1 and 2 will remain incomplete even under MW irradiation. Such reactions include the amidation and thioesterification of phosphinic acids (see subsequent discussion).

To justify the previously outlined scope and limitations of the application of MW irradiation in organic syntheses, three case studies taken from the field of derivatiza-

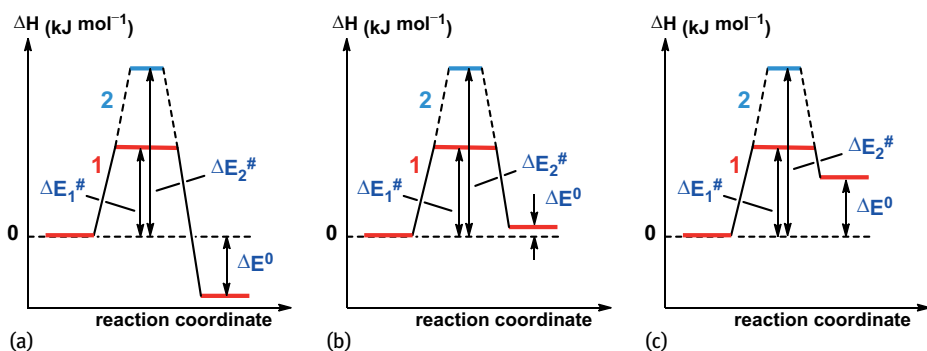


Fig. 4.1: Typical enthalpy profiles for organic chemical reactions.

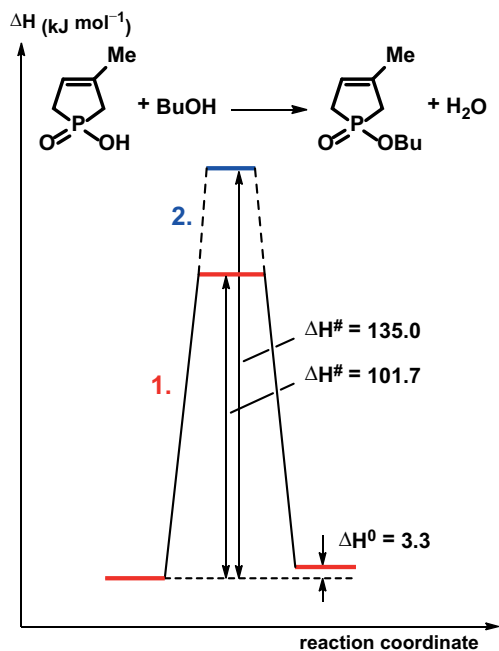


Fig. 4.2: Enthalpy profile for esterification of 1-hydroxy-3-methyl-3-phospholene 1-oxide.

tions of phosphinic acids (a direct esterification, a thioesterification, and an amidation) are discussed briefly. It is well known that phosphinic acids cannot be esterified directly by reaction with alcohols; it is more accurate to say that the conversions, in the best cases, will remain low [24]. However, on MW irradiation at 200–220 °C using alcohols in a 15-fold excess, the esterification of phosphinic acids did take place [25–27]. A reaction of 1-hydroxy-3-methyl-3-phospholene 1-oxide taking place with butanol in a conversion of 58% after 3 h irradiation at 200 °C was selected as the model. Its energetics was calculated by the B3LYP/6-31++G(d,p) method (Figure 4.2/1). More complex calculations utilizing the explicit–implicit solvent model at the B3LYP/6-31G(d,p) level of theory led to an even higher  $\Delta H^\ddagger$  of 135.0 kJ mol<sup>-1</sup> (Figure 4.2/2) [28]. The B3LYP/6-31++G(d,p) method may have obviously underestimated the  $\Delta H^\ddagger$ . As a comparison, the esterification of acetic acid was also calculated (Figure 4.3). It is noted that the practical method for the preparation of ethyl acetate involves refluxing the mixture of acetic acid and ethanol and distilling out a ternary azeotropic mixture. One can see from Figures 4.2 and 4.3 that both esterifications are practically thermoneutral, but the derivatization of the phosphinic acid has a significantly higher  $\Delta H^\ddagger$  of 101.7–135.0 kJ mol<sup>-1</sup>, compared to the barrier (75.0 kJ mol<sup>-1</sup>) of the esterification of acetic acid [29].

In an MW-assisted esterification at 200 °C for 3 h, 1-butoxy-3-methyl-3-phospholene oxide was obtained in a conversion of 58%. Carrying out the esterification in

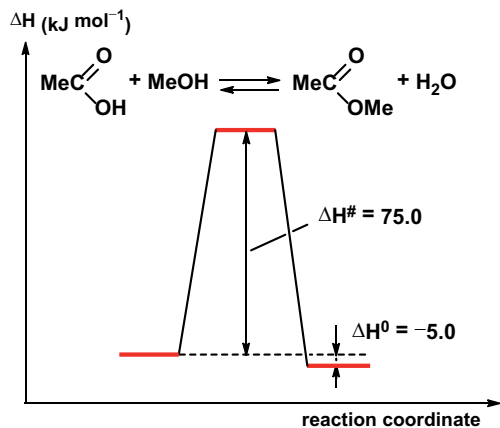


Fig. 4.3: Enthalpy profile for esterification of acetic acid.

the presence of 10% butylmethylimidazolium hexafluorophosphate, even at a lower temperature of 180 °C and after a shorter time of 0.5 h, the yield was 83% [30]. In a comparative thermal experiment at 200 °C for 2 h, the conversion was only 17%.

The preceding example shows well that a thermoneutral transformation with a relatively high  $\Delta H^\ddagger$  may be satisfactorily performed under MW conditions.

At the same time, the thioesterification of 1-hydroxy-3-methyl-3-phospholene oxide with thiobutanol at 200 °C under MW irradiations remained incomplete, and stopped at a conversion of ca. 30%. This was justified by the significant endothermicity of this reaction ( $\Delta H^0 = 48.5 \text{ kJ mol}^{-1}$ ) suggested by B3LYP/6-31++G(d,p) calculations. The thioesterification exhibited a high  $\Delta H^\ddagger$  of  $145.4 \text{ kJ mol}^{-1}$  (Figure 4.4) [31].

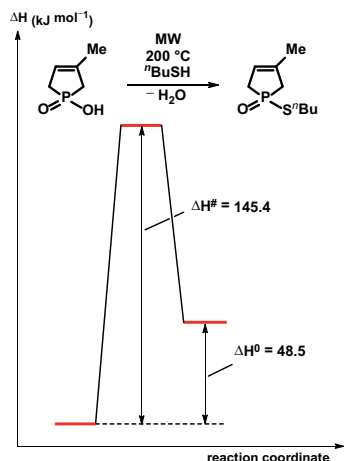


Fig. 4.4: Enthalpy profile for thioesterification of 1-hydroxy-3-methyl-3-phospholene 1-oxide.

The MW-assisted amidation of 1-hydroxy-3-methyl-3-phospholene oxide with cyclohexylamine at 220 °C also remained incomplete at a 33% conversion. Theoretical calculations revealed again the endothermicity ( $\Delta H^0 = 32.6 \text{ kJ mol}^{-1}$ ), but the  $\Delta H^\ddagger$  was rather low ( $79.4 \text{ kJ mol}^{-1}$ ) (Figure 4.5) [32].

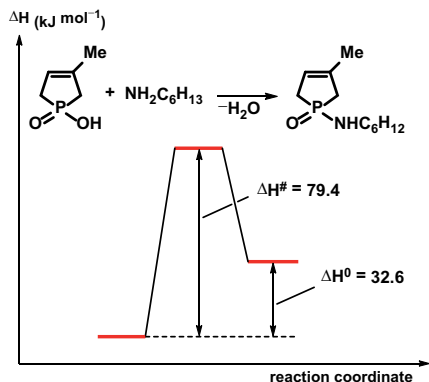


Fig. 4.5: Enthalpy profile for amidation of 1-hydroxy-3-methyl-3-phospholene 1-oxide.

The examples shown in Figures 4.4 and 4.5 demonstrate well that endothermic transformations cannot be performed well even under MW conditions.

#### 4.4 Modeling the rate-enhancing effect of MWs

The role of MWs is to enhance reactions with a higher ( $>135 \text{ kJ mol}^{-1}$ ) enthalpy of activation. MW assistance is optimal for thermoneutral transformations. But how does MW irradiation promote organic reactions? The potential of MW heating resides in the beneficial effects of local overheatings that may occur statistically in the bulk of a mixture. Even a slight overheating may have a significant impact on the rate, but quite high overheatings can also be imagined. Randomly occurring overheating may be rather efficient at overcoming a higher enthalpy of activation barriers.

To model the thermal effects of local overheating, the key is the Arrhenius equation (Equation (4.1)) that makes it possible to calculate the rate constants in the bulk of a mixture, and in overheated segments:

$$k = Ae^{-\frac{\Delta H^\ddagger}{RT}}, \quad (4.1)$$

where

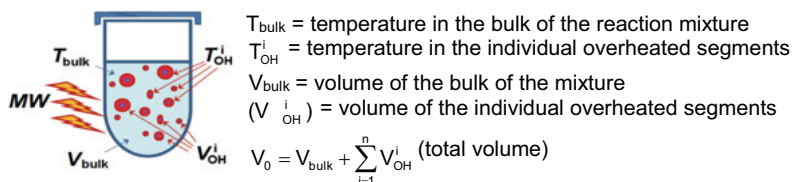
$\Delta H^\ddagger$ : activation enthalpy ( $\text{kJ mol}^{-1}$ ),

$T$ : reaction temperature ( $T_{\text{bulk}}$  or  $T_{\text{OH}} [T_{\text{OH}}^i]$ ),

$R$ : universal gas constant.



The different volume ( $V$ ) and temperature ( $T$ ) parameters are defined in Figure 4.6.



**Fig. 4.6:** Definition of volume ( $V$ ) and temperature ( $T$ ) parameters necessary for modeling.

The overall rate constant ( $k_{\text{overall}}$ ) is the weighted sum of  $k_{\text{bulk}}$  and the individual rate constants ( $k^i - s$ ) of the overheated segments as shown by Equation (4.2), where  $k_{\text{bulk}}$  and  $k_{\text{OH}}^i$  may be obtained as indicated by Equations (4.1-1) and (4.1-2):

$$k_{\text{overall}} = \frac{V_{\text{bulk}}}{V_0} \cdot k_{\text{bulk}} + \sum_{i=1}^n \frac{V_{\text{OH}}^i}{V_0} \cdot k_{\text{OH}}^i, \quad (4.2)$$

$$k_{\text{bulk}} = A \cdot e^{-\frac{\Delta H^\ddagger}{RT_{\text{bulk}}}}, \quad (4.1-1)$$

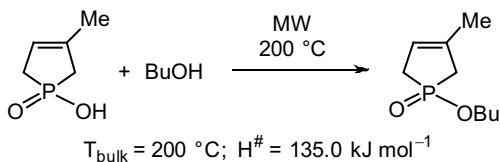
$$k_{\text{OH}}^i = A \cdot e^{-\frac{\Delta H^\ddagger}{RT_{\text{OH}}^i}}. \quad (4.1-2)$$

The increase may be characterized by  $k_{\text{rel}} = k_{\text{overall}}/k_{\text{bulk}}$ .

First, let us model the thermal effect of MWs according to a simplified approach assuming a percentage segment ( $V_{\text{OH}}/V_0$ ) with a distinct overheating ( $T_{\text{OH}} - T_{\text{bulk}}$ ) [33]. In this case, Equation (4.2) takes a simpler form (4.2'):

$$k_{\text{overall}} = \frac{V_{\text{bulk}}}{V_0} \cdot k_{\text{bulk}} + \frac{V_{\text{OH}}}{V_0} \cdot k_{\text{OH}}. \quad (4.2')$$

Regarding the esterification of 1-hydroxy-3-methyl-3-phospholene oxide with butanol at 200 °C, and using the  $\Delta H^\ddagger$  of 135 kJ mol<sup>-1</sup> calculated (Figure 4.7) [19], rate enhancements up to 3.2 were obtained as a function of the overheating and the proportion of this segment within the selected range (Table 4.1).

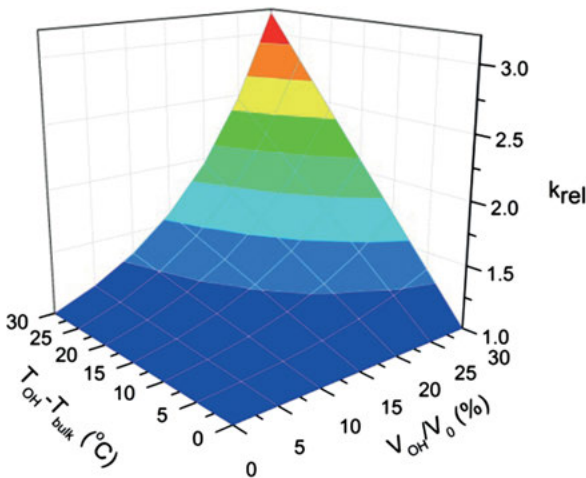


**Fig. 4.7:** The model esterification selected.

**Tab. 4.1:** Relative accelerations as a function of overheated segment ( $V_{OH}/V_0$ ) and overheating ( $T_{OH} - T_{bulk}$ ).

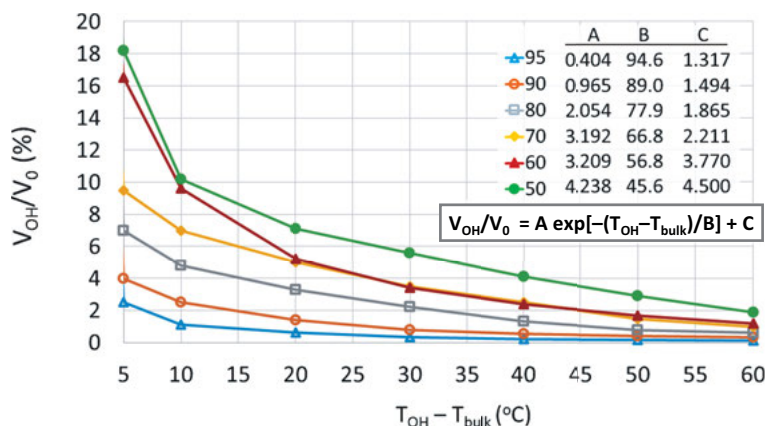
$V_{OH}/V_0$ (%)	0	5	10	15	20	30
$T_{OH} - T_{bulk}$ (°C)						
0	1.00	1.00	1.00	1.00	1.00	1.00
5	1.00	1.02	1.04	1.07	1.09	1.13
10	1.00	1.05	1.11	1.16	1.22	1.32
15	1.00	1.10	1.20	1.29	1.39	1.59
20	1.00	1.16	1.32	1.48	1.64	1.96
25	1.00	1.24	1.49	1.73	1.98	2.47
30	1.00	1.36	1.72	2.09	2.45	3.17

The results are also illustrated in a three-dimensional diagram (Figure 4.8).



**Fig. 4.8:** Relative accelerations as a function of  $V_{OH}/V_0 - T_{OH} - T_{bulk}$ .

The preceding simplification is obviously not an acceptable one because the extent of the local overheatings must be different throughout the reaction mixture. It is clear that the extent of the overheating ( $T_{OH} - T_{bulk}$ ), with respect to its tendency, is inversely proportional to its relative proportion ( $V_{OH}/V_0$ ). To approach the reality better, an exponentially decreasing relationship was freely assumed between the overheating and its proportion [34]. Regarding the proportion of the overheated segment, six distinct cases were differentiated. The overheated segments were chosen arbitrarily to be 5, 10, 20, 30, 40, and 50% (Figure 4.9). Hence, 95%, 90%, 80%, 70%, 60% and 50% in Figure 4.9 refer to the proportion of the bulk.



**Fig. 4.9:** Volume percentage ( $V_{OH}/V_0$ ) – overheating ( $T_{OH} - T_{bulk}$ ) relationships assumed in overheated segments of 5–50%.

Within the six cases, distinct overheatings of 5, 10, 20, 30, 40, 50 and 60 °C were assumed. The relative accelerations were calculated on the basis of the partial rate constants obtained for  $V_{bulk}$  and the individual segments ( $V_{OH}^i$ ) as obtained above. The list of the details, and the eventual accelerations are summarized in Table 4.2.

After modeling the effect of local overheatings assuming an exponentially decreasing relationship between  $V_{OH}/V_0$  and  $T_{OH} - T_{bulk}$ , and six different overheated segments, let us calculate the experimental acceleration. This is possible on the basis of the experimental data summarized in Table 4.3 [35]. The conversion( $x$ ) – time ( $t$ ) data pairs for the MW-assisted and thermal esterification of 1-hydroxy-3-methyl-3-phospholene oxide should be substituted in the logarithmic pseudo-first-order kinetic Equation (4.3).

$$k' = B \cdot \frac{\ln[(100 - x)/100]}{t} \quad (4.3)$$

where

$k'$ : pseudo-first-order rate constant,

$x$ : conversion,

$t$ : time.

The experimental relative acceleration ( $k_{rel}^{exp}$ ) may be calculated as the ratio of the virtual pseudo-first-order rate constant for the MW-assisted reaction and the pseudo-first-order rate constant for the thermal variation, as shown by Equation (4.4):

$$k_{rel}^{exp} = \frac{k'^{MW}}{k'^{\Delta}} = 3.10. \quad (4.4)$$

**Tab. 4.2:** Dependence of relative rate enhancement ( $k_{rel}$ ) on overheated segment ( $V_{OH}/V_0$ ) assuming an exponential distribution of  $T_{OH} - T_{bulk}$ 

Model ( $V_{bulk}/V_0$ )		Reference	A	B	C	D	E	F	G	H	Overall effect ( $k_{rel}$ )
			(bulk)								
I (95%)	$T_{OH} - T_{bulk}$ (°C)	0	0	5	10	20	30	40	50	60	
	$V_{OH}/V_0$ (%)	0	0	2.5	1.1	0.6	0.32	0.2	0.155	0.125	
	$k_{rel}$	1.00	0.95	0.04	0.02	0.03	0.03	0.03	0.05	0.07	$\Sigma = 1.20$
II (90%)	$T_{OH} - T_{bulk}$ (°C)	0	0	5	10	20	30	40	50	60	
	$V_{OH}/V_0$ (%)	0	0	4	2.5	1.4	0.8	0.55	0.4	0.35	
	$k_{rel}$	1.00	0.90	0.06	0.05	0.06	0.07	0.09	0.12	0.19	$\Sigma = 1.53$
III (80%)	$T_{OH} - T_{bulk}$ (°C)	0	0	5	10	20	30	40	50	60	
	$V_{OH}/V_0$ (%)	0	0	7	4.8	3.3	2.2	1.3	0.8	0.6	
	$k_{rel}$	1.00	0.80	0.10	0.10	0.14	0.18	0.20	0.24	0.32	$\Sigma = 2.08$
IV (70%)	$T_{OH} - T_{bulk}$ (°C)	0	0	5	10	20	30	40	50	60	
	$V_{OH}/V_0$ (%)	0	0	9.5	7	5	3.5	2.5	1.5	1	
	$k_{rel}$	1.00	0.70	0.14	0.15	0.21	0.29	0.39	0.44	0.54	$\Sigma = 2.85$
V (60%)	$T_{OH} - T_{bulk}$ (°C)	0	0	5	10	20	30	40	50	60	
	$V_{OH}/V_0$ (%)	0	0	16.5	9.6	5.2	3.4	2.4	1.70	1.2	
	$k_{rel}$	1.00	0.60	0.24	0.20	0.22	0.28	0.38	0.50	0.64	$\Sigma = 3.06$
VI (50%)	$T_{OH} - T_{bulk}$ (°C)	0	0	5	10	20	30	40	50	60	
	$V_{OH}/V_0$ (%)	0	0	18.2	10.2	7.1	5.6	4.1	2.9	1.9	
	$k_{rel}$	1.00	0.50	0.26	0.21	0.30	0.46	0.65	0.85	1.02	$\Sigma = 4.26$

**Tab. 4.3:** Experimental data for esterification of 1-hydroxy-3-methyl-3-phospholene 1-oxide and butanol at 200 °C under thermal ( $\Delta$ ) or MW-assisted conditions.

$T_{set} =$ 200 °C	t (h)	x (%)
$\Delta$	2	17
MW	3	58

Consulting Table 4.2, one can see that the real situation is well described by Model V, when the overheated segment was assumed to be 40%. The predicted acceleration of 3.06 is in good agreement with that determined experimentally (see Equation (4.4)).

The conversion–time curves for the thermal and MW-assisted esterifications are shown in Figure 4.10.

This is the first case, where the distribution of the local overheatings was modeled, and their effect was calculated on the basis of the Arrhenius equation. Hence, the beneficial effect of MWs could be treated quantitatively assuming a simple thermal effect [34–36]. This may encourage all chemists capable of applying the MW technique.

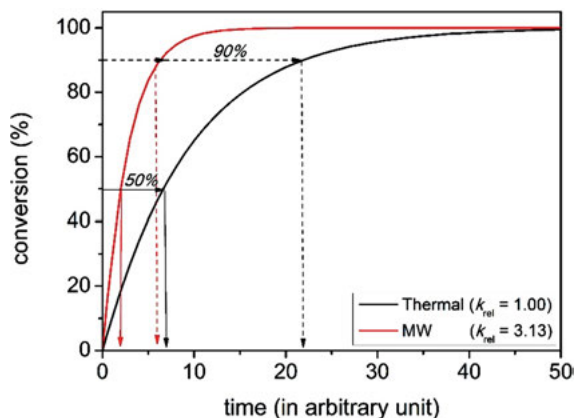


Fig. 4.10: Conversion–time diagram for thermal and MW-assisted esterifications.

## Acknowledgement

This project was supported by the Hungarian Research Development and Innovation Fund (K119202).

## Bibliography

- [1] Tierney JP, Lidsröm P, eds. *Microwave-Assisted Organic Synthesis*. Blackwell, Oxford, 2005.
- [2] de la Hoz A, Loupy A, eds. *Microwaves in Organic Synthesis*. Wiley-VCH, Weinheim, 2012.
- [3] Keglevich G, ed. *Milestones in Microwave Chemistry – SpringerBriefs in Molecular Science*. Springer, Switzerland, 2016.
- [4] Kranjc K, Kočevar M. Microwave-assisted organic synthesis: General considerations and transformations of heterocyclic compounds. *Curr. Org. Chem.* 2010, 14, 1050–1074.
- [5] Guenin E, Meziane D. Microwave-assisted phosphorus organic chemistry: A review. *Curr. Org. Chem.* 2011, 15, 3465–3485.
- [6] Keglevich G, Grün A, Bálint E, Kiss NZ, Jablonkai E. Microwave-assisted organophosphorus synthesis. *Curr. Org. Chem.* 2013, 17, 545–554.
- [7] Keglevich G, Greiner I. The meeting of two disciplines: organophosphorus and green chemistry. *Curr. Green Chem.* 2014, 1, 2–16.
- [8] Keglevich G, Kiss NZ, Mucci Z, Jablonkai E, Bálint E. The Synthesis of Phosphinates – Traditional Versus Green Chemical Approaches. *Green Process. Synth.* 2014, 3, 103–110.
- [9] Keglevich G, Novák T, Vida L, Greiner I. Microwave irradiation as an alternative to phase transfer catalysis in the liquid–solid phase, solvent-free C-alkylation of active methylene containing substrates. *Green Chem.* 2006, 8, 1073–1075.
- [10] Keglevich G, Szekrényi A. Eco-friendly accomplishment of extended Kabachnik-Fields reaction; a solvent- and catalyst-free microwave-assisted synthesis of  $\alpha$ -aminophosphonates and  $\alpha$ -aminophosphine oxides. *Lett. Org. Chem.* 2008, 5, 616–622.

- [11] Keglevich G, Jablonkai E, Balázs LB. A “green” variation of the Hirao reaction: the P–C coupling of diethyl phosphite, alkyl phenyl-*H*-phosphinates and secondary phosphine oxides with bromoarenes using P-ligand-free Pd(OAc)<sub>2</sub> RSC Adv. 2014, 4, 22808–22816.
- [12] Perreux L, Loupy A. A tentative rationalization of microwave effects in organic synthesis according to the reaction medium, and mechanistic considerations. Tetrahedron 2001, 57, 9199–9223.
- [13] Miklavc A. Strong acceleration of chemical reactions occurring through the effects of rotational excitation on collision geometry. ChemPhysChem 2001, 2, 552–555.
- [14] Binner JGP, Hassine NA, Cross TE. The possible role of the preexponential factor in explaining the increased reaction-rates observed during the microwave synthesis of titanium carbide. J. Mat. Sci. 1995, 30, 5389–5393.
- [15] Yadav GD, Bisht PM. Fundamental analysis of microwave irradiated liquid–liquid phase transfer catalysis (MILL-PTC): Simultaneous measurement of rate and exchange equilibrium constants in selective O-alkylation of *p*-tert-butylphenol with benzyl chloride. J. Mol. Catal. A: Chem. 2005, 236, 54–64.
- [16] Kappe CO, Pieber B, Dallinger D. Microwave effects in organic synthesis: Myth or reality? Angew. Chem. Int. Ed. 2013, 52, 1088–1094.
- [17] Kuhnert N. Microwave-assisted reactions in organic synthesis – Are there any nonthermal microwave effects? Angew. Chem. Int. Ed. 2002, 41, 1863–1866.
- [18] Hayes BL. Microwave Synthesis: Chemistry at the Speed of Light, CEM Publishing, Matthews, NC, USA, 2002.
- [19] Yeboah KA, Boyd JD, Kyeremateng KA, Shepherd CC, Ingersoll IM, Jackson DL Jr., Holland AW. React. Kinet. Mech. Cat. 2014, 112.
- [20] Rosana MR, Tao Y, Stiegman AE, Dudley GB. On the rational design of microwave-actuated organic reactions. Chem. Science 2012, 3, 1240–1244.
- [21] Rosana MR, Hunt J, Ferrari A, Southworth TA, Tao Y, Stiegman AE, Dudley GB. Microwave-specific acceleration of a Friedel-Crafts reaction: Evidence for selective heating in homogeneous solution. J. Org. Chem. 2014, 79, 7437–7450.
- [22] Chen PK, Rosana MR, Dudley GB, Stiegman AE. Parameters affecting the microwave-specific acceleration of a chemical reaction. J. Org. Chem. 2014, 79, 7425–7436.
- [23] Bana P, Greiner I. in: Milestones in Microwave Chemistry – SpringerBriefs in Molecular Science, Keglevich G ed., Springer, Switzerland, 2016, Chapter 4, Interpretation of the effects of microwaves. pp. 77–110.
- [24] Kiss NZ, Keglevich G. An overview of the synthesis of phosphinates and phosphinic amides. Curr. Org. Chem. 2014, 18, 2673–2690.
- [25] Kiss NZ, Ludányi K, Drahos L, Keglevich G. Novel synthesis of phosphinates by the microwave-assisted esterification of phosphinic acids. Synth. Commun. 2009, 39, 2392–2404.
- [26] Keglevich G, Bálint E, Kiss NZ, Jablonkai E, Hegedűs L, Grün A, Greiner I. Microwave-Assisted Esterification of Phosphinic Acids. Curr. Org. Chem. 2011, 15, 1802–1810.
- [27] Kiss NZ, É. Böttger, Drahos L, Keglevich G. Microwave-assisted direct esterification of cyclic phosphinic acids. Heteroatom Chem. 2013, 24, 283–285.
- [28] Mucci Z, Kiss NZ, Keglevich G. A quantum chemical study on the mechanism and energetics of the direct esterification, thioesterification and amidation of 1-hydroxy-3-methyl-3-phospholene 1-oxide. RSC Adv. 2014, 4, 11948–11954.
- [29] Keglevich G, Kiss NZ, Mucci Z, Körtvélyesi T. Insights into a surprising reaction: The microwave-assisted direct esterification of phosphinic acids. Org. Biomol. Chem. 2012, 10, 2011–2018.
- [30] Kiss NZ, Keglevich G. Microwave-assisted direct esterification of cyclic phosphinic acids in the presence of ionic liquids. Tetrahedron Lett. 2016, 57, 971–974.

- [31] Keglevich G, Kiss NZ, Drahos L, Körtvélyesi T. Direct esterification of phosphinic acids under microwave conditions; Extension to the synthesis of thiophosphinates and new mechanistic insights. *Tetrahedron Lett.* 2013, 54, 466–469.
- [32] Keglevich G, Kiss NZ, Körtvélyesi T. Microwave-assisted functionalization of phosphinic acids; amidations versus esterifications. *Heteroatom Chem.* 2013, 24, 91–99.
- [33] Keglevich G, Kiss NZ, Jablonkai E, Bálint E, Mucsi Z. *Phosphorus, Sulfur, Silicon* 190, 2015, 647–654.
- [34] Keglevich G, Greiner I, Mucsi Z. An Interpretation of the Rate Enhancing Effect of Microwaves – Modelling the Distribution and Effect of Local Overheating – A Case Study. *Curr. Org. Chem.* 2015, 19, 1436–1440.
- [35] Keglevich G, Kiss NZ, Mucsi Z. Milestones in microwave-assisted organophosphorus chemistry. *Pure Appl. Chem.* 2016, 88, 931–939.
- [36] Keglevich G, Kiss NZ, Mucsi Z. A Comparative Study on the Thermal and Microwave-Assisted Direct Esterification of Phenyl-*H*-phosphinic Acid – Modeling the Rate Enhancing Effects of MWs. *Curr. Phys. Chem.* 2016, 6, 307–311.

Marilena Radoiu

## 5 Industrial microwave reactors: components and set up

As safety concerns have been alleviated by improved technology and cost concerns by increased efficiency, industrial microwave (MW) applications have expanded beyond food cooking. There are many nonfood applications for industrial MW systems that utilize MW properties for drying and heating. Examples include timber processing, coal drying, and biowaste treatment. New applications are being tested and proven every day. The purpose of this chapter is to provide scientists and industry practitioners (end users) with the basic elements of MW equipment and some practical issues associated with industrial processing using MWs so as to enable a better understanding of MW-assisted processes and what it takes to scale them up. Some general advice and useful recommendations are given. To keep the chapter short, the basics of MW interaction with materials and the measurement of dielectric parameters are not discussed. Similarly, just a brief summary of the design of MW applicators and impedance components is given. For a more in-depth discussion of the field, the reader is referred to published work; most references are accessible online. A practical short guide with the basics of MWs is given in the final chapter.

### 5.1 MW heating and process scale-up

The use of MW heating as an industrial process dates back to the late 1940s. The engineering aspects of many applications in terms of, for example, scale-up, continuous operation, and automatic control, have been repeatedly addressed. At present MWs are used industrially in heating processes, especially of foodstuffs, in drying solids, and in plasma-assisted processes, especially in synthetic diamond deposition. In the field of chemistry, MW heating/processing has been a subject that has also generated a lot of excitement over the last 30–40 years. In many cases, MW heating has dramatically reduced reaction times and increased product yields and product purity by reducing unwanted side reactions due to a better control of energy in reactions via better settings of, for example, time, power level, and final temperature. Although MWs have revolutionized so-called kitchen chemistry over the last 30 years, MW energy is not a panacea for all energy required in laboratory and industrial applications. The use of MW energy has increased in the laboratory and it is used routinely in drug discovery; the short reaction times make it ideal for route scouting and optimization. The commercial scale-up of MW heating has been achieved in many other industries, including food processing, ceramics, and mineral processing, but it has not proved easy

<https://doi.org/10.1515/9783110479935-005>



in organic synthesis since the first academic publications in 1986 [1]. Several large laboratory MW systems are available that use a variety of approaches to achieve kilogram-scale parallel vessels, stopped flow, and continuous flow, for example, although some of these systems have inherent limitations [2].

Understanding how MWs can enhance technology requires a good knowledge of not only the fundamentals of MWs and their interactions with matter, but also of the hardware, including the practical advantages and limitations of the available tools. Understanding the pros and cons of MW energy is very important in deciding when and where MWs can replace other energy sources. The principles behind and the factors determining the successful scale-up of MWs at the industrial scale – frequency, power, and penetration depth, to name just a few – are not broadly familiar to researchers and industry.

To achieve the best performance when performing MW heating and to enable at least a feasibility study, the following relevant aspects concerning effective MW utilization and scale-up are a must:

- Knowledge and choice of MW equipment;
- Knowledge of product and the desired results to be achieved/good engineering practice;
- Knowledge of the economics.

## 5.2 MW equipment

Many distinct frequency bands have been allocated for industrial, scientific, and medical (ISM) use with the principal frequencies centered at 915 MHz (USA)/896 MHz (UK) and 2450 MHz for which equipment can be readily purchased; equipment at 5.8 GHz is presently developed, but the use of this frequency for industrial purposes has not been reported.

Although the examination of the MW frequency effect in connection with interactions with matter is not the subject of this chapter, it is worth mentioning that MW frequency effects were examined a long time ago in the heating of food. If the frequency changed, it was known that the heating efficiency and the penetration depth of the MWs would also change. However, owing to the availability of MW kitchen ovens that operate at 2.45 GHz, the in-depth examination of frequency effects has very often been disregarded.

The general setup of any industrial equipment consists of three main components: MW generator, MW power transmission line, and the applicator within which the product to be heated is placed (Figures 5.1–5.3).

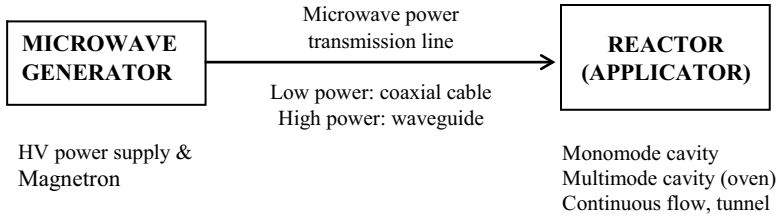


Fig. 5.1: General setup of MW equipment

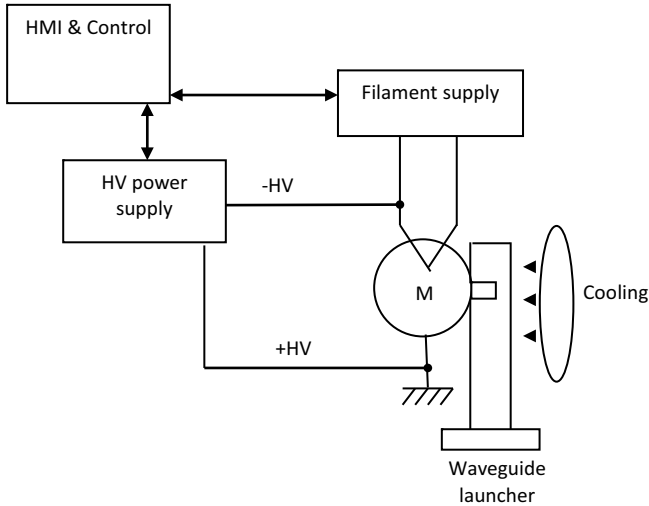


Fig. 5.2: General schematics of a magnetron (M) MW generator.

### 5.2.1 The MW generator

Generally speaking, an MW generator consists of a high-voltage (HV) DC power supply (L/C transformer or switch mode) and a magnetron; the power supply and the magnetron can be a single block or packaged up in two different metal frames interconnected via cables.

The magnetron is the heart of any MW generator, and the operation of laboratory and industrial equipment requires a thorough understanding of its operation.

A magnetron is a high-powered vacuum tube consisting of an external cylindrical anode usually made out of copper and a heated axial cathode made out of tungsten impregnated with highly emissive material; the cathode is directly or indirectly heated – temperatures of  $\sim 1750$  °C are required to insure the emission of electrons. The anode and cathode are separated by an interaction space where the magnetic and electric fields interact. A high potential is applied between anode and cathode, and there is a strong magnetic field along the axis of the tube; for low powers, usually  $< 6$  kW,

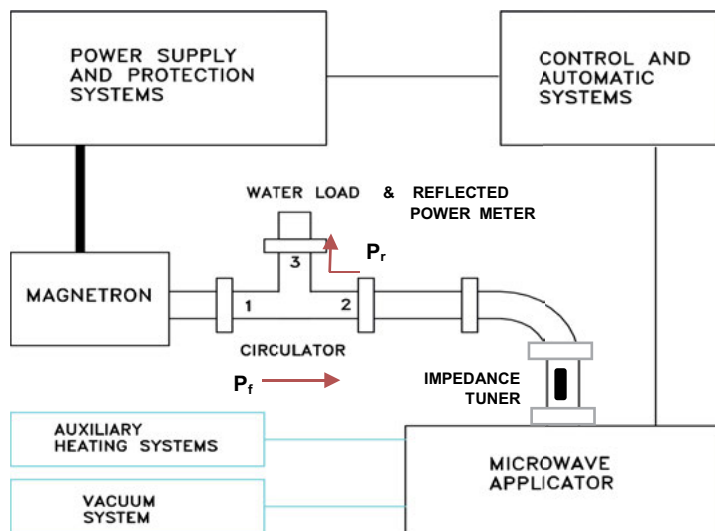


Fig. 5.3: Block diagram of an MW heating system.

the magnetic field is applied using a permanent magnet, while for higher powers an electromagnet is used. Under the influence of the crossed electric and magnetic fields, electrons emitted by the heated cathode (kept at negative voltage) travel toward the anode (grounded) following a cycloidal path.

The most usual form of an anode is the *hole-and-slot* type (Figure 5.4); each resonant cavity forms a tuned circuit, the cavity wall forming the inductive component

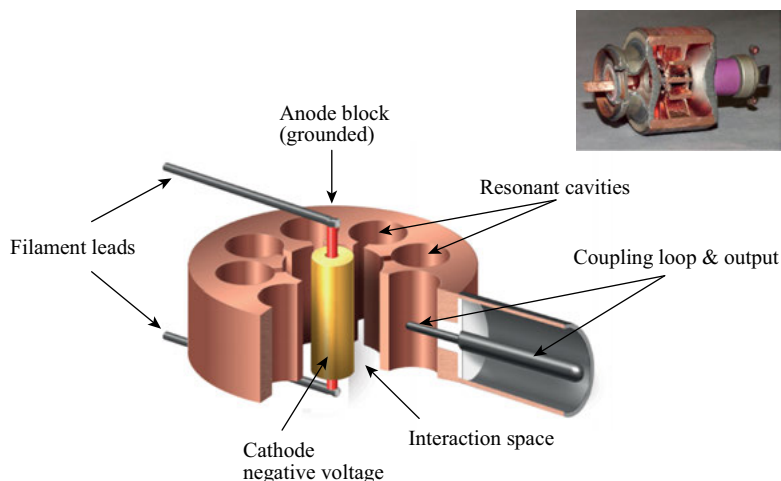


Fig. 5.4: Construction of a *hole-and-slot* magnetron and cutaway view [4, 5].

**Tab. 5.1:** Main parameters of industrial MW generators vs. frequency

Frequency, MHz		915	2450
Mains electrical efficiency, %	HV power supply (switching mode/transformer)	90–95	90–95
	Magnetron	90	70
Overall mains electrical efficiency, %		~80	~65
Magnetron lifetime (average) <sup>a,b</sup> , h		6000	7000
Max. power/unit, kW		100	6

<sup>a</sup>Continuous operation, 24 h/24 h; <sup>b</sup> Depends on max. rated power and max. operating power

and the slot the capacitive component. The size of the hole and slot determine the resonant frequency of each cavity. The relatively simple construction has the disadvantage that the magnetron usually can work only on a constructively fixed frequency, which is given by the geometry of the magnetron (size of anode resonant cavities and the interaction space); the maximum power and the electrical efficiency of a magnetron (mains electrical power transformed into MW power) are also directly related to this geometry.

Within the magnetron, the conversion of electronic energy into useful energy is a wasteful process. The impact of electrons with the anode results in considerable heat, which must be dissipated. These losses are given by the frequency of the magnetron and not by the quality of manufacture; as a general rule, the lower the frequency, the lower the losses within the magnetron. In practice we can express this efficiency as the mains electrical efficiency, that is, the mains electrical power required to produce a given level of MW power. The mains electrical efficiency of the magnetron together with that of the HV power supply give a very good idea of the overall mains electrical efficiency of the MW generator. For example, to generate 6 kW MWs at 2.45 GHz, the mains electrical power consumption will be ~9.5 kW, while if one is using 915 MHz, then the same level of MW power will require 7.5 kW from the mains (Table 5.1).

To maintain an adequate thermal gradient from the internal surface of the anode to the ambient air, the external surface of the anode is cooled by forced air or water. Generally low-power magnetrons (kitchen MW ovens and < 2 kW) are air cooled and high-power magnetrons are water cooled (Figure 5.5). The water used for cooling MW generators must not be lost, and cooling should be done using a closed water recirculation system with controlled temperature and water pressure to ensure good dissipation of the heat generated by the magnetron. The operating characteristics of a magnetron and its lifetime depend on its load but also on the environment, humidity, temperature, mechanical fixation to avoid vibrations, especially during operation. For more details on magnetrons, refer to Decareau and Peterson [3].



**Fig. 5.5:** Examples of air and air-/water-cooled magnetrons.

A magnetron is a consumable and must be replaced once the emission of electrons by the cathode ceases. Industrial magnetrons differ from kitchen magnetrons; industrial magnetrons are designed to operate in harsher conditions, for example, at much higher power levels, have longer ON times than kitchen magnetrons, and have several ON/OFF cycles during a day. In principle, the lifetime of a magnetron is expressed in the total number of MW-emitting hours. For example, if an MW generator operates 24 h/day, that is, ~8500 h/year, then, taking the average lifetime given in Table 5.1, it follows that the magnetron must be replaced three times in 2 years; however, if the MW generator operates 8 h/day, the magnetron will be replaced after more than 2 years. This calculation should make it easier to understand why a kitchen magnetron *never dies* – if we consider an average operating time of 5–10 min/day  $\times$  365 days, this means 30–60 h/year, which can result in many years of operation.

*In much simpler words: the emissions, losses, and cooling of a magnetron can be simplified to the same phenomena that occur in an incandescent light bulb.*

---

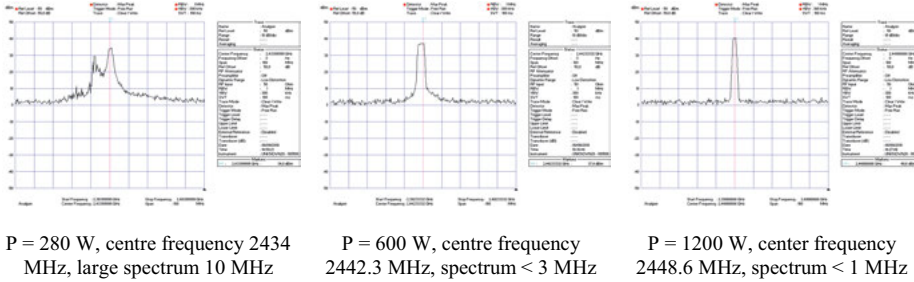
*Did you know?*

Industrial magnetrons should be operated between 10% of the nominal (rated) power and nominal power, for example, a 6 kW magnetron operates optimally between 600 and 6000 W. Low power levels could lead to instability of the magnetron's emission and operation. Operation at lower power depends on the quality of the power supply but also on the magnetron.

The operating frequency of magnetrons changes with the power level (Figure 5.6). Although the frequency stays within the ISM frequency band (2425–2475 MHz, 902–915 MHz), changing the power level during operation will change the frequency of the magnetron; hence, for very high Q-factor cavities and high precision applications (e.g., synthetic diamond deposition), retuning during operation (manually or automatically) is necessary.

---

The power supply applies a negative voltage to the filament to accelerate the electrons to the anode. For most commercial and consumer (kitchen) MW ovens a half-double power circuit is utilized to provide this voltage. In simple words, the magnetron supplied by such power supply supplies the MW power in bursts/pulses of 8.33 ms. Except for some MW excited plasmas, the heating of the load with short MW pulses can-



**Fig. 5.6:** Variation of magnetron's center frequency and spectrum (frequency bandwidth) with delivered power; 2.45 GHz magnetron 1200 W, ref YJ1540-3 (water cooling). [6]

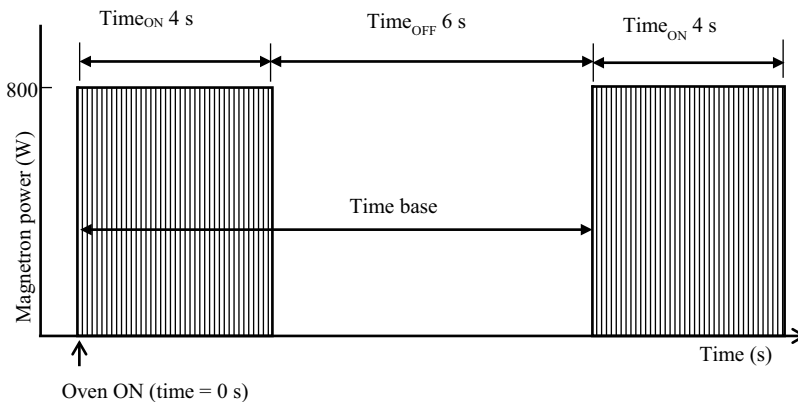
not be distinguished from continuous MW power. However, in terms of MW power output from the magnetron, the technique used is very important especially in scientific research. Most commercial MW laboratory equipment and virtually all consumer (kitchen) MW ovens use duty cycle control for varying the output power. This technique turns the oven on and off at full power automatically, the power delivered to the load is an average power determined by the number of cycles (Figure 5.7).

The oven is turned on for a  $\text{Time}_{\text{ON}} = 4 \text{ s}$  and then turned off for a time  $\text{Time}_{\text{OFF}} = 6 \text{ s}$ ; the duty cycle is continuously repeated. The main parameters, time base and duty cycle, are defined as follows:

$$\text{Time base} = \text{Time}_{\text{ON}} + \text{Time}_{\text{OFF}}, \quad (5.1)$$

$$\text{Duty cycle} = \frac{\text{Time}_{\text{ON}}}{\text{Time base}}. \quad (5.2)$$

The duty cycle represents the fraction of time that MW power is applied to a load and is commonly expressed as a percentage.



**Fig. 5.7:** Duty cycle control of output power of a magnetron, average power 40% (rectangular shaped pulses for better understanding; in reality pulses are far from equal and rectangular shaped.)

Therefore, the average power  $P_{\text{avg}}$  applied to a load is

$$P_{\text{avg}}(\text{W}) = \text{Duty cycle} \times \text{magnetron output power.} \quad (5.3)$$

In the preceding example, the duty cycle is 40% and the  $P_{\text{avg}} = 0.4 \times 800 = 320 \text{ W}$ .

*Did you know?*

In most cases, the power calculated using the preceding formula (e.g., 320 W) is not entirely absorbed by the sample. The power absorption by a sample depends on many parameters, for example, the sample size and geometry of the vessel the sample is placed in and its position inside the equipment. The user has no direct information from the equipment related to the power dissipated inside the sample.

Most industrial magnetrons can emit MW power continuously (CW) using low ripple power supplies; these power supplies are different, more complicated, and more expensive than transformers; for more references refer to Metaxas [7].

In addition to the environment and the type of power supply/power control, the frequency stability and spectrum of a magnetron are highly dependent on the load, that is, the sample to be heated and the cavity where the sample is placed. Badly designed cavities and small and poorly absorbing (low loss) samples can create reflected power, which will affect the operation characteristics and lifetime of the magnetron. From a hardware point of view, most manufacturers of industrial MW generators have built-in circulators/isolators to protect the magnetron against reflected power; systems to measure the reflected power are also provided – see *MW power transmission line* in what follows. However, most commercially available laboratory equipment manufacturers do not install isolators or reflected power measurement in their systems, probably because of their practicality (kitchen ovens) and the high cost of such components (laboratory and industrial equipment). Most available laboratory MW heating systems are not far from kitchen ovens – low power settings commonly displayed on fancy LCD screens are average powers resulting from duty cycle power control. In addition, the MW absorbance of most load materials varies with changes in temperature, phase, and chemical composition. This results in a gradual or rapid shift in the power absorbed by the load and therefore, for a fixed forward power, an increase in reflected power and changes in the frequency and temperature of the magnetron, which is a common problem in obtaining reproducible results.

*Did you know?*

- The turntable installed in MW kitchen ovens is made out of a glass-loaded material that absorbs MWs;
- The walls of the oven are made out of magnetic metal – they also absorb MWs;
- The magnetron is protected against high temperatures (caused by reflected power) by a thermal snap switch mounted on the magnetron's body. If the temperature reaches 40 °C, the magnetron will stop and can restart once its temperature is lower than 40 °C.

These construction features ensure that the magnetron will have a certain protection and that most of the reflected power will be dissipated inside if the oven is operated while empty, with a small or nonabsorbing load. The removal of the rotating plate or making holes through the walls will disturb the operation of the oven, which will also change the heating pattern, leading to random heating results and, ultimately, to the destruction of the magnetron.

### 5.2.2 The MW power transmission line

The transmission line passes the MW forward power ( $P_f$ ) from the MW generator to the load/sample and back if reflected power ( $P_r$ ) is created. Most common MW power transmission lines are based on waveguide configurations. In general, a waveguide consists of a hollow metallic tube; waveguide shapes are rectangular, circular, or ridged. The most common waveguide in use is the rectangular type. Waveguide dimensions are standardized according to the frequency and the power to be transmitted (Table 5.2). The rectangular waveguide has a width  $a$  and height  $b$  as shown in Figure 5.8. Commonly used rectangular waveguides have an aspect ratio  $b/a$  of  $\sim 0.5$ . Waveguides are made out of high-thermal-conductivity/low-electrical-resistivity metals like copper, aluminum, and brass, although stainless steel is used in the pharmaceutical and food industries owing to regulations.

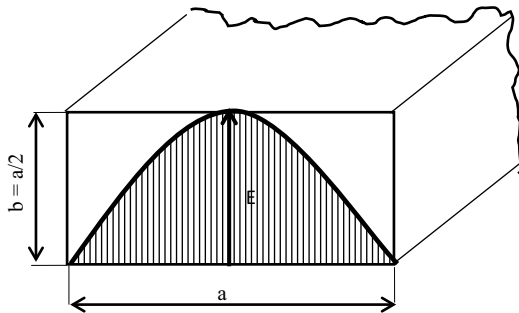


Fig. 5.8: Rectangular waveguide section; electric field in  $TE_{01}$  mode represented

Tab. 5.2: Main characteristics of waveguides vs. MW frequency

Frequency MHz/band	Waveguide standard			a		b		Guided wavelength mm	Max. power <sup>b</sup> kW
	US	UK	IEC	mm	inch	mm	inch		
2450/S	WR284	WG10	R32	72.13	2.84	36.06	1.44	230.8	12
	WR340 <sup>a</sup>	WG9A	R26	86.36	3.40	43.18	1.70	173.3	20
	WR430	WG8	R22	109.2	4.30	54.60	2.15	147.6	35
915/L	WR975	WG4	R9	247.65	9.75	123.825	4.875	495.9	100 <sup>c</sup>

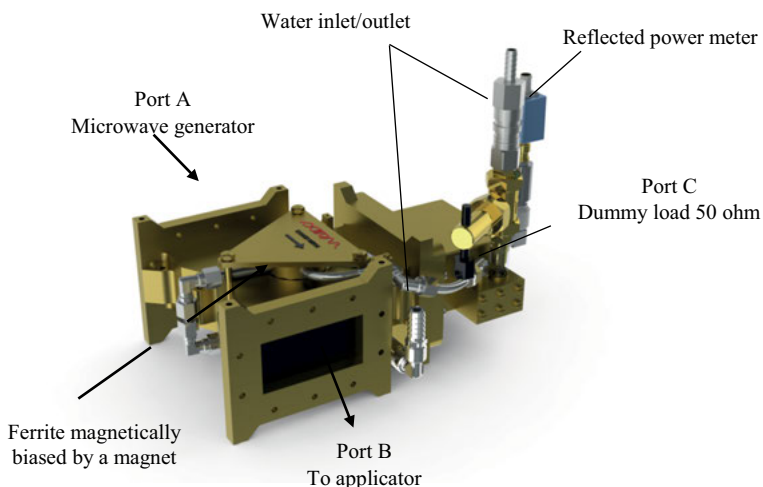
<sup>a</sup> Most common    <sup>b</sup> CW max. total power    <sup>c</sup> Owing to availability of magnetrons at higher power



### 5.2.2.1 Isolators and circulators

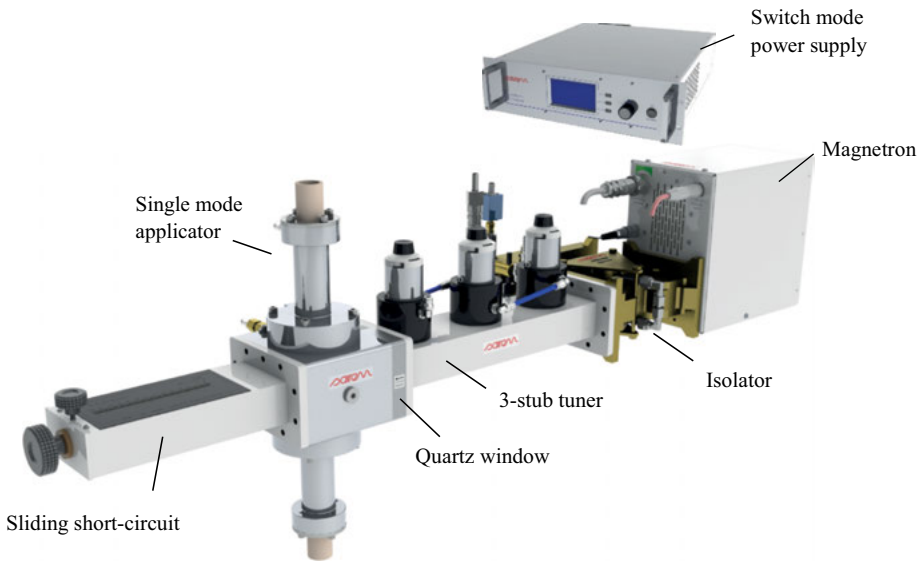
Isolators are two-port devices that allow MW power to pass from the MW generator to the applicator (forward power) but not in the reverse direction (reflected power). The most common use of such devices is to protect the magnetron from the damaging effects of reflected power. Another device often used for isolation purposes is a waveguide circulator, a three-port device ideally having no power attenuation capability. Because circulators are not designed to absorb power, a separate so-called dummy waveguide load (dry or wet) is connected to the circulator and used to absorb the reflected power. Ideally, all of the forward power entering the input port A will exit via the output port B toward the applicator and all reflected power coming back to B will be absorbed by the dummy load connected to port C (Figure 5.9). In practice, however, a small amount of forward power is absorbed by the isolator or reflected back to the source, and a small amount of reflected power inevitably passes through back to the generator.

The position of the circulator within the MW power transmission line ought to be as close as possible to the magnetron output (Figure 5.10). Very often manufacturers measure the MW reflected power using an antenna inserted in the dummy load. The reflected power ( $P_r$ ) is an important parameter in operating MW installations; generally speaking, the difference between the forward power ( $P_f$ ) and the reflected power ( $P_r$ ) is the closest and easiest estimation of the power absorbed ( $P_a$ ) by the load. The optimization (minimization) of the reflected power from very early stages of the research will assure reliable results in the laboratory and a good estimation of the required power and cost of the equipment if scale-up is desired.



*Power is coupled only from Port A to B, Port B to C and Port C to A*

**Fig. 5.9:** Isolator (circulator + water dummy load) and reflected power measurement – courtesy SAIREM SAS [8]



**Fig. 5.10:** A 6 kW, 2.45 GHz MW setup including manual tuning elements and single-mode applicator (reactor for plasma production or for continuous-flow liquid synthesis) – courtesy SAIREM SAS

### 5.2.2.2 Impedance matching components

In an energy-efficient MW system the transfer of energy from generator to workload must clearly be achieved with minimum loss. Because the insertion of a sample into the cavity changes the resonant frequency, a variety of manual or automatic MW waveguide components are used for impedance matching:

- Short circuits – waveguide components used to adjust the phase angle of 100% reflected energy = choke system;
- Capacitive or inductive waveguide impedance elements in the form of obstacles inserted into the waveguide (tuning screws, apertures, iris, and posts). The efficiency of matching can be controlled by the measurement of forward and reflected power by a network analyzer;
- Tuners – allow for regulating the matching of an MW system by optimizing the power transmitted to the applicator by matching the impedance of the applicator to that of the generator.

### 5.2.3 MW applicators

MW applicators or cavities/chambers/Faraday cages are metallic enclosures into which a launched MW signal and the sample to be heated are introduced. MW cavities can be classified into two main categories, single-mode resonant and multimode

cavities. Once in the cavity, an electromagnetic wave will suffer multiple reflections. The superposition of the incident and reflected waves give rise to a standing wave pattern that is very well defined in space for single-mode cavities and very complex for multimode structures.

### 5.2.3.1 Single-mode resonant cavities

Single-mode resonant cavities are structures with a well-defined distribution of the electric field; their size is determined by the wavelength. Monomode cavities are connected to a single MW source (generator) and they can establish a much higher electric field strength than multimode applicators, making them more useful for the treatment of low-loss dielectrics and small samples (Figure 5.8).

### 5.2.3.2 Multimode cavities

Multimode cavities come in at least two basic forms – oven type and conveyor belt – and are by far the most commonly used form of MW applicators. In essence, any metal enclosure a few times larger than the wavelength can serve as a basic multimode MW applicator. The MW energy, carried by a waveguide or a transmission line into the cavity, is deposited into a lossy material placed within (Figure 5.11a,b).

## 5.3 Good engineering practice

When performing MW heating the parameters to be taken into consideration are related to the *sample*, for example, size, dielectric parameters and their temperature dependence, boiling point, viscosity, penetration depth, and temperature distribution inside the sample, and to the *equipment*, for example, the power rating of all MW components, reactor selection – MW transparent and suitable for the intended process, CW or pulse generator, forward power, reflected power, single or multimode applicator, temperature control.

To enable correct operation of the equipment and the reliability of the results, in addition to the aforementioned considerations, simple rule-of-thumb calculations and reflections must be performed before using MW equipment.

### 5.3.1 Quick estimation of theoretical power $P_a$

To heat up a sample (without phase change) in static or continuous-flow conditions:

$$P_a(W) = \frac{m}{t} \times C_p \times \Delta T, \quad (5.4)$$

$m/t$ : sample weight per unit of time ( $\text{g s}^{-1}$ ),

$\Delta T$ : temperature gradient (K);  $\Delta T = T_{\text{final}} - T_{\text{initial}}$ ,



**Fig. 5.11:** Multimode cavities for laboratory purposes and small production. (a) 2.45 GHz, (b) 915 MHz [8–10, 12]

$C_p$ : specific heat capacity ( $\text{J g}^{-1} \text{K}^{-1}$ ).

### Examples

(a) Heating up 250 mL ethanol,  $\delta = 789 \text{ g/L}$ ,  $C_p = 2.46 \text{ J}/(\text{g} \times \text{C})$  from 15 to 61 °C in 2 min. The theoretical required power will be

$$P_a = \frac{0.25 \times 789}{120} \times 2.46 \times 46 = 186 \text{ W.}$$

Let us suppose the MW equipment available for tests is rated at 800 W, fixed power. The time to heat the sample is

$$t = \frac{0.25 \times 789 \times 2.46 \times 46}{800} = 28 \text{ s.}$$

These basic calculations give a very fair idea of the initial MW heating parameters when starting a test; losses to the environment by heat transfer from the sample and the efficiency of the MW applicator are not considered.

(b) From published work; the names of the authors are not relevant for the scope of this chapter, and no reference is given.

*A sample of 4 g (90% water) was heated in commercial MW equipment.* The authors claim that after optimization based on analyzing the results, 2000 W was required to heat the sample from 4 °C to 100 °C in 20 s. Applying Equation (5.4) we can calculate the theoretical power required to achieve these results:

$$P_a = \frac{4}{20} \times 4.18 \times 96 = 80 \text{ W},$$

meaning most of the power from the MW generator was lost by reflection back to the magnetron and within the cavity where the sample was heated.

It is easy to see from the preceding calculations there is a certain flexibility in playing with these parameters to ensure reliable results. For example, if the rated power of the available equipment is high, choosing a higher volume of sample to allow for a longer test time will lead to more accurate MW power emission from the MW generator.

### 5.3.2 Simple calorimetry to assess available MW power of equipment

Let us suppose we need to perform a reaction in 250 g water (solvent) in a piece of commercial equipment rated 300 W. Performing two to three sets of calorimetric measurements will help the operator determine whether the power will be absorbed by the sample and if information on delivered power corresponds to the power rating of the equipment.

Place 250 g water in the same reactor/recipient in which the reaction will occur. If the MW equipment does not have a built-in contact thermometer (fiber optic), measure the initial temperature of the water with the equipment off; turn on the equipment for 20 s, turn off, and, after a quick shake (stirring) of the reactor, measure the final temperature; this sequence can be repeated three to four times – care must be taken to avoid boiling or evaporation of water and injuries related to hot surfaces.

Results: Test 1 – initial temperature 20 °C, final temperature 31 °C, that is,  $\Delta T = 11$ .

Test 2 & 3 – initial temperature 20 °C, final temperature 33 °C, that is,  $\Delta T = 13$

Average temperature increase ~12 °C:

$$P_a = \frac{250}{20} \times 4.18 \times 12 = 627 \text{ W}.$$

The foregoing result reveals a much higher power than rated by the manufacturer, which, unfortunately, is still the case with some commercial equipment [11].

## 5.4 Economics and process scale-up

To reduce hazards and costs to an acceptable level and to enable scale-up, a good knowledge of dielectric processing is required. At the same time, to enable automatic operation of the processes in a continuous and repetitive manner, the electromagnetic power and treatment time need to be adapted to the product and optimized before large-scale processing.

The plant is not a laboratory – once production has started it is difficult to stop and change one or two parameters *to make it work*. The greatest opportunity to impact project costs is at the beginning, during planning and conceptual development; as the project progresses, this capability diminishes. The consequences of the decisions made in early phases of a project will dictate the viability of the project from a financial perspective and also have long-term effects on operations and cost of ownership.

When using MWs, the possibility to estimate a few parameters like power requirements, frequency, and power density will make it easier to estimate the total cost (equipment and operation) and the feasibility of scale-up.

### 5.4.1 Power requirements for heating a product

A quick evaluation of the theoretical power required for processing can be done using Equation (5.4).

#### Examples

- Heating 500 L/h ethanol from 15 °C to 61 °C

$$\begin{aligned}\delta &= 789 \text{ g/L}, \quad C_p = 2.46 \text{ J/(g} \times \text{C)} \\ P_a &= (789 \times 500)/3600 \times 2.46 \times (61 - 15) \text{ W} = 12\,400 \text{ W} \\ &\sim 13 \text{ kW}\end{aligned}$$

- Heating 500 L/h water from 15 °C to 61 °C

$$\begin{aligned}\delta &= 1000 \text{ g/L}, \quad C_p = 4.18 \text{ J/(g} \times \text{C)} \\ P_a &= (1000 \times 500)/3600 \times 4.18 \times (61 - 15) \text{ W} = 26\,705 \text{ W} \\ &\sim 27 \text{ kW}\end{aligned}$$

- Drying 500 L/h water at 15 °C

$$\begin{aligned}\delta &= 1000 \text{ g/L}, \quad C_p = 4.18 \text{ J/(g} \times \text{C)}, \quad \lambda_{\text{evap}} = 2260 \text{ J/g} \\ P_a &= (1000 \times 500)/3600 \times 4.18 \times (100 - 115) \text{ W} + (1000 \times 500)/3600 \times 2260 \text{ W} \\ &= 49,347 \text{ W} + 313,889 \text{ W} \\ &\sim 365 \text{ kW}\end{aligned}$$

### 5.4.2 Choice of MW frequency

Usually, the selection of 2.45 GHz or 915 MHz is a *product choice* – type, shape, dimensions, production capacity – but is also dictated by the regulations specific to the country and place of operation.

*However, let us suppose two frequencies are possible, 915 MHz and 2.45 GHz, in the following process:*

Reducing water content (drying) from 35 to 2% of a 1500 kg/h humid solid product, that is, ~500 kg/h of water to remove  $T_{\text{ini product}} = 25\text{ }^{\circ}\text{C}$ , thermal losses to the environment and for solid heating by thermal conduction are ignored.

The total theoretical required power to heat up the water to the boiling temperature and evaporate is

$$P_a = \frac{1000 \times 500}{3600} \times 4.18 \times (100 - 125) \text{ W} + \frac{1000 \times 500}{3600} \times 2260 \text{ W}$$

$$= 43,541 \text{ W} + 313,890 \text{ W} \sim 358 \text{ kW}$$

Let us now suppose that the industrial equipment will be built up with a total power of 400 kW MWs. The main parameters for estimating the cost of the equipment are given in Table 5.3.

Examination of the main components and costs shows a lower investment and lower operational cost at 915 MHz than at 2450 MHz. Generally speaking, industrial equipment capital expenditure (CAPEX) costs vary between 2500 USD and 5000 USD per kilowatt installed depending on the power range and the sophistication of auxiliary equipment.

**Tab. 5.3:** Main parameters of MW equipment for estimating main equipment and utility costs

Frequency	915 MHz <sup>a</sup>	2450 MHz <sup>a</sup>
Number of generators to deliver 390 kW	4 (× 100 kW)	65 (× 6 kW)
Generator price <sup>b</sup>	4 × 150 kUSD	65 × 15 kUSD
Total MW generators	= 600 kUSD	= 975 kUSD
Equipment estimated price <sup>c</sup>	1100 kUSD	1800 kUSD
Main consumable, magnetron		
– Lifetime <sup>d</sup>	6000 h	7000 h
– Price/unit	8 kUSD	2.6 kUSD
– Total	= 32 kUSD	= 170 kUSD
Mains electricity consumption	~480 kW	~550 kW

<sup>a</sup> Using switch mode power supply

<sup>b</sup> Price including isolator

<sup>c</sup> MW equipment only, upstream and downstream equipment not included

<sup>d</sup> Calculated for continuous operation 24 h/24 h

## 5.5 What can be improved – good engineering practice, good manufacturing practice

To decrease MW equipment costs (by lowering the total requested power) or the operational costs, a number of other parameters must be considered during the development stage:

- Synergetic treatments/additional energy: hot air, IR, steam, pressure, vacuum;
- Change of solvent: heating up ethanol requires ~50% less power than water;
- Minimization of heat losses (insulation) and heat recovery;
- Maximization of power absorbed by product through good applicator design;
- If product is not fragile, maximization of power density (W/volume) to decrease length/dimensions of applicator.

## 5.6 Industrial applications

MW heating has been established in some key industries and applications: food, plasma, chemical, drying, and rubber. In these applications the use of MW energy for heating has had a significant impact on processing time, quality control, minimization of waste, and residual water, and it has also helped to create new products (for example, with various organoleptic, mechanical, and electrical properties or brand new products never obtained via conventional heating methods).

### 5.6.1 Food processing

The use of MWs in food processing has found application in the following areas:

- Food tempering and thawing of frozen meat, fish, fruit, butter and other foodstuff from storage temperature approximately  $-20\text{ }^{\circ}\text{C}$  to approximately  $-2\text{ }^{\circ}\text{C}$  (tempering) and  $0\text{ }^{\circ}\text{C}$  (thawing) to enable easier further processing like gridding, portioning, or blending;
- Food blanching;
- Food drying at atmospheric or vacuum pressure;
- Food pasteurization and sterilization.

Because there is no physical contact between the MW equipment and food, appropriate working conditions can be optimized and guaranteed by equipment manufacturers. The higher the temperature uniformity within the product, the faster the heating speed and the quicker the processing by MW heating vs. conventional heating to prevent bacterial contamination; material savings are also possible because less fluid is lost when using MWs, especially in thawing food. In sterilizing and pasteurizing



processes, optimal processing conditions can be established because the structure of proteins and fats does not change during processing.

Examples of MW batch and tunnel equipment are shown in Figures 5.12–5.14.



**Fig. 5.12:** MIP12 – 75 kW, 915 MHz CF preheater (boost heating), courtesy Ferrite Inc. USA [12]



**Fig. 5.13:** 20 kW (10 generators x2 kW 2.45 GHz CF cooking and pasteurization of liquids, courtesy Puschner, Germany [13]



**Fig. 5.14:** 225 kW (3 generators x75 kW) 915 MHz for meat tempering, courtesy Sairem SAS, France

### 5.6.2 Drying at atmospheric or vacuum pressure

The processing times of certain materials can be up to 1000 times faster using MW heating over conventional heat sources [13]. This is likely based on very absorptive materials with a high dielectric loss tangent. However, even materials that do not absorb MWs very well are excellent candidates for drying. In drying applications, the aim is to only evaporate the water/polar solvent in the material bed. Therefore, in such cases, it can actually be an advantage for the base material to have a low dielectric loss tangent. That way, the water/solvent will be evaporated with minimal impact on the surrounding material and also consume less total energy to achieve the desired evaporation. In particular, MW (as well as radio frequency) heating has a unique advantage over other drying techniques. In the case of materials with low thermal conductivity, there is a self-limiting heating effect. As the solid products are dried, moisture content decreases, less energy is absorbed, and the heating rate decreases, thereby also avoiding overheating of the solid. By measurements of changes in the output power of the installation, a correlation can be made with the moisture content of the product, which can be used as feedback for process control. Various materials like textiles, ceramics, polymers, paper, and foodstuffs have been dried using MWs, usually in combination with conventional systems (e.g., hot air, IR). Some materials (e.g., fruits, plants, pharmaceutical powders, and pellets) are heat sensitive and must be dried at lower temperatures, that is, at slightly reduced pressures, 0.1–0.3 bar (50–70 °C), to avoid arcing or plasma formation. Some examples of continuous-flow (in a tunnel) or static conditions (batch) are shown in Figures 5.15–5.17.



**Fig. 5.15:** 300 kW (4 generators × 75 kW) 915 MHz, multipurpose continuous-flow dryer, Ferrite, USA



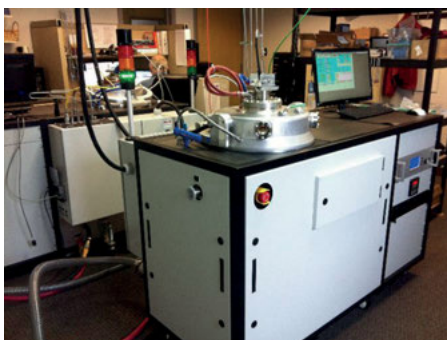
**Fig. 5.16:** 70 kW, 2.45 GHz continuous flow dryer for chemical powders, Union Microwaves, China [14]



**Fig. 5.17:** 36 kW (6 generators × 6 kW) batch vacuum dryer for pharmaceutical powder/pellets, Sairem SAS, France

### 5.6.3 Plasma processing

Since the use of electrodes in plasma processing has many disadvantages, for example, contamination or corrosion, MWs are frequently used to produce high-density plasmas at atmospheric or low pressure. Stable and reliable MW plasma equipment based on magnetrons and designed for automatic control of the operating parameters has already proved its efficiency in low-temperature diamond deposition (Figure 5.18), exhaust gas abatement (Figure 5.19), thin film deposition, metal surface cleaning, and sterilization, for example.



**Fig. 5.18:** CTS6U reactor – 6 kW, 2.45 GHz for chemical vapor deposition of diamond for jewellery, courtesy Carat Systems, USA [15]



**Fig. 5.19:** ZENITH Etch Plasma – Atmospheric MW plasma for semiconductor exhaust gas abatement, 2 kW or 6 kW, 2450 MHz, courtesy Edwards High Vacuum, UK [16]

#### 5.6.4 Chemistry

MW energy is extremely efficient in the selective heating of materials because no energy is wasted in the bulk heating of samples. MW heating processes are currently undergoing investigation for application in a number of fields where the advantages of MW energy may lead to significant savings in energy consumption, process time, and environmental remediation. However, apart from highly specialized applications like biomass extraction of different molecules used in cosmetics [17], MW heating applications have seen little commercialization in the field of synthetic chemistry. This is due to several reasons. First, little fundamental data exist regarding the dielectric properties of materials as a function of temperature and frequency. The second reason for the lack of development of MW heating processes is a lack of knowledge concerning the design of MW heating equipment. The third reason is badly designed laboratory research by chemists as a result of insufficient knowledge of equipment along with badly designed equipment by some MW manufacturers. All of this leads to nonreproducible results, magic effects, and varying kinetics, for example, which makes it very difficult to scale up the processes and attract the interest of industry.

As continuous manufacturing reaches new heights, the industry is adopting rigorous and robust measures to minimize risks and avoid batch failures. Proper modeling and simulation tools for the design of equipment would make it possible to produce very accurate models, but there is a bottleneck that currently prevents scaling up chemical reactions: a lack of knowledge of material parameters over the course of reactions.

There is a need to explore new reactor concepts by emphasizing dedicated designs that ensure the controllability and monitoring of process conditions. A number

of variables affect MW reactor output and its scale, with electric field intensity, power dissipation rate, and the temperature of heated mixtures being the most important. It is equally important to point out that MW technology cannot be implemented in a straightforward manner in just any industrial process involving heating. The development of MW equipment/installations needs to be studied individually on a system-by-system basis to achieve the desired benefits. Moreover, given the desire of the chemical industry to make the transition from batch to continuous processing, MW flow reactors have generated tremendous interest in the industry.

## 5.7 Conclusions

In general, industrial MW installations are not available as standard systems. Therefore, equipment performance is determined on the basis of discussions between end users, who indicate their needs in terms of production capacity, number of shifts, required temperature and temperature evolution, moisture, and so forth, and equipment manufacturers, who offer specifications related to such parameters as frequency, power, and applicator design.

It was shown in an earlier chapter that energy efficiency is a parameter to be considered in industrial processing. From a scientific point of view, energy efficiency is defined as the ratio between useful energy and total energy consumption. However, MW-assisted processes do not rely on benefits from reduced energy consumption alone [18]; energy efficiency is a further check point when other parameters have already pointed to the choice of electricity. The real interest in industrial processing is production efficiency, meaning the ratio between production yield and production effort. The main benefits of MW processing include process time savings, increased process yield and environmental compatibility. Processes where a number of these benefits are apparent may be considered to be likely candidates for further development.

Compared with conventional heating techniques, other claimed benefits of MW heating include the following:

- Higher heating rates and shorter production times;
- No direct contact between heating source and heated material;
- Selective heating;
- Greater control of process;
- Reduced equipment size and floor space;
- Flexible modular design;
- More friendly to the environment by lowering waste and production losses: MW installations do not produce dust, small particles, noise, exhaust gas, vibrations or ambient temperature increase;
- Gentle or rapid heating, depending on the product.

An important drawback of MW heating, which very often goes unmentioned, is the high cost of equipment and the relatively short (~1 year) lifetime of magnetrons. However, in terms of MW technology being implemented in industry, a more complex analysis of the benefits is required: technical and economic advantages as well as process-specific benefits must be analyzed together. MW equipment manufacturers have a significant role to play in technology implementation because they are the main contact between research and end users. They must make available to users enough in-depth information about their equipment and training to allow for correct and safe operation. On the other hand, users, either laboratory or industrial, must express sufficient interest in understanding the equipment (so that it does not remain a black box) and the limits of the technology for reproducible and scientifically sound results at the laboratory scale and successful operation in large-scale production.

## 5.8 A two-page definition guide to MW energy for beginners

### 5.8.1 What is MW energy?

Electrical energy is normally transmitted through wires, but as electromagnetic energy it can travel through space or along tubes. From electricity we obtain light, heat, and power. From electromagnetic energy, MWs, we receive radio and television, long-distance phone calls, and radar. MWs are naturally present in the atmosphere from the Sun and other stars and during thunderstorms.

### 5.8.2 How are MWs generated?

A magnetron converts electricity into MW energy. The magnetron produces high-frequency, 2.45 GHz electromagnetic waves (MWs). The MWs pass along a metal structure (waveguide) into a metal applicator.

### 5.8.3 What are dielectric properties?

The composition of a substance determines how much MW energy is absorbed, transmitted, reflected, and concentrated by it, and these are known as the dielectric properties. Described as the *loss factor* and *dielectric constant*, they can be calculated/measured for each substance. A high-loss substance like water is a very good absorber of MW energy. Low-loss substances like ice and plastic are poor absorbers of MW energy.

### 5.8.4 What happens to other materials?

Metals and other metallic materials reflect MW energy, and as a result, MW energy cannot pass through them. However, the energy can pass through other materials such as glass, china, paper, and most plastics.

### 5.8.5 Ionizing and nonionizing radiation

The subject of MW radiation is still regarded as mysterious and something of a black art. This is no doubt due to the fact that it cannot be seen or touched. Perhaps because MWs are unseen, they have also become confused with ionizing radiation. It is essential to understand the difference between the two since, given our present state of knowledge, it can be confidently asserted that exposure to these two different types of radiation carries very different consequences.

By definition, *ionizing radiation* is radiation that is capable of ejecting electrons from atoms and molecules with the resultant production of harmless radicals. There is a minimum quantum energy below which this disruption cannot take place. Since the human body is largely water, water molecules are used to define this minimum level. Different referent sources give different figures for this, varying between 12 and 35 eV. The actual value does not matter for the purpose of this comparison. A value of 12 eV corresponds to a wavelength of  $1.03 \times 10^{-7}$  m (103 nm), which, as is evident from Tables 5.4–5.6, lies just above the ultraviolet (UVC) spectrum. It should be noted that the term *radio frequency* (RF) is used here across the whole spectrum as a generic term and the term *microwave* refers to a portion of the RF spectrum.

The highest RF used in standards for RF safety is 300 GHz, which corresponds to a wavelength of  $10^{-3}$  m and lies in the extra high frequency (EHF) band of the RF spectrum. If the calculation is done the other way around, 300 GHz corresponds to an energy of 0.00125 eV, which is too small by about four orders of magnitude to cause ionization (Tables 5.7 and 5.8).

However, in radio transmitters using very high supply voltages, ionizing radiation in the form of X-rays are produced. It should be clear that this ionizing radiation is not inherent in RF energy but rather that both forms of radiation can coexist inside equipment and the RF engineer or technician needs to be aware of the hazards involved.

**Tab. 5.4:** Radiation wavelengths relative to 300 GHz (WHO). [7]

Ionizing radia- tions	UVC	UVB	UVA	Visible	Infrared	Radio frequencies
Wavelength	100 nm	280 nm	315 nm	400 nm	780 nm	1 mm, 300 GHz

**Tab. 5.5:** Frequency band designation

Frequency	Band code	Band description
300 Hz – 3 kHz	ELF	Extra low frequency
3 kHz – 30 kHz	VLF	Very low frequency
30 kHz – 300 kHz	LF	Low frequency
300 kHz – 3 MHz	MF	Medium frequency
3 MHz – 30 MHz	HF	High frequency
30 MHz – 300 MHz	VHF	Very high frequency
300 MHz – 3 GHz	UHF	Ultra high frequency
3 GHz – 30 GHz	SHF	Super high frequency
30 GHz – 300 GHz	EHF	Extra high frequency

**Tab. 5.6:** MW band letters (IEEE)

Frequency (GHz)	Band letter
1–2	L
2–4	S
4–8	C
8–12.5	X
12.5–18	Ku
18–26.5	K
26.5–40	Ka

**Tab. 5.7:** MW energy in comparison with other electromagnetic energy

Radiation type	Typical frequency (MHz)	Quantum energy (eV)
Gamma ray	$3.0 \times 10^{14}$	$1.24 \times 10^6$
X-Ray	$3.0 \times 10^{13}$	$1.24 \times 10^5$
UV	$1.0 \times 10^9$	4.1
Visible	$6.0 \times 10^8$	2.5
Infrared	$3.0 \times 10^6$	0.012
MW	2450	0.0016
Radio	1	$4 \times 10^{-9}$

**Tab. 5.8:** Chemical bonds with related energies

Chemical bond type	Chemical bond energy (eV)
H-OH	5.2
H-CH <sub>3</sub>	4.5
H-NHCH <sub>3</sub>	4.0
H <sub>3</sub> C-CH <sub>3</sub>	3.8
PhCH <sub>2</sub> -COOH	2.4
Hydrogen bond (water)	0.21



## Bibliography

- [1] Gedye R, Smith F, Westaway K, Ali H, Baldisera L, Laberge L, Rousell J. The use of microwave ovens for rapid organic synthesis. *Tetrahedron Letters*. 1986, 27(3): 279–282.
- [2] Moseley JD, Lenden P, Lockwood M, Ruda K, Sherlock JP, Thomson AD, Gilday JP. A Comparison of Commercial Microwave Reactors for Scale-Up within Process Chemistry, *Organic Process Research & Development*, 2008, 12:30–40
- [3] Decareau R, Teterson R. *Microwave Processing and Engineering*. Chicester, England: Ellis Horwood, 1986.
- [4] Radar basics – Magnetron, publisher Christian Wolff, on-line at [www.radartutorial.eu/08.transmitters/Magnetron.en.html](http://www.radartutorial.eu/08.transmitters/Magnetron.en.html), accessed on July 14th, 2017.
- [5] Cavity magnetron – Wikipedia on-line at [en.wikipedia.org/wiki/Cavity\\_magnetron](http://en.wikipedia.org/wiki/Cavity_magnetron), accessed on July 14th, 2017.
- [6] YJ1540-3NL-Magnetron-CW – Magnetrons – Richardson Electronics on-line at <http://www.relltubes.com/products/Magnetrons/Magnetron-CW/YJ1540-3NL.html?q=magnetron>, accessed on July 14th, 2017.
- [7] Metaxas AC, Meredith RJ. *Industrial Microwave Heating*, Peter Peregrinus Ltd, 1988.
- [8] Your partner in [microwave and radio-frequency] professional solutions: Sairem, publisher DWF Communications, on-line at [www.sairem.com](http://www.sairem.com), accessed on July, 15th, 2017.
- [9] Microwave Sample Preparation Instrumentation for Laboratories – Milestone Srl on-line at [www.milestonesrl.com](http://www.milestonesrl.com), accessed on July 15th, 2017.
- [10] CEM France on-line at [cem.com](http://cem.com), accessed on July 15th, 2017.
- [11] Sturm GSJ. Microwave field applicator design in small scale chemical processing. TU Delft, Faculty of Mechanical, Maritime and Materials Engineering, 11 November 2013. Available at: <http://repository.tudelft.nl/>, doi:10.4233/uuid:0407019d-248c-4061-b349-f9ea81085da1
- [12] Industrial Microwave Systems/Components & Integrated Assemblies on-line at [ferriteinc.com](http://ferriteinc.com), accessed on July 15th, 2017.
- [13] Puschner – Microwave Power Systems on-line at [www.pueschner.com](http://www.pueschner.com), accessed on July 5th, 2016.
- [14] Muegge Industrial Microwave and Plasma Systems on-line at [www.muegge.de](http://www.muegge.de), accessed on July 5th, 2016.
- [15] Jones DA, Lelyveld TP, Mavrofidis SD, Kingman SW, Miles NJ. Microwave heating applications in environmental engineering – a review. *Resources, Conservation and Recycling*, 2002, 34, 75–90,
- [16] Union Microwave Kesu Machinery & Equipment (Zhegzhou) Co.,Ltd. on-line at [www.unionmicrowave.com](http://www.unionmicrowave.com), accessed on July 5th, 2016.
- [17] Carat systems – Plasma CVD Deposition Equipment, Lab Grown Diamond Products and Advanced Deposition Processes on-line at [caratystems.com](http://caratystems.com), accessed on May 29th, 2016.
- [18] Vacuum and Abatement Solutions – Edwards on-line at [www.edwardsvacuum.com](http://www.edwardsvacuum.com), accessed on May 29th, 2016.
- [19] Radient Technologies: Advanced Extraction Solutions on-line at [www.radiantinc.com](http://www.radiantinc.com), accessed on May 29th, 2016.
- [20] Van Reusel K. Context and technology bound motives for use of electricity in industrial thermal processing, From ‘Electroheat’ to ‘Electromagnetic processing of materials’. PhD Thesis, KU Leuven, October 2010. Available at: <https://lirias.kuleuven.be/handle/123456789/270988>

## 6 The impact of microwaves in organic synthesis

The aim of this chapter is to provide a general overview of the utility of microwave irradiation in organic synthesis from a practical point of view. The chapter is structured considering the main effects of microwave irradiation and the reactions that can be improved using this enabling technique. The use of computational calculations as a tool that enables the prediction of whether a given reaction can be improved under microwaves is also covered.

### 6.1 Introduction

Since the publication of the seminal papers by Giguere and Gedye [1, 2] on the use of domestic microwave ovens in organic synthesis, microwave irradiation has emerged as a useful methodology to introduce energy into chemical reactions in chemistry in general and in organic synthesis in particular [3]. Early experiments were performed in domestic microwave ovens, but today most microwave chemistry is performed using instruments that are specifically designed for chemistry. More than 3000 articles have been published on microwave-assisted organic chemistry, with a significant increase since the introduction of dedicated monomode instruments.

Microwave-assisted organic synthesis (MAOS) has been defined as the *preparation of an organic compound from available starting materials via some (multistep) procedure involving microwave irradiation*. This statement implies that microwave irradiation could be the method of choice to introduce thermal energy in all steps of a chemical synthesis and supports the statement that microwaves will become the Bunsen burners of the twenty-first century [4].

Microwave chemistry is characterized by the efficient in-core volumetric heating of materials, and this is in contrast to the superficial nature of conventional heating. Dielectric heating depends on the ability of a material to absorb microwave energy and convert it into heat. In this regard, microwave heating is more selective than conventional conductive heating.

Considering these characteristics, some reactions can be clearly improved under microwave irradiation; such reactions include the following:

– *Condensation reactions:*

In most condensation reactions a polar low-boiling-point molecule is released that can be easily heated and thus removed under microwaves. In this regard it is worth highlighting heterocyclic synthesis or Knoevenagel reactions;

– *Equilibria:*

An example of an equilibrium is an esterification reaction. Similarly, many equi-

<https://doi.org/10.1515/9783110479935-006>

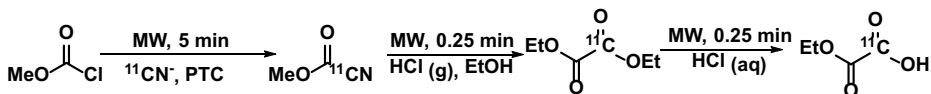
libria could be displaced to full conversion by the removal of a polar low-boiling-point molecule such as water;

- *Reactions that require harsh conditions (temperature and time):*  
Most cycloaddition and pericyclic reactions require long reaction times and high temperature. These conditions may produce extensive decomposition of the starting materials and products and, in cases like the Diels–Alder reaction, favor the reversibility of the reaction. The short reaction times observed under microwave irradiation are clearly beneficial in terms of yield and product purity;
- *Reactions with sensitive reagents and products:*  
Examples include reactions with organometallic reagents where, once again, the short reaction times avoid decompositions of the reagent;
- *Reactions on solid supports:*  
Many solid supports do not conduct heat very well, whereas they do absorb microwaves efficiently. It is possible to take advantage of the selective heating of the catalyst and the presence of so-called hot spots and consequently increase the turnover number (TON). In this way, it is also possible to replace mineral acids and oxidants with more benign solid heterogeneous acids and oxidants.

## 6.2 Acceleration effects

The best-known characteristic of microwave chemistry is the extraordinary reduction in reaction times – a phenomenon that leads to higher yields, higher product purity, fewer side products, and, in some cases, modification of the selectivity.

The extraordinarily short reaction times are particularly important in the preparation of radiopharmaceuticals [5]. The preparation with microwave methods of  $^3\text{H}$ -,  $^{11}\text{C}$ -, and  $^{18}\text{F}$ -labeled compounds used in PET may double the radioactive yield while maintaining the high degree of control, reproducibility, and predictability required to use these materials in humans (Scheme 6.1).



**Scheme 6.1:** Preparation of [ $^{11}\text{C}$ ] diethyl oxalate under microwave irradiation.

In a similar way, the application of microwave radiation in combinatorial and parallel chemistry opened new and interesting avenues due to the possibility of preparing a wide variety of products in a very short reaction time [6, 7]. Exploratory reactions can be conducted in minutes instead of hours and higher-risk ideas can be pursued with minimal time investment while still testing a hypothesis completely.



**Fig. 6.1:** Commercially available systems for microwave-assisted combinatorial synthesis (MACOS).

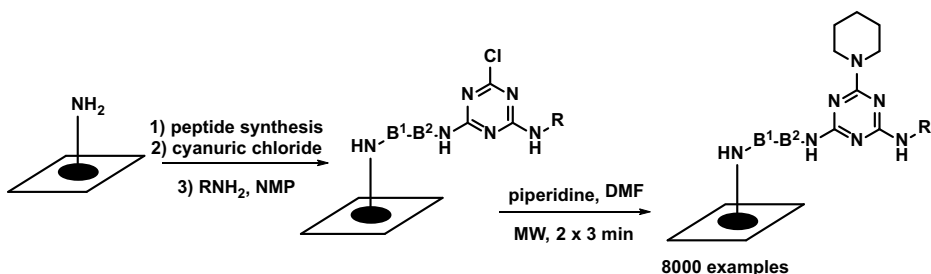
Multimode reactors can easily be used for most combinatorial applications such as parallel library synthesis, reactions on solid-supported reagents, multicomponent reactions, thin layer chromatography-supported reagents, and SPOT synthesis, among others, using commercially available systems. Most microwave systems can be adapted for use with rotor systems and microtiter plates (Figure 6.1).

Monomode reactors have a small cavity for use in combinatorial chemistry since they cannot accommodate a carousel or a multiplate. In these systems, a high process efficiency can be achieved by automatization. Most monomode systems can be used in conjunction with autosamplers, and this allows the efficient preparation of a variety of compounds (Figure 6.2).

An interesting example of SPOT synthesis (simultaneous parallel synthesis at different positions on a membrane support) was described by Scharn et al. [8], who reported the preparation of aminotriazines on cellulose and polypropylene membranes. Microwave irradiation was used for the synthesis of triazine membranes and the generation of a library of 8000 triazines (Scheme 6.2).



Fig. 6.2: Commercially available robotic microwave systems.



Scheme 6.2: SPOT synthesis of triazine membranes.

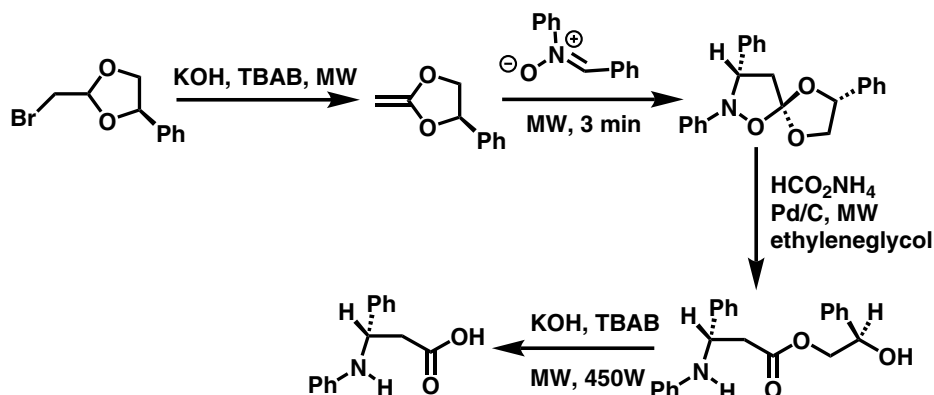
### 6.3 Multistep synthesis

The definition of MAOS implies the use of microwave irradiation in multistep synthesis, which means that microwaves can be applied for most reaction types and should be the technique of choice rather than a last resort.

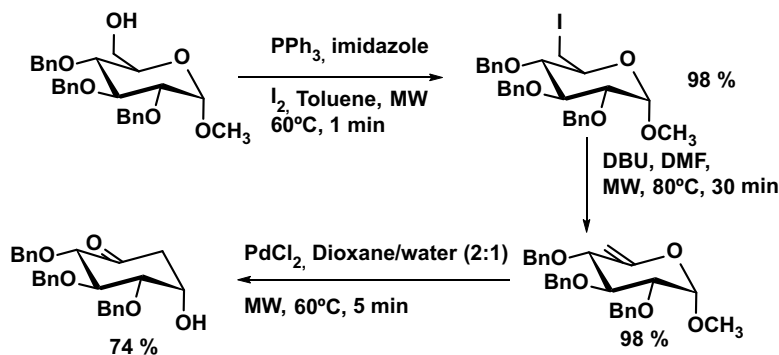
Very few multistep syntheses have been reported that involve microwave irradiation. Díaz-Ortiz et al. described the multistep preparation of  $\beta$ -amino acids from ketene acetals in four steps using microwave irradiation and solvent-free conditions in three cases [9]. On using an enantiomerically pure ketene acetal, the chirality is maintained in the  $\beta$ -amino acid (Scheme 6.3).

Similarly, Pohl et al. [10] described a three-step procedure for the preparation of carbocyclic systems as analogs of glucose-1-phosphate under microwave irradiation. The reaction involves a Ferrier-type rearrangement in which the reaction time can be shortened and the use of mercury can be avoided (Scheme 6.4).

Kappe et al. [11] reported a multistep microwave-assisted procedure for the preparation of biologically active 4-aryl-substituted quinolin-2(1*H*)-ones. The procedure has six steps, and palladium-catalyzed coupling reactions are the key steps for the introduction of substituents (Scheme 6.5).



Scheme 6.3: Multistep synthesis of  $\beta$ -amino acids.

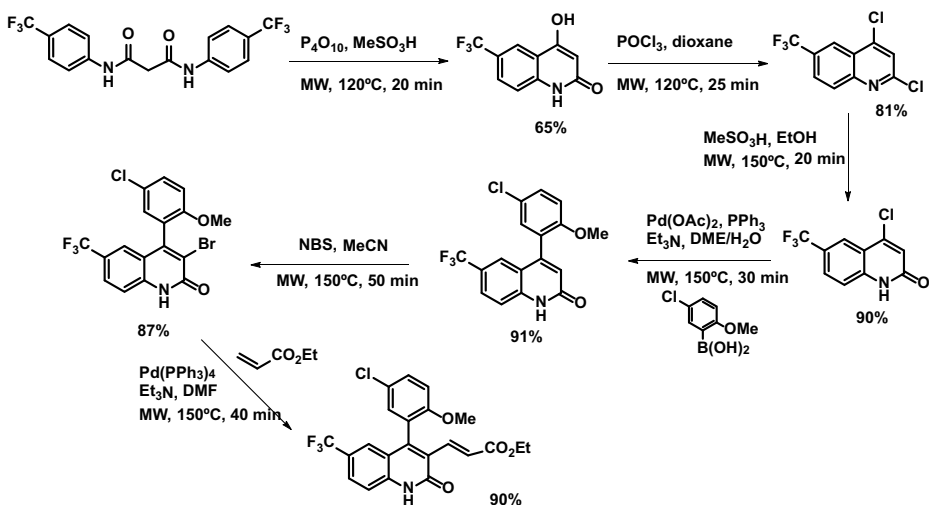


Scheme 6.4: Multistep synthesis of carbaglucose derivatives.

## 6.4 Natural products

Most natural products are characterized by a complex structure and are usually thermally sensitive. The use of microwave irradiation has a beneficial effect in the chemistry of natural products since the short reaction times required with microwaves have improved the yields of target compounds. Moreover, in many cases the key step in a multistep synthesis requires harsh conditions, and the use of microwave irradiation allows this to be achieved without decomposition of the natural product.

Ageliferin is an antiviral agent isolated from *Agelas conifera*. The biosynthetic origin of ageliferin was unknown, and the authors proved that ageliferin could be obtained from sceptrin by a vinyl cyclobutane rearrangement [12]. When sceptrin was dissolved in water and heated to 195 °C for 1 min using microwave irradiation (Scheme 6.6), ageliferin was obtained in 40% yield along with recovered sceptrin

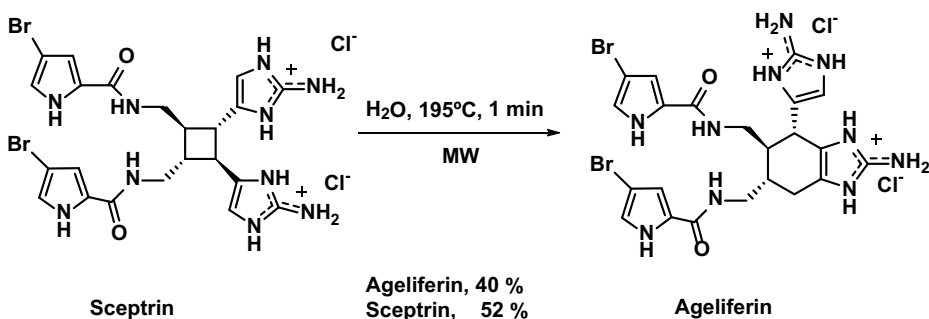


**Scheme 6.5:** Multistep synthesis of 4-aryl-substituted quinolin-2(1*H*)-ones.

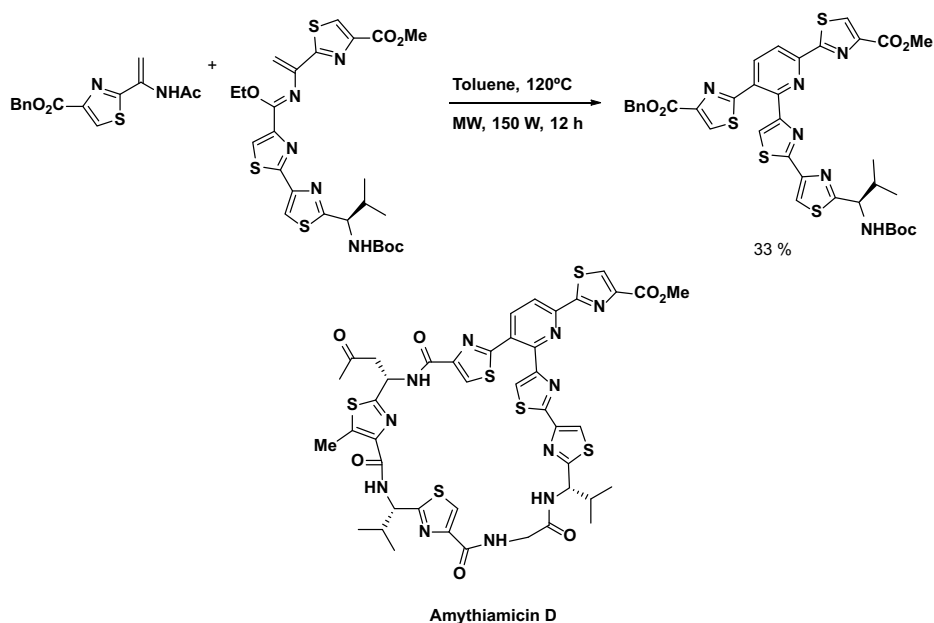
(52%). The use of any other procedure, for example, thermal heating or photochemical reaction, led to the complete decomposition of the starting material.

Moody et al. reported the first total synthesis of the thiopeptide antibiotic amythiamicin D [13]. The key step of the synthesis was a biomimetic hetero-Diels–Alder aromatization sequence that was performed under microwave irradiation for 1 h to provide a pyridine ring in modest yield (Scheme 6.7). This result could not be reproduced by conventional heating because of the harsh conditions required.

Similarly, Leigh et al. [14], in an improved methodology for the preparation of artificial molecular machines, prepared a machine that adds four amino acid blocks in a strand in sequence. Peptide bond formation was performed in acetonitrile/DMF (3 : 1) in the presence of DIPEA and  $(\text{HO}_2\text{CH}_2\text{CH}_2)_3\text{P}$  by heating at 60 °C under microwave



**Scheme 6.6:** Transformation of sceptrin into ageliferin.



**Scheme 6.7:** Key step in total synthesis of amythiamin D.

irradiation for 48 h (Scheme 6.8). This unusually long reaction time under microwaves implies that the reaction would not proceed under conventional heating.

Santra and Andreana [15] described a bioinspired Ugi/Michael/aza-Michael cascade reaction for the preparation of natural-product-like compounds under microwave irradiation. The reactions gave a high yield in 1.3 h and were performed in the absence of any additive, with water as the solvent, and they produced fused azaspiro tricyclic and tetracyclic compounds in one step (Scheme 6.9).

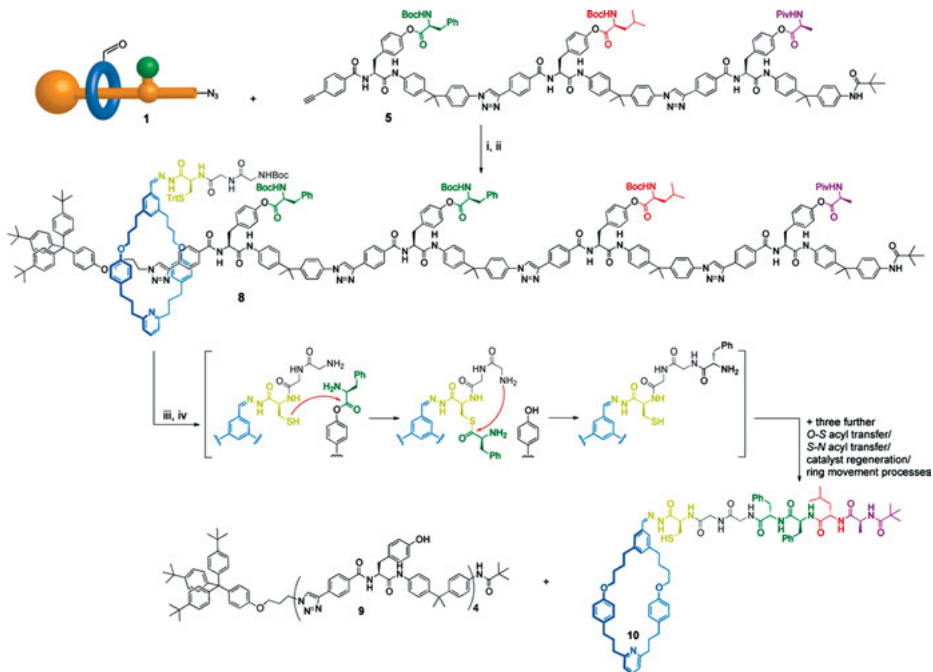
## 6.5 Homogeneous and heterogeneous catalysis

Microwave irradiation has had a profound impact in catalysis, not just in homogeneous [16, 17] and heterogeneous [18, 19] catalysis but also in nanocatalysis [20], which has profited from the characteristics of this methodology, namely flash and selective heating. The use of catalysis in benign solvents has also promoted a green and sustainable approach.

In some sections of this book emphasis will be placed on these topics, so only selected examples will be discussed in this chapter.

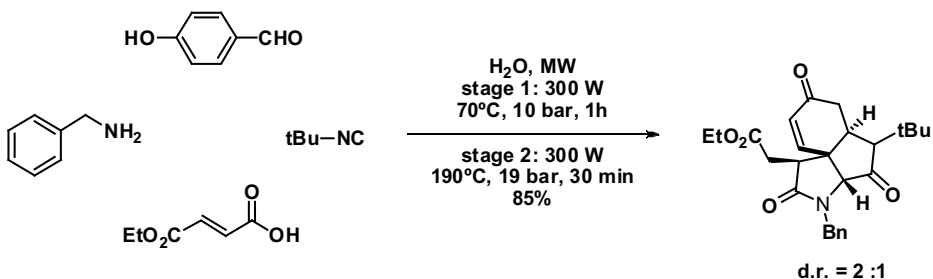
In homogeneous catalysis it is possible to design robust and reliable methodologies. Most results show spectacular acceleration along with improved yields and product purity, and in some cases, the selectivity can be modified. Some advantages are





**Scheme 6.8:** Molecular machines for the preparation of peptides under microwave irradiation.

also related to the design of green and sustainable procedures. These advantages include (1) the use of metallic catalysts in water as solvent, or other neoteric solvents, and without the need for an inert atmosphere; (2) addition of lower catalyst loading, including in the nanomolar range; (3) replacement of toxic reagents; (4) the design of new mild catalysts for use at high temperature; and (5) the integration of nonchro-

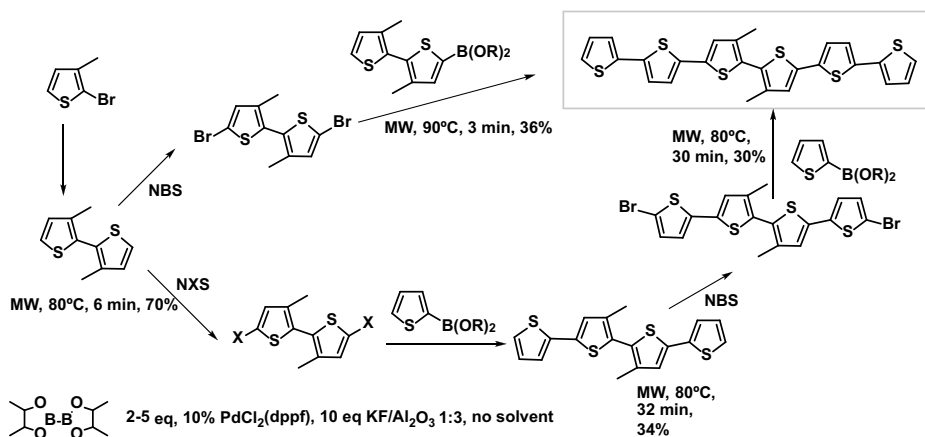


**Scheme 6.9:** Bioinspired Ugi/Michael/aza-Michael cascade reaction in aqueous media.

matographic separation techniques such as solid phase separations or fluoruous separations.

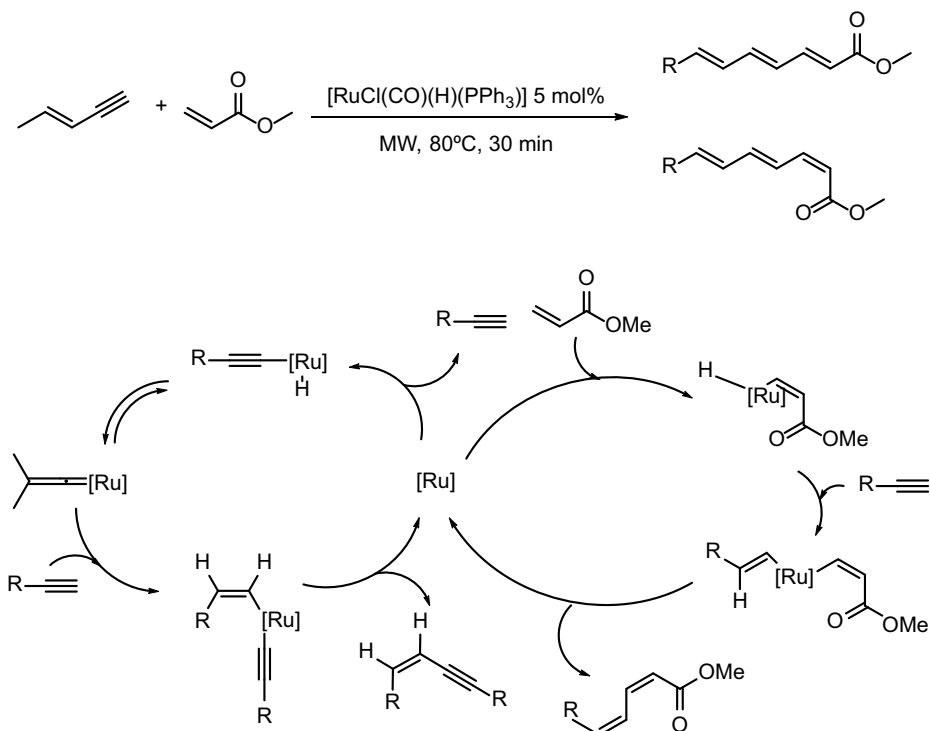
Green approaches have been developed in heterogeneous catalysis. It is possible to take advantage of the selective heating of polar catalysts or of the presence of hot spots in heterogeneous media. The catalyst can be heated rapidly to temperatures higher than the boiling point of the solvent. In this way the reaction occurs very rapidly on the surface of the catalyst (flash reaction) and the product can be collected in the solvent, which is at a lower temperature, and can even be cooled externally (cooling while heating) to avoid decomposition of the final product. In most cases these conditions produce an increase in the TON of the catalyst.

Cross-coupling reactions are among the most important catalyzed reactions that can be assisted by microwave irradiation, and they represent a fundamental methodology for the formation of C–C and C–heteroatom bonds. Almost any kind of palladium-catalyzed (or other metal-catalyzed) reaction has been performed and improved under microwave irradiation. For example, Barbarella et al. [21] described the preparation of thiophene oligomers by Suzuki coupling under microwave irradiation in solvent-free conditions. Reactions were performed in short reaction times (6–30 min) to obtain the oligomers in moderate to good yields (Scheme 6.10).



**Scheme 6.10:** Preparation of thiophene oligomers by Suzuki reactions.

Schabel and Plietker [22] described a ruthenium-catalyzed hydrovinylation of alkynes and enynes under microwave irradiation to obtain 1,3-dienes and 1,3,5-trienes (Scheme 6.11). The reaction required long reaction times (18–48 h) and elevated temperatures (100 °C), and a serious limitation was found in the fact that a homocoupling product was obtained instead of the desired heterocoupling reaction product. However, on using a large excess of acrylate and microwave irradiation as the heating



**Scheme 6.11:** Ru-catalyzed hydrovinylation of alkynes and enynes.

source in solvent-free conditions, the homocoupling reaction was observed exclusively to give a high yield in shorter reaction times (30 min) and under milder conditions ( $80^\circ\text{C}$ ). This reaction was not possible with conventional heating. The authors consider that this result is a consequence of the selective heating induced by microwaves.

Selective heating is more evident in heterogeneous reactions, and the different transmission of microwaves in the two phases can produce hot spots at the interphase. This situation can be exploited to obtain results that are not easy to achieve under conventional heating. As an example, Ley et al. [23] described the Suzuki reaction of arylboronic acids catalyzed by PdEncat (Figure 6.3). Under microwaves, the reaction time was shortened from 8 h to 10 min. They consider that enhanced catalytic activity is produced by the selective absorption of the metal particles, which can be heated directly without heating the support material as a result of the marked difference in their dielectric constants. A library synthesis was carried out, but of the 341 reactions undertaken, only 131 (38%) generated pure products. The use of a cooling-while-heating system led to a dramatic improvement in product purity. Reactions heated at 50 W reached global temperatures that did not exceed  $76^\circ\text{C}$ , that is, significantly cooler than

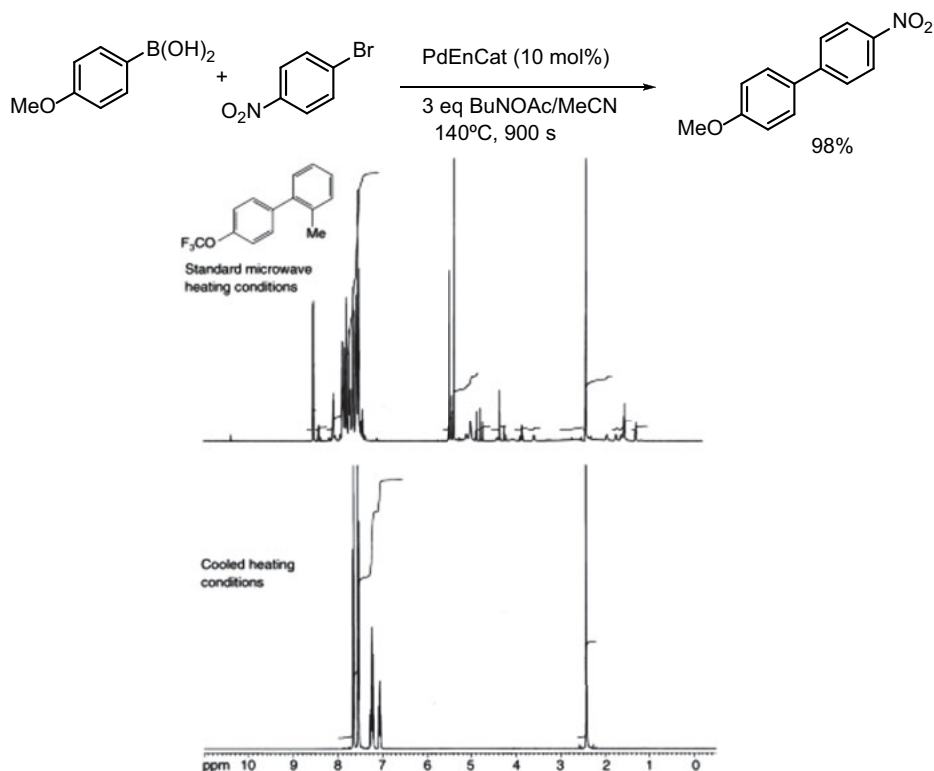


Fig. 6.3: Suzuki reactions with PdEnCat and cooling-while-heating conditions.

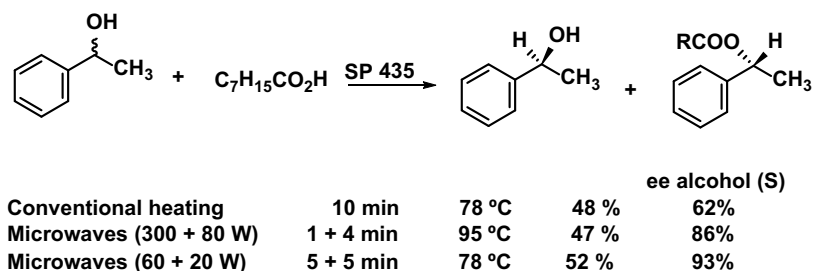
the 120 °C used in the standard reaction conditions (Figure 6.3). This finding confirms the selective heating of the catalyst. The reaction occurs at high temperature on the surface of the catalyst, and then the product goes into solution, which is cooler and thus avoids decomposition of the final product.

## 6.6 Biocatalysis

Considering that proteins and peptides have large dipole moments, they may be susceptible to rapid and selective heating under microwaves. This effect has been used to improve biocatalytic reactions with applications in organic synthesis and proteomics. Once again, in most cases a decrease in the reaction time was observed but in some cases modifications in the stereoselectivity and microwave effects were described.

Guibé-Jampel and Loupy [24] showed that the yield and stereoselectivity of the acylation of 1-phenylethanol catalyzed by supported enzymes can be improved under microwave irradiation. They explained this result by considering that, with microwaves, it is possible to reach the optimum temperature of the enzyme very rapidly,

especially when compared to conventional heating, and this leads to an increase in the stereoselectivity (Scheme 6.12).



**Scheme 6.12:** Acylation of 1-phenylethanol catalyzed by SP 435.

Deiters et al. [25] described specific microwave effects in enzymatic catalysis with the use of hyperthermophilic enzymes, which have minimal catalytic activity at temperatures below 40 °C and denature at much higher temperatures than their mesophilic counterparts.

A  $\beta$ -glucosidase (CeIB) from the hyperthermophilic archaeon *Pyrococcus furiosus* was examined for biocatalytic function under microwave irradiation; this enzyme is optimally active at ~110 °C. *P. furiosus* CeIB cleaves exoglycosidic linkages in both natural and synthetic substrates (Figure 6.4). Under identical thermal conditions (–20 to 40 °C) significant enzymatic activity ( $< 10\text{--}11 \text{ mol min}^{-1} \mu\text{g}^{-1}$ ) was not detected in the absence of microwave irradiation.

The authors consider that the observed specific microwave effect (enzyme activity at unusually low temperatures) is probably the result of molecular motion induced by a rapid dipole alignment of the peptide bonds with the oscillating electric field. In fact, Pfu CeIB activity at biocatalytically suboptimal temperatures is a function of the input of microwave power (Figure 6.4).

## 6.7 Reactions involving radicals

Special attention should be paid to reactions involving radicals owing to the spectacular results obtained under microwave irradiation.

Kilburn et al. [26] described the cyclization of alkenyl- and alkynylisonitriles with benzene and ethanethiol and 2-mercaptoethanol to give *cis* and *trans* pyrrolidines. Reactions under microwaves gave higher yields and required shorter reaction times, but they could be performed in the absence of a radical initiator (Scheme 6.13).

Ericsson and Engman [27] reported the microwave-assisted group transfer cyclization of organotellurium compounds. They found that under microwave irradiation

similar yields were obtained with shorter reaction times (6–10 min) when compared to those obtained by photolysis in refluxing benzene in the presence of 40 mol % hexabutylditin (Scheme 6.14). However, the selectivity was significantly reduced. The predominant formation of *exo* and *trans* isomers, respectively, is consistent with the Beckwith–Houk model for ring closure of 5-hexenyl radicals assuming a chairlike transition state, and this rule is probably not predominant under microwaves.

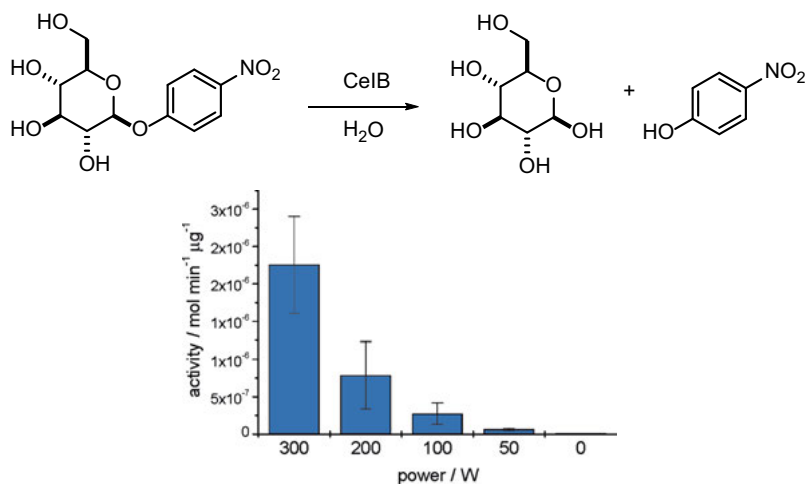
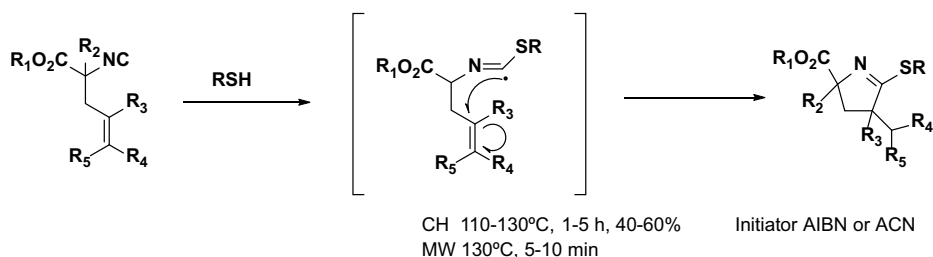
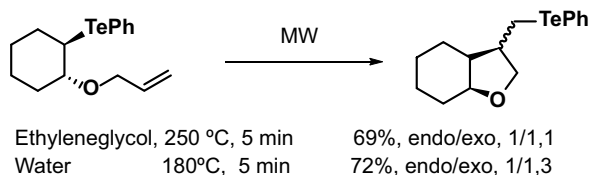


Fig. 6.4: Catalytic activity of CelB under microwave irradiation.

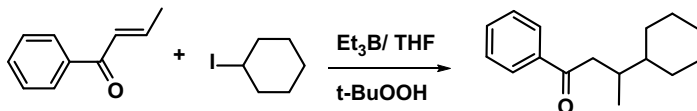


Scheme 6.13: Radical cyclizations under microwave irradiation without radical initiator.



Scheme 6.14: Stereoselectivity in radical cyclizations of organotellurium compounds under microwave irradiation.

Horikoshi et al. [28] reported the microwave-enhanced synthesis of 3-cyclohexyl-1-phenyl-1-butanone from crotonophenone and iodocyclohexane in the presence of *t*-BuOOH and triethylborane at ambient temperature and under reflux conditions (Scheme 6.15).



**Scheme 6.15:** Stereoselectivity in radical cyclizations of organotellurium compounds under microwave irradiation.

The yields were higher under microwave irradiation at low temperature using an internal cooling system that is more efficient than the traditional external system (Scheme 6.15 and Figure 6.5). As indicated in Figure 6.5 in traditional external cooling systems the coolant is situated in the exterior of the sample. Since the temperature is lower at the surface than in the internal part of the sample owing to the volumetric nature of microwaves, this cooling system is very inefficient. Moreover, condensation of water at the surface may hinder the penetration of microwave irradiation to the sample owing to the absorption of the radiation by the polar water. In this way internal cooling is more efficient and solves all the problems associated with external cooling; cooling is produced in the internal part of the sample, which absorbs microwave irradiation and condensation is avoided.

The authors considered that the higher yields observed for the microwave-induced reaction over those obtained by conventional heating for identical temperature conditions are related to some specific microwave effect.

## 6.8 Selectivity under microwave irradiation

One of the major issues in organic synthesis is obtaining the required selectivity (chemo-, regio-, and stereoselectivity). Selectivity, yield, and atom economy are the most important parameters to describe the efficiency of a reaction. The use of reaction conditions (e.g., temperature, time, solvent), kinetic vs. thermodynamic control, protecting or activating groups (e.g., chiral auxiliaries), and catalysts (including chiral catalysts) have all been used to obtain the desired isomer. The selective heating induced by microwave irradiation has been used to modify the selectivity of many reactions. In this regard, the possibility of obtaining the desired selectivity by simply changing the heating system is very attractive [29]. Some examples of this behavior are described in what follows.

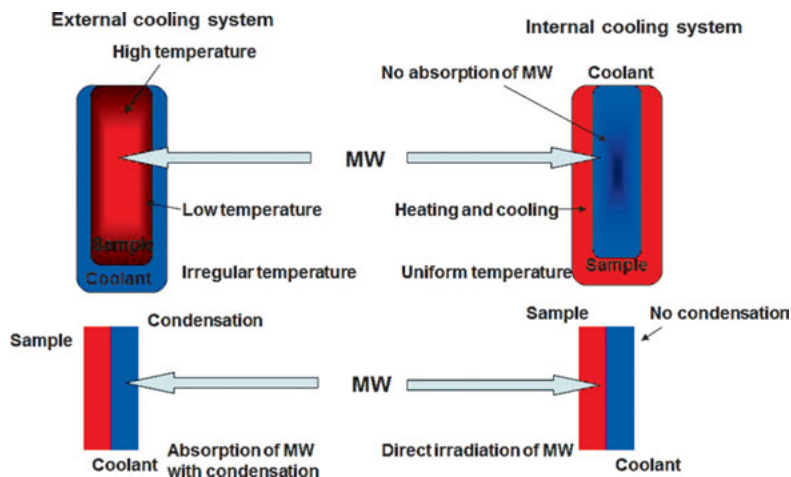


Fig. 6.5: Comparison of outside and inside cooling-while-heating systems.

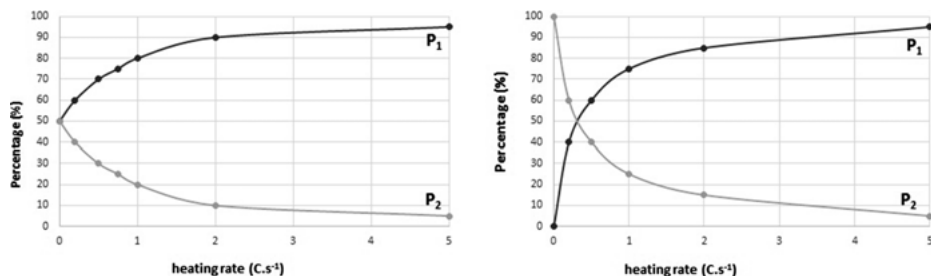


Fig. 6.6: Examples of induced selectivity (right) and inversion of selectivity (left) as a function of the heating rate.

Stuerga et al. [30] reported the sulfonation of naphthalene under microwave irradiation where the selectivity between 1- and 2-naphthalenesulfonic acids is controlled by the irradiation power, that is, the heating rate. In this study, it was shown how it was possible to induce selectivity or to produce an inversion of selectivity as a function of the heating rate (Figure 6.6), with conventional heating considered a slow heating system and microwave irradiation a fast heating system.

In the reaction of 2-pyridone with benzyl halides in the absence of solvent [31], microwave irradiation led to C-alkylation, whereas the classical route leads to *N*-alkylation (Scheme 6.16). Computational calculations showed that classical heating led to *N*-alkylation through a kinetically favorable  $S_N2$  mechanism. In contrast, under microwave irradiation a thermodynamic control product (C-alkylation) was obtained.

The cycloaddition of 6,6-dimethylfulvene with alkenes, as reported by Hong et al. [32], led to different polycyclic ring systems depending on the heating source (Scheme 6.17). Under conventional heating, the kinetically controlled Diels–Alder



cycloaddition of 6,6-dimethylfulvene occurred exclusively. In contrast, microwave irradiation resulted in the formation of intriguing polycyclic ring systems that are thermodynamically favored.

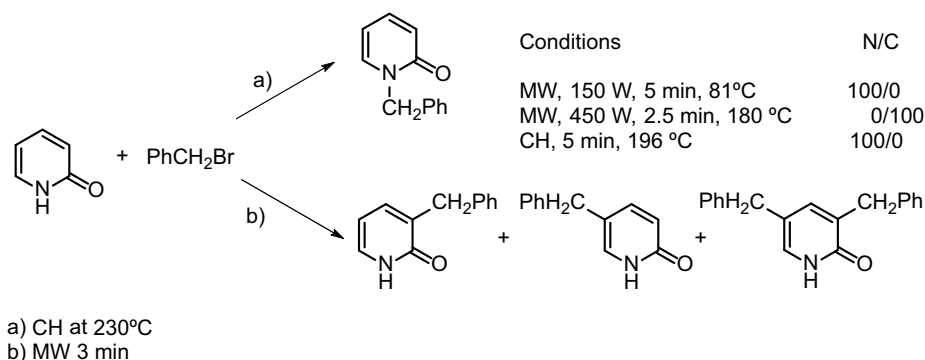
Fustero et al. [33] reported a tandem cross-metathesis intramolecular aza-Michael reaction (Scheme 6.18). When the reaction was performed under microwave irradiation, the reaction time was dramatically reduced (20 min), and the stereochemistry of the final products was reversed.

## 6.9 Computational calculations in MAOS

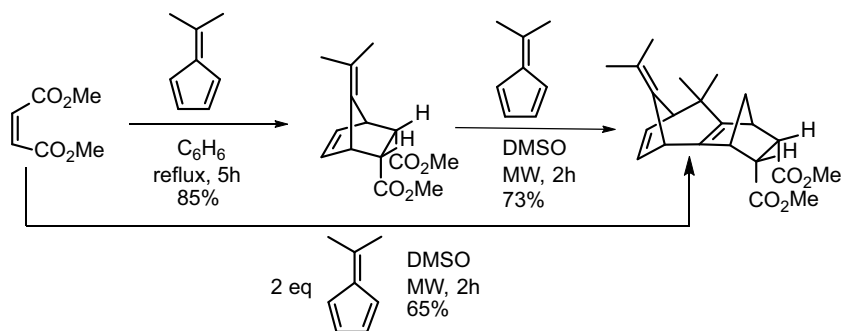
Exploitation of the benefits that microwave irradiation have in chemistry is still hindered by a lack of understanding of the physical principles of the interaction of microwave irradiation with the components of a reaction and the difficulty in reproducing the reaction conditions under conventional and microwave heating. Separation of thermal heating and the electromagnetic effects are experimentally impossible.

In this regard, computational chemistry [34] constitutes a powerful tool since it can determine both thermodynamic parameters (e.g., activation energy, enthalpy) and some variables, such as dipolar moments, polarity, and polarizability, that govern interactions with microwaves. As a consequence, computational chemistry has been used to understand and predict the effect of microwave irradiation in organic synthesis [35].

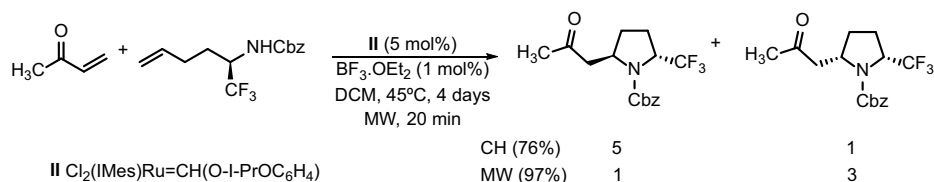
Prieto et al. [36] performed a computational study on previously described reactions that were improved under microwave reaction to determine the influence of thermodynamic parameters in MAOS. The main conclusions are collected in Table 6.1. It was quantified that exothermic reactions with low activation energies (type I) occur easily by conventional heating and improvements are not expected under microwaves. Endothermic reactions and reactions with moderate and high activation en-



**Scheme 6.16:** Benzoylation of 2-pyridone under conventional heating and microwave irradiation.



**Scheme 6.17:** Cycloadditions of 6,6-dimethylfulvene.



**Scheme 6.18:** Stereoselective synthesis of pyrrolidines.

ergies (types II–IV) can be improved under microwave irradiation. Finally, reactions with activation energies above  $30 \text{ kcal mol}^{-1}$  can be improved only if a polar component is present and they are exothermic (type V); otherwise, they do occur under conventional heating or microwave irradiation (type VI).

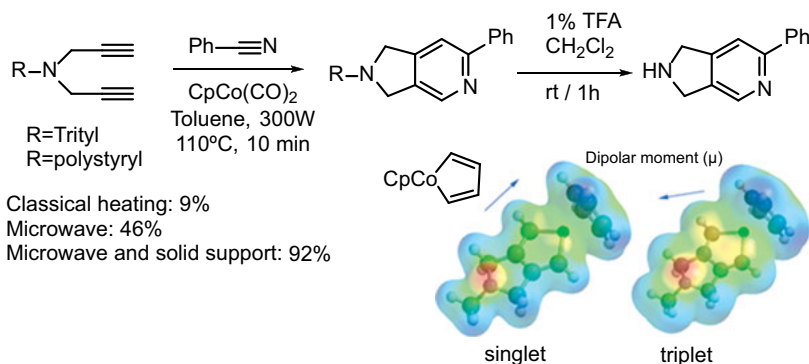
In cases where selectivity is subject to kinetic and thermodynamic control, microwave irradiation can modify the selectivity by favoring the thermodynamically controlled products [37].

The polarities of the components that take part in a reaction is the most indicative property that influences the heating rate under microwave irradiation. Three aspects should be highlighted: The polarity of the species involved in the reaction [38], the use of microwave susceptors [39], and the evolution of polarity along the reaction

**Tab. 6.1:** Influence of microwave irradiation as a function of thermodynamic parameters.

Reaction	Ea	$\Delta H$	Conclusion
Type I		$< 0$	Not improved
Type II	$< 20 \text{ kcal mol}^{-1}$	$> 0$	Improved
Type III		$< 0$	Improved
Type IV	$20\text{--}30 \text{ kcal mol}^{-1}$	$> 0$	Improved
Type V		$< 0$	Improved with susceptors
Type VI	$> 30 \text{ kcal mol}^{-1}$	$> 0$	Do not occur





**Fig. 6.9:** Influence of radicals in triplet state on cyclotrimerization reactions.

Langa et al. [43] described how the cycloaddition of *N*-methylazomethine ylides to  $C_{70}$  gave three regioisomers **a–c** (Figure 6.8) by reaction at the 1–2, 5–6, and 7–21 bonds, respectively (Figure 6.8). Under classical heating, isomer **a** was found to predominate and isomer **c** was formed in a low proportion. In contrast, isomer **c** was not formed under microwave irradiation regardless of the irradiation power, and isomer **b** predominated at higher power. The computational study performed at RHF/PM3 indicated that the reaction was stepwise and, in agreement with the experimental results, microwave irradiation favored the formation of the product corresponding to the hardest and least polarizable transition state, which corresponds to isomer **b** (Figure 6.8).

As mentioned earlier, reactions that involve radicals have been greatly affected by microwave irradiation – especially those that involve triplet states – since microwave irradiation has been reported to stabilize radicals in the triplet state [44].

It is worth highlighting a computational study of the [2+2+2] cyclotrimerization reaction between a trityl-protected dipropargylamine and benzonitrile using  $\text{CpCo(CO)}_2$  as catalyst (Figure 6.9) [45]. This reaction was reported to be markedly improved under microwave irradiation [46]. The outcomes indicate that the evolution of one radical intermediate from the singlet to the triplet state plays an important role in the mechanism. In this evolution, an inversion of the dipolar moment vector of this intermediate was detected (Figure 6.9). Thus, in agreement with the previous results [44], microwave irradiation can increase triplet lifetime and improve reaction results.

## Conclusions

In this chapter we have tried to rationalize how microwave irradiation can be applied successfully in organic synthesis. We included select examples to illustrate the advantages of this methodology in several fields related to the synthesis of organic compounds, such as multistep synthesis, combinatorial chemistry, natural products,

catalysis, and reactions with radicals, among others. Finally, we showed how computational chemistry can be used to predict efficiently the advantageous use of microwave irradiation.

## Bibliography

- [1] Gedye R, Smith F, Westaway K, Ali H, Baldisera L, Laberge L, Rousell J. The use of microwave ovens for rapid organic synthesis. *Tetrahedron Lett* 1986, 279–282.
- [2] Giguere RJ, Bray TL, Duncan SM, Majetic G. Application of commercial microwave ovens to organic synthesis. *Tetrahedron Lett* 1986, 4945–4948.
- [3] *Microwaves in Organic Synthesis*. de la Hoz A, Loupy A, eds. 3rd edn. Weinheim, Wiley, 2012.
- [4] Bose AK, Banik BK, Lavlinskaia N, Jayaraman M, Manhas MS. MORE chemistry in a microwave. *Chemtech* 1997, 27, 18–24.
- [5] Elander N, Jones JR, Lu SY, Stone-Elander S. Microwave-enhanced radiochemistry. *Chem Soc Rev* 2000, 29, 239–249.
- [6] Blackwell HE. Out of the oil bath and into the oven – microwave-assisted combinatorial chemistry heats up. *Org Biomol Chem* 2003, 1, 1251–1255.
- [7] de la Hoz A, Díaz-Ortiz A, eds. *Microwaves in High Throughput Synthesis*. *Comb Chem High T Scr* 2007, 9-10, 777–933.
- [8] Scharn D, Germeroth L, Schneider-Mergener J, Wenschuh H. Sequential Nucleophilic Substitution on Halogenated Triazines, Pyrimidines, and Purines: A Novel Approach to Cyclic Peptidomimetics. *J Org Chem* 2001, 66, 507–513.
- [9] Moreno A, Díaz-Ortiz A, Díez-Barra E, de la Hoz A, Prieto P. Transformations of isoxazolidine and dihydropyran derivatives to optically active compounds. *J Chem Soc Perkin Trans 1* 1996, 259–263 and references therein.
- [10] Ko KS, Zea CJ, Pohl NL. Surprising Bacterial Nucleotidyltransferase Selectivity in the Conversion of Carbaglucose-1-phosphate. *J Am Chem Soc* 2004, 126, 13188–13189.
- [11] Glasnov TN, Stadlbauer W, Kappe CO. Microwave-Assisted Multistep Synthesis of Functionalized 4-Arylquinolin-2(1H)-ones Using Palladium-Catalyzed Cross-Coupling Chemistry. *J Org Chem* 2005, 70, 3864–3870.
- [12] Baran PS, O'Malley DP, Zografos AL. Scepterin as a Potential Biosynthetic Precursor to Complex Pyrrole–Imidazole Alkaloids: The Total Synthesis of Ageliferin. *Angew Chem Int Ed* 2004, 43, 2674–2677.
- [13] Hughes RA, Thompson SP, Alcaraz L, Moody CJ. Total synthesis of the thiopeptide amythiamicin D. *Chem Commun* 2004, 946–948.
- [14] De Bo G, Kuschel S, Leigh DA, Lewandowski B, Pappmeyer M, Ward JW. Efficient Assembly of Threaded Molecular Machines for Sequence-Specific Synthesis. *J Am Chem Soc* 2014, 136, 5811–5814.
- [15] Santra S, Andreana PR. A Bioinspired Ugi/Michael/Aza-Michael Cascade Reaction in Aqueous Media: Natural-Product-like Molecular Diversity. *Angew Chem Int Ed* 2011, 50, 9418–9422.
- [16] Larhed M, Moberg C, Hallberg A. Microwave-Accelerated Homogeneous Catalysis in Organic Chemistry. *Acc Chem Res* 2002, 35, 717–727.
- [17] Mehta VP, Van der Eycken EV. Microwave-assisted C–C bond forming cross-coupling reactions: an overview. *Chem Soc Rev* 2011, 40, 4925–4936.
- [18] Daştan A, Kulkarnia A, Török B. Environmentally benign synthesis of heterocyclic compounds by combined microwave-assisted heterogeneous catalytic approaches. *Green Chem* 2012, 14, 17–37.

- [19] Horikoshi S, Serpone N. Role of microwaves in heterogeneous catalytic systems. *Catal Sci Technol* 2014, 4, 1197–1210.
- [20] Polshettiwar V, Varma RS. Green chemistry by nano-catalysis. *Green Chem* 2010, 12, 743–754.
- [21] Melucci M, Barbarella G, Sotgiu G. Solvent-Free, Microwave-Assisted Synthesis of Thiophene Oligomers via Suzuki Coupling. *J Org Chem* 2002, 67, 8877–8884.
- [22] Schabel T, Plietker B. Microwave-Accelerated Ru-Catalyzed Hydrovinylation of Alkynes and Enynes: A Straightforward Approach toward 1,3-Dienes and 1,3,5-Trienes. *Chem Eur J* 2013, 19, 6938–6941.
- [23] Baxendale IR, Griffiths-Jones CM, Ley SV, Tranmer GK. Microwave-Assisted Suzuki Coupling Reactions with an Encapsulated Palladium Catalyst for Batch and Continuous-Flow Transformations. *Chem Eur J* 2006, 12, 4407–4416.
- [24] Carrillo JR, Bouvet D, Guibé-Jampel E, Loupy A, Petit A. Microwave-Promoted Lipase-Catalyzed Reactions. Resolution of ( $\pm$ )-1-Phenylethanol. *J Org Chem* 1996, 61, 7746–7749.
- [25] Young DD, Nichols J, Kelly RM, Deiters A. Microwave Activation of Enzymatic Catalysis. *J Am Chem Soc* 2008, 130, 10048–10049.
- [26] Lamberto M, Corbett DF, Kilburn JD. Microwave assisted free radical cyclisation of alkenyl and alkynyl isocyanides with thiols. *Tetrahedron Lett* 2003, 44, 1347–1349.
- [27] Ericsson C, Engman L. Microwave-Assisted Group-Transfer Cyclization of Organotellurium Compounds. *J Org Chem* 2004, 69, 5143–5146.
- [28] Horikoshi C, Tsuzuki J, Kajitani M, Abe M, Serpone N. Microwave-enhanced radical reactions at ambient temperature Part 3: Highly selective radical synthesis of 3-cyclohexyl-1-phenyl-1-butanone in a microwave double cylindrical cooled reactor. *New J Chem* 2008, 32, 2257–2262.
- [29] Díaz-Ortiz A, de la Hoz A, Carrillo JR, Herrero MA. Selectivity Modifications under Microwave Irradiation In: de la Hoz A, Loupy A, eds. *Microwaves in Organic Synthesis*. 3rd ed. Weinheim, Wiley, 2012, 209–244.
- [30] Stuerger D, Gonon K, Lallemand M. Microwave heating as a new way to induce selectivity between competitive reactions. Application to isomeric ratio control in sulfonation of naphthalene. *Tetrahedron* 1993, 49, 6229–6234.
- [31] de la Hoz A, Prieto M P, Rajzmann M, de Cózar A, Díaz-Ortiz A, Moreno A, Cossío FP. Selectivity under microwave irradiation. Benzoylation of 2-pyridone: an experimental and theoretical study. *Tetrahedron* 2008, 64, 8169–8176.
- [32] Hong BC, Shr YJ, Liao JH. Unprecedented Microwave Effects on the Cycloaddition of Fulvenes. A New Approach to the Construction of Polycyclic Ring Systems. *Org Lett* 2002, 4, 663–666.
- [33] Fustero S, Jiménez D, Sánchez-Roselló M, del Pozo C. Microwave-Assisted Tandem Cross Metathesis Intramolecular Aza-Michael Reaction: An Easy Entry to Cyclic  $\beta$ -Amino Carbonyl Derivatives. *J Am Chem Soc* 2007, 129, 6700–6701.
- [34] Bachrach SM ed. *Computational Organic Chemistry*. 2nd edn. New York, John Wiley and Sons, Inc, 2014.
- [35] Prieto P, de la Hoz A, Díaz-Ortiz A, Rodríguez AM. Understanding MAOS through Computational Chemistry. *Chem Soc Rev* 2017, 46, 431–451.
- [36] Rodríguez AM, Prieto P, de la Hoz A, Díaz-Ortiz A, Martín R, García JI. Influence of Polarity and Activation Energy in Microwave-Assisted Organic Synthesis (MAOS). *ChemistryOpen* 2015, 4, 308–317.
- [37] Almena I, Díaz-Ortiz A, Díez-Barra E, de la Hoz A, Loupy A. Solvent-free benzoylation of 2-pyridone. Regiospecific N- or C-alkylation. *Chem Lett* 1996, 333–334.
- [38] Gabriel C, Gabriel S, Grant EH, Halstead BS, Mingos DMP. Dielectric parameters relevant to microwave dielectric heating. *Chem Soc Rev* 1998, 27, 213–224.
- [39] Besson T, Kappe CO. Microwave susceptors In: de la Hoz A, Loupy A, eds. *Microwaves in Organic Synthesis*. 3rd edn. Weinheim, Wiley, 2012, 297–346.

- [40] Perreux L, Loupy A. A tentative rationalization of microwave effects in organic synthesis according to the reaction medium, and mechanistic considerations. *Tetrahedron* 2001, 57, 9199–9223.
- [41] Sasaki S, Ishibashi N, Kuwamura T, Sano H, Matoba M, Nisikawa T, Maeda M. Excellent acceleration of the Diels-Alder reaction by microwave irradiation for the synthesis of new fluorine-substituted ligands of NMDA receptor. *Bioorg Med Chem Lett* 1998, 8, 2983–2986.
- [42] Stuerge DAC, Gaillard P. Microwave athermal effects in Chemistry: A myth's autopsy. *J Microwave Power E E* 1996, 31, 87–100.
- [43] Langa F, de la Cruz P, de la Hoz A, Espíldora E, Cossío FP, Lecea B. Modification of Regioselectivity in Cycloadditions to  $C_{70}$  under Microwave Irradiation. *J Org Chem* 2000, 65, 2499–2507.
- [44] Wasielewski MR, Bock CH, Bowman MK, Norris JR. Controlling the duration of photosynthetic charge separation with microwave radiation. *Nature* 1983, 303, 520–522.
- [45] Rodríguez AM, Cebrián C, Prieto P, García JI, de la Hoz A, Díaz-Ortiz A. DFT Studies on Cobalt-Catalyzed Cyclotrimerization Reactions: The Mechanism and Origin of Reaction Improvement under Microwave Irradiation. *Chem Eur J* 2012, 18, 6217–6224.
- [46] Young D, Deiters A. A General Approach to Chemo- and Regioselective Cyclotrimerization Reactions. *Angew Chem Int Ed* 2007, 46, 5187–5190.

Yuji Wada, Dai Mochizuki, Taishi Ano, Masato M. Maitani,  
Shuntaro Tsubaki, and Naoto Haneishi

## 7 Chemical reactions on the interfaces of solids under microwaves

### 7.1 Introduction

Chemists often encounter chemical reactions enhanced under microwave (MW) irradiation. They observe shortening of the reaction times required to complete the reactions or decrease of the reaction temperatures necessary for the progress of chemical reactions. Those unusual behaviors observed under MW irradiation have been often called *MW special effects*, *MW specific effects*, or *MW nonthermal effects*.

However, these MW effects are still in veil. Some chemists are skeptical about them, but others demonstrate their confidence in the presence of these MW effects. One of the leading chemists of so-called MW chemistry, Kappe, pointed out the importance of the *precise measurement of the temperatures of reaction systems*, especially for homogeneous reaction systems of organic syntheses [1]. Certainly chemists should agree with his comment. We would describe this chapter as showing and discussing thermal effects especially as observed for chemical reactions occurring at the interfaces of solids, specifically observed under MW irradiation. This should be recognized as being among the MW-specific thermal effects but it can never be observed under conventional heating because it originates from the intrinsic physics of the interactions of MWs with substances.

Now let us provide an overview of several works dealing with chemical reactions occurring at the solid interfaces under MW irradiation listed in Table 7.1. We can raise as examples works dealing with methanol reforming [2], hydrodesulfurization of thiophene and the decomposition of hydrogen sulfide [3], dehydrogenation of ethylbenzene [4], dry reforming of methane [5, 6], decomposition of NO [7], steam–carbon reaction [8], reduction of TiO<sub>2</sub> [9], carbothermic reduction of hematite [10], and the reduction of CuO [11, 12].

It is natural to point out the presence of the distribution of temperatures in their reaction systems containing the interfaces of solids. Perry et al. demonstrate that MW heating can provide an effective and efficient method for transferring heat to the catalyst used for endothermic reactions, such as methanol–steam reforming [2]. However, several authors have observed enhanced reaction rates, lowering the reaction temperatures, or shortening the reaction times for chemical reactions carried out under MW irradiation as described in what follows. Zhang et al. observed the hydrodesulfurization of thiophene (exothermic) and the decomposition of hydrogen sulfide (endothermic) on MoS<sub>2</sub>/Al<sub>2</sub>O<sub>3</sub> under MW irradiation and showed that the apparent equilibrium

<https://doi.org/10.1515/9783110479935-007>



**Tab. 7.1:** An overview of works dealing with chemical reactions occurring at the solid interfaces under MW irradiation.

Reaction	Catalyst	Condition	Ref.
$\text{CH}_3\text{OH} + \text{H}_2\text{O} \rightarrow \text{CO}_2 + 3 \text{H}_2$	$\text{Al}_2\text{O}_3/\text{CuO}/\text{ZnO}$	500~600 K MW	2
$\text{H}_2\text{S} \leftrightarrow \text{H}_2 + 1/2 \text{S}_2$	$\text{MoS}_2/\gamma\text{-Al}_2\text{O}_3$	700~1100 K MW	3
$\text{C}_4\text{H}_4\text{S} + 4 \text{H}_2 \rightleftharpoons \text{C}_4\text{H}_{10} + \text{H}_2\text{S}$	C2634	450~900 K MW	3
$\text{CH}_4 + \text{CO}_2 \leftrightarrow 2 \text{H}_2 + 2 \text{CO}$	Activated carbon (Filtracarb FY5)	873~1173 K MW	5
$\text{C} + \text{H}_2\text{O} \rightleftharpoons \text{CO} + \text{H}_2$	–	760~1000 K MW	8
$\text{CO} + \text{H}_2\text{O} \rightleftharpoons \text{CO}_2 + \text{H}_2$			
$\text{C} + \text{CO}_2 \rightleftharpoons 2 \text{CO}$			
$\text{C} + 2 \text{H}_2 \rightleftharpoons \text{CH}_4$			
$4 \text{CuO} \rightarrow 2 \text{Cu}_2\text{O} + \text{O}_2$	–	~1000 K MW Emax Hmax	11
$2 \text{Cu}_2\text{O} \rightarrow 4 \text{Cu} + \text{O}_2$			
$2 \text{CuO} \rightarrow 2 \text{Cu} + \text{O}_2$			

constants of both reactions were shifted in opposite directions [3]. They attributed this observation to the occurrence of the hot spots at the catalyst surface indicated by the formation of sintered melt particle containing  $\text{MoS}_2$  and  $\text{Al}_2\text{O}_3$ . Zhan published a review article with Hayward mentioning that hot spots generated at the surface of catalysts under MW irradiation are responsible for the enhancement of catalytic reactions [13].

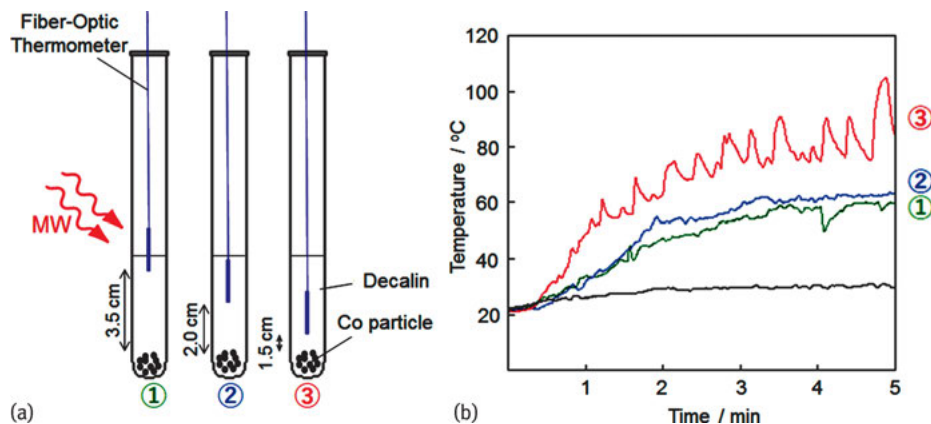
In addition to the occurrence of hot spots at the interface, various explanations were proposed for the enhanced chemical reactions under MWs. Fidalgo et al. explained the enhanced dry reforming of methane with carbon dioxide by the formation of microplasma in proximity to the interface [5]. Conner et al. insisted on the presence of an *effective temperature* of individual species at interfaces. They mentioned that MWs could change the effective temperature on the basis of Monte Carlo simulation [14]. On the other hand, Stiegman proposed a new aspect that enthalpy change, free energy change, and entropy change in chemical reactions are affected by MWs for enhanced reactions of steam–carbon and water–gas shift reactions [8]. Fukushima and Takizawa explained the enhanced reduction of copper oxide under MW magnetic-field (*H*-field) irradiation by the coupling of *H*-field with the Fermi-level electrons of  $\text{CuO}$ , resulting in the cleavage of the  $\text{Cu}$ – $\text{O}$  bond [11, 12].

Now we have still a lot of hypothetical understandings of enhanced chemical reactions under MWs, and we must emphasize the need to investigate *in situ* the chemical reaction systems under MWs, as Gregory et al. summarized in their review article [15]. We would like to introduce our own approach to this problem and discuss the future objective of clarifying the MW-specific thermal effects and contribute to understanding and expanding this research field. We believe that chemical technology using MWs as an energy source holds promise for future manufacturing technology.

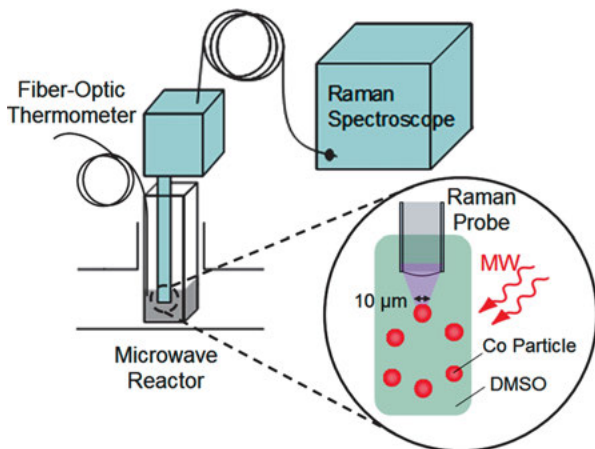
## 7.2 In situ observation of selective heating of inorganic particles dispersed in solution

As described in the previous section, we need to observe, *in situ*, the local temperatures of the heterogeneous systems used for catalyses and solid reactions in order to clearly recognize MW-specific thermal effects. Hot spots generated at interfaces under MW irradiation should be identified as a possible origin of MW-specific thermal effects. First of all, we need to check the requirements for *in situ* temperature measurements carried out for this purpose, that is, the size of the local area and the time resolution of the measurements. Unfortunately, we actually have no idea of how large the hot spot generated on the surface of a solid is or the lifetime of the hot spot, so we need to start figuring out how to measure the temperature and its distribution on a solid surface irradiated by MWs, even though we have no clear strategy.

First of all, let us see a simple experiment in which Co metal particles are selectively heated by MWs in a dispersed state in a solvent with low MW loss. Figure 7.1 shows an experimental setup for measuring the temperature rise of decalin depending on the distance from cobalt particles placed at the bottom of a glass test tube under MW irradiation. The test tube was placed in an MW applicator and irradiated by MWs. A probe of a fiber thermometer was placed above the Co particles at 1.5, 2, and 3.5 cm. The temperature measured at 1.5 cm was raised most rapidly, demonstrating that heat was generated from the Co particles by the loss of MW energy, converting that energy to heat. It was assumed that only Co particles were heated by MWs but the decalin was not. This simple result drove Tsukahara et al. to design a more sophisticated ex-



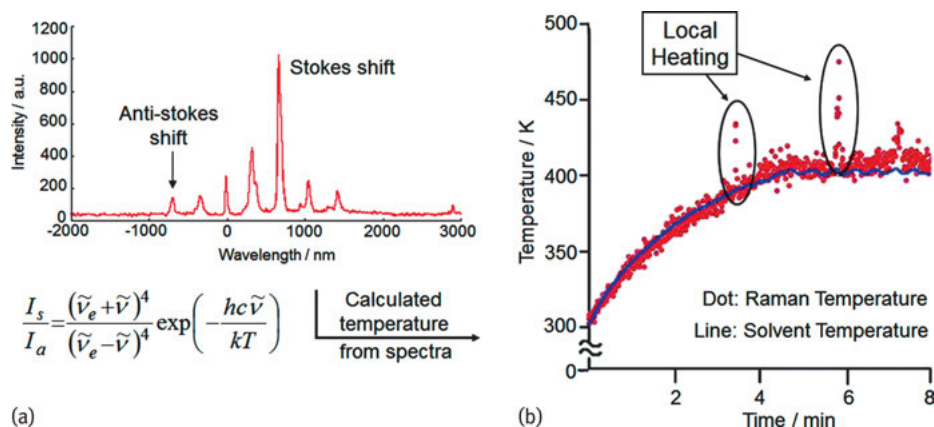
**Fig. 7.1:** (a) A simple experiment to show the heat generation from Co particles dispersed in decalin under microwave irradiation. A probe of the optic-fiber thermometer was placed above the sunk Co particles in decalin with three different distances. (b) Temperature rises observed for the three cases under microwave irradiation.



**Fig. 7.2:** In situ measurement of Raman spectroscopy of a solution containing dispersed Co particles under microwave irradiation.

periment to observe in situ *nonequilibrium local heating* of Co particles dispersed in organic solvent.

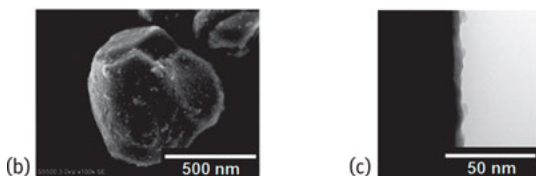
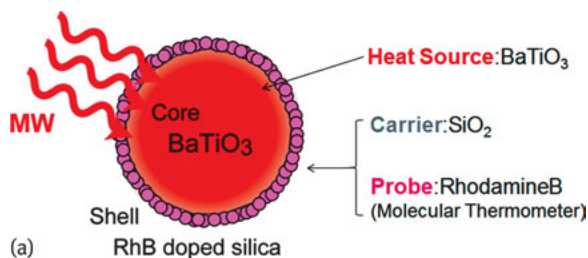
Tsukahara et al. succeeded in detecting *nonequilibrium local heating* on Co particles dispersed in dimethylsulfoxide (DMSO) under MW irradiation [16]. They designed and constructed a measuring system of Raman spectroscopy for a solvent solution containing dispersed inorganic particles (Figure 7.2). A probe was inserted into the solution and irradiated by MWs. Raman spectra were collected *in situ* under MW irradiation of the solution. The size of the area observed by the probe was 10–20 μm and the time resolution was 0.25 s. The measured Raman spectra were used as a molecular-level thermometer by deriving a temperature dependence of the intensity ratio of the Stokes line and anti-Stokes line (see equation in Figure 7.3). Here a DMSO solution containing dispersed Co particles was placed in a vessel and subjected to observation. Figure 7.3a shows a typical Raman spectrum observed for DMSO, giving the temperature of the DMSO molecules. Figure 7.3b exhibits the rise of the temperatures observed under MW irradiation determined by a fiber-optic thermometer (an average temperature of the solvent) and the Raman probe. The red dots correspond to the temperature of the DMSO molecules derived by the Raman spectra at each MW irradiation time. The blue line shows the temperature rise observed by means of the fiber-optic thermometer as the average temperature of the solvent on a scale of several millimeters. The points of the temperatures obtained by the Raman spectra measurements were slightly scattered around the smooth temperature rise obtained by the fiber-optic thermometer, showing good agreement between the temperatures obtained by the two methods. However, several points corresponding to unusually high temperatures were observed only for the temperature measurements made by Raman spectroscopy, demonstrating the occurrence of high temperatures of 30–80 °C. We believe that this is evidence of



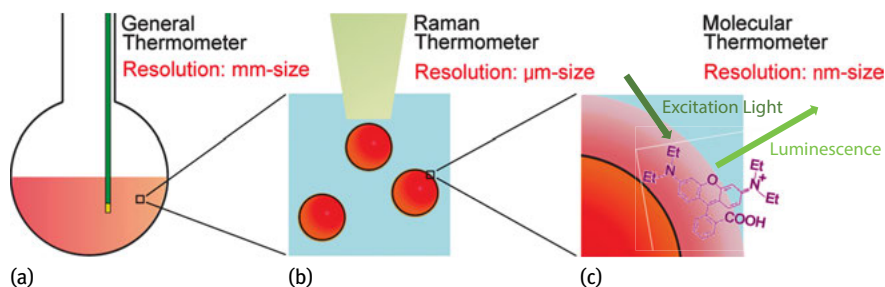
**Fig. 7.3:** Temperature measurements of the solution containing the dispersed Co particles using the Raman spectroscopic system shown in Figure 7.2. (a) A Raman spectrum of DMSO observed under microwave irradiation and an equation used to derive temperatures by the ratios of the Stokes shift and Anti-stokes shift peaks. (b) Dots: Temperatures calculated from the Raman spectra. Line: Temperatures measured by a fiber-optic thermometer.

the nonequilibrium local heating of Co particles dispersed in DMSO. Co particles are moving in the solution under MW irradiation. Only when a heated Co particle comes into the area measured by the Raman probe does the probe detect a high temperature of DMSO molecules placed in proximity with the Co particle experiencing nonequilibrium local heating by interacting with MWs.

Let us introduce another example in which nonequilibrium local heating was confirmed by *in situ* measurement of the temperature of the surface of inorganic particles. Ano et al. synthesized BaTiO<sub>3</sub> nanoparticles covered by a porous silica shell (denoted by BaTiO<sub>3</sub>@SiO<sub>2</sub> as shown in Figure 7.4a) [17]. Rhodamine B was adsorbed into the pores of the silica shell, which was supposed to act as a molecular thermometer, because the lifetime of the photoluminescence (PL) of Rhodamine B is dependent on the temperature. One can see scanning electron microscopy (SEM) and transmission electron microscopy (TEM) images of BaTiO<sub>3</sub>@SiO<sub>2</sub> in Figure 7.4b, c, respectively, showing the particle size of around 500 nm covered by a silica shell around 10 nm thick containing Rhodamine B molecules as a temperature probe (denoted by BaTiO<sub>3</sub>@RhB-SiO<sub>2</sub>). Figure 7.5 illustrates how Ano et al. tried to detect the nonequilibrium local heating of the silica shell covering the BaTiO<sub>3</sub> core acting as a heat generator under MW irradiation. In addition, this figure shows that we can change the size of the temperature measurement area by our choice of temperature measurement method. We can measure temperatures of the area at the millimeter scale using a fiber-optic thermometer under MW irradiation. The Raman method employed by Tsukahara et al. can provide temperatures at a micron-level spatial resolution, but we can obtain temperatures at a molecular size level using the temperature dependence of PL of a proper molecule



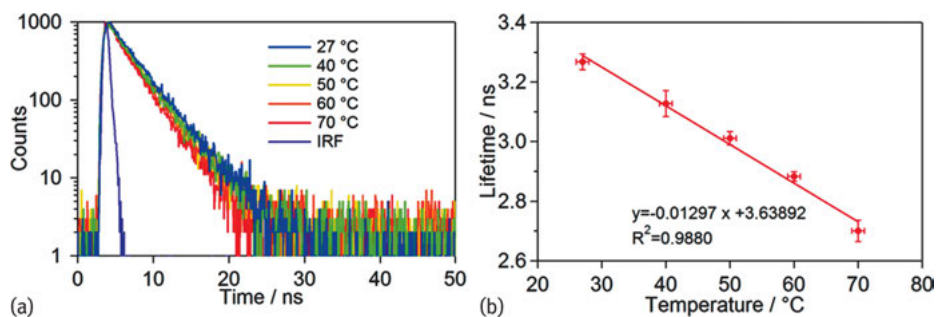
**Fig. 7.4:** Resolution of thermometers, and temperature distribution nearby a solid surface under microwave local heating.



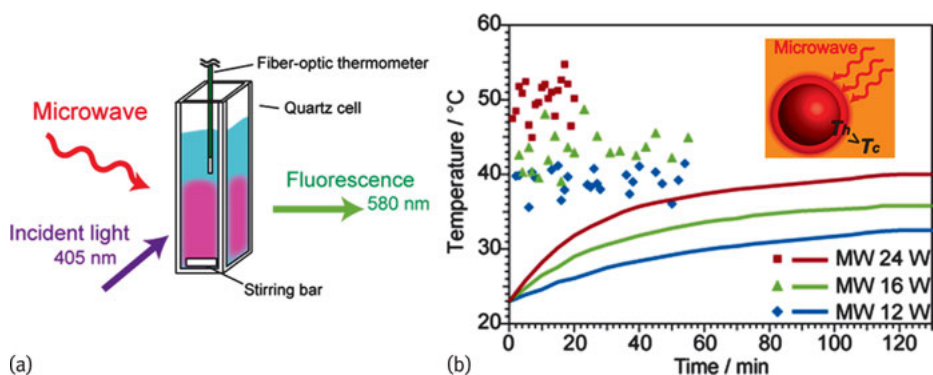
**Fig. 7.5:** BaTiO<sub>3</sub>@RhB-SiO<sub>2</sub> Core-shell particle. (a) A schematic structure, (b) SEM image of BaTiO<sub>3</sub>@RhB-SiO<sub>2</sub>, (c) TEM image of BaTiO<sub>3</sub>@RhB-SiO<sub>2</sub> surface. A gray layer is the silica shell part of BaTiO<sub>3</sub>@RhB-SiO<sub>2</sub>.

located in the measured area. The lifetime of the PL of Rhodamine B adsorbed in the silica shell in BaTiO<sub>3</sub>@SiO<sub>2</sub> changes depending on the temperature, as shown in Figure 7.6a, giving the linear relationship between the lifetimes and the temperatures, as shown in Figure 7.6b.

Figure 7.7a shows a setup for experimental measurements of the lifetime of Rhodamine B in BaTiO<sub>3</sub>@RhB-SiO<sub>2</sub> dispersed in heptane under MW irradiation. The experiments were started from the left side (21–24 °C) to the right side (32 °C) along with the temperature rise of the whole solution under MW irradiation, which was determined by a fiber-optic thermometer, as shown by the colored smooth lines. The colored symbolic dots indicate the temperatures derived from the PL lifetime measurements against the MW irradiation times. The higher the MW power is, the higher the temperature becomes, proving that the local temperature of the silica shell rises up un-



**Fig. 7.6:** (a) PL decays of Rhodamine B in BaTiO<sub>3</sub>@RhB-SiO<sub>2</sub> at 27, 40, 50, 60 and 70 °C under conventional heating, (b) Relationship between the lifetimes and the temperatures.



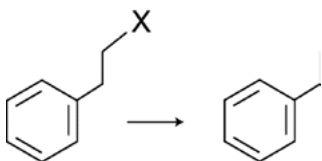
**Fig. 7.7:** (a) In situ PL-measuring system under microwave irradiation, (b) Dots: Temperatures estimated from the PL lifetimes for the nanospace in the silica shell, Lines: Temperatures measured by a fiber-optic thermometer.

der MW irradiation through the heat supply from the selectively heated core of BaTiO<sub>3</sub>. Sasaki et al. arrived at the conclusion that heat generated in the BaTiO<sub>3</sub> core was transported to the silica shell, resulting in a higher temperature of the silica shell than the surrounding heptane solution phase. Under prolonged MW irradiation, the local temperatures of the silica reached steady state, that is, 38.5 °C (20 W), 43.3 °C (40 W), and 50.4 °C (50 W), which were 6 °C, 7.5 °C, and 10.4 °C higher than the whole solution, as shown in Figure 7.7b.

This section describes direct observations of the nonequilibrium local heating of the interface of inorganic particles with solvents under MW irradiation. Nonequilibrium local heating was observed as local heating by Raman spectroscopy and PL lifetime measurements of a dye molecule as molecular thermometer. This nonequilibrium local heating can never be obtained by conventional heating, and therefore it can be the origin of MW-specific thermal effects occurring at the interface of solid in liquid. These effects should be more remarkable when the tangent delta of the solid is larger than that of the liquid.

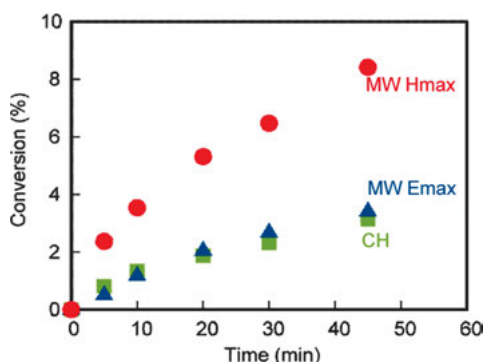
### 7.3 Accelerated chemical reactions by nonequilibrium local heating of solid interfaces

The previous section demonstrates the occurrence of nonequilibrium local heating under MW irradiation. Thus we can expect that chemical reactions proceeding at the interface of solids experiencing nonequilibrium local heating under MW irradiation can be accelerated. This section describes an example of this.

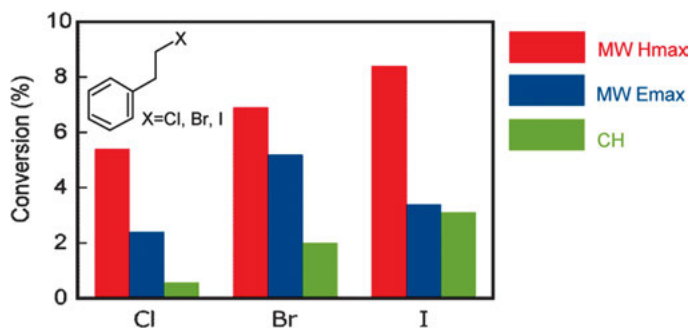


**Scheme 7.1:** Dehalogenation reaction of halogenated ethylbenzene

The dehalogenation reaction of halogenated ethylbenzene (Scheme 7.1) was performed in a decaline solution containing dispersed Fe particles at 190 °C close to the boiling point of decaline [18]. Fe particles acted as a catalyst and electron donor in the reaction. Halogenated ethylbenzene is adsorbed on the surface of Fe particles and reduced through an electron transfer from Fe as the initiation of the reaction. The surface of Fe particles is a reaction field in this reaction. Mochizuki et al. carried out this reaction under MW irradiation and compared it with that under conventional heating (electric heating). Figure 7.8 shows the time profile of conversions of iodide derivative under a maximum of magnetic field ( $H$ -field), a maximum of electric field ( $E$ -field) irradiation, and conventional heating. The reaction proceeded most rapidly under the  $H$ -



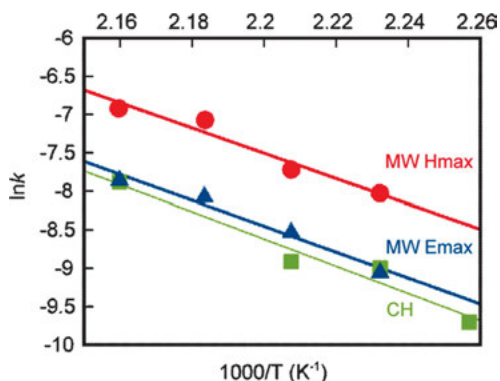
**Fig. 7.8:** Time profile in the conversions of phenethyl iodide under microwave irradiation at the maximum position of magnetic field (MW Hmax, red circles) and electric field (MW Emax, blue triangles) and conventional heating (CH, green squares).



**Fig. 7.9:** Comparison of the conversions of phenethyl iodide, phenethyl bromide and phenethyl chloride obtained under microwave irradiation for 45 min at the maximum position of magnetic field (MW Hmax, red) and electric field (MW Emax, blue) and conventional heating (CH, green).

field irradiation of MWs, while similar conversions were observed for both field irradiation and conventional heating. Figure 7.9 compares the conversions of the three halo-genated ethylbenzenes, that is, chloro-, bromo-, and iodo-derivatives, within 45 min under three heating modes. The iodide derivative was most efficiently dehalogenated under *H*-field, *E*-field, and conventional heating. Bromide and chloride derivatives were also dehalogenated, but their reactivity decreased in this order.

The temperature dependence of the rate constants obtained from the initial rate of dehalogenation of iodide derivatives is shown in Figure 7.10 in the form of an Arrhenius plot for *H*-field MW irradiation, *E*-field MW irradiation, and conventional heating. The activation energies obtained for MW irradiation coincided with each other within the experimental errors, which were  $137 \text{ kJ mol}^{-1}$  for *H*-field,  $140 \text{ kJ mol}^{-1}$  for *E*-field, and  $147 \text{ kJ mol}^{-1}$  for conventional heating. This coincidence in the activation



**Fig. 7.10:** Arrhenius plots for dehalogenation of phenethyl iodide under microwave irradiation at the maximum position of magnetic field (MW Hmax, red circles) and electric field (MW Emax, blue triangles) and conventional heating (CH, green squares).



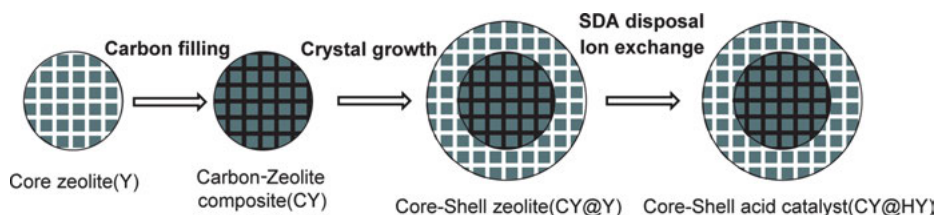
energies strongly suggests that the reaction mechanism is the same for the three systems. It would be reasonable to assume as a reaction mechanism of this reaction that one electron is transferred from the surface of the Fe particles to the substrate, giving its radical anion, and then the halogen anion is eliminated from the resulting radical anion. Using the activation energy obtained for conventional heating, Mochizuki et al. arrived at the conclusion that the temperature of the surface of Fe particles functioning as the reaction field was 15 °C higher than the surrounding solvent owing to nonequilibrium local heating induced by *H*-field MW irradiation. The decaline solvent used in these experiments was not heated by *H*-field MW irradiation owing to a lack of magnetism; however, Fe particles are ferromagnetic and therefore is heated very effectively through the magnetic loss of MW energy. The heat flow from the Fe particles experiencing nonequilibrium local heating to the surrounding solvent induces a temperature gradient corresponding to 15 °C.

#### 7.4 Strategic design of zeolite filled with carbon at its core: application of nonequilibrium local heating under MWs to solid catalysis

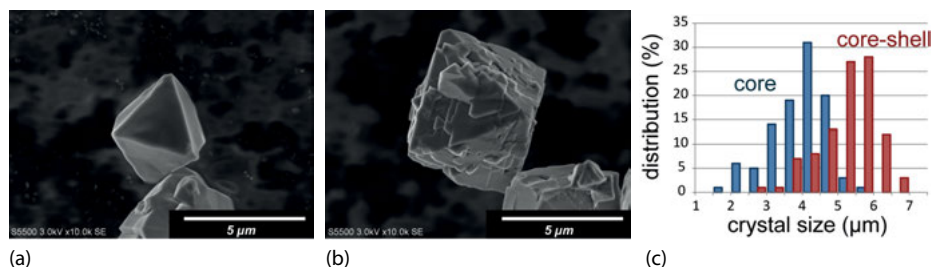
Now we are ready to design and construct a catalytic system utilizing nonequilibrium local heating to enhance catalytic reactions. Mochizuki et al. designed a zeolite filled with carbon at its core based on a strategy of heating it locally at the core filled with carbon under MW irradiation; the porous shell zeolite covering the core provides a catalytic reaction field heated by the heat transport from the heated core [19]. The authors aimed to enhance solid acid catalysis under MW irradiation.

Figure 7.11 shows a procedure to synthesize the structure of the zeolite described earlier.

Furfural alcohol was introduced into the pores of faujasite zeolite synthesized as the core and converted into carbon by calcination under anaerobic conditions. Then it was covered by successively synthesized faujasite. Following removal of the template molecules from the shell faujasite, the shell faujasite was converted into H-type (acid type) by ion exchange with ammonium ions and thermal decomposition. The



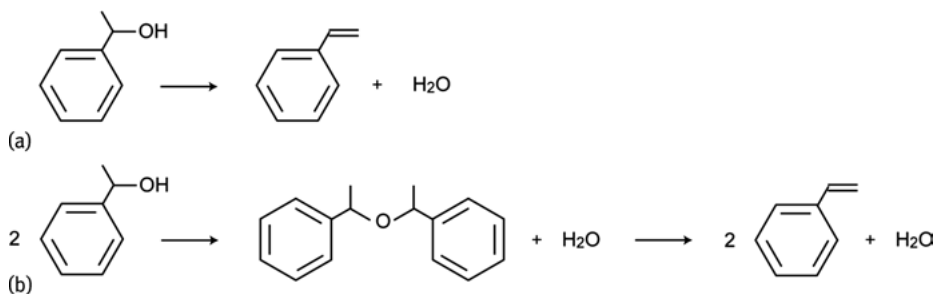
**Fig. 7.11:** Synthetic scheme of carbon-filled core-shell zeolites (CY@HY).



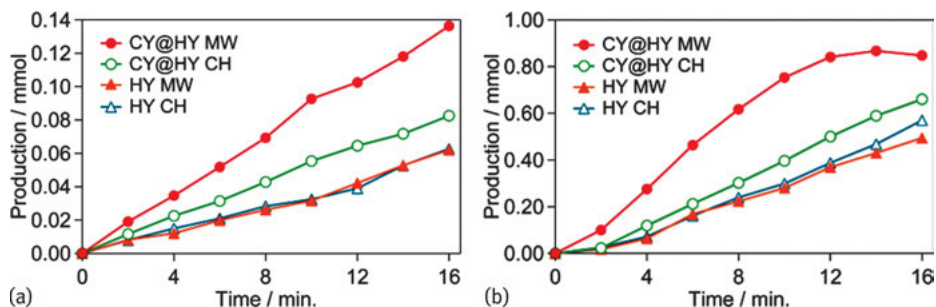
**Fig. 7.12:** FE-SEM images of (a)CY, (b)CY@Y and particle size distributions of CY and CY@Y (c). The particle size distribution was determined by counting 300 particles in SEM images.

SEM images of the core faujasite filled with carbon (denoted by CY) and that covered with faujasite (denoted by CY@HY) are shown in Figure 7.12a, b, respectively. The histograms of the particle diameters of both samples show the growth in the diameter by 2–3 nm by adding the shell, showing the thickness of the shell (2–3 nm).

Dehydration of 1-phenylethanol (Scheme2) was selected as a test reaction for demonstrating the acceleration of the reaction rates in solid acid catalysis on the resulting faujasite zeolite filled with carbon at its core (CY@HY). This reaction gives two products, styrene as an intramolecular dehydration product and *bis-α*-methyl benzyl ether as an intermolecular dehydration product (Scheme 7.2). Figure 7.13a shows the time profile of the formation of the two products using CY@HY and conventional H-faujasite zeolite (HY) under MW irradiation and conventional heating, respectively, at the boiling point of the solvent used in the experiment, namely, heptane (100 °C). The amounts of the products were standardized for a unit amount of H-faujasite zeolite functioning as a reaction field considering that the reaction molecules were not accessible to the core filled with carbon because of physical blocking. The obtained results demonstrated the acceleration of the formation of styrene by 1.5 times and that of *bis-α*-methyl benzyl ether by 2.3 times under MW irradiation for CY@HY compared to HY. Note that the conventional faujasite zeolite, HY, did show the same reaction rates



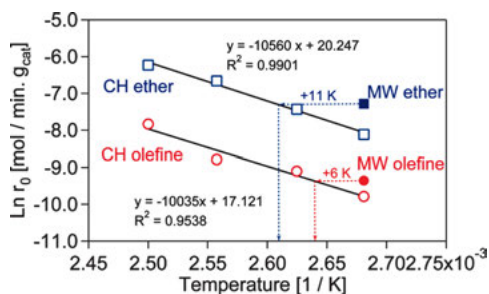
**Scheme 7.2:** Reaction scheme of 1-phenylethanol dehydration over acid catalysts. (a) intramolecular dehydration. (b) intermolecular dehydration.



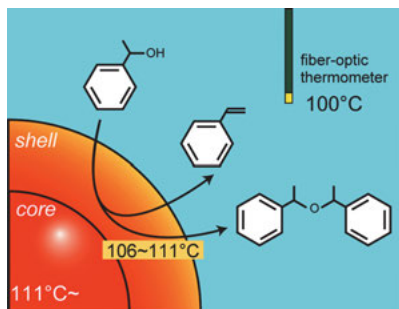
**Fig. 7.13:** Reaction scheme of dehydration of 1-phenylethanol over acid catalysts. (a) time profile of the production of styrene and (b) that of bis(a-methyl-benzyl) ether for (circle) CY@HY (1.0 g) and (triangle) HY (0.58 g) with (close) microwave (MW) and (open) conventional (CH) heating.

under both heating modes, MW irradiation and conventional heating, rationalized by the homogeneous temperature distribution in these reaction systems.

To obtain the activation energies for the two reaction products, it was necessary to obtain the reaction solutions with different boiling points. Then reaction experiments were carried out using heptane, octane, and mixtures of these two solvents, giving 100, 108, 118, and 127 °C as the boiling points under conventional heating. The apparent activation energies were determined to be 83 kJ mol<sup>-1</sup> and 88 kJ mol<sup>-1</sup> for styrene and *bis*- $\alpha$ -methyl benzyl ether, respectively, as shown in the mode of the Arrhenius-type plot in Figure 7.14. Estimating the temperature gradient present between the shell and the surrounding solvents using these activation energies, 1-phenylethanol is supposed to have experienced 6 °C higher temperature for olefin formation and 11 °C higher temperature for ether formation. These temperature gradients should be created by the heat supply from the carbon core selectively heated by MWs to the shell acting as the reaction field.



**Fig. 7.14:** Arrhenius plots for dehydration of 1-phenylethanol over CY@HY under oil bath heating in different solvents (*n*-heptane, *n*-octane, and binary mixtures of *n*-heptane-*n*-octane (1 : 2 and 2 : 1 v/v)) with the different boiling points (373, 400, 381, 391 K, respectively) to estimate the real reaction temperature at the shell of CY@HY under microwave irradiation.



**Fig. 7.15:** Conceptual illustration of non-equilibrium local heating occurring to the core–shell zeolites.

A similar acceleration in the solid acid catalysis was observed also for other substrates, such as the dehydration of 1-(2-methylphenyl) ethanol and 2-octanol. The dehydration of 1-(2-methylphenyl) ethanol yielded two products, olefin and ether. The results showed clear acceleration in both products under MW irradiation, as observed in the experiment involving 1-phenylethanol, by 2.9 times and 2.3 times. The dehydration of 2-octanol yielded only olefin, showing an acceleration by 1.7 times under MW irradiation.

Figure 7.15 exhibits nonequilibrium local heating created artificially using a designed nanostructure of zeolite. Carbon present at the core of zeolite particles transforms the MW energy into heat, which is transported to the shell functioning as a reaction field for solid catalysis. The reaction molecules experience a higher temperature in the shell functioning as a reaction field than the surrounding solvent, resulting in the acceleration of the reaction rate. This is the origin of MW-specific thermal effects, understood as one of the thermal effects of MWs observed in chemical reactions, but it can never be obtained by conventional heating.

## 7.5 Summary

This chapter introduced an aspect in understanding MW-specific thermal effects induced by a special mode of heating achieved by the interaction of MWs with substances. This is characteristic in supplying heat to an interface functioning as a reaction field between solids and solvents.

In addition to nonequilibrium local heating, Maitani et al. discovered a new heating mode that occurs at the interface of different solids [20], which can be called *selective interfacial heating* by MWs, which is observed as the interfacial heating between platinum particles and alumina or titania used as a support, for example. This selective interfacial heating was also observed at the interface between a paste containing titania and organic thickener and a transparent conductive glass. This new phenomenon is under scientific investigation by Wada's group.

Furthermore, Wada's group is revealing that an electric field is concentrated at the contact points between solids in which a large amount of heat is produced. We need to understand the behavior of oscillating electromagnetic fields in interactions with solid substances and will be able to prevent characteristic heating behaviors observed only for MWs.

The authors direct readers' attention to a very useful review article written by Bana and Greiner, "Interpretation of the effects of microwaves." This article summarizes the theme broadly [21].

## Bibliography

- [1] Herrero MA, Kreamsner JM, Oliver C Kappe, *J. Org. Chem.*, 2008, 73, 36–47
- [2] Perry WL, Datye AK, Prinja AK. *AIChE Journal*, 2002, 48, 4, 820–831
- [3] Zhang X, Hayward DO, Michael D, Mingos P. *Catalysis Letters*, 2003, 88, 1–2
- [4] Nigrovski B, Zavyalova U, Scholz P, Pollok K, Muller M, Ondruschka B. *CARBON*, 2008, 46, 1678–1686
- [5] Fidalgo B, Dominguez A, Pis JJ, Menendez JA. *international journal of hydrogen energy* 2008, 33, 4337–4344)
- [6] Fidalgo B, Menendez JA. *Fuel Processing Technology* 2012, 95, 55–61
- [7] Xu W, Zhou J, Su Z, Ou Y and You Z. *Catal. Sci. Technol.*, 2016, 6, 698
- [8] Ferrari A, Hunt J, Lita A, Ashley B, Stiegman AE. *J. Phys. Chem. C* 2014, 118, 9346–9356
- [9] Fukushima J, Kashimura K, Takayama S, Sato M. *Chem. Lett.* 2012, 41, 39–41
- [10] Hayashi M, Takeda K, Kashimura K, Watanabe T, Nagata K. *ISIJ International*, 2013, 53, 7, 1125–1130
- [11] Fukushima J, Kashimura K, Takayama S, Sato M, Sano S, Hayashi Y, Takizawa H. *Materials Letters*, 2013, 91, 252–254
- [12] Fukushima J, Takizawa H. *Materials Chemistry and Physics* 2016, 172, 47–53
- [13] Zhang X, Hayward DO. *Inorganica Chimica Acta*, 2006, 359, 3421–3433
- [14] Conner WC, Tompsett GA. *J. Phys. Chem. B*, 2008, 112, 2110–2118
- [15] Kitchen HJ, Vallance SR, Kennedy JL, Tapia-Ruiz N, Carassiti L, Harrison A, Whittaker AG, Drysdale TD, Kingman SW, Gregory DH. *Chem. Rev.* 2014, 114, 1170–1206)
- [16] Tsukahara Y, Higashi A, Yamauchi T, Nakamura T, Yasuda M, Baba A, Wada Y. *J. Phys. Chem. C*, 2010, 114, 8965–8970
- [17] Ano T, Kishimoto F, Sasaki R, Tsubaki S, Maitani MM, Suzuki E, Wada Y. *Physical Chemistry Chemical Physics*, 2016, 18, 13173–13179
- [18] Mochizuki D, Shitara M, Maitani MM, Wada Y. *Chem. Lett.*, 2012, 41, 1409–1411
- [19] Mochizuki D, Sasaki R, Maitani MM, Okamoto M, Suzuki E, Wada Y. *J. Catal.*, 2015, 323, 1–9
- [20] Maitani MM, Inoue T, Tsukushi Y, Hansen NDJ, Mochizuki D, Suzuki E, Wada Y. *Chem. Commun.*, 2013, 49, 10841–10843
- [21] Bana P and Greiner I. "Milestones in Microwave Chemistry", Springer, 77–110, 2016.

Satoshi Horikoshi and Nick Serpone

## 8 Some aspects of catalysis with microwaves

### 8.1 Historical aspects of catalyzed reactions under microwave radiation

A study carried out in the early days of the calcination and sintering of ceramics by microwaves (MWs) was reported as early as 1972 [1], with fundamental and application studies following thereafter around 1980. The early industrial use of MWs as a heat source was to remove water from inorganic materials. It was soon discovered [2], however, that ceramics could also be heated with MWs (the latter half of the 1970s), which led to the effective sintering of ceramic powders. Conventional heating methods for such tasks are typically heat conduction and radiation heating. With regard to MW irradiation, the sample being irradiated can generate heat and yields a sintered compact product at low temperatures in a short time. A symposium held at a conference on materials science in 1989 by the Materials Research Society (MRS) revealed that materials processing by MWs was a topic that drew a great deal of interest [3]. Indications from the conference revealed that MWs could not only be used to determine the quantity of water in ceramics but could also be used as a technique to detect and analyze the formation of fissures in ceramics and metals [3]. Basic interactions between MWs and materials were also widely discussed. Various kinds of ceramics have been treated by the MW method (e.g., [4]). In recent years, the calcination of special ceramics with a specific MW method has been reported [5].

Several interesting review articles have appeared in the last few years that describe the use of MW radiation in several processes [6–10]. Other relevant studies germane to the present chapter are summarized in Table 8.1 [11–33]. The 2012 review article by Luque and coworkers [6] discussed the synergy that exists between heterogeneous catalysis and MWs and that was exploited in MW-assisted organic syntheses to provide access to valuable chemicals from natural products to biomass-derived compounds; the utilization of MWs in a series of heterogeneous catalyzed processes from acid-catalyzed and base-catalyzed reactions to redox and coupling chemistries was also presented. The intensification of the production of fatty acid methyl esters from waste cooking oil (WCO) using MW reactors was reviewed by Mazubert et al. [7] who addressed the transformation of WCO feedstock by transesterification, esterification, and hydrolysis reactions together with catalyst choice and product separation. Protasova and coworkers [8], on the other hand, reviewed 2011/2012 studies on liquid-phase organic syntheses that take place in microreactors; noncatalytic and homogeneously catalyzed reactions, multistep syntheses, heterogeneously catalyzed reactions, MW-assisted reactions, and photocatalytic reactions were discussed. The

<https://doi.org/10.1515/9783110479935-008>

**Tab. 8.1:** Other articles of interest and germane to the discussion on the use of MW radiation to effect catalyzed organic syntheses and transformation of products.

Title of articles	Year	Ref.
K-10 and KSF clays as green and recyclable heterogeneous catalysts for the Cannizzaro reaction using DABCO under MWI and solvent-free conditions	2016	[11]
Post-polymerization modification of bio-derived unsaturated polyester resins via Michael additions of 1,3-dicarbonyls	2016	[12]
Utility of a heterogeneous palladium catalyst for the synthesis of a molecular semiconductor via Stille, Suzuki, and direct heteroarylation cross-coupling reactions	2015	[13]
Solid-supported rhodium(0) nano-/micro-particles: an efficient ligand-free heterogeneous catalyst for microwave-assisted Suzuki–Miyaura cross-coupling reaction	2012	[14]
Imidazolium chloride immobilized SBA-15 as a heterogenized organocatalyst for solvent free Knoevenagel condensation using microwave	2012	[15]
Heterogeneous versus homogeneous palladium catalysts for ligandless Mizoroki–Heck reactions: a comparison of batch/microwave and continuous-flow processing	2009	[16]
Kinetics of transesterification of palm oil under conventional heating and microwave irradiation using CaO as heterogeneous catalyst	2016	[17]
Lanthanum immobilized on chitosan: a highly efficient heterogeneous catalyst for facile synthesis of novel ( $\alpha,\beta$ -unsaturated) $\beta$ -amino ketones	2016	[18]
Transesterification of used vegetable oil catalyzed by barium oxide under simultaneous microwave and ultrasound irradiations	2014	[19]
Microwave-assisted reactions of natural oils: transesterification and hydroformylation/isomerization as tools for high value compounds	2015	[20]
Microwave assisted esterification of free fatty acid over a heterogeneous catalyst for biodiesel production	2013	[21]
Industrial eggshell wastes as the heterogeneous catalysts for microwave-assisted biodiesel production	2012	[22]
Improved microwave-assisted ligand-free Suzuki–Miyaura cross-coupling of 5-iodo-2'-deoxyuridine in pure water	2013	[23]
Toward the synthesis of 6-hydroxyquinoline starting from glycerol via improved microwave-assisted modified Skraup reaction	2014	[24]
Quinoline and phenanthroline preparation starting from glycerol via improved microwave-assisted modified Skraup reaction	2014	[25]
Original access to 5-arylracils from 5-iodo-2'-deoxyuridine via a microwave assisted Suzuki–Miyaura cross-coupling/ deglycosylation sequence in pure water	2014	[26]
Natural phosphate-supported palladium: a highly efficient and recyclable catalyst for the Suzuki–Miyaura coupling under microwave irradiation	2014	[27]
Microwaves under pressure for the continuous production of quinoline from glycerol	2015	[28]
Microwave-aided dehydration of D-xylose into furfural by diluted inorganic salts solution in a biphasic system	2015	[29]
Conversion of xylose, xylan and rice husk into furfural via betaine and formic acid mixture as novel homogeneous catalyst in biphasic system by microwave-assisted dehydration	2016	[30]
Furfural production from D-xylose and xylan by using stable Nafion NR50 and NaCl in a microwave-assisted biphasic reaction	2016	[31]
A new and original microwave continuous reactor under high pressure for future chemistry	2017	[32]
Copper-containing rod-shaped nanosized silica particles for microwave-assisted synthesis of triazoles in aqueous solution	2015	[33]

MW-assisted polycondensation reactions and curing of polycondensation polymers with a focus on the effect of process conditions have been described by Komorowska-Durka et al. [9]. Specifically, these authors addressed the lack of applicable guidelines necessary to experimentalists on process conditions and experimental design as experiments are often based on empirical trial-and-error approaches. Accordingly, their article examined the role of important process parameters (e.g., the presence and type of solvent, the dielectric properties of mixtures and the individual phases, the use of heterogeneous catalysts, pressure, stirring, reflux conditions, temperature measurement methods, and MW-absorbing fillers), all of which determine the occurrence and magnitude of the benefits enabled by MWs during polycondensation reactions. The use of MW technology (including multifeedstock) in MW-assisted heterogeneously catalyzed processes for the production of biodiesel through the transesterification of plant oils and animal fats was discussed in the 2015 article by Soltani and coworkers [10], who also discussed reaction variables that impact the transesterification process (e.g., heating system, MW power, type and amount of heterogeneous catalyst, oil/methanol molar ratio, reaction time, temperature, and mixing intensity).

This chapter describes some of the advantages of the MW-assisted heterogeneous catalytic method, followed by the MW catalytic systems in heterogeneous gas–solid phases (e.g., degradation of volatile organic compounds (VOCs),  $\text{NO}_x$ , and  $\text{SO}_x$  and hydrogen evolution from organic hydrides), and in heterogeneous liquid–solid phases such as the MW-/photo-driven photocatalytic treatment of wastewater; finally, it discusses some of the problems with the MW catalytic method and provides possible solutions.

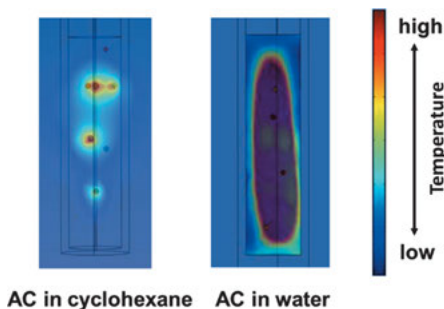
## 8.2 Heterogeneously catalyzed reactions

### 8.2.1 Advantages of MW-assisted heterogeneous catalytic method

A study of ceramic sintering by MW radiation led to the synthesis of MW-assisted solid catalyzed reactions and to syntheses of solid catalysts. Since the 1990s, several reactions have been carried out in the presence of solid catalysts for potential application of MW radiation in chemical syntheses, for example, the synthesis of acetylene by oxidization of methane using particulate metal catalysts [34]. In contrast to MW heating, with which the reaction proceeded to about 90% completion, when conventional heating was used, catalyst activity stopped when the reaction was ca. 25% complete. Research into the dechlorination of chlorinated substrates with heterogeneous metal catalysts was also examined in the initial stages (1990s) of utilization of MW radiation. The influence of both MW frequency and pulsed MW irradiation has been investigated and optimal reaction conditions determined in the presence of a solid catalyst [35].

When MW selective heating is desired, it is possible to carry out organic syntheses using some of the features of MW radiation. For example, when MW nonabsorb-





**Fig. 8.1:** Simulated temperature distribution in water and cyclohexane solvents in the presence of Pt/AC catalyst particles subjected to MW radiation. The simulation was carried out using an RF module and the COMSOL Multiphysics software Version 4.3a. Reproduced with permission from Horikoshi and coworkers [36]. Copyright 2014 by the Royal Society of Chemistry.

ing substrates, such as a nonpolar solvent or nonpolar sample or gas sample, are involved in a catalyzed chemical process, only the solid catalyst may be heated selectively. Figure 8.1 illustrates the results of a simulation experiment of the temperature distributions in water and in cyclohexane (a poor MW absorber) in the presence of an activated carbon (AC) catalyst support (a strong MW absorber) exposed to MW radiation [36]. The AC was selectively heated in cyclohexane by Joule loss heating, while selective heating of AC did not occur in aqueous media as water is a strong MW absorber. Chemical reactions typically occur at the catalyst particle surface so that when only dispersed catalyst particles are selectively heated by MWs, not only does the reaction take place but significant energy conservation can be achieved.

Germane to the present discussion, a study by Mastuzawa and coworkers [37] examined the synthesis of 4-phenyltoluene by a Suzuki–Miyaura coupling reaction using both heterogeneous and homogeneous Pd-based catalysts. The heterogeneously catalyzed process was enhanced by the MWs, while the same reaction in homogeneous media was only slightly enhanced under similar conditions. Moreover, when carried out in a heterogeneous solvent-free system, the reaction was only slightly enhanced by the MWs. Another example is the synthesis of the monoglycerylcetyl-dimethylammonium chloride (MGCA) surfactant from the 3-chloro-1,2-propanediol (CP) and *N,N*-dimethylhexadecylamine (DMHA) precursors in 2-propanol solvent and under solvent-free conditions [38] to reveal the possible existence of specific effects in MW-assisted reactions. Results showed no specific MW effects when the synthesis was carried out in homogeneous 2-propanol media under temperature conditions otherwise identical to those of conventional heating with an oil bath. However, when the reaction was performed under heterogeneous, solvent-free conditions with MW dielectric heating and oil-bath heating at 130 °C for a 30 min heating period, specific MW effects were evidenced by differences in product yields (62% by MW heating versus 47% by conventional heating). Hence, a heterogeneous system provides optimal

conditions to delineate the MW effects in chemical reactions. By contrast, specific MW effects have tended to be very difficult to ascertain in chemical syntheses carried out in homogeneous media.

The foregoing comments notwithstanding, however, though a heterogeneous catalyst system may appear to be ideal in performing a catalyzed reaction by the MW-assisted method, the nature of the solvent medium remains an important factor to contend with. For instance, if a polar solvent were used in carrying out a Suzuki–Miyaura cross-coupling reaction in the presence of palladium/activated carbon (Pd/AC) catalyst in heterogeneous media, the advantages of MWs are diminished as the MWs will heat nonselectively the whole of the bulk solution. Despite this, however, Arvela and Leadbeater [39] have witnessed significant enhancement effects by MWs using a novel methodology of MW heating and simultaneously cooling externally in the synthesis of biphenyl compounds from the Suzuki–Miyaura cross-coupling reaction. This led to significant product yields under such experimental conditions.

## 8.2.2 Microwave heterogeneous gas-phase catalytic systems

### 8.2.2.1 Degradation of VOCs, NO<sub>x</sub>, and SO<sub>x</sub>

MW-assisted catalysis has some benefits in systems designed for environmental detoxification where oxidative and reductive reactions, such as the elimination of VOCs, NO<sub>x</sub>, and SO<sub>x</sub>, occur on the solid surface of metal-oxide catalysts [40]. Using appropriate devices, heating can be concentrated on the catalyst mass, resulting in downsizing of the catalytic reactors and shortening of the heating time with very little energy absorption by the reactants adsorbed on supports [41]. Application of the MW heating method to catalytic processes for environmental purification is a most commendable effort. The MW dielectric heating effect uses the ability of some solid materials of absorbers or catalysts to transform electromagnetic energy into heat *via* dielectric loss and thus able to drive catalytic reactions [42]. Table 8.2 reports typical temperature data measured for a number of pure metal-oxide catalysts subjected to MW heating. Such metal-oxide catalysts as CuO, Co<sub>2</sub>O<sub>3</sub>, NiO, V<sub>2</sub>O<sub>5</sub>, and MnO<sub>2</sub> are susceptible to incident MW radiation and are rapidly heated to about 200 °C (or higher) after eight cycles of 5 s irradiation and 10 s rest periods (i.e., no irradiation). Similar results on NiO, Co<sub>2</sub>O<sub>3</sub>, V<sub>2</sub>O<sub>5</sub>, and CuO have been reported [43]. The reason these oxides are easily heated under MW irradiation has not been elucidated. However, it is speculated that the increase in conduction with temperature of these oxides may be associated with the thermal activation of electrons that migrate from the oxygen 2*p* valence band to the 3*s*3*p* conduction band [44]. In addition, electrical conduction may be enhanced by the presence of defects in oxides. Defects such as oxygen vacancies may form at higher temperatures and lead to the emergence of an *extrinsic* bandgap of the metal oxide (i.e., an effective energy gap between the vacancy levels and the conduction band) in contrast to an *intrinsic* bandgap.

**Tab. 8.2:** Heating profiles of pure oxides (catalysts or catalyst supports) by pulsed MW irradiation at 2.45 GHz; 2 s irradiation and then 10 s rest periods (eight cycles); starting temperature: 25 °C. Data reproduced with permission from Ref. [40]; copyright 2016 by Wiley-VCH Verlag GmbH.

Oxide	Temperature (°C)	Oxide	Temperature (°C)	Oxide	Temperature (°C)
CaO	58	Ta <sub>2</sub> O <sub>5</sub>	55	NiO	260
BaO	57	Cr <sub>2</sub> O <sub>3</sub>	54	CuO	341
CeO <sub>2</sub>	46	MoO <sub>3</sub>	41	ZnO	131
TiO <sub>2</sub>	40	WO <sub>3</sub>	188	γ-Al <sub>2</sub> O <sub>3</sub>	85
ZrO <sub>2</sub>	47	MnO <sub>2</sub>	194	SiO <sub>2</sub>	106
V <sub>2</sub> O <sub>5</sub>	221	Fe <sub>2</sub> O <sub>3</sub>	165	SnO <sub>2</sub>	143
Nb <sub>2</sub> O	51	Co <sub>2</sub> O <sub>3</sub>	272	Bi <sub>2</sub> O <sub>3</sub>	59

Comparing the heating properties determined for several metal oxides reveals that most transition metal oxides can absorb MWs and be heated. By contrast, rare earth metal oxides, alkaline earth group oxides, SiO<sub>2</sub>, and γ-Al<sub>2</sub>O<sub>3</sub> are weak absorbers of MW radiation and thus exhibit little rise in temperature. From a practical viewpoint such as in the oxidation of VOCs or NO<sub>x</sub> reduction catalysts, the most active catalysts have been derived from platinum group metals deposited on suitable supports: γ-Al<sub>2</sub>O<sub>3</sub> is normally used as a catalyst support in automobiles to control emissions. Supported platinum group metals of Pt, Rh, and Pd are the most efficient and active catalysts. However, considering the effectiveness of MW radiation, catalysts composed of transition metal oxides are more suitable for use in reactors irradiated by MWs than are metal catalysts on supports because materials normally used for supports such as γ-Al<sub>2</sub>O<sub>3</sub>, SiO<sub>2</sub>, and CeO<sub>2</sub> do not possess a high susceptibility to incident MWs (Table 8.2).

Several kinds of commercial catalysts that consist of mixed oxides, including transition metal elements, frequently used for improving or protecting the environment as a result of their high oxidation and reduction properties, have been investigated to assess their heating properties under MW irradiation [45]. The catalysts examined were G-3A, consisting of Fe<sub>2</sub>O<sub>3</sub> (90%) and Cr<sub>2</sub>O<sub>3</sub> (10%); G-132, consisting of CuO (40%) and ZnO (60%); G-53D, consisting of NiO (70%) and SiO<sub>2</sub> (30%); N-140, consisting of CuO (40%) and MnO<sub>2</sub> (60%); N-150, consisting of Fe<sub>2</sub>O<sub>3</sub> (40%) and MnO<sub>2</sub> (60%); and NF-9, consisting of pure NiO. Since every catalyst is typically shaped as a tablet, small amounts of graphite are added at concentrations between 0.5% and 1% to stabilize the tablets. The quantities of graphite are too small to influence MW heating. These mixed metal-oxide catalysts used in environmental purification were repeatedly pulse-heated by MWs at 2 s irradiation and 10 s rest periods; resulting temperatures reached after several pulsed cycles are given in Table 8.3 – measured dielectric constants of the catalysts at the MW frequency of 2.45 GHz and at 25 °C are also listed. Among the catalysts tested, NF-9, N-140, and N-150 show a rapid temperature rise, while G-132 and G-53D show a slow temperature rise.

**Tab. 8.3:** Surface area,  $\tan \delta$ , and temperature reached in commercial catalysts subjected to pulsed MW irradiation at 2.45 GHz; 2 s irradiation, 10 s rest; starting temperature: 25 °C. Data reproduced with permission from Ref. [40]; copyright 2016 by Wiley-VCH Verlag GmbH.

Catalyst	Surface area(m <sup>2</sup> g <sup>-1</sup> )	$\tan \delta$	Temperature (°C)
G-3A (Fe <sub>2</sub> O <sub>3</sub> -Cr <sub>2</sub> O <sub>3</sub> )	78	0.13	61
G-132 (CuO-ZnO)	35	0.12	49
G-53D (NiO-SiO <sub>2</sub> )	193	0.15	48
N-140 (CuO-MnO <sub>2</sub> )	133	0.19	96
N-150 (Fe <sub>2</sub> O <sub>3</sub> -MnO <sub>2</sub> )	175	0.13	79
NF-9 (NiO)	152	0.18	101

A comparison of the rates of temperature rise for the mixed oxides with those of pure oxides revealed little correlation; that is, the commercial catalysts N-140 and NF-9 containing CuO and NiO, respectively, showed relatively higher temperature rise, whereas, even though G-132 and G-53D contained CuO and NiO, the temperature rises are smaller under MW irradiation. The N-150 system that contained both Fe<sub>2</sub>O<sub>3</sub> and MnO<sub>2</sub> displayed a relatively higher temperature rise, while the two separate metal oxides showed smaller rises. These results indicate that the coexistence of different metal oxides in a catalyst system changes the MW susceptibility from those of separate catalyst oxides, meaning the dielectric loss of mixed oxides is significantly altered. The existence of two types of sites in perovskite-type oxides leads to different dipole strengths and results in the formation of hot spots during MW dielectric heating [46].

VOCs that also include odorants are major contributors to atmospheric pollution; their removal is best achieved at the source of contamination. Catalytically aided oxidation of such pollutants is a preferred method over thermal combustion because of lower processing temperatures and higher selectivity toward CO<sub>2</sub> evolution [47]. Lowering the temperature at which these processes occur with great efficiency can consequently reduce energy costs. From this point of view, it is important to utilize a catalyst for these MW-assisted processes because of such advantages as volumetric and high heating rates, indirect contact, and facile control of heating and minimization of equipment size.

For purposes of oxidative removal of environmental pollutants, MW-heated catalytic processes have been investigated extensively. For instance, aliphatic hydrocarbons with propane as a model substrate are more difficult to oxidize than aromatic hydrocarbons (e.g., benzene, toluene, and xylene) and CO over such doped perovskite catalysts as La<sub>0.5</sub>Co<sub>0.2</sub>MnO<sub>3</sub> [48]. There is no indication that MW heating and conventional heating lead to different reaction pathways because only small differences in selectivity were observed. However, the mechanism of propane oxidation and of CO oxidation is different; that is, CO is oxidized by reaction with adsorbed oxygen at low temperatures, while propane is oxidized by reaction with lattice oxygen at high temperatures according to a Mars/van Krevelen mechanism. MW energy enables fast and

efficient heating of the perovskite-type catalysts of complex oxides, where only the catalyst is selectively heated. Direct heating with MW irradiation is rapid, effective, and much more suitable for periodic operation than conventional heating.

$\text{NO}_x$  and  $\text{SO}_x$  are major air pollutants emitted from fossil fuel combustion in mobile and stationary sources.  $\text{NO}_x$  contributes significantly to photochemical smog, acid rain, ozone depletion, and greenhouse effects;  $\text{SO}_x$  is also an important precursor to acid rain [35]. MW-assisted catalysis has been applied to topics of environmental concern including the degradation of  $\text{NO}_x$  and  $\text{SO}_x$  [49]. Among many technologies to reduce the emission of  $\text{NO}_x$  and  $\text{SO}_x$ , the catalytic technology of direct and reductive decomposition of these oxides is more attractive because of the compact apparatus used and for its high efficiency and because there is no need for a reducing agent. Reduction of  $\text{NO}_x$  can reach as much as 98% conversion when MW energy is applied continuously [50]. On the other hand, where a reducing agent is used, the use of both catalyst and ammonium bicarbonate combined with MW energy can significantly increase the catalytic reductions of both  $\text{NO}_x$  and  $\text{SO}_x$ .

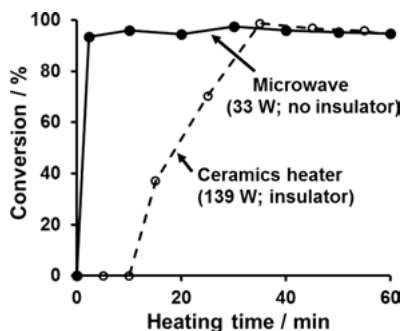
### 8.2.2.2 Hydrogen evolution from organic hydrides

As a clean energy carrier, hydrogen is expected to make a significant contribution toward a sustainable society [51]. Hydrogen is a regenerative and an environmentally friendly energy vector that reacts cleanly with oxygen in a highly exothermic reaction yielding pure water as the unique exhaust product, as occurs in a hydrogen fuel cell. However, this is not without its problems. The drawbacks of hydrogen as an energy vector are its storage, transport, and energy costs because the energy density of hydrogen on a per-volume basis is relatively low compared to other commonly used fuels. Organic hydrides are efficient and high-density materials for use as hydrogen storage, transportation, and supply to fuel cell systems in a hydrogen society. The organic hydride storage method (no need for low temperatures and high pressures) can make use of the infrastructure currently used for transport (Lorries and ships) and to store (reservoir tanks) gasoline. After storing the hydrogen gas, the aromatic hydrocarbon is collected by known infrastructure equipment, or else the infrastructure equipment to store the hydrogen energy can share the equipment used to store gasoline. Aromatic hydrocarbons can also be used as fuels in times of natural disasters. The cyclohexane  $\leftrightarrow$  benzene cycle is a system capable of storing and releasing hydrogen. However, benzene is strongly carcinogenic, and as such the benzene present in gasoline is regulated to less than 1 volume%. Consequently, the use of the cyclohexane  $\leftrightarrow$  benzene cycle is not desirable as an organic hydride carrier. The decalin  $\leftrightarrow$  naphthalene cycle is highly efficient for hydrogen evolution, so that it is possible to extract most of the hydrogen from the decalin molecule. Unfortunately, the melting point of naphthalene is 80 °C, so that when it is cooled in the reactor or in the flow pipe after the reaction, the naphthalene tends to solidify, which can clog the reactor or the pipes. On the other hand, the presence of a methyl group in naphthalene lowers the melting

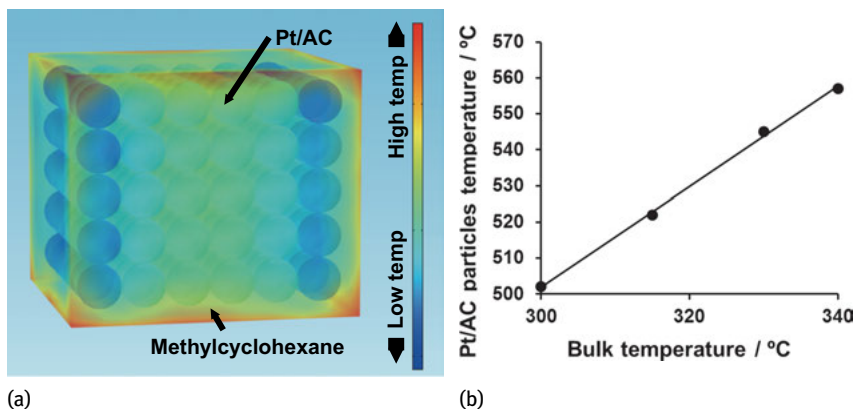
point compared with naphthalene. Unfortunately, these materials are not available in large, industrial-scale quantities. Moreover, a higher temperature reaction field is needed because the boiling point of ring compounds tends to be rather high. Accordingly, the methylcyclohexane (MCH)  $\leftrightarrow$  toluene cycle is the most suitable carrier of hydrogen for the organic hydride method in industry.

Hydrogen production from MCH as the source of hydrogen has been investigated by subjecting MCH to MW heating [52]. The most commonly used catalyst in dehydrogenation reactions is Pt supported on activated carbon particulates (Pt/AC). Current research focuses on enhancing the efficiency of hydrogen evolution using conditions that require low applied energy for the thermal activation of the catalysts. Energy conservation for hydrogen evolution can be achieved by MW selective heating of the solid catalysts (e.g., Pt/AC). Features pertaining to hydrogen evolution from MCH with the MW method are described next.

The reaction temperature for the dehydrogenation of MCH begins at ca. 200 °C [53], following which the yield of hydrogen is saturated at ca. 330 °C. Platinum (5 wt.%) deposited as particulates onto activated carbon as the support (Pt/AC) has been used as the catalyst in the dehydrogenation reactions of MCH carried out under atmospheric pressure in a quartz fixed-bed tubular reactor loaded with 2.5 g Pt/AC catalyst. Results from the dehydrogenation of MCH under MW heating and conventional heating with a ceramic heater and insulator are displayed in Figure 8.2 [54]. The packed Pt/AC catalyst particulates were heated to 330 °C within 1 min by MW heating, which resulted in ca. 94% dehydrogenation of MCH occurring in less than 90 s. On the other hand, when using a ceramics heater, dehydrogenation needed more than 30 min to reach 330 °C, even though an insulator was used. MW heating led to hydrogen evolution in much shorter time. On interruption of MW irradiation, the catalyst particulates promptly cooled and hydrogen evolution stopped, whereas interruption of conventional heating led to continuous hydrogen gas evolution for more than 30 min. Total power consumption of the MW system was 36 W (MW applied power, 17 W), while the ceramic heater consumed 115 W. Hence, MW heating is to be favored in terms of power consumption and is thus an attractive profitable energy-saving system, in addition



**Fig. 8.2:** Dependence of conversion of MCH to hydrogen gas and toluene over Pt/AC catalyst under MW heating and conventional heating with ceramic heater (temperature: 330 °C). Reproduced with permission from Ref. [54]. Copyright 2016 by Elsevier B.V.



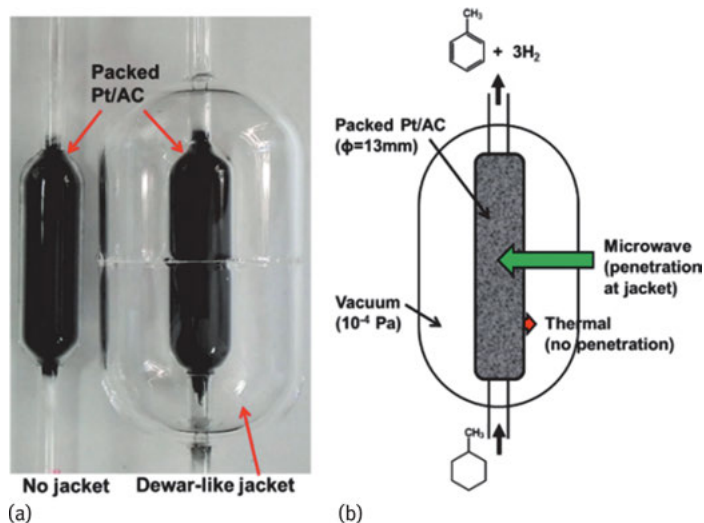
**Fig. 8.3:** Relation between Pt/AC particle temperatures and bulk temperatures. (a) Simulation image and (b) relationship between Pt/AC particle temperatures and bulk temperatures. Reproduced with permission from Ref. [54]. Copyright 2016 by Elsevier B.V.

to having shorter times for hydrogen evolution. Recall that electrical energy is being used to produce hydrogen energy.

Heat convection from Pt/AC in MCH solution was investigated by simulation using the COMSOL Multiphysics software package (version 4.3a). For the simulation, selective heating of 180 particles of Pt/AC dispersed in MCH was considered; the model geometry is displayed in Figure 8.3a [54]. The correlation between bulk temperature and the temperature of the Pt/AC particles is illustrated in Figure 8.3b. Results of the simulation demonstrated that to bring MCH from room temperature (25 °C) to 330 °C necessitated the temperature of the Pt/AC particles to be at 547 °C. Under MW irradiation, the Pt/AC particles were continuously heated by the MW radiation field, with much of the resulting thermal energy spent to heat MCH.

Studies reported so far have demonstrated that selective heating of a solid catalyst in a heterogeneous reaction is an ideal occurrence when using MWs. The combination of catalyst or catalyst support with high absorption of MWs and a nonpolar solvent satisfy this condition. A fixed-bed reactor is also an effective component of a reaction system. The temperature distribution peculiar to MW irradiation can enhance adsorption and desorption (contact efficiency) of the substrate on the catalyst surface and also lead to energy savings during heating stages. However, the heat developed on the catalyst can escape to the atmosphere through the reactor walls. Therefore, to avoid such heat losses, insulation of the reactor is most desirable.

Normally, one makes use of heat insulating materials (e.g., fiberglass) wrapped around the external walls of the reactor to prevent escape of heat to the surroundings. Unfortunately, such materials can also attenuate the MW radiation reaching the reacting substrates in the reaction vessel. Accordingly, a novel reactor design was conceived to avoid heat losses and attenuation of the MWs (Figure 8.4) [55]. The proposed



**Fig. 8.4:** (a) Photograph and (b) sketch of conventional MW reactor and MW Dewar-like vacuum reactor. Reproduced with permission from Ref. [55]. Copyright 2016 by Wiley-VCH Verlag GmbH.

reactor system consists of a double-walled glass vessel in which the double wall is vacuum-filled and typifies the Dewar-like structure used to preserve cold fluids. In this case, MW irradiation of the sample is not obstructed by the vacuum-filled double walls, while any heat emanating from the heated sample is intercepted by the reactor's double walls.

### 8.2.3 Microwave heterogeneous liquid-phase catalytic systems

#### 8.2.3.1 Microwave-/photo-driven photocatalytic treatment of wastewater

Some 15 years have passed since the discovery that led to the improvement in photocatalyst activity on exposure to MW radiation. The photocatalyst is a material that absorbs the energy of electromagnetic waves (UV light) and changes it into chemical energy. In this regard, MW radiation also consists of electromagnetic waves. The notion of irradiating  $\text{TiO}_2$  with MWs may appear strange at first because the photon energy ( $1 \times 10^{-5}$  eV) of the MWs of frequency 2.45 GHz is several orders of magnitude lower than the bandgap energy required (3.0–3.2 eV) to activate the  $\text{TiO}_2$  semiconductor. Moreover, MW radiation brings other effects to bear to a photocatalyst other than heat. MW nonthermal effects have been deduced to contribute significantly to the enhancement of  $\text{TiO}_2$ -photoassisted reactions, as it may affect both the surface and the crystalline structure of the metal oxide toward reactions taking place at the surface. The mechanism of the effect of MW radiation on photocatalyzed reactions has evolved gradually. The enhanced treatment of wastewater through improvements in photocat-

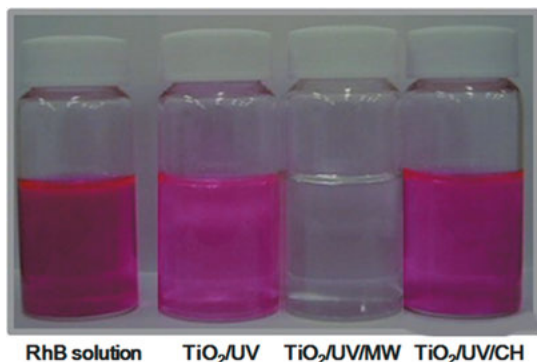


alyst activity when exposed to MW radiation is now a clear possibility. In fact, coupling MW radiation with UV light in TiO<sub>2</sub>-photoassisted processes can contribute significantly to the treatment of wastewater as a novel advanced oxidation technology (AOT).

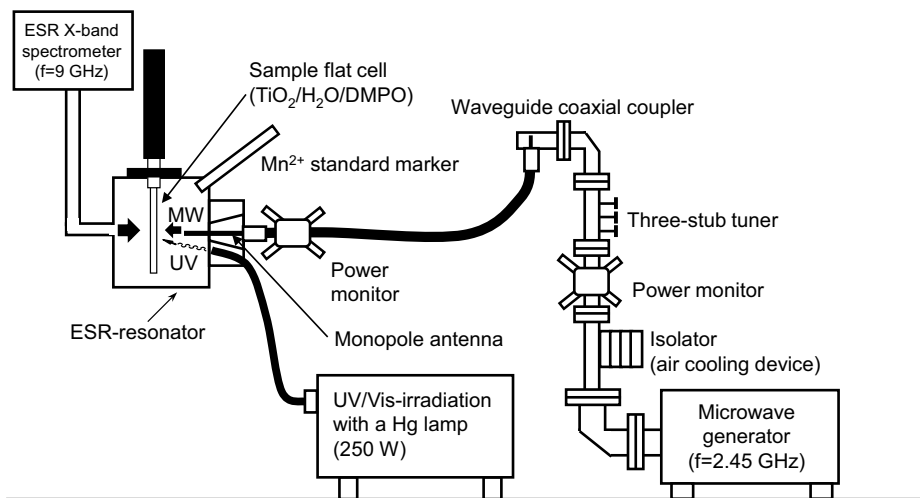
The photoassisted oxidative (and reductive) decomposition of pollutants by means of TiO<sub>2</sub> photocatalyst nanoparticulates is an effective and attractive oxidation (reduction) method in the general area of advanced oxidation technologies. Applications of photoassisted treatments to air pollution have been developed by TiO<sub>2</sub> fixation on several suitable substrate supports such as, for example, in filters found in air conditioners [56]. However, this photoassisted degradation methodology is not suitable for large-scale wastewater treatment because the rates of degradation of organic compounds dissolved in wastewaters tend to be rather slow. In this regard, relatively little has been done in this area in the last decade as large-scale treatments of organic pollutants in aquatic environments have not been without some problems, not least of which is the low photodegradation efficiency, a result of several factors. To remedy such a situation, Horikoshi and coworkers proposed some time ago [57] to couple MW radiation with UV radiation to enhance the activity of photocatalysts.

Some dyes are poorly photodecomposed and so are not useful in assessing the photoactivity of a metal-oxide photocatalyst. For example, the rate of photodegradation of the cationic Rhodamine-B (RhB) dye is slow in acidic aqueous media because the surface of the TiO<sub>2</sub> particles is positively charged ( $\text{Ti} - \text{OH}_2^+$ ;  $pI = 6.3$ ). However, RhB has proven an interesting model compound for examining the MW effect. In earlier studies, the major focus was on the degradation of organic pollutants, as exemplified by the degradation of the RhB dye catalyzed by TiO<sub>2</sub> semiconductor particles under both UV and MW irradiation [57]. Changes in color intensity of the RhB dye solutions occurring under various conditions are illustrated in Figure 8.5 [58]. The photodegradation of RhB is clearly evident on using the TiO<sub>2</sub>-assisted UV/MW method. These observations demonstrated that a method that can treat large quantities of pollutants in wastewater by a hybrid combination of MWs and TiO<sub>2</sub> photoassisted technologies is conceivable. The photodegradation of RhB by this metal oxide is unaffected by conventional heating – compare, for example, the results from the UV and the UV/CH methods in the presence of TiO<sub>2</sub> (Figure 8.5).

The possible enhancement of the photoactivity of TiO<sub>2</sub> photocatalysts subsequent to being exposed to MW radiation from the viewpoint of the amount of  $\cdot\text{OH}$  radicals generated has also been investigated [59]. The formation of  $\cdot\text{OH}$  radicals during TiO<sub>2</sub>-assisted photooxidations that were driven simultaneously by UV light and MW radiation was probed by electron spin resonance (ESR) spectroscopy employing a novel setup in which the ESR sample (containing the DMPO spin-trap agent and various TiO<sub>2</sub> particles in aqueous media) was irradiated by both UV light and MW radiation [59]. In this case, MW radiation was produced using a magnetron MW generator (frequency: 2.45 GHz), a three-stub tuner, a power monitor, and an isolator (Figure 8.6). The UV irradiation source was an Ushio 250 W mercury lamp; the emitted UV light irradiated the sample at an angle to the horizontal plane using a fiber-optic light guide.



**Fig. 8.5:** Visual comparison of color fading in degradation of RhB solutions (0.05 mM) subsequent to being subjected to various degradation methods for 150 min. Left to right: initial RhB solution; RhB subjected to photoassisted degradation (UV); RhB subjected to integrated MW-/photoassisted degradation (UV/MW); RhB subjected to thermal- and photoassisted degradation (UV/CH). Reproduced with permission from Ref. [58]. Copyright 2009 by Elsevier B.V.



**Fig. 8.6:** Setup used to generate  $\cdot\text{OH}$  radicals in water alone under MW irradiation, in an aqueous  $\text{TiO}_2$  dispersion by MW irradiation alone, and by the UV and UV/MW methods, together with assessing the quantity of radicals formed. Reproduced with permission from Ref. [59]. Copyright 2003 by Elsevier B.V.

The number of  $\cdot\text{OH}$  radicals generated under various experimental conditions is given in Table 8.4. For P25 titania, the number of  $\cdot\text{OH}$  radicals produced by the UV/MW method was nearly 30% greater than the quantity generated by the UV method alone [59]. A fivefold increase in incident MW power from 3 to 16 W led to a significant increase (*ca.* 40%) in the number of  $\cdot\text{OH}$  radicals. Such an increase was sufficient to increase the efficiency of the photooxidation of organic pollutants in water.

**Tab. 8.4:** Number of DMPO- $\cdot$ OH spin adducts produced in the various heterogeneous systems under MW irradiation, UV irradiation, and MW/UV irradiation relative to those formed in the rutile  $\text{TiO}_2$  specimen for the  $\text{TiO}_2/\text{H}_2\text{O}/\text{MW}$  heterogeneous system; data reproduced with permission from Ref. [59]. Copyright 2003 by Elsevier B.V.

Methodology	P25 $\text{TiO}_2$	UV100 $\text{TiO}_2$	Anatase	Rutile
UV	182	45	110	110
UV/MW (3 W)	259	51	92	76
UV/MW (16 W)	369	–	–	–

For the UV100 sample, the increase in the number of  $\cdot$ OH radicals produced was only 10% greater on increasing the MW power five times. On the other hand, the number of  $\cdot$ OH radicals generated for the pristine anatase and rutile  $\text{TiO}_2$  samples decreased under MW irradiation. The P25 specimen was clearly influenced by the MWs, generating a significant number of  $\cdot$ OH radicals. Therefore, under such conditions, the rate of decomposition of pollutants can be enhanced when P25 is used to detoxify wastewaters by the combined UV/MW method. On the other hand, to the extent that the quantity of  $\cdot$ OH radicals produced by the other three  $\text{TiO}_2$  systems does not increase even when irradiated by MWs, the rate of decomposition is not expected to be greatly affected by the MWs.

### 8.3 Problems with the MW catalytic method and possible solutions

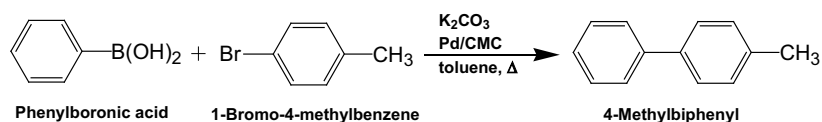
The term *hot spot* in MW chemistry and materials processing refers to an inhomogeneous dissipation of MW energy through selective heating of different parts of a material that causes the generation of temperature gradients within various domains of the material or the sample. Whenever high-temperature microdomains (so-called hot spots) are formed when the material is MW-irradiated, they must undergo fast heat transfer processes for the material to come into thermal equilibrium. However, where conditions are such that the rate of heat transfer is slow, the formation of steady-state hot spots occurs, which in principle can enhance the rate of a chemical process occurring within or near those hot spots. However, the formation of hot spots can also prove deleterious to a chemical process.

Several studies have been conducted to elucidate the existence of hot spots in chemicals subjected to MW irradiation. Indeed, heating a solid catalyst by MW radiation frequently generates hot spots as a result of differential heating. For example, an initial report by Mingos and coworkers [60] showed significant apparent shifts in the equilibrium constant in the MW-assisted decomposition of  $\text{H}_2\text{S}$  in the gas phase catalyzed by metal sulfides on a  $\gamma\text{-Al}_2\text{O}_3$  support (solid/gas system). The authors at

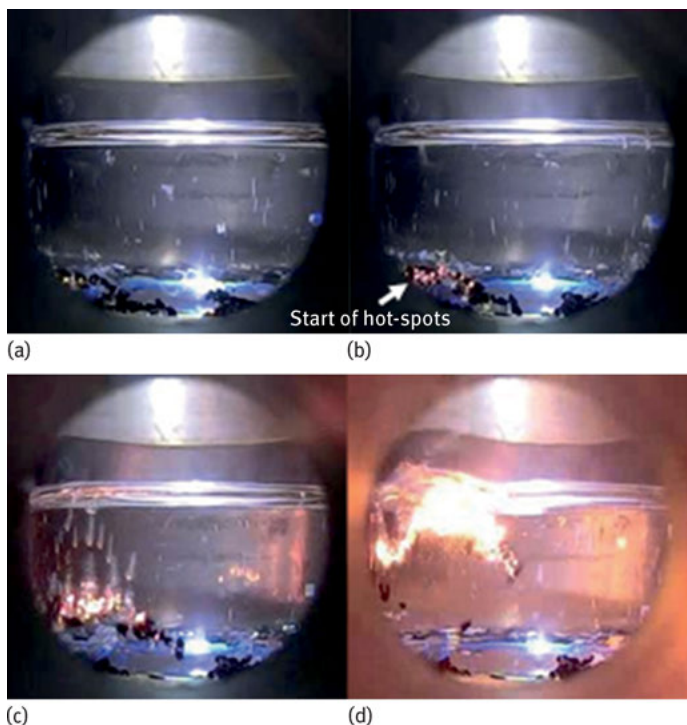
tributed the shifts to the development of hot spots with dimensions of 90 to 1000  $\mu\text{m}$  in the catalytic beds. In solid/liquid systems, hot spots can reach temperatures from 100 to 200 K above the temperature of the remaining bulk and cause a possible reorganization of the catalyst under MW irradiation conditions. In this regard, Tsukahara and coworkers [61] observed the occurrence of nonequilibrium local heating of DMSO molecules in the proximity of Co and Fe particles as a result of a faster input of MW power than heat loss induced by temperature gradients established between the high-temperature microdomains and the surrounding low-temperature domains. Such nonequilibrium local heating led to enhanced dechlorination of 2-chloroethylbenzene and 4-phenyl-butylchloride. In that instance, the reaction temperature of the MW system was ca. 55 K greater than the bulk solution temperature (473 K) under MW irradiation.

The occurrence and the existence of hot spots induced by MW radiation on materials have often been described by indirect suppositions but have seldom been observed visually. For instance, Gutmann and coworkers [62] showed that the formation of an organomagnesium Grignard reagent could be both activated and deactivated by the MWs' electric field (*E*-field) and attributed the activation event as originating either from a so-called cleansing effect of the Mg surface or from the formation of more reactive spherical Mg particles owing to mild electrostatic discharges (arcing, hot spots) between individual Mg turnings. However, neither the cause of the generation of hot spots nor their features were examined [62].

Accordingly, it was pertinent to examine and explain the mechanism of generation as well as the minimization or suppression of hot spots. Events occurring during the synthesis of 4-methylbiphenyl with the Suzuki–Miyaura coupling reaction (Scheme 8.1) under MW irradiation were investigated by Horikoshi and coworkers [63] using a high-speed camera. Results provided the basis to explain the occurrence of hot spots. Figure 8.7 displays photographs recorded in real time, which show that the Pd/AC catalyst particulates immersed in toluene solvent were selectively heated by the MWs' *E*-field radiation. In the case considered, as soon as MW irradiation was initiated, bubbles immediately formed on the activated carbon surface after only 3 s (Figure 8.7a) owing to differential heating of the AC particles. Also observed was the aggregation of the AC particulates as though they had been magnetized by the MW radiation. An orange light was observed from the aggregated activated carbon particles after 16 s (see lower left side in Figure 8.7b). Subsequently, the light emanating



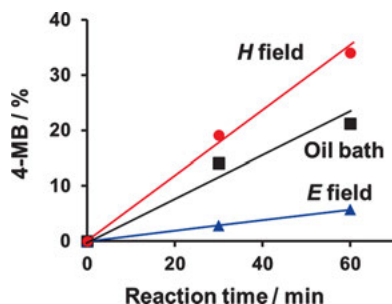
**Scheme 8.1:** Synthesis of 4-methylbiphenyl by Suzuki–Miyaura coupling reaction under MW irradiation [63].



**Fig. 8.7:** High-speed camera photograph of electrical arc discharge occurring on AC in toluene solvent under MW *E*-field irradiation: (a) after 3 s of MW irradiation, (b) after 16 s of irradiation, (c) under continuous irradiation, and (d) emitted light reaching maximal intensity. Reproduced with permission from Ref. [63]. Copyright 2013 by Elsevier B.V.

from the AC surface increased, as did its intensity, together with a greater number of bubbles formed around the emitted light (Figure 8.7c). The emitted light became even more intense on the AC surface under exposure to continued MW radiation. Figure 8.7d shows the light from the hot spots reaching maximum intensity, after which the luminescence from the AC surface disappeared, and the aggregated AC particles were redispersed.

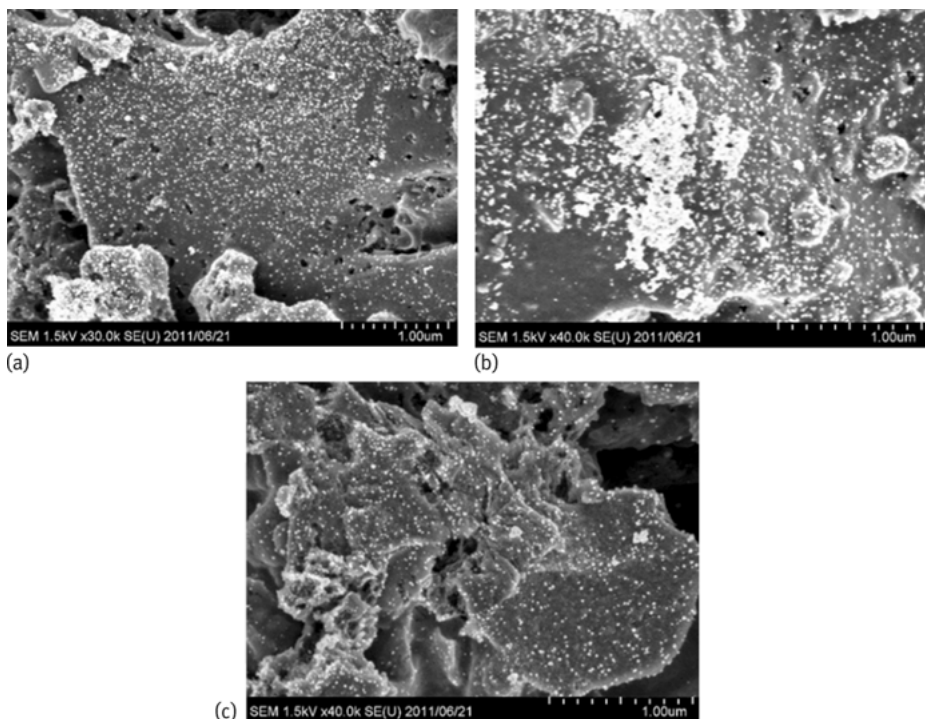
Chemical yields of 4-methylbiphenyl produced in toluene solvent from the Suzuki–Miyaura coupling reaction (Scheme 8.1) subjected to MW *E*-field and *H*-field irradiation, together with those from the more conventional oil-bath heating method, are displayed in Figure 8.8. Under *E*-field conditions, the yield was about 6% after a 60 min irradiation period at an input MW power of 70 W, whereas the corresponding yields under *H*-field irradiation conditions was 34% (also after 60 min). For comparison, with the oil-bath heating method, the chemical yield of 4-methylbiphenyl was 21% for a heating time of 60 min. When hot spots did form, the efficiency of the synthesis of 4-methylbiphenyl tended to decrease [63]. On the other hand, when



**Fig. 8.8:** Product yields of 4-methylbiphenyl in toluene solvent under irradiation with MW *H*-field and *E*-field components, and oil-bath heating. Reproduced with permission from Ref. [63]. Copyright 2013 by Elsevier B.V.

no hot spots formed, as occurred under *H*-field irradiation, the synthesis efficiency of 4-methylbiphenyl was nearly sixfold greater (Figure 8.8). Accordingly, the authors [63] also investigated the influence that hot spots may have on possible occurrence of side reactions other than the principal Suzuki–Miyaura cross-coupling reaction. With an electrical power input of MWs fixed at 70 W, hot spots were generated under *E*-field irradiation, but none under *H*-field irradiation.

When hot spots do occur, the decrease in the yields in a chemical synthesis is likely due to a decline in catalyst activity. The formation of hot spots on the catalyst surface did decrease the yield of 4-methylbiphenyl, while the amount of byproduct(s) generated increased. To elucidate this assertion, Figure 8.9 illustrates scanning electron microscopy (SEM) images of the Pd/AC surface before and after the formation of hot spots [63]. The Pd catalyst particles are dispersed rather uniformly on the AC surface prior to MW irradiation (Figure 8.9a). However, large Pd aggregates formed after 30 min of MW irradiation of the Pd/AC catalyst under *E*-field heating conditions (Figure 8.9b). By contrast, no aggregation of Pd particles occurred and no hot spots formed under conditions when heating was carried out by the MW magnetic field (Figure 8.9c). Evidently, the aggregation of Pd particles and the generation of hot spots (electric discharge) on the catalyst surface are events that occurred concurrently under *E*-field heating conditions. Accordingly, the lower chemical yields of 4-methylbiphenyl (12% vs. 22% after 2 h of MW irradiation) are due, in part, to the formation of less reactive larger Pd aggregates as one of several related factors that affect yields, for example, such factors as (i) a lower number of reactive sites on Pd particles through annihilation by the Joule heating effect, (ii) possible obstruction of reactive sites on Pd particles by a small layer of carbonaceous residue that might have formed by dielectric heating of the AC support under the MWs' *E*-field, and lastly (iii) an excessive number of hot spots formed on the Pd/AC catalyst surface. The decrease in efficiency was due to aggregation of the Pd catalyst because of the hot spots on the AC surface [63].



**Fig. 8.9:** SEM images of Pd/AC catalyst surface: (a) 0 min irradiation, (b) after 30 min of MW irradiation and the formation of hot spots, and (c) under conditions of no formation of hot spots. Reproduced with permission from Horikoshi et al. [63]. Copyright 2011 by American Chemical Society.

What the preceding discussion tells us is that the formation of hot spots needs to be controlled whenever they form. To achieve this, Horikoshi and coworkers [64] examined some possible methods to control or otherwise minimize/suppress the generation of these microplasmas. These methods involved (1) exposing the reaction only to the magnetic field (H-field) component of the MW radiation so as to minimize, or otherwise suppress, the formation of hot spots [63]; (2) making use of carbon microcoils rather than AC particles as supports for the Pd catalyst particles [64]; (3) using 5.8 GHz MWs rather than the 2.45 GHz MWs commonly used [65]; (4) improve the dispersion of the heterogeneous catalyst in the solution [66]; (5) keep the catalyst warm using thermal insulating material; and (6) finally decrease the MW power levels [56].

## 8.4 Conclusions

In the twentieth century, the development of chemistry was essentially based on the use of substrates that acted as catalysts. For example, at the beginning of the last

century, whatever soil nitrogen (mostly nitrates) was available proved insufficient for the intensive production of crops. Accordingly, several commercial processes to produce nitrogen-based fertilizers were developed, with the best-known process being the Haber–Bosch process (discovered by Fritz Haber in 1906 and produced industrially by Carl Bosch in 1913) that converted air nitrogen into ammonia using iron-based catalysts. The challenges of the twenty-first century will be, among others, the development of processes that achieve lower greenhouse gas (e.g., CO<sub>2</sub>) emissions and the discovery of novel energy-saving catalysts and catalyzed reactions. A natural choice to achieve such goals might likely involve both catalysis and MW radiation. An in-depth discussion on this subject is available elsewhere [67].

## Bibliography

- [1] Shimomura K, Miyazaki T, Taniguchi N, Tutiya A. Study of ceramics processing, Annual Report, RIKEN, Japan, 48, 1972, 11–19.
- [2] Kingston HM, Haswell SJ (Eds.). *Microwave-Enhanced Chemistry*, American Chemical Society, Washington D.C. 1997.
- [3] Sutton WH. Microwave processing of ceramic materials, *Am. Ceram. Soc. Bull.* 68, 1989, 376–386.
- [4] Folz DC, Booske JH, Clark DE, Gerling JF (Eds.) *Microwave and Radio Frequency Applications, Proceedings from the Third World Congress on Microwave and RF Processing*, American Ceramic Society, Westerville, OH, 2003.
- [5] Takizawa H. Microwave non-equilibrium chemistry in an inorganic chemistry and material chemistry, *Institute Elect. Eng. Jpn.*, 132, 2012, 17–19.
- [6] Luque R, Balu AM, MacQuarrie DJ. Microwave-assisted heterogeneously catalyzed processes, in *Microwaves in Organic Synthesis*, De la Hoz A, Loupy A (Eds.), 3<sup>rd</sup> Edn., vol. 2, pp. 811–842, Chapter 18, 2012, Wiley-VCH Verlag GmbH & Co. KGaA, Germany.
- [7] Mazubert A, Poux M, Aubin J. Intensified processes for FAME production from waste cooking oil: A technological review, *Chem. Engin. J.*, 233, 2013, 201–223.
- [8] Protasova LN, Bulut M, Ormerod D, Buekenhoudt A, Berton J, Stevens CV. Latest highlights in liquid-phase reactions for organic synthesis in microreactors, *Org. Proc. Res. Develop.*, 17, 2013, 760–791.
- [9] Komorowska M-Durka, Dimitrakis G, Bogdal D, Stankiewicz AI, Stefanidis CD. A concise review on microwave-assisted polycondensation reactions and curing of polycondensation polymers with focus on the effect of process conditions, *Chem. Engin. J.*, 264, 2015, 633–644.
- [10] Soltani S, Rashid U, Yunus R, Taufiq YH-Yap, Synthesis of biodiesel through catalytic transesterification of various feedstocks using fast solvothermal technology: A critical review, *Catal. Rev.: Sci. Engin.*, 57, 2015, 407–435.
- [11] Marvi O, Talakoubi M, K-10 and KSF clays as green and recyclable heterogeneous catalysts for the Cannizzaro reaction using DABCO under MWI and solvent-free conditions, *Oriental J. Chem.*, 32, 2016, 359–365.
- [12] Farmer TJ, Clark JH, Macquarrie DJ, Ogunjobi JK, Castle RL. Post-polymerization modification of bio-derived unsaturated polyester resins via Michael additions of 1,3-dicarbonyls, *Polymer Chem.*, 7, 2016, 1650–1658.



- [13] McAfee SM, McCahill JS, Macaulay CM, Hendsbee AD, Welch GC. Utility of a heterogeneous palladium catalyst for the synthesis of a molecular semiconductor via Stille, Suzuki, and direct heteroarylation cross-coupling reactions, *RSC Adv.*, 5, 2015, 26097–26106.
- [14] Guha NR, Reddy CB, Aggarwal N, Sharma D, Shil AKB, Das P. Solid-supported rhodium(0) nano-/micro-particles: An efficient ligand-free heterogeneous catalyst for microwave-assisted Suzuki-Miyaura cross-coupling reaction, *Adv. Syn. Catal.*, 354, 2012, 2911–2915.
- [15] Mst. Parvin N, Jin H, Ansari MB, Oh SM, Park SE. Imidazolium chloride immobilized SBA-15 as a heterogenized organocatalyst for solvent free Knoevenagel condensation using microwave, *Appl. Catal. A: General*, 413–414, 2012, 205–212.
- [16] Glasnov TN, Findenig S, Kappe CO. Heterogeneous versus homogeneous palladium catalysts for ligandless Mizoroki-Heck reactions: A comparison of batch/microwave and continuous-flow processing, *Chem. Eur. J.*, 15, 2009, 1001–1010.
- [17] Ye W, Gao Y, Ding H, Liu M, Liu S, Han X, Qi J. Kinetics of transesterification of palm oil under conventional heating and microwave irradiation, using CaO as heterogeneous catalyst, *Fuel*, 180, 2016, 574–579.
- [18] Tarannum S, Siddiqui ZN. Lanthanum immobilized on chitosan: a highly efficient heterogeneous catalyst for facile synthesis of novel ( $\alpha,\beta$ -unsaturated)  $\beta$ -amino ketones, *Appl. Organomet. Chem.*, 30, 2016, 473–480.
- [19] Martinez E-Guerra, Gude VG. Transesterification of used vegetable oil catalyzed by barium oxide under simultaneous microwave and ultrasound irradiations, *Energy Conv. Manag.*, 88, 2014, 633–640.
- [20] Pereira MM, Pineiro M, Calvete MJF, Aquino G, Abreu AR, Carrilho RMB, Ruas JC, Costa GN, Damas L. Microwave-assisted reactions of natural oils: Transesterification and hydroformylation/isomerization as tools for high value compounds, *Current Microwave Chem.*, 2, 2015, 53–60.
- [21] Liu W, Yin P, Liu X, Chen W, Chen H, Liu C, Qu R, Xu Q. Microwave assisted esterification of free fatty acid over a heterogeneous catalyst for biodiesel production, *Energy Conv. Manag.*, 76, 2013, 1009–1014.
- [22] Khemthong P, Luadthong C, Nualpaeng W, Changsuwan P, Tongprem P, Viriya N-Empikul, Faungnawakij K. Industrial eggshell wastes as the heterogeneous catalysts for microwave-assisted biodiesel production, *Catal. Today*, 190, 2012, 112–116.
- [23] Gallagher-Duval S, Herve G, Sartori G, Enderlin G, Len C. Improved microwave-assisted ligand-free Suzuki-Miyaura cross-coupling of 5-iodo-2'-deoxyuridine in pure water, *New J. Chem.*, 37, 2013, 1989–1995.
- [24] Saggadi H, Luat D, Thiebault N, Polaert I, Estel L, Len C. Toward the synthesis of 6-hydroxyquinoline starting from glycerol *via* improved microwave-assisted modified Skraup reaction, *Catal. Commun.*, 44, 2014, 15–18.
- [25] Saggadi H, Luat D, Thiebault N, Polaert I, Estel L, Len C. Quinoline and phenanthroline preparation starting from glycerol *via* improved microwave-assisted modified Skraup reaction, *RSC Adv.*, 4, 2014, 21456–21464.
- [26] Lussier T, Herve G, Enderlin G, Len C. Original access to 5-arylracils from 5-iodo-2'-deoxyuridine *via* a microwave assisted Suzuki-Miyaura cross-coupling/deglycosylation sequence in pure water, *RSC Adv.*, 4, 2014, 46218–46223.
- [27] Hassine P, Bouhrara M, Sebti S, Solhy A, Luat D, Len C, Fihri A. Natural phosphate-supported palladium: a highly efficient and recyclable catalyst for the Suzuki-Miyaura coupling under microwave irradiation, *Curr. Org. Chem.*, 18, 2014, 3141–3148.
- [28] Saggadi H, Polaert I, Luat D, Len C, Estel L. Microwaves under pressure for the continuous production of quinoline from glycerol, *Catal. Today*, 255, 2015, 66–74.

- [29] Le Guenic S, Delbecq F, Ceballos C, Len C. Microwave-aided dehydration of D-xylose into furfural by diluted inorganic salts solution in a biphasic system, *J. Mol. Catal. A: Chem.*, 410, 2015, 1–7.
- [30] Delbecq F, Wang Y, Len C. Conversion of xylose, xylan and rice husk into furfural via betaine and formic acid mixture as novel homogeneous catalyst in biphasic system by microwave-assisted dehydration, *J. Mol. Catal. A: Chem.*, 423, 2016, 520–525.
- [31] Le Guenic S, Gergela D, Ceballos C, Delbecq F, Len C. Furfural production from D-xylose and xylan by using stable Nafion NR50 and NaCl in a microwave-assisted biphasic reaction, *Molecules*, 21, 2016, 1102–1112.
- [32] Polaert I, Estel L, Luart D, Len C, Delmotte M. A new and original microwave continuous reactor under high pressure for future chemistry, *AIChE J.*, 63, 2017, 192–199.
- [33] Mnasri N, Nyalosaso JL, Colacino E, Derrien G, Lamaty F, Martinez J, Zajac J, Charnay C. Copper-containing rod-shaped nanosized silica particles for microwave-assisted synthesis of triazoles in aqueous solution, *ACS Sustain. Chem. Engin.*, 3, 2015, 2516–2525.
- [34] Wan JKS. Microwaves and chemistry: The catalysis of an exciting marriage, *Res. Chem. Intermed.*, 2, 1993, 147–158.
- [35] Wan JKS, Ioffe MS. Surface heating and energy transfer in pulsed microwave catalytic systems: A microwave-induced acoustic study, *Res. Chem. Intermed.*, 20, 1994, 115–132.
- [36] Horikoshi S, Serpone N. Role of microwaves in heterogeneous catalytic systems, *Catal. Sci. Technol.*, 4, 2014, 1197–1210.
- [37] Matsuzawa M, Togashi S, Hasebe S. Investigation of microwave effects on transition metal catalyzed reaction using an isothermal reaction, *Chem J. Eng. Jpn.*, 45, 2012, 429–435.
- [38] Horikoshi S, Fukui M, Tsuchiya K, Abe M, Serpone N. Microwave specific effects in organic synthesis: A proposed model from the solvent-free synthesis of monoglyceryldimethylammonium chloride, *Chem. Phys. Lett.*, 491, 2010, 244–247.
- [39] Arvela RK, Leadbeater NE. Suzuki coupling of aryl chlorides with phenylboronic acid in water using microwave heating with simultaneous cooling, *Org. Lett.*, 7, 2005, 2101–2104.
- [40] Hirano T. In *Microwaves in Catalysis*, Horikoshi S, Serpone N (Eds.), Wiley-VCH Verlag GmbH: Weinheim, Germany, Chapter 18, 2016.
- [41] Jones DA, Leyveld TP, Mavrofidis SD, Kingman SW, Miles NJ. Microwave heating applications in environmental engineering – Review, *Resourc. Conservat. Recycl.*, 34, 2002, 75–90.
- [42] Liu CC, Na BK, Walters AB, Vannie MA. Microwave absorption measurements of the electrical conductivity of small particles, *Catal. Lett.*, 26, 1994, 9–24.
- [43] Mignos DMP, Baghurst DR. Applications of microwave dielectric heating effects to synthetic problems in chemistry, *Chem. Soc. Rev.*, 20, 1991, 1–47.
- [44] Tamura H, *Amer. Ceramics Soc. Bull.*, 73, 1994, 92–95.
- [45] Hirano T, Matsuda Y. *Proceedings of the 2<sup>nd</sup> Kyushu-Taipei International Congress on Chemical Engineering*, 1997, 335–338.
- [46] Steenwinkel YZ, Castricum HL, Beckers J, Eiser E, Blieke A. Dielectric heating effects on the activity and SO<sub>2</sub> resistance of La<sub>0.8</sub>Ce<sub>0.2</sub>MnO<sub>3</sub> perovskite for methane oxidation, *J. Catal.*, 221, 2004, 523–531.
- [47] Spivery JJ. Complete catalytic oxidation of volatile organics, *Ind. Eng. Chem. Res.*, 26, 1987, 2165–2180.
- [48] Beckers J, van der Zande LM, Rothemberg G. Clean diesel power via microwave susceptible oxidation catalysts, *ChemPhysChem*, 7, 2006, 747–755.
- [49] Wan JKS, Tse MY, Husby H, Depew MC. High-power pulsed microwave catalytic processes: Decomposition of methane, *J. Microwave Power Electromag. Rad.*, 25 1990, 32–38.
- [50] Zang DX, Yu AM, Jin QH. Studies on microwave-carbon reduction method for the treatment of nitric oxide, *Chem. J. Chinese Univ.*, 18, 1997, 1271–1280.

- [51] Winter CJ. Into the hydrogen energy economy – Milestones, *Int. J. Hydrogen Energy*, 30, 2005, 681–685.
- [52] Horikoshi S, Osawa A, Sakamoto S, Serpone N. Control of microwave-generated hot spots. Part V. Mechanisms of hot-spot generation and aggregation of catalyst in microwave-assisted reaction in toluene catalyzed by Pd-loaded AC particulates, *Appl. Catal. A: General*, 460–461, 2013, 52–60.
- [53] Hodoshima S, Shono A, Kuwano J, Saito Y. Chemical recuperation of low-quality waste heats by catalytic dehydrogenation of organic chemical hydrides and its energy analysis, *Energy Fuels*, 22, 2008, 2559–2569.
- [54] Horikoshi S, Kamata M, Sumi T, Serpone N. Hydrogen evolution from organic hydrides through microwave selective heating in heterogeneous catalytic systems, *Int. J. Hydrogen Energy*, 41, 2016, 12029–12037.
- [55] Horikoshi S, Kamata M, Serpone N. Energy savings through microwave selective heating of Pd/AC catalyst particulates in a fixed-bed reactor, *Chem. Eng. Technol.*, 39, 2016, 1575–1577.
- [56] Fujishima A, Hashimoto K, Watanabe T, *TiO<sub>2</sub> Photocatalysis: Fundamentals and Applications*; BKC Incorporated: Tokyo, Japan, 1999.
- [57] Horikoshi S, Hidaka H, Serpone N. Environmental remediation by an integrated microwave/UV illumination method. 1. Microwave-assisted degradation of rhodamine-B dye in aqueous TiO<sub>2</sub> dispersions, *Environ. Sci. Technol.*, 2002, 36, 1357–1366.
- [58] Horikoshi S, Serpone N. Photochemistry with microwaves: catalysts and environmental applications, *J. Photochem. Photobiol. C: Photochem. Rev.*, 10, 2009, 96–110.
- [59] Horikoshi S, Hidaka H, Serpone N. Hydroxyl radicals in microwave photocatalysis. Enhanced formation of •OH radicals probed by ESR techniques in microwave-assisted photocatalysis in aqueous TiO<sub>2</sub> dispersions, *Chem. Phys. Lett.*, 376, 2003, 475–480.
- [60] Zhang S, Hayward DO, P Mingos DM, Apparent equilibrium shifts and hot-spot formation for catalytic reactions induced by microwave dielectric heating, *Chem. Commun.*, 1999, 975–976.
- [61] Tsukahara Y, Higashi A, Yamauchi T, Nakamura T, Yasuda N, Baba A, Wada Y. In situ observation of nonequilibrium local heating as an origin of special effect of microwave on chemistry, *J. Phys. Chem. C*, 114, 2010, 8965–8970.
- [62] Gutmann B, Schwan AM, Reichart B, Gspan C, Hofer F, Kappe CO. Activation and deactivation of a chemical transformation by an electromagnetic field: Evidence for specific microwave effects in the formation of Grignard reagents, *Angew. Chem. Int. Ed.*, 50, 2011, 4636–4640.
- [63] Horikoshi S, Osawa A, Abe M, Serpone N. On the generation of hot spots by microwave electric and magnetic fields and their impact on a microwave-assisted heterogeneous reaction in the presence of metallic Pd nanoparticles on an activated carbon support, *J. Phys. Chem. C*, 115, 2011, 23030–23035.
- [64] Horikoshi S, Suttisawat Y, Osawa A, Takayama C, Chen X, Yang S, Sakai H, Abe M, Serpone N. Organic syntheses by microwave selective heating of novel metal/CMC catalysts – The Suzuki–Miyaura coupling reaction in toluene and the dehydrogenation of tetralin in solvent-free media, *J. Catal.*, 289, 2012, 266–271.
- [65] Horikoshi S, Serpone N. In *Microwaves in Organic Synthesis*, 3<sup>rd</sup> Edn.; de la Hoz A, Loupy A, Eds.; Wiley-VCH Verlag GmbH: Weinheim, Germany, 2012.
- [66] Horikoshi S, Kamata M, Mitani T, Serpone N. Control of microwave-generated hot spots. 6. Generation of hot spots in dispersed catalyst particulates and factors that affect catalyzed organic syntheses in heterogeneous media, *Ind. Eng. Chem. Res.* 53, 2014, 14941–14947.
- [67] Horikoshi S, Serpone N (Eds.). *Microwaves in Catalysis*, Wiley-VCH Verlag GmbH: Weinheim, Germany, 2016.

## 9 Microwaves in flow chemistry

### 9.1 Introduction

The chemical industry generates a large variety of products including (1) basic chemicals, namely polymers, petrochemicals, and basic inorganics; (2) specialty chemicals for crop protection, paints, inks, colorants, textiles, paper, and engineering; and (3) consumer chemicals, for example, detergents and soaps. To date, most chemical production relies on fossil fuel resources, but petroleum reserve depletion is at hand. Aiming to replace petroleum chemistry processing or improve the process intensification, chemists have recently established chemical reactions based on renewable resources, the atom economy, less hazardous chemical steps, safer (least toxic) solvents and auxiliaries, and alternative technologies such as continuous flow, microwave irradiation, and ultrasound irradiation. In this chapter, the combination of microwave irradiation and flow chemistry is described as an alternative technology using either petroleum resources or bio-based starting materials.

Since the early days of microwave chemistry [1, 2], a large number of green and sustainable approaches to microwave-assisted organic reactions have been reported showing different advantages compared to conventional heating protocols that include energy efficiency, safer solvents, material reusability, catalysis, fewer steps, and increases in product yield or selectivity [3, 4]. Microwave technology also allows reactions at temperatures up to 300 °C and pressures up to 80 bar with safety as a priority and excellent parameter controls. Nevertheless, some disadvantages of this technology have been identified, and the major limitation is the penetration depth (almost a few centimeters) into absorbing materials, that is, solvent or reaction mixtures due to the use of microwave reactors with a typical operating frequency of 2.45 GHz. This property excludes the use of high-volume reactors since the microwave power density inside a large batch reactor may only be a small fraction of the density on the surface. The solution to scale-up issues in microwave chemistry must come from a continuous-flow processing approach.

Academic and industrial chemists have developed various chemical reactions in batch-type reactors including flasks and beakers. Compared with the chemistry in human and other living organisms, nature promotes a number of bioorganic reactions in flow systems instead of batch-type conditions. Continuous-flow systems can be conveniently divided into four types (Figure 9.1): (1) all reagents flow through the reactor; (2) one of the reactants is supported on a solid and confined in the reactor with the substrate passing through the reactor; (3) a homogeneous catalyst is used, and the catalyst and reactant flow through the reactor; and (4) a heterogeneous catalyst is used in the reactor [5, 6].

<https://doi.org/10.1515/9783110479935-009>

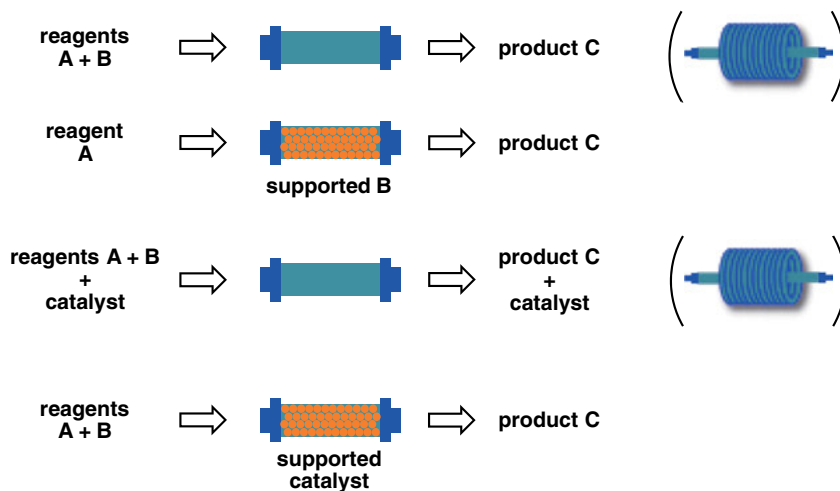
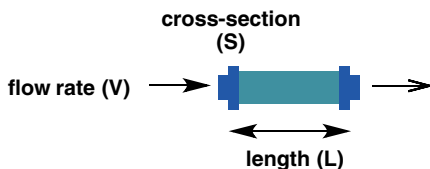


Fig. 9.1: Types of continuous-flow systems.

Different parameters can be controlled under flow chemistry conditions: fluid dynamics, residence time and reaction time, temperature, flow, pumped volume, and pressure. A flow reaction can be studied using a flow of gas, a flow of liquid, and a flow of critical fluid depending on the fluid dynamics. Sometimes a combination of flow of gas and liquid via a heterogeneous solid catalyst is used in the case of hydrogenation. The residence time is the time in which the solution resides inside the tube or reactor. This residence time is also calculated from the volume of the reactor and the flow rate through it (Figure 9.2). A reaction is considered to start when reagents are introduced at one end of the tube and undergo reaction inside the tube. The difference between time of reaction and residence time is very important. The time of reaction is generally the time at which most materials react and convert to the target product.

The way a reaction occurs in a flow reactor is basically similar to the way one happens in a batch reactor (Figure 9.3). On the other hand, the concentration at each location in the flow reactor does not change with time. The starting materials and reagents are pumped into the inlet, usually at a constant concentration and at a constant rate,



$$\text{Residence time} = \text{reactor volume} / \text{flow rate} = (S \times L) / V$$

Fig. 9.2: Residence time in a continuous-flow system.

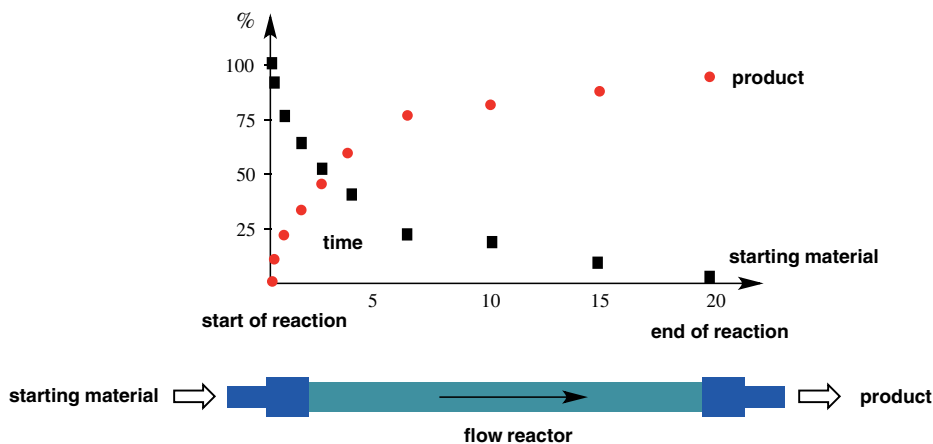


Fig. 9.3: Progress of a reaction in a flow reactor.

and such a continuous-flow condition makes the concentrations of all the materials involving the reaction constant at each location in the reactor. For these reasons, the residence time is a very important parameter to control in flow chemistry since when the residence time is set too short, the solution generally leaves the flow reactor before the reaction is completed. In contrast, the target products may decompose or lead to side reactions when the residence time is too long inside the flow reactor. The operator may assume that the reaction is just terminated when the solution is discharged from the reactor with a concentration of the starting material reaching almost zero and the concentration of the product becoming sufficiently high. In continuous flow, a synthetic process can be rapidly optimized because the results of any set of reaction parameters can be assessed from the first drop of eluent. Of course, the residence time can be varied by changing the flow rate and the volume of the reactor. Concerning the flow rate, its change can modify the mixing rate and the reaction kinetics.

Continuous-flow chemistry as an alternative technology offers significant processing advantages, including improved thermal management, mixing control, application to a wider range of reaction conditions, scalability, energy efficiency, waste reduction, safety, and the possibility to use heterogeneous catalysis and multistep synthesis [7–12]. Two different main reactors, micro and meso (or flow) reactors, exist and the devices depend on channel dimensions: from 10 to 300  $\mu\text{m}$  for microreactors (also called milli or mini), and from 300  $\mu\text{m}$  to more than 5 mm for mesoreactors. Several advantages and disadvantages are associated with micro- and mesoreactors. The main advantages of microreactors are the low material input, low waste output, excellent mass transfer properties, fast diffusive mixing, with disadvantages being low throughput, tendency to experience channel blockage, and high pressure drops. For mesoreactors, the advantages include high throughput, low pressure drops, and

the ability to handle solids for heterogeneous catalysis. The few disadvantages of mesoreactors are the poor mass transfer property and slower mixing.

Although there are many comprehensive reviews and book chapters on the topics of microwave synthesis and flow chemistry, few have been specially dedicated to microwaves in flow chemistry [13–15]. Most often the publications compared microwave chemistry in batch with continuous-flow chemistry. For the sake of clarity, this chapter describes continuous flow under microwave irradiation integrating microwave chemistry in microfluidic systems, in mesofluidic systems, and then its application in nanoparticle (NP) production and organic synthesis. The stop-flow mode is not included in this chapter because it is considered to be part of automated batch processing.

## 9.2 Different flow reactors for microwave applications

Several reports have described the combination of microwave technology and flow reactor, such as microfluidic systems, mesofluidic systems, and more. Most often the systems are homemade apparatus, even if commercial microwave flow reactors are available.

### 9.2.1 Microfluidic systems for chemistry

During the last decade, different microreactors and microcapillary reactors have been explored using either a commercial single-mode microwave cavity or a commercial multimode microwave oven [16–21]. Varma described a microfluidic system using a commercial oven and a homemade microreactor in polytetrafluoroethylene (PTFE) for organic reactions ( $2.7 \cdot 10^{-7} \text{ m}^3$ ), including an aluminum section for the heat transfer side that employs water as liquid ( $6 \cdot 10^{-6} \text{ m}^3$ ) [18]. With this equipment, the authors reported that they achieve near 100% transparency to microwaves in reaction zones and 0% transparency on the heat transfer side (Figure 9.4).

A homemade parallel capillary microreactor has also been reported by Organ [19–21]. The device was composed of an high-performance liquid chromatography (HPLC) pump or syringe pump with three inlets and a stainless steel mixing chamber. The mixed stream was introduced to one capillary tube with the possibility of varying the internal diameter (200–1200  $\mu\text{m}$ ), and microwave irradiation was monitored (Figure 9.5). The application of this process to eight inlets and four capillary tubes for combinatorial applications was developed by the authors.

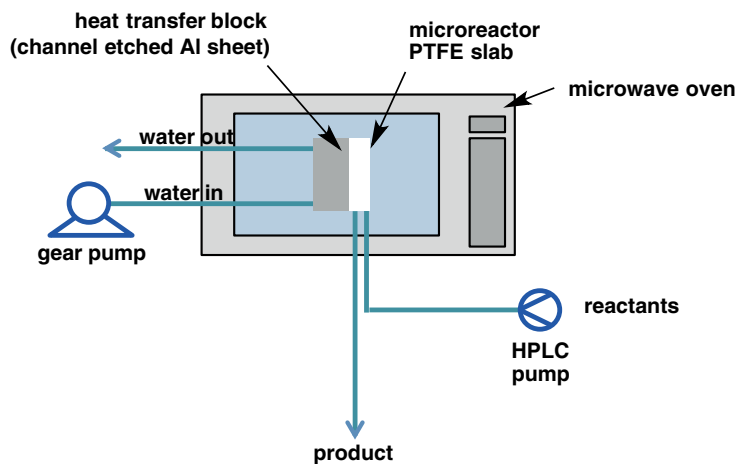


Fig. 9.4: Isothermal continuous-flow microreactor.

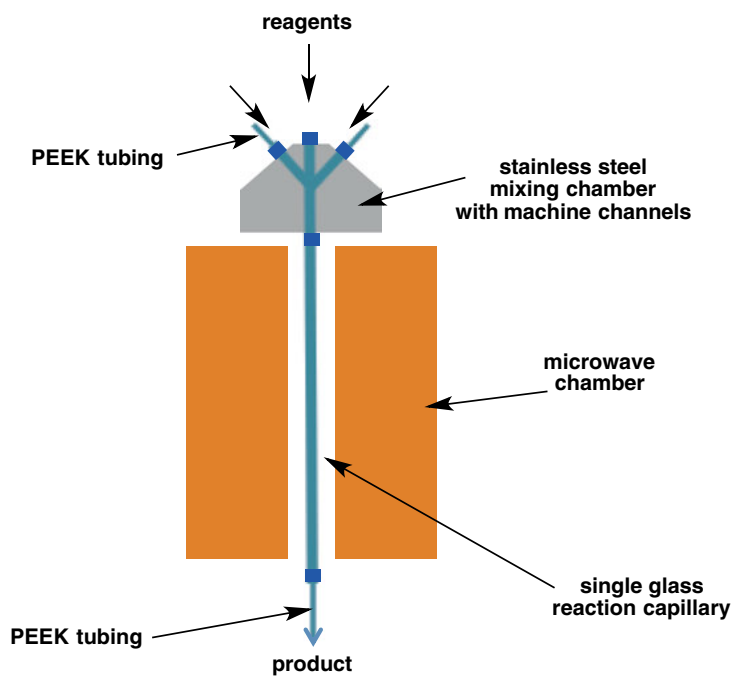
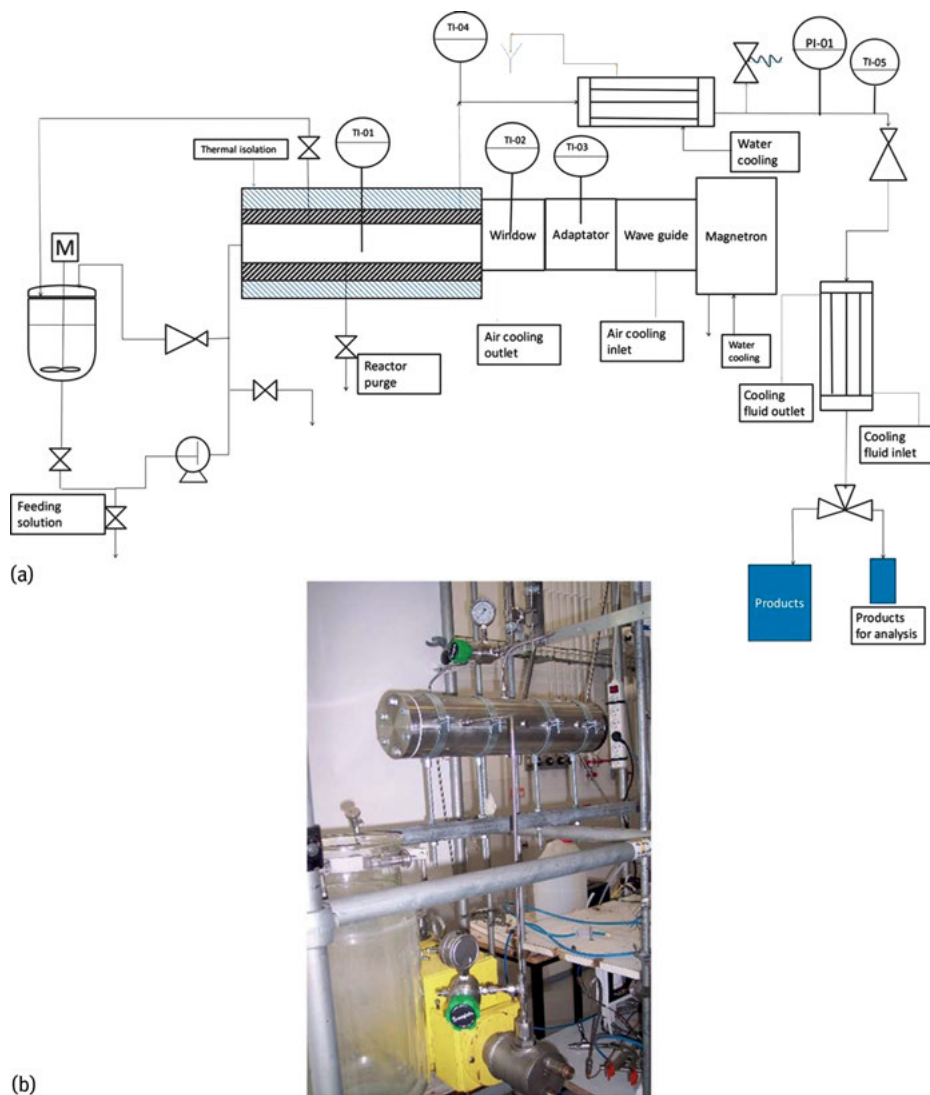


Fig. 9.5: Microreactor design under microwave irradiation for a single sample processing.

### 9.2.2 Mesofluidic system for chemistry

Chemists have very recently transferred their knowledge from microfluidic to mesofluidic systems. To date, various commercial microwave apparatus exist, including the





**Fig. 9.6:** (a) Experimental setup for continuous microwave synthesis under high temperature and pressure. (b) Photo of high-pressure microwave reactor.

Emrys Synthesizer from Biotage, Voyager from CEM, Flow Synth from Milestone, and MiniFlow 200SS from SAIREM. In parallel, different groups have attempted to develop their own processes by varying different parameters [22–27].

Len's group developed in collaboration a new and original high-pressure reactor for continuous-flow chemistry under microwaves at the industrial scale (Figure 9.6) [28]. Interestingly, the concept explores a microwave applicator as reactor,

allowing the use of metallic and thick walls adapted for use at high pressures and temperatures. After optimization, the design can be applied to minimize wave reflections and maximize energy transfers in the reacting medium. This leads to extremely good energy yields. Experiments confirmed that the microwave energy can be fully absorbed by the reacting medium. The reactor allows continuous chemical reactions at a  $\text{kg h}^{-1}$  scale, under microwave heating, up to 7 MPa and 200 °C. Also notable is the fact that in 2014 other groups also described a continuous-flow microwave reactor for high-temperature and high-pressure chemical reactions [29].

## 9.3 Applications of microwaves in flow chemistry

The combination of microwave irradiation and continuous flow has recently surged in use. The advantages of microwaves no longer need to be demonstrated. Nevertheless, the low depth of irradiation does not allow for the use of a large volume of solvent and, thus, scale-up. Hence, the passage of microwaves in a continuous flow can limit this drawback. Different groups have shown that the synthesis of NPs and the synthesis of conventional organic molecules can be successfully carried out.

### 9.3.1 Production of nanoparticles

In recent decades, noble-metal, especially silver and gold, NPs have received increasing attention in connection with their unique size and shape-dependent optical and electric properties. Silver NPs have found various applications in the areas of plasmonics, surface enhanced Raman scattering, catalysis, biosensing, and medicine, as well as in ultra-high-density storage and film growth seeding. For all the aforementioned reasons, various industries have attempted to develop new processes to produce large amounts of these NPs in a short amount of time. Commonly, silver nanoparticles (Ag NPs) are synthesized on a small scale from silver salt precursors in aqueous media or in organic solvents. In aqueous solution, the method is usually simpler, rapid, and environmentally friendly. To avoid the aggregation of nanocrystals, a colloidal process is generally employed involving a capping agent such as a carboxylate (fatty acid, citrate) or a polymer such as poly(vinylpyrrolidone) (PVP) or  $\beta$ -cyclodextrin. At the end of the reaction, the formed NPs need to be extracted by centrifugation or coprecipitated with insoluble inorganic materials such as alumina  $\text{Al}_2\text{O}_3$  or silicon dioxide  $\text{SiO}_2$ . Many reactions parameters can affect the size and shape of *in situ* generated Ag NPs such as the pH, the strength of the reducing agent ( $\text{NaBH}_4$ , formaldehyde, alcohol, and ascorbic acid), and the general nature and concentration of the salt precursor.

Horikoshi et al. studied the formation of small Ag NPs under microwave irradiation coupled with a continuous flow [30]. They started from the thermal decomposi-

tion at 100 °C of an *in situ* formed  $[\text{Ag}(\text{NH}_3)_2]^+$  complex stabilized with carboxymethyl cellulose. Herein, the capping agent could partially act as reducing agent. Interestingly, under both microwave and conventional heating, the nucleated Ag NPs were obtained in a narrow distribution, with a diameter of ca. 10 nm. However, significantly smaller NPs (0.7 and 2.8 nm in diameter) could be obtained keeping unchanged the narrow size distribution by transferring the reaction to a microwave-heated continuous-flow apparatus, according to transmission electron microscopy results. The entire process remained temperature-dependent and could minimize contamination caused by the presence of an external reducing agent.

On the other hand, the recent work of Dzido et al. detailed a successful microwave-assisted Ag NP synthesis under continuous-flow conditions [31]. Silver acetate (AgOAc) was utilized as the optimum metallic salt precursor and proved to be superior to silver nitrate  $\text{AgNO}_3$  in producing the smallest Ag NPs (ca. 10–20 nm average diameter). A solution of a selected polyol, such as ethylene glycol, propan-1,2-diol, or butan-1,4-diol, with polyvinylpyrrolidone (PVP) and a chosen salt in a 1 : 7 ratio (v/v) was prepared and pumped through a PTFE tubular reactor (8 mm internal diameter, 42 mm length) under microwave activation at controlled flow rates of 0.318, 0.635, 1.27, and  $2.5 \text{ dm}^3 \text{ h}^{-1}$  to reach residence time values of 3, 6, 12, and 24 s, respectively. All NPs were also particularly homogeneous in shape and size. Like the others, the capping agent could have been ethylene glycol, and it could act as reducing agent when the well-prepared solution was heated at a temperature between 90 and 170 °C. The synthesis of the target Ag NPs was then achieved in a few seconds with the flow set at  $41 \text{ mL min}^{-1}$ . AgOAc was found to be comparatively more reactive than  $\text{AgNO}_3$ , especially when heated at shorter residence times or lower temperatures (< 170 °C). These Ag NPs exhibited remarkable activity against Gram-positive *Bacillus subtilis* and Gram-negative *Escherichia coli*.

Dzido and Jarzebski already demonstrated the superior potential of a monomodal microwave-assisted polyol process for the generation of Ag NPs compared to a bimodal model. A polyol process is known to be comparatively slower at bringing about Ag NPs synthesis compared to an aqueous system. In batch conditions, microwave heating is not suitable for scaling up a process (because of the difficulty of using microwaves for deep penetration of reactors), while a continuous flow coupled to a microwave oven appears to be a good alternative.

In this second procedure [32], silver acetate was the precursor for Ag NP synthesis, dissolved in ethylene glycol or glycerol, which was employed as both reaction solvent and reducing agent. The reaction was carried out at 80 °C, the flow rate was set at  $0.5 \text{ L h}^{-1}$ , and the size and stability of the generated NPs were controlled with PVP of sufficient molecular weight. According to the results obtained in this study, the particle size distribution was directly connected to the silver precursor concentration and it was possible to observe the appearance of a second group of smaller Ag NPs on the same histogram of around 10 nm. Interestingly, no comment was made about a possible influence of the current flow rate on the quality of the formed Ag NPs.

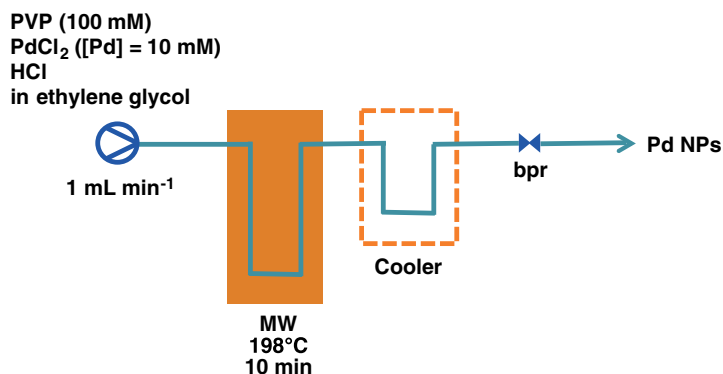


Fig. 9.7: Synthesis of Pd NPs under microwave continuous-flow conditions.

Tab. 9.1: Influence of metal and its concentration on different particle sizes.

Entry	Metal	Metal concentration (mM)	Particle size (nm)
1	Pd	5	5.5
2	Pd	10	6.7
3	Rh	10	3.4
4	Ru	10	2.0
5	Pt	10	3.6

Other types of metallic NPs could be prepared using similar protocols. In a recent paper, Harada used palladium and some related metallic salt precursors, including rhodium (Rh), ruthenium (Ru), and platinum (Pt), to design their well-dispersed and PVP-capped corresponding NPs [33]. This process required ethylene glycol and glycerol as reducing agents, and the reaction temperature was set at 198 °C. To develop a strategy to promote the scale-up of the noble metal NPs, microwave-heated continuous flow was employed giving Pd NPs, Rh NPs, Ru NPs, and PtNPs of 5.5, 3.4, 2.0, and 3.6 nm of average diameter respectively (Figure 9.7 and Table 9.1). However, only Rh, Ru, and Pt NPs remained regular in shape and size without showing undesired aggregation at any time.

Another paper, written by Nishioka and coworkers, reported the synthesis of Pt NPs using a single-mode microwave flow reactor [34]. They described a rapid and continuous polyol process for Pt NP synthesis using a single-mode monowave reactor. Among three tested polyols as reducing agents, propan-1,3-diol was found to be most effective. The principal source of platinum was H<sub>2</sub>[PtCl<sub>6</sub>], 6 H<sub>2</sub>O. The dispersion of the NPs was created in ethylene glycol solution containing 1 wt% of PVP as the capping agent and pumped into the reactor (Figure 9.7).

**Tab. 9.2:** Variation in Pt NP size based on the nature of the reducing agent and residence time of the reaction.

Entry	Polyol	Time (s)	Particle size (nm)
1	Ethylene glycol	28.3	5.9
2	Glycerol	28.3	6.5
3	Glycerol	2.8	3.4
4	propan-1,3-diol	2.8	4.1

When heated at 160 °C for 2.8–28.3 s of residence time, a simple increase of the flow rate from 10 to 100 mL h<sup>-1</sup> could serve as size control of the generated Pt NPs. In fact, after 2.8 s small Pt Nps 3.4 nm in diameter were formed. Pt NPs with average sizes of 2 to 5 nm were obtained with ethylene glycol or glycerol as reducing agent (Table 9.2). The authors did not mention anywhere in the text the influence of the initial platinum salt precursor concentration on the size of the resultant Pt NPs.

Later, the same team attempted to extend their proposed protocol to produce core-shell bimetallic NPs of both palladium/platinum and copper/silver combinations [35]. The preparation required a double injection process. First, smaller Pd and Cu NPs displaying respectively diameters of 6.5 and 90 nm were obtained from an ethylene glycol solution containing one of each of the metallic salt precursors, for example, Na<sub>2</sub>[PdCl<sub>4</sub>] and Cu[OAc]<sub>2</sub>, in the presence of 15 wt% of PVP. The resulting solutions were then heated at 200 °C in microwave-continuous flow. The solution was pumped through a pump at a flow rate of 50 mL h<sup>-1</sup> into the reactor, which corresponded to a residence time of 6 s. Once formed, the aqueous dispersion of Pd NPs was mixed through a binary flow with another H<sub>2</sub>[PtCl<sub>6</sub>], 6 H<sub>2</sub>O aqueous solution of pH adjusted to 12. The same procedure was repeated for the Cu NP solution, replacing the previous platinum solution by AgNO<sub>3</sub> dissolved in water. But this time the solution needed to show a pH adjusted to 9 with NaOH. Finally, the respective stable desired Pd@Pt and Cu@Ag core-shell NPs were obtained at room temperature outside the apparatus. Unfortunately, no further information about the influence of the flow rate on the formed bimetallic size was given in this paper.

The use of microwave-assisted continuous-flow conditions is not exclusive to the synthesis of metallic NPs. It could become an essential tool to gain access to a large variety of nanosized structured materials. Akram et al. produced different types of nanosized titania useful for their photocatalytic properties [36]. In this regard, they did not indicate the concrete influence of the flow rate on the size of the particles and their relative degree of crystallinity (Figure 9.8).

Nanosized titania was obtained using continuous microwave flow synthesis for its ability to be used as photocatalyst and as photovoltaic solar cell material, water splitting, and electrochemical fuel cells. In this regard, Hussain described the formation of phase-pure, visible-light active anatase TiO<sub>2</sub> at relatively low temperature and pressure. The volume of the NPs changed as a function of the power (450, 600, and 800 W)

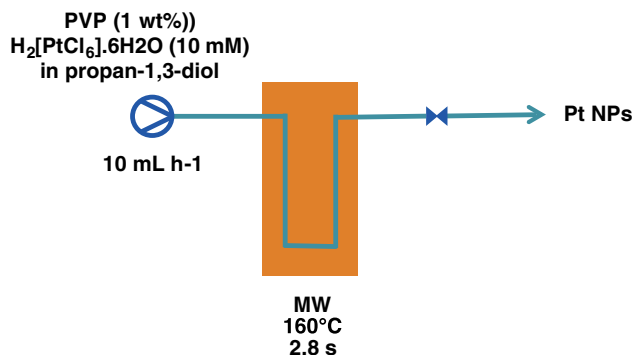


Fig. 9.8: Synthesis of Pt NPs under microwave continuous-flow conditions.

to give 4.35/4.71, 4.83/5.07, and 6.98/7.10 nm, respectively. It was noticeable that photocatalytic effect of  $\text{TiO}_2$  on methylene blue (MB) was effective from NPs obtained with a microwave power of 450 W.

However, only the microwave power had a strong impact on the quality of the material displaying a great number of crystallized areas and overall less porosity. In addition, the average size of the particle also increased with the power of the microwave irradiation until they reached a diameter limit of 7.0 nm. The most evident advantage of the method included the possibility for scaling up the process due to the deepest penetration of microwaves inside the reactor. Regarding these promising results, they decided to apply the same method to get small tin NPs from  $\text{SnCl}_4$ ,  $\text{H}_2\text{O}$  immersed in  $\text{NaOH}$ /ethanol solution [37]. Thus, they observed the same reaction behavior leading to the formation of the smallest NPs with low porosity and a higher degree of crystallinity at the higher power of 800 W.

The same research team also investigated the impact of a similar procedure on the manufacture of nanostructured mesoporous hydroxyapatite [38]. Two distinct aqueous solutions of  $\text{Ca}(\text{NO}_3)_2$ ,  $4 \text{H}_2\text{O}$  and  $(\text{NH}_4)_2\text{HPO}_4$  were pumped through two distinct peristaltic pumps and mixed in a domestic microwave oven. During the process the pH of the solutions was adjusted by the addition of ammonia solution  $\text{NH}_4\text{OH}$  (28%). The process produces different structured  $\text{Ca}_{10}(\text{PO}_4)_6\text{OH}_2$  solids obtained by varying both precursors' concentrations, microwave power, and retention time. Despite a real increase of the particle diameter within 15 and 24 nm, the degree of crystallinity was improved with higher microwave power, demonstrated by the result of the X-ray diffraction analysis. Interestingly, at the maximum level of 800 W, a slight decrease of the porosity was confirmed by a simple Brunauer–Emmett–Teller (BET) analysis. Herein, for all synthesized materials, longer residence times could promote the formation of a solid with a high crystallinity level and lower porosity.

Bayazit et al. have developed a process to produce self-assembled hierarchical hematite superstructures using a continuous-flow device equipped with a microwave oven [39]. This original procedure used iron (III) nitrate monohydrate  $(\text{Fe}(\text{NO}_3)_3$ ,

9 H<sub>2</sub>O) as the sole precursor without the addition of any promoter or stabilizer. Just by heating a solution loaded with the iron precursor salt at 120 °C under a flow rate of 1 mL min<sup>-1</sup>, after 6 min of residence time, pure and crystalline ellipsoid hematite superstructures were obtained prior to further structural and physicochemical characterizations. At higher flow rates, these structures were not observed. This paper confirmed the superiority of the microwave-assisted process compared to a conventionally heated system. This process was reported to be highly reproducible.

Cannio and his collaborators have already demonstrated the potential of microwave-heated continuous flow for the hydrothermal synthesis of aqueous magnetite nanofluids, or more precisely for obtaining a dispersion of magnetic NPs in aqueous medium [40]. The starting point of the experiments was the preparation of various solutions loaded with iron (II) chloride FeCl<sub>2</sub>, sodium hydroxide NaOH, hydrazine hydrate N<sub>2</sub>H<sub>4</sub>, and H<sub>2</sub>O in deionized water pumped through a tubular system at a fixed flow rate. The residence time never exceeded 15 min. The resulting solutions were heated at 100 °C under a fixed flow rate. Unfortunately, only the pH had a strong effect on the main characteristics of the generated Fe<sub>3</sub>O<sub>4</sub> magnetic NPs.

The last example described the preparation of sprayable kesterite NPs (Cu<sub>2</sub>ZnSnS<sub>4</sub>) dispersed under a microwave-assisted continuous-flow process [41]. These composite NPs were expected to be potent for the inkjet fabrication of thin films. Their preparation required a mixture of three different salt precursors: SnCl<sub>4</sub>, Cu(OAc)<sub>2</sub>, H<sub>2</sub>O, and Zn(OAc)<sub>2</sub>, 2 H<sub>2</sub>O. The pH of the aqueous solution was adjusted with hydrochloric acid (HCl) and heated in the presence of 3-mercapto acetic acid and sodium sulfide Na<sub>2</sub>S in a homemade continuous-flow system equipped with a microwave unit. When the solution was pumped and heated at 100 °C, the feed solution circulated in the reactor under a flow rate of 18.5 mL min<sup>-1</sup>. In this condition, the process was able to release the desired NPs displaying an average diameter of 3–5 nm in association with a semiamorphous pattern. All generated NPs kept a regular distribution of each chemical element inside the material. This work again served as a good example of the scalable preparation of more complex nanostructured NPs.

### 9.3.2 Organic synthesis

In recent decades, microwave-assisted continuous-flow organic synthesis (MACOS) has been developed for conventional organic chemistry (e.g., heterocyclic chemistry, metal-catalyzed chemistry) and particularly for the multigram organic synthesis of aromatic compounds [42, 43]. In the literature, the dehydration of diol, transesterification, Petasis olefination, multistep reactions, and multicomponent reactions have been performed by MACOS.

Trivertal (2,4-dimethylcyclohex-3-enecarboxaldehyde) is an industrial fragrance and flavor material. Following a retrosynthetic pathway, trivertal can be produced in two steps by (1) dehydration of hexylene glycol (2-methylpentan-2,4-diol) in acidic

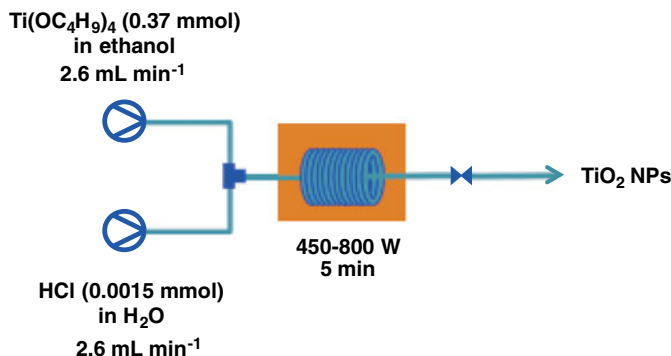


Fig. 9.9: Synthesis of  $\text{TiO}_2$  NPs under microwave continuous-flow conditions.

medium to form 2-methylpenta-1,3-diene (M2P) and then by (2) Diels–Alder reaction with acrolein. Len’s and Estel’s groups reported the dehydration of hexylene glycol to a mixture of M2P and 2-methylpenta-2,4-diol (M4P) on a kilogram-per-hour scale of under 2.5 MPa at 150 °C [28]. In our hands, the conversion was 85% yield and the two diastereoisomers (63 : 37) were produced in 58% yield (Figure 9.9). Notably, the obtained mixture could be distilled to yield pure M2P.

Biodiesel is composed of fatty acid methyl esters (FAMES), which are derived from renewable oils or fats instead of petroleum. It is therefore an alternative and so-called green fuel that has the potential to replace fossil fuels, thereby ensuring the sustainability of energy sources and the environment. Currently in industrial processes, biodiesel is produced via the transesterification of refined vegetable oils or animal fats with methanol or ethanol in the presence of basic catalysts in heated stirred tanks. Cravotto and collaborators reported biodiesel production in a novel continuous-flow microwave reactor [44]. Using a commercial FlowSynth apparatus, the authors reported that starting from oil in methanol (methanol-oil, 12 : 1, v/v) in the presence of NaOH (1 wt%), FAME was obtained in 99% yield after a residence time of 1.75 min at 70 °C. In these conditions, the energy consumption is  $0.1167 \text{ kWh L}^{-1}$ , which is about half the energy consumed by the conventional reaction.

Petasis olefination for the production of *exo*-glycals from sugar lactones was also demonstrated to be possible in a continuous-flow microwave reactor [45]. Among the olefination reactions, Petasis reaction allowed the formation of the corresponding alkenes in nonbasic media. Kunz and collaborators developed different sugar derivatives with an *exo* double bond in an anomeric position (Figure 9.10). The fucose derivative is conventionally olefinated at 70 °C within 16 h with an identical yield as in the continuous-flow reaction in a residence time of 8.5 min. The homemade apparatus consists of an HPLC pump for delivering the mixture of solvent and the reagents, and the sample loop and reactor are capillaries (PTFE, 3.2 mm o.d. and 1.6 mm i.d.).

Among all the works developed by Organ, the synthesis of sultam derivatives in a multistep process was reported using microwave-assisted continuous flow organic



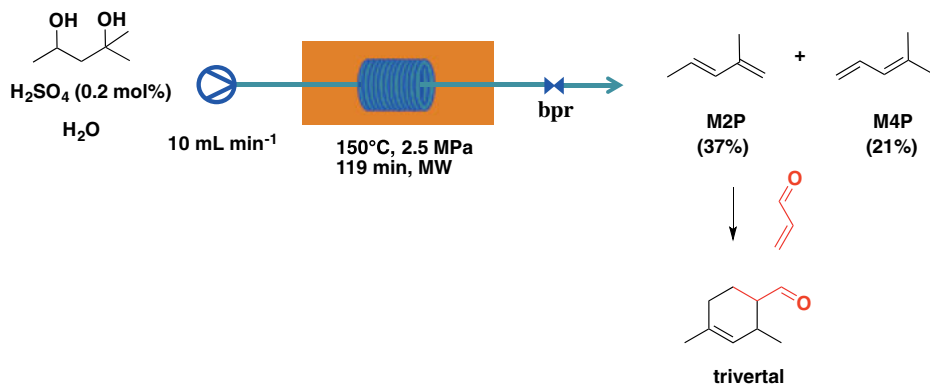


Fig. 9.10: Synthesis of 2-methylpenta-1,3-diene (M2P) under microwave continuous-flow conditions.

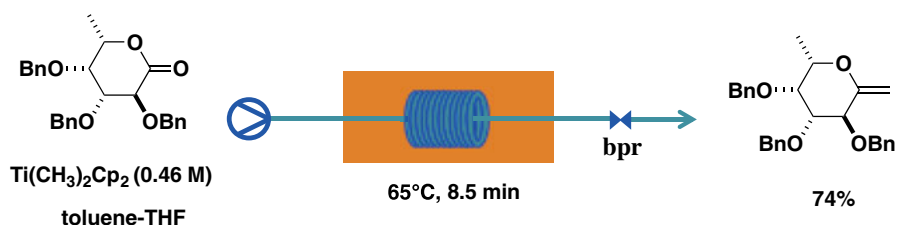


Fig. 9.11: Synthesis of exo-glycal from lactone *via* Petasis olefination under microwave continuous-flow conditions.

synthesis [46–50]. The strategy used successive MACOS processes or conventional batch organic chemistry with one MACOS process.

Collaboration between Li and Organ resulted in the development of a multicomponent reaction (MCR) protocol in the presence of transition-metal films for the production of propargyl amine as an intermediate for drug development [50]. With the metal-coated capillaries ( $1700 \mu\text{m}$  i.d.), a toluene solution of aldehyde, secondary amine, and terminal alkyne was injected with a flow rate of  $20 \mu\text{L mL}^{-1}$ , and the stream was introduced to the reactor at  $950^\circ\text{C}$  under microwave irradiation (Figure 9.11). In these conditions, the propargyl amines were produced in good yield in the presence of copper as metal. This was the first time that the temperature exceeded  $900^\circ\text{C}$  when a thin-metal film was used.

## Summary and conclusion

This contribution has been aimed at providing an overview of the possibilities of continuous-flow processes combined with microwave irradiation. In view of the future challenges facing the chemical industry, the role of microwave and particularly

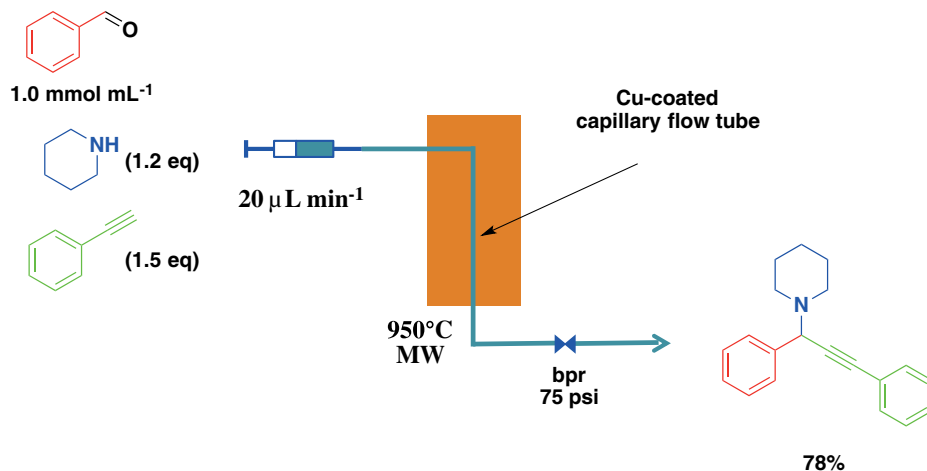


Fig. 9.12: Multicomponent reaction for the production of propargyl amine via MACOS. [50]

its combination with continuous-flow processes can be considered as highly advantageous for scaling-up purposes. A number of different examples of microfluidic and mesofluidic systems as part of this work illustrate the potential of such synergy that includes multiple applications of microwaves in flow chemistry for the production of NPs and different organic compounds. To date, microfluidic systems under microwave irradiation can provide significant advantages compared to separate microwave/flow systems, because they are more appropriate for the multigram synthesis of new compounds/nanomaterials at laboratory scale. Varying the nature of the materials and reactor designs, the possibility of working under high temperatures and pressures (near critical point of the solvent) represent new avenues to explore in the future. Chemists and chemical engineers have the means to pave the way to a more widespread implementation of microwave-assisted continuous flow production for the production of industrially relevant products in the future. Importantly, we hope that the demonstrated advantages of combining microwaves in flow processes can stimulate further advances in the field from younger generations for the benefit of the chemical industry.

## Bibliography

- [1] Gedye R, Smith F, Westaway K, Ali H, Baldisera L, Laberge L, Rousell J. The use of microwave ovens for rapid organic synthesis, *Tetrahedron Lett.* 27, 1986, 279–282
- [2] Giguere RJ, Bray TL, Duncan SM, Majetich G. Application of commercial microwave ovens to organic synthesis, *Tetrahedron Lett.* 27, 1986, 4945–4948.
- [3] Gawande MB, Shelke SN, Zboril R, Varma RS. *Acc. Chem. Res.* 47, 2014, 1338–1348.

- [4] Rathi AK, Gawande MB, Zboril R, Varma RS. Microwave-assisted synthesis – Catalytic application in aqueous media, *Coord. Chem. Rev.* 291, 2015, 68–94.
- [5] Baumann M, Baxendale IR, Ley SV. The flow synthesis of heterocycles for natural product and medicinal chemistry applications, *Mol. Divers.* 15, 2011, 613–630.
- [6] Baxendale IR. The integration of flow reactors into synthetic organic chemistry, *J. Chem. Technol. Biotechnol.* 88, 2013, 519–552.
- [7] Haswell SJ, Watts P. Green chemistry: synthesis in micro reactors, *Green Chem.* 5, 2003, 240–249.
- [8] Frost CG, Mutton L. Heterogeneous catalytic synthesis using microreactor technology, *Green Chem.* 12, 2010, 1687–1703.
- [9] Wiles C, Watts P. Continuous flow reactors: a perspective, *Green Chem.* 14, 2012, 38–54.
- [10] Newman SG, Jensen KF. The role of flow in green chemistry and engineering, *Green Chem.* 15, 2013, 1456–1472.
- [11] Wiles C, Watts P. Continuous process technology: a tool for sustainable production, *Green Chem.* 16, 2014, 55–62.
- [12] Vaccaro L, Lanari D, Marrochi A, Strappaveccia G. Flow approaches towards sustainability, *Green Chem.* 16, 2014, 3680–3704.
- [13] Glasnov TN, Kappe CO. Microwave-assisted synthesis under continuous-flow conditions, *Macromol. Rapid Commun.* 28, 2007, 395–410.
- [14] Estel L, Poux M, Benamara N, Polaert I. Continuous flow-microwave reactor: where are we? *Chem. Engin. Process.* 113, 2017, 56–64.
- [15] Rebrov EV. Microwave-assisted organic synthesis in microstructured reactors, *Russ. J. Gen. Chem.* 82, 2012, 2060–2069.
- [16] He P, Haswell SJ, Fletcher PD. Microwave heating of heterogeneously catalyzed Suzuki reactions in a micro reactor, *Lab Chip* 4, 2004, 38–41.
- [17] He P, Haswell SJ, Fletcher PD. Microwave-assisted Suzuki reactions in a continuous flow capillary reactor, *Appl. Catal.* 274, 2004, 111–114.
- [18] Jachuck RJJ, Selvaraj DK, Varma RS. Process intensification: oxidation of benzyl alcohol using a continuous isothermal reactor under microwave irradiation, *Green Chem.* 8, 2006, 29–33.
- [19] Comer E, Organ MG. A microreactor for microwave-assisted capillary (continuous flow) organic synthesis, *J. Am. Chem. Soc.* 127, 2005, 8160–8167.
- [20] Shore G, Morin S, Organ MG. Catalysis in capillaries by Pd thin films using microwave-assisted continuous flow organic synthesis (MACOS), *Angew. Chem. Int. Ed.* 45, 2006, 2761–2766.
- [21] Comer E, Organ MG. A microcapillary system for simultaneous, parallel microwave-assisted synthesis, *Chem. Eur. J* 11, 2005, 7223–7227.
- [22] Wilson NS, Sarko CR, Roth G. Development and application of a practical continuous flow microwave cell, *Org. Process. Res. Dev.* 8, 2004, 535–538.
- [23] Bagley MC, Lenkins RI, Lubinu MC, Mason C, Wood R. A simple continuous flow microwave reactor, *J. Org. Chem.* 70, 2005, 7003–7006.
- [24] Wada D, Sugiyama JI, Zushi H, Murayama H. Temperature distribution monitoring of a coiled flow channel in microwave heating using an optical fiber sensing technique, *Sensors Actuators B* 232, 2016, 434–441.
- [25] Zhou P, Yang X, Huang K, Jia G. Microwave-assisted continuous-flow reactor based on a ridged waveguide, *Chem. Eng. Technol.* 38, 2015, 1334–1339.
- [26] Nishioka M, Miyakawa M, Daino Y, Kataoka H, Koda H, Sato K, Suzuki TM. Single-mode microwave reactor used for continuous flow reactions under elevated pressure,
- [27] Sturm GSJ, Van Braam Houckgeest AQ, Verweij MD, Van Gerven T, Stankiewicz AI, Stefanidis GD. Exploration of rectangular waveguide as a basis for microwave enhanced continuous flow chemistries, *Chem. En. Sci.* 89, 2013, 196–205.

- [28] Polaert I, Estel L, Luart D, Len C, Delmotte M. A new and original microwave continuous reactor under high pressure for future chemistry, *AIChE Journal* 63, 2017, 192–199.
- [29] Sauks JM, Malliks D, Lawryshyn Y, Bender T, Organ M. A continuous-flow microwave reactor for conducting high-temperature and high-pressure chemical reactions, *Org. Process Res. Dev.* 18, 2014, 1310–1314.
- [30] Horikoshi S, Abe H, Torigoe K, Abe M, Serpone N. Access to small size distributions of nanoparticles by microwave-assisted synthesis. Formation of Ag nanoparticles in aqueous carboxymethylcellulose solutions in batch and continuous flow reactors, *Nanoscale*, 2, 2010, 1441–1447.
- [31] Dzido G, Markowski P, Malachowska-Jutsz A, Prusik K, Jarzebski AB. Rapid continuous microwave-assisted synthesis of silver nanoparticles to achieve very high productivity and full yield: from mechanistic study to optimal fabrication strategy, *J. Nanopart. Res.* 2015, 17, 27–43.
- [32] G Dzido, Jarzebski AB. Fabrication of silver nanoparticles in a continuous flow, low temperature microwave assisted polyol process, *J. Nanopart. Res.* 13, 2011, 2533–2541.
- [33] Harada M, Cong C. Microwave-Assisted Polyol Synthesis of Polymer-Protected Monometallic Nanoparticles Prepared in Batch and Continuous-Flow Processing, *Ind. Eng. Chem. Res.* 55, 2016, 5634–5643.
- [34] Nishioka M, Miyakawa M, Daino Y, Kataoka H, Koda H, Sato K, Suzuki TM. Rapid and Continuous Polyol Process for Platinum Nanoparticle Synthesis Using a Single-mode Microwave Flow Reactor, *Chem Lett.* 40, 2011, 1327–1329.
- [35] Miyakawa M, Hiyoshi N, Nishioka M, Koda H, Sato K, Miyazawa A, Suzuki TM. Continuous syntheses of Pd@Pt and Cu@Ag core-shell nanoparticles using microwave-assisted core particle formation coupled with galvanic metal displacement, *Nanoscale* 6, 2014, 8720–8725.
- [36] Akram M, Butt FK, Alshemary AZ, Goh YF, Ibrahim WAW, Hussain R. Continuous microwave flow synthesis (CMFS) of nanosized titania: Structural, optical and photocatalytic properties, *Mater. Lett.* 158, 2015, 95–98.
- [37] Akram M, Alshemary AZ, Butt FK, Goh YF, Ibrahim WAW, Hussain R. Continuous microwave flow synthesis and characterization of nanosized tin oxide, *Mater. Lett.* 160, 2015, 146–149.
- [38] Akram M, Alshemary AZ, Goh YF, Ibrahim WAW, Lintang HO, Hussain R. Continuous microwave flow synthesis of mesoporous hydroxyapatite, *Mater. Sci. Eng. C* 56, 2015, 356–362.
- [39] Bayazit MK, Cao E, Garrilidis A, Tang J. A microwave promoted continuous flow approach to self-assembled hierarchical hematite superstructures, *Green Chem.* 18, 2016, 3057–3065.
- [40] Cannio M, Ponzoni C, Gualtieri ML, Lugli E, Leonelli C, Romagnoli M. Stabilization and thermal conductivity of aqueous magnetite nanofluid from continuous flows hydrothermal microwave synthesis, *Mater. Lett.* 173, 2016, 195–198.
- [41] Martini T, Chubilleau C, Poncelet O, Ricaud A, Blayo A, Martin C, Tarasov K. Spray and inkjet fabrication of Cu<sub>2</sub>ZnSnS<sub>4</sub> thin films using nanoparticles derived from a continuous-flow microwave-assisted synthesis, *Sol. Energy Mater. Sol. Cells*, 144, 2016, 657–663.
- [42] Alcazar J, de Munoz M. Microwave-assisted continuous flow organic synthesis (MACOS) in: *Microwaves in organic synthesis*, vol 1, third edn., A de la Hoz, Loupy A(Eds), Wiley-VCH Verlag GmbH, Weinheim, Germany, chap 25, 2012, pp 1173–1204.
- [43] Morschhauser R, Krull M, Kayser C, Boberski C, Bierbaum R, Puschner PA, Glasnov TN, Kappe CO. Microwave-assisted continuous flow synthesis on industrial scale, *Green Process Synth.* 1, 2012, 281–290.
- [44] Choedkiatsakul I, Ngaosuwan K, Assabumrungat S, Mantegna S, Cravotto G. Biodiesel production in a novel continuous flow microwave reactor, *Renew. Energy* 83, 2015, 25–29.
- [45] Koch S, Lowe H, Kunz H. Petasis olefination in a continuous-flow microwave reactor: exoglycals from sugar lactones, *Synlett*, 14, 2011, 1978–1982.

- [46] Ullah F, Zang Q, Javed S, Porubsky P, Neuenswander B, Lushington GH, Hanson PR, Organ MG. Synthesis of an isoindole-annulated, tricyclic sultam library *via* microwave-assisted, continuous-flow organic synthesis (MACOS), *Synthesis* 44, 2012, 2547–2554.
- [47] Ullah F, Samarakoon T, Rolfe A, Kurtz RD, Hanson PR, Organ MG. Scaling out by microwave-assisted continuous flow organic synthesis (MACOS): multi-gram synthesis of bromo- and fluoro-benzofused sultams benzthioxazepine-1,1-dioxides, *Chem. Eur. J.* 16, 2010, 10959–10962.
- [48] Ullah F, Zang Q, Javed S, Zhou A, Knudtson CA, Bi D, Hanson PR, Organ MG. Multicapillary flow reactor: synthesis of 1,2,5-thiadiazepane 1,1-dioxide library utilizing one-pot elimination and inter-/intramolecular double aza-Michael addition *via* microwave-assisted continuous-flow organic synthesis (MACOS), *J. Flow Chem.* 2, 2012, 118–123.
- [49] Zang Q, Javed S, Ullah F, Zhou A, Knudtson CA, Bi D, Basha FZ, Organ MG, Hanson PR. Application of a double aza-Michael reaction in a ‘click, click, Cy-click’ strategy: from bench to flow, *Synthesis* 17, 2011, 2743–2750.
- [50] Shore G, Yoo WJ, Li CJ, Organ MG. Propargyl amine synthesis catalyzed by gold and copper thin films by using microwave-assisted continuous-flow organic synthesis (MACOS), *Chem. Eur. J.* 16, 2010, 126–133.

## 10 Microwaves in green and sustainable chemistry

### 10.1 Microwaves and the 12 principles of green chemistry. Energy Efficiency

Green chemistry has been considered to be one of the last chemical revolutions because it protects the environment, not by cleaning it up, but by developing new chemical processes that prevent pollution (*benign by design*) [1]. Green chemistry had its origins with the publication of a book by Anastas and Warner in 1998 [2], and this area has increased in importance in recent years in research [3], industry [4], and education [5].

Anastas and Warner defined the 12 principles of green chemistry to design environmentally benign processes (Table 10.1).

Microwave radiation is an alternative source of energy that has been employed to introduce energy into reactions. Microwave heating exploits the ability of some compounds (liquids and solids) to transform electromagnetic energy into heat. At first glance, microwave chemistry is related to the fifth, sixth, and ninth principles of green chemistry. The use of microwave irradiation in conjunction with environmentally benign solvents or solvent-free conditions have been advertised as green (fifth principle), and similar arguments can be applied with respect to the catalytic transformations that are very common in microwave chemistry (ninth principle) [6].

The absorption and transmission of energy in microwave chemistry is completely different from the conventional mode of heating. Whereas microwave irradiation produces an efficient, rapid, and internal heating by direct coupling of microwaves with

**Tab. 10.1:** The 12 principles of green chemistry [2]

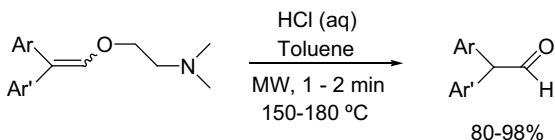
- 
1. Prevent waste
  2. Maximize the atom economy
  3. Design less hazardous chemical syntheses
  4. Design safer chemicals and products
  5. Use safer solvents and reaction conditions
  6. Increase energy efficiency
  7. Use renewable feedstocks
  8. Avoid chemical derivatives
  9. Use catalysts, not stoichiometric reagents
  10. Design chemicals and products to degrade after use
  11. Analyze in real time to prevent pollution
  12. Minimize the potential for accidents
-

the molecules that are present in the reaction mixture, conventional forms of heating are rather slow and inefficient as a result of superficial heating. In this context, the use of microwaves in green chemistry could relate to the sixth principle owing to increased energy efficiency. However, several authors have expressed doubts about the greenness of microwave-assisted reactions (the magnetron transforms only 65% of electrical energy into electromagnetic radiation) [6]. Indeed, it has even been considered that ball milling could be more efficient in terms of energy consumption [7]. In contrast, a complete cost study on a production plant concluded that integrated microwave heating and microflow processing employing a micropacked-bed reactor represent a cost-efficient system compared with a wall-coated microreactor [8].

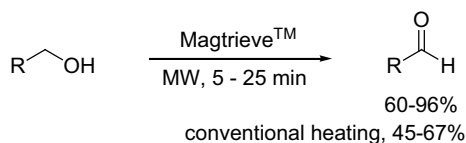
### 10.1.1 Dielectric properties (solvents and polar compounds)

The magnitude of microwave heating depends on the dielectric properties of the molecules that are present in the reaction mixture: compounds with a high dielectric constant tend to absorb microwave energy efficiently, whereas less polar materials and highly ordered crystalline substances do not absorb radiation and are not heated (*selective heating*). This characteristic was usefully exploited by Strauss using a two-phase water/chloroform system to perform a Hofmann elimination [9] and by Hallberg in the preparation of  $\beta,\beta$ -diarylated aldehydes in a toluene/ $\text{HCl}_{(\text{aq})}$  system (Scheme 10.1) [10]. In contrast to the low yield and extensive byproduct formation in conventional acid-catalyzed hydrolysis, diaryl aldehydes were isolated with high purity and in high yield through a two-phase microwave approach. Despite reaction temperatures reaching up to 180 °C in the acidic media, sensitive aldehydes were isolated after partitioning into the weakly microwave-absorbing toluene layer. The two-phase (microwave-absorbant/microwave-transparent) system explains the different temperatures and reactivities of both solvents under microwaves and the outcomes observed in the last examples.

Selective heating has also been exploited in catalysis. In homogeneous catalysis several environmental advantages have been reported [11]: the combination of metal catalysts with water as the solvent in air, the use at high temperatures of milder and less toxic reagents, and the prospect of combining efficient synthesis without the need for chromatographic purifications. In heterogeneous catalysis heating is concentrated



**Scheme 10.1:** Preparation of  $\beta,\beta$ -diarylated aldehydes under microwaves in a two-phase (absorbant/transparent) system [10]



**Scheme 10.2:** Preparation of carbonyl compounds by microwave selective heating [13]

on the mass of the catalyst, while the rest of the reaction medium remains relatively cool [12]. Thus, an efficient oxidation of alcohols using Magtrieve™ was reported by Bogdal [13] (Scheme 10.2). Magtrieve™ can reach temperatures up to 360 °C after 2 min of microwave irradiation, although when toluene was added to the reaction mixture, the reaction medium reached ca. 140 °C with a uniform temperature distribution.

Several authors have described the concept and advantages of *molecular radiators* in microwave chemistry [14]. These strongly absorbing reagents act by channeling energy from the microwave radiation to bulk heat, thereby improving the reaction conditions and providing cleaner reaction mixtures with high yields of products.

### 10.1.2 Use of susceptors

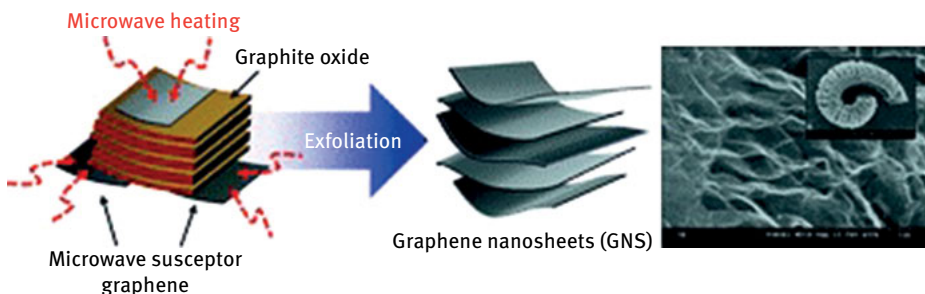
As mentioned in Section 10.1.1, nonpolar substances are poorly heated by microwaves. In other cases, the temperature required by the reaction cannot be achieved by the absorption inherent in the substances present in the medium. These problems can be solved by the use of a susceptor: an inert material that efficiently absorbs microwave radiation and transfers the thermal energy to other substances that are poor radiation absorbers.

Numerous substances have been used as passive heating elements in microwave chemistry. Most forms of carbon, for example graphite, interact strongly with microwaves and rapidly reach very high temperatures upon irradiation (1 min > 1000 °C). The Diels–Alder cycloaddition of anthracene with diethyl fumarate supported on graphite in a dry medium was described by Dubac in 1996 [15], and since then, numerous examples of the use of this susceptor have been reported in the literature.

In 2011 Kim described the preparation within 1 min of high-quality graphene nanosheets by microwave irradiation under a hydrogen atmosphere of a mixture of graphite oxide and graphene nanosheets (10 wt.%) (Figure 10.1) [16]. Graphene acts as a microwave susceptor and provides sufficiently rapid heating for the efficient exfoliation of graphite oxide. The hydrogen atmosphere promotes the reduction of graphite oxide and prevents the formation of defects, thereby improving the quality of the graphene nanosheets.

Silicon carbide (SiC, melting point 2700 °C) is compatible with any solvent or reagent, is practically indestructible, and can be reused almost indefinitely without loss of efficiency. These characteristics have made SiC cylinders excellent microwave





**Fig. 10.1:** Preparation of graphene nanosheets by exfoliation of graphite oxide using graphene as a microwave susceptor [16]

**Tab. 10.2:** Microwave-induced temperatures of nonpolar solvents in the presence and absence of SiC as a microwave susceptor (150 W constant magnetron output power, 2 mL solvent, sealed 10 mL quartz (pure solvent) or Pyrex (solvent with SiC) vessels) [17]

Solvent	<i>T</i> without SiC(°C)	<i>T</i> with SiC(°C)	Time(s)	B. p.(°C)
CCl <sub>4</sub>	40	172	81	76
Dioxane	41	206	114	101
Hexane	42	158	77	69
Toluene	54	231	145	111
THF	93	151	77	66

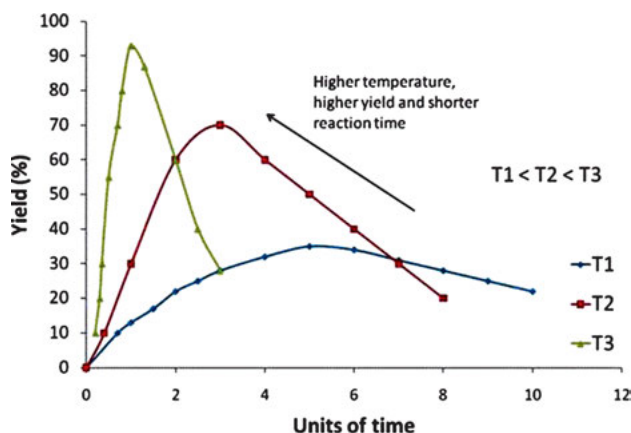
passive heating elements that are capable of rapidly raising the temperature of non-polar solvents (Table 10.2) [17].

### 10.1.3 Thermal effects

On using conventional methodologies (oil baths, heating mantles, or autoclaves) the response time is slow, and heating to high temperatures with the subsequent cooling usually requires long times. Additionally, it is difficult to avoid temperature gradients, and it is therefore common to observe pyrolytic degradation of compounds on or close to the inner walls of a vessel.

Vessels for microwave chemistry are normally made from microwave-transparent materials, and direct bulk heating, combined with efficient mechanical stirring, helps to minimize temperature gradients since the energy is absorbed directly by the components of the reaction rather than the vessel.

Depending on the kinetics of the individual processes and the thermal stability of the products, rapid and precise heating is a significant tool for obtaining high yields of products in short times. On using thermally sensitive products or in competitive reactions in which it is a prerequisite to avoid overreaction, it may be necessary to perform



**Fig. 10.2:** Schematic plots depicting influence of time and temperature on yield of a product for the same competitive thermal process conducted at temperatures of T1 (lowest), T2, and T3 (highest) [18].

rapid heating and rapid postreaction cooling. For these reasons, Strauss [18] stated that “thermal reactions proceed optimally when they are rapidly heated to the highest tolerable temperature, held there for the shortest possible time and then quenched” (Figure 10.2). These conditions can be nicely achieved in microwave chemistry.

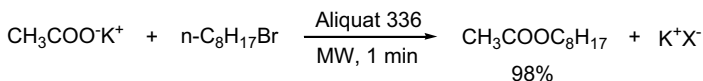
## 10.2 Reactions in green solvents

### 10.2.1 Solvent-free reactions

Microwave-assisted processes in the absence of organic solvents lead to a clean, efficient, and sustainable technology. Additionally, safety is increased significantly, the work-up is considerably simpler, costs are reduced, larger quantities of reactants can be used, the reactivity is enhanced, and, in some cases, the selectivity is modified. In the absence of solvent the microwaves are directly absorbed by the reagents, thereby increasing the energy savings and having effects on yield and selectivity [19].

Loupy classified microwave-assisted processes in dry media into three types [20]: (1) reactions with neat reactants requiring at least one liquid polar compound; (2) reactions with supported reagents by adsorption of compounds on alumina, silica, or clays; and (3) phase transfer catalysis in solvent-free conditions with a liquid compound acting as both a reagent and an organic phase.

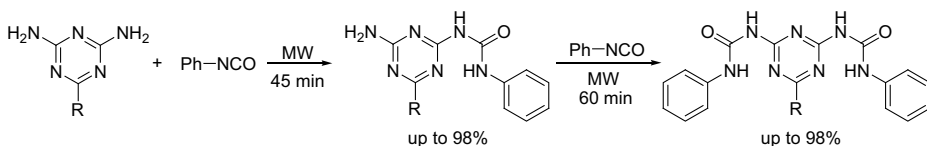
This methodology was first described by Loupy in 1993 when he reported the alkylation of potassium acetate using equivalent amounts of salt and alkylating agent in the presence of Aliquat 336 (10% mol) (Scheme 10.3) [21]. After 1–2 min of microwave irradiation, practically quantitative yields were obtained in these reactions regard-



**Scheme 10.3:** Solvent-free preparation of esters under microwave irradiation [21]

less of the nature of the halide leaving group, the chain length, and the scale (up to 500 mmol).

As a recent example, de la Hoz et al. [22] described an efficient and sustainable microwave-assisted approach for the preparation of a wide range of 1,3,5-triazinyl mono- and bisureas in the absence of solvent (Scheme 10.4). The unreactive amino groups attached to the triazine ring are able to react with phenylisocyanate under these conditions. Products were obtained with an economical and sustainable purification procedure that involved simply washing with a solvent (diethyl ether or ethanol).



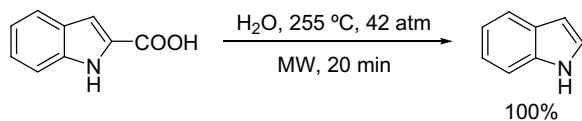
**Scheme 10.4:** Sustainable preparation of 1,3,5-triazinyl bisureas in absence of solvent [22].

### 10.2.2 Reactions in water

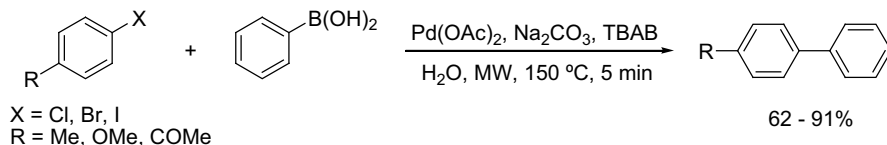
Water is a naturally abundant, nontoxic, noncorrosive, and nonflammable compound. These properties make water a truly sustainable solvent. The main drawback with water is that most organic substrates are insoluble in it [23]. However, the dielectric constant of water decreases from 78 at 25 °C to 20 at 300 °C (comparable to the dielectric constant of acetone at room temperature). As a consequence, water behaves as a pseudo-organic solvent at high temperatures. In addition, the isolation of products is normally facilitated by the decrease in the solubility of the organic substances upon postreaction cooling. Moreover, the dissociation constant of water increases from  $10^{-14}$  at 25 °C to  $10^{-11.3}$  at 300 °C. Hence, water is a much stronger acid and base at high temperatures.

Strauss exploited the rapid heating induced by microwaves in the decarboxylation of indole-2-carboxylic acid in water at 255 °C and 42 atm to obtain quantitative yields within 20 min (Scheme 10.5) [9].

Leadbeater and Marco described microwave-assisted Suzuki reactions in aqueous media (Scheme 10.6) [24]. These processes generally afforded good yields and required short reaction times, although with aryl chlorides poorer results were obtained. This



**Scheme 10.5:** Decarboxylation of carboxylic acids in water under microwaves [9]



**Scheme 10.6:** Suzuki reactions in aqueous media under microwaves with simultaneous cooling. TBAB: tetrabutylammonium bromide [24]

problem was solved by carrying out the process in an aqueous medium using a simultaneous cooling technique in conjunction with microwave heating to raise the irradiation power.

### 10.2.3 Reactions in ionic liquids

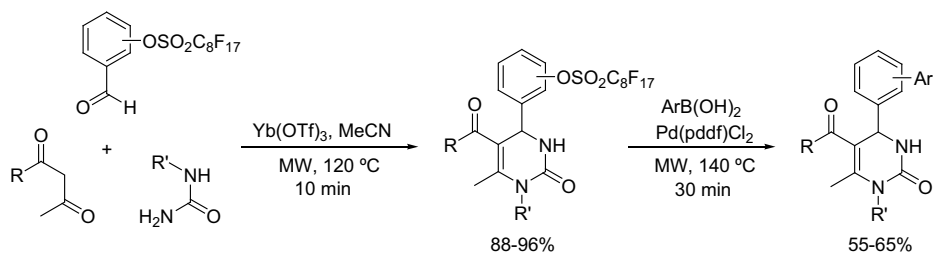
Ionic liquids (ILs) are molten salts that are formed by an array of heterocyclic cations and different anions. ILs have negligible vapor pressure, are recyclable and compatible with most organic compounds and organometallic catalysts, and they can be easily separated from reaction products.

Owing to their polar and ionic character, ILs couple with microwave irradiation very efficiently and reach very high temperatures in short times [25]. Leadbeater and Torrenius [26] studied the effect of adding a small amount of ionic liquid to several solvents. As shown by the results in Table 10.3, the addition of 10–55 mg IL to 2 mL solvent can raise the temperature well above its boiling point. In this sense, an ionic liquid can be employed as a microwave susceptor.

Varma and Namboodiri [27] described the preparation of ionic liquids, such as 1,3-dialkylimidazolium tetrachloroaluminate, and their use as recyclable catalysts for the protection of alcohols as tetrahydropyranyl (THP) ethers and for the deprotection of THP ethers.

Catalytic transfer hydrogenation of conjugated compounds has been performed with an IL, namely 1-butyl-3-methylimidazolium hexafluorophosphate (bmimPF<sub>6</sub>), as solvent under microwave irradiation with ammonium formate as a hydrogen source and palladium on carbon as the catalyst (Scheme 10.7) [28]. The catalyst/solvent system can be easily recycled.





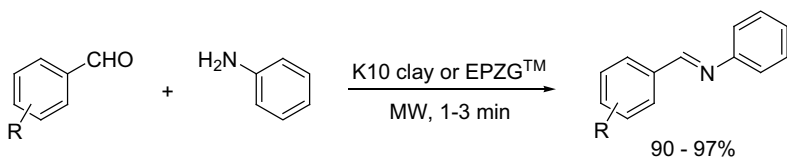
**Scheme 10.9:** Sustainable processes using fluoros chemistry under microwave irradiation [31].

### 10.3 Reactions with solid supports

The use of organic reagents within or on an inert inorganic support provides a large effective reaction area and also makes separation of the products easier. The application of microwave irradiation in supported reactions has had a profound impact on such heterogeneous processes. Mineral oxides are, in many cases, poor conductors of heat, but they behave as efficient microwave absorbers, providing rapid and homogeneous heating of the reaction mass and less decomposition of final products when compared to classical heating [32].

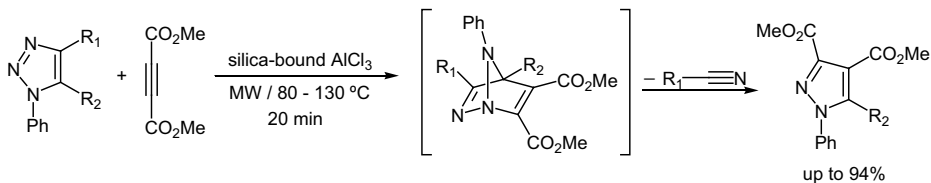
Generally, reactants are impregnated onto the solid support and reactions are performed in the absence of solvent under microwave irradiation. Alumina, silica, clay, or doped surfaces have all been used as solid supports. This methodology has been applied to deprotection, condensation, cyclization, rearrangement, oxidation, and reduction processes [33].

Imines and enamines can be easily prepared in a supported process using montmorillonite K10 or Envirocat reagent (EPZG<sup>TM</sup>) (Scheme 10.10) [34]. The authors employed low-power irradiation or intermittent heating to avoid the loss of low boiling reactants.



**Scheme 10.10:** Preparation of imines under microwaves with solid supports [34].

1,2,3-Triazoles can act as dienes in Diels–Alder cycloadditions catalyzed by silica-bound  $\text{AlCl}_3$  with extrusion of a nitrile molecule to afford pyrazole derivatives (Scheme 10.11) [35]. The recyclable supported Lewis acid catalyst can be reused five times without a decrease in activity.



**Scheme 10.11:** Diels–Alder reaction of 1,2,3-triazoles catalyzed by a recyclable Lewis acid [35].

## 10.4 Synergy with other sustainable technologies

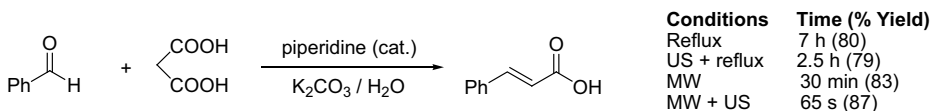
### 10.4.1 Ultrasound

Improvements in the reactivity with ultrasound (US) waves are not due to direct interaction between US and matter but to a phenomenon called cavitation: the formation and effects of gas or vapor bubbles and bubble clouds in a liquid. Cavitation results in the formation of fine emulsions between immiscible phases and creates liquid streams that violently hit the surface of the reagents, thus cleaning it and inducing fragmentation. Consequently, the combination of microwaves and US increases the reactive surface and heat transfer, and this has several advantages: (1) stronger activation with catalysts or poorly reactive substrates; (2) reduction in the catalyst load; (3) improvements in homogenization of heterogeneous systems; (4) lower reaction temperatures; (5) higher conversion rates in shorter reaction times to afford purer products; and (6) greener protocols in general [36].

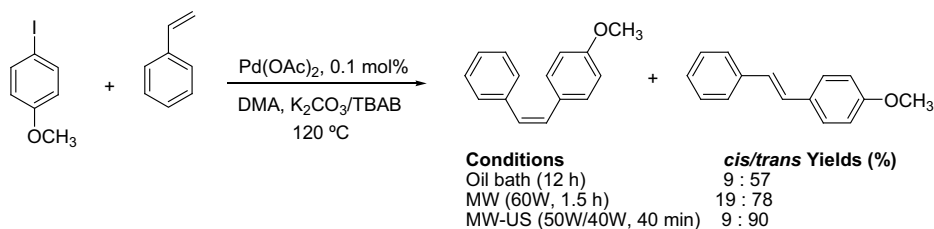
In the field of natural products an efficient extraction of flavonoids has been reported that employs US for cell disruption and extraction followed by microwave drying under vacuum, thus increasing the extraction yield without any change in the product bioactivity [37].

Peng and Song [38] described significant improvements in several organic transformations, including hydrazinolysis of esters in dry media, Williamson ether synthesis without a phase-transfer catalyst, and aqueous Knoevenagel–Doebner reactions to obtain 3-aryl acrylic acids (Scheme 10.12).

Likewise, Cravotto et al. [39] described the utility of simultaneous microwave–US irradiation in Heck reactions to obtain good yields and diastereomeric *cis/trans* stilbene ratios within 1 h of irradiation and employing low ligandless catalyst loads (Scheme 10.13).



**Scheme 10.12:** Knoevenagel–Doebner reaction under combined reaction conditions [38].

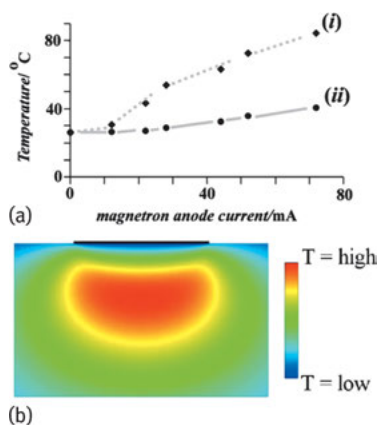


**Scheme 10.13:** Heck reaction in different reaction conditions [39].

### 10.4.2 Electrochemistry

Electrochemical processes are heterogeneous in nature and, consequently, they are dependent on transport by diffusion-convection, adsorption-desorption processes, electron transfer at the solid/liquid interface, and so forth. All of these steps may be modified by microwaves, not only by a direct polarization effect but by thermal effects, thermal gradients as a result of localized heating, and transport effects owing to microwave-induced convection [40].

Microwave activation in electrochemistry and electrosynthesis was introduced in 1998 [41]. In large-electrode processes microwaves are responsible for the preferential heating of the electrode material in comparison with the solution phase dielectric (Figure 10.3a). This effect can be exploited in electrodeposition processes [42]. Smaller electrodes have the ability to *focus* the microwave radiation on a small region, generally in front of the electrode, and this results in significant temperature-gradient effects (so-called antenna effects) (Figure 10.3b) [43]. These effects are based on the formation of microwave-induced hot spots.



**Fig. 10.3:** (a) Plot of average electrode surface temperature determined potentiometrically under flow (i) and the solution outlet temperature vs. magnetron anode current (applied microwave intensity) (ii). (b) Gradient temperature in critical region close to electrode surface [40, 43]



In these processes microwaves are also responsible for the extremely high mass transport. At low microwave power, solution heating induces convective flow of the liquid (due to hot spots), whereas at high power this changes to an oppositely directed liquid jet (owing to the formation of vapor bubbles). On using carbon electrodes, heating to the boiling point and mass transport enhancement are observed due to the direct heating of the electrode [40].

The first quantitative account of the effects of microwave irradiation on electrochemical processes in nonaqueous media was described by Marken et al. [44]. The authors studied the oxidation of ferrocene (E process) and the electroreduction of some halogenated nitrobenzenes (ECE process).

### 10.4.3 Photochemistry

A combination of the action of UV/Vis light and microwave radiation on chemical substances to achieve synergic effects has been called *microwave photochemistry* or *microwave photocatalysis*. The energy of microwaves ( $E = 0.98 \text{ J mol}^{-1}$  at  $\nu = 2.45 \text{ GHz}$ ) is much lower than that of UV/Vis radiation ( $E = 600\text{--}170 \text{ kJ mol}^{-1}$  at  $\lambda = 200\text{--}700 \text{ nm}$ ) and is clearly insufficient to break common organic bonds. Thus, it can be assumed that UV/Vis radiation is responsible for photochemical transformations, and microwaves affect the course of the reaction [45].

Photoreactors used in microwave-assisted experiments in a batch flask are classified according to the different arrangements of the lamp (external vs. internal UV/Vis source). Reactors with an internal UV/Vis source generally employ an electrodeless discharge lamp (EDL). An EDL consists of a glass tube filled with an excitable substance (frequently Hg) and an inert gas that is sealed under low pressure. The microwave field provokes gas discharge, and this causes the emission of UV/Vis radiation. Owing to the absence of electrodes, EDLs are usually characterized by lower contamination and a longer lifetime [46]. The use of EDLs in microwave photochemistry has several advantages and disadvantages (Table 10.4) [45].

Microwave photochemistry in flow-through reactors has also been developed in the last decade with both UV lamps and EDL employed. Four types of techniques for flow-through setups have been implemented: (1) internal classical UV lamp; (2) annular reactor with internal EDL; (3) cylindrical reactor surrounded by EDL; and (4) mixed reactor with internal EDL.

As a *green* application, Hidaka and Serpone showed that microwave photocatalysis can be an efficient, attractive, and clean technology for pollution abatement in water under mild conditions [47]. They studied the  $\text{TiO}_2$ -photocatalyzed degradation of substances bearing various functional groups. Titanium(IV) oxide has an inherent photocatalytic activity, and it is inexpensive, chemically and thermally stable, non-toxic, and available in large quantities. Additionally, this compound can be easily recovered and reused in immobilized form as a thin film on glass substrates.

**Tab. 10.4:** Advantages and disadvantages of EDLs in microwave photochemistry [45]

Advantages	Disadvantages
<ul style="list-style-type: none"> <li>– Simultaneous UV/Vis and microwave irradiation of reaction mixture</li> <li>– Simplicity of experimental setup (commercial microwave oven and EDL)</li> <li>– Low cost of EDL</li> <li>– Possibility to perform photoexperiments at high temperatures</li> <li>– Good photo-efficiency (EDL is inside the reaction mixture)</li> <li>– Appropriate choice of EDL material can modify its spectral output</li> </ul>	<ul style="list-style-type: none"> <li>– Technical difficulties on carrying out experiments at temperatures below the solvent boiling point</li> <li>– Intensity of EDL strongly depends on experimental conditions:               <ul style="list-style-type: none"> <li>(a) boiling point, polarity and transmittance of solvent</li> <li>(b) output and type of microwave reactor</li> <li>(c) type and intensity of cooling</li> </ul> </li> </ul>

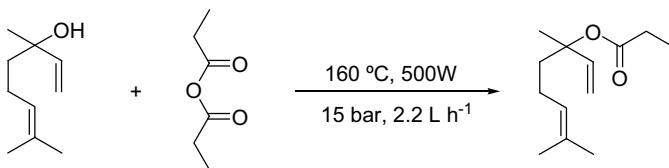
#### 10.4.4 Flow chemistry

Despite the sustainable and eco-friendly advantages of microwave radiation, significant technological drawbacks are encountered in scaling this approach beyond a few grams due to the limited penetration depth of microwaves into absorbing materials: for example, at 2.45 GHz, the frequency of most commercial microwave reactors, the penetration depth is on the order of a few centimeters. To overcome this problem, microwave continuous- or stop-flow reactors have been developed. In these systems the reaction mixture is passed through a relatively small microwave cavity. This green synthetic methodology is called microwave-assisted continuous-flow organic synthesis (MACOS) [48]. Continuous flow enables excellent control over reaction parameters and can increase the rate, yield, and selectivity of reactions, as well as enhancing the safety and reproducibility of the processes. Additionally, microwave technology can take advantage of these capabilities to process large amounts of reagents.

Since the synergy between microwave irradiation and flow was described by Strauss et al. in 1994 [49] various excellent reviews and book chapters have been published in the literature [48, 50]. Chapter 12 of this book is dedicated to microwaves in flow chemistry. Therefore, commercially available instrumentation or methodological considerations will not be included in this section. Our aim here is to highlight some sustainable examples.

Methylation reactions normally require the use of very toxic compounds, such as methyl iodide, or unsafe reagents, such as diazomethane. Dialkyl carbonates are safer alkylating agents that allow environmentally friendly procedures – the corresponding alcohol and CO<sub>2</sub> are the only byproducts formed. Since the conventional use of these green chemicals requires high temperatures and long reaction times, the combination of microwave and flow chemistry provides dramatic rate enhancements and a safer scalability [51].

The esterification of tertiary alcohols can be a problematic process if other functional groups are present or the process must be scaled up from the laboratory scale to production scale. Ondruschka et al. [52] carried out the esterification of linalool under microwave irradiation on a 25 kg scale employing a high flow rate of 2.2 L h<sup>-1</sup> (Scheme 10.14).



**Scheme 10.14:** Preparation of linalool on a production scale using MACOS [52].

## 10.5 Conclusions

In this chapter we have described how microwave irradiation can be employed under green and sustainable conditions. We have attempted to highlight the sustainable applications of this methodology and the synergy with other green technologies that has allowed the expansion of microwave radiation in all fields of chemistry.

## Bibliography

- [1] Varma RS. Journey on greener pathways: from the use of alternate energy inputs and benign reaction media to sustainable applications of nano-catalyst in synthesis and environmental remediation. *Green Chem* 2014, 16, 2027–2041.
- [2] Anastas PT, Warner J. *Green Chemistry. Theory and Practice*. Oxford University Press, Oxford, 1998.
- [3] Li C-J, Anastas PT eds. *Chem Soc Rev* 2012, 41 (4).
- [4] Dunn PJ. The importance of green chemistry in process research and development. *Chem Soc Rev* 2012, 41, 1452–1461.
- [5] Burmeister M, Rauch F, Eilks I. Education for sustainable development (ESD) and chemical education. *Chem Educ Res Pract* 2012, 13, 59–68.
- [6] Moseley JD, Kappe CO. A critical assessment of the greenness and energy efficiency of microwave-assisted synthesis. *Green Chem* 2011, 13, 794–806.
- [7] Schneider F, Szuppa T, Stolle A, Ondruschka B, Hopf H. Energetic assessment of the Suzuki-Miyaura reaction: a curttate life cycle assessment as an easily understandable and applicable tool for reaction optimization. *Green Chem* 2009, 11, 1894–1899.
- [8] Benaskar F, Ben-Abdelmoumen A, Patil NG, Rebrov EV, Meuldijk J, Hulshof LA, Hessel V, Krtschil U, Schouten JC. Cost analysis for a continuously operated fine chemicals production plant at 10 kg/day using a combination of microprocessing and microwave heating. *J Flow Chem* 2011, 2, 74–89.

- [9] Strauss CR, Trainor RW. Developments in microwave-assisted organic chemistry. *Aust J Chem* 1995, 48, 1665–1692.
- [10] Nilsson P, Larhed M, Hallberg A. Highly regioselective, sequential, and multiple palladium-catalyzed arylations of vinyl ethers carrying a coordinating auxiliary: an example of a Heck triarylation process. *J Am Chem Soc* 2001, 123, 8217–8225.
- [11] Larhed M, Moberg C, Hallberg A. Microwave-accelerated homogeneous catalysis in organic chemistry. *Acc Chem Res* 2002, 35, 717–727.
- [12] Moyes RB, Bond G. Microwave heating catalysis. In: *Handbook of heterogeneous catalysis*. Wiley, 1997.
- [13] Bogdal D, Lukasiewicz M, Pielichowski A, Miciak A, Bednarz S. Microwave-assisted oxidation of alcohols using Magtrieve™. *Tetrahedron* 2003, 59, 649–653.
- [14] (a) Kaiser NFK, Bremberg U, Larhed M, Moberg C, Hallberg A. Fast, convenient, and efficient molybdenum-catalyzed asymmetric allylic alkylation under noninert conditions: an example of microwave-promoted fast chemistry. *Angew Chem Int Ed Engl* 2000, 39, 3595–3598. (b) Steinreiber A, Stadler A, Mayer SF, Faber K, Kappe CO. High-speed microwave-promoted Mitsunobu inversions. Application toward the deracemization of sulcatol. *Tetrahedron Lett* 2001, 42, 6283–6286.
- [15] Garrigues B, Laporte C, Laurent R, Laporterie A, Dubac J. Microwave-assisted Diels-Alder reaction supported on graphite. *Liebigs Ann* 1996, 739–741.
- [16] Park S-H, Bak S-M, Kim K-H, Jegal J-P, Lee S-I, Lee J, Kim K-B. Solid-state microwave irradiation synthesis of high quality graphene nanosheets under hydrogen containing atmosphere. *J Mater Chem* 2011, 21, 680–686.
- [17] Kremsner JM, Kappe CO. Silicon carbide passive heating elements in microwave-assisted organic synthesis. *J Org Chem* 2006, 71, 4651–4658.
- [18] Strauss CR, Rooney DW. Accounting for clean, fast and high yielding reactions under microwave conditions. *Green Chem* 2010, 12, 1340–1344.
- [19] (a) Loupy A, Petit A, Hamelin H, Texier-Boullet F, Jaquault P, Mathé D. New solvent-free organic synthesis using focused microwaves. *Synthesis* 1998, 1213–1234. (b) Gawande MB, Bonifácio VDB, Luque R, Branco PS, Varma RS. Solvent-free and catalysts-free chemistry: a benign pathway to sustainability. *ChemSusChem* 2014, 7, 24–44.
- [20] Bougrin K, Loupy A, Soufiaoui M. Microwave-assisted solvent-free heterocyclic synthesis. *J Photochem Photobiol C* 2005, 6, 139–167.
- [21] Loupy A, Petit A, Ramdani M, Yvanaef C, Majdoub M, Labiad B, Villemin D. The synthesis of esters under microwave irradiation using dry-media conditions. *Can J Chem* 1993, 71, 90–95.
- [22] Ruiz-Carretero A, Ramírez JR, Sánchez-Migallón A, de la Hoz A. Microwave-assisted selective and efficient synthesis of 1,3,5-triazinyl mono and bisureas. *Tetrahedron* 2014, 70, 1733–1739.
- [23] Polshettiwar V, Varma RS. Aqueous microwave chemistry: a clean and Green synthetic tool for rapid drug Discovery. *Chem Soc Rev* 2008, 37, 1546–1557.
- [24] Leadbeater NE, Marco M. Rapid and amenable Suzuki coupling reaction in water using microwave and conventional heating. *J Org Chem* 2003, 68, 888–892.
- [25] Martinez-Palou R. Ionic liquid and microwave-assisted organic synthesis: A “green” and synergic couple. *J Mex Chem Soc* 2007, 51, 252–264.
- [26] Leadbeater NE, Torrenius HM. A study of the ionic liquid mediated microwave heating of organic solvents. *J Org Chem* 2002, 67, 3145–3148.
- [27] Namboodiri VV, Varma RS. Microwave-assisted preparation of dialkylimidazolium tetrachloroaluminate and their use as catalysts in the solvent-free tetrahydropyranlation of alcohols and phenols. *Chem Commun* 2002, 342–343.
- [28] Berthold H, Schotten T, Höning H. Transfer hydrogenation in ionic liquids under microwave irradiation. *Synthesis* 2002, 1607–1610.

- [29] Kadam A, Zhang Z, Zhang W. Microwave-assisted fluororous multicomponent reactions- A combinatorial chemistry approach for green organic synthesis. *Curr Org Synth* 2011, 8, 295–309.
- [30] Larhed M, Hoshino M, Hadida S, Curran DP, Hallberg A. Rapid fluororous Stille coupling reactions conducted under microwave irradiation. *J Org Chem* 1997, 62, 5583–5587.
- [31] Piqani B, Zhang W. Synthesis of diverse dihydropyrimidine-related scaffolds by fluororous benzaldehyde-based Biginelli reactions and post-condensation modifications. *Beilstein J Org Chem* 2011, 7, 1294–1298.
- [32] Kranjc K, Kočevar M. From conventional reaction conditions to microwave-assisted catalytic transformations of various substrates. State of the art in 2012 (Part A: general). *Curr Org Chem* 2013, 17, 448–456.
- [33] Varma RS, Baig N. Organic synthesis using microwaves and supported reagents. In: *Microwaves in organic synthesis*, 3rd edn., de la Hoz A, Loupy A, eds. Weinheim, Wiley-VCH, 2012. Pg. 427–479.
- [34] (a) Varma RS, Dahiya R, Kumar S. Clay catalyzed synthesis of imines and enamines under solvent-free conditions using microwave irradiation. *Tetrahedron Lett* 1997, 38, 2039–2042. (b) Varma RS, Dahiya R. Microwave-assisted facile synthesis of imines and enamines using envirocat EPZG™ as a catalyst. *Synlett* 1997, 1245–1246.
- [35] Díaz-Ortiz A, de Cózar A, Prieto P, de la Hoz A, Moreno A. Recyclable supported catalysts in microwave-assisted reactions: first Diels-Alder cycloaddition of a triazole ring. *Tetrahedron Lett* 2006, 47, 8761–8764.
- [36] (a) Cravotto G, Cintas P. Power ultrasound in organic synthesis: moving cavitation chemistry from academia to innovative and large-scale applications. *Chem Soc Rev* 2006, 35, 180–196. (b) Cravotto G, Cintas P. The combined use of microwaves and ultrasound. Methods and practice. In: *Microwaves in organic synthesis*, 3rd edn., de la Hoz A, Loupy A, Eds. Weinheim, Wiley-VCH, 2012. Pg. 541–560.
- [37] Hu Y, Wang T, Wang M-X, Han S, Wan P, Fan M-H. Extraction of isoflavonoids from *Pueraria* by combining ultrasound with microwave vacuum. *Chem Eng Process* 2008, 47, 2256–2261.
- [38] Peng Y, Song G. Combined microwave and ultrasound accelerated Knoevenagel–Doebner reaction in aqueous media: a green route to 3-aryl acrylic acids. *Green Chem* 2003, 5, 704–706.
- [39] Palmisano G, Bonrath W, Boffa L, Garella D, Barge A, Cravotto G. Heck reactions with very low ligandless catalyst loads accelerated by microwaves or simultaneous microwaves/ultrasound irradiation. *Adv Synth Catal* 2007, 349, 2338–2344.
- [40] Dale SEC, Compton RG, Marken F. Microwaves and electrochemistry. In: *Microwaves in organic synthesis*, 3rd edn., de la Hoz A, Loupy A, Eds. Weinheim, Wiley-VCH, 2012. Pg. 525–537.
- [41] Compton RG, Coles BA, Marken F. Microwave activation of electrochemical processes at micro-electrodes. *Chem Commun* 1998, 2595–2596.
- [42] Rassaei L, Jaber R, Flower SE, Edler KJ, Compton RG, James TD, Marken F. Microwave-electrochemical formation of colloidal zinc oxide at fluorine doped tin oxide electrodes. *Electrochim Acta* 2010, 55, 7909–7915.
- [43] Marken F, Tsai YC, Coles BA, Matthews SL, Compton RG. Microwave activation of electrochemical processes: convection, thermal gradients and hot spot formation at the electrode solution interface. *New J Chem* 2000, 24, 653–658.
- [44] Tsai Y-C, Coles BA, Compton RG, Marken F. Microwave activation of electrochemical processes: enhanced electrodehalogenation in organic solvent media. *J Am Chem Soc* 2002, 124, 9784–9788.
- [45] Církva V. Microwaves in photochemistry and photocatalysis. In: *Microwaves in organic synthesis*, 3rd edn., de la Hoz A, Loupy A, eds. Weinheim, Wiley-VCH, 2012. Pp. 563–598.
- [46] Církva V, Relich S. Microwave photochemistry. Applications in organic synthesis. *Mini-Rev Org Chem* 2011, 8, 282–293.

- [47] (a) Horikoshi S, Hojo F, Hidaka H, Serpone N. Environmental remediation by an integrated microwave/UV illumination technique. 8. Fate of carboxylic acids, aldehydes, alkoxy-carbonyl and phenolic substrates in a microwave radiation field in the presence of TiO<sub>2</sub> particles under UV irradiation. *Environ Sci Technol* 2004, 38, 2198–2208. (b) Horikoshi S, Serpone N. Photochemistry with microwaves. Catalysts and environmental applications. *J Photoch Photobio C* 2009, 10, 96–110.
- [48] Alcázar J, Muñoz J de M. Microwave assisted continuous-flow organic synthesis (MACOS). In: *Microwaves in organic synthesis*, 3<sup>rd</sup> edn., de la Hoz A, Loupy A, eds. Weinheim, Wiley-VCH, 2012. Pg. 1173–1204.
- [49] Cablewski T, Faux AF, Strauss CR. Development and application of a continuous microwave reactor for organic synthesis. *J Org Chem* 1994, 59, 3408–3412.
- [50] Baxendale IR, Hayward JJ, Ley SV. Microwave reactions under continuous flow conditions. *Comb Chem High T Scr* 2007, 10, 802–836.
- [51] Shieh W-C, Dell S, Repič O. 1,8-Diazabicyclo[5.4.0]undec-7-ene (DBU) and microwave-accelerated green chemistry in methylation of phenols, indoles, and benzimidazoles with dimethyl carbonate. *Org Lett* 2001, 3, 4279–4281.
- [52] Nüchter M, Ondruschka B, Bonrath W, Gum A. Microwave assisted synthesis – a critical technology overview. *Green Chem* 2004, 6, 128–141.

Abhishek Sharma and Erik Van der Eycken

# 11 Synthesis of medium-sized heterocycles under microwave irradiation

## 11.1 Introduction

Medium-sized (i.e., seven- to nine-membered) [1] heterocycles constitute an important structural component of a diverse range of biologically active natural compounds and pharmaceuticals [2–7]. Their structural framework endows them with several special properties, like the proper presentation of functional groups to the binding site of biomolecules and the introduction of conformational constraint. The latter often leads to increased binding affinity and improved bioavailability. In principle, such ring systems can be constructed by three distinct approaches, viz., intramolecular cyclization, annulation, and ring expansion. However, all of the aforementioned synthetic strategies are hampered by unfavorable transannular interactions leading to large enthalpies of activation [1, 8, 9]. Moreover, ring closure by cyclization is also hindered by entropic factors. Consequently, the synthesis of seven- to nine-membered rings has posed a significantly greater challenge in comparison to the construction of their five- and six-membered or larger ring counterparts [1].

In recent times, microwave-assisted chemistry has heralded a paradigm shift in organic synthesis as it offers several unique advantages like drastic acceleration of sluggish transformations, enhanced yields, and cleaner reactions [10, 11]. Moreover, sustained technological improvements in this arena have provided new high-throughput platforms such as microwave-assisted continuous-flow and parallel synthesis, thereby allowing rapid synthesis of biologically important chemical libraries [12]. The application of focused microwave irradiation has also opened new avenues in the traditionally challenging domain of the synthesis of medium-sized rings while circumventing bottlenecks like low yields, prolonged reaction time, and formation of side products. In this context, several elegant synthetic approaches for a diverse range of N-, O-, and S-containing seven- to nine-membered heterocycle ring systems have been devised employing microwave-assisted techniques.

This chapter will highlight the remarkable effectiveness of microwave irradiation in overcoming barriers to the efficient synthesis of otherwise challenging medium-sized heterocycles [1]. In particular, the emphasis of this chapter will be on applications of dedicated microwave instruments for the synthesis of seven- to nine-membered N-, O-, and S-containing rings.

<https://doi.org/10.1515/9783110479935-011>

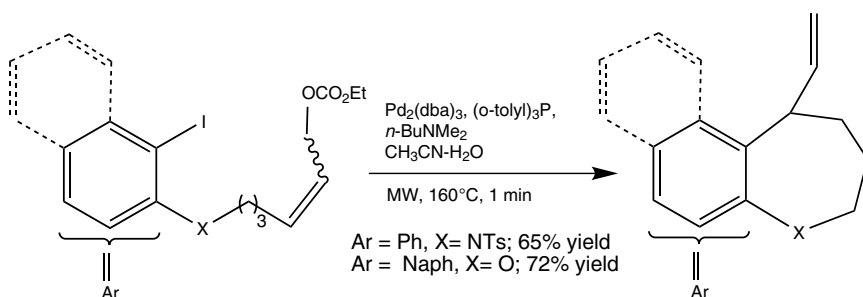
## 11.2 Microwave-assisted synthesis of seven-membered heterocycles

### 11.2.1 Benzazepine and benzoxazepine derivatives

Seven-membered heterocyclic ring systems have attracted a great deal of attention from synthetic chemists due to their preponderance in several pharmaceutically important compounds. In this context, the application of microwave irradiation has been found to be particularly useful in devising several conceptually interesting methodologies.

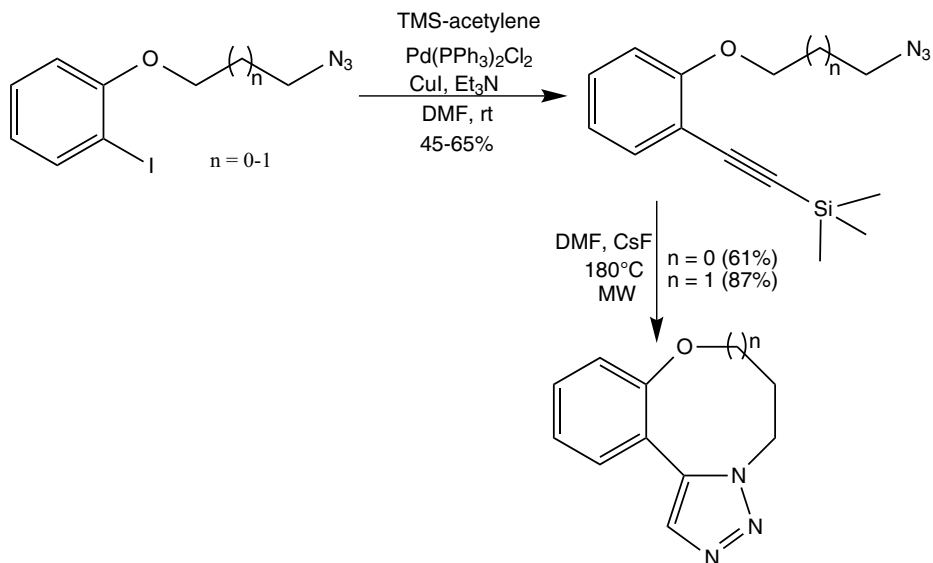
The palladium-catalyzed intramolecular coupling between an aryl halide and allyl moieties is a powerful strategy for the construction of valuable carbocyclic or heterocyclic scaffolds. In a pioneering study, Lautens and coworkers utilized allyl acetates and carbonates for microwave-assisted intramolecular coupling with aryl iodides, leading to the synthesis of seven-membered N- and O-containing heterocycles (Scheme 11.1) [13]. The initial reaction conditions involving heating under the reflux of allyl carbonates in the presence of  $\text{Pd}_2(\text{dba})_3$ , tri-*o*-tolylphosphine, and *N,N*-dimethylbutylamine in  $\text{CH}_3\text{CN}-\text{H}_2\text{O}$  led to a low yield of the desired cyclized products. However, the authors reported a tremendous enhancement in yield from 49 to 72% upon the application of microwave irradiation.

The synthesis of 1,2,3-triazoles by 1,3-dipolar cycloaddition (click chemistry) has attracted considerable attention in different domains of chemical, biological, and material sciences. Bell and coworkers recently described an elegant approach to triazolobenzoxazepines and triazolobenzoxazocines via a one-pot, two-step intramolecular cycloaddition of silicon containing azidoalkynes (Scheme 11.2) [14]. The application of microwave irradiation was found to be critical to achieve the high temperature (180 °C) needed for the annulation step as well as a very short reaction time (30 min). Interestingly, the aforementioned reaction also selectively afforded the 1,5-regioisomer of the triazole.



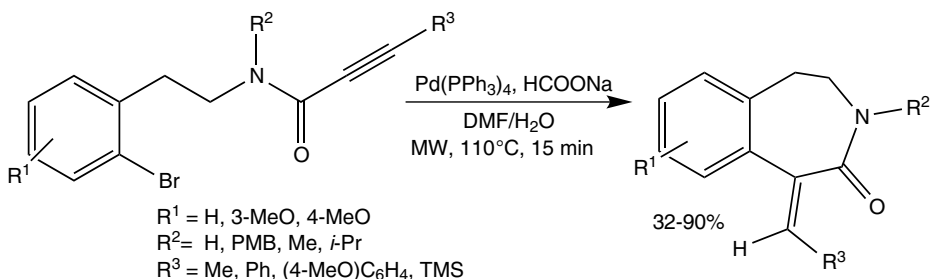
**Scheme 11.1:** Microwave-assisted intramolecular coupling between allyl acetates/carbonates and aryl halides.



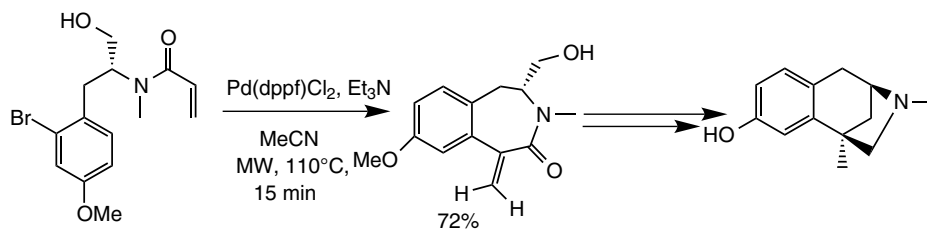


**Scheme 11.2:** Microwave-assisted synthesis of triazolobenzoxazepine via an intramolecular click reaction.

Our group has been interested in exploring the utility of microwave irradiation for the rapid and efficient synthesis of medium-sized heterocyclic ring systems. In this context, the 1-substituted 3-benzazepine framework represented an attractive target as it constitutes the core of several NMDA receptor antagonists. A fully regio- and stereoselective synthesis of 1-substituted 3-benzazepinones was developed via a microwave-assisted intramolecular Heck reductive cyclization strategy (Scheme 11.3) [15]. Thus, a series of propynoic acid amides could be rapidly cyclized into the desired seven-membered 3-benzazepinones in the presence of  $\text{Pd(PPh}_3)_4$ ,  $\text{HCOONa}$  in dimethylformamide (DMF)/ $\text{H}_2\text{O}$  at a ceiling temperature of  $110^\circ\text{C}$  in a



**Scheme 11.3:** Microwave-assisted intramolecular Heck reductive cyclization for the synthesis of 1-substituted 3-benzazepinones.

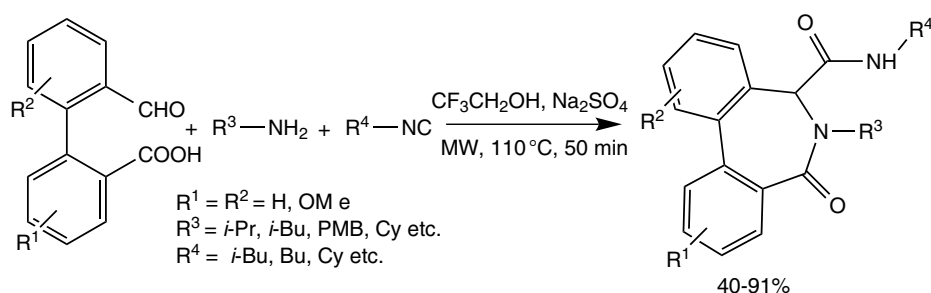


**Scheme 11.4:** Microwave-assisted formal total synthesis of 3-benzazepine alkaloid (–)-aphanorphine.

mere 15 min. In comparison, a similar reaction under conventional heating proceeded in lower yields and required a longer reaction time (3 h).

A few years later, we became interested in applying our previously described reductive cyclization approach to a formal total synthesis of the 3-benzazepine alkaloid (–)-aphanorphine (Scheme 11.4) and its analogs. However, it soon became apparent that the corresponding substrates, namely, unprotected propynoic acid amides, were unstable under the aforementioned conditions [16]. Consequently, an alternative strategy was adopted wherein a microwave-assisted intramolecular Heck reaction of an acrylamide substrate in the presence of Pd(dppf)Cl<sub>2</sub>, triethylamine in MeCN at 110 °C provided the required 3-benzazepinone (72% yield) in 15 min (Scheme 11.4). The obtained 3-benzazepinone was subsequently subjected to an intramolecular radical cyclization to afford the tricyclic core of (–)-aphanorphine.

Having explored the synthesis of seven-membered ring systems through palladium-catalyzed approaches, we wondered whether greater structural diversity could be installed on such scaffolds via a microwave-assisted multicomponent reaction (MCR). In particular, the dibenzo-[*c,e*]azepinone framework drew our attention as it bears structural resemblance with the  $\gamma$ -secretase inhibitor LY411575, developed by Eli Lilly. Subsequently, we found that the Ugi 4-component reaction of an appropriate biaryl compound bearing the required aldehyde and carboxylic acid moiety could be accomplished under microwave irradiation (110 °C) to afford the desired dibenzo-[*c,e*]azepinones in excellent diastereoselectivities (Scheme 11.5) [17]. In comparison to



**Scheme 11.5:** Microwave-assisted synthesis of dibenzo-[*c,e*]azepinones via Ugi 4 component reaction.

conventional heating, the use of microwave irradiation drastically curtailed the reaction time from 24 h to 50 min while simultaneously providing a significant increase in reaction yield.

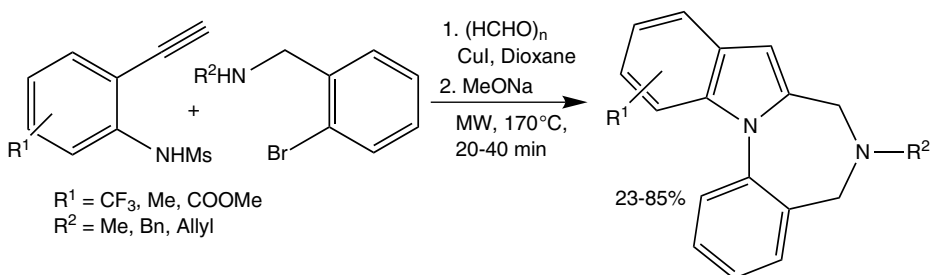
The critical step involved an acid-promoted intramolecular Friedel–Crafts cyclization of oxazolidinones via an *N*-acyliminium ion. The authors screened various Lewis acids at different reaction temperatures and found that the best results were generally obtained using  $\text{TiCl}_4$  at 80 °C. Further, the aforementioned microwave-assisted methodology proved advantageous in comparison to earlier protocols as it led to only minute racemization during the cyclization step.

### 11.2.2 Diazepines and their analogs

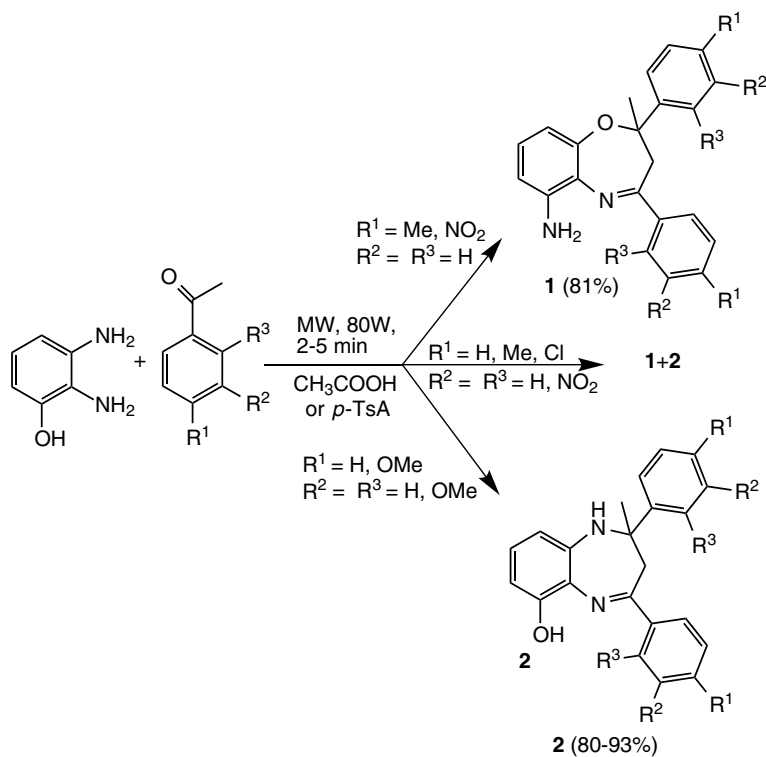
The 1,4-benzodiazepine scaffold is an important component of pharmaceuticals used for the treatment of neurological disorders. Consequently, the previously described framework has attracted considerable attention for the incorporation of greater structural diversity. Thus, Fujii, Ohno, and coworkers elaborated a microwave-assisted, novel, concise route to indole-fused 1,4-benzodiazepines. The authors utilized *N*-mesyl-2-ethynylanilines and secondary amines as precursors for a copper-catalyzed, one-pot, three-component coupling-indole formation-*N*-arylation sequence conducted at 170 °C for 20–40 min (Scheme 11.6) [18].

It was observed that the corresponding reactions under conventional heating involved long reaction times and produced lower yields. The developed microwave-assisted methodology is noteworthy as it constitutes a rare example of a copper-catalyzed reaction involving a one-pot formation of one carbon-carbon bond and three carbon-nitrogen bonds.

Stephanidou-Stephanatou and coworkers investigated the competitive formation of 6-hydroxybenzodiazepines versus 6-aminobenzoxazepines through a microwave-assisted condensation between 2,3-diaminophenol and substituted acetophenones in the presence of acetic acid or paratoluenesulfonic acid at 80 W for 2–5 min (Scheme 11.7) [19].



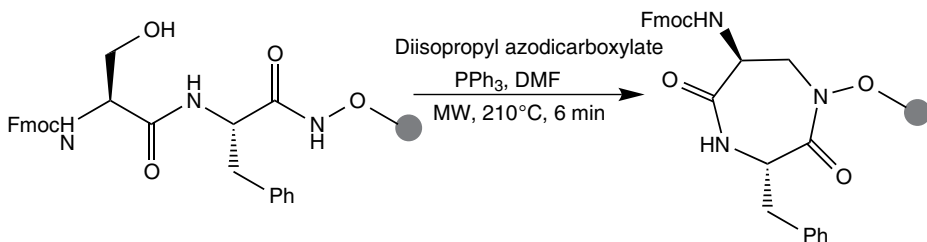
**Scheme 11.6:** Microwave-assisted, one-pot, three-component coupling-indole formation-*N*-arylation sequence for the synthesis of indole-fused 1,4-benzodiazepines.



**Scheme 11.7:** Microwave-assisted condensation between 2,3-diaminophenol and substituted acetophenones for the synthesis of benzoxazepines and benzodiazepines.

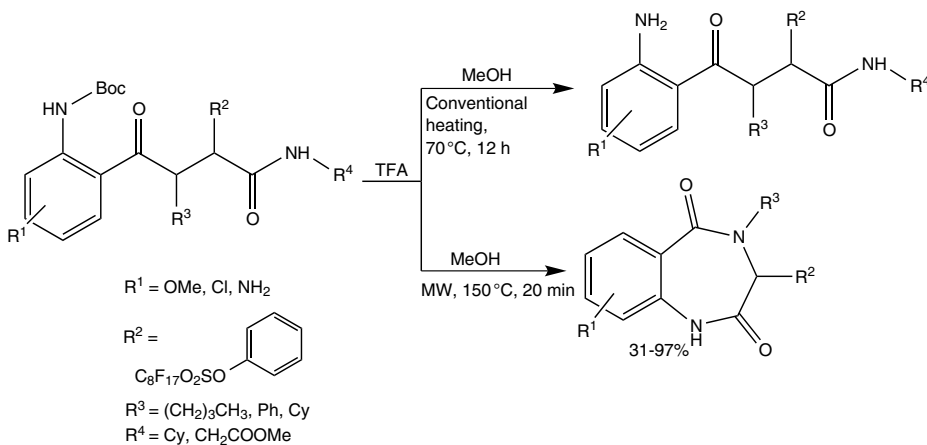
Interestingly, the nature of the seven-membered ring product depended on the type of substituents on the acetophenone moiety as the benzodiazepines constituted the kinetic products, with benzoxazepines being the thermodynamic ones. The authors also found that use of *p*-nitro substituted acetophenones afforded the respective benzoxazepines, while unsubstituted, *p*-methyl/chloro- or *m*-nitro-substituted acetophenones provided a mixture of benzoxazepines and benzodiazepines.

The conformational strain associated with medium-sized heterocycles, a factor that initially inhibits the construction of such rings, has increasingly become a cherished attribute as the introduction of these constraints in peptides can lead to more selective or potent peptide mimetics. Taddei and coworkers utilized a microwave-promoted solid-phase approach for the synthesis of 3,6-disubstituted-perhydro-diazepin-2,5-diones as conformationally constrained peptidomimics [20]. The methodology involved a Mitsunobu cyclization of a hydroxamic dipeptide (anchored to PS-DVB 2-chlorotrytyl resin) in the presence of diisopropyl azodicarboxylate, PPH<sub>3</sub> in DMF at 210 °C (Scheme 11.8).



**Scheme 11.8:** Microwave-assisted Mitsunobu cyclization of a hydroxamic dipeptide for the synthesis of 3,6-disubstituted-perhydro-diazepin-2,5-diones.

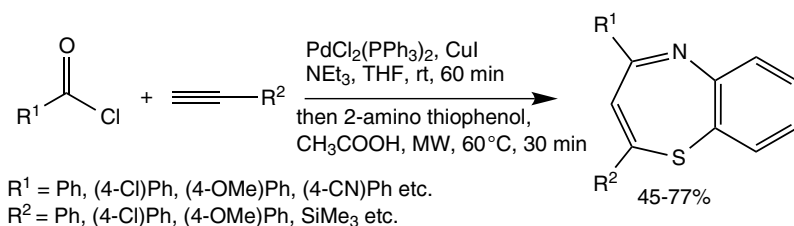
Apart from the well-known benefits of microwave-assisted synthesis like enhanced yields and reduced reaction times, the superheating effect offered by microwave irradiation can also drive a reaction that is otherwise not feasible under conventional conditions. Yan and coworkers reported such an example, where Ugi products, possessing a protected amino group and an amide, underwent sequential deprotection/cyclization at a ceiling temperature of 150 °C in 20 min, to produce the respective 1,4-benzodiazepine-2,5-diones (Scheme 11.9) [21]. In contrast, under conventional heating in refluxing methanol at 70 °C for 12 h, only the Boc-deprotected product was formed. Subsequently, the authors were able to apply this unique microwave-assisted protocol for a solution phase fluororous parallel synthesis of a library of biaryl-substituted 1,4-benzodiazepine-2,5-diones.



**Scheme 11.9:** Microwave-assisted sequential deprotection/cyclization reaction for synthesis of 1,4-benzodiazepine-2,5-diones.

### 11.2.3 Thiazepine and thiadiazepine derivatives

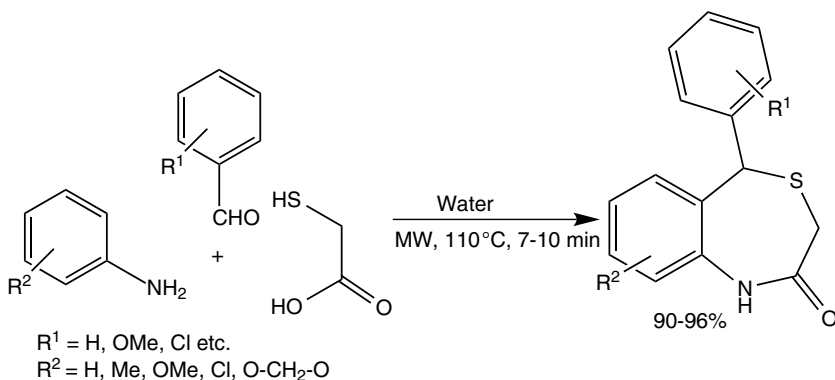
The 1,5-benzothiazepine framework has emerged as a versatile pharmacophore since its derivatives exhibit a broad range of medicinal applications such as anti-HIV, anticancer, angiotensin converting enzyme inhibitors, and antimicrobial compounds. Willey and Müller reported a one-pot, three-component synthesis of 2,4-disubstituted benzo[*b*][1,5]thiazepines [22]. The methodology comprised an initial Sonogashira coupling of acid chlorides with terminal alkynes to give the corresponding alkynones that subsequently underwent a Michael addition–cyclocondensation reaction with *ortho*-amino thiophenol in the presence of acetic acid. The authors explored the cyclocondensation step under conventional as well microwave conditions at identical temperature (60 °C), where the yield of reaction was found to have more than doubled in the case of the latter (81%) (Scheme 11.10).



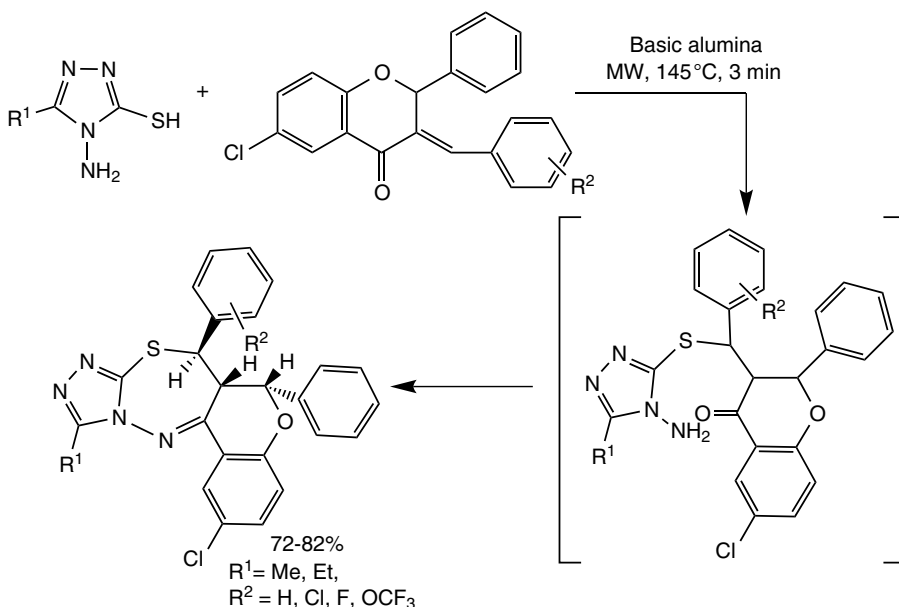
**Scheme 11.10:** Microwave-promoted Michael addition–cyclocondensation reaction for synthesis of 2,4-disubstituted benzo[*b*][1,5]thiazepines.

One of the unique benefits of microwave-assisted synthesis lies in the remarkable acceleration of reactions conducted in unconventional reaction media. In this context, the use of water as an economical and nonflammable alternative to traditional organic solvents has attracted a great deal of attention as the high dielectric constant of the former allows efficient absorption of microwave irradiation [23]. Tu and coworkers developed such a microwave-assisted reaction under aqueous conditions for an efficient synthesis of benzo[*e*][1,4]thiazepin-2-ones, which are potential therapeutic agents against Type II diabetes. The protocol involved a multicomponent reaction between a benzaldehyde, an aromatic amine and mercaptoacetic acid at 110 °C for 7–10 min using water as the only solvent (Scheme 11.11) [24]. The methodology affords a convenient route to such heterocycles as these were earlier mainly prepared through multiple steps requiring long reaction times or harsh conditions.

In addition to the use of unconventional solvents, microwave irradiation also allows the unique possibility of conducting reactions in the solid phase, that is, under solventless conditions. Dandia and coworkers disclosed a microwave-promoted synthesis of thiadiazepines possessing fused benzopyrano-triazole rings via a tandem Michael addition–condensation reaction between 3-arylidene flavanones and 4-



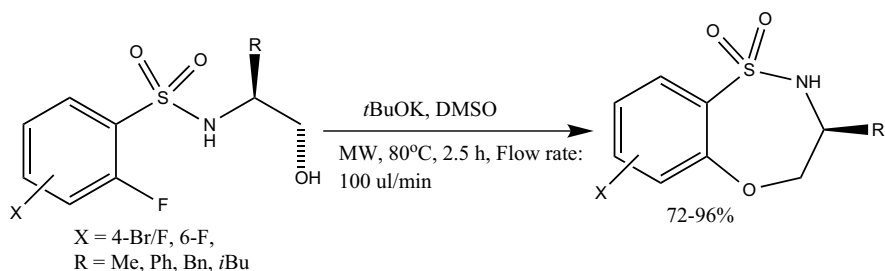
**Scheme 11.11:** Microwave-assisted multicomponent synthesis of benzo[e][1,4]thiazepin-2-ones.



**Scheme 11.12:** Microwave-promoted solid-phase synthesis of thiadiazepines.

amino-5-alkyl 3-mercaptotriazole using basic alumina as solid support at 145 °C (72–82% yield) for 3 min (Scheme 11.12) [25]. In contrast, a similar reaction under thermal conditions involved a long reaction time (60 h) and lower yields (40–47%).

The apparent limitation of vessel size and scale-up in traditional microwave-promoted synthetic approaches has led to the emergence of microwave-assisted continuous-flow organic synthesis (MACOS) as a valuable alternative. Such a MACOS-based process involving an intramolecular  $S_NAr$  O-arylation of  $\beta$ -hydroxy  $\alpha$ -fluoro benzene sulfonamides allowed Hanson, Organ, and coworkers to develop a multi-

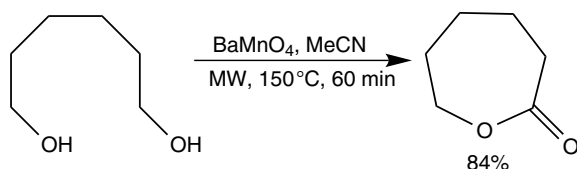


**Scheme 11.13:** Microwave-assisted continuous-flow synthesis of benzothiazepine-1,1-dioxides via an intramolecular  $S_NAr$  O-arylation of  $\beta$ -hydroxy- $\alpha$ -fluoro benzene sulfonamides.

gram synthesis of a small library of pharmaceutically important benzothiazepine-1,1-dioxides [26]. Initially, the intramolecular cyclization was explored using a standard microwave synthesizer, wherein the best reaction conditions involved a 0.1M concentration of the substrate at 140 °C for 30 min in DMF. To further increase the batch size, the authors resorted to a flow platform wherein a flow rate of 100  $\mu$ L/min at 80 °C in dimethyl sulfoxide proved to be optimum (Scheme 11.13) [26]. These conditions were subsequently applied to the synthesis of 19 benzofused sultams in 5–10 g quantities at an average production time of 2.5 h.

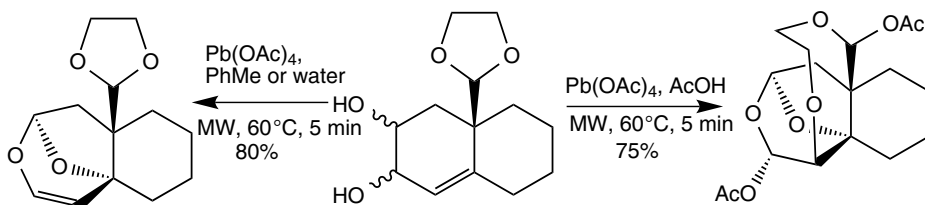
#### 11.2.4 Oxacycles

In comparison to the N- and S-containing medium-sized rings, the corresponding oxacycles have remained significantly more challenging synthetic targets. For instance, the medium-sized lactones have attracted considerable attention as these are considered to be a rare class of organic compounds that are even difficult to produce in natural biosynthetic pathways [27]. Bagley and coworkers revealed a microwave-assisted synthesis of seven-membered lactones through a tandem oxidation-cyclocondensation of 1,6-hexanediol (Scheme 11.14) [28]. Among the various oxidants screened,  $BaMnO_4$  was found to provide the best reaction performance in acetonitrile at a ceiling temperature of 150 °C for 60 min.



**Scheme 11.14:** Microwave-assisted tandem oxidation-cyclocondensation approach for the synthesis of seven-membered lactones.



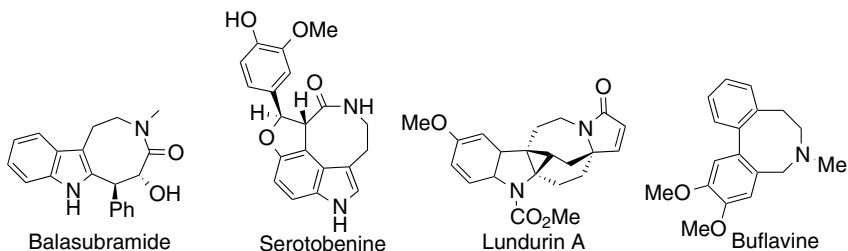


**Scheme 11.15:** Microwave-assisted domino synthesis of tri- and tetracyclic ring systems.

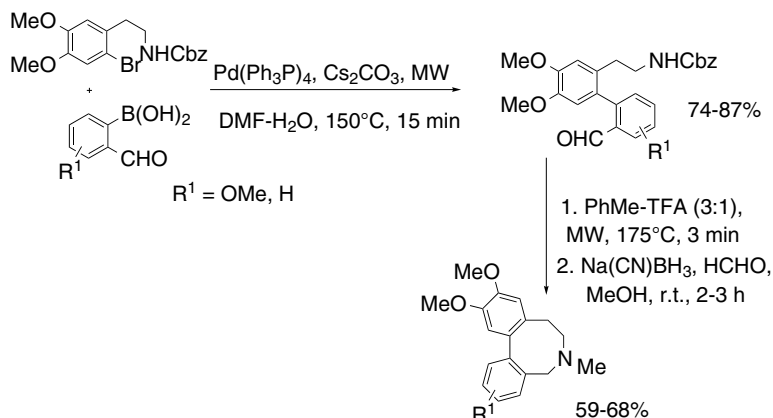
Another interesting and modular strategy for seven- or eight-membered oxygen-containing rings was presented by Arseniyadis and coworkers. The authors described a microwave-promoted and  $\text{Pb}(\text{OAc})_4$ -mediated domino transformation of octaline diols (Scheme 11.15) [29]. The methodology proved modular as just a change in solvent from toluene or water to acetic acid led to switching of product from a tricyclic to a tetracyclic compound at 60 °C. The application of microwave irradiation was also critical for this transformation as it led to a significant rate enhancement (up to tenfold) in comparison to thermal conditions.

### 11.3 Microwave-assisted synthesis of eight-membered heterocycles

Target molecules bearing an eight-membered heterocycle have attracted extensive synthetic interest in recent years owing to their presence in a large number of naturally occurring molecules like balasubramide [30], serotobenine [31], lundurine A [32], and buflavine [33] (Scheme 11.16). However, owing to the difficulty of generating the constrained eight-membered ring, published studies on the synthesis of such highly interesting targets have been scarce in the literature. In recent years, the emergence of microwave-assisted techniques as a tool for driving the otherwise improbable reactions pathways has led to a more focused research on the chemistry of these eight-membered ring systems.



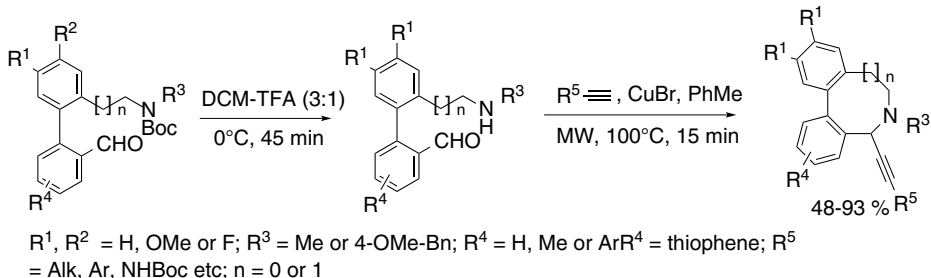
**Scheme 11.16:** Some naturally occurring compounds bearing eight-membered ring skeleton.



**Scheme 11.17:** Microwave-assisted synthesis of apogalanthamine analogs.

As part of our explorations toward the synthesis of natural product analogs featuring structurally constrained eight-membered rings, we have investigated novel and efficient pathways for the synthesis of apogalanthamine analogs (Scheme 11.17) [34]. These target molecules have a rare 5,6,7,8-tetrahydrobenzo[*c,e*]azocine skeleton composed of a biaryl-fused eight-membered *N*-heterocyclic ring and are close structural relatives of the naturally occurring *Amaryllidaceae* alkaloid bufllavine (Scheme 11.16) [33]. Our protocol chiefly depended on the combination of a microwave-assisted Suzuki–Miyaura reaction between an electron-rich phenethylamine and various boronic acids bearing an electron-withdrawing formyl group in the ortho position, followed by a microwave-assisted, rapid ring-closure reaction (Scheme 11.17). It is particularly noteworthy that the meager yields of Suzuki–Miyaura reactions between these unfavored coupling partners under conventional heating were drastically improved from 11–20% to an excellent 74–87% when performed under microwave irradiation. Furthermore, microwave-assisted conditions were helpful in promoting the formation of the highly constrained eight-membered ring system, which failed to proceed under classical ring-closure conditions.

The aforementioned strategy also enabled us to develop another protocol for the generation of biaryl-fused seven- and eight-membered *N*-heterocyclic rings. In our new approach, we investigated an intramolecular A<sup>3</sup>-coupling reaction as a key, ring-generation step under microwave-assisted conditions (Scheme 11.18) [35]. Thus the amino and aldehyde functionalities were made to react with suitable alkynes in the presence of CuBr in toluene at  $100^\circ\text{C}$  for 15 min under focused microwave irradiation, and the desired 6,7-dihydro-5*H*-dibenzo[*c,e*]azepines and 5,6,7,8-tetrahydrodibenzo[*c,e*]azocines were isolated in good to excellent yields. Altering the reaction temperature and time to  $150^\circ\text{C}$  and 5 min respectively, it was also possible to successfully transfer the microwave batch procedure to a continuous-flow process using an

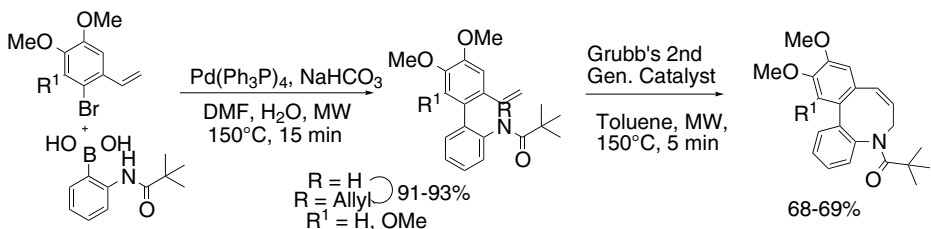


**Scheme 11.18:** Microwave-assisted intramolecular A<sup>3</sup>-coupling reactions for the synthesis of structurally diverse dibenzo[*c,e*]azocine and dibenzo[*c,e*]azepine analogs.

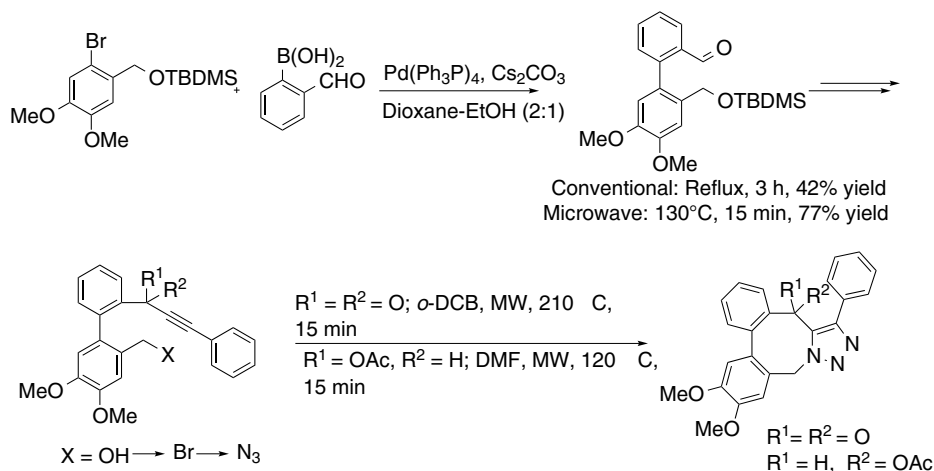
X-Cube reactor. The desired intramolecular A<sup>3</sup>-coupling product was isolated in 67% yield using a flow rate of 1.5 mL/min.

Our interest in the synthesis of structurally intriguing natural product analogs bearing highly constrained medium-sized rings led us to explore a novel protocol for the synthesis of N-shifted buflavine analogs (Scheme 11.19) [36]. The combination of a microwave-assisted Suzuki–Miyaura reaction and ring-closing metathesis (RCM) reaction was explored to successfully generate the key eight-membered ring system of these molecules (Scheme 11.19). Once again, the use of microwave irradiation was highly beneficial in promoting the cross coupling between a highly hindered and electron-rich aryl halide with a boronic acid bearing a bulkier group on the ortho position. Furthermore, microwave irradiation was found to play a pivotal role in promoting the RCM reaction to generate the highly strained ring system of the target molecules, as is evident from the shortening of the reaction time from 3 h to 5 min as well as from the increased yields of 68–69% in comparison with the 55–58% under conventional heating.

Apart from the N-shifted buflavine analogs, we have also utilized the aforementioned microwave-assisted Suzuki–Miyaura reaction between an electron-rich aryl halide and a boronic acid toward the synthesis of various other medium-sized ring-containing natural product analogs. Thus, the core biaryl skeleton of (–)-steganacin and (–)-steganone 7-aza-analogs bearing a 1,2,3-triazole subunit was assembled via a



**Scheme 11.19:** Microwave-assisted synthesis of N-shifted buflavine analogs.

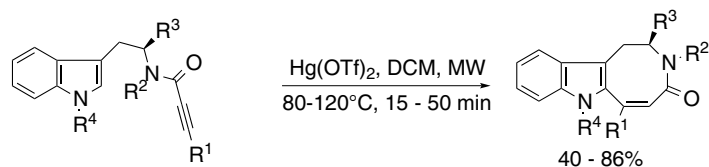


**Scheme 11.20:** Microwave-assisted synthesis of steganacin and steganone 7-aza-analogs.

microwave-assisted Suzuki reaction (77% yield) [37] in a mere 15 min, in comparison with a meager 42% yield in 3 h under conventional heating conditions (Scheme 11.20).

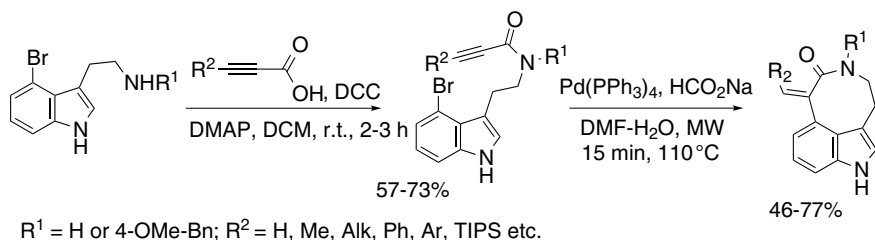
Continuing our efforts at developing novel protocols for the synthesis of N-containing medium-sized rings, we have explored an intramolecular carbocyclization mediated by  $Hg(Otf)_2$  under microwave irradiation to access the highly interesting indoloazocine framework (Scheme 11.21) [38]. A suitably decorated tryptamine or tryptophan derivative was converted into the corresponding amide to introduce a so-called cyclization handle. The final microwave-assisted carbocyclization was effected in dry dichloromethane at 80–120 °C with 5–20 mol% of  $Hg(Otf)_2$ . It is of particular interest that the reaction times of 24–40 h under conventional heating were dramatically shortened to merely 15–50 min under focused microwave irradiation while the reaction yields were similar or even higher.

As an extension of our microwave-assisted,  $Hg(Otf)_2$ -mediated carbocyclizations toward fused-indole frameworks, we have also studied a stereo- and regioselective, Pd-catalyzed, intramolecular acetylene hydroarylation reaction for accessing the



$R^1 = H, Me, Alk, Ph, Ar$  etc.;  $R^2 = H, Me, Bn$  etc.;  $R^3 = H$  or  $CH_2OTIPS$ ;  $R^4 = H, Ts$  or  $Ac$

**Scheme 11.21:** Microwave-assisted intramolecular carbocyclization for the synthesis of indoloazocines.

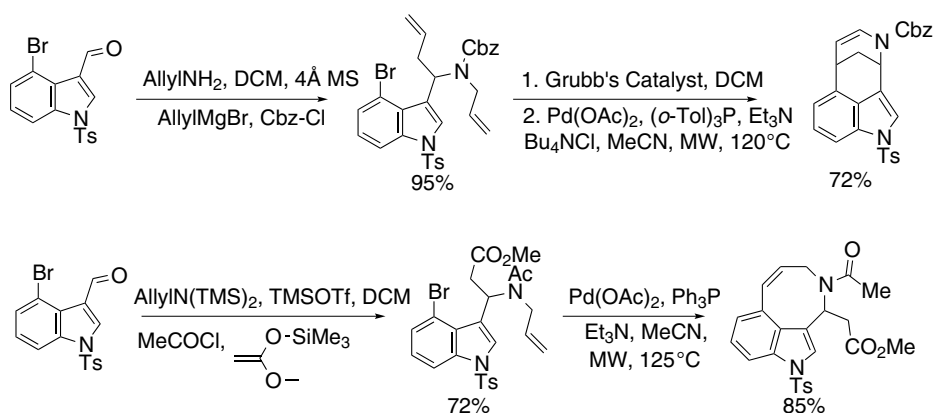


**Scheme 11.22:** Microwave-assisted synthesis of azocino[*c,d*]indoles.

highly interesting azocino[*c,d*]indole framework (Scheme 11.22) [39] often found in naturally occurring compounds like decursivine and serotobenine [40, 41]. Precursors for the intramolecular cyclizations were generated by the *N,N'*-dicyclohexylcarbodiimide-mediated amidation of suitably functionalized 4-bromotryptamines and a variety of propiolic acid derivatives. The microwave-assisted cyclizations were then carried out in a 3 : 1 mixture of DMF and water at 110 °C for 15 min using a reagent mixture of  $\text{Pd}(\text{PPh}_3)_4$  (3 mol%) and  $\text{HOONa}$  (1.5 equiv). The desired azocino[*c,d*]indole derivatives were isolated in good to excellent yields of 46–77%.

An interesting case study on the synthesis of indole-fused medium-sized ring heterocycles was delineated by Martin and coworkers [42], where the authors used an ingenious combination of a MCR and an RCM reaction together with a microwave-assisted, intramolecular Heck reaction to access the highly constrained heterocyclic cores (Scheme 11.23).

The acyclic precursors were conveniently generated from a suitably functionalized 4-bromoindole-3-carbaldehyde, which was converted into the required intermediate for cyclization in specific cases via an RCM reaction. The intramolecular Heck



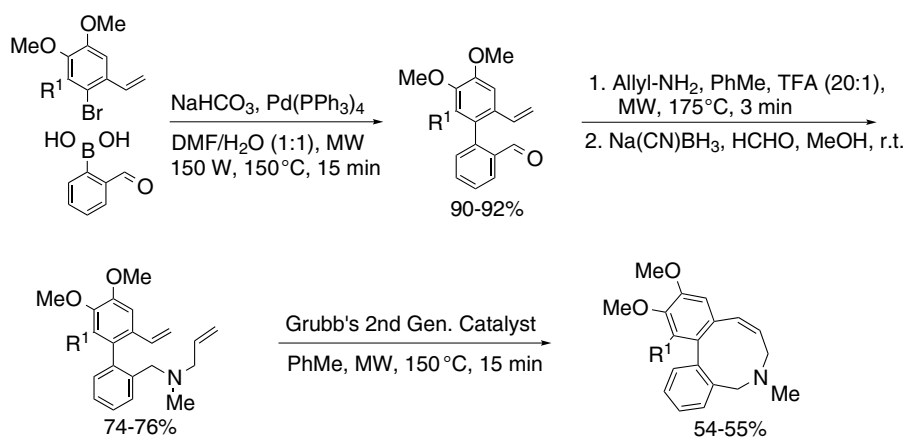
**Scheme 11.23:** Microwave-assisted RCM and intramolecular Heck reaction for the synthesis of fused ring heterocyclic systems.

reaction was then effected under microwave-assisted conditions in MeCN using Et<sub>3</sub>N as a base at 125 °C, using the combination of Pd(OAc)<sub>2</sub> and suitable phosphines as the catalyst system (Scheme 11.23). The beneficial nature of microwave irradiation is particularly evident in the synthesis of the bridged bicyclic tetracycle in 72% yield, where the highly constrained nature of the ring system makes the intramolecular cyclizations rather sluggish under conventional conditions.

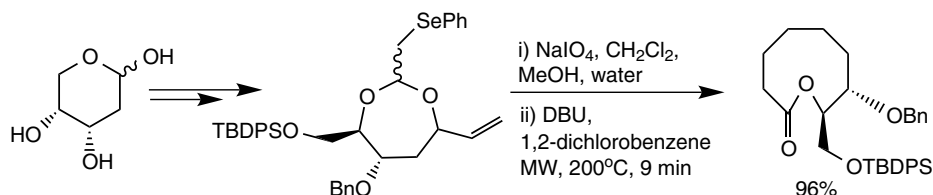
## 11.4 Microwave-assisted synthesis of nine-membered heterocycles and beyond

Despite their potential applications as valuable pharmacophores, reports on the synthesis of heterocyclic targets bearing nine- and ten-membered ring systems are scarcely available in the literature [43–45]. The primary reason for the lack of synthetic methods can be attributed to the extremely high conformational strain associated with these molecules, thereby requiring very high activation energy for the ring closure. In view of this, the emergence of microwave irradiation as a highly valued tool for facilitating hitherto difficult reaction pathways has led to significant breakthroughs in the synthesis of these intriguing classes of target molecules.

During the course of the last few years, our laboratory has carried out extensive research on the microwave-assisted synthesis of novel heterocyclic moieties bearing medium-sized rings. Once again, the formation of the key biaryl intermediate was effected by a microwave-assisted Suzuki reaction at 150 °C for 15 min in a 1:1 mixture of DMF and H<sub>2</sub>O, using NaHCO<sub>3</sub> as the base and Pd(PPh<sub>3</sub>)<sub>4</sub> as the catalyst (Scheme 11.24). The key RCM reaction for the generation of the rigid, biaryl-bearing, nine-membered ring system of the dibenzo[*c,e*]azonine skeleton was carried out under



**Scheme 11.24:** Microwave-assisted synthesis of ring-expanded bufavine analogs.



**Scheme 11.25:** Microwave-assisted synthesis of nine-membered lactone via a tandem elimination/Claisen rearrangement sequence.

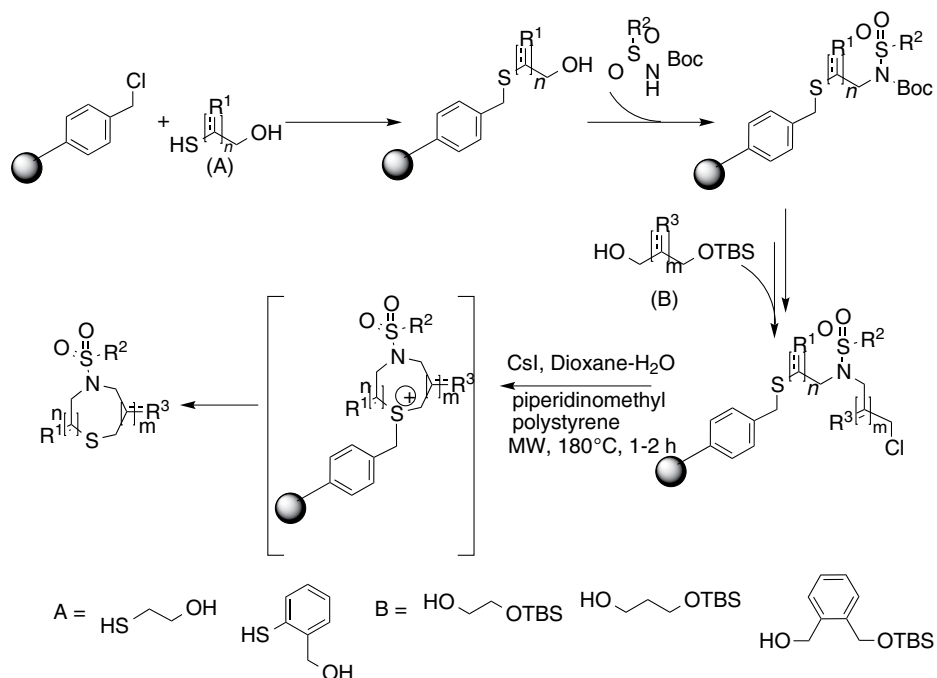
focused microwave irradiation in toluene at 150 °C for 15 min, wherein the fused-ring targets were isolated in 54–55% yield. It is noteworthy that the RCM has resulted in a far inferior yield of 15% when performed under conventional heating conditions, clearly underlining the beneficial effect of microwave irradiation on the synthesis of these nine-membered ring systems (Scheme 11.24) [46].

In the course of their total synthesis of naturally occurring oxacycle (+)-obtusenyne and its analogs, Burton, Holmes, and coworkers elaborated a microwave-assisted approach to a nine-membered lactone. The methodology utilized 2-deoxy-D-ribose as substrate for the initial formation of a selenoacetal that was oxidized into the corresponding selenoxide. Subsequently, the selenoxide was subjected to a tandem elimination/Claisen rearrangement sequence in the presence of 1,8-diazabicyclo[5.4.0]undec-7-ene under microwave irradiation at a ceiling temperature of 200 °C for 9 min to deliver the corresponding nine-membered lactone (96% yield) (Scheme 11.25) [47]. The authors found that the application of microwave irradiation afforded an improved yield in comparison to conventional heating.

Compounds possessing a sulfonamide-containing cyclic sulfide skeleton exhibit a diverse array of intriguing biological activities such as antimalarial and antiobesity effects [48, 49]. Saruta and coworkers explored the traceless, solid-supported synthesis of a variety of seven-, eight-, and nine-membered ring sulfides bearing multiple sulfonamide groups under microwave irradiation (Scheme 11.26) [50].

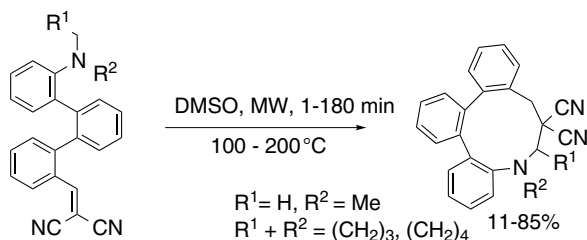
The authors carried out the key ring closure and the subsequent iodide-mediated traceless cleavage of the resin in the presence of a polymer-supported base as HCl scavenger. The microwave-assisted ring closure was undertaken in a dioxane–water mixture at 180 °C using CsI and piperidinomethyl polystyrene, wherein the desired seven-, eight-, and nine-membered sulfides were isolated in excellent yields of 53–93%. Once again, careful comparison of the cyclization reaction of a typical substrate revealed that the microwave-assisted protocol yielded an excellent 88% yield in comparison with a meager 24% yield under conventional heating.

In comparison to their seven-, eight-, and nine-membered counterparts, the ten-membered N-heterocyclic ring systems are scarce in the literature. However, the latter have also invited a lot of current interest owing to their structural semblance with various biologically interesting molecules like the alkaloids dysazecine [51] and



**Scheme 11.26:** Microwave-assisted solid-supported synthesis of cyclic sulfides.

protopine [52, 53] (a potent antimalarial lead compound) as well as the nanomolar dopamine receptor antagonist LE300 [54]. Mátyus and coworkers have recently reported a straightforward, microwave-assisted synthesis of tribenzo[*b, d, f*]- and pyridazino[*d*]dibenzo[*b, f*]azecines, employing the so-called tert-amino effect (Scheme 11.27) [55]. The desired compounds were furnished via an open-vessel, microwave-assisted cyclization of the corresponding triphenyl intermediates at 100–200 °C for 1–180 min.



**Scheme 11.27:** Microwave-assisted synthesis of novel fused azecines via application of tert-amino effect.



## 11.5 Conclusion

This chapter has highlighted the tremendous impact of the application of microwave irradiation on the development of new and efficient synthetic approaches to the generation of medium-sized heterocycles. All three classical approaches, viz., cyclization, annulation, and ring expansion, have greatly benefited from microwave-assisted techniques. It is also apparent that the application of focused microwave irradiation is often helpful in efficiently overcoming the formidable entropic/enthalpic barriers associated with the formation of such ring systems. Thus, a diverse array of N-, O-, and S-containing seven- to nine-membered heterocycles have been constructed in higher yields and shorter reaction times compared to conventional conditions. Moreover, newer innovations like microwave-assisted continuous-flow synthesis have enabled fast and efficient synthesis of multigram quantities of such heterocycles for the eventual generation of diverse chemical libraries.

The aforementioned developments also augur well for addressing some of the limitations associated with the current state of the art. One of the most cherished features is the introduction of greater diversity into medium-sized heterocyclic systems. As demonstrated by our work as well that of others, microwave-assisted MCRs offer a promising route for the rapid diversity-oriented synthesis of such heterocycles. It is expected that these results would spur further exploration of MCRs for library syntheses of structurally diverse and novel seven-, eight-, and nine-membered heterocyclic scaffolds. On the other hand, palladium-catalyzed reactions have greatly benefited from the application of microwave irradiation, and these also constitute one of the most widely used approaches to the construction of structurally challenging medium-sized ring systems. Thus, a major challenge for the future would be to explore the utility of microwave-assisted palladium-catalyzed protocols for the synthesis of hitherto inaccessible and highly strained ring systems. Another important domain of investigation would concern further refinements in microwave reactor technologies such as sequential and continuous-flow synthesis for the generation of multigram quantities of complex medium-sized ring heterocycles. It is hoped that microwave-assisted techniques and their future technological advancements will continue to facilitate newer strategies for medium-sized ring formation, further enriching the landscape of these fascinating scaffolds.

### Acknowledgement

Reproduced by permission of The Royal Society of Chemistry from Chem. Commun. 2012, 48, 1623–1637. All rights reserved.

## Bibliography

- [1] Yet L. *Chem. Rev.*, 2000, 100, 2963–3008.
- [2] Nubbemeyer U. Synthesis of Medium-Sized Ring Lactams, *Top. Curr. Chem.* 2001, 216, 125–196.
- [3] Arnold LA, Luo W, Kiplin GR. *Org. Lett.* 2004, 6, 3005–3007.
- [4] Bauer RA, Wenderski TA, Tan DS. *Nat. Chem. Biol.* 2013, 1, 21–29.
- [5] Hadac EM, Dawson ES, Darrow JW, Sugg EE, Lybrand TP, Miller LJ. *J. Med. Chem.* 2006, 49, 850–863.
- [6] Lee J, Gauthier D, Rivero RA. *J. Org. Chem.* 1999, 64, 3060–3065.
- [7] Cepanec I, Litvić M, Pogorelić I. *Org. Proc. Res. Dev.* 2006, 10, 1192–1198.
- [8] Illuminati G, Mandolini L. *Acc. Chem. Res.* 1981, 14, 95–102.
- [9] Michaut A, Rodriguez J. *Angew. Chem. Int. Ed.* 2006, 45, 5740–5750.
- [10] Kappe CO. *Angew. Chem. Int. Ed.* 2004, 43, 6250–6284.
- [11] Van der Eycken E, Kappe CO. *Microwave-Assisted Synthesis of Heterocycles*, Springer, Berlin-Heidelberg-New York, 2006, vol. 1.
- [12] Baxendale IR, Hayward JJ, Ley SV. *Comb. Chem. High Throughput Screen.* 2007, 10, 802–836.
- [13] Lautens M, Tayama E, Herse C. *J. Am. Chem. Soc.* 2005, 127, 72–73.
- [14] Ellison A, Boyer R, Hoogestraat P, Bell M. *Tetrahedron Lett.* 2013, 54, 6005–6007.
- [15] Donets PA, Van der Eycken E. *Org. Lett.* 2007, 9, 3017–3020.
- [16] Donets PA, Goeman JL, Van der Eycken J, Robeyns K, Van Meervelt L, Van der Eycken E. *Eur. J. Org. Chem.* 2009, 793–796.
- [17] Mehta VP, Modha SG, Ruijter E, Hecke KV, Meervelt LV, Pannecouque C, Balzarini J, Orru RVA, Van der Eycken E. *J. Org. Chem.* 2011, 76, 2828–2839.
- [18] Ohta Y, Chiba H, Oishi S, Fujii N, Ohno H. *Org. Lett.* 2008, 10, 3535–3538.
- [19] Neochoritis CG, Tsoleridis CA, Stephanatou JS, Kontogiorgis CA, Litina DJH. *J. Med. Chem.* 2010, 53, 8409–8420.
- [20] Lampariello LR, Piras D, Rodriguez M, Taddei M. *J. Org. Chem.* 2003, 68, 7893–7895.
- [21] Zhou H, Zhang W, Yan B. *J. Comb. Chem.* 2010, 12, 206–214.
- [22] Willy B, Müller TJJ. *Mol. Divers.* 2010, 14, 443–453.
- [23] Dallinger D, Kappe CO. *Chem. Rev.* 107 (2007) 2563–2591.
- [24] Tu SJ, Cao XD, Hao WJ, Zhang XH, Yan S, Wu SS, Han ZG, Shi F. *Org. Biomol. Chem.* 2009, 7, 557–563.
- [25] Dandia A, Singh R, Khaturia S. *Bioorg. Med. Chem.* 2006, 14, 1303–1308.
- [26] Ullah F, Samarakoon T, Rolfe A, Kurtz RD, Hanson PR, Organ MG. *Chem. Eur. J.* 2010, 16, 10959–10962.
- [27] Shiina I. *Chem. Rev.* 2007, 107, 239–273.
- [28] Bagley MC, Lin Z, Phillips DJ, Graham AE. *Tetrahedron Lett.* 2009, 50, 6823–6825.
- [29] Elkhayat Z, Safir I, Aquino M, Perez M, Gandara Z, Retailleau P, Arseniyadis S. *Eur. J. Org. Chem.* 2009, 2687.
- [30] Remer B, Hofer O, Greger H. *Phytochemistry.* 1997, 45, 337–341.
- [31] Sato H, Kawagishi H, Nishimura T, Yoneyama S, Yoshimoto Y, Sakamura S, Furusaki A, Katsuragi S, Matsumoto T. *Agric. Biol. Chem.* 1985, 49, 2969–2974.
- [32] Kam T, Yoganathan K, Chuah C. *Tetrahedron Lett.* 1995, 36, 759–762.
- [33] Viladomat F, Bastida J, Codina C, Campbell WE, Mathee S. *Phytochemistry.* 1995, 40, 307–311.
- [34] Appukkuttan P, Dehaen W, Van der Eycken E. *Comb. Chem. High Throughput Screen.* 2007, 10, 790–801.
- [35] Bariwal JB, Ermolat'ev DS, Glasnov TN, Van Hecke K, Mehta VP, Van Meervelt L, Kappe CO, Van der Eycken EV. *Org. Lett.* 2010, 12, 2774–2777.

- [36] Appukkuttan P, Dehaen W, Van der Eycken E. *Org. Lett.* 2005, 7, 2723–2726.
- [37] Beryozkina T, Appukkuttan P, Mont N, Van der Eycken E. *Org. Lett.* 2006, 8, 487–490.
- [38] Donets PA, Van Hecke K, Van Meervelt L, Van der Eycken E. *Org. Lett.* 2009, 11, 3618–3621.
- [39] Peshkov VA, Van Hove S, Donets PA, Pereshivko OP, Van Hecke K, Van Meervelt L, Van der Eycken E. *Eur. J. Org. Chem.* 2011, 1837–1840.
- [40] Zhang H, Qiu S, Tamez P, Tan GT, Aydogmus Z, Van Hung N, Cuong NM, Angerhofer C, Soejarto DD, Pezzuto JM, Fong HHS. *Pharm. Biol.* 2002, 40, 221–224.
- [41] Koizumi Y, Kobayashi H, Wakimoto T, Furuta T, Fukuyama T, Kan T, *J. Am. Chem. Soc.* 2008, 130, 16854.
- [42] Sunderhaus JD, Dockendorff C, Martin SF. *Org. Lett.*, 2007, 9, 4223.
- [43] Fürstner A, Radkowski K, Wirtz C, Goddard R, Lehmann CW, Mynott R. *J. Am. Chem. Soc.* 2002, 124, 7061–7069.
- [44] Rodríguez C, Ravelo JL, Martín VS. *Org. Lett.* 2004, 6, 4787–4789.
- [45] Kim YJ, Lee D. *Org. Lett.* 2004, 6, 4351–4353.
- [46] Appukkuttan P, Dehaen W, Van der Eycken E. *Chem. Eur. J.* 2007, 13, 6452–6460.
- [47] Mak SYF, Curtis NR, Payne AN, Congreve MS, Wildsmith AJ, Francis CL, Davies JE, Pascu SI, Burton JW, Holmes AB. *Chem. Eur. J.* 2008, 14, 2867–2885.
- [48] Plouffe D, Brinker A, McNamara C, Henson K, Kato N, Kuhen K, Nagle A, Adrián F, Matzen JT, Anderson P, Nam T, Gray NS, Chatterjee A, Janes J, Yan SF, Trager R, Caldwell JS, Schultz PG, Zhou Y, Winzeler EA. *Proc. Nat. Acad. Sci.* 2008, 105, 9059–9064.
- [49] Huryñ DM, Konradi AW, Ashwell S, Freedman SB, Lombardo LJ, Pleiss MA, Thorsett ED, Yednock T, Kennedy JD. *Curr. Top. Med. Chem.* 2004, 4, 1473–1484.
- [50] Saruta K, Ogiku T, Fukase K. *Tetrahedron Lett.* 2009, 50, 4364–4367.
- [51] Aladesanmi AJ, Kelley CJ, Leary JD. *J. Nat. Prod.* 1983, 46, 127–131.
- [52] Xiao X, Liu J, Hu J, Zhu X, Yang H, Wang C, Zhang Y. *Eur. J. Pharmacol.* 2008, 591, 21–27.
- [53] Saeed SA, Gilani AH, Majoo RU, Shah BH. *Pharmacol. Res.* 1997, 36, 1–7.
- [54] Mohr P, Decker M, Enzensperger C, Lehmann J. *J. Med. Chem.* 2006, 49, 2110–2116.
- [55] Dunkel P, Túrós G, Bényei A, Ludányi K, Mátyus P. *Tetrahedron.* 2010, 66, 2331–2339.

Jacek Wojnarowicz, Tadeusz Chudoba, Andrzej Majcher, and Witold Łojkowski

## 12 Microwaves applied to hydrothermal synthesis of nanoparticles

### 12.1 Introduction

The main aim of the present chapter is to draw attention to the peculiarities of microwave reactors for nanoparticle (NP) synthesis.

After more than 70 years since Percy Lebaron Spencer's discovery of the phenomenon of heating caused by microwave radiation, microwave technologies have been commonly employed in the kitchen, laboratory practice, and industry. Attempts to use microwaves for initiating chemical reactions were made already in the early 1960s [1, 2]. The theoretical background for the use of microwaves in heating, providing a base for planning applications in numerous fields of technology, was developed in the early 1950s [3]. Computer software for equipment design purposes, for example QuickWave (by QWED) [4], was introduced as a result of the experiences of numerous programmers and scientists. The early 1980s saw the first publications describing the possibility of applying microwaves in chemistry, mainly in the area of organic compound syntheses. Specialized reactors used for chemical analyses and syntheses in laboratories have been designed. One of the significant prerequisites of the development of this field was the establishment of methods of controlling the chemical processes initiated by microwaves and carried out in closed pressure vessels. Despite ongoing progress in this field, microwaves as an energy source remain rather difficult to control [5]. The most important advantage of microwave heating is that it delivers energy directly to the substance/matter without thermal-conductivity-related constraints. This allows for heating different media at rates up to 100 × greater than conventional heating [6]. Despite extensive discussion about possible nonthermal activation of chemical reactions by microwaves [7, 8], it is more practical to assume that the main reason for their effectiveness is that they cause thermal effects, perhaps reinforced by forming *super-heated* areas (sometimes called hot spots) as a result of interference patterns in closed spaces.

### 12.2 Benefits of microwave synthesis in a Teflon® reaction chamber

Microwave radiation energy is absorbed directly by polar particles (e.g., water, organic solvents, acids) and in these cases constitutes a significantly quicker and more effec-

<https://doi.org/10.1515/9783110479935-012>

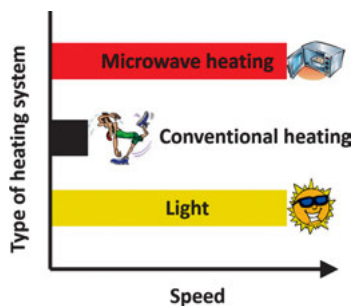


Fig. 12.1: Comparison of speed of microwave heating with conventional heating.

tive energy source than classical heating based on convection and thermal conductivity (Figure 12.1).

Figure 12.2 shows the differences between conventional heating and microwave heating. Precursor (solution, suspension) heating by conventional heating is unfavorable for the products of NP synthesis. In conventional heating, thermal energy coming from an external heat source first of all heats the walls of the reaction vessel and then the precursor. As a consequence, during heating, the precursor temperature at the vessel wall is much higher than in the remaining vessel volume. With time, the remaining precursor volume is heated by convection currents, that is, movement of matter that transfers thermal energy in the precursor (Figure 12.2a). For structural reasons (reaction chamber tightness), it is impossible to place a mechanical stirrer in a reaction vessel; this would enable a quick and uniform distribution of precursor temperature and concentration in the whole feedstock volume. The less uniform the temperature distribution in the reaction vessel, the broader the NP size distribution obtained. The type of material in which a tight reaction vessel is formed is very important. In the case of convection heating, the material must be characterized by a high coefficient of thermal conductivity, which determines the precursor heating speed achieved.

The structural material commonly used in microwave technology is polytetrafluoroethylene (PTFE)  $(-C_2F_4-)_n$ , a very interesting plastic. PTFE was discovered by an

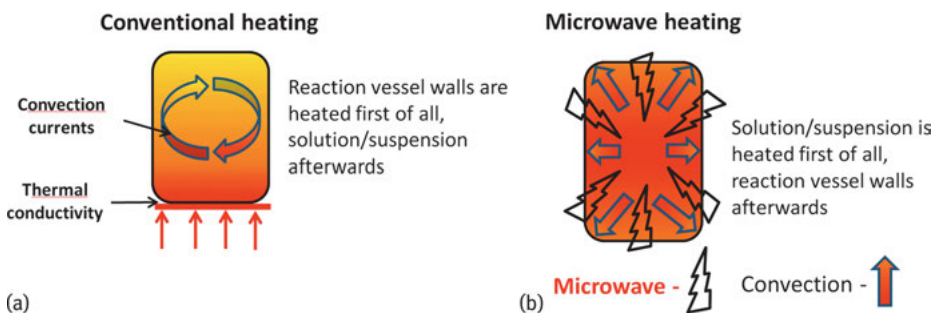
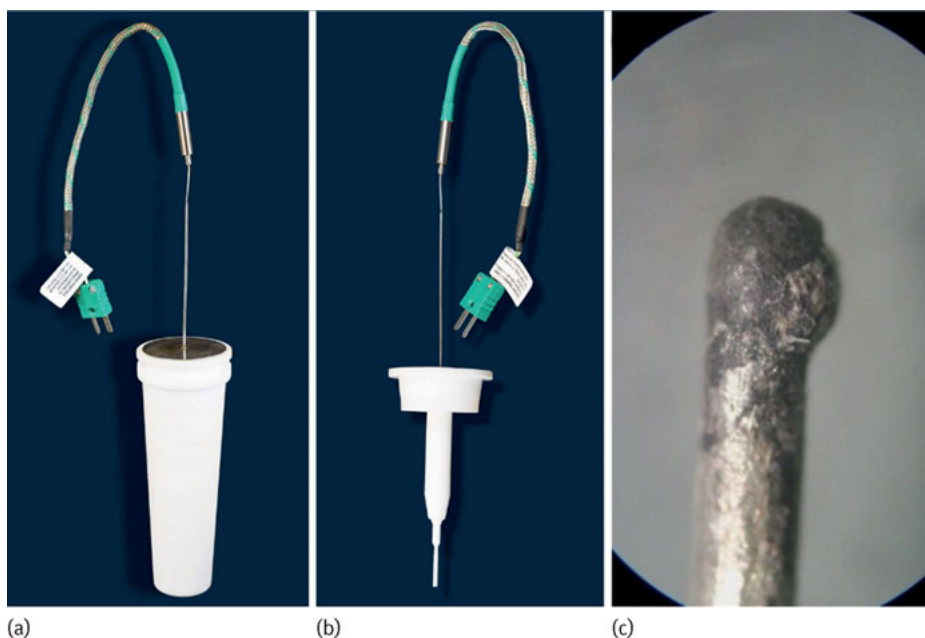


Fig. 12.2: Indicative illustration showing differences between conventional (a) and microwave heating (b).

American scientist, Dr. Roy J. Plunkett, on 6 April 1938 in New Jersey. Just like in the case of most discoveries, this one happened by pure accident. Plunkett, who was working for DuPont at the time, conducted research on substances that could be used in refrigerators (gases related to Freon® refrigerants). The company gave the trade name Teflon® to the new compound. Teflon® synthesis was patented by DuPont in 1956. Although the patent for that product expired long ago, the name Teflon® is a proprietary trademark of DuPont. Teflon® is a thermoplastic polymer, which is very widely applied as a structural material. It is relatively easy to process mechanically, for example, by machining or turning. It is characterized as having the best thermal resistance among plastics with applications in technology and industry within a temperature range of – 200 to 260 °C. It is nonflammable and begins decomposing only at a temperature of circa 330 °C. It is chemically inert and insoluble in virtually all inorganic and organic solvents. It does not undergo hydrolysis. It is distinguished by exceptionally high chemical resistance to acids and bases. When unmodified, it is physiologically neutral (odorless, tasteless, nontoxic). The most important property of Teflon®, which enabled its wide application in microwave structures, is transparency to microwaves. The high chemical and temperature resistance as well as transparency to microwaves are the greatest strengths of that material and make Teflon® the most frequently applied material for constructing tight reaction chambers in microwave reactors.

Figure 12.2b presents characteristics of microwave heating. The most important feature of microwave heating is the direct supply of energy to the precursor – during microwave heating the precursor is heated first and the walls of the reaction vessel afterward. The microwave heating method is very commonly designated as endogenous or volumetric heating. In an aqueous precursor, microwaves with a frequency of 2.45 GHz penetrate circa 2.5 cm deep inside the precursor. Because of this, the temperature increases uniformly in the whole precursor volume immediately upon switching the microwave heating on. The coefficient of thermal conductivity of Teflon® is 0.25 W/(m · K) [25 °C] and is 12 times lower than that of quartz (3 W/(m · K) [25 °C]) and 64 times lower than that of stainless steel (16 W/(m · K) [25 °C]). The low coefficient of thermal conductivity of Teflon® allows that material to act as a thermal insulator. The walls of a Teflon® reaction chamber slow down the heat loss during microwave heating, which permits a rapid increase in the precursor temperature and at the same time the emergence of a small temperature gradient.

The speed of precursor heating in a Teflon® reaction chamber depends on the used microwave power and on the precursor quantity in the reaction vessel. Microwave power attributable to the precursor quantity in a Teflon® cup can be expressed by dividing the microwave reactor's rated power (Watts, W) by the quantity (milliliters, mL) of the precursor poured into the Teflon® reaction chamber. Teflon® is relatively easy to process, which is another of its great advantages, since it enables making new experimental designs of reaction vessels. Figure 12.3 shows the special cover constructed by us of a Teflon® reaction chamber, which permits an exact measurement of precursor temperature during the microwave heating. A K-type



**Fig. 12.3:** (a, b) A system for direct temperature measurement in a Teflon<sup>®</sup> reaction vessel in Magnum II reactor by ERTEC-Poland; (c) Ø1 mm thermocouple damaged by microwaves during the precursor temperature measurement.

grounded thermocouple was inserted by us centrally into a spindle ending with a thin capped Teflon<sup>®</sup> tube. Our design remains tight at pressures reaching even 60 bar. It should be emphasized that the reaction vessel design serves only for experimental purposes, for example, verification of readouts of the reactor software and for examination of the kinetics of precursor microwave heating. Despite the central position of the thermocouple in the precursor, which protects it against the destructive action of microwaves, the thermocouple may still burn out during microwave heating (Figure 12.3b). Our experience shows that the thermocouple withstands merely between 10 and 20 measurement cycles.

Figure 12.4 presents a comparison of changes of deionized water temperature depending on its volume (50, 60, 70 mL) in a Teflon<sup>®</sup> cup for the applied constant microwave power (100%, 600 W). The water's boiling point (100 °C) was reached after 2–3 min of heating. As expected, heating speed decreased in line with the water quantity increase in the Teflon<sup>®</sup> cup. However, the most interesting data in the chart are the temperature change after the 10<sup>th</sup> minute of heating. It is a well-known fact that the dielectric constant of pure solvents depends strongly on temperature and decreases in line with its increase. The result is that, despite the adopted constant power of microwave heating, after a certain time the water heating speed reaches a value equal virtually to 0 °C/min. In our experiment, a temperature of circa 210 °C may be used as the

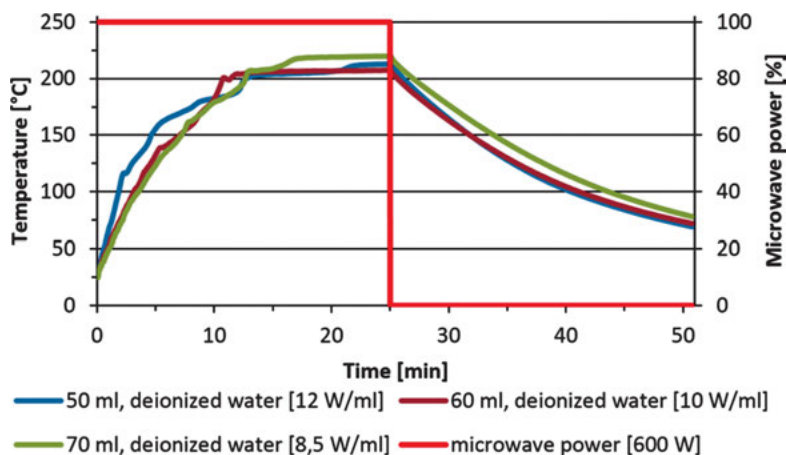


Fig. 12.4: Characteristics of microwave heating of deionized water. Experimental data obtained in ERTEC-Poland Magnum II.

limit temperature of microwave heating of deionized water ( $0.07 \mu\text{S}/\text{cm}$ ). For the 25<sup>th</sup> minute of heating the temperature in the reaction vessel reached  $213^\circ\text{C}$  (50 mL),  $208^\circ\text{C}$  (60 mL) and  $220^\circ\text{C}$  (70 mL). The achievement of the highest temperature of  $220^\circ\text{C}$  for the highest sample volume (70 mL) is quite interesting and probably results from the geometry of the distribution of so-called hot spots in deionized water [9].

Figure 12.5 presents a comparison of changes of ethylene glycol (EG) temperature depending on volume (50, 60, 70 mL) in a Teflon<sup>®</sup> cup for the adopted constant microwave power (100%, 600 W). Ethylene glycol's boiling point ( $198^\circ\text{C}$ ) was reached af-

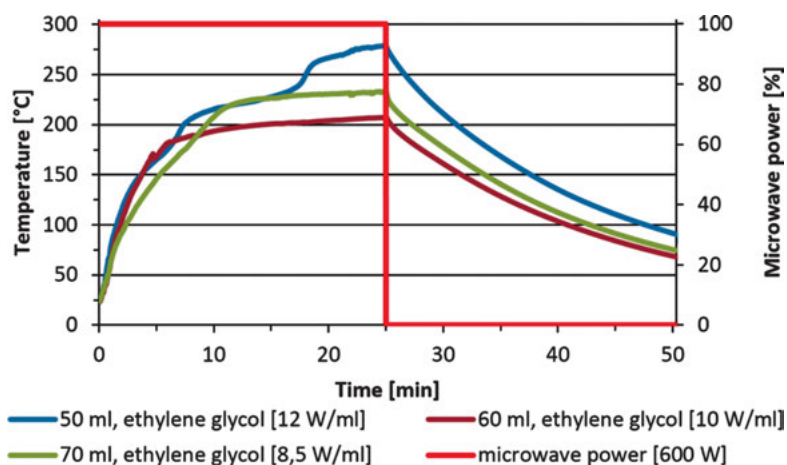


Fig. 12.5: Characteristics of EG heating (0.5 wt.%  $\text{H}_2\text{O}$ ). Experimental data obtained in ERTEC-Poland Magnum II.



ter 7 min (50 mL), 9 min (70 mL), and 12 min (60 mL) of heating. As expected, similarly to the case of deionized water, the heating speed decreased in line with the increase in the EG quantity in the Teflon<sup>®</sup> cup. Surprising results of temperature measurement emerge after the eighth minute of microwave heating. Heating speed decreases but does not reach a value close to 0 °C/min. In addition, in this experiment a limit temperature of microwave heating cannot be provided, unlike in the previous example (water). Average heating speed calculated in the temperature range from 10 to 25 min was 4 °C/min (50 mL), 0.9 °C/min (60 mL), and 1.7 °C/min (70 mL). Interestingly, the following temperatures were reached for the 25<sup>th</sup> minute of microwave heating of EG: 278 °C (50 mL), 207 °C (60 mL), and 232 °C (70 mL). Reaching virtually the same temperature of 207–208 °C after 25 min of heating the volume of 60 mL of both water and glycol is quite a surprising result. Large differences in the speed of EG heating, particularly for the 60 mL sample, probably result primarily from the geometry of distribution of hot spots and polymerization or decomposition of EG.

The presented results of the heating characteristics of solvents (water, EG) serve as an example of how the selection of precursor volume and temperature in the Teflon<sup>®</sup> reaction chamber can be optimized. This is a practical approach to microwave syntheses of NPs. It reduces the time of synthesis parameter selection and enables learning and tracking the real temperature profile of microwave syntheses of NPs. These data are necessary, for example, for determining the mechanisms of NP synthesis reactions and for controlling NP properties through changes in temperature and synthesis time. Such an approach to the microwave synthesis of NPs is possible only through the use of Teflon<sup>®</sup> as the material for constructing reaction chambers. This material enables constructing tight reaction chambers with different complex shapes using, for example, readily available lathes and milling machines. But the most important advantage of Teflon<sup>®</sup> reaction chambers is the achieved purity of NPs as a result of microwave synthesis. The synthesis in a Teflon<sup>®</sup> chamber does not contaminate NPs. This is very significant, for example, in the case of synthesis of NPs for biomedical applications. Teflon<sup>®</sup> reaction chambers are currently widely used in such microwave processes as the following:

- hydro- and solvothermal synthesis of nanopowders
- sample mineralization
- organic syntheses
- polymerization and polycondensation
- biofuel and oil processing

### 12.3 Reactions initiated by microwaves in a liquid environment

Microwaves can easily and quickly heat the majority of popular solvents to temperatures exceeding the boiling point under atmospheric pressure, and this phenomenon in tight reactors is accompanied by autogenous pressure increase (in compliance with

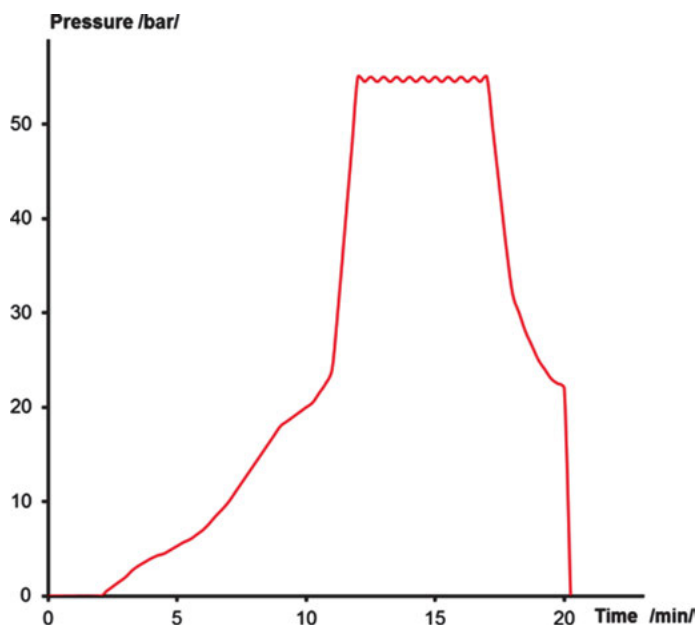


Fig. 12.6: Heating curve, microwave reactors MSS1 and MSS2 (IHPP PAS, ITeE-PIB, ERTEC-Poland).

the basic thermodynamic correlations). In such a situation, measurement of the equilibrium pressure of the reaction is a convenient manner of control, and this parameter is used most often for controlling processes in the liquid phase.

Figure 12.6 shows the characteristic curve of the aqueous solution pressure rise in MSS1 and MSS2 microwave reactors constructed by the Institute of High Pressure Physics of the Polish Academy of Science (IHPP PAS), Institute for Sustainable Technologies – National Research Institute (ITE-PIB) and ERTEC-Poland Company. Pressure measurement is done with a strain gauge or a pressure gauge. Irregularities exceeding 2.5–3 bar and at ca. 20 bar are observed most often, and they are probably caused by many factors (changes in the dielectric and ohmic properties of water, changes in the reaction chamber volume due to the high thermal expansion of Teflon<sup>®</sup>, changes in the seal mechanics, and perhaps some other factors). Above 25 bar, heating and pressure rises are rapid, and their course corresponds to the known concept of *thermal escape*. The reactor was opened under a pressure of 22 bar, a chamber volume of 470 mL, and a filling rate of 70%.

Reactions occurring in a closed system in liquid phase at a pressure higher than atmospheric pressure are called solvothermal reactions, and if water is the solvent, they are known as hydrothermal reactions [10]. Hydrothermal and solvothermal reactions have been developed for many years, despite an incomplete theoretical background, and are one of the fundamental and most widely employed technologies of advanced chemical syntheses, in particular in the field of controlled crystallization

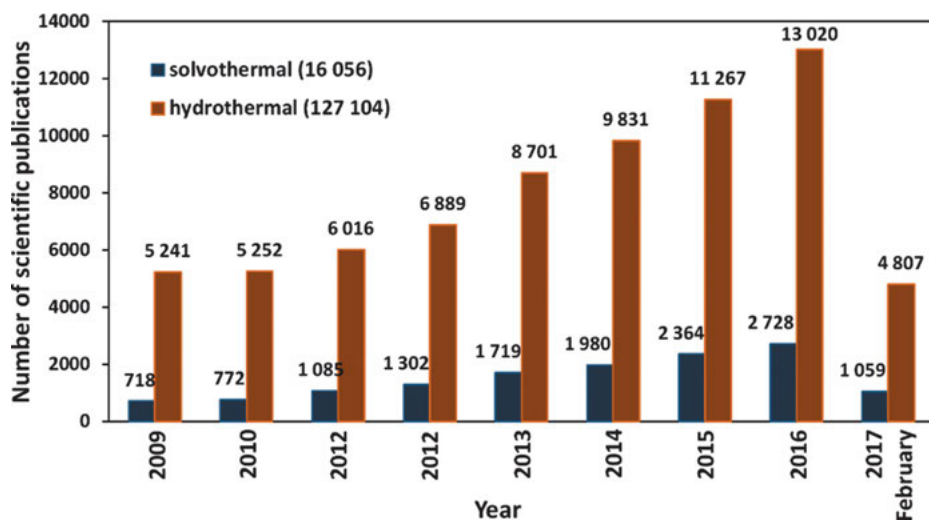


Fig. 12.7: Number of scientific publications on solvothermal and hydrothermal syntheses published in the period 2008–2016. Source: ScienceDirect search engine, dated 2017-02-09.

of substances. The development and popularity of these processes are demonstrated, for example, by search results on the terms *solvothermal* and *hydrothermal* in a scientific search engine and in a patent search engine (Figures 12.7 and 12.8). Owing to the properties of water as solvent, such materials are mainly obtained in traditional

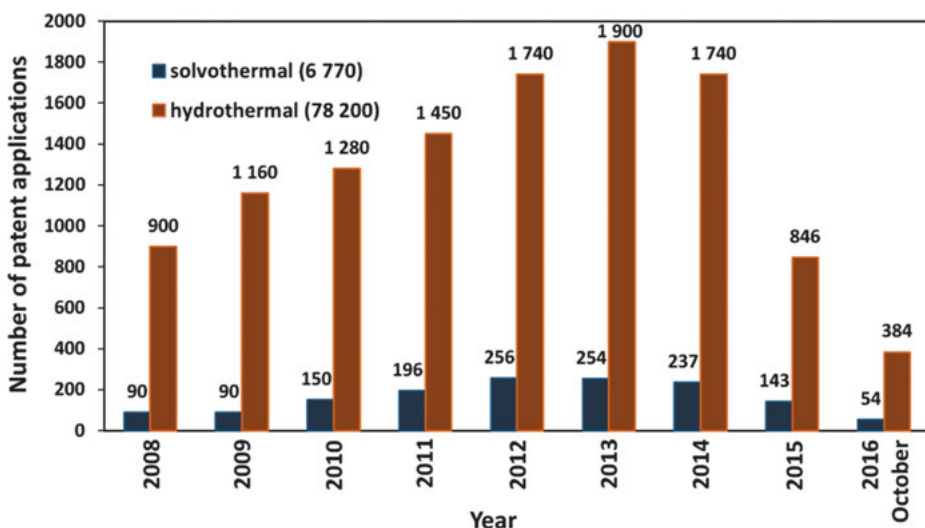


Fig. 12.8: Number of patent applications containing “solvothermal” and “hydrothermal” in the period 2008–2016. Source: Google search engine, dated 2016-10-10.

hydrothermal processes as oxide materials (simple oxides and complex oxides) [11]. These materials can contain hydroxide and oxyhydroxide residues. Methods of obtaining various structures have been developed: from massive single crystals (e.g., synthetic quartz  $\text{SiO}_2$  [12]) to such nanostructures as nanocrystals covered by nanolayers of substances changing the physicochemical properties of materials (e.g.,  $\text{SiO}_2$  layer coatings on  $\text{BaTiO}_3$  [13]). Well-known products of hydrothermal reactions include oxides of the majority of metals (e.g.,  $\text{ZnO}$ ,  $\text{ZrO}_2$ ,  $\text{SiO}_2$ ,  $\text{TiO}_2$ ,  $\text{Al}_2\text{O}_3$ ,  $\text{Fe}_2\text{O}_3$ ,  $\text{CeO}_2$ ,  $\text{Sb}_2\text{O}_5$ ,  $\text{SnO}_2$ ,  $\text{Co}_3\text{O}_4$ ,  $\text{HfO}_2$ ), chalcogenides [14], and pure or doped metal compounds [15]. In certain cases hydrothermal processes have long been used for producing powder products, for example,  $\text{ZrO}_2$ ,  $\text{ZnO}$ ,  $\text{KTiOPO}_4$ ,  $\alpha\text{-Al}_2\text{O}_3$ ,  $\text{Be}_3\text{Al}_2(\text{SiO}_2)_6$ , carbon nanotubes, and zeolite powders (zeolite beta, mordenite, Na-P1, ZSM-5) [11, 16, 17]. Obtaining nonoxide materials, in particular metal particles, most often requires employing solvothermal syntheses [18] with limited and precisely controlled water access. Using microwave reactors, IHPP PAS has carried out hydrothermal syntheses of  $\text{ZrO}_2$  and doped  $\text{ZrO}_2$  [19],  $\text{TiO}_2$  (nanorods and nanopipes),  $\text{FeO}$ ,  $\text{Fe}_2\text{O}_3$ ,  $\text{Fe}_3\text{O}_4$ ,  $\text{ZnO}$  and doped  $\text{ZnO}$  [20–23],  $\text{Bi}_2\text{Se}_3$  and  $\text{Sb}_2\text{Te}_3$  [24], and hydroxyapatite (HAP) [25–27].

## 12.4 Obtaining nanometric ZnO in hydrothermal processes

$\text{ZnO}$  is a good example for the purpose of assessing the suitability of diverse methods of obtaining NPs in various production scales. Known to humanity for several hundred years, it has been used in an exceptionally large number of fields – from medicine to the automotive sector [28–30]. Global production is estimated to exceed 1.5 million tons, and to a major extent it is obtained in metallurgical processes of ore and recyclable material processing as a result of sublimation refining of concentrates. As a rule, oxides obtained in this way are micrometric, although it is possible to carry out the process to obtain submicron powders [32]. Growing market requirements leading to the cheapest possible production of metallic zinc will result in an increasingly wider application of hydrometallurgical processes in its processing, and the application of those processes currently accounts for 80% of the total global zinc production [33]. The total global production of  $\text{ZnO}$  nanopowder ( $\text{ZnO}$  NPs) is many times lower than that of metallic zinc and  $\text{ZnO}$  micropowders, but  $\text{ZnO}$  NPs are indispensable for numerous applications. They are applied in cosmetics and medicine, the production of pigments, lubricants, plastics, ceramic materials, and electronic instruments, in biosensors, photocatalysis, UV filters, antiseptics, and many more [28–30]. Biocompatibility, antibacterial action, antifungal action, and the biodegradability of  $\text{ZnO}$  NPs explain why they are an object of considerable interest in biomedicine [34–37]. Methods of  $\text{ZnO}$  NP production have been the subject of numerous studies; sol-gel technologies, precipitation, hydrothermal, solvothermal, and plasmatic methods have been used [31]. Hydrothermal and solvothermal methods are regarded as being among the most popular ways to obtain  $\text{ZnO}$ . They are being gradually developed by

constructing new types of reactors, for example, microwave stop-flow and continuous-flow reactors [38, 40, 43].

We carried out tests of efficiency of heating precursors containing suspensions of  $\text{Zn}(\text{OH})_2$  by various methods, including by traditional electrical heating, heating by immersion heater, heating by direct current flow through  $\text{Zn}(\text{OH})_2$  suspension, and microwave heating [44]. It was proved that when comparable conditions were preserved, similar products were obtained, but nevertheless powders obtained as a result of microwave heating were beneficially distinguished by the purity level and better homogeneity. This was an effect of greater heating speed than in other methods, and the lack of contact of reaction liquids with the metal components of heaters or electrodes, for example. Microwave heating proved least energy-consuming. Further tests proved that fully crystalline nanometric ZnO was obtained after soaking the precursor in a water environment at a minimum temperature of 200 °C, which corresponds to an equilibrium pressure of 16 bar. However, the relevant literature provides temperatures of hydrothermal synthesis of nano ZnO ranging from 100 to 250 °C. The primary parameter of ZnO crystallinity is density, which is 5.61 g/cm<sup>3</sup> for fully crystalline ZnO. The majority of publication authors do not provide density results for the obtained ZnO nanostructures. They assess ZnO crystallinity in their papers based on the powder X-ray diffraction (XRD) results [45]. Nevertheless, it should be borne in mind that the limit of detectability of a foreign phase in the diffraction method (XRD) can be even up to 5–6 at. %. If the synthesis temperature is too low, it is very likely to obtain an incompletely reacted product, which can contain small quantities of a foreign phase, such as  $\text{Zn}(\text{OH})_2$ . When  $\text{ZnCl}_2$  is used as the feedstock, stable simonkolleite  $\text{Zn}_5(\text{OH})_8\text{Cl}_2 \cdot \text{H}_2\text{O}$  is an often observed impurity that is difficult to avoid. Therefore, the Laboratory of Nanostructures, IHPP, performs the following primary measurements for each nanomaterial: density (in accordance with ISO 12154:2014), specific surface area (in accordance with ISO 9277:2010), and XRD (in-house procedure). The parameters of the syntheses carried out by IHPP PAS correspond perfectly to the definition of hydrothermal reactions. The popular microwave reactor MAGNUM II (ERTEC-Poland [46]) proved to be the best equipment for testing the properties of and conditions for obtaining pure and doped ZnO NPs in laboratory conditions.

## 12.5 Obtaining ZnO nanopowders in microwave reactors

The MAGNUM II reactor (Figure 12.9) design enables carrying out a reaction in the liquid phase in a tight Teflon<sup>®</sup> chamber with a usable volume of 70 mL, a temperature of up to 260 °C, and a pressure of up to 100 bar. The reactor is controlled by a pressure sensor, and the temperature measurement for control purposes is performed under the bottom of the reaction chamber. The heating speed with a power of circa 600 W can reach 4 °C/s, and the cooling time before opening the reactor can reach circa 20 min.

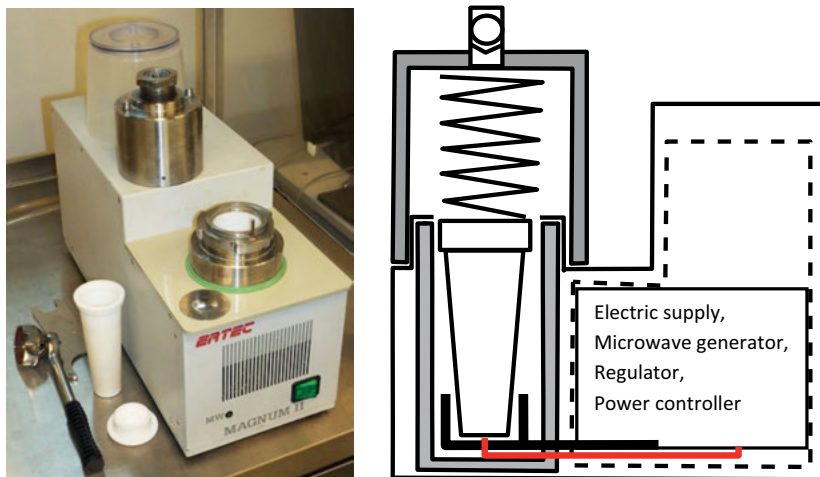


Fig. 12.9: MAGNUM II reactor, design diagram, control temperature shown in red.

The practical productivity is up to 10 g of ZnO NPs per day. It is possible to carry out hydrothermal and solvothermal processes.

The MAGNUM II reactor is an ideal laboratory instrument. Although the basic handling operations have to be performed by hand, the reagents are not in contact with the metal, and cleaning the reaction chambers after the process is very easy. Its design enables quick and convenient replacement of reaction vessels/chambers.

Tests on the course of ZnO NP synthesis made use also of semi-industrial reactors, designated MSS1 and MSS2 (Figure 12.10) [38]. Both these devices enable reaching a temperature of 260 °C and a pressure of up to 60 bar. In both of them the reaction occurs inside Teflon<sup>®</sup> chambers (Figure 12.11). The system chemicals feeding the MSS1 reactor contains fittings with metal fragments and valves of acid-resistant steel. In the MSS2 reactor, in turn, reaction fluids are not in contact with metal components at any stage of the synthesis process (for design details see [38]).

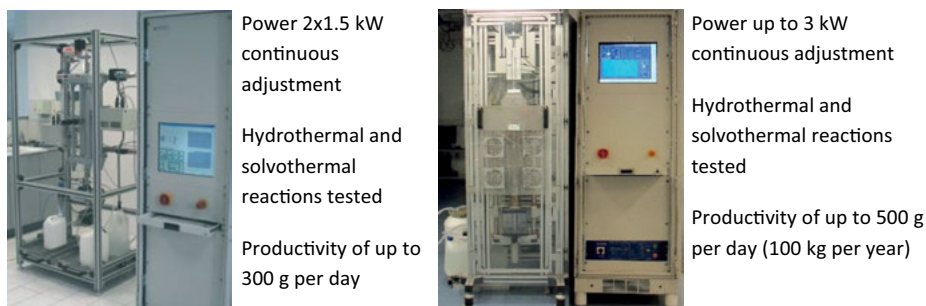


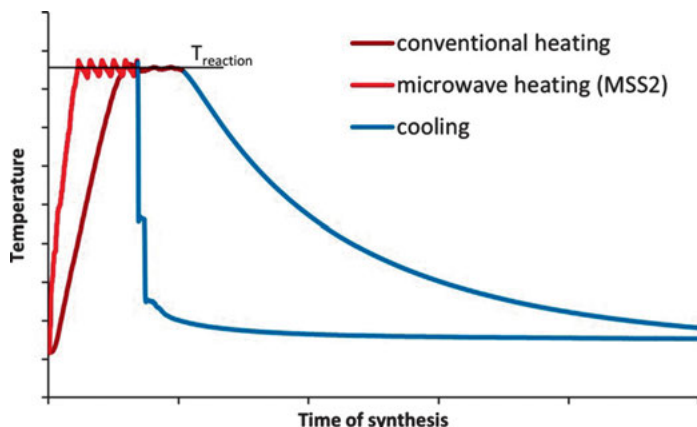
Fig. 12.10: MSS1 and MSS2 reactors [38].



**Fig. 12.11:** Reaction chambers of MSS1 (left) and MSS2 (right).

For comparison purposes, Figure 12.11 shows the reaction chambers of MSS1 and MSS2 reactors. MSS1 reactor can be operated in the continuous-flow mode, but based on our experience we have found that better results are achieved in the stop-flow mode. An MSS2 reactor is intended by design for batch-mode reactions. The designs of these reactors ensures easy and quick replacement of their reaction chambers, thereby avoiding the threat of their nanopowder suspension product contamination.

MSS1 and MSS2 reactors can be emptied under pressure, which all in all reduces the synthesis time and increases the output. Products leave the reactor in the frozen reaction state, which secures against undesirable recrystallization processes during long cooling (Figure 12.12). Product outflow under pressure causes the effective atomization of the suspension and its rapid cooling, thanks to which agglomeration processes are significantly limited.

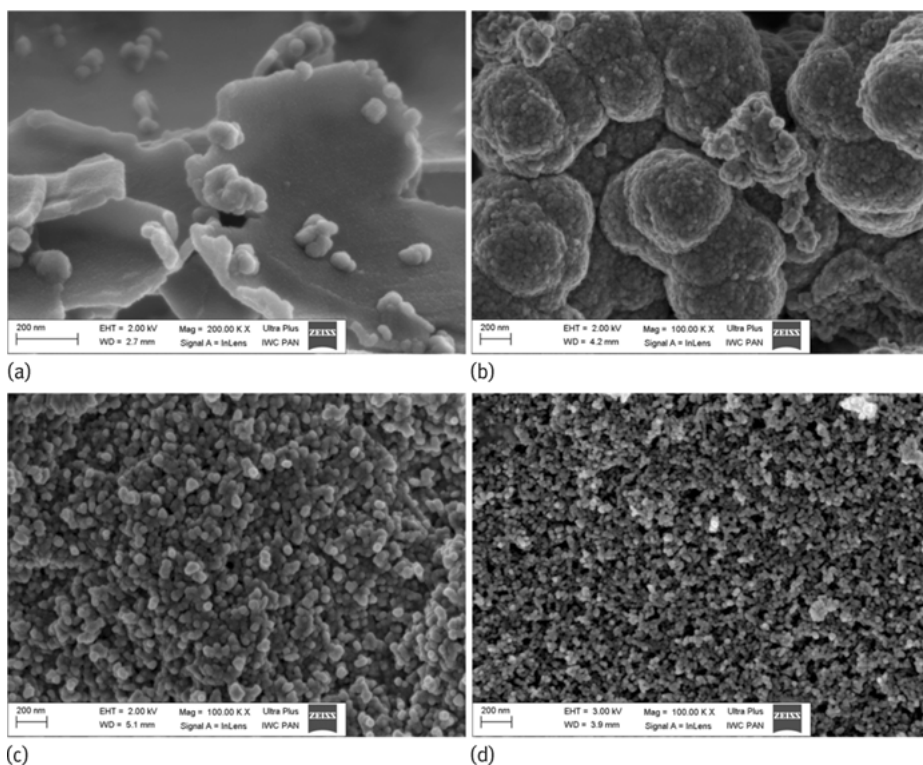


**Fig. 12.12:** Reference drawing illustrating the temperature profile of EG in a reactor with conventional heating and in MSS2 microwave reactor with power of 3 kW.

## 12.6 Solvothermal production of ZnO nanopowders in microwave reactors

Solvothermal syntheses of ZnO NPs were carried out in all the aforementioned reactors. We carried out numerous syntheses of ZnO NPs in order to optimize the technology. The finally developed method is single-stage controlled crystallization of ZnO NPs with a designed particle size from the  $\text{Zn}(\text{Ac})_2$  solution in EG [20]. The optimization of our technology of ZnO NP synthesis can be divided into the following stages:

1. Selection of reagents ( $\text{Zn}(\text{Ac})_2$ , EG), time and temperature of reaction: The main goal of this stage was to obtain crystalline ZnO NPs, pure in terms of phase. At this stage, we also tested intermediates of the solvothermal synthesis of ZnO NPs (Figure 12.13a). We noticed a very strong tendency of ZnO NPs to agglomerate/aggregate during synthesis (Figure 12.13b).



**Fig. 12.13:** Scanning electron microscopy photographs of ZnO solvothermal synthesis products for synthesis times: (a) 5 min (intermediates, metal-organic products with lamellar structure); (b) 25 min (conglomerates/congloaggregates of ZnO NPs); (c) 25 min (powder after synthesis optimization); (d) 25 min (powder after drying optimization).

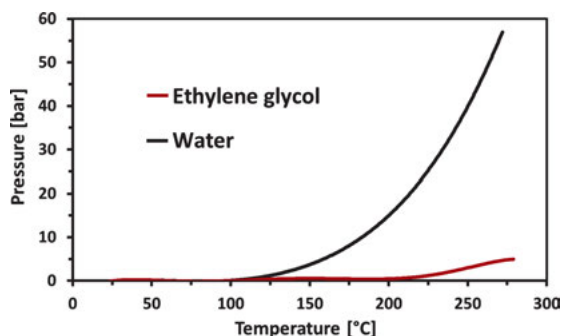


2. Control of particle size: Control of water content in the precursor turned out to be the key parameter for particle size programming [20].

3. Elimination of the phenomenon of agglomeration/aggregation of ZnO NPs: The most significant parameter that affects the agglomeration/aggregation process is synthesis temperature. Too high temperature causes degradation/polymerization of EG. EG degradation/polymerization products are deposited on the surface of ZnO particles and are a cause of permanent combination of particles into large conglomerates/congloaggregates (Figure 12.13b).

4. Powder drying: Drying of ZnO NPs in a lyophilizer proved to be the most effective method of drying ZnO NPs, which enabled preserving the structure of single particles or small agglomerates/aggregates. Figure 12.13c presents a dense structure of ZnO NPs dried by the traditional method on laboratory paper. Figure 12.13d shows homogeneous ZnO NP powder dried by the lyophilizer, with a loose structure.

The primary advantage of the technology of microwave solvothermal synthesis of ZnO NPs developed by IHPP PAS is the use of precursor solutions – rather than settling suspensions of hydroxides, as in the case of hydrothermal syntheses in water. This permits avoiding a range of problems, among others, with heterogeneity and unrepeatability of hydroxide suspensions. The necessity of mixing the precursor continuously during the mineralization and heating in the reactor critically affects the quality and homogeneity of the obtained products. It should be noted that the precursor in the form of Zn(Ac)<sub>2</sub> solution in EG is less aggressive to the chemical apparatus in comparison with aqueous solutions or suspensions. No corrosive reagents (acids, bases, salts) are used in this case, for example, ZnCl<sub>2</sub>. EG enables a considerable reduction in the synthesis pressure (Figure 12.14) with simultaneous achievement of the necessary temperature and a reduction in the process time in relation to the ZnO synthesis in water [30]. However, EG is a flammable and toxic substance, which increases the level of necessary safety precautions and the costs of the synthesis process. In addition, it is more expensive than water, and the purification of ZnO synthesis prod-



**Fig. 12.14:** Chart presenting dependency of pressure on temperature for pure glycol ethylene (0.27 wt.% H<sub>2</sub>O) and water. Experimental data obtained in MSS3 microwave reactor (IHPP PAS).

ucts is more costly. This makes the technology of solvothermal synthesis of ZnO more expensive than hydrothermal synthesis. However, the solvothermal method enables obtaining ZnO NPs with a designed particle size in an exceptionally beneficial range of 20–100 nm, without the fear of contamination by other products [20].

**Experiences gained while operating the described reactors have made possible several significant observations:**

- Feeding suspensions to the reactor that operates in automatic mode leads to contamination, difficult to remove, of the precursor feeding system. Pumps, valves, and other components quickly become worn. In addition, zinc salts display strong caustic action even to acid-resistant steel. Magnum and MSS2 reactors, which are devoid of any metal components of fixtures and have no precision valves, are advantageous in these conditions.
- Synthesized powders tend to deposit on the walls of reaction chambers and all other components. Even repeated flushing with acids does not prevent gradual accumulation of contamination. In this situation, it is advantageous to flush the reaction chamber from time to time after the process, which is easiest in the case of Magnum II laboratory reactors.
- The use of zinc acetate solution as the precursor that does not require initial mineralization of the precursor makes it possible to batch the feedstock into the reactor, but unfortunately it does not prevent the observed settling of reaction products on the reactor walls.
- The use of glycol (or other organic solvents) is very advantageous from the point of view of reduction of reaction pressure and easy control of product properties. Unfortunately, their flammability (it is necessary to take special precautions against fire or explosion), toxicity, price, and waste disposal cost are disadvantages.

## 12.7 Comparison of different methods of obtaining ZnO NPs

We tried to compare solvothermal and hydrothermal microwave-driven reactions to other routes of solvothermal ZnO NP production, like ultrasound irradiation [39] or supercritical water (SCW) technology [40–42]. The essence of the SCW method is heating the reagents with superheated steam, which makes the very fast reaction proceed in the presence of a considerable amount of water even if nonaqueous precursors are used. In the case of ultrasonic irradiation phenomena, areas of high-temperature and high-pressure microbubbles inside liquids are used to induce chemical reactions. The results are presented in Table 12.1 and data from the literature are given for comparison purposes.

Tab. 12.1: Comparison of several methods of ZnO production.

Method	Key process parameters Pressure/temperature	Most important properties of obtained ZnO NPs	Output
Microwave hydrothermal IHPP PAS	16 bar/200 °C Alkalized precursor (suspension)	Average particle size 100 nm	Up to 300 g/day
Microwave solvothermal IHPP PAS [20]	3 bar/210 °C Soluble precursor (solution)	Controlled particle size 20–80 nm	200 g/day
Microwave hydrothermal [47]	40 bar/240 °C Alkalized precursor (suspension)	Particle size 80–150 nm	15 g per day
Solvothermal [48]	150 °C Alkalized precursor (suspension)	Particle size 18–436 nm	A few grams per day
Supercritical water reaction [42]	( $T = 410$ °C and $P = 305$ bar) from $Zn(NO_3)_2$ and KOH (suspension)	Controlled particle size 20–300 nm	–
Ultrasonic [39]	$Zn(Ac)_2 \cdot 2 H_2O$ and DEG (solution)	Particle size 15 nm	–

What follows from the comparison is that the most advantageous, in our opinion, properties are acquired by ZnO NPs obtained as a result of microwave solvothermal synthesis. We believe that this technology offers the highest product purity as well as high productivity, and it is easy to control NP properties (particle dimensions).

## 12.8 Summary

The described results of the use of microwaves for hydrothermal synthesis exhibit many advantages in laboratory conditions this method. Apparatuses for these processes that are available on the market (e.g., Milestone, Kilolab, Labotron, Sairem) can reach a working temperature of 300 °C and enable the synthesis of the majority of oxide materials. The operation and maintenance costs of microwave devices are not high. The main limitations concern the materials used in microwave technology. Reactor enclosures must ensure electromagnetic shielding and, in the case of increased pressure, appropriate safety level. Reaction chambers should be made of materials that are chemically and thermally resistant but transparent for microwaves. Currently the group of materials that are suitable for this purpose is not big – it includes above all Teflon<sup>®</sup> and certain chemically similar materials, PEEK, and quartz. The use of quartz will probably be more widespread in line with the development of technologies en-

abling pressure compensation (see Anton Paar [50]), but at very high temperatures quartz dissolves in water. The reduction of solvent (water) loss factors at high temperatures might be a significant limitation. So far, no possibilities of direct heating of liquids with microwaves to temperatures exceeding 320 °C have been reported.

An important limitation of solvothermal reactions is the lower critical parameters of organic liquids than those of water. The majority of solvents undergo unfavorable reactions at an increased temperature – for example, decomposition, polymerization, and redox. For instance, the onset of the initial decomposition of EG is 240 °C. Water, which is an excellent medium for use even at temperatures above 500 °C, interfaces with the microwave field poorly already below 300 °C [49]. The works executed by IHPP PAS and oriented toward reaching the water critical point using microwave heating encountered severe difficulties on exceeding 320 °C.

Limitations also relate to temperature at which nonaqueous solvents can be applied. Since they are most often toxic, flammable, or even explosive, the necessary safety precautions limit their application. In addition, inorganic compounds tend to decompose at an increased temperature, which is often facilitated by chemicals that serve as the feedstock of the performed reactions. In this approach, water, as a rather universal solvent with exceptionally high stability and exceptionally high critical parameters, proves most advantageous.

Microwave hydrothermal syntheses are regarded as so-called green processes since they are energy-efficient owing to the lower process temperature and the use of an effective heating process. Aqueous solutions/suspensions of common chemical compounds, which can be safely prepared as well as processed or disposed of, are used for syntheses. The lower synthesis process temperature in comparison with the conventional nanoceramic synthesis (combustion, calcination, volatilization, pyrolysis) enables a considerable reduction in:

- greenhouse gas CO<sub>2</sub> production,
- air pollution in the form of, for example, SO<sub>x</sub>, NO<sub>x</sub>, Cl<sub>2</sub>,
- air pollution with particulate matter, for example, coal dust.

Such factors as the development of new types of microwave reactors and a lack of adverse environmental impacts of microwave hydrothermal synthesis will contribute to the increasing popularity of these methods in commercial production of various nanomaterials.

The past 30 years have seen a small revolution in the chemical laboratory technology and some industrial applications thanks to microwave apparatuses. Use them and love them.

## Bibliography

- [1] Whittaker G. Microwave chemistry. *School Science Review* 2004, 85, 87–94.
- [2] American Laboratory, LabTips: Would You Benefit From Microwave-Assisted Organic Synthesis in Your Lab? (Accessed August 8, 2016, at [www.americanlaboratory.com/Lab-Tips/157805-LabTips-Would-You-Benefit-From-Microwave-Assisted-Organic-Synthesis-in-Your-Lab/](http://www.americanlaboratory.com/Lab-Tips/157805-LabTips-Would-You-Benefit-From-Microwave-Assisted-Organic-Synthesis-in-Your-Lab/))
- [3] Von Hippel AR. *Dielectrics and Waves*, John Wiley & Sons, Inc., New York, 1954, republished by Artech House Publishers, 1995.
- [4] Discover accurate EM modelling: QW-Modeller for QuickWave (Accessed 9 August 2016, at [www.qwed.com.pl/quickwave.html](http://www.qwed.com.pl/quickwave.html))
- [5] Pert E, Carmel Y, Birnboim A et al. Temperature Measurements during Microwave Processing: The Significance of Thermocouple Effects. *J. Am. Ceram. Soc.* 2001, 84, 1981–1986.
- [6] Kappe CO, Dallinger D. The Impact of Microwave Synthesis on Drug Discovery. *Nature Reviews* 2006, 5, 51–63.
- [7] Loupy A. *Microwaves in Organic Synthesis*. Wiley-VCH Verlag GmbH & Co. KGaA, 2nd edn., 2006.
- [8] Leonelli C, Lojkowski W. Main development directions in the application of microwave irradiation to the synthesis of nanopowders. *Chemistry Today* 2007, 25, 34–38.
- [9] Chandra D, Nusantara I, Imron MA, Basuki. On the Formation of Hotspot in Microwave Heating. In: van Groesen van E, Soewono E. *Differential Equations Theory, Numerics and Applications* Springer Netherlands, 1997, 245–255.
- [10] Yoshimura M, Byrappa K. Hydrothermal processing of materials: past, present and future. *Journal of Materials Science* 2008, 43, 2085–2103.
- [11] Suchanek WL, Riman RE. Hydrothermal Synthesis of Advanced Ceramic Powders. *Advances in Science and Technology* 2006, 45, 184–193.
- [12] Nishinaga T. *Handbook of Crystal Growth*. 2nd edn., Elsevier 2014.
- [13] Hur MG, Masaki T, Choi BK et al. Homogenous SiO<sub>2</sub> layer coating on BaTiO<sub>3</sub> particle by hydrothermal hydrolysis method. *Journal of the Ceramic Society of Japan* 2013, 121, 702–705.
- [14] Rajamathi M, Seshadri R. Oxide and chalcogenide nanoparticles from hydrothermal/solvothermal reactions. *Current Opinion in Solid State and Materials Science* 2002, 6, 337–345.
- [15] Horikoshi S, Serpone N. *Microwaves in Nanoparticle Synthesis: Fundamentals and Applications*. Wiley-VCH Verlag GmbH & Co. KGaA, 2013.
- [16] Bućko MB, Haberko K. Crystallization of Zirconia under Hydrothermal Conditions. *Jour. of Am. Ceramic Soc.* 1995, 78, 3397–3400.
- [17] Suchanek WL, Riman RE. Hydrothermal routes to advanced ceramic powders and materials. In Riedel R, Chen IW. *Ceramics Science and Technology*, Volume 3, 1st edn. Weinheim, Germany: Wiley-VCH. 2012, 63–88.
- [18] Demazeau G. Solvothermal reactions: an opening-up on the synthesis of novel materials or the development of new processes. *High Pressure Research* 2007, 27, 173–177.
- [19] Opalinska A, Hreniak D, Lojkowski W et al. Structure, morphology and luminescence properties of Pr-doped nanocrystalline ZrO<sub>2</sub> obtained by hydrothermal method. *Solid State Phenomena* 2003, 94, 141–144.
- [20] Wojnarowicz J, Opalinska A, Chudoba T et al. Effect of water content in ethylene glycol solvent on the size of ZnO nanoparticles prepared using microwave solvothermal synthesis. *Journal of Nanomaterials* 2016, ID 2789871, 1–15.
- [21] Wojnarowicz J, Mukhovskiy R, Pietrzykowska et al. Microwave solvothermal synthesis and characterization of manganese doped ZnO nanoparticles. *Beilstein J. Nanotechnol.* 2016, 7, 721–732.

- [22] Wojnarowicz J, Kusnieruk S, Chudoba T et al. Paramagnetism of cobalt-doped ZnO nanoparticles obtained by microwave solvothermal synthesis, *Beilstein J. Nanotechnol.* 2015, 6, 1957–1969.
- [23] Lojkowski W, Gedanken A, Grzanka E et al. Solvothermal synthesis of nanocrystalline zinc oxide doped with Mn<sup>2+</sup>, Ni<sup>2+</sup>, Co<sup>2+</sup> and Cr<sup>3+</sup> ions. *Journal of Nanoparticle Research* 2009, 11, 1991–2002.
- [24] Maradudina ON, Lyubushkin RA, Lojkowski W, Ivanov ON. Preparation of nanocrystalline Bi<sub>2</sub>Te<sub>3</sub> via microwave-solvothermal synthesis and hot isostatic pressure, *Journal of Thermoelectricity International Research Quarterly* 2012, 14, 17–21.
- [25] Smolen D, Chudoba T, Malka I et al. Highly biocompatible, nanocrystalline hydroxyapatite synthesized in a solvothermal process driven by high energy density microwave radiation. *Int J Nanomedicine.* 2013, 8, 653–668.
- [26] Smolen D, Chudoba T, Gierlotka S et al. Hydroxyapatite Nanopowder Synthesis with a Programmed Resorption Rate, *Journal of Nanomaterials* 2012, Article ID 841971, 1–9.
- [27] Kusnieruk S, Wojnarowicz J, Chodara A et al. Influence of hydrothermal synthesis parameters on the hydroxyapatite nanostructure, *Beilstein J. Nanotechnol.* 2016, 7, 1586–1601.
- [28] Klingshirn C, Fallert J, Zhou H. 65 years of ZnO research – old and very recent results. *Physica Status Solidi (B)* 2010, 247, 1424–1447.
- [29] Özgür Ü, Alivov Yal, Liu C et al. A comprehensive review of ZnO materials and devices. *J. Appl. Phys.* 2005, 98, 45–148.
- [30] Salzano de Luna M, Galizia M, Wojnarowicz J et al. Dispersing hydrophilic nanoparticles in hydrophobic polymers: HDPE/ZnO nanocomposites by a novel template-based approach. *eX-PRESS Polymer Letters* 2014, 8/5, 362–372.
- [31] Kołodziejczak-Radzimska A, Jesionowski T. Zinc Oxide-From Synthesis to Application: A Review, *Materials* 2014, 7, 2833–2881.
- [32] Moezzi A, McDonagh AM, Cortie MB. Review Zinc oxide particles: Synthesis, properties and applications. *Chemical Engineering Journal* 2012, 185–186, 1–22.
- [33] The production processes of lead, zinc and cadmium (Accessed 9 August 2016, at [ipcc.mos.gov.pl/ipcc/custom/BAT\\_met\\_niez\\_r5.pdf](http://ipcc.mos.gov.pl/ipcc/custom/BAT_met_niez_r5.pdf))
- [34] Cierech, Wojnarowicz J, Szmigiel D et al. Preparation and characterization of ZnO-PMMA resin nanocomposites for denture bases. *Acta of Bioengineering and Biomechanics* 2016, 18, 31–41.
- [35] Sirelkhatim A, Mahmud S, Seeni A et al. Review on Zinc Oxide Nanoparticles: Antibacterial Activity and Toxicity Mechanism. *Nano-Micro Lett.* 2015, 7, 219–242.
- [36] Zhang Y, Nayak TR, Hong H, Cai W. Biomedical applications of zinc oxide nanomaterials. *Curr Mol Med.* 2013, 13, 1633–1645.
- [37] Cierech M, Kolenda A, Grudniak AM and et al. Significance of polymethylmethacrylate (PMMA) modification by zinc oxide nanoparticles for fungal biofilm formation. *International Journal of Pharmaceutics* 2016, 510, 323–335.
- [38] Majcher A, Wiejak J, Przybylski J and et al. A Novel Reactor for Microwave Hydrothermal Scale-up Nanopowder Synthesis. *Int. J. Chem. React. Eng.* 2013, 11, 361–368.
- [39] Hosni M, Farhat S, Schoenstein F et al. Ultrasound assisted synthesis of nanocrystalline zinc oxide: Experiments and modelling. *Journal of Alloys and Compounds* 2014, 615, 472–475.
- [40] Dunne PW, Munn PW, Starkey CL and et al. Continuous-flow hydrothermal synthesis for the production of inorganic nanomaterials. *Phil. Trans. R. Soc. A* 2015, 373.
- [41] Golmohammadia M, Towfighia J, Hosseinpourb M, Ahmadi SJ. An investigation into the formation and conversion of metalcomplexes to metal oxide nanoparticles in supercritical water. *J. of Supercritical Fluids* 2016, 107, 699–706.

- [42] Demoisson F, Piolet R, Ariane M, Leybros A, Bernard F. Influence of the pH on the ZnO nanoparticle growth in supercritical water: Experimental and simulation approaches. *J. of Supercritical Fluids* 2014, 95, 75–83.
- [43] Lojkowski W, Leonelli C, Chudoba T and et al. High-Energy-Low-Temperature Technologies for the Synthesis of Nanoparticles: Microwaves and High Pressure. *Inorganics* 2014, 2, 606–619.
- [44] Strachowski T, Chudoba T, Reszke E. and et al. Otrzymywanie nano tlenku cynku z zastosowaniem różnych technik pobudzenia reakcji chemicznych. *Glass and Ceramic* 2007, 4, 27–33.
- [45] Clearfield A, Reibenspies J, Bhuvanesh N. Principles and Applications of Powder Diffraction. Wiley-Blackwell, 2008.
- [46] Ertec microwave reactors (Accessed 9 August 2016, at [www.ertec.pl/en](http://www.ertec.pl/en))
- [47] Strachowski T, Grzanka E, Palosz BF et al. Microwave Driven Hydrothermal Synthesis of Zinc Oxide Nanopowders. *Solid State Phenomena* 2003, 94, 189–192.
- [48] Li S, Meierott S, Kohler JM. Effect of water content on growth and optical properties of ZnO nanoparticles generated in binary solvent mixtures by micro-continuous flow synthesis. *Chemical Engineering Journal* 2010, 165, 958–965.
- [49] Loupy A. Microwave-Material Interactions and Dielectric Properties, Key Ingredients for Mastery of Chemical Microwave Processes. In: Loupy A. *Microwaves in Organic Synthesis*. 2nd edn. Wiley-VCH Verlag GmbH & Co. KGaA, 2006.
- [50] Multiwave 3000 (Accessed 24 July 2017, at <http://www.rofa.at/Leaflet/Apaar/MW3000.pdf>)

Rodrigo González-Prieto, Santiago Herrero, Reyes Jiménez-Aparicio, Emilio Morán, Jesús Prado-Gonjal, José Luis Priego, and Rainer Schmidt

## **13 Microwave-assisted solvothermal synthesis of inorganic compounds (molecular and non molecular)**

The purpose of this chapter is more ambitious than simply to provide an overview of the advantages of the solvothermal synthesis of inorganic compounds under microwave (MW) radiation. The chapter focuses on the influence of different parameters and reaction conditions that allow the optimization of yield, the formation of a particular compound, or even the fine-tuning of its properties. The possibilities of this synthetic method are also presented with select examples of the application of microwave-assisted solvothermal synthesis (MWSS) to the preparation of molecular coordination compounds with different dimensionality and nonmolecular inorganic compounds. Specific aspects related to the MWSS of inorganic species, such as catalysis, nanomaterials, or green chemistry, are covered in other chapters of this book. It is important to underline that synthetic procedures in ambient atmosphere or in open vessels are not considered in this chapter.

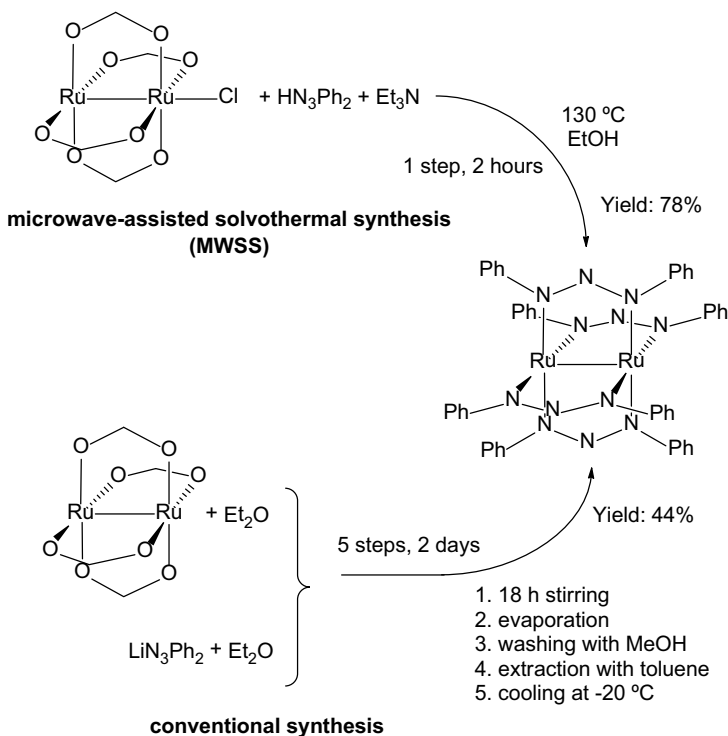
### **13.1 Introduction**

Microwave-assisted solvothermal synthesis (MWSS) has been extended to all territories covered by inorganic chemistry. The advantages and new opportunities that provide this new method with respect to traditional heating approaches were evident from the very beginning, despite the fact that it is often difficult to make direct comparisons (temperature, pressure, and reactant concentration are usually higher in MWSS than in conventional heating procedures) [1]. The heating due to the interaction of the microwave (MW) radiation with the reaction mixture and the heat transfer during the absorption process are usually considered the origin of the improvements found in MW synthesis. The heating mechanism is complex and depends on the nature of the material. Thus, nonmagnetic materials are basically affected by the MW electrical field, dipolar losses and conduction losses being the two main loss mechanisms. However, magnetic materials are also affected by the magnetic field component of MWs. Therefore, hysteresis and eddy current losses constitute additional heating mechanisms, as do other residual losses such as domain wall resonance and electron spin resonance losses [2]. Moreover, some authors also claim the existence of nonnegligible nonthermal effects. Direct and indirect heating and nonthermal effects are taken into account in some approximations to explain the MW effect [3].

<https://doi.org/10.1515/9783110479935-013>



One of the advantages of MWSS is the improvement in reaction times [4]. This general fact is also true of solid-state and organometallic reactions and particularly for substitutionally inert transition metal ions, for which the reaction time can be reduced by more than thousand times [5]. The MWSS of polymetallic cluster compounds also started to be used one decade ago with similar results [6]. Even MWSS may improve the results obtained by MW activation under atmospheric conditions [7]. In addition to the reduction of the reaction times, many other advantages usually accompany MWSS, such as energy saving, high yields, high selectivity, atom economy, reduction of reaction steps, and the use of less solvent, that cause MWSS to be considered as an environmentally benign method (Chapter 10). The synthesis with good yields of some elusive paddlewheel diruthenium compounds with  $N,N'$ -donor ligands is an example of simple, efficient, fast, and cheap MWSS (Scheme 13.1) [8, 9].



**Scheme 13.1:** MWSS (top) and conventional synthesis (bottom) of  $[Ru_2(PhNNNPh)_4]$ . Adapted from Ref. [8] with permission from The Royal Society of Chemistry.

Furthermore, this technique can allow access to alternative kinetic pathways to produce compounds or phases that cannot be synthesized using other solvothermal methods [10, 11].

The use of solvothermal synthesis under MW radiation also has some disadvantages with respect to conventional electric heating solvothermal synthesis (CESS). Since reactions usually progress faster in the presence of MWs, the pressure can increase more rapidly when a gas is produced. Therefore, the risk of explosion is higher in MWSS than in CESS, which must be taken into account when a procedure is set up [12]. Also, MWSS usually produces smaller crystals than traditional solvothermal procedures, which limits the study of new products [13], although this restriction may be overcome by a careful design of the reaction conditions [14]. Another disadvantage is a possible accidental cleavage of a bond that can occur during reactions under solvothermal MW activation conditions [15].

MWSS sometimes does not provide a significant improvement over other conventional heating methods. In some reactions, similar or even better yields in shorter times may be obtained by other means [11, 16–19].

## 13.2 Influence of parameters and reaction conditions

In MWSS, it is possible to vary and control several parameters, such as irradiation power, solvent, temperature, time, stirring, and ramp rates or cooling time, in addition to reactant ratio and concentration/dilution of the mixture. This fact improves reproducibility with respect to conventional solvothermal synthesis, although it depends on the particular design of the MW oven that is employed. Much care must be taken to set up a particular experiment, not only to work safely and limit the risks but also to find the best conditions to obtain the desired product. In this section, several examples in which the variation of a parameter leads to significant differences in the results are shown.

### 13.2.1 Solvent

Different solvents have their own characteristics that influence reactions, as in other synthetic procedures (e.g., polarity, solvation, redox properties). However, in MWSS the capacity of solvents to absorb MW radiation must also be considered, which is strongly related to its polarity. Thus, polar solvents and the presence of ionic species lead to a rapid increase in temperature, and temperatures above the boiling points of the solvents are easily reached. This fact raises the pressure of the system and modifies the viscosity of the reaction mixture. Therefore, the solvent determines the autogenic pressure of the reaction vessel, but it may also be incorporated into the final compound. Moreover, high pressures could shift the reaction toward the incorporation of species from the solvent. Thus, hydroxide groups are incorporated in  $[\text{Co}_7(\mu_3\text{-OH})_6\text{L}_6](\text{ClO}_4)_2$  when the reaction takes place in water/acetonitrile, while methoxide species are coordinated instead in  $[\text{Co}_7(\mu_3\text{-CH}_3\text{O})_6\text{L}_6](\text{ClO}_4)_2$  when

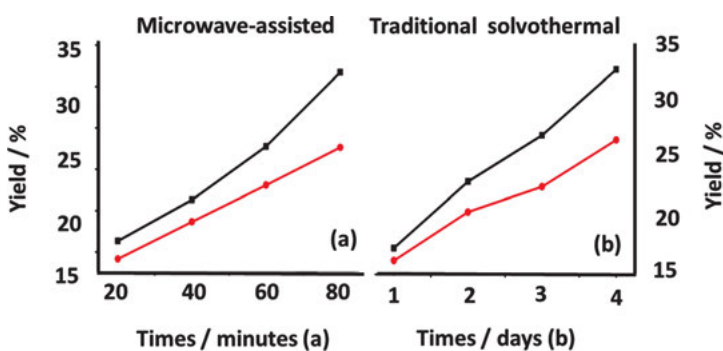
methanol/acetonitrile are used ( $L = 2\text{-methoxy-6-}[(\text{methylimino})\text{methyl}]\text{phenolate}$ ) [20]. More interestingly, it has been reported that  $[\text{Ni}(\text{OH}_2)_4(4\text{-pyc})_2]$  (4-pyc-isonicotinate) is transformed into the metal organic framework (MOF)  $[\text{Ni}(4\text{-pyc})_2]_n$  in (THF), but another MOF with much better adsorption capacity,  $[\text{Ni}_5(\text{OH}_2)_3(4\text{-pyc})_{10}]_n$ , is obtained when the reaction takes place in a THF/water mixture [21].

### 13.2.2 Reaction time

This parameter must be carefully controlled in order to get a particular compound in good yield. The dependence of the yield versus time has been studied for the preparation of  $[\text{Co}_4(\mu_3\text{-OMe})_4(L)_4(\text{MeOH})_4]$  ( $L$  is the deprotonated form of 2-hydroxy-3-methoxy-benzaldehyde or 2-hydroxy-3-ethoxy-benzaldehyde) [22] (Figure 13.1). The longer the reaction times, the higher the yields. However, traditional solvothermal synthesis needs to increase the reaction time from minutes to days in order to get yields similar to the corresponding MWSS ones for the same compounds.

The average size of the crystals also increases with time (Figure 13.2), and the size distribution is more homogeneous and narrow under MW radiation than for the conventional method.

The size, quality, and yield of crystals of the heterobimetallic clusters  $[\text{Ni}_3\text{ML}_3(\text{OH})(\text{CH}_3\text{CN})_3]_2$  ( $M = \text{K}$  or  $\text{Na}$ ;  $L$  is an anion of 2-[(2-hydroxy-3-methoxy-benzylidene)-amino]-ethanesulfonate) are also augmented when the reaction time is increased progressively from 29 to 149 min [23]. The crystal size of the MOF Cr-MIL-101 also increases with increasing radiation time [24]. In other cases, longer times are necessary to obtain pure phases because it happens in the synthesis of  $[\text{Ce}_2(\text{pydc})_3(\text{OH}_2)_2]$  (pydc = 2,5-pyridinedicarboxylate) [25].



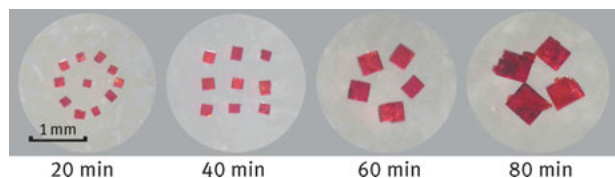
**Fig. 13.1:** Yield versus time in preparation of  $[\text{Co}_4(\mu_3\text{-OMe})_4L_4(\text{MeOH})_4]$  ( $L$  is the deprotonated form of 2-hydroxy-3-methoxy-benzaldehyde (black) or 2-hydroxy-3-ethoxy-benzaldehyde (red) by MWSS (a) and traditional solvothermal conditions (b). Adapted from Ref. [22] with permission from The Royal Society of Chemistry.

On the other hand, short times in MWSS have been employed to obtain kinetic compounds as in the preparation of unstable porous materials with enhanced properties. The reaction of  $\text{CrCl}_3 \cdot 6 \text{H}_2\text{O}$  with terephthalic acid in water at  $210^\circ\text{C}$  in an MW oven produces basically the chromium terephthalate phase MIL-101, with a huge pore volume ( $1.9 \text{ mL/g}$ ), while in a conventional electric oven mainly MIL-53 is formed, with a lower pore volume ( $0.6 \text{ mL/g}$ ). Study of the reaction products with several reaction times demonstrated that MIL-101 is the kinetic phase. This phase-selective synthesis of MIL-101 is ascribed to a fast crystallization of the material [26].

Sometimes, longer reaction times lead to the transformation of the initial product toward the formation of other compounds. The reaction of  $[\text{Ru}_2\text{Cl}(\text{O}_2\text{CMe})_4]$  with *N,N'*-diphenyltriazene ( $\text{HN}_3\text{Ph}_2$ ) produces initially the substitution of the equatorial ligands to form the  $\text{Ru}_2^{5+}$  compound  $[\text{Ru}_2\text{Cl}(\text{N}_3\text{Ph}_2)_4]$ , but 2 h are needed to obtain a pure reduced  $\text{Ru}_2^{4+}$  derivative  $[\text{Ru}_2(\text{N}_3\text{Ph}_2)_4]$  [8]. Some systems can allow the isolation of several compounds keeping the same reaction conditions except the reaction time:  $[\text{FeCl}_2(\text{TzH})_4]$  (10 mg in 0.5 mL toluene at  $150^\circ\text{C}$  under an inert gas atmosphere) is transformed by MW irradiation into two different one-dimensional (1D) polymers:  $[\text{FeCl}(\text{TzH})_2]\text{Cl}$  (82%) in 20 min and  $[\text{FeCl}_2(\text{TzH})]$  (86%) in 45 min (TzH = 1,2,4-1H-triazole) [27].

### 13.2.3 Temperature

Temperature is generally a key factor when reactivity is studied and, of course, is also very important in MWSS. Increasing the temperature may lead to a reduction of the reaction time and an improvement of the yield as observed in the preparation of iso-butyl-2-(trimethylstannyl)isonicotinate from the bromo derivative and  $\text{Sn}_2\text{Me}_6$  in toluene in the presence of  $[\text{Pd}(\text{PPh}_3)_4]$ . At  $110^\circ\text{C}$  for 2 h, the product is isolated in 79% yield, while at  $150^\circ\text{C}$ , a yield of 85% is reached in only 4 min [28]. When the formation of several compounds is possible from the same reaction, increasing the temperature is usually more effective than increasing the time to obtain the thermodynamic product [29]. Nevertheless, high temperatures can also lead to decomposition species [30] or produce crystal degradation and surface defects that can affect the properties of the



**Fig. 13.2:** Photos of crystals of  $[\text{Co}_4(\mu_3\text{-OMe})_4(\text{L})_4(\text{MeOH})_4]$  (L is the deprotonated form of 2-hydroxy-3-ethoxy-benzaldehyde) obtained by MWSS for 20, 40, 60, and 80 min. Adapted from Ref. [22] with permission from The Royal Society of Chemistry.

final product [25, 31]. Therefore, it is always desirable to optimize the temperature to increase the yield without favoring decomposition [32].

Checking the products after several time intervals can be useful in order to know the steps of the reaction mechanism as has been seen in the previous section. However, varying the temperature with fixed periods of reaction has also been employed to determine the step in which an isomerization of the ligand takes place, before, after, or when the coordination occurs [33].

It is also worth mentioning that the morphology of the final product can be tailored by controlling the temperature, as was found in several metal sulfides. CuS, NiS/Ni<sub>3</sub>S<sub>2</sub>, FeS<sub>2</sub>, and Co<sub>9</sub>S<sub>8</sub> can be obtained with various morphologies including nanoparticles, nanobuds, nanosheets, and interlinked nanosheets [34].

### 13.2.4 Reactant ratio

The reactant ratio often influences the final compound to be isolated. MWSS can afford different arrangements of magnesium 1,2,4,5-benzenetetracarboxylate compounds, varying the ratio of the reacting species (which also varies the pH of the reaction mixtures): lamellar [Mg<sub>2</sub>(BTEC)(OH<sub>2</sub>)<sub>6</sub>] (pH = 4.2), MOF [Mg<sub>2</sub>(BTEC)(OH<sub>2</sub>)<sub>4</sub>] · 2 H<sub>2</sub>O (pH = 4.6), or the one-dimensional polymer [Mg<sub>2</sub>(BTEC)(OH<sub>2</sub>)<sub>8</sub>] (pH = 4.8) [35]. The pH value of the precursor solution is also crucial to control the particle size and morphology of NH<sub>4</sub>V<sub>3</sub>O<sub>8</sub> microcrystals [36].

Species generated *in situ* can also determine the final product, and the formation of those species can depend on the reactant ratio. Thus, the reaction between Cu(HCO<sub>2</sub>)<sub>2</sub> · H<sub>2</sub>O and 2-dpds (2-dpds = 2,2'-dipyridyldisulfide) gives [Cu<sub>2</sub>(μ-Hpvt)<sub>2</sub>(Hpvt)<sub>4</sub>](SO<sub>4</sub>) · ~ 5 EtOH and [Cu<sub>6</sub>(μ-pyt)<sub>6</sub>] in a 1:1 ratio (Hpvt = pyridine-2(1H)-thione). However, [Cu(OH<sub>2</sub>)<sub>6</sub>][Cu<sub>6</sub>(μ-Hpvt)<sub>12</sub>](SO<sub>4</sub>)<sub>4</sub> · 4 H<sub>2</sub>O is formed additionally in a 1:2 ratio. A 2:1 or 3:1 ratio produces [Cu<sub>6</sub>(μ-pyt)<sub>6</sub>], [Cu(OH<sub>2</sub>)<sub>6</sub>][Cu<sub>6</sub>(μ-Hpvt)<sub>12</sub>](SO<sub>4</sub>)<sub>4</sub> · 4 H<sub>2</sub>O, and [Cu(2-dps)(μ-SO<sub>4</sub>)(OH<sub>2</sub>)<sub>2</sub>] · 3 H<sub>2</sub>O [37].

Nevertheless, there are reactions in which the selectivity for a particular compound is so remarkable that the ratio only affects the yield of that compound. The reaction in refluxing THF of [Ru<sub>2</sub>Cl(O<sub>2</sub>CMe)<sub>4</sub>] with *N,N'*-diphenylformamidine (HDPHF) to form [Ru<sub>2</sub>Cl(DPhF)<sub>4</sub>] is stepwise. Therefore, an adjustment of the reactant ratio allows the synthesis of the intermediate compound [Ru<sub>2</sub>Cl(DPhF)<sub>3</sub>(O<sub>2</sub>CMe)] [38]. However, the solvothermal reaction in an MW oven produces exclusively [Ru<sub>2</sub>Cl(DPhF)<sub>4</sub>]. When there is not enough formamidine, the presence of [Ru<sub>2</sub>Cl(O<sub>2</sub>CMe)<sub>4</sub>] and [Ru<sub>2</sub>Cl(DPhF)<sub>4</sub>] is observed, but no intermediate species were detected [9].

It is also worth mentioning that larger crystals and higher yields can also be obtained, increasing the ligand:metal ratio, as was observed in the synthesis of MOF-5. Unfortunately, the crystallinity of the product was inferior with a lower surface area [31].

### 13.2.5 Other variables

Irradiation power and pressure are important parameters that usually are not reported. When the irradiation power is higher than what is necessary to reach the designated temperature, the irradiation is more discontinuous and could influence the final result. Pressure is autogenic and depends on many factors such as the temperature, the volume of the vessel, the nature and quantity of solvent, and others that could be *a priori* unknown, such as the formation of gaseous products.

Other reaction conditions or parameters that usually are not considered essential and, hence, are not often provided in the published recipes can affect the yield, the purity, or the properties of the product. Thus, cooling time or dilution influences the crystallinity of the final product for discrete species [8, 9]. In the synthesis of polymeric species as MOF-5, it was already observed that more diluted substrates produce higher-quality crystals [31]. Even the crystal size of IRMOF1 can be fine-tuned from the micrometer to the submicrometer scale by diluting progressively the starting mixtures [39].

Stirring and heating rates can also be determining parameters in some synthetic procedures. For example, the yield in the synthesis of  $Y(O_3P-C_2H_4-SO_3)$  depends on the stirring rate: with no stirring the yield is 71%, which decreases to 45–43% for 420–600 rpm to 32% at 900 rpm [40]. The use of a rapid heating rate (2 min from 25 to 220 °C) is the key point to obtain  $[ZrO(O_2CC_6H_4CO_2)]$  (MIL-140A-MW) in highly pure and crystalline form. When the ramp time is increased from 2 min to 1 h, the UiO-66 phase appears as an impurity [41].

## 13.3 Molecular solids

Many types of reactions have been carried out showing the advantages of the use of MW activation in the synthesis of coordination and organometallic compounds, including coordination polymers. In this section, several significant examples of MWSS are presented. Structural differences (often differences in solubility) prompt the separation between discrete mononuclear species and clusters on the one hand and polynuclear compounds on the other.

### 13.3.1 Discrete species

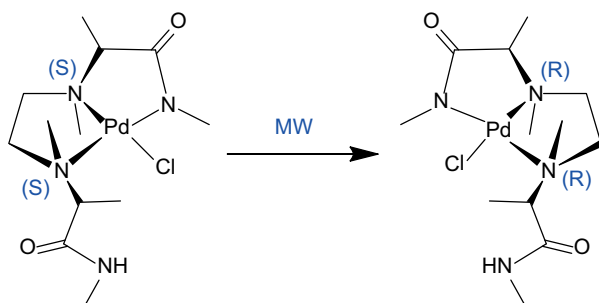
Molecular compounds are usually soluble in several solvents, which allows for a quick coupling between the MW radiation and the reacting molecules, and consequently the reaction time is frequently reduced from days and hours to minutes [42]. This fact is especially appealing for the synthesis of some coordination compounds of metals from the first, and especially from the second- and third-row transition metals,

which are usually inert toward the substitution of ligands when the metal centers are in their common oxidation states. Reaction times, yields, and some reaction conditions for the preparation of several compounds are collected in Table 13.1. As can be seen, the MW activation procedure not only leads usually to lower reaction times but also to higher yields than conventional methods. This trend is observed, for example, in the synthesis of  $[\text{AuCl}_2(\text{N-N})](\text{PF}_6)$  complexes (N-N = 2,2'-bipyridine and related ligands), whose preparation is greatly improved by the use of MW heating. For these compounds the reactions were complete within minutes, and generally the products are analytically pure yellow solids that do not require recrystallization. In addition, MWSS can favorably replace procedures that employ toxic organomercury reagents in some cases [43].

The same tendency is observed in the preparation of different functionalized tetraarylcyclopentadienones and the corresponding dinuclear ruthenium hydride Shvo-type complexes. Specifically, in the case of  $[3, 4-(R\text{-C}_6\text{H}_4)_2\text{-}2, 5\text{-Ph}_2(\eta^5\text{-C}_4\text{CO})]_2 \text{H-Ru}_2(\text{CO})_4(\mu\text{-H})$ , the reaction time is reduced from 40 h to 50 min. Other advantages are the relatively low amount of solvent used and the fact that the process does not require solvent-consuming purification steps [32].

An additional advantage of using MW activation is to promote many important metal-mediated organic transformations to yield organometallic compounds that cannot be readily obtained under traditional thermal conditions. For example, under MW conditions diarylacetylenes with cyclopentadienyl cobalt dicarbonyl provide the access to metallocenes in both cyclobutadiene ( $\text{Ar}_4\text{C}_4\text{CoCp}$ ) and cyclopentadienone ( $\text{Ar}_4\text{C}_4(\text{C=O})\text{CoCp}$ ) families [54].

The MW radiation also permits the separate synthesis of a pair of right- and left-handed square planar Pd(II) complexes [55],  $N_S, N_S\text{-}[\text{Pd}(\text{HL})\text{Cl}]$  and  $N_R, N_R\text{-}[\text{Pd}(\text{HL})\text{Cl}]$ , from a single chiral precursor,  $N, N'\text{-ethylene-bis}[N''\text{-methyl-(S)-alanine methyl amide (H}_2\text{L)}$ .



**Scheme 13.2:** Helicity inversion of  $N_S, N_S\text{-}[\text{Pd}(\text{HL})\text{Cl}]$  under MW radiation. Adapted from Ref. [55] with permission from The Royal Society of Chemistry.

**Tab. 13.1:** Comparison of reaction time and yield for the preparation of selected compounds by MW and conventional methods.

Compound	Conventional methods		Microwave method		References	
	Reaction time	Other data	Yield (%)	Reaction time		Other data
$[\text{AuCl}_2(\text{bpy})](\text{PF}_6)$	16 h	$\text{CH}_3\text{CN}/\text{H}_2\text{O}$ reflux.	96	10 min	110 °C, $\text{CH}_3\text{CN}/\text{H}_2\text{O}$	[43, 44]
$[\text{Bi}(\text{MBT})_3]_3^{\text{a}}$	6 h	Recrystallization Toluene reflux, dry $\text{N}_2$	65	8 min	Toluene, 115 °C, dry $\text{N}_2$	[45]
$[\text{Cr}(\text{BSAP})(\text{H}_2\text{O})_3] \text{Cl}^{\text{c}}$	8.2 h	Ethanol reflux	59.6	7.9 min	Dry ethanol	[46]
$[\text{Cr}_2\text{O}_4(\text{dap})_2]^{2\text{c}}$	8 h	Abs. ethanol reflux	60	20 min	absolute ethanol, 250 W, 50 °C	[47]
$\text{GdL}_3 \cdot 3\text{H}_2\text{O}^{\text{b}}$	14.5 h	45 mL methanol reflux	74	6 min	2 mL methanol	[48]
$[\text{Os}_3(\mu\text{-I})_2(\text{CO})_{10}]$	37.5 h	Benzene reflux, $\text{N}_2$ atmosphere	16	13 min	Cyclohexane, 150 °C	[49, 50]
$[(\text{C}_6\text{H}_6)\text{RuLC}][\text{Cl} \cdot 2\text{H}_2\text{O}]^{\text{a2}}$	4 h	60 °C	63.5	30 min	$\text{CH}_2\text{Cl}_2$ , 60 °C	[51]
$[\text{Ru}_2(\text{DPhT})_4]$	18 h	$\text{Et}_2\text{O}$ , Ar atmosphere	44	8 min	$\text{EtOH}$ , 130 °C, air atmosphere	[9, 52]
$[\text{VO}(\text{C}_{14}\text{H}_8\text{N}_2\text{OCIF}_2)_2]\text{SO}_4$	7.2 h	Methanol reflux	68	8.9 min	Dry ethanol	[53]

<sup>a</sup> MBT = 4-methylthiazole-2-thiol    <sup>a2</sup>L = phenanthroimidazole

<sup>b</sup> L<sup>1</sup>H = 3-formyl-4-chlorocoumarinhydrazinecarbothioamide

<sup>c</sup> H<sub>2</sub>BSAP = 2-[(5-bromo-2-hydroxybenzylidene)amino]pyridin-3-ol    <sup>c2</sup> dap = 2,6-diaminopyridine

<sup>d</sup> PHEHAT = 1,10-phenanthroline[5,6-b]1,4,5,8,9,12-hexaazatriphenylene.



MW activation is also useful to prepare dinuclear species such as dimolybdenum [56] and diruthenium compounds [6, 7, 9]. In some cases, the metallic atom is reduced or oxidized without any addition of redox agent. Thus, the use of MW radiation allows the easy and clean substitution of the acetate groups in  $[\text{Ru}_2\text{Cl}(\text{O}_2\text{CMe})_4]$  by 1,3-diphenyltriazene ( $\text{DPhT}^-$ ), 1,3-diphenylformamidinate ( $\text{DPhF}^-$ ), or 1,3,4,6,7,8-hexahydro-2H-pyrimido[1,2-a]pyrimidinate ( $\text{hpp}^-$ ). In every case, the use of MW activation promotes the total substitution of the acetate ligands by *N,N*-donor ligands, although the selective substitution of the acetate group in  $[\text{Ru}_2\text{Cl}(\text{DPhF})_3(\text{O}_2\text{CMe})]$  by another carboxylate can also be achieved. The MW methods lead to different results depending on the donor character of the equatorial ligand ( $\text{hpp}^- > \text{DARF}^- > \text{DART}^-$ ), giving a  $\text{Ru}_2^{4+}$  compound when the ligand is  $\text{DART}^-$ ,  $\text{Ru}_2^{5+}$  complex when the ligand employed is  $\text{DARF}^-$ , and a  $\text{Ru}_2^{6+}$  compound when  $\text{hpp}^-$  is used. Hence, the synthesis of the  $[\text{Ru}_2\text{Cl}_2(\text{hpp})_4]$  complex containing a  $\text{Ru}_2^{6+}$  unit can be very easily carried out instead of the tedious procedures followed in other methods [57, 58].

MWSS has also proven to be a useful tool for the preparation of higher nuclearity complexes. For example,  $[\text{Mn}_6\text{O}_2(\text{sao})_6(\text{O}_2\text{CH})_2(\text{CH}_3\text{OH})_4] \cdot 2 \text{MeOH}(\text{sao})\text{H}_2 = \text{salicylaldoxime}$ , a single-molecule magnet, is obtained when the reaction mixture in 8 mL of methanol is heated at 110 °C and 110 psi for 5 min. The compound is isolated in an 80% yield. The synthesis in the absence of MW activation requires longer reaction periods, and only a 39% yield is achieved [6]. Synthetic conditions play an important role in the structural diversities of the clusters. Thus, the formation of *4f-3d* complexes frequently depends on the competitive reactions between *3d* and *4f* metals chelating to the same bridging ligand. A good example is the preparation of the nonanuclear metal cluster  $[\text{La}_3\text{Ni}_6(\text{IDA})_6(\text{OH})_6(\text{H}_2\text{O})_{12}] \cdot 3 \text{NO}_3 \cdot 15 \text{H}_2\text{O}$ , (IDA = iminodiacetate) in 40% yield under MW irradiation and only in 28.5% yield in standard conditions [59].

In many circumstances, the MW activation leads to a different complex than the conventional method. For example, when a solution of  $\text{MnCl}_2 \cdot 4 \text{H}_2\text{O}$  and  $\text{NiCl}_2 \cdot 6 \text{H}_2\text{O}$  in MeCN/EtOH is stirred at room temperature with 3,5-di-*tert*-butylsalicylic acid ( $\text{SALOH}_2$ ), 3-dimethylamino-1-propanol, and  $\text{NEt}_3$ , the Mn/Ni complex  $[\text{Mn}_5\text{Ni}_4(\text{OH})_4(\text{C}_5\text{H}_{12}\text{NO})_4(\text{SALOH})_6(\text{SALO})_4] \cdot 6 \text{C}_2\text{H}_3\text{N} \cdot 3 \text{C}_2\text{H}_6\text{O}$  is obtained, whereas a similar reaction under MW irradiation leads to  $[\text{Mn}_7(\text{OH})_3(\text{C}_5\text{H}_{12}\text{NO})_2(\text{C}_5\text{H}_{13}\text{NO})(\text{SALO})_6(\text{SALOH})_3]$ , in which the Ni(II) ions have not been incorporated in the complex [60].

In other instances, this technique permits one to synthesize coordination compounds in which classical ligands such as  $\text{NO}_2^-$  present unknown coordination modes ( $\eta^1, \eta^1, \eta^1, \mu_3\text{-NO}_2^-$ ) [61].

### 13.3.2 Polymeric species

MW heating under solvothermal conditions to prepare coordination polymers has advantages similar to those mentioned for discrete species. For example, the 1D polymer  $[\text{NiLn}(\text{L})(\text{NO}_3)_2(4\text{-pyp})(\text{EtOH})]$  (Ln = Nd, Eu;  $\text{H}_2\text{L} = 1,3\text{-bis}((3\text{-methoxysalicylidene})-$

amino)propane; 4-pyp = 4-pyridinepropionate) is formed in 1 min while most of the coordination polymers based on *d-f* metals and pyridine carboxylates require several days in solvothermal conditions [62]. The synthesis of the catalyst 2D-CCB (2D cobalt–cysteate coordination polymer) is another example of fast MWSS (10 min, 100 W) that improves the time employed by the conventional solvothermal method (50 h, 140 °C) and avoids the lack of purity found by other conventional procedures [63].

MWSS has also been extensively used in the synthesis of 3D MOFs [10, 14, 64–66] to reduce reaction times from days or hours to minutes. Very short reaction times have also been found in the synthesis of lanthanide compounds. Thus, MOF [Ln(Hpmd)(OH<sub>2</sub>)] materials (Ln<sup>3+</sup> = Eu<sup>3+</sup>, Gd<sup>3+</sup>, and Tb<sup>3+</sup>; H<sub>4</sub>pmd = 1,4-phenylenebis-(methylene)diphosphonic acid) can be achieved in only 5 s by MWSS at 40 °C with 50 W of irradiation power [67]. However, under conventional hydrothermal conditions 3 days at 180 °C and 5 min by ultrasound-assisted synthesis at room temperature are required. The three synthetic approaches yielded phase-pure and highly crystalline products, demonstrating that it is possible to get quantitative yields in considerably reduced temperature and reaction time using MWSS.

MW solvothermal conditions may lead a reaction through alternative pathways, which permit the isolation of compounds or phases that are not accessible by other means. Thus, a reaction in ambient conditions of a copper(II) salt, 1-H'' pyrazole, and [W(CN)<sub>8</sub>]<sup>3-</sup> (3 : 9 : 2) in the presence of an organic acid forms Cu<sub>3</sub><sup>II</sup>(Hpyr)<sub>6</sub>[W<sup>V</sup>(CN)<sub>8</sub>]<sub>2</sub> · 3.5 H<sub>2</sub>O, regardless of the nature of the copper salt and acid. However, varying the Cu(II) salt and the carboxylic acid, three different compounds with diverse dimensionality are obtained under MW solvothermal conditions:

- Cu<sub>2</sub><sup>II</sup>(Hpyr)<sub>5</sub>(H<sub>2</sub>O)[W<sup>V</sup>(CN)<sub>8</sub>](NO<sub>3</sub>)<sub>3</sub> · 3 H<sub>2</sub>O (1D),
- Cu<sub>5</sub><sup>II</sup>(Hpyr)<sub>18</sub>[W<sup>V</sup>(CN)<sub>8</sub>]<sub>4</sub>[Cu<sup>II</sup>(Hpyr)<sub>4</sub>(H<sub>2</sub>O)<sub>2</sub>] · 9 H<sub>2</sub>O (2D), and
- Cu<sub>4</sub><sup>II</sup>(Hpyr)<sub>10</sub>(H<sub>2</sub>O)[W<sup>V</sup>(CN)<sub>8</sub>]<sub>2</sub>(HCOO)<sub>2</sub> · 4.5 H<sub>2</sub>O (3D).

Conventional heating of the mixture leads to the reduction of the tungsten centers [68]. The formation of a 1D structure for [NdCl<sub>3</sub>(H<sub>2</sub>O)(phen)] has also been ascribed to the MW heating procedure [69] since conventional solvothermal synthesis leads to the formation of monomeric or dimeric discrete species.

There are many examples of subsequent transformations with longer reaction times such as the already mentioned [FeCl(TzH)<sub>2</sub>]Cl into [FeCl<sub>2</sub>(TzH)], in which both are 1D coordination compounds [27]. Another example is the synthesis of [La(H<sub>4</sub>bmt)(H<sub>5</sub>bmt)(H<sub>2</sub>O)<sub>2</sub>] · 3 H<sub>2</sub>O (1D) and [La<sub>2</sub>(H<sub>3</sub>bmt)<sub>2</sub>(H<sub>2</sub>O)<sub>2</sub>] · H<sub>2</sub>O (3D). Both are produced from the reaction between H<sub>6</sub> bmt[(benzene-1,3,5-triyltris(methylene))triphosphonic acid] and LaCl<sub>3</sub> hydrate under MW radiation. The former compound is obtained pure at low temperatures and short times while the formation of the latter is preferred at longer times and, especially, at high temperatures [29].

There are even some examples of reversibility among structures with the same or different dimensionality. Thus, the 1D coordination polymer [Pb(O<sub>2</sub>CCH<sub>2</sub>Ph)<sub>2</sub>(OH<sub>2</sub>)] is transformed into the 2D polymer [Pb(O<sub>2</sub>CCH<sub>2</sub>Ph)<sub>2</sub>] by dehydration. This latter com-

pound is transformed back into the former by hydrothermal treatment [70]. Another possibility is the co-crystallization of two molecules, as in  $[\text{Cu}(\mu_{1,1}\text{-N}_3)_2(\text{H}_2\text{O})][\text{CuL}_2]$  ( $\text{L} = 5\text{-methylpyrazine-2-carboxylate}$ ), which form a 2D supramolecular structure owing to the interactions between the 1D and 0D components [71].

The synthesis of kinetic compounds is sometimes due to a fast crystallization of the species [26], which is often related to the low solubility of polymeric structures. This fact can induce the formation of too small crystals to solve their structure by single-crystal X-ray diffraction. Nevertheless, the purity of the phases allows in some cases the use of X-ray powder diffraction instead [4].

The completion of a reaction is more difficult to survey for polymeric species, especially for paramagnetic ones. In those cases, mass spectrometry may be a useful tool. This technique was employed to optimize the reaction time in the step substitution of the acetate ligands in the 1D polymer  $[\text{Ru}_2\text{Cl}(\text{O}_2\text{CMe})_4]_n$  by amidates to synthesize  $[\text{Ru}_2\text{Cl}(\mu\text{-NHOCR})_4]_n$ , also 1D [16].

Microwave activation also permits, in some MOFs, the control of the size of the crystals. For example, Kitagawa and coworkers have used MWSS to control the crystal size of the porous coordination polymer  $[\text{Cu}_3(\text{BTC})_2]$  ( $\text{BTC} = \text{benzene-1,3,5-tricarboxylate}$ ) [72]. Thus, applying MW irradiation (140 °C, 10 min) and with several ratios of dodecanoic acid to benzene-1,3,5-tricarboxylic acid, nanocrystals of  $[\text{Cu}_3(\text{BTC})_2]$  were obtained in high yields with controlled and homogeneous sizes ranging from nanometers to micrometers (Figure 13.3).

The use of MWSS to obtain MOFs is usually limited to small-scale preparation. However, in 2015, Bag and coworkers [73] reported the laboratory large-scale synthesis of nine isostructural lanthanide MOFs. The authors were able to obtain in 5 min up to 2 g of microcrystalline  $[\text{Ln}(\text{TTTPC})(\text{NO}_2)_2\text{Cl}] \cdot 10\text{H}_2\text{O}$ , where  $\text{Ln} = \text{La, Ce, Pr, Nd, Eu, Tb, Dy, Ho, or Yb}$ , and  $\text{H}_3\text{TTTPC}$  is the flexible 1,1',1''-tris(2,4,6'' trimethylbenzene-1,3,5-triyl)-tris(methylene)-tris(pyridine-4'' carboxylic acid).

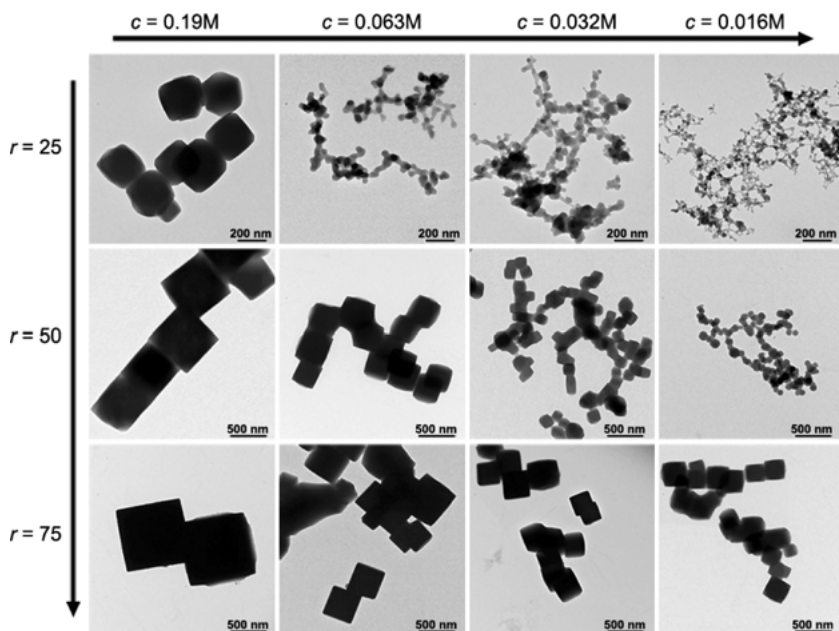
### 13.4 Nonmolecular solids

Nonmolecular solids are those characterized by strong chemical bonding, that is, ionic-covalent. Since many of them, such as transition metal halides, oxides, and nitrides, possess useful properties, they can also be considered inorganic materials. Metals, semimetals, and alloys are obviously nonmolecular solids but are beyond the scope of this section. The use of MWs as a fast chemistry method for the preparation of different inorganic nonmolecular materials in liquid media is growing very rapidly. Taking into account that there are some recent reviews covering the topic with a large number of references [74, 77], the goal of this section is to provide an overview of the field with some selected examples rather than making an exhaustive study.

Dr. Komarneni must be mentioned here since he launched a pioneering work in the 1990s [78] in connection with studying and comparing the conventional hydro-

thermal syntheses of different ceramic powders and the corresponding hydrothermal syntheses performed by MW heating using special autoclaves. This group paved the way for this kind of research showing that a plethora of nonmolecular inorganic materials can be rapidly and easily produced by these means. Lately, they have extended this novel synthetic route to the production of other nanophase materials including metals [79–85].

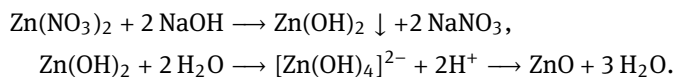
Although many types of nonmolecular solids can be prepared using MWSS (e.g., metals, oxides, chalcogenides, nitrides), this section is focused only on the well-represented oxygen-containing compounds because the mechanisms of reaction are easier to imagine and understand than in other families of compounds. Microwave-hydrothermal synthesis (MWHS) has been successfully used for materials ranging from binary metallic oxides, oxyhydroxides, and ternary oxides to more complex materials and structures such as zeolites or other mesoporous materials. It is also an effective method for producing nanoparticles with short reaction times. The control of the particle size and morphology is also feasible by varying nucleation and growth kinetics parameters, although, up till now, most of the results have been based on a trial-and-error procedure. Some selected examples of oxygen-containing materials are listed in what follows.



**Fig. 13.3:** TEM images of samples obtained with various concentrations of dodecanoic acid and benzene-1,3,5-tricarboxylic acid. Samples were prepared under MW irradiation (140 °C, 10 min). Reprinted with permission from Ref. [72]. Copyright (2010). American Chemical Society.

### 13.4.1 Binary metallic oxides

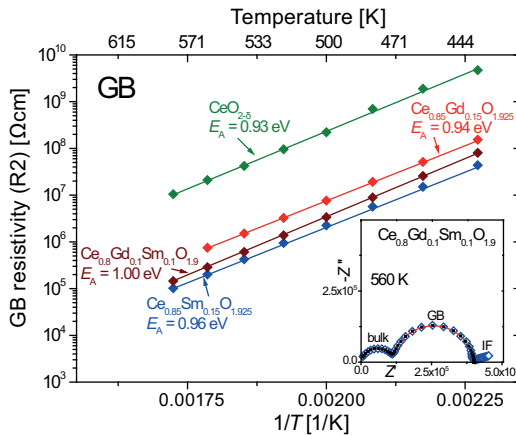
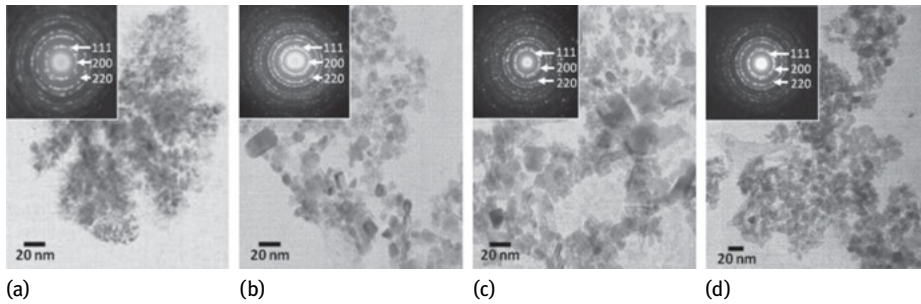
Oxides such as ZnO, CuO, PdO, CoO, MnO, TiO<sub>2</sub>, CeO<sub>2</sub>, SnO<sub>2</sub>, HfO<sub>2</sub>, ZrO<sub>2</sub>, Nd<sub>2</sub>O<sub>3</sub>, In<sub>2</sub>O<sub>3</sub>, Tl<sub>2</sub>O<sub>3</sub>, Fe<sub>2</sub>O<sub>3</sub>, Fe<sub>3</sub>O<sub>4</sub>, and Mn<sub>3</sub>O<sub>4</sub> can be synthesized in just a few minutes using MWHS, many of them nanometer sized [see for example Refs. [78] and [86]]. In particular, there is broad interest in ZnO, a direct bandgap semiconductor (3.37 eV) with near-UV photoemission, because of potential applications in different fields, mostly in electronics. It can be prepared in the form of different nanostructures (e.g., nanorods, nanowires, spindles) using zinc salts (e.g., nitrate, chloride, acetate) in strongly alkaline aqueous solutions, sometimes in the presence of complexing agents such as organic amines [87, 88]. Interestingly enough, it has been shown that the Zn(II) concentration (0.8 to 1.6 M) and the temperature (100–180 °C) have a marked influence on the different morphologies obtained [89]. The reaction mechanism can be simply considered as a hydrolysis-condensation one:



Another interesting example among binary oxides, TiO<sub>2</sub>, is one of the most widely studied and is used in different industrial and technological applications: as a white pigment, in photocatalysis, for water splitting in H<sub>2</sub> and O<sub>2</sub>, and so forth. Moreover, it may adopt different structures depending on the preparation conditions (brookite, anatase, rutile, and others that show different properties) and in all cases, MW-assisted synthesis works properly. Morishima et al. [90] have reported that brookite-type nanoparticles can be prepared at 200 °C in just 5 min starting from the titanium peroxoglycolate complex in basic media while the anatase phase, well crystallized and with high surface area, with potential uses in energy and environmental applications, is obtained if citrate precursors are used as reported by Huang et al. [91]. These mesoporous anatase nanocrystals made at 180 °C were used to prepare film photoanodes by the screenprinting deposition method. Finally, Chen et al. [92] have shown that rutile, the high-temperature polymorph, is produced as a metastable phase at quite moderate temperatures when working in acidic media (HCl) instead of an alkaline one and using a different precursor. More recently, the rapid MW-assisted hydrothermal synthesis of hierarchical micro/nanostructured TiO<sub>2</sub> with tunable nanomorphologies has been described [93].

Cerium oxide (ceria) is a refractory material featuring the fluorite structure and is widely used, for instance, as support for metal nanoparticles in catalysis. Ceria nanospheres can be prepared by MWHS [94, 95]. On the other hand, gadolinium and samarium-doped ceria have been extensively studied owing to their high ionic oxygen conductivity, higher than that of yttria-stabilized zirconia (YSZ) in the intermediate temperature range (500–800 °C).

The partial replacement of Ce(IV) by trivalent rare earths produces oxygen vacancies that increase the ionic conductivity, and this makes them promising candidates



**Fig. 13.4:** TEM micrographs of nanosized cerias: (a)  $\text{CeO}_{2-\delta}$ ; (b)  $\text{Ce}_{0.85}\text{Gd}_{0.15}\text{O}_{2-\delta}$ ; (c)  $\text{Ce}_{0.85}\text{Sm}_{0.15}\text{O}_{2-\delta}$ ; (d)  $\text{Ce}_{0.8}\text{Gd}_{0.1}\text{Sm}_{0.1}\text{O}_{2-\delta}$ . The insets show the corresponding SAED patterns. On the right are shown Arrhenius plots for grain-boundary resistivity and activation energies for ionic conductivity. Taken from Ref. [96].

to serve as electrolytes in solid oxide-fuel cells (SOFCs). Nanosized ceria powders, either pure or Sm- and Gd-doped, can be obtained under MWS at 200 °C for 30 min (autogenous pressure ~16 bar) from aqueous solutions containing the corresponding metal nitrates and 1.2 M KOH under constant stirring. A typical transmission electron microscopy (TEM) micrograph of these materials, together with the corresponding electron diffraction pattern, is shown in Figure 13.4, and the cubic morphology of the nanosized crystals is apparent. It is worth noting that these nanosized crystals can be pressed and sintered at high temperatures (1450 °C) in order to get high-density pellets that show better conductivities than materials with the same composition obtained by a conventional ceramic procedure [96].

### 13.4.2 Oxides also containing hydrogen

Oxides of vanadium containing also hydrogen have attracted much attention owing to their diverse physicochemical properties. They adopt a large number of different structures and the metal center may present different oxidation states from 2+ to 5+, in some cases with a mixed metal valence. On the other hand, many of them present open structures and 1D nanostructures such as nanobelts, nanoribbons, or nanorods. All these features make these compounds excellent candidates as electrode materials for lithium or sodium rechargeable batteries with a large specific capacity, good cyclability, and low cost.

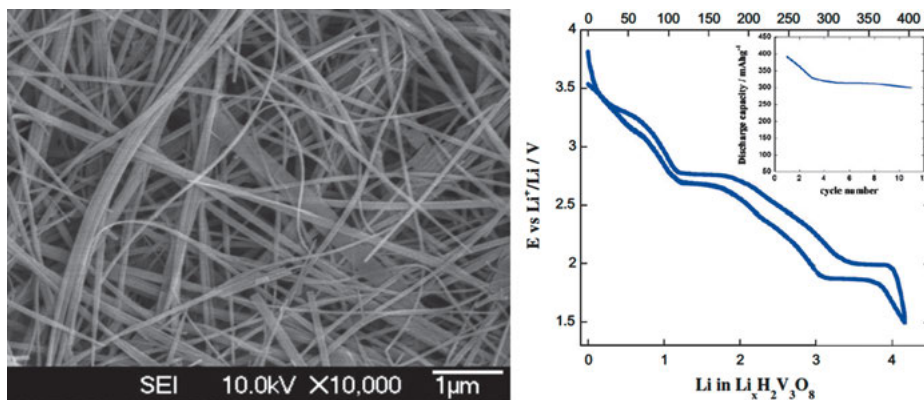
In this connection, the hydrogen trivanadate  $\text{H}_2\text{V}_3\text{O}_8$ , also formulated as a hydrated vanadium oxide  $\text{V}_3\text{O}_7 \cdot \text{H}_2\text{O}$ , with a layered structure formed by two different polyhedral (octahedra and trigonal bipyramids) and two different vanadium oxidation states (4+ and 5+), is a very attractive option. It can be synthesized in the form of nanobelts through a fast and environmentally friendly MWHS (200 °C, 2 h, power limited to 500 W). A quartz pressure vessel is required rather than the usual Teflon one in order to avoid failure of the vessel owing to the formation of uncontrolled hot spots on the autoclave walls. This is also true for any MWSS where metallic conducting particles are formed. Nanobelts about 100 nm wide and several micrometers long are easily prepared, but if the reaction is stopped at lower times of reaction (15–20 min), another, quite different, hydrated vanadium oxide with a flakelike morphology is obtained. An electrochemical study revealed the reversible insertion of ca. 4 Li per formula unit ( $400 \text{ mAh g}^{-1}$ ), through several pseudo-plateaus in the 3.75–1.5 V versus  $\text{Li}^+/\text{Li}$  voltage range, and this makes this material an interesting candidate an electrode for lithium rechargeable batteries. Nevertheless, after the first cycle a significant capacity loss is observed, probably due to the acidic character of the hydrogen ions. Interestingly, the reduction of vanadium down to V(III) in various steps, as seen in the electrochemistry plot, is also confirmed by electron energy loss spectroscopy (EELS) experiments [97].

With a similar approach, ammonium trivanadate  $\text{NH}_4\text{V}_3\text{O}_8$  was recently prepared and its cathodic performance in rechargeable lithium ion batteries successfully tested [36].

The synthesis of oxyhydroxides is also possible:  $\gamma\text{-AlOOH}$  nanoparticles,  $\alpha\text{-FeOOH}$  hollow spheres, and  $\beta\text{-FeOOH}$  architectures have been synthesized using the MWHS with temperature and pressure control [98, 99].

### 13.4.3 Ternary oxides

Ternary oxides such as some of the well-known and ubiquitous perovskites have been synthesized using this technique, for example,  $\text{ATiO}_3$  ( $A = \text{Ba}, \text{Pb}$ ),  $\text{AMnO}_3$  ( $A = \text{La}, \text{Sr}$ ),  $\text{KNbO}_3$ , and  $\text{NaTaO}_3$  [78, 100–102]. Spinelns such as  $\text{ZnM}_2\text{O}_4$  ( $M = \text{Al}, \text{Ga}$ ) [103] and fer-



**Fig. 13.5:** SEM micrograph of  $\text{H}_2\text{V}_3\text{O}_8$  nanobelts obtained by MWSS. The variation of voltage versus composition and the corresponding specific capacity of  $\text{H}_2\text{V}_3\text{O}_8$  discharged down to 1.5 V are shown on the right. The inset shows the discharge capacity of the cell upon cycling. Taken from Ref. [97].

rites  $\text{AFe}_2\text{O}_4$  ( $\text{A} = \text{Zn}, \text{Ni}, \text{Mn}, \text{Co}$ ) [81] and garnets such as  $\text{Y}_3\text{Fe}_5\text{O}_{12}$ , also known as YIG, have also been successfully prepared [104].

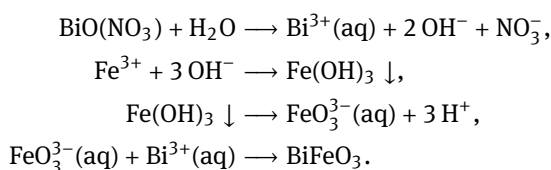
Perovskite oxides, of general formula  $\text{ABO}_3$ , are among the most studied materials because of the variety of properties that they can exhibit and the versatility of their structure. Usually, A accounts for a quite large cation (in dodecahedral coordination) and B for a smaller one (typically a transition metal ion in octahedral coordination). Although the literature is abundant, here only two different and important materials are reported: barium titanate and bismuth ferrite.

Starting with  $\text{BaTiO}_3$  (a classical ferro-piezoelectric material with interesting phase transitions), it has been shown that its synthesis can be accomplished by MWS means in the range of 150–200 °C after 30 min of MW irradiation at the usual 2.45 GHz. The growth rate with MW irradiation was one order of magnitude larger than in a conventional hydrothermal process. Hydroxyl concentration has an enhancement effect on the growth of particles, especially at lower base concentrations or at lower reaction temperatures. The reagents are  $\text{Ba}(\text{OH})_2 \cdot 8\text{H}_2\text{O}$  and amorphous  $\text{TiO}_2$  obtained from the hydrolysis of  $\text{TiCl}_4$ , with an initial Ba/Ti molar ratio of 3 : 2 [105]. On the other hand, the role of *in situ* stirring on morphology and growth has been investigated [84], and the different MW frequencies used on the hydrothermal synthesis of the tetragonal polymorph of barium titanate (the piezoelectric one) have also been reported [106]. Nanoparticles of the material doped with different cations, either on the A site, that is Sr(II) or Sn(II) [107, 108], or in the B site can also be prepared by these means and the piezoelectric properties modulated so far.

Regarding the second perovskite material presented here,  $\text{BiFeO}_3$ , it is a scarce multiferroic material and, thus, has been intensively studied. It features simultaneously ferroelectric behavior and weak ferromagnetism at room temperature. The fer-



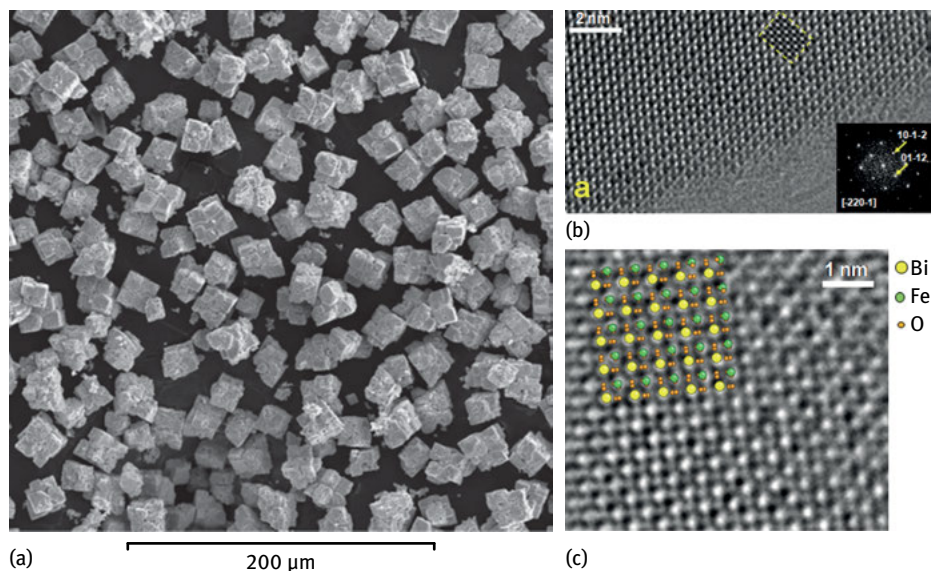
roelectricity arises from a rhombohedrally distorted perovskite structure, where Bi(III) has a so-called lone pair effect and the critical temperature for the ferro-paraelectric transition is as high as 1100 K, while the magnetic behavior is due to the Fe(III) ions, which are antiferromagnetically ordered up to 643 K but with an imperfect antiparallel alignment (spin canting). The general interest in multiferroic materials derives from the possibility of modulating the magnetic properties using an electric field or, conversely, changing the ferroelectric properties via a magnetic field, something directly applicable in memories. BiFeO<sub>3</sub> synthesis when performed by the high-temperature ceramic method has many drawbacks, in particular the appearance of very stable, secondary phases such as the sillenite-type Bi<sub>25</sub>FeO<sub>39</sub> or the high volatility of Bi<sub>2</sub>O<sub>3</sub>, which makes the high-temperature processing troublesome. The MWHS of this material has been proven to overcome all these difficulties, and the material can be easily prepared in very pure form in 30 min using the corresponding bismuth and iron nitrates in a strongly alkaline KOH medium (from 2 to 8 M). The temperature is set at 200 °C (limiting the power to a maximum of 500 W), and the autogenous pressure reaches 13 bar [109]. The reactions involved can be schematized as follows:



Furthermore, the KOH concentration and the reaction times have a clear effect on the morphology and size of the cubic, not nanoparticles (Figure 13.6). The authors later reported the synthesis of this material using FeCl<sub>3</sub> · 6 H<sub>2</sub>O instead of bismuth nitrate, the same mineralizer (1.5 KOH) and Tween 80 as surfactant at the same temperature and longer times (1 h) [110]. This material was not used as multiferroic but as a UV photocatalyst [111]. If a strong acid medium (HNO<sub>3</sub>) is used to dissolve the bismuth nitrate followed by the addition of ammonia, nanoparticles of this material, 30–50 nm in size, can be obtained after MW heating at 100 °C for 20 min followed by annealing at different temperatures, 400–600 °C, in air [112]. Nanostructures with spherical (15–55 nm) and rectangle-like morphologies can be obtained by changing the synthesis conditions [113].

#### 13.4.4 Other materials

In the last decade different kinds of porous materials, with different structures, such as zeolites, usually prepared by hydrothermal synthesis, have also been prepared by MWHS. The quick MW syntheses of a large number of aluminosilicates and aluminophosphates, namely MFI, sodalite, NaY (FAU), LSX (FAU), analcime, Na-P1 (Gis),



**Fig. 13.6:** SEM micrograph of  $\text{BiFeO}_3$  crystals obtained by MWSS. (a) High-resolution TEM image and electron diffraction pattern (inset) of a crystal along the  $[-220-1]$  direction; (c) TEM image showing cation arrangement and good agreement between experimental image and structural model. Taken from Ref. [110].

Ti-ZSM-5 (MFI),  $\text{AlPO}_4$ , toad, cloverite, MnAPO-5VAPSO-44, MnAPO-5, MCM-41, SBA-15, UDF-1, PSU-1, and others have been reviewed [114].

Last but not least, other phosphate materials, such as the phospholivine  $\text{LiFePO}_4$  (commonly used as a cathode in rechargeable batteries) and similar materials like  $\text{LiVOPO}_4$  [115, 116], phosphonates (used in catalysis) [117], hydroxyapatite, and calcium phosphates (some of the most important biomaterials) [118] have been successfully prepared as well.

## Bibliography

- [1] De la Hoz A, Díaz-Ortiz A, Moreno A. *Chem. Soc. Rev.* 2005, 34, 164–178.
- [2] Mishra RR, Sharma AK. *Composites: Part A* 2016, 81, 78–97.
- [3] Ma J. *J. Phys. Chem. A* 2016, 120, 7989–7997.
- [4] Cortijo M, Herrero S, Jiménez-Aparicio R, Matesanz E. *Inorg. Chem.* 2013, 52, 7087–7093.
- [5] Baghurst DR, Cooper SR, Greene DL, Mingos DMP, Reynolds SM. *Polyhedron* 1990, 9, 893–895.
- [6] Milios CJ, Vinslava A, Whittaker AG, Parsons S, Wernsdorfer W, Christou G, Perlepes SP, Brechin EK. *Inorg. Chem.* 2006, 45, 5272–5274.
- [7] Servaty K, Moucheron C, Kirsch-De Mesmaeker A. *Dalton Trans.* 2011, 40, 11704–11711.

- [8] Herrero S, Jiménez-Aparicio R, Perles J, Priego JL, Urbanos FA. *Green Chem.* 2010, 12, 965–967.
- [9] Herrero S, Jiménez-Aparicio R, Perles J, Priego JL, Saguar S, Urbanos FA. *Green Chem.* 2011, 13, 1885–1890.
- [10] Khan NA, Nhung SH. *Coord. Chem. Rev.* 2015, 285, 11–23.
- [11] Cortijo M, Delgado-Martínez P, González-Prieto R, Herrero S, Jiménez-Aparicio R, Perles J, Priego JL, Torres MR. *Inorg. Chim. Acta* 2015, 424, 176–185.
- [12] Garringer SM, Hesse AJ, Magers JR, Pugh KR, O'Reilly SA, Wilson AM. *Organometallics* 2009, 28, 6841–6844.
- [13] Cortijo M, Herrero S, Jiménez-Aparicio R, Perles J, Priego JL, Torroba J. *Cryst. Growth Des.* 2014, 14, 716–722.
- [14] Klinowski J, Paz FAA, Silva P, Rocha J. *Dalton Trans.* 2011, 40, 321–330.
- [15] Constable EC, Housecroft CE, Murray NS, Zampese JA. *Polyhedron* 2013, 54, 110–118.
- [16] Delgado P, González-Prieto R, Jiménez-Aparicio R, Perles J, Priego JL, Torres RM. *Dalton Trans.* 2012, 41 11866–11874.
- [17] Delgado-Martínez P, González-Prieto R, Gómez-García C, Jiménez-Aparicio R, Priego JL, Torres RM. *Dalton Trans.* 2014, 43, 3227–3237.
- [18] Delgado-Martínez P, Elvira-Bravo A, González-Prieto R, Priego JL, Jiménez-Aparicio R, Torres MR. *Inorganics* 2014, 2, 524–536.
- [19] Cortijo M, Herrero S, Jerez B, Jiménez-Aparicio R, Perles J, Priego JL, Torroba J, Tortajada J. *ChemPlusChem* 2014, 79, 951–961.
- [20] Zhou YL, Zeng MH, Wei LQ, Li BW, Kurmoo M. *Chem. Mater.* 2010, 22, 4295–4303.
- [21] Cortijo M, Herrero S, Jiménez-Aparicio R, Perles J, Priego JL, Torralvo MJ, Torroba J. *Eur. J. Inorg. Chem.* 2013, 2580–2590.
- [22] Zhang K, Dai J, Wang YH, Zeng MH, Kurmoo M. *Dalton Trans.* 2013, 42, 5439–5446.
- [23] Zhang SH, Zhou YL, Sun XJ, Wei LQ, Zeng MH, Liang H. *J. Solid State Chem.* 2009, 182, 2991–2996.
- [24] S. Nhung H, Lee JH, Yoon JW, Serre C, Férey G, Chang JS. *Adv. Mater.* 2007, 19, 121–124.
- [25] Silva P, Ananias D, Bruno SM, Valente AA, Carlos LD, Rocha J, Paz FAA. *Eur. J. Inorg. Chem.* 2013, 5576–5591.
- [26] Khan NA, Nhung SH. *Cryst. Growth Des.* 2010, 10, 1860–1865.
- [27] Brede FA, Heine J, Sxetl G, Müller-Buschbaum K. *Chem. Eur. J.* 2016, 22, 2708–2718.
- [28] Barolo C, Yum JH, Artuso E, Barbero N, Di Censo D, Lobello MG, Fantacci S, De Angelis F, Grätzel M, Nazeeruddin MK, Viscardi G. *ChemSusChem* 2013, 6, 2170–2180.
- [29] Vilela SMF, Firmino ADG, Mendes RF, Fernandes JA, Ananias D, Valente AA, Ott H, Carlos LD, Rocha J, Tome JPC, Paz FAA. *Chem. Commun.* 2013, 49, 6400–6402.
- [30] Dömötör O, Aicher S, Schmidlehner M, Novak MS, Roller A, Jakupec MA, Kandioller W, Hartinger CG, Keppler BK, Enyedy EA. *J. Inorg. Biochem.* 2014, 134, 57–65.
- [31] Choi JS, Son WJ, Kim J, Ahn WS. *Microporous Mesoporous Mater.* 2008, 116, 727–731.
- [32] Cesari C, Sambri L, Zacchini S, Zanotti V, Mazzoni R. *Organometallics* 2014, 33, 2814–2819.
- [33] Louie AS, Harrington LE, Valliant JF. *Inorg. Chim. Acta* 2012, 389, 159–167.
- [34] Xiao S, Li X, Sun W, Guan B, Wang Y. *Chem. Eng. J.* 2016, 306, 251–259.
- [35] H.-K. Liu, T.-H. Tsao, Y.-T. Zhang, C.-H. Lin. *CrystEngComm* 2009, 11, 1462–1468.
- [36] Zakharova GS, Ottmann B, Ehrstein B, Klingeler R. *Mater. Res. Bull.* 2016, 83, 225–229.
- [37] Delgado S, Santana A, Castillo O, Zamora F. *Dalton Trans.* 2010, 39, 2280–2287.
- [38] Barral MC, Herrero S, Jiménez-Aparicio R, Torres MR, Urbanos FA. *Inorg. Chem. Commun.* 2004, 7, 42–46.
- [39] Ni Z, Masel RI. *J. Am. Chem. Soc.* 2006, 128, 12394–12395.
- [40] Sonnauer A, Stock N. *J. Solid State Chem.* 2008, 181, 3065–3070.

- [41] Liang W, D'Alessandro DM. *Chem. Commun.* 2013, 49, 3706–3708.
- [42] Pons-Balagué A, Heras Ojea MJ, Ledezma-Gairaud M, Reta Mañeru D, Teat SJ, Sánchez Costa J, Aromi G, Sañudo EC. *Polyhedron* 2013, 52, 781–787.
- [43] Shaw AP, Tilset M, Heyn RH, Jakobsen S. *J. Coord. Chem.* 2011, 64, 38–47.
- [44] Casini A, Diawara MC, Scopelliti R, Zakeeruddin SM, Grätzel M, Dyson PJ. *Dalton Trans.* 2010, 39, 2239–2245.
- [45] Luqman A, Blair VL, Brammananth R, Crellin PK, Coppel RL, Kedzierski L, Andrews PC. *Eur. J. Inorg. Chem.* 2015, 725–733.
- [46] Jain RK, Mishra AP. *J. Serb. Chem. Soc.* 77 2012, 1013–1029.
- [47] Soliman AA, Ali SA, Marei AH, Nassar DH. *Spectrochim. Acta A* 2012, 89, 329–332.
- [48] Kapoor P, Singh RV, Fahmi N. *J. Coord. Chem.* 2012, 65, 262–277.
- [49] Deeming AJ, Johnson BFG, Lewis J. *J. Chem. Soc. A* 1970, 897–901.
- [50] Pyper KJ, Kempe DK, Jung JY, Loh LHJ, Gwini N, B, Lang D, Newton BS, Sims JM, Nesterov VN, Powell GL. *J. Clust. Sci.* 2013, 24, 619–634.
- [51] Wu Q, Fan C, Chen T, Liu C, Mei W, Chen S, Wang B, Chen Y, Zheng W. *Eur. J. Med. Chem.* 2013, 63, 57–63.
- [52] Lindsay AJ, Wilkinson G, Motevalli M, Hursthouse MB. *J. Chem. Soc., Dalton Trans.* 1987, 2723–2736.
- [53] Mishra AP, Mishra R, Jain R, Gupta S. *Mycobiology* 2012, 40, 20–26.
- [54] Harcourt EM, Yonis SR, Lynch DE, Hamilton DG. *Organometallics* 2008, 27, 1653–1656.
- [55] Miyake H, Ueda M, Murota S, Sugimoto H, Tsukube H. *Chem. Commun.* 2012, 48, 3721–3723.
- [56] Johnson KD, Powell GL. *J. Organomet. Chem.* 2008, 693, 1712–1715.
- [57] Bear JL, Li Y, Han B, Kadish KM. *Inorg. Chem.* 1996, 35, 1395–1398.
- [58] Cotton FA, Murillo CA, Wang X, Wilkinson CC. *Inorg. Chim. Acta* 2003, 351, 191–200.
- [59] Zhuang GL, Sun XJ, Long LS, Huang RB, Zheng LS. *Dalton Trans.* 2009, 4640–4642.
- [60] Ledezma-Gairaud M, Pineda LW, Aromi G, Sañudo EC. *Polyhedron* 2013, 64, 45–51.
- [61] Pons-Balagué A, Ioanidis N, Wernsdorfer W, Yamaguchi A, Sañudo EC. *Dalton Trans.* 2011, 40, 11765–11769.
- [62] Im HJ, Lee SW. *Polyhedron* 2015, 101, 48–55.
- [63] Kathalikkattil AC, Roshan R, Tharun J, Soek HG, Ryu HS, Park DW. *ChemCatChem* 2014, 6, 284–292.
- [64] Gangu KK, Maddila S, Mukkamala SB, Jonnalagadda SB. *Inorg. Chim. Acta* 2016, 446, 61–74.
- [65] Jin LN, Liu Q, Sun WY. *CrystEngComm* 2014, 16, 3816–3828.
- [66] Stock N, Biswas S. *Chem. Rev.* 2012, 112, 933–969.
- [67] Vilela SMF, Ananias D, Fernandes JA, Silva P, Gomes AC, Silva NJO, Rodrigues MO, Tomé JPC, Valente AA, Ribeiro-Claro P, Carlos LD, Rocha J, Paz FAA. *J. Mater. Chem. C* 2014, 2, 3311–3327.
- [68] Stefanczyk O, Korzeniak T, Nitek W, Rams M, Sieklucka B. *Inorg. Chem.* 2011, 50, 8808–8816.
- [69] Lhoste J, Henry N, Loiseau T, Abraham F. *Inorg. Chem. Commun.* 2011, 14, 1525–1527.
- [70] Akhbari K, Morsali A. *CrystEngComm* 2011, 13, 2047–2053.
- [71] Zeng MH, Zhou YL, Zhang WX, Du M, Sun HL. *Cryst. Growth Des.* 2009, 10, 20–24.
- [72] Diring S, Furukawa S, Takashima Y, Tsuruoka T, Kitagawa S. *Chem. Mater.* 2010, 22, 4531–4538.
- [73] Bag PP, Wang XS, Cao R. *Dalton Trans.* 2015, 44, 11954–11962.
- [74] Bilecka I, Niederberger M. *Nanoscale* 2010, 2, 1358–1374.
- [75] Kharisov BI, Kharisova OV, Ortiz-Méndez U. Microwave Hydrothermal and Solvothermal Processing of Materials and Compounds, in *The Development and Application of Microwave Heating*, W. Cao ed., Intech. Publishers. 2012, Chapter 5, 109–140.
- [76] Zhu YJ, Chen F. *Chem. Rev.* 2014, 114, 6462–6555.
- [77] Leonelli C, Komarneni S. *Inorganics* 2015, 3, 388–391.

- [78] Komarneni S, Roy R, Li QH. *Mat. Res. Bull.* 1992, 27, 1393–1405.
- [79] Komarneni S, Pidugu R, Li QH, Roy R. *J. Mater. Res.* 1995, 10, 1687–1692.
- [80] Komarneni S, Hussein MZ, Liu C, Breval E, Malla PB. *Eur. Sol J. State Inor. Chem.* 1995, 32, 837–849.
- [81] Komarneni S, D'Arrigo MC, Leonelli C, Pellacani GC, Katsuki H. *J. Amer. Ceram. Soc.* 1998, 81, 3041–3043.
- [82] Komarneni S, Katsuki H. *Pure Appl. Chem.* 2002, 74, 1537–1543.
- [83] Komarneni S. *Curr. Sci.* 2003, 85, 1730–1734.
- [84] Komarneni S, Katsuki H. *Ceram. Int.* 2010, 36, 1165–1169.
- [85] Komarneni S, Noh YD, Kim JY, Kim SH, Katsuki H. *Z. Naturforsch. B* 2010, 65, 1033–1037.
- [86] Bilecka I, Djerdj I, Niederberger M. *Chem. Comm.* 2008, 886–888.
- [87] Shojae N, Ebadzadeh T, Aghaei A. *Mater. Charact.* 2010, 61, 1418–1423.
- [88] De Moura AP, Lima RC, Moreira ML, Volanti DP, Espinosa JWM, Orlandi MO, Pizani PS, Varela JA, Longo E. *Solid State Ionics* 2010, 181, 775–780.
- [89] Huang J, Xia C, Cao L, Zeng X. *Mat. Sci. Eng. B* 2008, 150, 187–193.
- [90] Morishima Y, Kobayashi M, Petrykin V, Kakihana M, Tomita K. *J. Ceram. Soc. Japan* 2007, 115, 826–830.
- [91] Huang CH, Yang YT, Doong RA. *Microporous Mesoporous Mater.* 2011, 142, 473–480.
- [92] Chen Z, Li W, Zeng W, Li M, Xiang J, Zhou A, Huang J. *Materials Letters* 2008, 62, 4343–4344.
- [93] Yang Y, Liang Y, Hu J, Zou J, Tang Q, Wan Z, Lu Y. *J. Mater. Sci.-Mater. Electron.* 2016, 27, 11606–11612.
- [94] Dos Santos ML, Lima RC, Riccardi CS, Tranquilin RL, Bueno PR, Varela JA, Longo E. *Mater. Lett.* 2008, 62, 4509–4511.
- [95] Cao CY, Cui ZM, Chen CQ, Song WG, Cai W. *J. Phys. Chem. C* 2010, 114, 9865–9870.
- [96] Prado-Gonjal J, Schmidt R, Espíndola-Canuto J, Ramos-Alvarez P, Morán E. *J. Power Sources* 2012, 209, 163–171.
- [97] Prado-Gonjal J, Molero-Sánchez B, Ávila-Brande D, Morán E, Pérez-Flores JC, Kuhn A, García-Alvarado F. *J. Power Sources* 2013, 232, 173–180.
- [98] Zhang L, Zhu YJ. *J. Phys. Chem. C* 2008, 112, 16764–16768.
- [99] Cao SW, Zhu YJ. *Acta Mater.* 2009, 57, 2154–2165.
- [100] Rizzuti A, Viviani M, Corradi A, Nanni P, Leonelli C. *Solid State Phenom.* 2007, 128, 21–24.
- [101] Shi J, Liu G, Wang N, Li C. *J. Mater. Chem.* 2012, 22, 18808–18813.
- [102] Zhu X, Wang J, Zhang Z, Zhu J, Zhou S, Liu Z, Ming N. *J. Amer. Ceram. Soc.* 2008, 91, 2683–2689.
- [103] Conrad F, Massue C, Kühn S, Kunkes E, Girgsdies F, Kasatkin I, Zhang B, Friedrich M, Luo Y, Armbrüster M, Parzke GR, Behrens M. *Nanoscale* 2012, 4, 2018–2028.
- [104] Sadhana K, Shinde RS, Murthy SR. *Int. J. Mod. Phys. B* 2009, 23, 3637–3642.
- [105] Sun W, Pang Y, Li J, Ao W. *Chem. Mat.* 2007, 19, 1772–1779.
- [106] Nyutu EK, Chen CH, Dutta PK, Suib SL. *J. Phys. Chem. C* 2008, 112, 9659–9667.
- [107] Simões AZ, Moura F, Onofre TB, Ramirez MA, Varela JA, Longo EJ. *J. Alloys Compd.* 2010, 508, 620–624.
- [108] Xie Y, Yin S, Hashimoto T, Kimura H, Sato T. *J. Mater. Sci.* 2009, 44, 4834–4839.
- [109] Prado-Gonjal J, Villafuerte-Castrejón ME, Fuentes L, Morán E. *Mat. Res. Bull.* 2009, 44, 1734–1737.
- [110] Prado-Gonjal J. Microwave-assisted synthesis and characterization of inorganic materials. PhD Thesis. Chapter 6. Universidad Complutense de Madrid. 2014.
- [111] Zheng Y, Tan G, Bo H, Miao H, Chang M, Xia A. *Guisuanyan Xuebao* 2011, 39, 1249–1253.
- [112] Wang L, Han Y, Jia G, Zhang C, Liu Y, Liu L, Wang C, Cao X, Yin K. *J. Nanosci. Nanotechnol.* 2011, 11, 5207–5209.

- [113] Zhu X, Yang Y, He K, Zhu J, Ye S, Zhou S, Liu Z. *Ferroelectrics* 2010, 409, 204–210.
- [114] Tompsett GA, Conner WC, Yngvesson KS. *Chem. Phys. Chem.* 2006, 7, 296–319.
- [115] Yang G, Ji H, Miao X, Hong A, Yan Y. *J. Nanosci. Nanotechnol.* 2011, 11, 4781–4792.
- [116] Harrison KL, Manthiram A. *Chem. Mater.* 2013, 25, 1757–1760.
- [117] Yang YF, Ma YS, Bao SS, Zheng LM. *Dalton Trans.* 2007, 4222–4226.
- [118] Lee BT, Youn MH, Paul RK, Lee KH, Song HY. *Mat. Chem. Phys.* 2007, 104, 249–253.

Satoshi Horikoshi and Nick Serpone

## 14 Microwave-assisted synthesis of nanoparticles

### 14.1 Introduction

One of the most central research topics in nanoscience and nanotechnology deals with nanoparticle synthesis since the availability of appropriate nanomaterials serves as the foundation to explore novel properties and applications associated with materials that are on the nanometer scale. It is therefore fitting that this chapter explores some of the ways that nanoparticles can be synthesized using microwave radiation as the energy source to effect the synthesis of such nanosized materials. Although we emphasize our own studies in this field, the interested reader should peruse through a recent book coedited by us [1] that treats in far greater detail the various protocols proposed and used by several other researchers.

This chapter is subdivided into various sections that first attempt to define what nanoparticles are, followed by how nanoparticles might originate from nucleating seeds and their growth to nano-sized materials. The chapter then delves into why microwave radiation is a useful energy source and what the advantages are in using microwaves, together with possible mechanistic information, the advantages of performing syntheses using microwaves of different frequencies, the ability to control the shapes of nanoparticles, and microwave local heating effects. Next, the chapter discusses the more interesting binary systems that consist of synthesizing core-shell nanoparticles, addresses the use of continuous-flow reactors, and, finally, takes a brief look at the synthesis of metal chalcogenides such as CdS and the related core-shell CdTe/CdS system with their multicolored displays.

### 14.2 Nanoparticle: definition

A nanoparticle is often thought of as a grain of nanometer ( $10^{-9}$  m) size; however, at least one side of the nanoparticle will have a size from 1 to 100 nm. Nanoparticles possess different physical and chemical properties from bulk materials (e.g., lower melting points, higher specific surface areas, specific optical properties, mechanical strengths, and specific magnetization) and find applications in various industrial fields. When seen from an industrial point of view the definition of a nanoparticle differs somewhat depending on the application field. Recent years have witnessed significant progress in controlling the shape of a nanoparticle because of advances in liquid synthesis methods and phase surface chemical technology that have led to the emergence of a variety of shapes [1], such as polygon shapes, nanorods, nanowires,

<https://doi.org/10.1515/9783110479935-014>

and nanoboards (among others); not of least importance, nanoparticles are found in core-shell structures.

Improving nanoparticle functions is not costly if one uses a mass-production technology that yields nanoparticles with a small particle size distribution. In this context, microwave heating has been used in recent years in nanoparticle syntheses. Using existing facile methods, it is possible to produce high-quality nanoparticles that are of importance to industry. Before proceeding to describe the several aspects of the use of microwave radiation in nanoparticle synthesis, it is instructive to consider both nucleation and growth facets in the formation of nanoparticles.

### 14.3 Homogeneous and heterogeneous nucleation

Nucleation is the first step in the formation of a new structure taking place either through self-assembly or self-organization and is usually understood to be the process that determines the time needed for an observer to witness the formation of a new phase or self-organized structure to appear. The process of nucleation is very sensitive to impurities that may be present in the system, which could mean the difference between witnessing the occurrence of either heterogeneous or homogeneous nucleation, with the former occurring at *nucleation sites* on surfaces [2], whereas homogeneous nucleation occurs away from such surfaces. Heterogeneous nucleation is far more common than homogeneous nucleation [2, 3].

The basic classical nucleation theory (CNT) that describes a new phase provides an approximate but physically reasonable prediction for the rate,  $R_{(\text{nucl})}$ , at which nuclei of a new phase form via nucleation on a set of identical nucleation sites; see Equation (14.1) [4]. The theory assumes, for instance, that a microscopic nucleus resembles a macroscopic droplet with a well-defined surface whose free energy can be estimated from an equilibrium property (e.g., interfacial tension):

$$R_{(\text{nucl})} = N_S \cdot Z \cdot j \cdot e^{\left(\frac{-\Delta G^*}{k_B T}\right)} \quad (14.1)$$

where  $\Delta G^*$  is the free energy cost of the nucleus at the top of the nucleation barrier;  $k_B T$  is the thermal energy, with  $T$  the absolute temperature and  $k_B$  Boltzmann's constant;  $N_S$  is the number of nucleation sites;  $j$  is the rate at which molecules attach to the nucleus, causing it to grow; and  $Z$  is the so-called Zeldovich factor, which is the probability that a nucleus at the top of the barrier will go on to form the new phase (but not dissolve). Equation (14.1) is the product of two factors. The first is the number of nucleation sites times the probability that a nucleus of critical size has grown around it given by  $N_S \exp(-\Delta G^*/k_B T)$ , which is taken as the average instantaneous number of nuclei at the top of the nucleation barrier. The probability that a nucleus will form at a site is proportional to  $\exp(-\Delta G^*/k_B T)$ , so that if  $\Delta G^*$  were large and positive, the probability of forming a nucleus would be very low and nucleation would be slow, and the average number would be  $\ll 1$ ; that is, it is likely that at any given time none of



the sites will have a nucleus. The second factor in the expression for the rate  $R_{(\text{nucl})}$  is the dynamic part given by  $Zj$ , where  $Z$  expresses the rate of incoming matter and  $j$  the probability that a nucleus of critical size (at the maximum of the energy barrier) will continue to grow (and not dissolve).

To the extent that homogeneous nucleation is simpler and easier to understand than heterogeneous nucleation, let us first examine some aspects of homogeneous nucleation by considering the CNT calculation for the homogeneous nucleation barrier  $\Delta G^*$  expressed by Equation (14.2):

$$\Delta G^* = \frac{4}{3}\pi r^3 \Delta g + 4\pi r^2 \sigma \quad (14.2)$$

The first term here is the volume term for a spherical nucleus of radius  $r$ , while  $\Delta g$  represents the difference in free energy per unit volume between the thermodynamic phase ( $\alpha$ ) where nucleation occurs and the nucleating phase ( $\beta$ ). The second term reflects the interface at the surface of the nucleus and is proportional to the surface area of a sphere, and  $\sigma$  denotes the surface tension of the interface between the nucleus and its surroundings (note that  $\sigma$  is always positive). For small  $r$ , the second surface term dominates so that  $\Delta G(r) > 0$ . The free energy is the sum of  $r^2$  and  $r^3$  terms, with the  $r^3$  term varying faster with the radius of the nucleus  $r$  than the  $r^2$  term does, so that for small values of  $r$  the  $r^2$  term dominates and the free energy is positive. By contrast, for large values of  $r$  the  $r^3$  term dominates and the free energy is negative. Note that the free energy barrier defined in the expression for  $R_{(\text{nucl})}$ , Equation (14.1), is given by (see Equation (14.3))

$$\Delta G^* = \frac{4\pi r^3}{3(\Delta g)^2} \quad (14.3)$$

Heterogeneous nucleation is characteristically much faster than homogeneous nucleation because the nucleation barrier  $\Delta G^*$  is much lower at a surface, given that the nucleation barrier emanates from the positive term in the free energy  $\Delta G^*$  (the surface term). For homogeneous nucleation, the nuclei are assumed to have a spherical shape so that the free energy equals the surface area of the sphere,  $4\pi r^2$ , times the surface tension  $\sigma$ .

Nucleation typically takes place at a surface, at an interface, on an impurity, or as a result of some heterogeneity in the system. The energy required for nucleation is reduced by a factor related to the contact angle  $\theta$  of the nucleus on the foreign surface as expressed by Equation (14.4):

$$\Delta G_{\text{hetero}}^* = \Delta G_{\text{homo}}^* f(\theta) \quad (14.4)$$

where

$$f(\theta) = \frac{(2 + \cos \theta)(1 - \cos \theta)^2}{4} \quad (14.5)$$

In comparison to nucleation, the growth process is relatively simple because it assumes that stable nuclei exist prior to growth followed by molecules being added

to form a stable cluster, with the process being driven by a decrease of the free energy of phase change, which is kinetically limited [5]. The rate of growth,  $R_{(\text{growth})}$ , per unit area of interface at a distance,  $a_0$ , across the interface (ca. 1 atomic diameter) and frequency,  $\nu$ , is given by Equation (14.6):

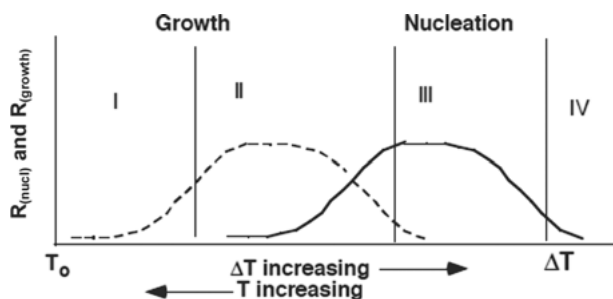
$$R_{(\text{growth})} = \nu a_0 \left( 1 - e^{-\frac{-\Delta G_{\text{mob}}}{kT}} \right) \quad (14.6)$$

where  $\Delta G_{\text{mob}}$  denotes the activation energy for mobility (or diffusion); the frequency factor,  $\nu$ , is given by Equation (14.7),

$$\nu = \frac{kT}{3\pi a_0^3 n} \quad (14.7)$$

where  $n$  refers to the atomic mobility of viscosity.

To summarize, the thermodynamic driving force for both nucleation and growth increases as cooling increases, both of which become limited by the atomic mobility, as illustrated in Figure 14.1.



**Fig. 14.1:** Plot showing the four regions of the rate of nucleation and rate of growth of nuclei as the system is cooled from the reaction temperature  $T_0$ . In region I, the  $\alpha$  phase is metastable and no  $\beta$  phase grows since no nuclei have formed; in region II, there is mixed nucleation and growth; in region III, only nucleation occurs; in region IV, there is neither nucleation nor growth because of atomic mobility. Reproduced from Ref. [5].

## 14.4 Microwave nanoparticle synthesis

Recent years have seen exponential growth in the application of microwaves in organic syntheses. By contrast, syntheses of inorganic nanoparticles, such as metallic and metal oxides, in particular, and metal chalcogenides, in general, and not least general microwave chemistry have yet to reach their full potential despite a growing number of publications in nanoscience and nanotechnology that have made effective use of the dielectric heating provided by microwave radiation [6]. Microwave heating has been demonstrated to reduce significantly not only reaction times but also the

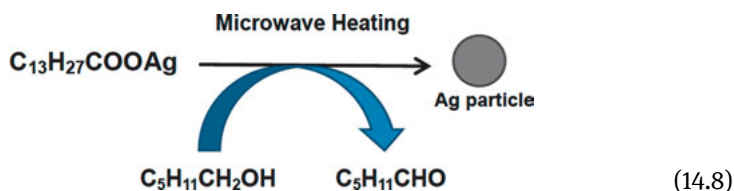
minimization, if not the suppression, of side reactions that lead to enhanced chemical yields and reproducible processes. The major features of microwaves in nanoparticle synthesis are uniform heating and the short times, points that will be emphasized throughout this chapter.

A simple and straightforward method for bulk- and shape-controlled synthesis of prisms, cubes, hexagonal, and spherical nanostructures of such noble metals as Au, Ag, Pt, and Pd by microwave-assisted reduction of their corresponding salts in aqueous glucose, sucrose, and maltose was recently reported by Mallikarjuna and Varma [7]. This filled the growing need for developing eco-friendly processes that avoid the use of toxic chemicals in preparative protocols. Uniform nano and bulk particle sizes are typically obtained by uniform nuclear growth through microwave specific heating. In this regard, synthetic methods that utilize conventional convective heating, because of the need for high-temperature-initiated nucleation followed by controlled precursor addition to the reaction media, rely on a conduction path to drive the synthetic process; here the reactor acts as the intermediary to transfer the thermal energy from the external heat source to the solvent and ultimately to the reactants [8]. Such a pathway typically leads to sharp thermal gradients throughout the bulk media and to inefficient and nonuniform reactions, which can cause serious issues when attempting process scale-up and, more importantly, in nanomaterial syntheses where uniform nucleation and growth rates are essential in maintaining product quality, not to mention the formation of a metallic coating in the inner walls of the reactor. Unlike convective heating, microwave internal heating can prevent formation of a metallic coating on the synthesis reactor walls in nanoparticle synthesis, and plays an important role in the wash-free, continuous flow production of metallic nanoparticles [9]. A clear need to clarify some of the features of microwaves in nanoparticle syntheses and develop novel microwave methodologies for possible process scale-ups is evident. This chapter will focus on nanoparticle synthesis that uses microwave heating efficiently; in most parts we describe the authors' own research. However, interested readers may wish to consult a recent book [1] that deals with nanoparticle synthesis in much greater details and describes various synthesis protocols.

## 14.5 Advantage(s) of the microwave method

### 14.5.1 Uniform nucleating particle size

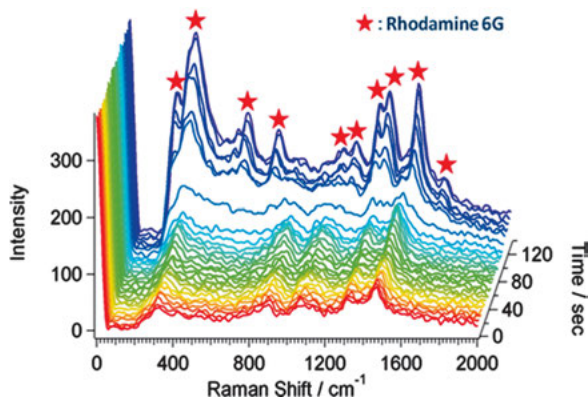
Tsukahara and coworkers reported that the size distribution of a nucleating particle becomes uniform by microwave heating [10], as was evidenced by *in situ* surface-enhanced Raman scattering (SERS) spectroscopy used to observe the early stage of the formation of silver nanoparticles in solution (reaction 14.8) generated under homogeneous and rapid heating by microwave irradiation.



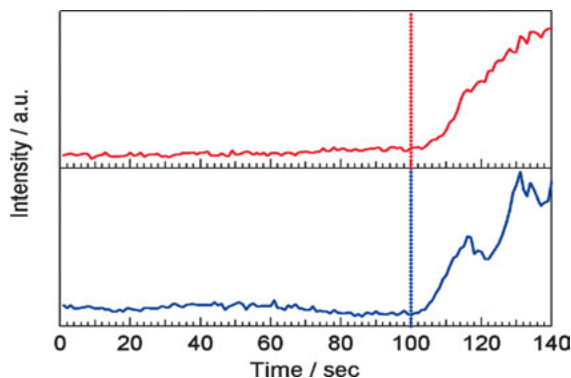
The subsequent appearance of the Raman spectrum of Rhodamine 6G, which was amplified by the surface-enhanced effect as seen by the rise of the band intensities, confirmed the homogeneous formation of silver nanoparticles. Experimental observations of the SERS spectra of Rhodamine 6G (Figure 14.2) showed that the spectra appeared simultaneously with the formation of the silver particles under microwave irradiation whether the Raman probe was located at the center of the reaction vessel or beside the wall of the vessel.

The increase in intensity of the Raman signal for the Rhodamine 6G adsorbed on silver particles occurred because of an enhancement in the electric field provided by the silver particle surface when struck by the incident light that caused localized surface plasmons to be excited, with the enhancement being greatest when the plasmon frequency,  $\omega_p$ , was in resonance with the radiation. For this scattering effect to occur, however, the plasmon oscillations must be perpendicular to the surface (note that when oscillations are in plane with the surface, no scattering occurs) [11].

When the reaction vessel was heated in a hot oil bath (Figure 14.3), the Raman spectrum appeared sooner than was the case when the Raman probe was positioned at the center of the reactor. The increase of the intensity of the Raman spectrum coincided completely with the increase of temperature when both microwave heating and oil bath heating were used [10]. This study demonstrated that a reaction solution



**Fig. 14.2:** *In situ* SERS spectra demonstrating the formation of silver nanoparticles in solution. Reproduced with permission from Ref. [10]. Copyright 2006 by the Japan Chemical Society.



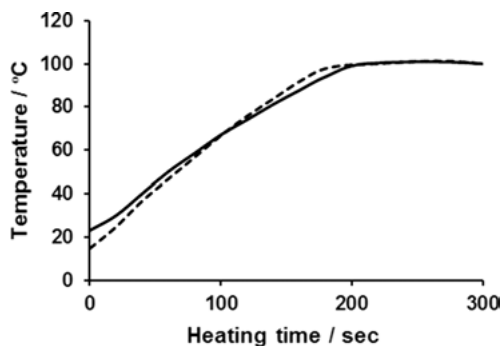
**Fig. 14.3:** Rises of *in situ* SERS observed at center (top) and on side of wall (bottom) under microwave irradiation. The peak intensities at  $1518\text{ cm}^{-1}$  (C–C) vibration are plotted against microwave irradiation time. Reproduced with permission from Ref. [10]. Copyright 2006 by Japan Chemical Society.

can be heated up in the inner parts of a solution, resulting in homogeneous reaction conditions that can be achieved under microwave irradiation.

#### 14.5.2 Synthesis of nanoparticles of uniform sizes: mechanism

This section discusses some of the thermal features of 2.45 GHz microwave radiation used in the synthesis of silver nanoparticles in comparison with the conventional heating method using an oil bath, with special emphasis on the temperature effects and the characteristics (if any) of different microwave synthesizers [9]. The following materials were used in the synthesis of silver nanoparticles. An aqueous solution of the diamine silver(I) complex and carboxymethyl cellulose (CMC) was introduced into a 150 mL Pyrex<sup>®</sup> glass batch-type cylindrical reactor. Continuous microwave irradiation (power: 64 W) was provided with a microwave single-mode resonance apparatus. The reactor was positioned such that irradiation was achieved by the microwaves' electric field at maximal density by adjustments with a short plunger and a three-stub tuner. The conventional heating source was a silicone oil bath. After heating the sample solution, either with microwaves or conventionally with an oil bath, the reactor contents were rapidly cooled in an ice/water bath to arrest the synthesis of the silver nanoparticles, which would have otherwise continued as a result of residual heat from the microwave and oil-bath heating.

The microwave-assisted synthesis of nanoparticles is characterized by rapid and homogeneous heating, in contrast to a conventional heat-assisted synthesis, even though the thermal effects are similar to those of other heating methods [12]. The observed rapid heating by microwaves was controlled and closely monitored so as to extract the characteristic thermal features of the microwaves. The temperature conditions of both heating methods were closely matched in the nanoparticle syn-

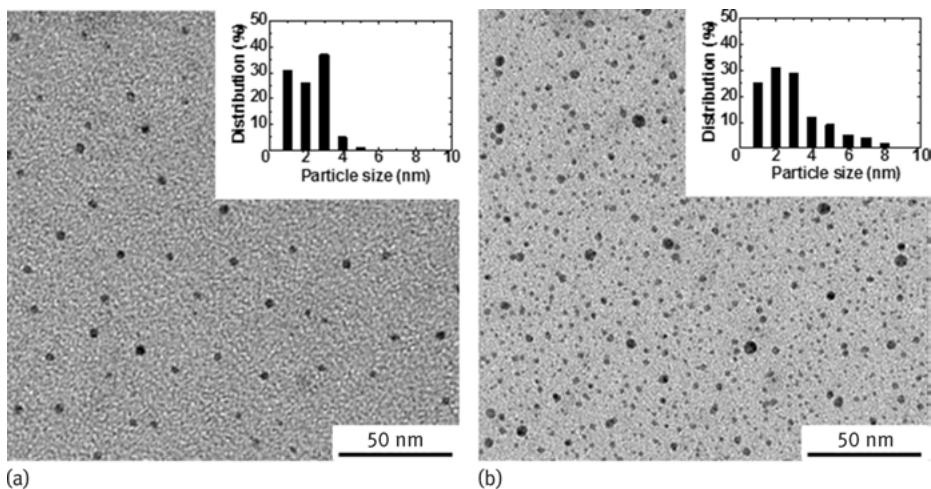


**Fig. 14.4:** Temperature-heating time profiles of aqueous CMC/diaminesilver(I) solution by microwave heating (applied power: 64 W, solid line) and oil-bath heating (consumed power: 400 W, dashed line). Reproduced with permission from Ref. [9]. Copyright 2010 by the Royal Society of Chemistry.

thesis. This was achieved by soaking the cylindrical reactor in the oil bath preheated to 190 °C, followed by determination of the temperature rise of the solution (dashed line in Figure 14.4). The rise in temperature of the solution exposed to microwave radiation was subsequently matched to the temperature rise in the oil-bath heating using microwave power levels in the range 60–70 W at 1 W increments controlled by a proportional–integral–derivative (PID) device present in the microwave apparatus. The solid line in Figure 14.4 represents the temperature rise in the solution exposed to the 64 W microwaves.

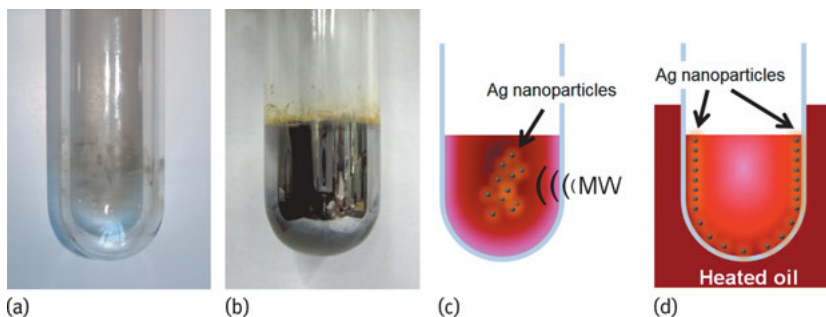
Following the temperature match between microwave heating and oil-bath heating, the formation of silver nanoparticles was monitored at heating times of 0.5, 1, 2, 3, 4, and 5 min by the surface plasmon resonance (SPR) band around 420 nm in the ultraviolet (UV)-visible absorption spectrum. Silver nanoparticles were formed after a 3 min heating period by both microwave and oil-bath methods. In both cases, the synthesis of silver nanoparticles necessitated a temperature of 100 °C, which was reached only after this time period. Figure 14.5a, b shows the corresponding transmission electron microscopy (TEM) images of the resulting silver nanoparticles after a 5 min heating time. A uniform particle size distribution was observed from the TEM image of the colloids obtained from microwave heating under temperature conditions that were otherwise identical to those under conventional heating. The results from light scattering indicate that silver nanoparticles prepared by microwave heating were in a range of 1 to 2.3 nm (Figures 14.5a, inset), whereas the oil-bath heating method yielded polydispersed nanoparticles, mostly in the 3 to 5.7 nm range (Figure 14.5b inset), with some up to 30 nm. Thus, even though the reaction temperature conditions for the microwave and oil-bath methods were identical, there was an otherwise noticeable difference in the rate of formation of the silver nanoparticles and their size distributions.

Variations in the two heating methods are clearly evident in the results illustrated in Figure 14.6. Five minutes into the microwave irradiation of the aqueous



**Fig. 14.5:** TEM images of silver nanoparticles produced by microwave and oil-bath heating methods (inset to figures: particle size distribution from light scattering experiments). Reproduced with permission from Ref. [9]. Copyright 2010 by the Royal Society of Chemistry.

CMC/diaminesilver(I) solution led to the formation of a slightly yellow colored sol in the reactor (Figure 14.6a), whose concentration did not change even after 60 min of irradiation. Silver nanoparticles that adsorbed on the reactor walls were easily removed by simple washing with water. By contrast, a silver film (mirror) coating formed in the inner reactor walls after 4 min by oil-bath heating (Figure 14.6b) under temperature conditions otherwise identical to those under the microwave method; the coating resisted such washings.



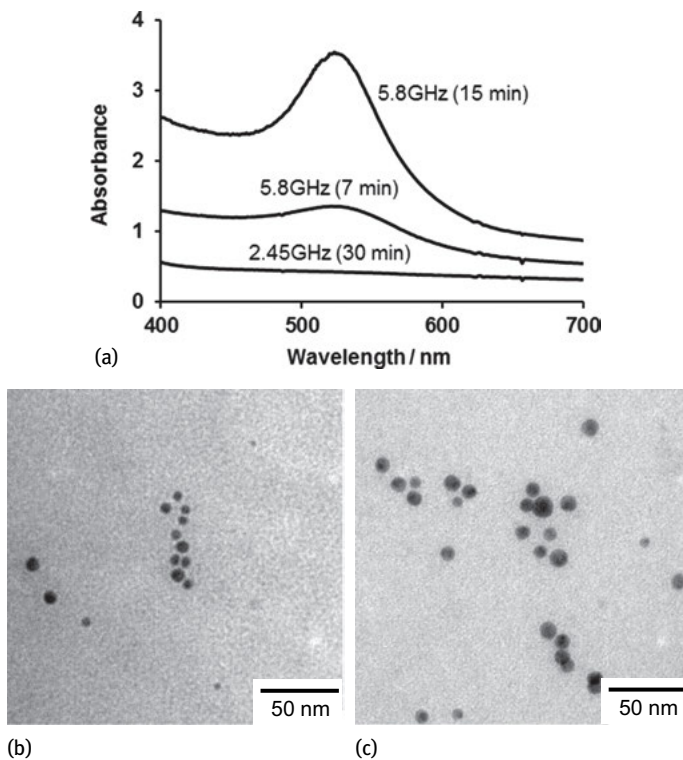
**Fig. 14.6:** Photographs of reactor after sample discharge: (a) after 4 min of microwave irradiation and (b) after 5 min of oil-bath heating. Cartoons representing the temperature distribution in the reactor: (c) after 4 min of microwave heating and (d) after 4 min of oil-bath heating. Note that the photographs in (a) and (b) were taken immediately after the 4 min heating time. Experiments were carried out under nonstirring conditions. Reproduced with permission from Ref. [9]. Copyright 2010 by the Royal Society of Chemistry.

The initial temperature distributions and formation of silver nanoparticles produced under nonstirring conditions by both microwave and oil-bath heating methods are illustrated, respectively, in the cartoons of Figure 14.6c and d. In the former case, microwave radiation penetrated the CMC/diamine silver(I) solution causing the temperature to rise by dielectric loss and to some extent by conduction loss heating, followed by subsequent loss of heat to the surroundings through the reactor walls. As such, the temperature near the inner walls of the reactor tended to be lower than at the center of the reactor. That is, the synthesis of silver nanoparticles by the microwave-assisted process progresses outward from the center of the reactor to the inner reactor walls owing to a temperature gradient that gave rise to a concentration gradient (thermophoretic migration, i.e., the Ludwig–Soret effect [13]). On the other hand, heat from the oil bath was most prominent at the reactor walls and was subsequently transmitted to the solution by thermal conduction and convection mechanisms. This ultimately led to the formation of a silver film at the reactor's inner walls as the concentration of the nanoparticles was greatest at this position. Germane to the present discussion, Schanche [14] has described temperature distributions produced from microwave and oil-bath heating methods in various organic syntheses. In a later study, the Kappe group noted that the temperature distribution in the microwave method may not always be uniform [12]. That is, the location where heat is generated may be different from the position where the endothermic process occurs. This called attention to the fact that even completely homogeneous solutions must be stirred/agitated when using single-mode microwave reactors so as to avoid temperature gradients from developing, a consequence of the inherent field inhomogeneities that exist inside a single-mode microwave cavity.

### 14.5.3 Efficient synthesis of metal nanoparticles at different microwave frequencies

The advantages of the 5.8 GHz microwave frequency are the prompt heating and superheating resulting from the shallow penetration depth of these microwaves and the greater heating efficiencies of nonpolar solvents at this frequency relative to the more commonly used 2.45 GHz frequency [15, 16]. The synthesis of gold nanoparticles in the nonpolar oleylamine solvent ( $C_{18}H_{35}NH_2$ ) was carried out using hydrogen tetrachloroaurate(III) tetrahydrate ( $HAuCl_4 \cdot 4 H_2O$ ) dissolved in oleylamine medium [17]. Initial rates of temperature increase for a 6 min irradiation period were  $16.5\text{ }^\circ\text{C min}^{-1}$  for the 5.8 GHz and  $2.79\text{ }^\circ\text{C min}^{-1}$  for the 2.45 GHz microwaves, respectively, under a continuous applied microwave power of 45 W. The rate of increase of temperature was nearly fivefold faster for the 5.8 GHz microwaves than for the 2.45 GHz microwaves, with the latter increasing gradually with irradiation time. The SPR absorption spectra at irradiation times of 7 and 15 min for the 5.8 GHz microwaves and 30 min for the 2.45 GHz microwaves are displayed in Figure 14.7a.





**Fig. 14.7:** (a) UV-visible absorption spectra of product from irradiating the oleylamine/aurochloric acid solution with 5.8 GHz and 2.45 GHz microwaves at times indicated; microwave power levels: 45 W. Absorption spectra were obtained after a twofold dilution of the respective colloidal sols. TEM images of gold nanoparticles produced after (b) 7 min and (c) 15 min of dielectric heating by 5.8 GHz microwave radiation. Note the larger gold nanoparticles produced at the longer irradiation time. Reproduced with permission from Ref. [18]. Copyright 2010 by the Royal Society of Chemistry.

A SPR band occurred at 528 nm on irradiation with the 5.8 GHz microwaves, in accordance with the absorption spectra of gold nanoparticles reported earlier by Mohamed and coworkers [18]. By contrast, no absorption bands were seen after a 15 min (not shown) and 30 min heating time with the 2.45 GHz microwaves, which indicated that no gold nanocolloids had formed under these conditions. Evidently, the  $\text{Au}^{3+}$  ions in  $\text{HAuCl}_4$  were reduced by the pure oleylamine under 5.8 GHz microwaves and the product displayed only one plasmon band at 528 nm, an indication of the formation of spherical gold nanoparticles. The oleylamine solvent acted as both the reducing agent and possibly as the capping agent.

TEM images of the resulting gold nanoparticles produced subsequent to heating with 5.8 GHz microwaves for 7 and 15 min are illustrated in Figure 14.7b,c, respectively. A fairly uniform particle size distribution of spherical nanocolloids was observed from the TEM images: a random sampling of 35 particles gave a size distribution of  $6 \pm 2$  nm

after 7 min and  $9 \pm 2$  nm after the 15 min heating time [18]. By contrast, the TEM images (not shown) from the 2.45 GHz microwave heating of the oleylamine/aurochloric acid mixture resulted in no formation of Au nanoparticles even after an irradiation period of 30 min, which confirms the results observed from the SPR spectra. Accordingly, these observations inferred a lack of formation of gold nanoparticles under irradiation by the 2.45 GHz microwaves probably the result of not reaching the appropriate reaction temperature.

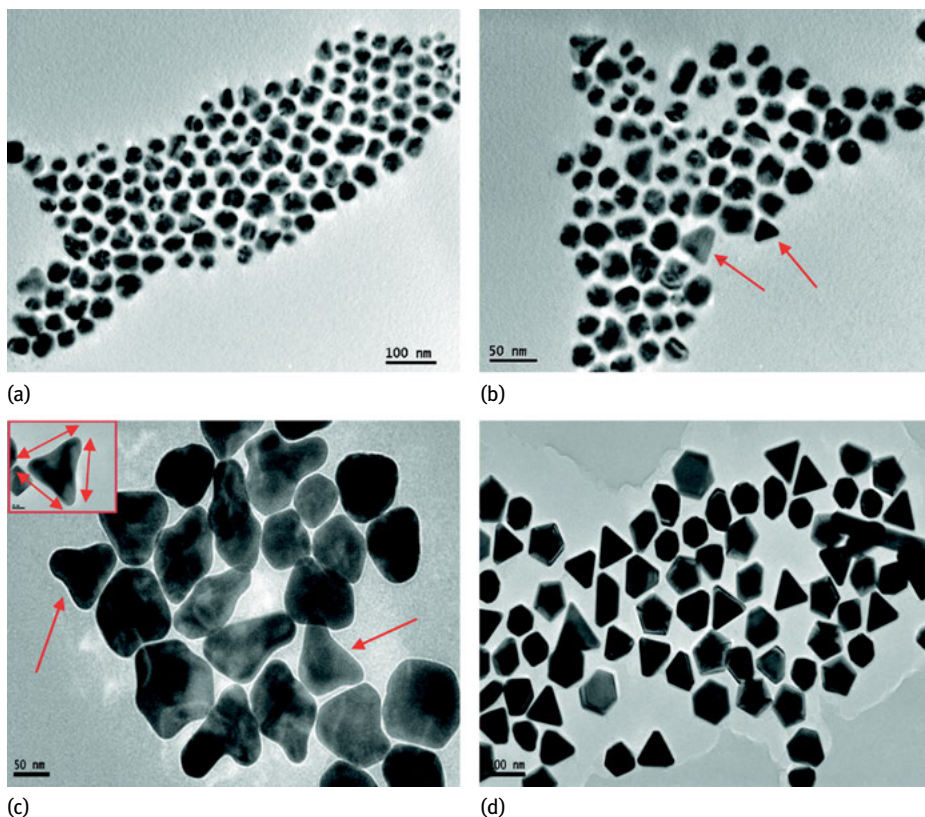
#### 14.5.4 Advantage(s) of shape control

Kundu and coworkers [19] described a highly effective, very fast microwave method to synthesize shape-controlled gold nanoparticles in the presence of 2,7-dihydroxynaphthalene (2,7-DHN) as a new reducing agent under microwave dielectric heating for 60–90 s. The growth of the particles with different shapes (spherical, polygonal, rodlike, and triangular/prismatic shapes) was governed by the surfactant-to-metal ion molar ratios and the concentration of 2,7-DHN. For instance, experiments carried out at different microwave irradiation times led to the formation and growth of triangular-shaped particles. Figure 14.8 displays TEM images of gold nanoprisms at various stages of microwave heating.

Figure 14.8a,b shows, respectively, the TEM images of the formation of gold nanoprisms after 30 and 45 s of microwave heating. The number of particles was about 40 (10 nm in diameter) having no defined shape, but started to grow into adopting a triangular shape. Figure 14.8c shows the low-magnification image after 60 s of microwave heating with particles perfectly grown into triangular shapes, whereas Figure 14.8d shows the different magnified images of nanoprisms after 90 s of microwave heating. The latter image contains more than 95% of prism-shaped particles with a few other shaped particles (ca. 65) with an average particle size of 10 nm. The contrast changes seen in the particles of Figure 14.8c might be due to an internal stress of the continually growing crystal layers. The thickness of the prisms was around 3.5–4 nm, calculated from the atomic force microscopy (AFM) height profile. Because it was possible to heat a sample uniformly, microwave irradiation may yield seed particles at first followed by crystal growth. Therefore, shape control may be facilitated by the presence of dispersing agents.

#### 14.5.5 Microwave local heating effects

When a microwave-assisted synthesis of nanomaterials is performed in the presence of a dispersing agent with a high dielectric loss factor, the dispersing agent becomes the local heat source in the sample solution. For example, when polyvinylpyrrolidone (PVP) was the dispersing agent, it was heated selectively in the sample solution by mi-



**Fig. 14.8:** TEM images for synthesis of gold nanoprisms under different microwave irradiation times: (a) 30 s, (b) 45 s, (c) 60 s, and (d) 90 s. Reproduced with permission from Ref. [19] Copyright 2008 by the American Chemical Society.

crowave radiation, which was then followed rapidly by the reduction of the metallic ions and production of seed particles [20]. In this connection, Yamamoto and coworkers reported that microwave local heating occurs at the junction between  $\text{Ag}^+$  ions and the PVP dispersing agent. Formation of prism-like particles did not occur at the stage of seed particle development (Figure 14.9), but later with the generation of globular particles and subsequent to aggregation it produced prism-shaped nanoparticles [21].

#### 14.5.6 Microwave synthesis of core-shell nanoparticles

Au@Ag core-shell nanoparticles were synthesized by Tsuji and coworkers in gold nanoparticle dispersions in the presence of a silver precursor using the microwave polyol method [22]. The shape of the core-shell was controlled by the shape of the gold core and by the ratio of the gold ( $\text{HAuCl}_4 \cdot 4 \text{H}_2\text{O}$ ) and silver ( $\text{AgNO}_3$ ) precursors. Fig-

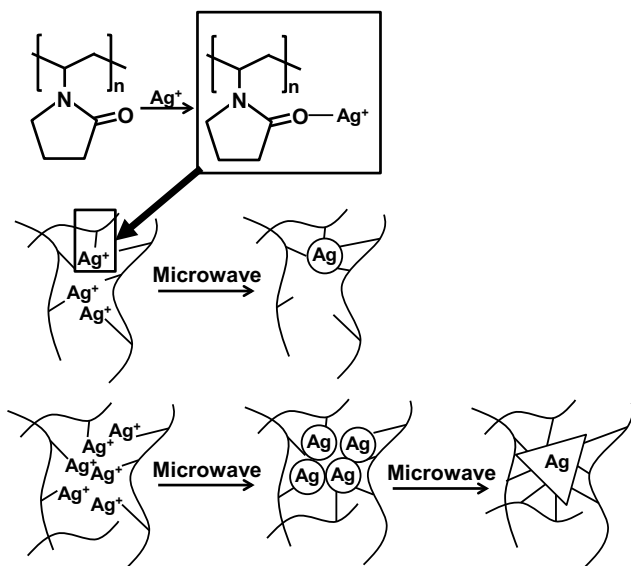
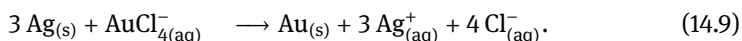
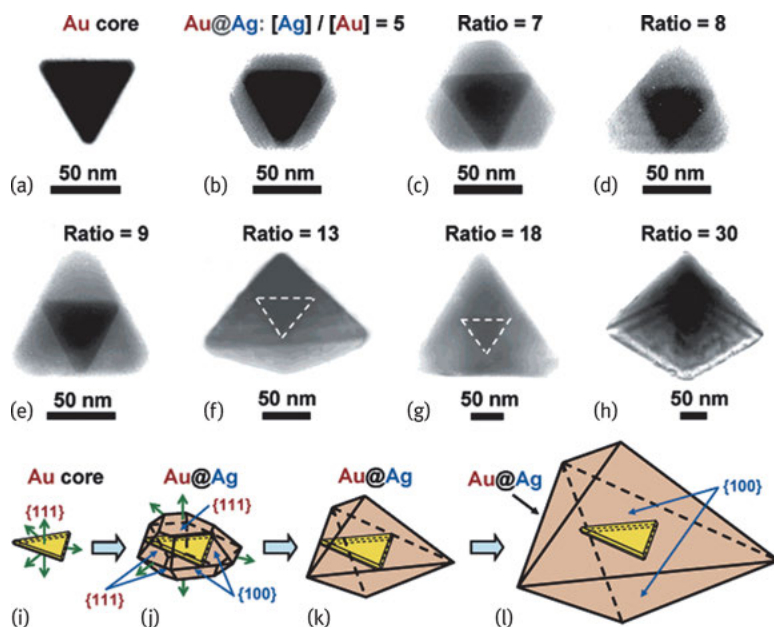


Fig. 14.9: Mechanistic view in formation of silver nanoparticles in a PVP network under microwave irradiation. Reproduced with permission from Ref. [21]. Copyright 2004 by the Japan Chemical Society

ure 14.10 displays TEM photographs of the gold core (Figure 14.10a) and the Au@Ag core-shell nanocrystals (Figure 14.10b-h) overgrown over TTBP-like gold cores in a  $[\text{AgNO}_3]/[\text{HAuCl}_4]$  molar ratio range from 5 to 30. At the low  $[\text{AgNO}_3]/[\text{HAuCl}_4]$  molar ratios of 5 to 9, truncated-triangular-bipyramidal (TTBP) crystals developed until the silver edge lengths observed from the top view became twice those of the gold core plates (Figure 14.10b–e). At higher  $[\text{AgNO}_3]/[\text{HAuCl}_4]$  molar ratios of 13 to 30, the same triangular-bipyramidal shells formed (Figure 14.10f–h).

The edge length of the silver shells increased on increasing the  $[\text{AgNO}_3]/[\text{HAuCl}_4]$  molar ratio and was about seven times larger than that of the TTBP-like gold core (~50 nm) at the highest  $[\text{AgNO}_3]/[\text{HAuCl}_4]$  molar ratio of 30 (Figure 14.10h). When the total sizes of Au@Ag crystals became large, it became difficult to see the exact position of the gold cores. However, TEM images with better contrast definitely demonstrated that all the cores located in the middle consisted of inverted outer larger triangular-bipyramidal silver shells. The position of the gold core was also confirmed by etching silver shells using  $\text{AuCl}_4^-$  ions. Owing to the displacement reaction between silver and gold (Reaction (14.9)), the silver shells could be broken partially and a gold core could then be observed in the center of the gold/silver alloy shells:



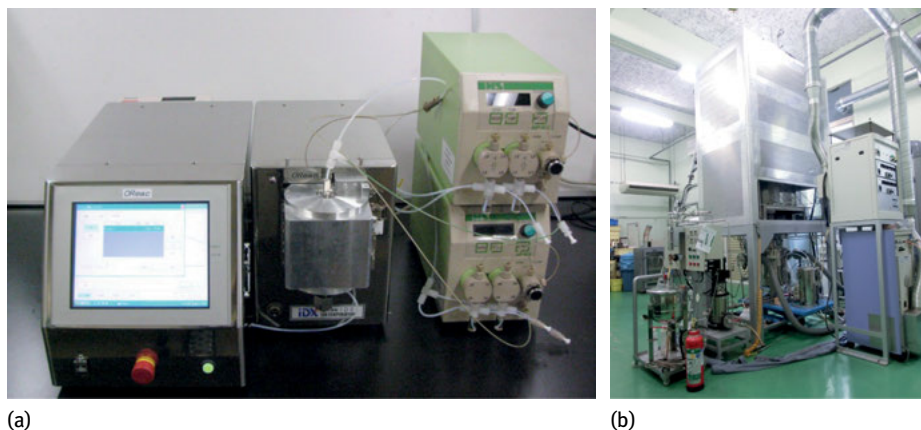


**Fig. 14.10:** TEM photographs of (a) triangular twin gold core and (b–h) Au@Ag nanocrystals prepared by addition of various amounts of AgNO<sub>3</sub> to gold cores with microwave heating for 2 min. Dotted lines denote the triangular twin gold core plates, which can be observed using photographs with better contrast. (i–l) Growth mechanism of triangular-bipyramidal Au@Ag crystals from triangular twin gold cores. Reproduced with permission from Ref. [22]. Copyright 2006 by the American Chemical Society

## 14.6 Microwave desktop system of nanoparticle synthesis in continuous-flow reactors

Nishioka and coworkers reported the synthesis of Ag@SiO<sub>2</sub> core-shell particles by a two-step reaction with microwave systems [23] in which a polytetrafluoroethylene (PTFE) tube (internal diameter 1 mm) was mounted coaxially in the center of the TM<sub>010</sub> single-mode cavity for use as a flow-type reactor (Figure 14.11a). Since the microwave system was a unit-type microwave heating device, the interesting feature of that equipment was that the reactor could be connected perpendicularly. Homogeneous heating of this long reactor was carried out with this microwave unit.

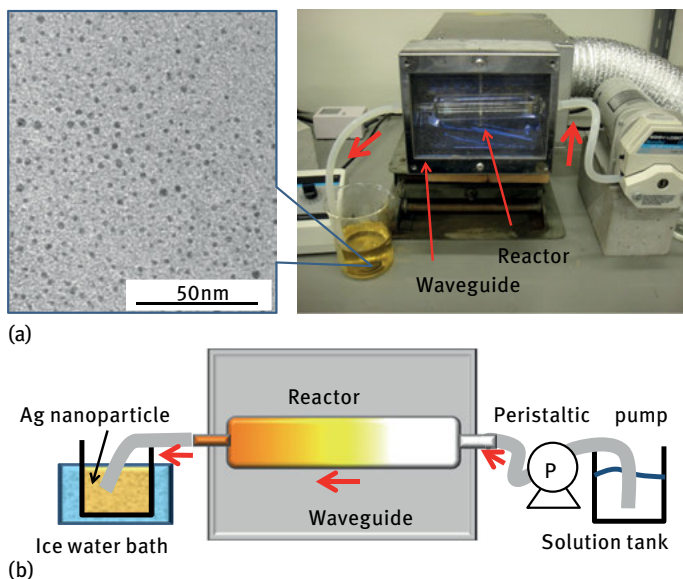
A large-scale ultrasonic atomization-type microwave nanoparticle continuous-flow synthesis equipment system (Kojundo Chemical Lab. Co. Ltd) is illustrated in Figure 14.11b. A 3.5 m reactor is contained at the center of the equipment; the sample solution is sprayed by an ultrasonic wave into the apparatus following which resistance heating and microwave heating lead to the formation of nanoparticles. This type of system has been used for the synthesis of ferrite, a material that absorbs electromagnetic waves [24].



**Fig. 14.11:** Continuous-flow microreactor nanoparticle synthesis systems. (a) Unit-type microwave heating device; (b) industrial-scale device comprising an ultrasonic atomization-type microwave nanoparticle continuous-flow synthesis equipment. Reproduced with permission from Ref. [24]. Copyright 2013 by Wiley-VCH Verlag GmbH.

Features of a microwave nanoparticle synthesis and a synthetic case will now be described. A continuous-flow reactor system that consisted of a Pyrex pipe (length: 135 mm; internal diameter: 8 mm) placed horizontally in a microwave waveguide through which an aqueous CMC/diaminesilver(I) solution was circulated by means of a peristaltic pump was proposed by Horikoshi et al. [9]. Irradiation of the reactor contents was performed with 1200 W microwaves obtained from a microwave generator (maximum power: 3000 W). In the photograph of Figure 14.12a, the microwaves emanate from the back toward the reactor with the maximum of the microwaves' electric field positioned at the center of the reactor. A metal mesh closed the waveguide to prevent microwave leakages and to observe events occurring in the reactor. For maximal heating efficiency, the flow rate of the peristaltic pump was set at  $600 \text{ mL min}^{-1}$ . The solution temperature increased rapidly to  $100 \text{ }^\circ\text{C}$  under microwave irradiation to yield a colloidal sol of silver nanoparticles, which were then collected in the receiver flask and rapidly cooled in an ice-water bath to arrest any further reaction.

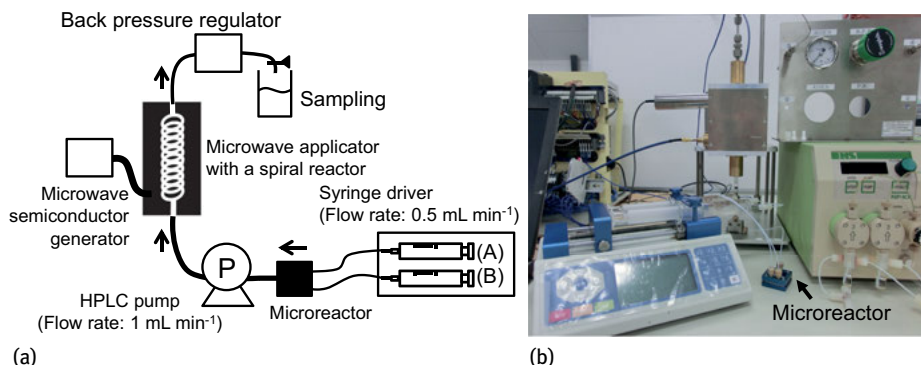
The TEM image of the nanoparticles displayed in Figure 14.12a confirmed the generation of a fairly narrow size distribution of silver nanoparticles (range: 1–4 nm) with this reactor setup. The cartoon in Figure 14.12b summarizes the reactor setup and our observations [9]. Interestingly, the internal reactor walls showed no visible evidence of a yellow stain (seen above in the batch reactor) by this continuous-flow synthesis of silver nanoparticles even after 7 min of microwave irradiation. With microwave power levels greater than 1200 W, we had some difficulty in controlling the temperature, which could (in principle) be corrected by cooling the reactor externally with a cooling device and by a faster solution flow rate to enhance synthesis efficiency. However, the addition of any cooling device (e.g., cooling jacket, cold wind) would



**Fig. 14.12:** (a) Photograph of continuous-flow reactor system for microwave-assisted synthesis of silver nanoparticles; a TEM image of the resulting silver colloids is also displayed. (b) Schematic image of overall experimental setup. Reproduced with permission from Ref. [9]. Copyright 2010 by the Royal Society of Chemistry.

unnecessarily complicate the reactor setup. In the present instance, with the 1200 W microwaves there was no necessity for cooling, and as such this microwave power level was maintained throughout the synthesis. Understandably, a similar continuous-flow rapid synthesis of silver nanoparticles of similar size distribution (i.e., 1–4 nm) would be somewhat difficult to achieve in a reactor system that relied on a conventional heating method.

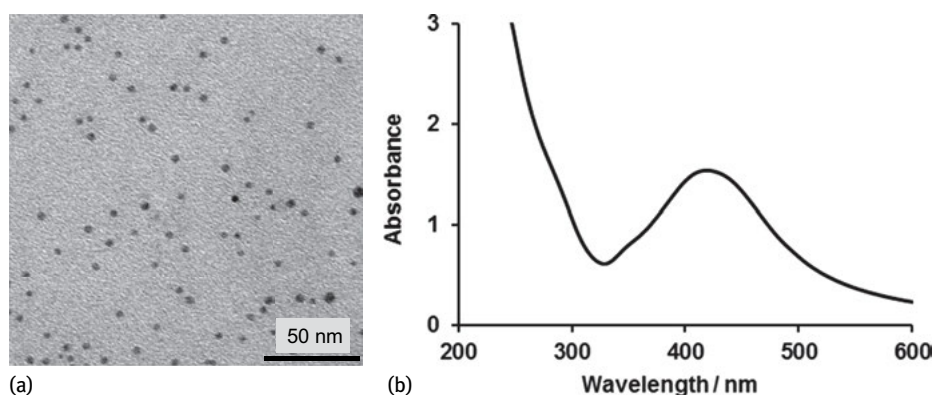
Microfluidic reactors have been used in the synthesis of various organic, inorganic, and biological materials [25, 26]. Such microreactors have also been successful in the synthesis of colloidal nanoparticles [27]. The microreactor method and the microwave method can lead to nanoparticles of uniform size. A uniform seed crystal is the principal feature of the microreactor. Incorporating the microwave method, in which the microreactor can generate a uniform seed crystal such that a uniform crystal growth is possible, results in nanoparticles with a narrower size distribution. A novel hybrid system that combines a microreactor and microwave radiation for the continuous nanoparticle synthesis has been proposed using the formation of silver nanoparticle as an example [27]. For instance, the addition of PVP as the dispersing agent and glucose as the reducing agent to produce nanoparticles in an aqueous medium will be referred to as *solution A* (Figure 14.13); *solution B* consisted of a diaminesilver(I) complex aqueous solution. The solutions were then mixed in the microreactor (YMC. Co.



**Fig. 14.13:** Experimental setup of a hybrid microreactor/microwave system: (a) detailed schematic; (b) whole photograph. Reproduced with permission from Ref. [27]. Copyright 2013 by Elsevier B.V.

Ltd Deneb mixer) using a syringe driver; subsequently, the solution flowed spiral reactor by means of a high-performance liquid chromatography pump. The reactor was heated rapidly using a microwave resonator (Saida FDS Inc); the temperature of the sample solution was adjusted to 162 °C, and the pressure was regulated to 1 MPa using a back-pressure regulator.

Heating the mixed solution in the microreactor with microwaves generated silver nanoparticles of uniform size (~5 nm) (Figure 14.14a). The maximum absorption of the SPR band of the silver colloids produced by the microreactor/microwave combination occurred at ca. 420 nm (Figure 14.14b). Control experiments were carried out in which both solutions A and B were mixed in the microreactor system, yet no silver nanoparticles formed under these conditions or in the presence of glucose as the reducing agent, no doubt due to a very slow reducing rate in the absence of microwaves [27]. When the



**Fig. 14.14:** TEM images and plasmon resonance absorption of silver nanoparticles produced by hybrid microreactor/microwave system [27]. Copyright 2013 by Elsevier B.V.



mixed solution comprising solutions A and B was heated by microwaves, but without the microreactor, no silver nanoparticles were produced, at least none were observed, in spite of having arranged the appropriate temperature conditions under microwave irradiation. Silver nanoparticles did form, however, with the hydrothermal synthesis method utilizing a continuous-flow system and a synthesis apparatus that combined both microwaves and the microreactor.

## 14.7 Synthesis of core-shell metal chalcogenide nanoparticles

The synthesis of metal chalcogenides with microwave radiation can be accomplished either via the hydrothermal method or the polyol method (see, for example, Ref. [1] for more details). As an example, a novel microwave synthesis of water-dispersed and highly luminescent CdTe/CdS core-shell nanocrystals was reported nearly a decade ago by He and coworkers [28]. Their method allowed for the rapid synthesis of high-quality CdTe/CdS core-shell nanocrystals in aqueous phase under moderate conditions that displayed a variety of colors (Figure 14.15). Results demonstrated that the as-prepared CdTe/CdS core-shell nanocrystals required no postpreparative treatment and revealed a high photoluminescence quantum yield (up to 75%) and a narrow size distribution (full width at half maximum: ~35 nm). More importantly, their investigations demonstrated the suitability and the advantages of microwave irradiation for accelerating the epitaxial growth of a CdS shell; only 5 min were needed to form an optimal thickness of the CdS shell in the microwave synthesis compared with several days expended using an illumination method with ambient light. In



**Fig. 14.15:** Photograph of wide spectral range of bright luminescence from a sample of microwave-assisted synthesis of CdTe/CdS core-shell nanocolloids in aqueous media without any postpreparative treatment under irradiation with 365 nm UV light from a UV lamp [28]. Copyright 2006 by the American Chemical Society.

this regard, successful examples of the formation of core-shell structures have been reported in aqueous systems, such as citrate-stabilized CdSe/CdS nanocrystals by Wang and coworkers [29] and thioglycolic acid (TGA)-stabilized CdTe/CdS nanocrystals by Bao and coworkers [30], who prepared these systems by exposing citrate-stabilized CdSe nanocrystals in the presence of cadmium and sulfide ions or TGA-stabilized CdTe nanocrystals to ambient light in order to achieve the formation of the CdS shell through the photodegradation of the respective stabilizers. Both of the as-prepared core-shell nanocrystals also demonstrated high quantum yields of photoluminescence (QYPL) owing to the CdS shell, which passivated the core CdSe and CdTe nanocrystal surfaces by effectively smoothing out the surfaces and reducing the number of surface traps of these core nanocrystals. Enhancement of the QYPL also resulted from the disposal of the stabilizers through their photodegradation.

The illumination methods were quite time consuming, however, since 5 days or 20 days were required, respectively, to obtain citrate-stabilized CdSe/CdS nanocrystals [29] and TGA-stabilized CdTe/CdS nanocrystals [30] with the highest QYPL; in the latter case, a gradual and slow photooxidation of TGA was required to form the CdS shell. In addition, the long reaction times generated a broad size distribution of these systems.

In comparison to the thioglycolic acid method for synthesizing CdTe/CdS core-shell nanocrystals by the illumination method under ambient light, microwave synthesis can also be applied to synthesize core-shell nanocrystals capped with other thiols such as 3-mercaptopropionic acid [28]. Clearly, microwave synthesis has proven to be an extremely simple and convenient methodology that is free of complicated vacuum manipulation and expensive chemical reagents, not to mention that it is also environmentally and biologically friendly since the whole synthesis can be carried out in an aqueous medium.

## 14.8 Epilog

We have attempted in this chapter to describe some of the aspects and advantages in using microwave radiation to effect the synthesis of nanoparticles, which begins with a nucleation process first by the formation of nuclei of very small dimensions that ultimately grow into nanosized particles. While the authors' recent work has been particularly emphasized herein, several excellent research groups are working in this area of Materials Science to prepare, characterize, and investigate the properties of nanomaterials of various shapes and compositions. The interested reader may wish to consult Ref. [1] as a place to start and then consult the vast available references of the literature on the Internet.

## Bibliography

- [1] Horikoshi S, Serpone N (Eds.). *Microwaves in Nanoparticle Synthesis: Fundamentals and Applications*, Wiley-VCH Verlag GmbH & Co., 2013. Doi: 10.1002/9783527648122.
- [2] Pruppacher HR, Klett JD. *Microphysics of Clouds and Precipitation*, Kluwer, Dordrecht, Holland, 1997.
- [3] Sear RP. Quantitative Studies of Crystal Nucleation at Constant Supersaturation: Experimental Data and Models, *Cryst. Eng. Comm.*, 16, 2014, 6506. doi:10.1039/C4CE00344F.
- [4] Sear RP. Nucleation: theory and applications to protein solutions and colloidal suspensions, *J. Phys. Cond. Matt.* 19, 2007, 033101.
- [5] See, for example, the web site of Missouri University of Science and Technology, Rolla, MO, USA: [http://web.mst.edu/~billf/nuc\\_growth.pdf](http://web.mst.edu/~billf/nuc_growth.pdf) (accessed January 2017).
- [6] Bilecka I, Niederberger M. Microwave chemistry for inorganic nanomaterials synthesis, *Nanoscale*, 2, 2010, 1358–1374.
- [7] Mallikarjuna NN, Varma RS. Microwave-Assisted Shape-Controlled Bulk Synthesis of Noble Nanocrystals and Their Catalytic Properties, *Cryst. Growth Des.*, 7, 2007, 686–690.
- [8] Gerbec JA, Magana D, Washington A, Strouse GF. Microwave-enhanced reaction rates for nanoparticle synthesis, *J. Am. Chem. Soc.*, 127, 2005, 15791–15800.
- [9] Horikoshi S, Abe H, Torigoe K, Abe M, Serpone N. Access to small size distributions of nanoparticles by microwave-assisted synthesis. Formation of Ag nanoparticles in aqueous carboxymethylcellulose solutions in batch and continuous-flow reactors, *Nanoscale*, 2, 2010, 1441–1447.
- [10] Tsukahara Y, Nakamura T, Kobayashi T, Wada Y. Homogeneous Ag particle formation confirmed by real-time in situ surface-enhanced Raman scattering measurements under microwave irradiation, *Chem. Lett.* 35, 2006, 1396–1397.
- [11] Smith E, Dent G. *Modern Raman Spectroscopy: A Practical Approach*, John Wiley and Sons Ltd., Chichester, UK, 2005, pp 210.
- [12] Herrero MA, Kreamsner JM, Kappe CO. Nonthermal microwave effects revisited: on the importance of internal temperature monitoring and agitation in microwave chemistry, *J. Org. Chem.*, 73, 2008, 36–47.
- [13] Wiegand S. Thermal diffusion in liquid mixtures and polymer solutions, *J. Phys. Condens. Matter*, 16, 2004, R357–R379.
- [14] Schanche JS. Microwave synthesis solutions from personal chemistry, *Molec. Diversity*, 7, 2003, 291–298.
- [15] Nyutu EK, Chen CH, Dutta PK, Suib SL. Effect of microwave frequency on hydrothermal synthesis of nanocrystalline tetragonal barium titanate, *J. Phys. Chem. C*, 112, 2008, 9659–9667.
- [16] Horikoshi S, Iida S, Kajitani M, Sato S, Serpone N. Chemical reactions with a novel 5.8-GHz microwave apparatus. 1. Characterization of properties of common solvents and application in a Diels–Alder organic synthesis, *Org. Proc. Res. Dev.*, 12, 2008, 257–263.
- [17] Horikoshi S, Abe H, Sumi T, Torigoe K, Sakai H, Serpone N, Abe M. Microwave frequency effect in the formation of Au nanocolloids in polar and non-polar solvents, *Nanoscale*, 3, 2011, 169–172.
- [18] Mohamed MB, Abouzeid KM, Abdelsayed V, Aljarash AA, El-Shall MS. Growth mechanism of anisotropic gold nanocrystals via microwave synthesis: formation of dioleamide by gold nanocatalysis, *ACS Nano*, 4, 2010, 2766–2772.
- [19] Kundu S, Peng L, Liang H. A new route to obtain high-yield multiple-shaped gold nanoparticles in aqueous solution using microwave irradiation, *Inorg. Chem.*, 47, 2008, 6344–6352.
- [20] Tsuji M, Hashimoto M, Nishizawa Y, Kubokawa M, Tsuji T. Microwave-assisted synthesis of metallic nanostructures in solution, *Chem. Eur. J.*, 11, 2005, 440–452.

- [21] Yamamoto T, Yin H, Wada Y, Kitamura T, Sakata T, Mori H, Yanagida S. Morphology-control in microwave-assisted synthesis of silver particles in aqueous solutions, *Bull. Chem. Soc. Jpn.*, 77, 2004, 757–761.
- [22] Tsuji M, Miyamae N, Lim S, Kimura K, Zhang X, Hikino S, Nishio M. Crystal Structures and Growth Mechanisms of Au@Ag Core-Shell Nanoparticles Prepared by the Microwave-Polyol Method, *Cryst. Growth Des.*, 6, 2006, 1801–1807.
- [23] Nishioka M, Miyakawa M, Kataoka H, Koda H, Sato K, Suzuki TM. Facile and continuous synthesis of Ag@SiO<sub>2</sub> core-shell nanoparticles by a flow reactor system assisted with homogeneous microwave heating, *Chem. Lett.*, 40, 2011, 1204–1206.
- [24] Horikoshi S, Serpone N(Eds.). *Microwaves in nanoparticle synthesis*, Chapter 5, Wiley-VCH Verlag GmbH: Weinheim, Germany, 2013.
- [25] Ehrfeld W, Hessel V, Lowe H. *Microreactor*, Wiley-VCH Verlag GmbH, Weinheim, Germany (2001).
- [26] Zhao CX, He L, Qiao SZ, Middelberg APJ. Nanoparticle synthesis in microreactors, *Chem. Eng. Sci.*, 66, 2011, 1463–1479.
- [27] Horikoshi S, Sumi T, Serpone N. A hybrid microreactor/microwave high-pressure flow system of a novel concept design and its application to the synthesis of silver nanoparticles, *Chem. Engin. Proc.*, 73, 2013, 59–66.
- [28] He Y, Lu HT, Sai LM, Lai WY, Fan QL, Wang LH, Huang W. Microwave-assisted growth and characterization of water-dispersed CdTe/CdS core-shell nanocrystals with high photoluminescence, *J. Phys. Chem. B*, 110, 2006, 13370–13374.
- [29] Wang Y, Tang Z, Correa-Duarte MA, Pastoriza-Santos I, Giersig M, Kotov NA, Liz-Marzan LM. Mechanism of Strong Luminescence Photoactivation of Citrate-Stabilized Water-Soluble Nanoparticles with CdSe Cores, *J. Phys. Chem. B*, 108, 2004, 15461–15469.
- [30] Bao H, Gong Y, Li Z, Gao M. Enhancement Effect of Illumination on the Photoluminescence of Water-Soluble CdTe Nanocrystals: Toward Highly Fluorescent CdTe/CdS Core-Shell Structure, *Chem. Mater.*, 16, 2004, 3853–3859.

Dariusz Bogdal

## 15 Microwaves in polymer chemistry

The chemistry as well as processing of polymers can greatly benefit from the unique feature offered by modern microwave technology; thus, they have been the subject of extensive research during the last five decades. These can include such technical issues as shorter processing time, increased process yield, and temperature uniformity during polymerization and crosslinking. For example, three typical temperature/time stages can be observed during polymerization reactions. First, an initial temperature rise by direct heating of monomers where the temperature rises slowly. Second, a significant temperature peak with maximum temperature due to the exothermic reaction. Third, free convective cooling to an ambient temperature indicating the end of the exothermic reaction processes.

Fast exothermic reaction heating usually accelerates the temperature rise and gradient inside samples. Neither continuous microwave nor thermal processing can be effectively controlled in order to maintain constant temperature/time profile through the entire process. However, pulsed microwave heating can be used to control temperature and eliminate the exothermic temperature peak, maintaining the same temperature at the end of a reaction. Furthermore, a fundamental difference in the heat transfer during material processing in thermal and microwave fields is that microwave energy, in contrast to thermal heating, is supplied directly to a large volume, thereby avoiding the thermal lags associated with conduction or convection. Consequently, temperature gradients and the excessive heat build-up during thermal processing could be reduced by microwave power control [1].

Although microwave energy is more expensive than electrical energy owing to the low conversion efficiency from electrical energy (50% for 2.45 GHz and 85% for 915 MHz), the efficiency of microwave heating is often much higher than conventional heating and more than compensates for the higher energy cost. Thus, the process characteristics that have been suggested as being potentially attractive under microwave irradiation include those reactions and processes in which the size or thickness of the material is relatively large, the cost of the substrate is high and must be quickly processed, and improvements in reaction rates or the properties of materials obtained from microwave processing are significant while scaling up the processes [2].

An overview of the application of microwaves in polymer synthesis can be found in the review articles [1, 2] and in the comprehensive review with over 600 references cited in the recently published book and chapter [3, 4]. The purpose of this chapter is to provide some of the most representative examples of the application of microwaves to the synthesis of polymers [5, 6] and the preparation of composite/hybrid materials [7].

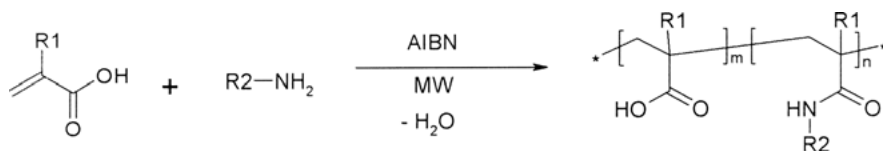
<https://doi.org/10.1515/9783110479935-015>

## 15.1 Free-radical polymerization

Regarding free-radical polymerization reactions, microwave irradiation was employed for the polymerization of vinyl monomers, fast curing of thermosetting resins and composites, rapid drying of aqueous solutions or the dispersion of polymers and resins, and heat drawing of polymer rods and tubings. Emulsion polymerization of various vinyl monomers, that is, styrene, acrylic and methacrylic esters, and acrylic and methacrylic acids, was also described for the radio frequency and microwave frequency range. Recently, it was shown that free-radical emulsion polymerization reactions activated by microwave irradiation as well as conventional heating could also be modeled using simulation software [8].

Using variable-power microwave irradiation, it was shown that the bulk polymerization of methyl methacrylate (MMA) led to a reaction rate enhancement of ca. 130–150% compared to conventional heating methods. However, thermal polymerization of MMA in a temperature range of 69 to 88 °C displayed a limiting conversion of ca. 90%, while limiting the conversion of microwave polymerization declined in the following order: 200 W, 88% > 300 W, 84% > 500 W, 78%. Finally, the nuclear magnetic resonance (NMR) spectroscopy analysis proved that the tacticity of the polymers for thermal and microwave polymerization are similar, suggesting that the polymerization process followed the same mechanism under microwave conditions [9].

Applying solvent-free conditions, a number of methacrylamides were synthesized from methacrylic acid and aliphatic and aromatic amines under microwave irradiation. Then it was found that the addition of a polymerization initiator (i.e., 2,2'-azobisisobutyronitrile (AIBN)) to the reaction mixture led directly to polymethacrylamides in a single reaction step (Figure 15.1) [10].



**Fig. 15.1:** Formation of poly(meth)acrylamides from the reaction of meth(acrylic) acid and various amines.

Later, it was demonstrated that under microwave conditions it was possible to obtain chiral (R)-*N*-(1-phenyl-ethyl)methacrylamide directly from methacrylic acid and (R)-1-phenylethylamine. An addition of AIBN led again in a single-step reaction to the formation of an optically active polymers that contained both methacrylamide and imide moieties. It was found that microwave irradiation accelerates considerable the process of condensation between the acid and amine, which is also more selective in comparison to thermal heating. The one-pot polymerization under microwave condi-

tions at 120 °C allowed the synthesis of the polymers with relatively high yields (80%), which depend on applied power. The yield under classical heating conditions (an oil bath) was only 40% [10].

More recently, the influence of microwave irradiation on polymerizations in the ionic liquids [EMIM]EtSO<sub>4</sub> and [BMIM]BF<sub>4</sub> was demonstrated. Different monomers (styrene, MMA, acrylonitrile) were homo- and co- polymerized at 60 and 80 °C in DMF or methanol and [EMIM]EtSO<sub>4</sub> or [BMIM]BF<sub>4</sub> as solvent. Either in a microwave or preheated heating block, the polymerizations were performed under N<sub>2</sub> in sealed ampoules, in which 1.5 g monomer, 0.05 g of an initiator, AIBN, or benzoyl peroxide, and 6 mL [EMIM]EtSO<sub>4</sub>, [BMIM]BF<sub>4</sub>, dimethylformamide (DMF), or methanol were weighted and then heated. The investigation showed that there were no differences in the rate of conversion between microwave irradiation and conventional heating when polymerizing in DMF or methanol. The rate of conversion in [EMIM]EtSO<sub>4</sub> and [BMIM]BF<sub>4</sub> was in all the cases higher than that in methanol and DMF when the reactions were carried out under conventional heating conditions. The overall polymerization rate under microwave conditions in comparison to conventional heating was in all cases lower in [EMIM]EtSO<sub>4</sub> and [BMIM]BF<sub>4</sub> but not in DMF and methanol. Nevertheless, there were no systematic differences in the molecular weights and in the copolymer compositions between microwave irradiation and conventional heating [11].

Catalytic chain transfer polymerization (CCTP) is a very efficient and versatile free-radical polymerization technique for the synthesis of functional macromonomers. The process is based on the ability of certain transition metal complexes, most notably of low-spin Co<sup>II</sup> complexes such as cobaloximes, to catalyze the chain transfer to monomer reaction. Microwave-assisted CCTP of MMA was presented to obtain low-molecular-weight oligomers. Various cobalt complexes have been tested as catalytic chain transfer agents. At a low amount of initiator (AIBN), both heating methods (conventional and microwave) were almost similar in terms of monomer conversion and the molecular weight of obtained oligomers (Table 15.1). However, with 1% of AIBN the polymerization mixture rapidly reached the temperature of 100 °C under microwave conditions. The total time of the process was shortened from 120 min (conventional heating) to 3 min (microwave irradiation). This phenomenon was explained by selective absorption of microwave energy by radicals generated by the decomposition of AIBN. Radical concentration had reached sufficient critical level (i.e., 1%), and energy dissipated by microwave-radical interactions contributed strongly to the overall heating process of the system [12].

In another study, the reactions were carried out in both a conventional oil bath and microwave oven using a cobalt-based catalyst that very expeditiously controls the molecular weight of the final polymer. Also, the temperature of both the reaction medium and reactor walls were precisely controlled by the use of internal fiber-optic sensors during the full period of the processes. It was shown that to monitor precisely the temperature, the application of fiber-optic sensor rather than the external IR sen-

**Tab. 15.1:** Catalytic chain transfer polymerization of MMA in bulk using 600. ppm of  $\text{CoBr}_2$  *in situ* catalyst at 80 °C adopting microwave heating and with no prestirring.

Heating method	Equatorial ligand	[AIBN] (wt.%)	Time (min)	Conv. <sup>a</sup> (%)	PDI	$M_n^b$ (g mol <sup>-1</sup> )
CH	dpg	0.5	120	35	1.34	300
MWH	dpg	0.5	120	35	1.39	300
CH	dmg	0.5	120	72	2.20	900
MWH	dmg	0.5	120	81	2.31	800
CH	dpg	1.0	120	47	2.50	200
MWH	dpg	1.0	3	31	1.29	200

<sup>a</sup> Determined by <sup>1</sup>H NMR.

<sup>b</sup> Determined by GPC.

sor supplied with the reactor is necessary. By using microwave irradiation, the reaction time was again reduced from 300 to 3 min and the yields of reaction were significantly greater [13].

## 15.2 Controlled radical polymerization

Concerning controlled radical polymerization methods, microwave techniques were used to obtain polymers with predetermined molecular weights, a low polydispersity index (PDI), specific functionalities, and more diverse architectures than in conventional free-radical polymerization. There are a number of reports where enhanced rates and low polydispersity indexes were observed for atom transfer radical polymerization (ATRP) (Section 15.2.1) under microwave conditions; similarly, significant rate enhancements were reported for reversible addition-fragmentation chain transfer (RAFT) (see Section 15.2.3) and nitroxide-mediated polymerization.

### 15.2.1 Atom transfer radical polymerization

ATRP of MMA under microwave irradiation was described in a number of reports. For example, for the reactions run with different activator-initiator systems including benzyl chloride and bromide/ $\text{CuCl}/2,2'$ -bipyridine,  $\text{AIBN}/\text{CuBr}_2/2,2'$ -bipyridine and  $\alpha,\alpha'$ -dichloroxylylene/ $\text{CuCl}/\text{N},\text{N},\text{N}',\text{N}'',\text{N}'''$ -pentamethyldiethylenetriamine, linear first-order rate plots, linear increase of the number average molecular weight with conversion and low polydispersities were observed, which indicated that ATRP of MMA was controlled under microwave conditions (Figure 15.2) [14].

In contrast, reverse ATRP was used to successfully synthesize polyacrylonitrile under microwave irradiation.  $\text{FeCl}_3$ , coordinated by isophthalic acid, was used as the



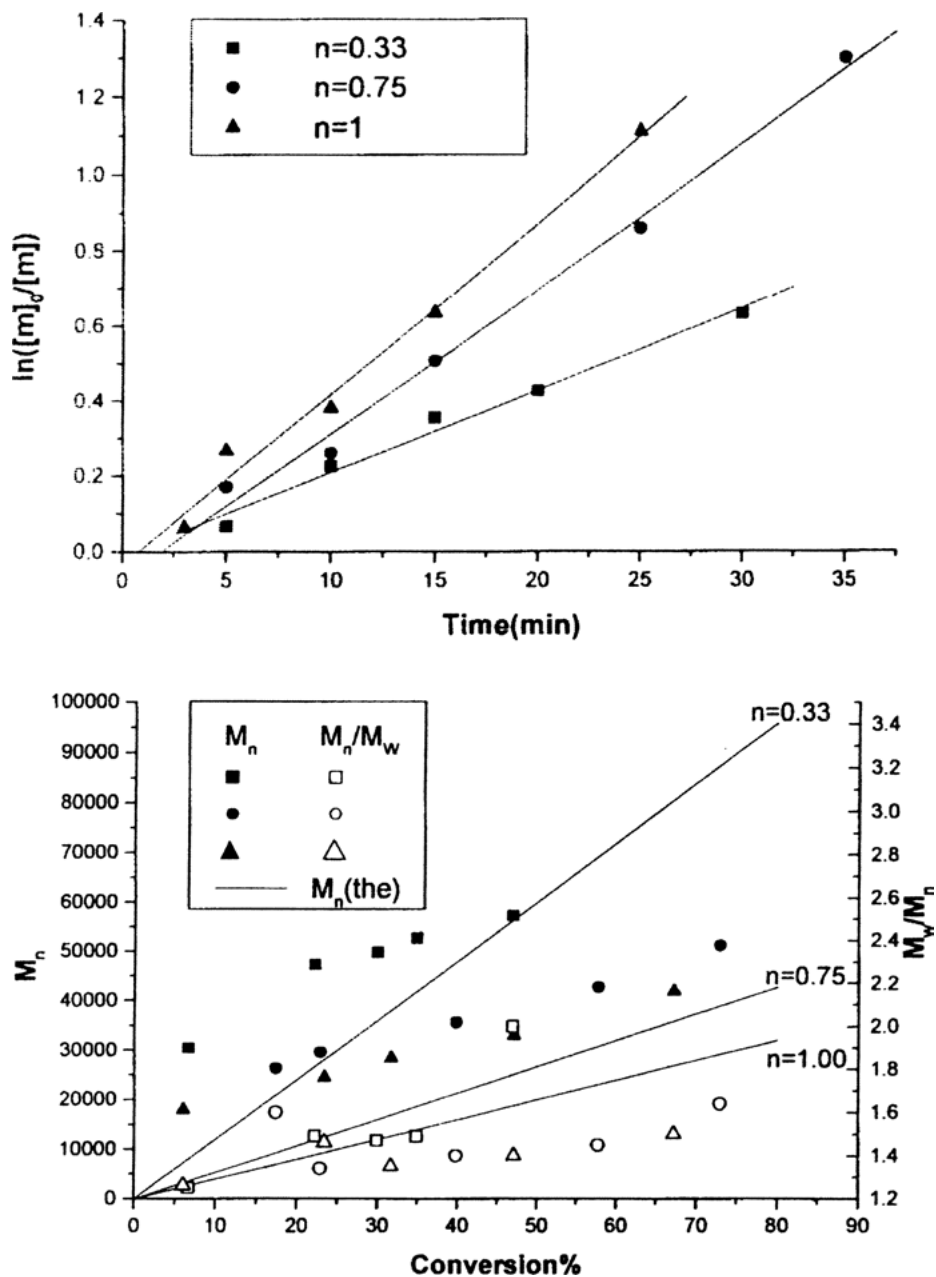


Fig. 15.2: Kinetics of ATRP for MMA at different initiator concentration and dependency of  $M_n$  and  $M_w/M_n$  on conversion for ATRPT of MMA

catalyst, and 2,2'-azobisisoheptonitrile was used as the initiator. *N,N*-DMF was used as the solvent to improve the solubility of the ligand. Under the same experimental conditions, the apparent rate constant under microwave irradiation was higher than that under conventional heating. The polymerization not only showed the best control of the molecular weight and its distribution but also provided a rather rapid reaction rate with the [acrylonitrile]/[2,2'-azobisisoheptonitrile]/[FeCl<sub>3</sub>]/[isophthalic acid] ratio of 300 : 1 : 1 : 2. The polymers obtained were used as macroinitiators to initiate the chain extension and successfully synthesize acrylonitrile polymers with a molecular weight higher than 50,000 and a narrow polydispersity as low as 1.30 [14].

### 15.2.2 Nitroxide-mediated polymerization

TEMPO-mediated bulk radical polymerizations of styrene were successfully performed under microwave irradiation. The polymerizations were well controlled in terms of linear kinetic plots and a linear increase in molecular weight with increasing conversion, and a narrow PDI (1.16–1.38) was obtained (Table 15.2).

The polymerization rates at appropriate power of microwave irradiation were faster than that under conventional heating conditions at same reaction temperature with or without benzoyl peroxide. Furthermore, it was proved by successful chain extension polymerization and NMR spectrum analysis that the nitroxide moiety did exist at the end of polymeric chain [15].

Solid-supported TEMPO-mediated controlled polymerization was also described for the preparation of novel high-loading functionalized styrenyl resins. The resin was prepared in a neat reaction of TEMPO-methyl resin with styrene derivatives. The resin with 7.25-fold increase in the mass was obtained. It was stressed that the microwave

**Tab. 15.2:** Experimental results of thermal initiated polymerization of styrene under microwave and conventional heating at 125 °C.

Heating method	Power [W]	Time [h]	Conversion [%]	$M_n$ [g/mol]	$M_w/M_n$
thermal	–	3	0	–	–
thermal <sup>a</sup>	–	3	16	4400	1.25
thermal	–	6	9	4650	1.18
mw	–	9	18	8100	1.23
mw <sup>a</sup>	100	3	3	2570	1.14
mw	100	3	41	9700	1.26
mw <sup>a</sup>	200	2	8	4600	1.15
mw	200	2	66	13600	1.38
	200	3	37	11100	1.38

<sup>a</sup> Conditions: [styrene]<sub>0</sub> = 8.7 M; [BPO]<sub>0</sub> = 0.0305 M; [OH-TEMPO]<sub>0</sub> = 0.0366 M. Others without BPO.

procedure was 150-fold faster in comparing to those described in literature under conventional conditions.

### 15.2.3 Reversible addition-fragmentation chain transfer

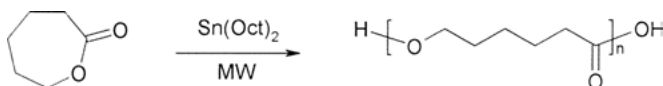
Similarly, microwave-mediated RAFT polymerization leads to fast polymerizations of common monomers (methyl acrylate, vinyl acetate, and styrene) while keeping excellent control over molecular weights and molecular weight distributions. When the experiments were conducted with more accurate temperature control, it was found that only polymerization of polar monomers like methyl acrylate and MMA led to a reaction rate enhancements of 152% and 254%, respectively; however, the polymerization rate of nonpolar monomers like styrene was not enhanced by the use of microwave irradiation. Moreover, the mechanism for the rate enhancement in RAFT polymerization under microwave irradiation was investigated by means of modeling using a numerical simulation [16].

For example, during the polymerization of methyl acrylate mediated by ethylsulfanylthioconyl sulfanyl-propionic acid ethyl ester (ETSPE) using an oil-bath heating (50 °C), an approximately 50% conversion was achieved in 4 h. Under microwave conditions, an enhancing of kinetics was observed that allowed a 60% monomer conversion in just 5 min and 80% conversion in 20 min. A study of the development of  $M_n$  and PDI relative to conversion throughout the two polymerization reactions showed excellent consistency, demonstrating that although the kinetics was significantly enhanced, it was not at the expense of the control of molecular weight or polydispersity [16].

## 15.3 Ring-opening polymerization

Ring-opening polymerization (ROP) reactions were investigated for a number of monomers like  $\epsilon$ -caprolactone, D,L-lactide, and oxazoline derivatives. For example, the ROP of  $\epsilon$ -caprolactone under microwave irradiation was carried out at different temperatures ranging from 80 to 210 °C in the presence of  $\text{Sn}(\text{Oct})_2$  and zinc powder as catalysts (Figure 15.3) [17].

Poly( $\epsilon$ -caprolactone) with an average molecular weight of 124,000 g/mol and yield of 90% was obtained after 30 min of irradiation using 0.1% mol/mol of  $\text{Sn}(\text{Oct})_2$ ,



**Fig. 15.3:** Ring opening polymerization of  $\epsilon$ -caprolactone in the presence of  $\text{Sn}(\text{Oct})_2$  and zinc powder as catalysts.

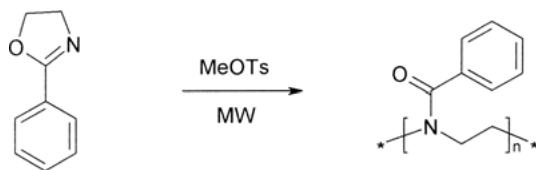
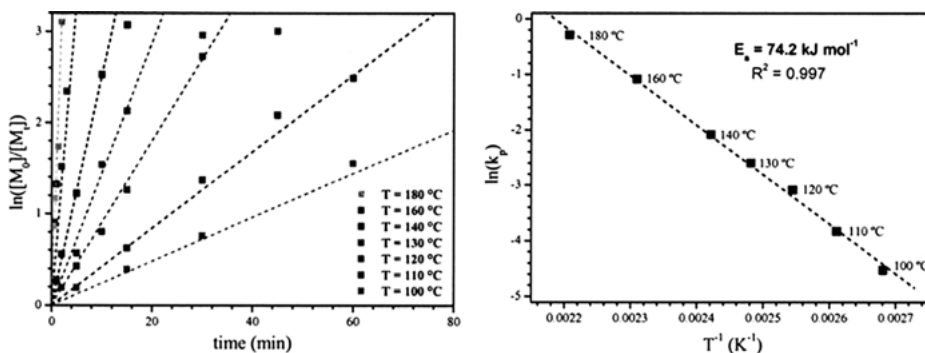


Fig. 15.4: Ring-opening polymerization of oxazoline derivatives.

whereas the polymerization catalyzed by zinc powder yielded poly( $\epsilon$ -caprolactone) with an average molecular weight of 92,300 g/mol after 30 min of irradiation using 1% mol/mol zinc powder. Without microwave irradiation, the polymerization rate was considerably slower; at 120 °C poly( $\epsilon$ -caprolactone) was afforded with an average molecular weight of 60,000 g/mol with  $Sn(Oct)_2$  after 24 h and 27,000 g/mol with zinc powder after 48 h [17].

Oxazoline derivatives were the next group of cyclic monomers studied for ROP under microwave irradiation. For instance, 2-phenyl-2-oxazoline mixed with methyl tosylate in an acetonitrile solution was irradiated in a microwave reactor for 30 to 150 min at 125 °C (Figure 15.4). A comparison with thermal heating experiments showed a great enhancement in the reaction rates while the living character of the polymerization was conserved. Under microwave irradiation after 90 min the monomer conversion was nearly quantitative, that is, 98%. In contrast, polymerization under conventional conditions showed only a 71% conversion after 90 min. Interestingly, the reaction rate coefficient under conventional conditions was the same for reactions in open and closed vessels, that is,  $1.1 \times 10^{-2} \text{ min}^{-1}$ , while for the microwave experiments the reaction rate coefficient was different for the reaction in open and closed reaction vessels, that is,  $3.6 \times 10^{-2} \text{ min}^{-1}$  and  $4.2 \times 10^{-2} \text{ min}^{-1}$ , respectively [10].

Then ROP reactions of a number of 2-substituted-2-oxazolines (i.e., 2-methyl, 2-ethyl, 2-nonyl, and 2-phenyl) in the presence of methyl tosylate as catalyst were studied in a temperature range of 80 °C to 200 °C (Figure 15.4). While enhancing the reaction rate by factors of 400 going from 80 to 200 °C (Figure 15.5), activation energies for the polymerization ( $E_A$ : 73 to 84 kJ/mol) were within the range of values obtained with conventional heating (Table 15.3). The first-order kinetics of the monomer conversion and livingness of the polymerization were maintained. A maximum number of 300 monomers can be incorporated into polymer chains under such conditions. Moreover, polymerization can be carried out in concentrated solutions or even bulk conditions to afford well-defined monomers (PDI < 1.20). Recently, it was observed that ROP of 2-oxazolines with fluorinated aromatic substituents was found to be strongly accelerated (ca. 10 times) by *o*-fluoro substituents. This observed acceleration is due to an interaction of the cationic reaction center on nitrogen atoms with an ortho-fluorine substituent that overcompensates for the negative electron-withdrawing effect and by the increased nucleophilic character of the monomer due to the nonplanarity of the oxazoline and the phenyl substituent [6].



**Fig. 15.5:** Monomer conversion against time plot for polymerization of 2-nonyl-2-oxazoline at different temperatures.

**Tab. 15.3:** Activation energies  $E_A$  and frequency factors  $A$  for the polymerization of 2-methyl-, 2-ethyl-, 2-phenyl-, and 2-nonyl-2-oxazoline.

Monomer	Frequency factor ( $A$ ) [ $10^8 \text{ L} \cdot \text{mol}^{-1} \cdot \text{s}^{-1}$ ]	Activation energy ( $E_A$ ) [ $\text{kJ} \cdot \text{mol}^{-1}$ ]
2-Methyl-2-oxazoline	$5.00 \pm 1.20$	$75.4 \pm 0.5$
2-Ethyl-2-oxazoline	$1.99 \pm 0.85$	$73.4 \pm 0.5$
2-Phenyl-2-oxazoline	$14.9 \pm 2.8$	$84.4 \pm 0.5$
2-Nonyl-2-oxazoline	$7.58 \pm 1.15$	$76.3 \pm 0.5$

A library of diblock copoly(2-oxazoline)s was prepared applying the same technique of ROP under microwave irradiation. A total number of 100 (50 + 50) monomer units were incorporated into the polymer chains. The reactions were initiated by methyl tosylate and carried out in an acetonitrile solution at 140 °C. After polymerization of the first monomer, the second monomer was added, and the reaction mixture was again irradiated in a microwave reactor. As a result, 16 polymers were obtained with a narrow PDI < 1.30 (Table 15.4).

Recently, the same method was used for the preparation of a library of 30 triblock copolymers starting from 2-methyl-, 2-ethyl-, 2-nonyl-, and 2-phenyl-2-oxazoline in a microwave reactor. The polymers exhibited narrow molecular weight distributions (PDI < 1.33) and showed only minor deviations from the targeted monomer ratio of 33 : 33 : 33. The glass transition temperature of the triblock copolymers ranged from 50 to 100 °C depending on the incorporated monomers. More recently, the successful synthesis of 2-(3-ethylheptyl)-2-oxazoline and polymerization under microwave conditions was reported. The corresponding homopolymer was the first poly(2-oxazoline) that is amorphous and exhibits a low glass-transition temperature at -6 °C. The significant differences in properties compared with its linear analog 2-(3-nonyl)-2-oxazoline polymer are caused by the branching of the side chain, resulting in a lower packing density, which is consistent with an easier molecular motion of the polymer. Thermal

**Tab. 15.4:** (Theoretical) average molecular weight  $M_n^{\text{th}}$  (g/mol)  $\times 10^3$  and polydispersity index PDI for the four chain-extended and 16 diblock copoly(2-oxazoline)s<sup>a</sup>.

First monomer	Second monomer			
	2-Methyl- 2-oxazoline	2-ethyl- 2-oxazoline	2-nonyl- 2-oxazoline	2-phenyl- 2-oxazoline
2-Methyl- 2-oxazoline	$M_n^{\text{th}} = 8.5$ PDI = -/1.16	$M_n^{\text{th}} = 9.2$ PDI = -/1.17	$M_n^{\text{th}} = 14.2$ PDI = -/-	$M_n^{\text{th}} = 11.6$ PDI = -/1.25
2-Ethyl- 2-oxazoline	$M_n^{\text{th}} = 9.2$ PDI = -/1.18	$M_n^{\text{th}} = 9.9$ PDI = 1.12/1.16	$M_n^{\text{th}} = 14.8$ PDI = 1.15/-	$M_n^{\text{th}} = 12.3$ PDI = 1.27/1.19
2-Nonyl- 2-oxazoline	$M_n^{\text{th}} = 14.2$ PDI = -/-	$M_n^{\text{th}} = 14.8$ PDI = 1.64/-	$M_n^{\text{th}} = 19.7$ PDI = 1.14/-	$M_n^{\text{th}} = 17.2$ PDI = 1.24/-
2-Phenyl- 2-oxazoline	$M_n^{\text{th}} = 11.6$ PDI = -/1.18	$M_n^{\text{th}} = 12.3$ PDI = 1.35/1.19	$M_n^{\text{th}} = 17.2$ PDI = 1.28/-	$M_n^{\text{th}} = 14.7$ PDI = 1.27/1.16

<sup>a</sup> in each cell, the first (second) entry for the polydispersity indices results from measurements in chloroform (*N,N*-dimethylformamide).

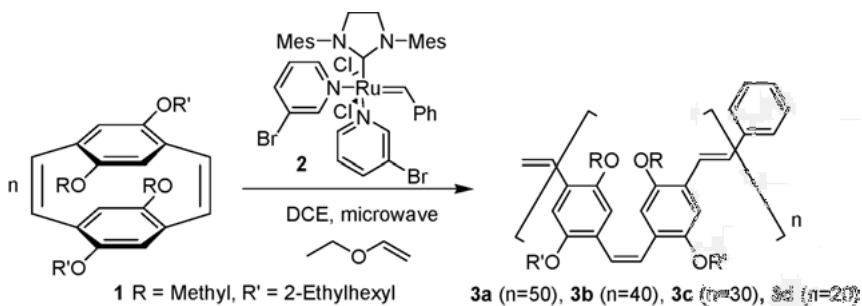
investigations of the random copolymers revealed a linear dependency of the  $T_g$  with a weight percent of 2-(3-ethylheptyl)-2-oxazoline monomer, allowing simple fine-tuning of the  $T_g$  from -6 to 59 °C for specific applications [6].

## 15.4 Ring-opening metathesis polymerization

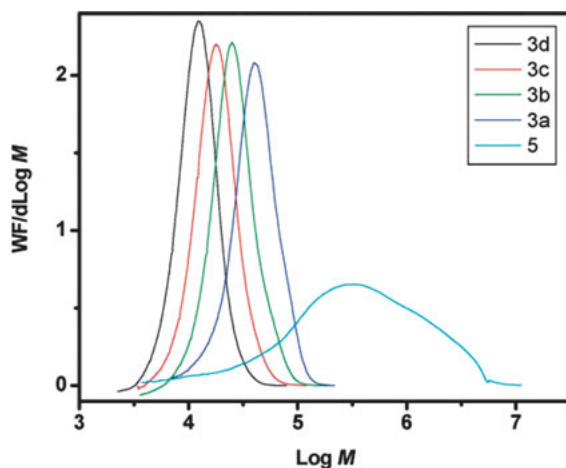
Ring-opening metathesis polymerization (ROMP) uses metathesis catalysts to generate polymers from cyclic olefins. ROMP is most effective on strained cyclic olefins and becomes an important reaction for obtaining polymers with predetermined molecular weights and low PDIs.

A new synthetic method of preparing soluble phenylenevinylene polymers by ROMP of 4,7,12,15-tetraoctyloxy-[2.2]paracyclophane-1,9-diene under microwave irradiation was described (Figure 15.6). The polymerization showed a living character and gave polymers of controlled molecular weight, with a narrow polydispersity, fewer chain defects, and an alternating cis,trans-microstructure [18].

As was shown, 4,12-di-20-ethylhexyloxy-7,15-dimethoxy-[2.2]paracyclophane-1,9-diene (1) was polymerized by a third-generation Grubbs catalyst when heated by microwave irradiation in anhydrous 1,2-dichloroethane. The optimum reaction conditions were found to be heating at 80 °C for 1 h. This compares with reaction times of up to 36 h required for complete monomer consumption using conventional heating in a tetrahydrofuran (THF) solution. Under microwave irradiation, polymers with a range of molecular weights were prepared by varying the initial monomer-to-catalyst ratio and the polydispersities were all low and in a range of 1.18 to 1.28 (Figure 15.7).



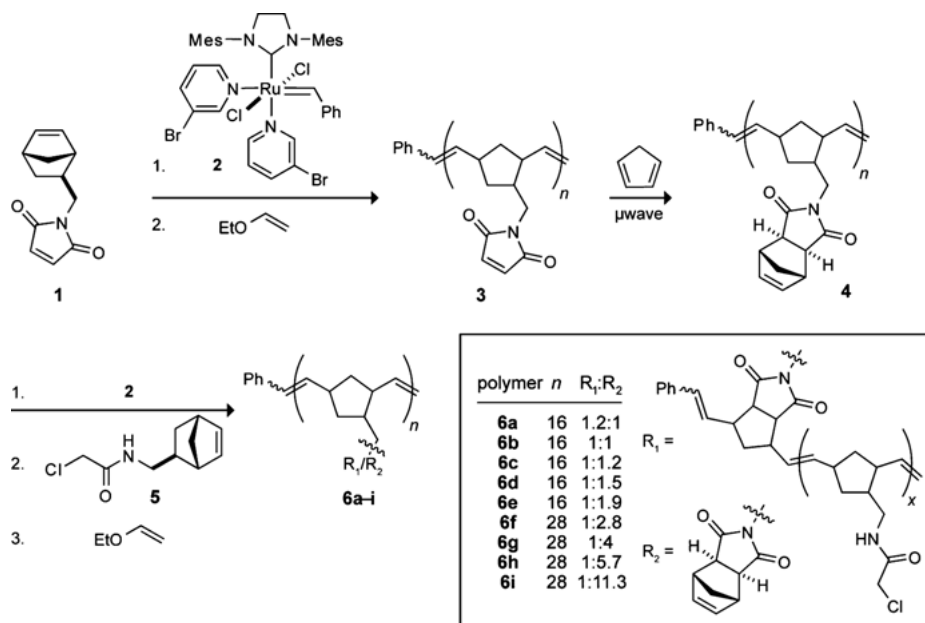
**Fig. 15.6:** Synthesis of poly[2-methoxy-5-(2'-ethylhexyloxy)-*p*-phenylene vinylene] (MEH-PPV) by microwave assisted ROMP.



**Fig. 15.7:** Molecular weight distributions for MEH-PPV prepared by microwave-assisted ROMP (3) and that prepared by the Gilch route (5) using calculated Mark–Houwink parameters.

Then the polymers were isomerized from the *cis*- to *trans*-vinylene form by prolonged irradiation at 365 nm in a THF solution (20 mg in 10 mL) [18].

Recently, ROMP was applied for the synthesis of maleimide-containing polymers from norbornene maleimide in the presence of Grubbs catalyst. Via a Diels–Alder reaction with cyclopentadiene, the resulting maleimide side-chain polymers were converted efficiently to the norbornene units of the polymer, which in turn were grafted by ROMP again (ROMP from ROMP) (Figure 15.8) under microwave irradiation.



**Fig. 15.8:** Synthetic route to graft copolymers (the *n* values refer to the degree of polymerization determined for the polymers by  $^1\text{H}$  NMR analysis).

## 15.5 Microwave-assisted acyclic diene metathesis (ADMET)

Microwave-assisted acyclic diene metathesis (ADMET) polymerization was reported for a series of  $\alpha,\omega$ -diene monomers in the presence of Grubbs G1 and G2 catalysts providing polymers up to  $M_w = 31,000$  g/mol, and these values were nearly triple those obtained with conventional heating (Figure 15.9). The reactions were performed in a 10 mL pressurized vessel, which was stopped repeatedly to apply a vacuum for the removal of ethylene; in addition, 1,2-dichlorobenzene was used to facilitate ethylene removal.

Both the pulsed-mode and continuous low-power operation of microwave irradiation provide an absolute advantage over an oil-bath heat source. The continuous low-power run yielded molecular weights ( $M_w = 22,000$  g/mol) lower than pulsed power in the same solvent ( $M_w = 31,000$  g/mol). Data provide clear evidence that the increased power (150 W) of the pulsed mode had a positive effect on polymer molecular weight in contrast to the low-power condition (<5 W) of fixed-temperature experiments [19].



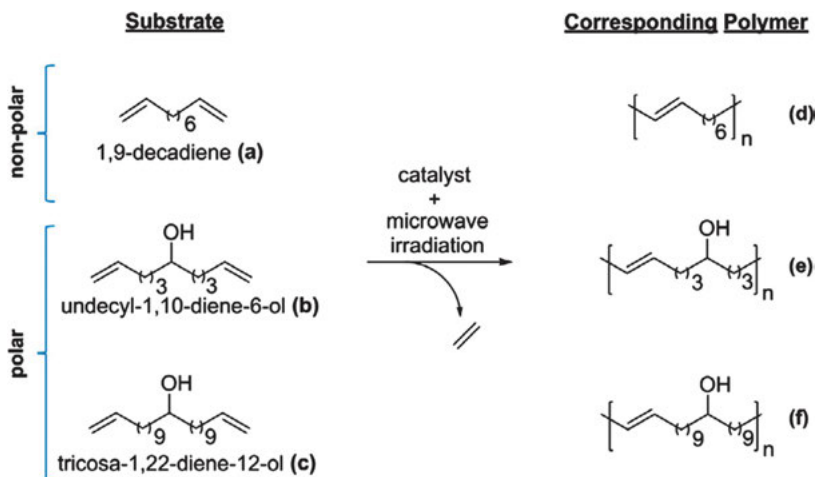


Fig. 15.9: Polymerization of polar and nonpolar dienes utilizing microwave-assisted ADMET polymerization.

## 15.6 Step growth polymerization and preparation of composite/hybrid materials

Regarding the step growth polymerization reactions, microwave-assisted curing of thermosetting polymers was one of the first applications in polymer chemistry and technology and represents the most widely studied areas under both continuous and pulse microwave conditions. It is worth stressing that most of the polymers, that is, thermoplastics, thermosets, and liquid resins, are in the microwave receptive region for the given frequency (Figure 15.10); however, a strict distinction between nonpolar and polar polymers, that is, polymers with nonpolar pendant groups and polar pendant groups, respectively, must be kept in mind [3].

Because thermosetting resins are cured, their dielectric loss factor decreases significantly because of the formation of cross-linked structures, increase in viscosity, and, finally, a decrease in the motion of polymer molecules. Thus, thermosetting resins absorb increasingly fewer microwaves when they are being cured, so microwaves easily penetrate the outer layers of cured specimens to in turn cure internal layers.

Furthermore, it has been shown that a computer-controlled pulsed microwave processing of epoxy systems could successfully eliminate the exothermic temperature peak and maintain the cure temperature to the end of the reaction [20]. Thus, it was possible to cure the epoxy systems under pulsed microwave irradiation at higher temperatures and faster without thermal degradation when compared to a continuous microwave or conventional processing, which is of the utmost importance during processing of composite and hybrid materials. Moreover, numerical simulation methods

were developed to predict the one-dimensional (1D) transient temperature profile of composites under both microwave and conventional heating and increase the quality of thick-section composites [20].

Novel polyaniline (PANI) nanocomposites were synthesized through the polymerization initiated by chemical oxidants. First, aniline was introduced into the interlayers of  $\text{HNb}_3\text{O}_8$ ,  $\text{HTiNbO}_5$ , and  $\text{HSr}_2\text{Nb}_3\text{O}_{10}$ ; then the PANI nanocomposites were prepared by polymerization under microwave irradiation in the presence of oxidants. The orientation of the aromatic rings and extent of oxidation and protonation of the interlayered PANI was closely related to the different layer properties. The nanocomposites were used as porous electrolytes and analyzed by equivalent circuit, cyclic voltammetry, and charge-discharge measurements. Compared with nanocomposites in which the aromatic rings are parallel with the inorganic slabs, nanocomposites in which the aromatic rings are perpendicular to the slabs demonstrate higher conductivity, electroactivity, and discharge capacity. Thus, a nanocomposite with enough interlayer space can provide a good  $\text{Li}^+$  transition and act as a good reservoir to store ions (Figure 15.11) [21].

One-dimensional nanorods from conducting polymers can lead to a wide range of potential applications, ranging from sensors, energy storage, and light emitting to photovoltaics. A rapid route to synthesizing self-assembled poly(aniline-co-*p*-phenylenediamine) nanorods via microwave-assisted interfacial polymerization (IP) using acid dopants was elaborated [22]. The IP method involves the step polymerization of two reactive monomers or agents, which are dissolved in two immiscible phases, and the reaction takes place at the interface of the two liquids. As a solvent, an aqueous/ionic liquid (IL) biphasic system was used with aniline and *p*-phenylenediamine. The reaction mixtures were irradiated for 30 min, and the proper reaction took place at an interface between the two layers (water and IL system), where, after

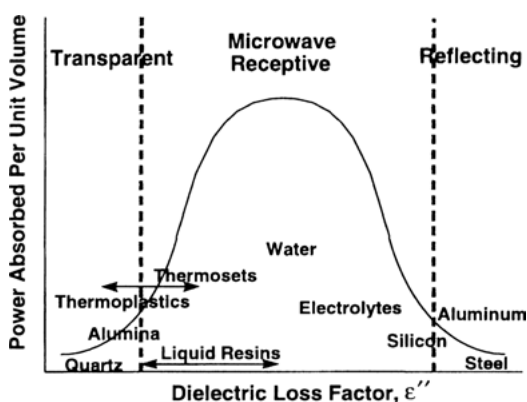


Fig. 15.10: Relationship between loss factor ( $\epsilon''$ ) and ability of some common materials to absorb microwave energy.

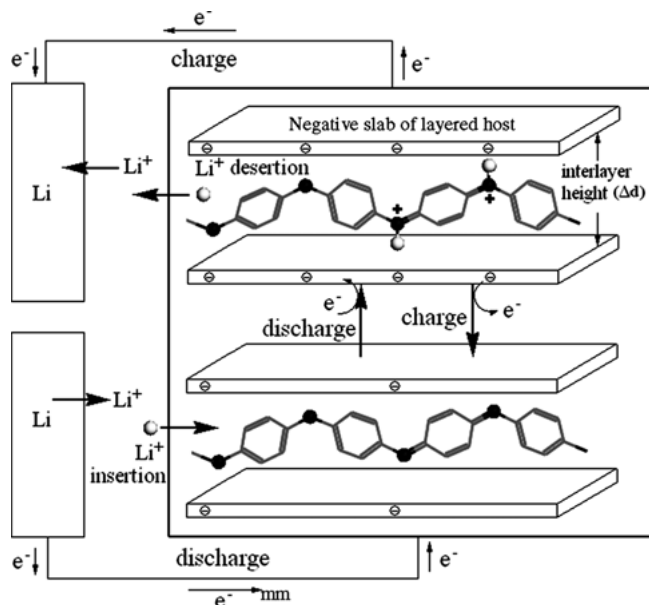


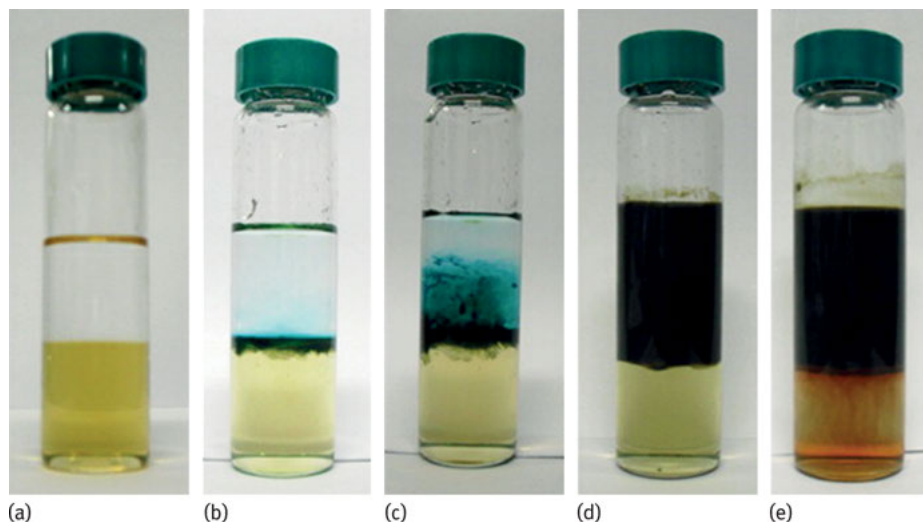
Fig. 15.11: Charge/discharge mechanism for electrochemical reaction in Li/nanocomposite cell.

a short induction period, a green copolymer appeared and diffused into the aqueous phase (Figure 15.12) [22].

After the reaction, the polymers were washed, dried, and characterized by a number of techniques including Fourier transform infrared spectroscopy, finite-element transmission electron microscopy, finite-element scanning electron microscopy (FE-SEM), ultraviolet–visible (UV–VIS) spectroscopy, thermogravimetric analysis, and X-ray diffraction. It was observed that the nanorods with an average diameter of 45–100 nm and lengths in a range up to a micrometer tended to agglomerate into an interconnected nanorod network (Figure 15.13). The conductivity of the self-assembled copolymer nanorods, which varied with the nature of the acid dopant used, i.e. HCl or *p*-toluene sulfonic acid (*p*-TSA), was found to be  $2.17 \times 10^{-3}$  and  $6.42 \times 10^{-2} \text{ S cm}^{-1}$ , respectively. Conducting copolymer nanorods can find potential applications in the construction of optoelectronic devices [22].

In other approaches, 1D polymer nanorods and nanotubes from polystyrene (PS) were successfully synthesized via a novel microwave-annealing-induced nanowetting (MAIN) method using porous anodic aluminum oxide (AAO) templates, which provided a new research direction on the microwave annealing of polymer chains in confined environments. A scheme of the experimental process is shown in Figure 15.14 [23].

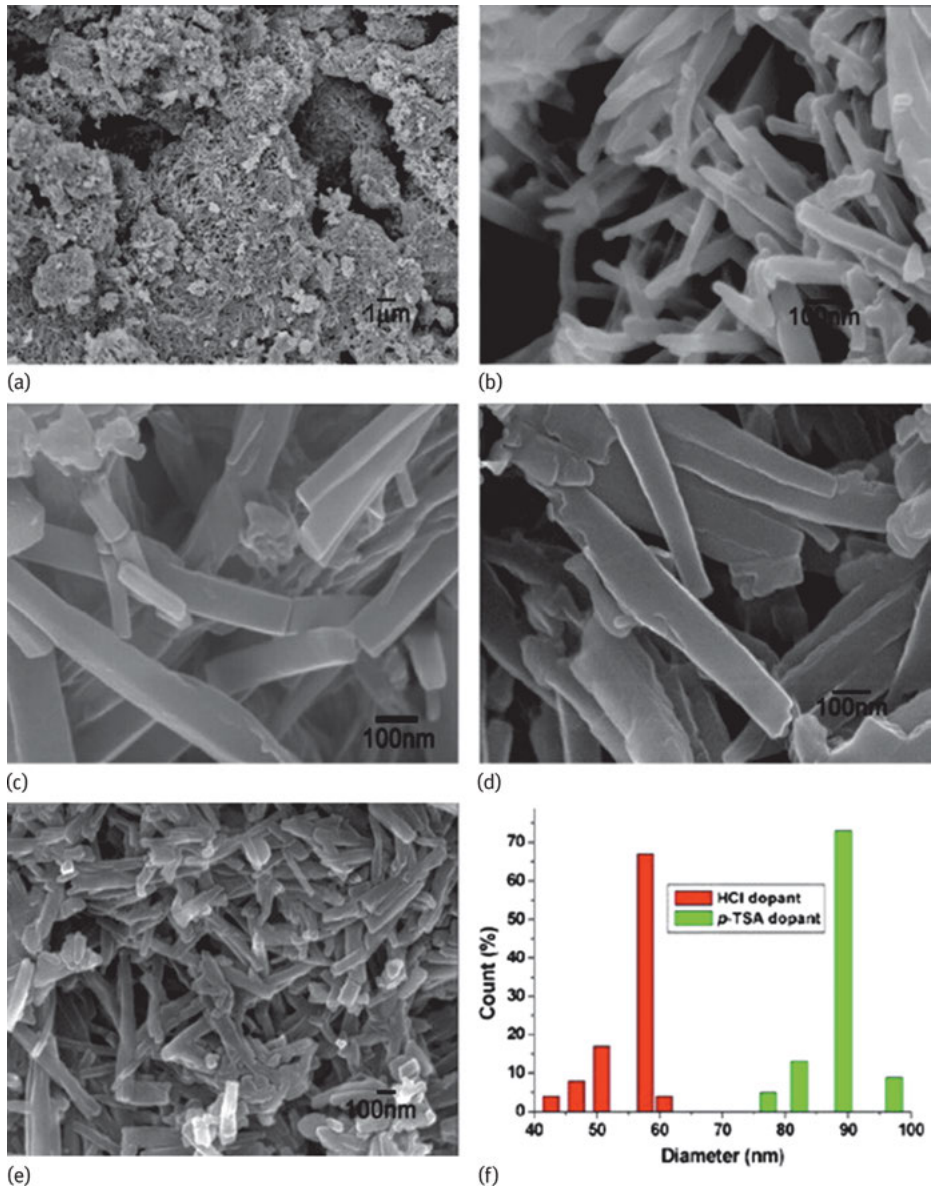
To obtain PS nanorods/nanotubes, an AAO template was placed on top of a PS-coated silicon wafer. Next, a glass substrate was placed on top of the AAO template



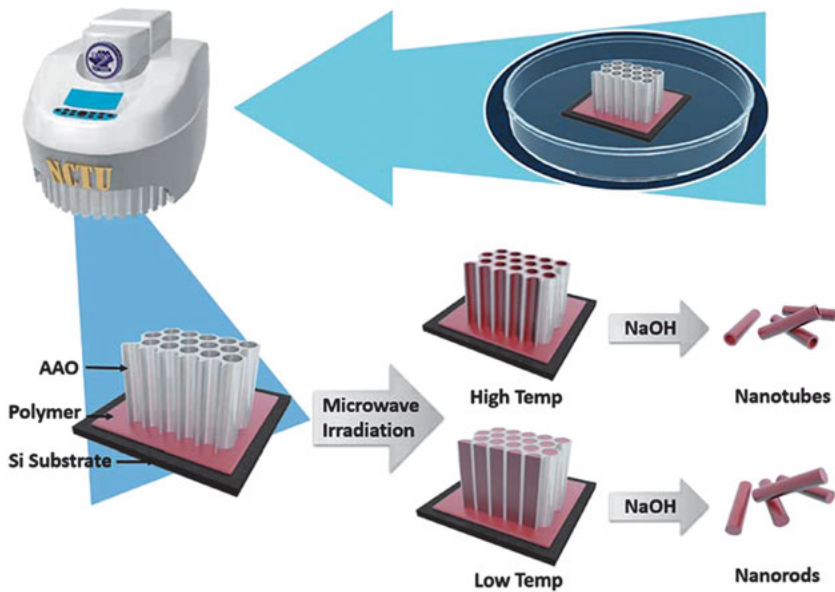
**Fig. 15.12:** Snapshots showing interfacial polymerization of comonomer in an aqueous/IL system. (a)–(e) The reaction times are 0, 1, 3, 10, and 30 min, respectively. Top phase: aqueous solution of dopant and potassium persulfate; bottom phase: comonomer/IL solution.

to ensure good contact between the template and the polymer film, and the sample was moved into a microwave-safe glass holder. The annealing process was carried out in a microwave reactor, where the temperatures were controlled by a built-in microwave feedback system. Finally, the samples were cooled and the AAO template was removed selectively using a 5 wt.% NaOH(aq) solution. It was shown that the formation of PS nanorods or nanotubes depended on the annealing temperature and time. PS nanorods were formed at lower temperatures (ca. 120 °C for 30 min), while at higher temperatures (ca. 190 °C for 30 min) nanotubes were produced. Figure 15.15 shows the SEM images of the PS nanorods and nanotubes prepared by the thermal annealing method under different annealing conditions [23].

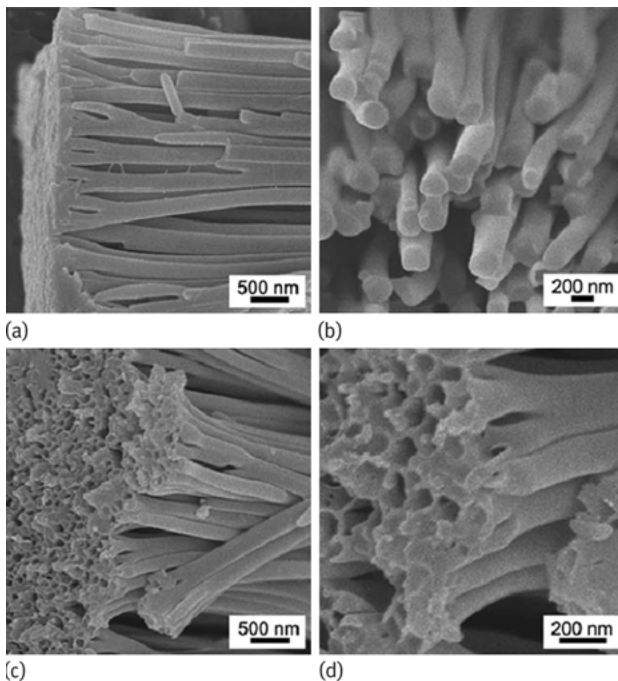
In turn, microwave irradiation was applied for *in situ* conversion of titania particles into titanate 1D nanofilaments such as nanotubes and nanorods in a polymer Nafion matrix. As a result, novel Nafion-titanate nanotube/nanorod composites for high-temperature direct ethanol fuel cells were fabricated [24]. First, spherical nanoparticles of titania anatase were homogeneously dispersed into the conducting phase of Nafion using *in situ* sol-gel process. Then titania particles were transferred *in situ* to titanate 1D nanofilaments by a microwave-assisted alkaline hydrothermal reaction. The process was carried out in a Teflon-covered stainless steel reactor placed in a microwave oven at 140 °C for 180 min. Figure 15.16 shows a schematic of the synthetic route for the preparation of Nafion-titanate nanotube/nanorod hybrid composites [24].



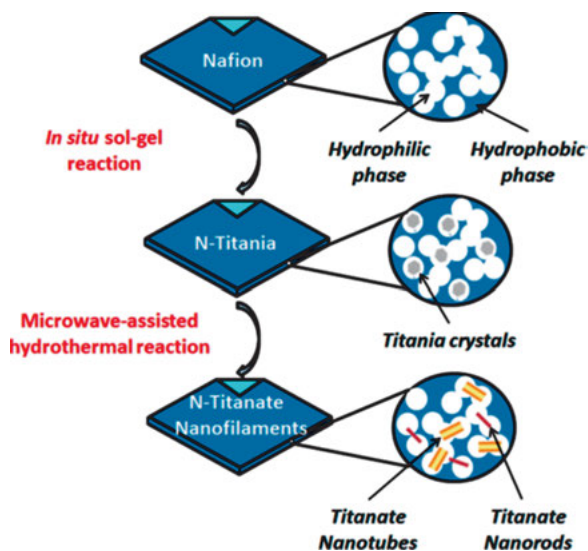
**Fig. 15.13:** FE-SEM images of self-assembled copolymer nanorods synthesized using HCl (a) low, (b, c) high magnifications, (d) *p*-TSA as dopants; (e) image obtained after gentle sonication of nanorods suspension for 20 s; (f) diameter distributions of nanorods.



**Fig. 15.14:** Schematic illustration of experimental processes to prepare 1D polymer nanostructures via a novel microwave-annealing-induced nanowetting (MAIN) method.



**Fig. 15.15:** SEM images of PS nanorods and nanotubes prepared by thermal annealing method under different annealing conditions.



**Fig. 15.16:** Schematic representation of synthetic route for preparation of Nafion-titanate nanotube/nanorod hybrids.

Metal nanostructures have been studied extensively because of their use in applications such as catalysis, optics, electronics, and optoelectronics. Metal oxide (ZnO)-containing nanoparticles with different morphologies were incorporated into poly(methyl methacrylate) (PMMA) and PMMA/polyurethane (PU) matrices, and ZnO/PMMA nanocomposite films of thickness 0.04 mm using the solution-casting method were prepared (Figure 15.17). In both cases the content of ZnO nanocrystallites in the polymer matrix was 0.1 wt%. By near infrared (NIR) reflectance and UV-VIS spectral analysis of the ZnO/PMMA and ZnO/PMMA/PU nanocomposites, it was shown that the addition of inorganic ZnO nanoparticles into the PMMA matrix improved the NIR reflectance efficiency significantly compared to pure PMMA. For instance, neat PMMA had low reflectance only 2% while ZnO/PMMA nanocomposites increased NIR reflectivity to ~55% at wavelength of 1100 nm [25].

Additionally, the NIR reflectance was investigated and correlated with ZnO particle size and morphologies. It was found that the morphology of ZnO particles plays a key role in obtaining a high NIR reflectance. The best result (about 55% at wavelength of 810 nm) was achieved using ZnO nanosheet morphology obtained with polyethylene glycol 300 capping under a microwave irradiation reaction. Taking into account the properties of the obtained ZnO/PMMA nanocomposite, these materials can find potential applications as solar thermal control interface films [25].

In another report, magnetic hybrid core-shell nanoparticles consisting of magnetite ( $\text{Fe}_3\text{O}_4$ ) cores surface-functionalized by glycolic acid and covered by polylactic acid were prepared by ROP in microwave-assisted synthesis. The synthesis consisted



Fig. 15.17: Photographic images of ZnO/PMMA and ZnO/PU/PMMA sheets.

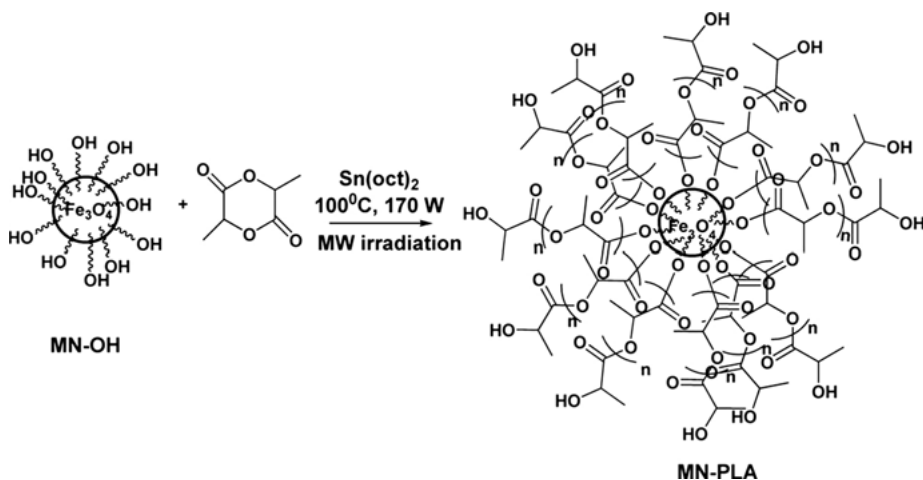
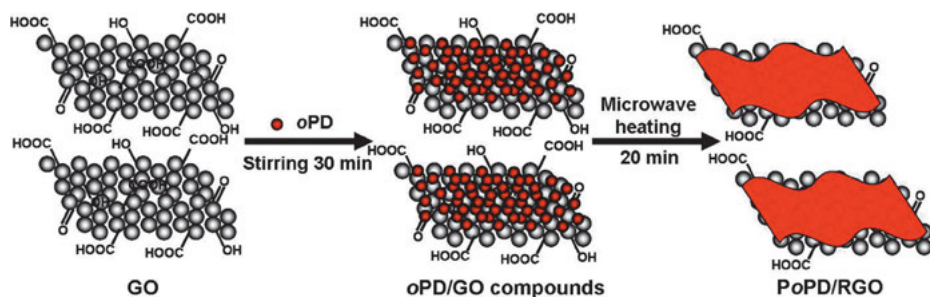


Fig. 15.18: Surface-initiated ROP of D,L-lactide onto stabilized magnetite MN-OH by microwave irradiation.

of a few steps (Figure 15.18), including the preparation of  $\text{Fe}_3\text{O}_4$  nanoparticles by coprecipitation, the stabilization of nanoparticles by chemical adsorption of glycolic acid on the surface (MN-OH), and finally surface modification with D,L-lactic acid by polycondensation (MN-PLA). The last stage was carried out under microwave heating for 11 min at 100 °C. Nearly spherical core-shell nanoparticles with diameters between 14 and 16 nm were obtained, which show superparamagnetic behavior with relatively high magnetization values [26].

Poly(*o*-phenylenediamine)/reduced graphene oxide (PoPD/RGO) composite nanosheets using microwave heating were described, and their effective adsorption of lead ions was examined. In a typical synthesis of a hybrid PoPD/RGO composite, a homogeneously dispersed mixture of graphene oxide and *o*-phenylenediamine (oPD) in water was placed in a microwave oven (210 W) for 20 min. The final prod-



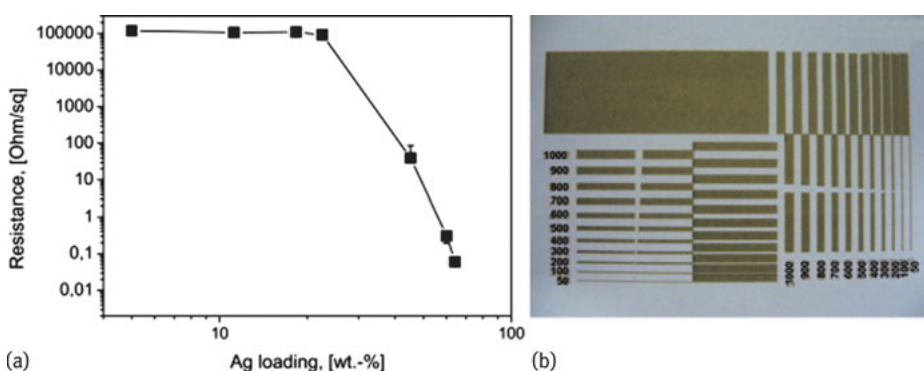


**Fig. 15.19:** Schematic diagram of fabrication of PoPD/RGO composite nanosheets.

uct was collected by filtration and washed with water. During the reaction process, graphene oxide nanosheets were used as oxidant to polymerize oPD monomer to form poly(*o*-phenylenediamine) (PoPD) on their surface, while they themselves were reduced (Figure 15.19) [27].

Finally, applying microwave techniques, it was possible to prepare composite films with high electrical conductivity. The application of hybrid colloids as building blocks for the formation of conducting films was feasible because of a combination of film-forming and conducting components in colloid form that can be used as inks in ink-jet printers for printing conducting elements in low-cost electronics for textiles or packaging. The preparation of colloids with a polymer core and an inorganic shell applied as building blocks for the manufacture of conducting composite films were carried out under microwave irradiation (Figure 15.20) [28].

The study presented in this chapter gives only some of the possibilities of the chemistry and processing of polymeric materials under microwave irradiation. The continuation of these studies could provide much stronger evidence that temperature



**Fig. 15.20:** Conductivity of composite films as a function of silver nanoparticle content (a). Array prepared by ink-jet printing of hybrid colloids containing 18.3 wt.% silver nanoparticles on paper substrate (the numbers near each line indicate line widths) (b).

gradients and excessive heat build-up during thermal processing could be reduced by a microwave power control that would result in a shorter processing time, increased yield, and more homogeneous properties of materials.

## Bibliography

- [1] Bogdal D, Penczek P, Pielichowski J, Prociak A. *Advances in Polymer Science*, 2003, 163, 193–263.
- [2] Bogdal D, Prociak A 2008. *Microwave-Enhanced Polymer Chemistry and Technology*, Blackwell-Wiley.
- [3] Bogdal D. *Microwave-assisted polymerization*, *Polymer Science: A Comprehensive Reference*, 2012, 4, 981–1027.
- [4] Bogdal D, Matras K 2006. In: *Microwaves in Organic Synthesis*, Wiley-VCH: Weinheim, pp. 653–684.
- [5] Wiesbrock F, Hoogenboom R., Schubert US, *Macromolecularl. Rapid Communication* 2004, 25, 1739–1764.
- [6] Hoogenboom R., Schubert US, *Macromolecularl. Rapid Communication* 2007, 28, 368–386.
- [7] Bogdal D, Bednarz S, Matras-Postalek K. *Advances in Polymer Science*, 2016, 274, 241–294.
- [8] Jaramillo-Soto G, Ramírez-Cupido M, Tenorio-López JA, Vivaldo-Lima E, Penlidis A. *Chemical Engineering and Technology*, 2010, 33, 1888–1892.
- [9] Chia LHL, Jacob J, Boey FYC. *Journal of Materials Processing Technology* 1995, 48, 445–449.
- [10] Sinwell S, Ritter H. *Australian Journal of Chemistry*, 2007, 60, 729–743.
- [11] Glück, T, Woecht I, Schmalfuß A, Smidt-Naaake G. *Macromolecular Symposia*, 275–2009, 276, 230–241.
- [12] Adlington K, McSweeney R, Dimitrakis G, Kingman SW, Robinson JP, Irvine DJ. *RSC Advances*, 2014, 4, 16172–16180.
- [13] Adlington K, Jones GJ, El Harfi J, Smith A, Kingman WW, Robinson JP, Irvine DJ. *Macromolecules*, 2013, 46, 3922–39300.
- [14] Finberger M, Wiesbrock F 2016. In: *Microwave Engineering of Nanomaterials: From Mesoscale to Nanoscale* (Ed. Guenin), PAN Stanford Publishing.
- [15] Li J, Zhu X, Zhu J, Cheng Z. *Radiation Physics and Chemistry*, 2006, 75, 253–258.
- [16] Zetterlund PB, Perrier S, *Macromolecules*, 2011, 44, 1340–1346.
- [17] Zhang C, Liao L, Gong S. *Green Chemistry* 2007, 9, 303–314.
- [18] Spring AM, Yu CY, Horie M, Turner ML. *Chem. Commun.* 2009, 2676–2678.
- [19] Gaines TW, Williams KR, Wagener KB, Rojas G. *Tetrahedron Letters*, 2015, 56, 3923–3927.
- [20] Thostenson ET, Chou TW, *Composites: Part A*, 1999, 30, 1055–1071.
- [21] Yang G, Hou WH, Feng XM, Xu L, Liu YG, Wang G, Ding WP. *Advanced Functional Materials*, 2007, 17, 401–412.
- [22] Haldorai Y, Zong T, Shim JJ. *Materials Chemistry and Physics*, 2011, 127, 385–390.
- [23] Chang CW, Chi MH, Chu CW, Ko HW, Tu YH, Tsai CC, Chen JT. *RSC Advances* 2015, 5, 27443–27448.
- [24] Matos BR, Isidoro RR, Santiago EI, Linardi M, Ferlauto AS, Tavares AC, Fonseca FC. *Journal of Physical Chemistry C*, 2013, 117, 16863–16870.
- [25] Soumya S, Mohamed AP, Paul L, Mohan K, Ananthakumar S. *Solar Energy Materials and Solar Cells*, 2014, 125, 102–112.
- [26] Nan A, Turcu R, Liebscher J. *Journal of Polymer Science Part A: Polymer Chemistry*, 2012, 50, 1485–1490.

[27] Yang L, Li Z, Nie G, Zhang Z, Lu X, Wang C. *Applied Surface Science*, 2014, 307, 601–607.

[28] Türke A, Fischer WJ, Adler HJ, Pich A. *Polymer*, 2010, 51, 4706–4712.

Sandrine Perino, Emmanuel Petitcolas, and Farid Chemat

## **16 Microwave extraction of natural products in the teaching laboratory: fundamentals of essential oils green extraction**

### **16.1 Introduction**

Chemists (scientists and engineers) do not ignore the potential consequences of their professions and realize that they have responsibilities in connection with educating others about green chemistry, its acceptance, and implementation (e.g., analysis, extraction, synthesis, separation). They recognize that their research will affect the future of the planet by creating new products and processes that improve the quality of life [1, 2]. The implementation of green chemistry technologies minimizes the use of materials that are hazardous to human health and the environment [3], decreases energy and water usage, and maximizes efficiency. Today, although many advances have been made in green chemistry in industrial and academic research, integrating these concepts into the teaching environment has not been sufficiently exploited. This phenomenon is due to the limited availability of educational tools that illustrate the methods, techniques, and principles of green chemistry, although education plays an important role in embodying the concepts and principles of green chemistry and engineering [4].

Teaching green chemistry serves several key functions. First, it provides fundamental knowledge related to new chemical products and processes and data that are necessary to develop cleaner technologies. Moreover, these new products and processes, which were developed in an academic setting, can, in some cases, have direct applications in industry. Finally, academia serves as the primary means to educate students about the need to design green chemistry technologies and provides tools to implement them.

To illustrate applications of green chemistry in teaching laboratories, we developed new green techniques and procedures employing microwave energy as the energy source to teach fundamental green extraction of essential-oil concepts. Essential oils are volatile secondary metabolites that plants produce for their own needs other than nutrition. They are widely used in foods, cosmetics, and pharmaceuticals [5]. In general, they are complex mixtures of organic compounds that give characteristic odors and flavors to aromatic plants. The objective of this chapter is to elucidate the potential for the extraction of essential oils of these green techniques, which typically use less or no solvent and energy, such as portable microwave-assisted extrac-

<https://doi.org/10.1515/9783110479935-016>

tion (PMAE), solvent-free microwave extraction (SFME), and microwave hydrodiffusion and gravity (MHG).

## 16.2 Microwave versus conventional heating

In conventional heating, heat transfer depends on thermal conductivity, on the temperature difference across the material, and on convection currents, this last term being quite often the most important. As a result, the temperature increase is often rather slow, while in microwave heating, owing to the mass heating effect, a much faster temperature increase can be obtained, depending on the microwave power and loss factor of the material being irradiated. But it is also well known that the microwave field distribution is not homogeneous in an irradiated material; therefore, energy is also not homogeneously dissipated, and so-called hot spots occur if heat generation is faster than heat transfers. This problem is also connected with penetration depth,  $D_p = \lambda_0 \epsilon' / 2\pi \epsilon''$ , the depth at which energy is reduced to  $1/e$  of the original intensity ( $\lambda_0$ : wavelength,  $\epsilon'$ : dielectric constant,  $\epsilon''$ : loss factor). For more transparent media, the occurrence of standing wave patterns will result in hot spots if the power dissipation is faster than the heat transfer to surrounding colder areas. The advantages of using microwave energy, a noncontact heat source, include faster energy absorption, reduced thermal gradients, and selective heating. For the extraction of essential oils from plant materials, the benefits could include more effective heating, fast heating, reduced equipment size, faster response to process heating control, faster startup, increased production, and elimination of process steps.

## 16.3 Experimental setup

### 16.3.1 Portable microwave-assisted extraction

Miniaturization (downscaling) is an important factor in modern science and technology [6], including in medicine, chemistry, ecology, and food safety [7]. The miniaturization of a procedure can be achieved simply by reducing the dimensions of the systems or by developing completely new setups or techniques. When compared to conventional systems, miniature systems can use similar methods with remarkably reduced consumption of plant matrices and solvents, size and power requirements, and system costs and at the same time faster analysis time and massively parallel analysis.

The idea has been to develop a method of PMAE that can be used directly in crops or forests [8, 9]. Given the reduced scale at which it works, this microwave technique requires a small amount of sample in a small glassware system that is designed as a miniature alembic to be placed inside a microwave oven. It was a challenge to develop a miniature alembic capable of allowing for the fast extraction of essential oils from

fresh samples and collecting the extract using a Vigreux column as an air-cooled condenser and suitable for placement inside a microwave oven. In this way, the PMAE apparatus can provide information about the actual state of fresh samples and their essential-oil content. This procedure is appropriate for a teaching laboratory because it requires no special microwave equipment. The experiment developed, in addition to providing information quickly on real samples, allows students to learn extraction and acquire chromatographic and spectroscopic analysis skills. It is a dramatic visual example of the rapid, sustainable, and green extraction of natural products.

A PMAE apparatus consists of a portable microwave oven that works on a car's battery (12 V). A miniature alembic employed for microwave-assisted extraction is illustrated in Figure 16.1.

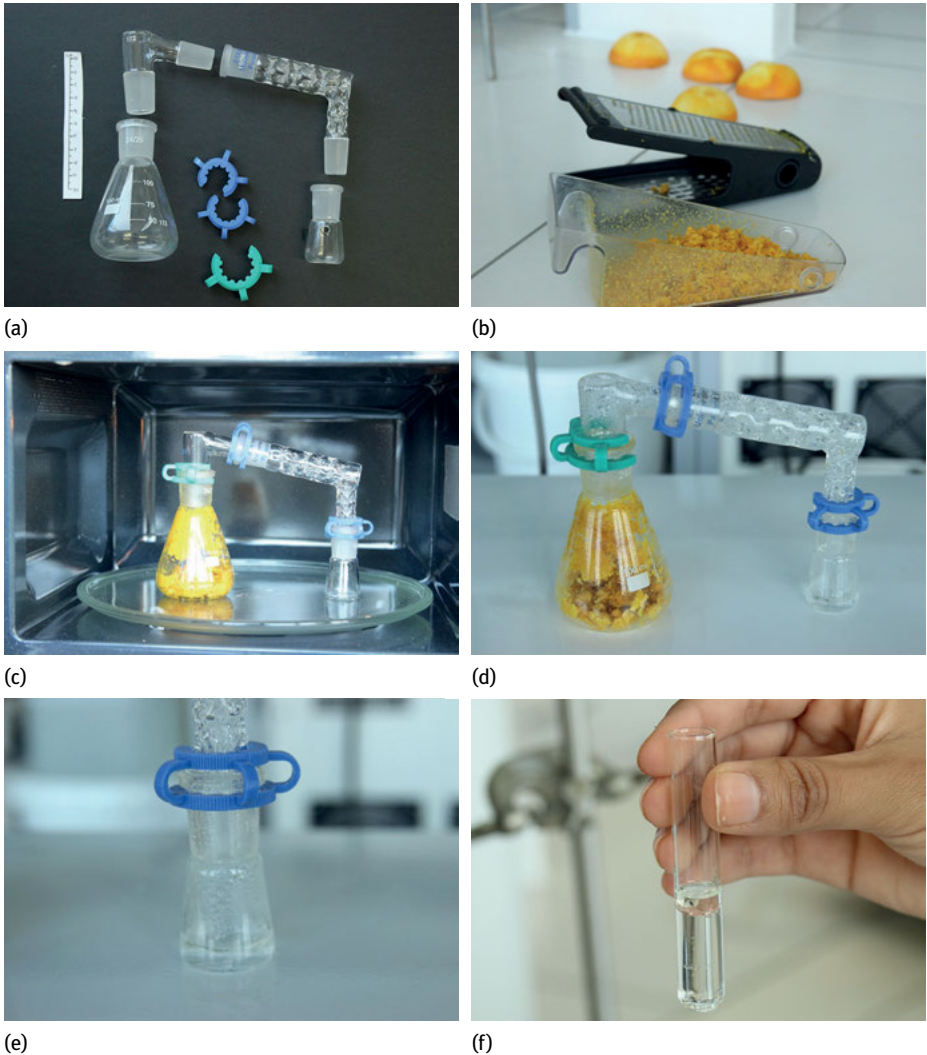
Example of application: 30 g of fresh rosemary leaves were added to a 100 mL Erlenmeyer flask with a ground socket. Then a Vigreux column as an air-cooled condenser followed by an Erlenmeyer flask drilled (at atmospheric pressure) to collect the distillate were adapted to the socket. The glass system was put into the microwave oven and heated for 15 min without any added solvent or water, using a fixed power of 100 W. The essential-oil layer was carefully transferred with a Pasteur pipette to a test tube. The oil was dried over anhydrous sodium sulfate and weighed with a portable balance before being stored prior to analysis.

### 16.3.2 Solvent-free microwave extraction

SFME was conceived for laboratory-scale applications in the extraction of essential oils from different kinds of aromatic plants and fruits [10–12]. An SFME apparatus is an original combination of microwave heating and distillation at atmospheric pressure (Figure 16.2).

Based on a relatively simple principle, this method involves placing plant material in a microwave reactor and extracting the oil without any added solvent or water. The internal heating of the *in situ* water within the plant material distends the plant cells and leads to a rupture of the glands and oleiferous receptacles. Thus, this process coevaporates the essential oil with the *in situ* water of the plant material. A cooling system outside the microwave oven condenses the distillate continuously. The excess water is refluxed to the extraction vessel to restore the *in situ* water to the plant material.

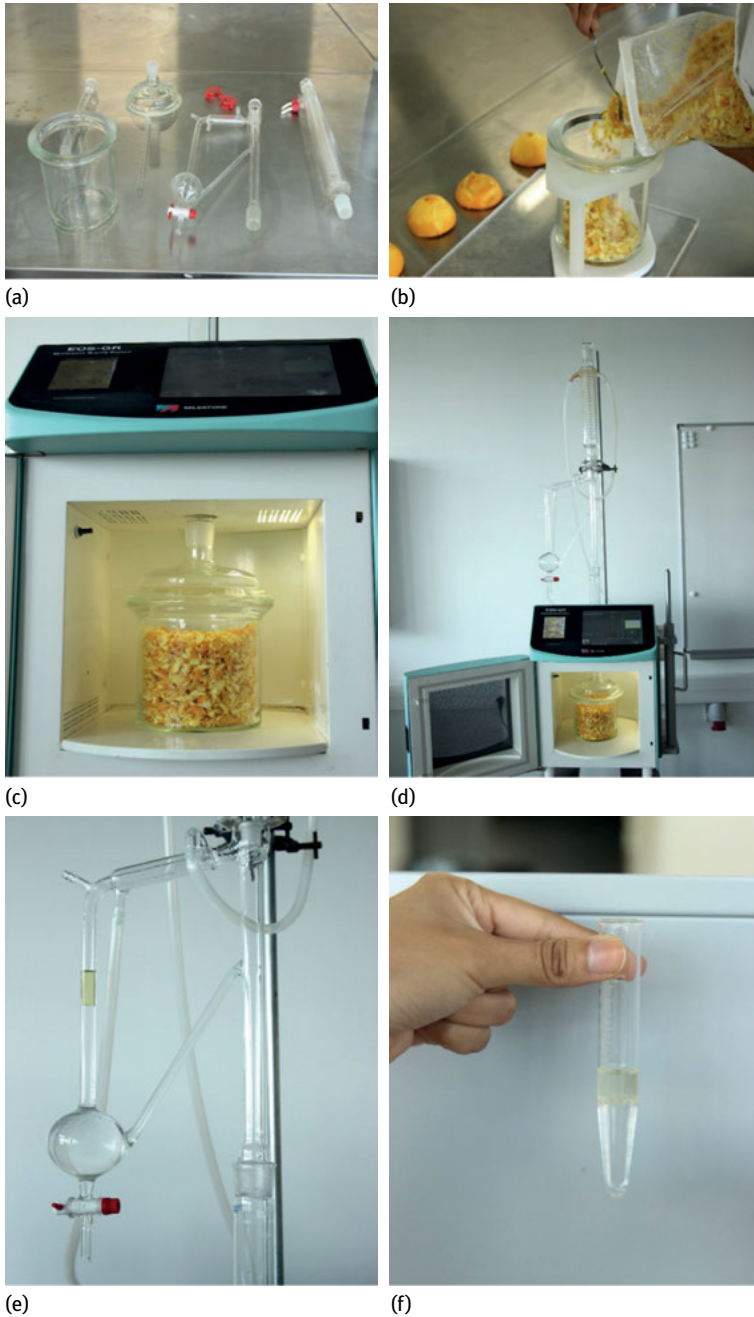
Example of application: 250 g of fresh plant material was heated using a fixed power of 500 W for 30 min without added any solvent or water. A cooling system outside the microwave cavity condensed the distillate continuously. Condensed water was refluxed to the extraction vessel in order to provide uniform conditions of temperature and humidity for extraction. The extraction was continued at 100 °C until no more essential oil was obtained. The essential oil was collected, dried under anhydrous sodium sulfate, and stored at 0 °C until used [11].



**Fig. 16.1:** (a) Glassware system for PMAE; (b) orange zest; (c) PMAE inside microwave oven; (d) PMAE following extraction; (e) essential oil and *in situ* water of orange peel; (f) essential oil of orange peels above the *in situ* water.

### 16.3.3 Microwave hydrodiffusion and gravity

This green extraction technique, patented by Chemat et al. [13], is an original so-called upside down microwave alembic combining microwave heating and Earth's gravity at atmospheric pressure. MHG was conceived for laboratory and industrial-scale applications for the extraction of food ingredients from different kinds of fruits, vegetables, and aromatic plants (Figure 16.3).



**Fig. 16.2:** (a) Glassware system for SFME; (b) microwave reactor with orange peels; (c) microwave reactor inside microwave oven; (d) SFME system; (e) system to collect essential oil and *in situ* water; (f) essential oil of orange peels above *in situ* water.





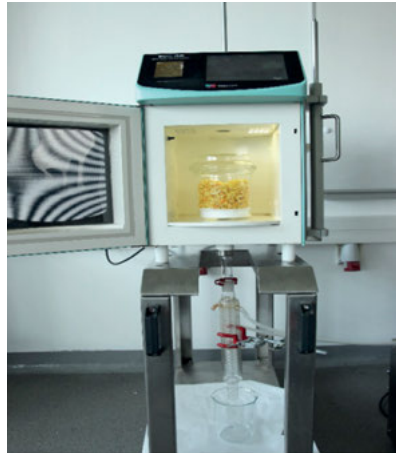
(a)



(b)



(c)



(d)



(e)



(f)

**Fig. 16.3:** (a) Glassware system for MHG; (b) microwave reactor; (c) microwave reactor with orange peels inside microwave oven; (d) MHG system; (e) system to collect essential oil and *in situ* water; (f) essential oil of orange peels above *in situ* water.

This method involves placing plant material in a microwave reactor, without adding any solvent or water. The internal heating of the *in situ* water within the plant material distends the plant cells and leads to the rupture of glands and oleiferous receptacles. The heating action of microwaves thus frees essential oil and *in situ* water, which are transferred from the inside to the outside of the plant material. This physical phenomenon, known as hydrodiffusion, allows the extract (water and essential oil), diffused outside the plant material, to drop by Earth's gravity out of the microwave reactor and fall through the perforated Pyrex disk. A cooling system outside the microwave oven cools the extract continuously. Water and essential oil are collected and separated in a vessel traditionally called the Florentine flask. The essential oil floats at the top while water goes to the bottom and can be easily separated. It is important to note that this green method allows one to extract essential oils without distillation and evaporation, which are the most energy-consuming processes between the unit operations.

Example of application: 250 g of lavandin (after soaking in 1 L distilled water for 10 min) was heated without the addition of solvent or water. The direct interaction of microwaves with biological water (i.e., steam produced from the water present in the plant material) facilitates the release of essential oil trapped inside the cells of plant tissues. Due to Earth's gravity, a mixture of hot so-called crude juice and steam (*in situ* water) naturally moves downward into a condenser outside the microwave cavity, where it is condensed. The oil condensate is collected continuously in a receiving flask, dried under anhydrous sodium sulfate, and stored at 4 °C until it is used [14].

## 16.4 Advantages

### 16.4.1 Green production rapidity

Microwave extraction is clearly quicker than the conventional method (hydrodistillation); an extraction time of 20 min provides yields comparable to those obtained after 3 h by hydrodistillation (HD), which is one of the reference methods in essential-oil extraction. For HD, SFME, PMAE, or MHG, the extraction temperature is equal to water's boiling temperature at atmospheric pressure (100 °C). To reach this temperature and thus distill the first oil droplet, it is necessary to heat for only 2 min with MHG or SFME versus 90 min for HD [11].

### 16.4.2 Green production efficiency

In general, the oils obtained from each experiment are very similar in their pale appearance and fragrancy. The essential oils isolated by microwave extraction are similar in their composition: the same number of volatile secondary metabolites is found in essential oils with equivalent relative amounts from both extraction methods [14].

### 16.4.3 Green production messages

Microwave extraction is a green method that avoids the use of large quantities of water and voluminous extraction vessels necessary in HD. The reduced cost of extraction is clearly advantageous for the proposed microwave methods in terms of energy and time. For example, the energy required using the two extraction methods are respectively 3 kW/h for the conventional method (HD) (electrical energy for heating and evaporating) and 0.1 kW/h for MHG (electrical energy for microwave supply). Regarding environmental impact, the calculated quantity of carbon dioxide ejected into the atmosphere is higher in the case of HD (3464 g CO<sub>2</sub> per g of essential oil) than for MHG (70 g CO<sub>2</sub> per g of essential oil) or for SFME (200 g CO<sub>2</sub> per g of essential oil). These calculations were made according to the literature: to obtain 1 kWh from coal or fuel, 800 g of CO<sub>2</sub> will be ejected into the atmosphere during the combustion of fossil fuel [15].

## 16.5 Future prospects

The ideal solvent for extraction or synthesis is no solvent. In this chapter we have discussed how the concept of microwave-induced, solvent-free extraction technique has already become an important issue in the extraction or synthesis of natural products. The understanding, on the molecular scale, of processes relevant to microwave solvent-free extraction techniques has not yet reached the degree of maturity at the industrial scale that other topics in analytical chemistry have. The challenge of reaching such a level is somewhat ambitious and will require a special approach. First, we must study the different mechanisms involved during microwave solvent-free extraction (selective heating, overboiling, detexturation, and microwave poration) and influencing parameters. It is also important to have special insight in terms of not only scaling up and industrial applications for microwave reactors and their possible combination with conventional or innovative techniques but also quality, safety considerations, and environmental impacts.

Nowadays, the choice of which technique to use to perform the extraction of a desired metabolite from a specific plant must be the result of a compromise between the efficiency and reproducibility of extraction and ease of procedure, together with considerations of cost, time, safety, and degree of automation. In this chapter we have discussed how the concept of a microwave solvent-free extraction technique has already become an important issue in the chemistry of natural products. A detailed analysis of earlier and current literature confirms explicitly the usefulness of this extraction method at the laboratory and industrial scales. We hope that this chapter will widen the scope of laboratory and commercial success in potential applications of microwave technology in the extraction of food and natural products.

## Bibliography

- [1] Chemat F. *Eco Extraction du Végétal*, Edn. Dunod, Paris, 2011.
- [2] Anastas PT, Warner JC. *Green Chemistry: Theory and Practice*, Oxford University Press, New York, 1998.
- [3] Warner MG, Succaw GL, Hutchison JE. Solventless syntheses of mesotetraphenylporphyrin: new experiments for a greener organic chemistry laboratory curriculum, *Green Chem.*, 2001, 3, 267–270.
- [4] Penas FJ, Barona A, Elias A, Olazar M. Implementation of industrial health and safety in chemical engineering teaching laboratories, *Journal of Chem. Health and Safety*, 2006, 19–23.
- [5] Arous K, Uquiche E, Del Valle JM. Matrix effects in supercritical CO<sub>2</sub> extraction of essential oils from plant material, *Journal of Food Engineering*, 2009, 92, 438–447.
- [6] Contreras JA, Murray JA, Tolley S.E, Oliphant JL, Tolley HD, Lammert S.A, Lee E.D, Later DW, Lee ML, *J. Am. Soc. Mass Spectrom.*, 2008, 1425–1434.
- [7] Kim SJ, Vengatajalabathy Gobi K, Harada R, Shankaran DR, Miura N. *Sensors and Actuators B*, 2006, 115, 349–356.
- [8] Ryvolova M, Preisler J, brabazon D, Macka M, *Trends in Analytical Chemistry*, 2010, 29, 339–353.
- [9] Sui X, Liu T, Ma C, Yang L, Zu Y, Zhang L, Wang H, *Food Chem.*, 2012, 131, 1399–1405.
- [10] Chemat F, Smadja J, Lucchesi ME. Brevet Européen, EP 1 439 218 A1, 2004.
- [11] Lucchesi ME, Chemat F, Smadja J. Solvent-free microwave extraction of essential oil from aromatic herbs: comparison with conventional hydro-distillation, 2004, *Journal of Chromatography A*, 1043, 323–327.
- [12] Li Y, Fabiano-Tixier A.S, Abert Vian M, Chemat F. Solvent-free microwave extraction of bioactive compounds provides a tool for green analytical chemistry, *Trends in Analytical Chemistry*, 2013, 47, 1–11.
- [13] Chemat F, Abert-Vian M, Visinoni F. Microwave hydro-diffusion for isolation of natural products, European Patent. EP 1 955 749 A1, 2008.
- [14] Périno-Issartier S, Giniès C, Cravotto G, Chemat F. Comparison of essential oils from lavender obtained by different extraction processes : ultrasound, microwave, steam and hydrodistillation. *Journal of Chromatography A*, 2013, 1305, 41–47.
- [15] Ferhat MA, Meklati BY, Chemat F. Comparison of different isolation methods of essential oil from Citrus fruits: cold pressing, hydrodistillation and microwave “dry” distillation, *Flavour and Fragrance Journal*, 2007, 22, 494–504.

Cláudia P. Passos and Manuel A. Coimbra

## **17 Microwave extraction of bioactive compounds from industrial by-products**

### **Abbreviations list:**

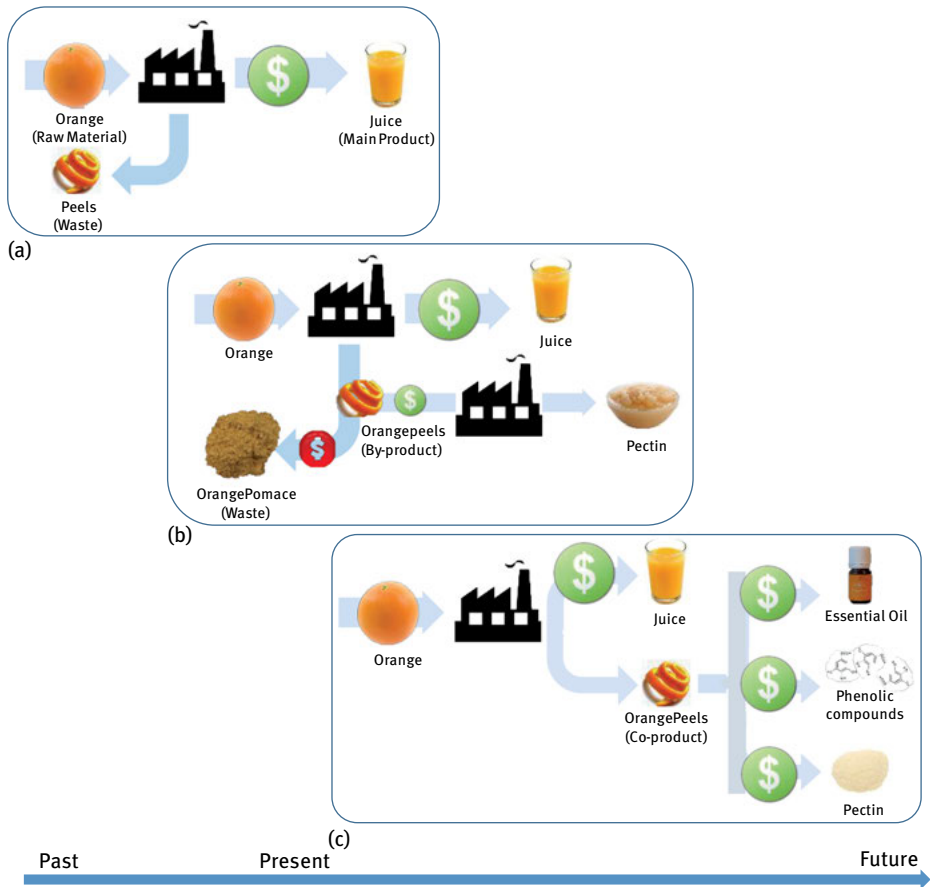
**AG**, Arabinogalactans  
**AGX**, Arabinoglucuronoxylans  
**AOA**, Antioxidant activity  
**ASE**, Accelerated Solvent Extraction  
**ASP**, Alkaline-Soluble Polysaccharide  
**AX**, Arabinoxylans  
**AXOS**, Arabinoxyloligosaccharides  
**BSG**, Brewer Spent Grain  
**CE**, Conventional Extraction  
**CGA**, Chlorogenic acids  
**CP**, Mechanical “Cold” Pressing  
**DPPH**, 2,2-diphenyl-1-picrylhydrazyl  
**EDTA**, Ethylenediaminetetraacetic acid  
**EO**, Essential Oils  
**EtOAc**, Ethyl acetate  
**EtOH**, Ethanol  
**Ext.Cycles**, Extraction Cycles  
**GAE**, Gallic Acid Equivalents  
**GM**, Galactomannans  
**GP**, Ginger Press cake  
**GR**, Ginger Rhizomes  
**GS**, Grape Seeds  
**HD**, Hydrodistillation  
**HG**, Homogalacturonan  
**HRE**, Heat Reflux Extraction  
**KOH**, Potassium Hydroxide  
**KOH**, Alkali concentration  
**m**, Mass  
**MAD**, Microwave-Accelerated Distillation  
**MAE**, Microwave-Assisted Extraction  
**MAEE**, Microwave-Assisted Enzymatic Extraction  
**MC**, Moisture  
**MeOH**, Methanol

<https://doi.org/10.1515/9783110479935-017>

**MHD**, Microwave Hydrodistillation  
**MHG**, Microwave Hydrodiffusion and Gravity  
**MSD**, Microwave Steam Distillation  
**MSD<sub>f</sub>**, Microwave Steam Diffusion  
**MW**, Microwave  
**Mw**, Molecular Weight  
**OK**, Olive kernel  
**OL**, Olive leaves  
**P**, Pressure  
**RG**, Rhamnogalacturonan  
**S:W**, Solid:water ratio  
**SD**, Steam Distillation  
**SD<sub>f</sub>**, Steam Diffusion  
**SE**, Solvent Extraction  
**SFE**, Supercritical Fluid Extraction  
**SFME**, Solvent-Free Microwave Extraction  
**SHLE**, Superheated Liquid Extraction  
**Steam<sub>Flow</sub>**, Steam flow  
**t**, time  
**T**, Temperature  
**t<sub>constant</sub>**, Constant period of time  
**t<sub>heating</sub>**, Heating period of time  
**UAE**, Ultrasound-Assisted Extraction  
**UHP**, Ultrahigh Pressure  
**UHP**, Ultra-High Pressure  
**V**, Volume  
**v<sub>MAE</sub>**, Vacuum Microwave-assisted extraction  
**v<sub>MHD</sub>**, Vacuum Microwave Hydrodistillation  
**v<sub>MHG</sub>**, Vacuum Microwave Hydrodiffusion and Gravity  
**W**, Power  
**W/m**, Power density

## 17.1 Industrial waste, byproducts, or coproducts?

To obtain a manufactured product, companies usually cannot avoid the generation of side compounds (Figure 17.1a). Because the companies have no alternative, these compounds are discarded as waste, requiring environmental treatment by incineration or landfill disposal, which nowadays represents an additional cost, reflected in the rise of the price of the product. The increasing environmental regulatory demands associated with the search for a reduction in costs of production have led companies to adopt, as much as possible, circular economic strategies involving integrated approaches that



**Fig. 17.1:** Industrial waste, byproduct, and coproduct scenarios based on a hypothetical orange juice company: (a) single high-profit product with waste disposal; (b) single high-profit product produced together with valuable byproducts and waste treatment required; (c) several coproducts produced together with the main product.

allow them to maximize their use of all raw materials and reduce to a minimum the production of waste. During the manufacturing process, other products that are produced unintentionally at the same time as the main product and that be used in other applications and by other companies are called byproducts. For this, an economic value needs to be identified. Most companies produce byproducts (Figure 17.1b) that have an economic value. However, because their production is not controlled, their characteristics are not standardized, which limits their applicability to new products. If industrial byproducts were controlled and standardized according to required specifications for application, they could be converted into high-value and profitable coproducts (Figure 17.1c). Under the best scenario possible, industrial waste is eliminated by the production of one or several coproducts together with the main product.

## 17.2 Availability and opportunities for industrial byproduct recycling

In Europe alone, in 2010, the total waste production amounted to 2.5 billion metric tons. It was estimated that in 2012, around 88 million of that was related to food waste, with associated costs estimated at 143 billion euros [1]. Along the food supply chain, food waste is divided into primary (agricultural) production, industrial processing, distribution (wholesale, retail, and food service), and food consumption (households). Of these, the food processing sector has the second highest contribution, 16.9 million metric tons, representing about 19% of the total food waste [1]. Industrial byproducts from food processing are divided, in decreasing order of abundance, into five main sectors: fruits and vegetables, milk, meat, fish, and wine [2]. With respect to just the fruit byproduct sector (pomace, peels, and press residues in general), the most representative genera are *Malus*, *Citrus*, and *Pyrus*, representing about 20–50% of the total fruit weight. The total fruit available for processing in the 2015/2016 season was, respectively, 65 million metric tons for apples [3], 19 million metric tons for oranges [4], 2 million metric tons for lemons/limes [4], 1.5 million metric tons for tangerines/mandarin oranges [4], and 2.6 million metric tons for pears [3]. These huge figures are only an example of the large amount of agricultural and food byproducts, representing environmental and economic potential and opportunity for food waste transformation [2, 5–7].

The window of opportunity for a food company to transform raw materials and byproducts into high-value products is usually narrow owing to the high water content and consequent perishability of these materials, which often results in waste. Nevertheless, resource depletion pushes companies to search for feasible alternatives to efficiently handle food byproducts, although a high investment is still required in basic research, extraction technologies, and adaptation of existent or even the creation of new production lines. Although, from an industrial point of view, established regular procedures should not be changed, the increasing demand for more efficient, cleaner, and environmentally friendly methodologies has led a search for so-called greener technologies. This includes the conversion of byproducts into coproducts able to be used as raw materials. In the case of companies involved in the extraction of bioactive compounds, their identification in industrial wastes and the definition of technological strategies for their extraction allow for a new paradigm of conversion of wastes into byproducts and, through the regulation of the extraction process, design of bioactive coproducts.

For an effective and optimized production process, the number of operations should be minimized while maximizing the extraction yield and reducing the solvent consumption, always maintaining product safety and quality. Under these guidelines, microwave extraction appears to be a promising technological tool for extraction, in most cases, in very short periods of processing time, which also allows for a significant



reduction of energy consumption. As 70% of all the energy for industrial processes is allocated to the extraction step [8], one can foresee relevant outcomes from this point of view. Also, microwave extraction represents a versatile and so-called green extraction technology [9] whose main achievements for bioactive extraction from industrial byproducts are presented in Table 17.1 on page 307 and discussed in this chapter.

### 17.3 Microwave extraction

The first report on the use of microwave-assisted extraction dates back to 1986 and aimed to speed sample preparation for chromatographic analysis [10]. With a conventional kitchen oven, the extraction of crude fat from different origins, mainly foods, faba bean alkaloids, cotton seed gossypol (a terpenic derived phenolic compound), and soil pesticides were successfully recovered in shorter times compared with conventional Soxhlet or shake-flask extraction with organic solvents. This alternative extraction technique has been subjected to different modifications according to the different applications, namely for the use of microwave-assisted extraction of bioactive compounds from industrial byproducts.

The extraction process, especially when applied to plant-derived components, should take into account the localization of the active compounds in the raw material, at both the cellular and subcellular levels. Many compounds of interest, namely phenolic compounds, are present in the cytoplasm, confined to subcellular membrane-bound organelle containers, the vacuoles, which are also filled with water, or oil glands, which contain essential oils (EOs). Polysaccharides are the components of the cell walls, which include the pectic polysaccharides from middle lamella and primary cell walls, the alkali-extracted polysaccharides usually referred to as hemicelluloses, and cellulose, each group representing one-third of the vascular plant cell wall polysaccharide composition. These polysaccharides are key components and provide rigidity and stability to cell walls [11]. When byproducts are the raw material, however, the well-defined plant structure may have made significant changes owing to the previous processing steps. When applying microwave heating to plant material, the moisture inside the cells heats up and evaporates and exerts pressure on the cell wall, promoting internal superheating and a vapor pressure difference between the interior and surface regions. It is a driving force behind swelling and an eventual bursting of the vacuoles and other organelles [12–15], facilitating the leaching of intracellular material into the surrounding solvent [16]. As a result, the two transport phenomena, mass and heat transfer (volumetric heating), are in the same direction: from the inside to the outside of the plant matrix [12, 13, 17]. The consequent moisture transfer in turn results in the drying of the plant material [18].

In the following sections, special attention is devoted to the application of microwave-assisted extraction from byproducts of EOs, phenolic compounds, and cell wall polysaccharides.

**Tab. 17.1:** Microwave-treated industrial byproducts, principles, conditions of operation, and highlights of extraction.

Byproduct (starting material)	Main compounds of interest (family)	Principle	MW conditions	Highlights on extraction	Ref.
<i>Malus</i>					
Apple pomace	Ursolic acid, oleoanolic acid (triterpenic compounds)	MAE	S:W = 1:20 g/mL; P = 1000 W; $t_{\text{constant}} = 30$ s; m = 1 g; Ext.Cycles: 1–3.	Regardless of the extraction method used, similar HPLC chromatographic profiles were observed. MAE led to the best extraction yield (54%). The use of a water:MeOH (90 : 10) mixture extracted preferentially the most polar solutes. EtOH and EtOAc solvents extracted less-polar compounds. EtOH seems to be a good compromise, solubilizing compounds with a larger polarity range.	[29]
Apple pomace	Polyphenols	MAE	T = 70 °C; S:W = 1 : 10–1 : 30 g/mL; W = 500–700 W ; $t_{\text{constant}} = 40–60$ s; EtOH = 50–70%; m = 5 g.	Compared to other extraction methods, namely SE and UAE, the proposed MAE is more efficient, with higher yields and lower solvent consumption: MAE yields 63 mg GAE/100 g, whereas SE and UAE yield, respectively, 46 mg GAE/100 g and 55 mg GAE/100 g.	[61]
Apple pomace	Pectin (polysaccharides)	MAE	S:W = 1 : 20–1 : 30 g/mL; $t_{\text{constant}} = 10–18$ min; pH = 1.2–1.8; W = 320–580 W; MC = 8%; m = 2 g.	Application of MAE significantly decreases extraction time.	[102]
Apple pomace	Polysaccharides	MAE	S:W = 1 : 2 g/mL; W = 550 W; $t_{\text{constant}} = 2$ min; m = 20 g.	Acid hydrolysis gave 10% soluble dietary fiber, whereas UAE yielded 16% after 40 min. MAE gave a slightly lower yield (15%) than UAE, but using only 2 min of irradiation time; hydrolysis using cellulase resulted in highest soluble dietary fiber recovery (19%).	[103]

Byproduct (starting material)	Main compounds of interest (family)	Principle	MW conditions	Highlights on extraction	Ref.
<i>Citrus</i>					
Lemon peels	Essential oil	(SFME) MHD	$t_{\text{constant}} = 30$ min; $W = 200$ W; $W/m = 1$ W/g; $m = 200$ g (fresh).	The microwaves, as an alternative tool of extraction, offered important advantages: (1) shorter extraction times (30 min vs. 3 h for HD and 1 h for CP); (2) better yields (0.24% vs. 0.21% for HD and 0.05% for CP); (3) reduction in environmental impact as the energy cost is higher for HD (4.33 kWh) and for mechanical motors in CP (1.00 kWh) than that required for rapid MAD extraction (0.25 kWh); (4) ejected CO <sub>2</sub> is higher for performing HD (3464 g) and CP (800 g) than that required for rapid MAD extraction (200 g); (5) cleaner features with no residues generated and no additional water or other solvent used; (6) increases antimicrobial activities; (7) provides a more valuable EO with high amounts of oxygenated compounds; (8) offers the possibility of good reproduction of natural aroma of EO from <i>Citrus</i> .	[30]
Lemon peels	Limonene	(SFME) MHG	$W = 500$ W; $t_{\text{constant}} = 15$ min; $m = 500$ g (fresh).	The energy requirements are respectively 3 kWh for HD and 0.2 kWh for MHG. The ejected CO <sub>2</sub> is higher with HD (2.4 kg) than with MHG (1.60 g). Limonene is the main EO component in all extraction methods. Differences associated with the matrix have been reported.	[17]
Lemon peels	flavonoids (Polyphenols)	MAE	$W = 300$ – $600$ W; $t_{\text{constant}} = 90$ – $240$ s; EtOH = 20–80%; S:W = 1 : 15–1 : 30 (g/mL).	MAE and UAE yielded 15.8 and 15.2 mg GAE/g, respectively. MAE conditions for total phenolic compound extraction were mostly affected by ethanol concentration, extraction power, and liquid–solid ratio. The proposed MAE method allowed higher recovery yield and specific antioxidant activity with a shorter working time and lower solvent consumption compared to UAE or CE. The better MAE results were due to more intense tissue degradation.	[62]

Byproduct (starting material)	Main compounds of interest (family)	Principle	MW conditions	Highlights on extraction	Ref.
Lime fruit flavedo, albedo, and pulp	Pectin	MAE	$t_{\text{constant}} = 1-10$ min; S:W = 1 : 25 g/mL; $m = 1$ g.	Molecular weight (Mw) of pectin extracted from lime flavedo/albedo/pulp decreased from 559 to 13 kDa, when MAE treatment time was increased from 2.5 to 10 min. Molar mass, viscosity, radius of gyration, and hydrated radius were found to decrease with heating time. Pectin molecules became less compact with increasing heating time. Molar mass, intrinsic viscosity, radius of gyration, and hydrated radius all decreased with time of heating during MAE.	[104]
Mandarin peels	Polyphenols	MAE	$T = 50-250$ °C; $t_{\text{constant}} = 1-15$ min; $W = 400-800$ W; S:W = 1 : 2-1 : 4:5 (g/mL).	The antioxidant activity of the extracted compounds is higher. Browning of extract started above 135 °C.	[50]
Mandarin pomace	Polyphenols	MAE	$W = 125-500$ W; $t_{\text{constant}} = 1, 5, 10$ min; MC = 8.4-9.7%; $m = 4$ g.	After MAE, the free phenolic fraction increased, leading to higher antioxidant activity, whereas the bound fractions decreased. This seems to be an efficient process to liberate and activate bound phenolic compounds. Higher power and longer treatment time seems to result in degradation of phenolic compounds.	[55]
Orange and lemon peels	Limonene and pectin	(SFME) MHD	$T = 80$ °C; $t_{\text{constant}} = 1$ h; MC = 85% $m = 20$ kg (fresh).	Pectin and EO were extracted both in a laboratory and at semi-industrial scales. About 0.5 mL/kg <sub>peel</sub> of EO and 0.15 kg/kg <sub>peel</sub> of pectin were recovered.	[31]
Orange peels	Pectin	MAE	$T = 120$ °C; S:W = 1 : 16 g/mL; $t_{\text{constant}} = 5, 10, 15$ min; $m = 2.5$ g.	10% ethanol and 0.05 M aqueous EDTA as extraction solvents in MAE extracted twice as much pectin compared to water. As a surfactant solvent, ethanol significantly reduced the wetting angle by modifying the drainage properties of the plant tissues. Under a yield similar to that of Soxhlet extraction, MAE showed a reduction in operation time from 3 h to 15 min.	[63]

Byproduct (starting material)	Main compounds of interest (family)	Principle	MW conditions	Highlights on extraction	Ref.
Orange peels	Pectin	MAE	$T = 80\text{ }^{\circ}\text{C}$ ; $t_{\text{constant}} = 21\text{ min}$ ; $MC = 15\%$ ; $W = 500\text{ W}$ ; $S:W = 1 : 50\text{ g/mL}$ ; $m = 50\text{ g}$ .	Extraction yield was 15% (60 min) for CE, 18% (21 min) for MAE, and 20% (10 min) for UHP. Intrinsic viscosity and viscosity" = average Mw of pectin extracted by UHP were higher than those extracted by CE, MAE, or commercial pectin. The viscosity of the pectin extracted by UHP was significantly greater than that extracted by MAE and CP, allowing the use of this pectin as texturizer or stabilizer. The shear stress as a function of shear rate indicated that the extraction methods had significant influence on the rheological behavior of pectin. The pectin gel's viscoelastic properties were similar when using UHP and MAE, and better than CP.	[89]
Orange peels	Limonene, polyphenols, and pectin	(SFME) MHG	$W = 200\text{--}700\text{ W}$ ; $t_{\text{constant}} = 25\text{ min}$ ; $MC = 59\%$ ; $m = 400\text{ g (fresh)}$ .	Combination of microwave, ultrasound, and recycled <i>in situ</i> water of citrus peels allowed the sequential recovery of EO, polyphenols, and pectin. Significant changes in EO yield were noticed: 4.22% and 4.16% for MHG and SD, respectively. MHG yielded 0.016 g GAE, whereas CE traction gave 8.25 g GAE. MAE recovered 24.2% of pectin in 3 min, whereas CE gave 18.32% in 120 min.	[34]
Orange peels	Limonene	(SFME) MSD	$W = 200\text{--}700\text{ W}$ ; $t_{\text{constant}} = 6\text{ min}$ ; $\text{Steam}_{\text{flow}} = 2\text{--}18\text{ g/min}$ ; $MC = 75\%$ ; $m = 100\text{ g (fresh)}$ .	MSD offers shorter extraction time (6 min) and cleaner features and provides an EO with better sensory properties. MSD could also be used to produce larger quantities of EOs by using existing large-scale extraction reactors, which are suitable for the extraction of 10, 20, or 100 kg of fresh plant material <i>per batch</i> .	[35]
Orange peels	Limonene	(SFME) MSDf	$W = 200\text{ W}$ ; $t_{\text{constant}} = 12\text{ min}$ ; $\text{Steam}_{\text{flow}} = 25\text{ g/min}$ ; $MC = 90\%$ ; $m = 250\text{ g (fresh)}$ .	The EOs extracted by MSDf in 12 min were quantitatively (yield) and qualitatively (aromatic profile) like those obtained by SDf in 40 min.	[13]

Byproduct (starting material)	Main compounds of interest (family)	Principle	MW conditions	Highlights on extraction	Ref.
<i>Vitis</i>					
Grape pomace	Polyphenols	MAE	<p><math>T = 50\text{ }^{\circ}\text{C}</math>;  <math>W = 200\text{ W}</math>;  <math>S:W = 1 : 50\text{ g/mL}</math>;  <math>t_{\text{constant}} = 60\text{ min}</math>;  <math>\text{EtOH} = 0</math>, and <math>50\%</math>  <math>\text{MC} = 59.5\%</math>;  <math>m = 2\text{ g}</math>.</p>	Under similar extraction yields, SE required a longer extraction time (360 min) than MAE (60 min). UAE extracts were found to be richer in phenolic compounds compared to MAE and SE.	[64]
Grape seeds	Polyphenols	MAE	<p><math>T = 40\text{--}60\text{ }^{\circ}\text{C}</math>;  <math>S:W = 1 : 10\text{--}1 : 50\text{ g/mL}</math>;  <math>\text{EtOH} = 10\text{--}90\%</math>;  <math>W = 100\text{--}200\text{ W}</math>;  <math>t_{\text{constant}} = 2\text{--}32\text{ min}</math>;  <math>T = 50\text{--}100\text{ }^{\circ}\text{C}</math>;  <math>S:W = 1 : 12\text{--}1 : 15\text{ g/mL}</math>;  <math>\text{MeOH} = 50\text{--}80\%</math>;  <math>W = 100\text{--}500\text{ W}</math>;  <math>t_{\text{constant}} = 5\text{--}20\text{ min}</math>;  <math>m = 2\text{ g}</math>.</p>	MAE yield $96\text{ mg GAE/g}_{65}$ , whereas UAE and CE yield respectively $54\text{ mg GAE/g}_{65}$ and $110\text{ mg GAE/g}_{65}$ .	[66]
Grape skins	Anthocyanins	MAE	<p><math>T = 50\text{--}100\text{ }^{\circ}\text{C}</math>;  <math>S:W = 1 : 12\text{--}1 : 15\text{ g/mL}</math>;  <math>\text{MeOH} = 50\text{--}80\%</math>;  <math>W = 100\text{--}500\text{ W}</math>;  <math>t_{\text{constant}} = 5\text{--}20\text{ min}</math>;  <math>m = 2\text{ g}</math>.</p>	MAE reduced the extraction time from 5 h to 5 min. Solvent was the most important variable to anthocyanin recovery. Three new acyl derivatives were extracted.	[58]
Grape peels	Polyphenols	MAE	<p><math>W = 100\text{--}540\text{ W}</math>;  <math>\text{EtOH} = 0\text{--}50\%</math>;  <math>t_{\text{constant}} = 3\text{--}10\text{ min}</math>.</p>	Polyphenols were extracted in 3 min using MAE.	[67]

Byproduct (starting material)	Main compounds of interest (family)	Principle	MW conditions	Highlights on extraction	Ref.
Grape press residues	Anthocyanins	(SFME) MHG	$W = 900 \text{ W}$ ; $W/m = 1 \text{ W/g}$ ; $t_{\text{constant}} = 20 \text{ min}$ ; $m = 400 \text{ g}$ .	MHG improved polyphenol extraction under short extraction time (20 min), low energy input, and no requirement of additional solvents. The organoleptic characteristics of a supplemented juice were considered acceptable, with an attractive color and a higher polyphenol content.	[65]
Vine shoots	Phenolic compounds	MAE	$W = 60\text{--}140 \text{ W}$ ; $S:W = 1 : 20 \text{ g/mL}$ ; EtOH = 20%; $t_{\text{constant}} = 3\text{--}15 \text{ min}$ ; $m = 1 \text{ g}$ .	MAE provided $401 \mu\text{g/mL}$ vs. $650 \mu\text{g/mL}$ obtained by SHLE and 546 with UAE, respectively. Hydroxymethylfurfural levels were reported in very low concentrations in MAE and UAE extracts and higher values in SHLE extracts.	[68]
<i>Rhizomes and roots</i>					
Carrot peels	$\beta$ -carotene	MAE	$S:W = 1 : 37$ ; $1 : 75 \text{ g/mL}$ ; $W = 180, 300 \text{ W}$ ; $m = 2 \text{ g}$ .	The use of intermittent microwave radiation made it possible to extend MAE without causing excessive thermal degradation of carotenoids.	[93]
Potato pulp byproduct	Galactan-rich RG I	MAE	$W = 14\text{--}86 \text{ W}$ ; KOH = 0–2 M; $t_{\text{constant}} = 0\text{--}8 \text{ min}$ ; $S:W = 1 : 25\text{--}1 : 500 \text{ g/mL}$ ; power density: 23–833 W/g; volume = 30 mL.	A compromise between the combined effects of high KOH concentration and solid to liquid ratio, or low power and extraction time were found to be key factors for efficient extraction of galactan-rich RG I with limited debranching. RG-enriched isolates were fractionated into two populations of polysaccharides: high (> 600 kDa) and low (< 600 kDa) Mw. Galactan-rich RG I, which was mainly recovered in the high Mw fraction (78%), exhibited higher solubility and emulsifying stability as compared to potato galactan and oranges HG, showing a Newtonian behavior at 25 and 73 °C, and pseudoplastic behavior at 49 °C.	[105]

Byproduct (starting material)	Main compounds of interest (family)	Principle	MW conditions	Highlights on extraction	Ref.
Sugar beet pulp	Polysaccharides	MAE	<p><math>T = 60\text{ }^{\circ}\text{C}</math>;  <math>t_{\text{constant}} = 3\text{ min}</math>;  <math>W = 1200\text{ W}</math>;  <math>S:W = 1 : 25\text{ g/mL}</math>;  <math>m = 1\text{ g}</math></p>	Using MAE, ASPs, showing moderate-viscosity properties, were extracted at times ranging from 3 to 20 min rather than hours as required by CE.	[91]
Sugar beet pulp	Polysaccharides	MAE	<p><math>T = 60\text{ }^{\circ}\text{C}</math>;  <math>W = 1200\text{ W}</math>;  <math>S:W = 1 : 25\text{ (g/mL)}</math>;  <math>t_{\text{heating}} = 2\text{ min}</math>;  <math>t_{\text{constant}} = 3\text{ min}</math>;  <math>m = 1\text{ g}</math>            Ext.Cycles: 2.</p>	MAE yielded two populations of ASP within Mw ranges of 532–1200 kDa and 83–299 kDa, both showing promising results as emulsifying agents.	[92]
Sugar beet pulp	Polysaccharides	MAE	<p><math>T = 60\text{ }^{\circ}\text{C}</math>;  <math>W = 1200\text{ W}</math>;  <math>S:W = 1 : 25\text{ g/mL}</math>;  <math>t_{\text{heating}} = 2\text{ min}</math>;  <math>t_{\text{constant}} = 3\text{ min}</math>;  <math>m = 1\text{ g}</math>            Ext.Cycles: 2.</p>	The residue remaining after removal of pectin and ASP is a rich source of carboxymethyl cellulose.	[90]
Yellow onion byproducts	Flavonoids	vMHG	<p><math>W/m = 1\text{ W/g}</math>;  <math>W = 100\text{--}900\text{ W}</math>  <math>t_{\text{heating}} = 2\text{ min}</math>;  <math>t_{\text{constant}} = 3\text{ min}</math>;  <math>m = 1\text{ g}</math>;            Ext.Cycles: 2.</p>	Vacuum MHG allowed the extraction of flavonols at lower temperature (81 °C) in 26 min, in the absence of additional solvent. Reduction of pressure up to 0.7 bar during MAE treatments allowed a 57% increase in total quercetin content and an increase in the antioxidant activity of onion extracts.	[15]



Byproduct (starting material)	Main compounds of interest (family)	Principle	MW conditions	Highlights on extraction	Ref.
Ginger fruit rhizomes and press cake	Essential oil rich in zingiberene	(SFME) MHG	Laboratory scale: MC = GR (10.7%) and GP (25.4%); $W/m = 0.6 - 1.8 \text{ W/g}$ ; $m = 500 \text{ g}$ (fresh). Pilot scale: $t_{\text{constant}} = 25 \text{ min}$ ; $m = 4 \text{ kg}$ (fresh).	A so-called dry bio-refinery concept was introduced using sequential procedures: pressing, followed by MHG, and UAE, for valorization of ginger byproducts by recovery of juice, EO, and phenolics, leaving a final solid residue rich in fibers and phenolic acids, without any additional water. Microwave power had no effect on EO extraction yields as $0.2 \text{ g EO}/100 \text{ g GP}$ was always recovered. The aromatic profiles of the EO were similar for MHG extraction conditions, except for $0.6 \text{ W g}^{-1}$ and $1.8 \text{ W g}^{-1}$ experiments, respectively subjected to a longer extraction time (90 min) and intense MW irradiation ( $1.8 \text{ W g}^{-1}$ ), which could induce degradation. Compared to HD and ethanol extraction, MHG and UAE enabled a time reduction from 540 min to 110 min and energy consumption reduction.	[40]
<b>Cereals</b>					
Hull-less barley bran	$\beta$ -glucan	MAE	S:W = 1 : 15 (g/mL); $W = 800 \text{ W}$ ; $t_{\text{constant}} = 2 \text{ min}$ ; $m = 10 \text{ g}$ ; Ext. Cycles: 1–4.	The use of ASE produced higher $\beta$ -glucans under environmentally friendly extraction conditions and shorter extraction times, yielding 16.39% of total extractable material.	[85]
Barley brewers' spent grain	Arabinoxylans	MAE	$T = 140 - 210 \text{ }^\circ\text{C}$ ; $m = 10 \text{ g}$ ; S:W = 1 : 6 (g/mL); $t_{\text{constant}} = 2 \text{ min}$ ; Ext. Cycles: 1–2.	The AX + AXOS yield increased with increases of temperature in a range of 140 to 210 °C for 2 min. Higher temperatures promoted depolymerization, debranching, and deesterification of the polysaccharides, with the formation of brown products. Using this sequential procedure, it was possible to extract 62% of BSG AX + AXOS, presenting degrees of polymerization ranging between 7 and 24 xylose residues, with a degree of phenolic acid esterification between 5 and 21%.	[78]

Byproduct (starting material)	Main compounds of interest (family)	Principle	MW conditions	Highlights on extraction	Ref.
Corn pericarp	Arabinoxylans	MAE	T = 140–220 °C; S:W = 1 : 10– 1 : 30 g/mL; $t_{\text{heating}} = 2–4$ min; $t_{\text{constant}} = 1–26$ min; $m = 0.5–1$ g.	MAE solubilization rate increased with increases in heating temperature, reaching 75.2% at 220 °C with predominant production of xylooligosaccharides.	[106]
Corn cob	Xylooligosaccharides	MAE	T = 130, 140, 150 °C; W = 400 W; S:W = 1 : 20 (g/mL); $t_{\text{constant}} = 0–40$ min; $m = 1$ g.	A maximum yield of 86% of xylose was achieved using a ball milling pretreatment for 60 min with 15 mM oxalic acid, followed by hydrothermal treatment at 130 °C for 30 min.	[107]
Corn fiber	Arabinoxylans and glucuronoxylans	MAE	T = 100–210 °C; $t_{\text{heating}} = 2$ min; $t_{\text{constant}} = 5$ min; $m = 10$ g.	Increasing yield in hemicelluloses recovery using MAE is achievable with increased temperatures at the cost of a lower Mw. About 30% of xylans were recovered at 210 °C, where the Mw was about half that measured at 160 °C ( $1.37 \times 10^5$ ). Addition of sodium hydroxide in the treatment led to higher yields (11%) with longer polysaccharide chains ( $1.3 \times 10^5$ ).	[75]
Okara	Arabinogalactans and isoflavones	MAE	T = 60–230 °C; S:W = 1 : 10– 1 : 40 g/mL; $t_{\text{heating}} = 2$ min; $t_{\text{constant}} = 5$ min.	Solubilization rate increased with temperature reaching higher than 70% at 200 °C and a heating time of 7 min. Formation of new polyphenolic compounds, with higher antioxidant activity, was observed above 180 °C.	[51]
Soybean waste	Isoflavones	MAE	T = 75 °C; W = 0–375 W; S:W = 1 : 5–1 : 25 (g/mL); EtOH = 80%; $t_{\text{constant}} = 1–5$ min; Ext.Cycles: 1–4.	MAE achieved yields (0.46%) comparable to CE (0.45%) without causing any degradation and with reduction in extraction time from 3 h to 3 min, while Soxhlet yielded a lower content (0.23%). Isoflavone content had the same yield for both MAE and CE processes (14.56 µg/g). More than 82% of the total isoflavone content was recovered by the first extraction cycle.	[69]

Byproduct (starting material)	Main compounds of interest (family)	Principle	MW conditions	Highlights on extraction	Ref.
<i>Seeds</i>					
Spent coffee grounds	Mannans	MAE	<p><math>T = 200\text{ }^{\circ}\text{C}</math>;</p> <p><math>t_{\text{heating}} = 3\text{ min}</math>;</p> <p><math>t_{\text{constant}} = 2\text{ min}</math>;</p> <p><math>m = 2.6\text{ g}</math>;</p> <p>S:W = 1 : 30 (g/mL);</p> <p>Ext. Cycles: 1–5.</p>	<p>A sequential microwave-assisted extraction (MAEn) showed an effective recovery of arabinogalactans by MAE1 and galactomannans in MAE2 and MAE3. With MAE3, mannose recovery reached 48%, increasing to 56% by MAE4, and reaching a maximum of 69% with MAE5. By increasing the number of extractions, the average degree of polymerization of the mannans decreased, and after the final MAE5, the remaining unextracted insoluble material, representing 22% of the initial spent coffee grounds, was composed mainly of cellulose (84%).</p>	[77]
Spent coffee grounds	Arabinogalactans and galactomannans	MAE	<p><math>T = 200\text{ }^{\circ}\text{C}</math>;</p> <p><math>t_{\text{heating}} = 3\text{ min}</math>;</p> <p><math>t_{\text{constant}} = 2\text{ min}</math>;</p> <p>S:W = 1 : 5–1 : 30 (g/mL);</p> <p>Ext. Cycles: 1–2.</p>	<p>A maximum of 0.57 g of polysaccharides were recovered using a 1 : 10 solid–water ratio in a batch process. All extraction conditions allowed recovery of arabinogalactans. A re-extraction of the insoluble material (MAE2) allowed a further extraction of polysaccharides (0.34 g/batch for 1 : 10), mainly galactomannans. A high amount of oligosaccharides, mainly derived from galactomannans, was obtained in MAE2 (0.96 g/batch for 1 : 10).</p>	[76]
Spent coffee grounds	Polysaccharides and chlorogenic acids	MAE	<p><math>T = 170\text{--}200\text{ }^{\circ}\text{C}</math>;</p> <p><math>t_{\text{heating}} = 5\text{ min}</math>;</p> <p><math>t_{\text{constant}} = 2\text{ min}</math>;</p> <p><math>m = 1\text{ g}</math>;</p> <p>S:W = 1 : 10 (g/mL);</p> <p>multiple reactors.</p> <p>Ext. Cycles: 1–2.</p>	<p>Application of two cycles of extraction allowed the recovery of water-soluble extracts rich in polysaccharides as sources of dietary fiber with antioxidant properties. When added to biscuit dough it increased the biscuits' antioxidant activity from 30 to 47%, with the biscuits' antioxidant activity remaining constant by a period of 55 days when using at least 2% of supplement.</p>	[70]

Byproduct (starting material)	Main compounds of interest (family)	Principle	MW conditions	Highlights on extraction	Ref.
<i>Shrub or bush</i>					
Rosemary residues	Antioxidants	SFME		Mass transfer rates of antioxidants from leaves increased as a result of previous extraction of EOs using SFME.	[86]
Sea buckthorn pomace	Flavonoids	MHG	$W/m = 1 \text{ W/g}$ ; $W = 300\text{--}900 \text{ W}$ ; $t_{\text{constant}} = 15 \text{ min}$ ; $T = 30\text{--}70 \text{ }^\circ\text{C}$	MHG extract has shown much higher phenolic content (114.7 mg GAE/g) vs. CE extract (74.1 mg GAE/g), with greater antioxidant activity determined by DPPH assay.	[47]
Yellow horn defatted kernels	Saponins	MAE	$W = 300\text{--}900 \text{ W}$ ; $S:W = 1 : 20\text{--}1 : 40 \text{ g/mL}$ ; $\text{EtOH} = 10\text{--}90\%$ ; $t_{\text{constant}} = 3\text{--}11 \text{ min}$ ; $m = 1 \text{ g}$ ; Ext.Cycles: 1–4.	Compared with the CE methods, UAE, and HRE, MAE showed higher efficiency for the extraction of triterpene saponins (11.62%).	[108]
<i>Wood</i>					
Marine pine bark lignocellulosic waste	$\alpha$ -Terpineol	(SFME) MSD	$W = 200\text{--}700 \text{ W}$ ; $t_{\text{constant}} = 300 \text{ min}$ ; $m = 100 \text{ g}$ .	A maximum extraction yield of 3.48% (g/100 g dry bark) was achieved under optimal extraction time of 92 min and an irradiation power of 804 W compared to 2.2% obtained for the conventional method (HD). SFME extract is richer in oxygenated compounds (40%) compared to HD (26%).	[109]
<i>Eucalyptus globulus</i> wood veneer trimmings	Phenolics	MAE	$T = 50\text{--}70 \text{ }^\circ\text{C}$ ; $W = 150 \text{ W}$ ; $t_{\text{constant}} = 5\text{--}15 \text{ min}$ ; $S:W = 1 : 5\text{--}1 : 10 \text{ g/mL}$ .	MAE yield increased with increasing temperature and reduced particle size; however, extract antioxidant properties decreased when temperature increased. MAE allowed a significant reduction on extraction time, although maceration led to best antioxidant properties.	[57]

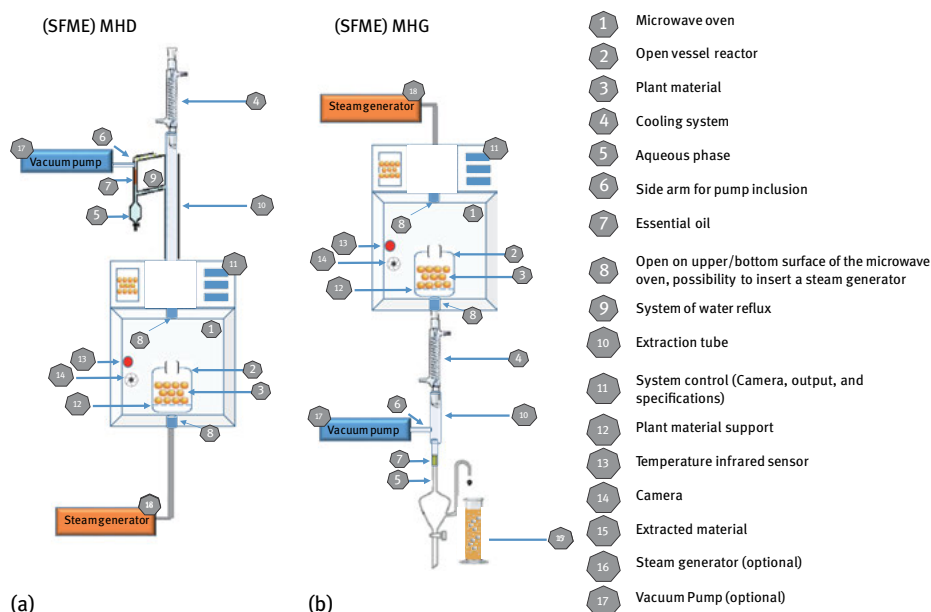
Byproduct (starting material)	Main compounds of interest (family)	Principle	MW conditions	Highlights on extraction	Ref.
Tree bark	Polyphenols	MAE	$T = 60\text{--}120\text{ }^{\circ}\text{C}$ ; $S:W = 1 : 10\text{ g/mL}$ ; $t_{\text{constant}} = 10, 20\text{ min}$ ; $m = 0.15\text{ g}$ .	Microwave treatment ensured inactivation of polyphenol-oxidizing enzymes. Ethanol-containing solutions are more efficient for extraction than the respective mixtures with methanol, but under pressurized high-temperature conditions, pure water can be as effective as alcohol-containing mixtures.	[59]
<i>Other</i>					
Berry fruit press residues	Pectin	MAE	$W = 550\text{ W}$ ; $W/m = 15\text{ W/g}$ ; $S:W = 1 : 10\text{ g/mL}$ ; $t_{\text{total}} = 30\text{ min}$ .	The rheological behavior of pectins extracted using MAE are weaker than commercial citrus pectin but stronger than that of commercial apple pectin. Red currant pectin was found to possess outstanding values regarding gel-forming capacity and thickening effect.	[110]
Tea residues	Polysaccharides, polyphenols, caffeine, and cutin	MAE	$T = 110\text{--}230\text{ }^{\circ}\text{C}$ ; $t_{\text{heating}} = 2\text{ min}$ ; $t_{\text{constant}} = 2\text{ min}$ ; $S:W = 1 : 20\text{ g/mL}$ ; $m = 1\text{ g}$ .	Heating at $200\text{--}230\text{ }^{\circ}\text{C}$ for 2 min extracted 40–50% of polysaccharides and 60–70% of polyphenols. Solubilization of arabinose and galactose by autohydrolysis occurred with heating above $170\text{ }^{\circ}\text{C}$ , whereas heating above $200\text{ }^{\circ}\text{C}$ was necessary to solubilize xylose. New polyphenols having strong antioxidant activity were produced above $200\text{ }^{\circ}\text{C}$ . Cutin remained in the residue after heating, as did cellulose and lignin/tannin. The predominant cutin monomer that was recovered was 9,10-epoxy-18-hydroxyoctadecanoic acid, followed by dihydroxyhexadecanoic acid and 9,10,18-trihydroxyoctadecanoic acid.	[52]
Low-grade tobacco leaves and powders	CGA (phenolics)		$S:W = 1 : 9\text{ g/mL}$ ; $W = 900\text{ W}$ ; $t_{\text{constant}} = 90\text{ s}$ ; acetone: 30%; $m = 10\text{ g}$ Ext. Cycles: 1–2.	MAE yield $4.9\text{ mg/mL}$ (90 s), whereas CE with ethanol $3.4\text{ mg/mL}$ ( $2\text{ h}$ , $78\text{ }^{\circ}\text{C}$ ); UAE yield $4.42\text{ mg GAE}$ (15 min).	[60]

Byproduct (starting material)	Main compounds of interest (family)	Principle	MW conditions	Highlights on extraction	Ref.
<i>Agaricus bisporus</i> L.	Ergosterol	MAE	$T = 60\text{--}210\text{ }^{\circ}\text{C}$ ; $t_{\text{constant}} = 3\text{--}20\text{ min}$ ; $S:W = 1:2\text{--}4:20\text{ g/L}$ ; $\text{EtOH} = 100\%$	Ergosterol yield (MAE: 556.1 mg/100 g) was like those obtained in other works when using Soxhlet extraction (SE: 352 mg/100 g) and other emerging techniques (UAE: 671.5 mg/100 g; and SFE: 550 mg/100 g), but with a significant decrease in the time of extraction and while avoiding the saponification step, which decreases the process complexity.	[97]
Olive kernel (OK)	Oleuropein, hydroxytyrosol, and rutin	MAE	$T = 40, 60\text{ }^{\circ}\text{C}$ ; $t_{\text{constant}} = 5, 10\text{ min}$ ; $W = 400\text{ W}$ ; MC (OK) = 45%; (OL) = 49%.	Similar results in total phenolic compounds (measured as GAE) and AOA (measured in Trolox equivalent) were obtained when using MAE, MAEE, and CE as extraction methodologies applied to olive kernel at 60 °C. However, time was reduced from 1 h for CE, to 30 min in MAE and MAEE. More significant differences were observed for olive leaves, with higher yields than olive kernel in all cases.	[111]
<p><b>Main compounds of interest:</b> Essential oil (EO); alkaline-soluble polysaccharide (ASP); arabinogalactans (AG); galactomannans (GM); arabinoxylyans (AX); arabinoxylooligosaccharides (AXOS); arabinoglucuronoxylans (AGX); Chlorogenic acid (CGA).</p> <p><b>Principles:</b> Heat reflux extraction (HRE); microwave-assisted extraction (MAE); solvent-free microwave extraction (SFME); microwave-accelerated distillation (MAD); hydrodistillation (HD); microwave hydrodistillation (MHD); microwave hydrodiffusion and gravity (MHG); steam diffusion (SD); microwave steam diffusion (MSD); steam distillation (SD); microwave steam distillation (MSD); microwave-assisted enzymatic extraction (MAEE); ultrasound-assisted extraction (UAE); superheated liquid extraction (SHLE); ultrahigh pressure (UHP); conventional extraction (CE); Soxhlet extraction (SE); cold pressing (CP); accelerated solvent extraction (ASE).</p> <p><b>MW conditions:</b> Solid: water ratio (S:W); temperature (T); heating period (<math>t_{\text{heating}}</math>); constant temperature period (<math>t_{\text{constant}}</math>).</p> <p><b>Highlights:</b> Gallic acid equivalent (GAE); molecular weight (Mw).</p>					

### 17.3.1 Essential oils

EOs have been reported as sources of compounds with antioxidant, anti-inflammatory, antimicrobial, antiviral, and antitumoral activities [19], which give them pharmaceutical and therapeutic potential against cancer, cardiovascular diseases, diabetes, and skin penetration enhancers for transdermal drug delivery [20]. Many applications for the microwave technology demonstrated up till now have been devoted to the extraction of EOs from raw plant material itself; examples include rosemary plant [12, 21, 22]; lavender, oregano, basil, thyme, sage cardamom, or mint spices [22–26]; and boldo [27] and laurel leaves [28]. But, using the same approach, applications to byproduct recovery are also emerging, mainly associated with fruit juice processing byproducts, including apple pomace [29], lemon peel [17, 30, 31], and orange peel [13, 31–33], with a focus on the recovery of the main active compounds such as limonene [13, 31, 34, 35] and triterpenic compounds [29] or EOs in general [17, 30]. Some of these compounds, namely limonene and  $\alpha$ -pinene (from pine, other trees, or even orange peel), have been applied as solvent media for microwave-assisted extraction of fat and oils [9, 36, 37], chosen based on their characteristics of being so-called green solvents, namely they are biodegradable, nontoxic, and nonflammable while having a high solvent power for this class of compounds [9].

The methodology most commonly used by companies for EO recovery is hydrodistillation, which is based on producing a water steam that carries away the aroma compounds present in the vapor phase, which are then condensed and separated. This is the principle of alembics, a process only affordable for EO extraction owing to their high commercial value. Alternatively, the lower costs associated with microwave hydrodistillation (MHD) seem to enhance its applicability in the recovery of byproduct volatile compounds, which are the active constituents of EOs [9, 12, 25, 27, 38]. For EO recovery, solvent-free microwave extraction may also have great advantages because it does not require the addition of solvent or water but rather uses *in situ* water instead [23, 39]. As the separation of EOs from water is due to their insolubility and density differences, the loss of volatile compounds promoted by solvent removal is avoided when the amount of water is minimal. This approach also represents a significant reduction in water consumption and wastewater produced, hence leading to a reduction in energy consumption [13, 17]. Solvent-free microwave extraction of EOs can be based on two principles: hydrodistillation or hydrodiffusion. Microwave hydrodiffusion is usually associated with gravity, which allows the diffusion of EOs from a matrix and their simultaneous separation by dropping in a receiving flask using gravity. This process is called microwave hydrodiffusion and gravity (MHG) [39]. Figure 17.2 shows schematic diagrams of both hydrodistillation-based (Figure 17.2a) and hydrodiffusion-based (Figure 17.2b) microwave approaches. Both processes have been applied to byproducts of EO extraction, namely from dried caraway (*Carum carvi*) seeds [14, 17] or citrus peels [17, 30, 31, 34, 35, 40]. The attachment of a vacuum pump to a microwave station has been described as an efficient alteration for the recovery of



**Fig. 17.2:** Schematic diagram of solvent-free microwave extraction (SFME) of EOs based on (a) hydrodistillation (MHD) and (b) hydrodiffusion (MHG) mechanisms (based on Refs. [13, 15, 23, 35, 39, 41, 45–47])

oxygen- and heat-sensitive compounds [41]. This principle has been applied also to EO extraction applications using vacuum microwave hydrodistillation (vMHD) [42, 43], although vacuum microwave hydrodiffusion and gravity (vMHG) could also use this approach. Microwave extraction of heat-sensitive compounds may also use microwave steam distillation (MSD) or microwave steam diffusion (MSD<sub>f</sub>). In these cases, the saturated steam is produced by an electrical steam generator, which passes through the matrix bed, while the mixture is continuously heated in the microwave cavity [13, 35, 44].

To exemplify the main advantage of using microwave technology, namely the reduction in extraction time, comparative studies for the extraction of EOs from *Citrus* peels showed a timeline of 30 min for the extraction of 0.24% of EO from 200 g lemon peels applying MHD [30], 15 min for the extraction of 1% of EO from 500 g lemon peels using MHG [17], or 12 min for the extraction of 1.54% of EO from 250 g orange peels by MSD [13] versus 3 h for conventional hydrodistillation (HD) [30], 1 h for mechanical pressing (CP) [30], and 40 min for steam distillation (SD) [13]. Similar yields were obtained when comparing HD-based processes for extracting EO from lemon peel, obtaining respectively 0.24 and 0.21% [30] and 5.43% and 5.45% [35] by MHD and HD. The same occurred when comparing hydrodiffusion-based processes, with 1.54% and 1.51% respectively, for MSD<sub>f</sub> and steam diffusion (SD<sub>f</sub>) [13]. Also, when comparing dif-



ferent mechanistic processes, 1.0% and 1.1% for MHG and HD [17], or 4.2% and 4.6% for MHG and SD, respectively, were obtained [34]. The resulting profiles have been described as being similar when comparing MHD and MHG approaches, as when the bioactive compound of interest in the EO is limonene, obtaining 70.9%, 71.2%, and 71.9% respectively for MHG, HD, and CP [17]. However, there has been a general tendency toward a higher content of oxygenated compounds in MHD and MHG in comparison with HD [17, 30]. Differences associated with the matrix have also been reported, exemplified in the different tendencies reported among *Citrus* species [17]. The main difficulty is still to compare results among different studies, as industrial processing has a high impact on byproduct characteristics. For example, moisture-content differences from 59 up to 90% have been described for orange peel [13, 31, 34, 35]. In addition, without a control process, byproducts may present a wide range of distinct characteristics as so-called fresh material, making it very difficult to compare, control, and normalize results. The environmental impact is higher when applying HD or mechanical pressing considering the energy cost (4.33 kWh and 1.00 kWh, respectively) and the ejected CO<sub>2</sub> (3464 g and 800 g, respectively) [17] compared to MHD (energy cost: 0.25 kWh, ejected CO<sub>2</sub>: 200 g) [30] or MHG (energy cost: 0.2 kWh, ejected CO<sub>2</sub>: 160 g).

### 17.3.2 Phenolics

Thanks to its widespread availability, hydrophilic behavior, and ease of application, microwave-assisted extraction also has a high applicability for the extraction of phenolic compounds. Fruits and vegetables are good raw materials for the extraction of phenolic compounds using microwave technology due to their high dielectric properties, promoted by the presence of water and salts [22, 48]. The fast heating rates of microwave treatments can lead to a fast inactivation of polyphenol oxidase, an enzyme responsible for phenolic compound oxidation and browning of products, which is associated with the loss of quality [49], making this feature an additional advantage of microwaves [48]. On the other hand, the high temperatures resulting from microwave treatments may promote other types of browning reactions, nonenzymatic, usually known as Maillard reaction. This occurs when, to increase the efficiency of an extraction, closed vessels are irradiated to obtain higher temperatures than those allowed by the boiling points of the solvents of extraction at atmospheric pressure. This was the case of polyphenols extracted from mandarin orange peels at temperatures above 135 °C [50]. The generation of new polyphenols at temperatures above 180 °C, resulting from a temperature-dependent decrease in the amount of extracted compounds, has also been reported [51, 52].

Plant phenolic compounds, which include phenolic acids, flavonoids, stilbenes, and tannins, have been associated with the improvement of human health, promoting healthy aging and quality of life [53], mainly due to their antioxidant activity, which is

a structure-related property [54]. Phenolic compounds can occur in plant cells in free form, ester-bound to other compounds, namely to polysaccharides, or glycosidically bound to mono- or oligosaccharides. The free forms have higher antioxidant activity than the bound forms, as observed for phenolics extracted from mandarin pomace, resulting in a significant increase of the antioxidant activity of the extracts [55]. Because bioactive compounds may be heat sensitive, the high yield of extraction does not ensure a high yield of the bioactive compounds in the extract [16]. Vacuum microwave-assisted extractions (vMAE, vMHD, or vMHG) have been applied for the extraction of heat-sensitive coloring nutrients and antioxidants [15, 39, 41, 56].

Owing to the great diversity of phenolic compounds, operational conditions must be chosen in accordance with the chemical composition of the active compounds to be extracted, including the choice of solvent. The use of hot-pressurized water is a common approach to phenolic microwave-assisted extraction [50–52, 55, 57]. For the extraction of lower polar compounds it is also common to combine water with less-polar solvents like methanol [29, 58, 59], ethyl acetate [29], acetone [60], or ethanol [29, 61–64]. To maintain a so-called green solvent label, ethanol is the best choice for most phenolic compounds [9]. Nevertheless, in some cases, the solvent can be the plant's in situ water, with no addition of external solvents, as discussed for EO extraction using MHD [57] and MGH [65].

Microwave-assisted extractions (MAEs) of phenolic compounds from byproducts are often compared to ultrasound extraction [29, 34, 55, 61, 62, 64, 66–68] as both represent innovative green technology approaches. Depending on the matrix and the conditions used, better results can be achieved by one or the other, where most of the times both give higher yields than conventional methods. For example, an improvement of up to 26% in yield, measured in gallic acid equivalents (GAE), was obtained by the application of MAE (62% ethanol) (62.68 mg GAE/100 g, dry weight (dw)) compared to reflux (46.33 mg GAE/100 g, dw) and ultrasound-assisted extraction (UAE) (54.76 mg GAE/100 g, dw) of phenolic compounds from apple pomace [61]. Similar yields were obtained for extraction from lemon peels (48% ethanol) respectively for MAE (15.78 mg GAE/g, dw) and UAE (15.22 mg GAE/g, dw) [62]. Under the application of MHG, sea buckthorn pomace yielded a higher value for MAE (1147 mg GAE/g, dw) compared to conventional extraction (741 mg GAE/g, dw) [47]. Grape press residues yielded 21.41 mg GAE/g by MAE [65], while grape pomace yielded about ten times more using MAE [64]. For the extraction of soybean waste phenolics in general, and isoflavones in particular, MAE yielded (146 mg/100 g) approximately the same as conventional reflux but in less time: only 3 min versus 3 h [69]. With the application of sequential microwave-assisted extractions (MAEn), which is the repetition of extraction using unextracted material in several cycles of extraction, for soybean byproducts, although more than 82% of isoflavone content was obtained with MAE1, using three extra cycles it was possible to extract all isoflavones [69]. This strategy of MAE repeating cycles was also used for the extraction of chlorogenic acids from spent coffee grounds, making it possible to obtain a yield of 5.2% in MAE1 and an additional 1.9% in MAE2 [70].

Although food products containing phenolics from byproducts using MAE are not yet available on the market, experiments have been successfully carried out, for example, on the use of antioxidant-rich extracts obtained from spent coffee grounds by MAE for incorporation in biscuit dough, increasing biscuit shelf life [70].

### 17.3.3 Polysaccharides

Plant polysaccharides have long been reported to present immunostimulatory, anticoagulating, and anticomplement activities [71]. However, only recently have systematic studies demonstrating the structure–function relationships of reported polysaccharide bioactivities become available to support those reports. An example is polysaccharide immunostimulatory activity [72].

When considering polysaccharide extraction from plant biomass, extreme conditions are usually required. Hot compressed water is one of the most environmentally friendly physicochemical substances with an ability to decompose and fractionate plant cell wall biomass [73, 74]. The production of hot compressed water at a fast heating rate can be achieved using microwaves. This has proved a feasible tool for extracting polysaccharides from various plant byproducts using only water as solvent, namely from tea [50] and okara [51], and diluting alkali conditions to extract corn fiber polysaccharides [75]. The use of diluted acids under microwave extraction conditions has been proposed for converting amylose into oligosaccharides [79] and free sugars, namely glucose, arabinose, and galactose, from carbohydrate-rich biomass residues, that is, sugar beet molasses, whey powder, wine yeast, potato peel sludge, spent hops, malt dust, and apple marc [80], galactose and mannose from galactomannan-rich seed gums [81], and glucose, mannose, and fructose from palm kernel cake [82]. In most cases, temperature (and pressure), time, and solid:water ratio are the operational parameters that require tight control.

Most byproducts that have been microwave treated are related to plant materials for the extraction of pectic polysaccharides and hemicelluloses, namely galactans,  $\beta$ -glucan, arabinoxylans, arabinogalactans, and galactomannans (Table 17.1). However, such a variety of structures makes it difficult to evaluate and compare the ease with which these different polysaccharides can be extracted from different matrices using MAE. Most publications only discuss the yield of material recovered, which is not relevant when considering that polysaccharides with different structural features, presenting different properties, may be extracted under different conditions. Under a constant operational time, increasing temperature leads to higher yields, but at the expense of the molecular weight of the isolated polysaccharides. This has been shown by scanning electron microscopy of plant cell walls from different byproducts, namely orange [32] and potato peels [83], soybean [51], and spent coffee grounds [77]. This phenomenon has been described as autohydrolysis [51, 75, 84]. The conditions in which polysaccharide degradation leads to oligosaccharides, or even to monosaccharides,

are dependent on the initial matrix composition. For example, acetylated polysaccharides, under the heat treatment conditions usually used, can release acetic acid, which is able to decrease the solution pH and accelerate the hydrolysis phenomenon [75, 76]. Because glycosidic linkages are stable in alkali medium, the use of diluted alkali MAE conditions allows the extraction of polysaccharides with a higher molecular weight, although with lower yields [75] due to the higher entrapment of the polymerized structures within the matrix. To extract different polysaccharide structures or when different polysaccharide types are present, it is also important to apply repeating consecutive cycles of MAE, as described in detail in the previous section for phenolic extraction. This sequential procedure was used to recover arabinogalactans, galactomannans, and mannan-oligosaccharides from spent coffee grounds [70, 76, 77]; arabinoxylans and arabinoxyloligosaccharides from brewers' spent grains [78], and  $\beta$ -glucan from dehulled barley bran [85]. This also allows the coextraction of different active compounds, namely phenolic compounds, both free and glycosidic-bound to polysaccharides. Examples of application have been found in the coextraction of free chlorogenic acids from spent coffee grounds [70] and in the coextraction of esterified ferulic and coumaric acids bounded to the arabinofuranosyl residues in brewers' spent grains [78]. The approach using repeating cycles of extraction has also been used as an integrated process for the extraction of different compounds, starting with EOs, followed by a second extraction of phenolic compounds from apple pomace [29], EOs from citrus peels, followed by pectin [31] and EOs from citrus peels, phenolic compounds, and pectin [34]. In addition, a previous microwave extraction of EOs increases the subsequent phenolic compound mass transfer rates [86].

In pectic polysaccharides, various fragments of linear and ramified regions can be covalently interlinked in three to four elements, namely homogalacturonan, rhamnogalacturonan-I, rhamnogalacturonan-II, and xylogalacturonan [87]. These pectic polysaccharides' different structural features give them different physical and biological properties [88]. The homogalacturonan, also known as pectin, is a linear region consisting of units of ( $\alpha$  1 $\rightarrow$ 4)-D-GalpA residues that can carry methyl ester groups and can be acetylated at the galacturonan backbone [72]. The ratio between pectin methylation and acetylation patterns determines the gelling properties and the final application: a high degree of methylation increases the capacity to form gels, whereas a high degree of acetylation inhibits gelling, conferring viscosity to the solutions. The pectin extracted from orange peels using MAE was shown to possess a lower intrinsic viscosity and viscosity-average molecular weight than conventional heating-extracted pectin, but better viscoelastic properties [89]. In contrast, pectin extracted from sugar beet, owing to its high degree of acetylation and high neutral-sugar content, does not gel under a high sugar and acid conditions. However, its extraction using MAE [90–92], due to the promotion of hydrolysis of acetyl groups, provides products with low- to moderate-viscosity behavior. Furthermore, this process occurs in a few minutes rather than hours, as reported for the conventional process.

### 17.3.4 Other MAE applications

Beyond the extraction of EOs, phenolic compounds, and cell wall polysaccharides, other valuable compounds could be extracted from industrial byproducts by application of microwaves. Some examples already applied include the extraction of pigments like carotenoids (focus on lycopene) from carrot peels [93] or tomato byproducts [94]. Carotenoids, as well as chlorophylls, and fucoxanthins have also been extracted using MAE from macro- [95] and microalgae [95, 96]. The extraction of valuable compounds from byproducts using MAE also includes the extraction of alkaloids from tea residues [52] and phytosterols (focusing on ergosterol) from the industrial processing byproducts of mushrooms [97]. Edible oil extraction from rice bran using ethanol as solvent [98] and protein from brewers' spent grains under alkali conditions [78] has also been proposed.

## 17.4 From laboratory to pilot – perspectives on the industrial scale

Although a large number of examples of microwave extraction of bioactive compounds are available on the laboratory scale, only a few studies cover the pilot scale. Continuous-flow processing [99, 100] or multimode reactors with a perforated drum (easy transfer of vapor and liquid phases) [22, 27, 40, 101] are the best approaches to scaling up the process. The extraction of EOs from aromatic herbs [22] and boldo leaves [27] has been proposed using a 75 L batch reactor under solvent-free microwave hydrodistillation (SFME-MHD) with highly reproducible results. The sequential extraction of EOs and pectin from lemon peels has also been proposed at the pilot scale using a single-step microwave hydrodiffusion-based process [31]. The pilot scale showed also a greater efficiency in energy use and was less time consuming, which reflects a more sustainable process [40]. The largest microwave extraction plant for the extraction of natural compounds (lipids, alkaloids, terpenes, proteins, phenolics, and glycosides) from plants [101] based on a microwave patented technology [37] opened in 2014, working with a peak processing capacity of 200 kg biomass/h [101], showing that the industrial application of the microwave extraction technology is already a reality.

## 17.5 Conclusion

This chapter showed that microwave technology can be a useful tool in converting valuable byproducts into profitable products by extracting bioactive compounds. This should usually occur in a short window of opportunity because this type of biore-source tends to deteriorate. Microwave-assisted extraction is a highly thermally effi-

cient alternative to conventional established extraction methods: (1) by lowering the total extraction time, ensuring lower energy consumption; (2) reducing the amount of solvent consumption, resulting also in a reduction in the energy used for sample concentration or drying. Furthermore, the absence of toxic solvents in most microwave-assisted extraction processes leads also to a reduction in environmental impacts, with minor waste production and low CO<sub>2</sub> emissions, while at the same time maintaining the quality of the bioactive compounds extracted.

The microwave operational conditions and the applicability of any extraction method are dependent on the characteristics of the matrix and the type of biomolecules to be extracted. The extraction of aroma-rich EOs from byproducts has shown good potential for application, especially when applying solvent-free-based microwave processes, where solvent consumption is significantly decreased compared to conventional methods. The extraction of microwave phenolic compounds, which exhibit antioxidant activities, is better achieved when using aqueous solvent combinations, such as water-ethanol, ensuring green processes of extraction. Hot-water-pressurized systems using microwaves can efficiently extract cell wall polysaccharides, which possess bioactive properties, and the main components of plant-derived industrial byproducts. All combined, the application of microwave technology represents a green technology with high potential to be applied to industrial byproducts, making it possible to obtain products with high yield and, above all, high quality. The extraction of bioactive plant compounds on an industrial scale using microwave technology makes it possible to forecast further increases in byproducts' value.

**Acknowledgment:** Thanks are due to Fundação para a Ciência e a Tecnologia (FCT, Portugal), European Union, QREN, FEDER and COMPETE for funding the QOPNA research unit (project PEst-C/UI0062/2013; FCOMP-01-0124-FEDER-037296). Cláudia Passos was supported by a post-doc grant by FCT (SFRH/BPD/107881/2015).

## Bibliography

- [1] Fusions – Estimates of European food waste levels (october 4, 2016 at [www.eu-fusions.org/phocadownload/Publications/Estimates%20of%20European%20food%20waste%20levels.pdf](http://www.eu-fusions.org/phocadownload/Publications/Estimates%20of%20European%20food%20waste%20levels.pdf)).
- [2] Baiano A. Recovery of biomolecules from food wastes – A Review. *Molecules* 2014, 19, 14821–14842.
- [3] Fresh deciduous fruit: world markets and trade (Apples, Grapes, & Pears) (September 1, 2016 at [apps.fas.usda.gov/psdonline/circulars/fruit.pdf](http://apps.fas.usda.gov/psdonline/circulars/fruit.pdf)).
- [4] Citrus: world markets and trade. (September 1, 2016 at [apps.fas.usda.gov/psdonline/circulars/citrus.pdf](http://apps.fas.usda.gov/psdonline/circulars/citrus.pdf)).
- [5] Pfaltzgraff LA, De bruyn M, Cooper EC, Budarin V, Clark JH. Food waste biomass: a resource for high-value chemicals. *Green Chem.* 2013, 15, 307–314.
- [6] Santana-Meridas O, Gonzalez-Coloma A, Sanchez-Vioque R Agricultural residues as a source of bioactive natural products. *Phytochem Rev* 2012, 11, 447–466.

- [7] Laufenberg G, Kunz B, Nystroem M Transformation of vegetable waste into value added products: (A) the upgrading concept; (B) practical implementation. *Bioresour. Technol.* 2003, 87, 167–198.
- [8] Clark J, Macquarrie D *Handbook of green chemistry and technology*. Weinhiem: Blackwell Science Ltd, 2002.
- [9] Chemat F, Vian MA, Cravotto G Green extraction of natural products: Concept and principles. *Int. J. Mol. Sci.* 2012, 13, 8615–8627.
- [10] Ganzler K, Salgó A, Valkó K Microwave extraction. A novel sample preparation method for chromatography. *J. Chromatogr. A* 1986, 371, 299–306.
- [11] Ochoa-Villarreal M, Aispuro-Hernández E, Martínez-Téllez MA, Vargas-Arispuro I plant cell wall polymers: function, structure and biological activity of their derivatives, Book chapter 4 in *Polymerization*. Edited by Ailton De Souza Gomes, under CC BY 3.0 license. 2012
- [12] Bousbia N, Vian MA, Ferhat MA, Petitcolas E, Meklati BY, Chemat, F. Comparison of two isolation methods for essential oil from rosemary leaves: Hydrodistillation and microwave hydrodiffusion and gravity. *Food Chem.* 2009, 114, 355–362.
- [13] Farhat A, Fabiano-Tixier AS, Maataoui ME, Maingonnat JF, Romdhane M, Chemat F Microwave steam diffusion for extraction of essential oil from orange peel: Kinetic data, extract's global yield and mechanism. *Food Chem.* 2011, 125, 255–261.
- [14] Farhat A, Fabiano-Tixier AS, Visinoni F, Romdhane M, Chemat F. A surprising method for green extraction of essential oil from dry spices: Microwave dry-diffusion and gravity. *J. Chromatogr. A* 2010, 1217, 7345–7350.
- [15] Zill-e-Huma, Abert-Vian M, Elmaataoui M, Chemat F. A novel idea in food extraction field: Study of vacuum microwave hydrodiffusion technique for by-products extraction. *J. Food Eng.* 2011, 105, 351–360.
- [16] Wang LJ, Weller CL. Recent advances in extraction of nutraceuticals from plants. *Trends Food Sci. Technol.* 2006, 17, 300–312.
- [17] Bousbia N, Vian MA, Ferhat MA, Meklati BY, Chemat F A new process for extraction of essential oil from Citrus peels: Microwave hydrodiffusion and gravity. *J. Food Eng.* 2009, 90, 409–413.
- [18] Maskan M Microwave/air and microwave finish drying of banana. *J. Food Eng.* 2000, 44, 71–78.
- [19] Shaaban HAE, El-Ghorab AH, Shibamoto T Bioactivity of essential oils and their volatile aroma components: Review. *J. Essent. Oil Res.* 2012, 24, 203–212.
- [20] Edris AE. Pharmaceutical and therapeutic potentials of essential oils and their individual volatile constituents: A review. *Phytother. Res.* 2007, 21, 308–323.
- [21] Okoh OO, Sadimenko AP, Afolayan AJ. Comparative evaluation of the antibacterial activities of the essential oils of *Rosmarinus officinalis* L. obtained by hydrodistillation and solvent free microwave extraction methods. *Food Chem.* 2010, 120, 308–312.
- [22] Filly A, Fernandez X, Minuti M, Visinoni F, Cravotto G, Chemat F Solvent-free microwave extraction of essential oil from aromatic herbs: From laboratory to pilot and industrial scale. *Food Chem.* 2014, 150, 193–198.
- [23] Lucchesi ME, Chemat F, Smadja J Solvent-free microwave extraction of essential oil from aromatic herbs: Comparison with conventional hydro-distillation. *J. Chromatogr. A* 2004, 1043, 323–327.
- [24] Bayramoglu B, Sahin S, Sumnu G Solvent-free microwave extraction of essential oil from oregano. *J. Food Eng.* 2008, 88, 535–540.
- [25] Binello A, Orio L, Pignata G, Nicola S, Chemat F, Cravotto G Effect of microwaves on the *in situ* hydrodistillation of four different Lamiaceae. *C. R. Chim.* 2014, 17, 181–186.

- [26] Lucchesi ME, Smadja J, Bradshaw S, Louw W, Chemat F Solvent free microwave extraction of *Elletaria cardamomum* L.: A multivariate study of a new technique for the extraction of essential oil. *J. Food Eng.* 2007, 79, 1079–1086.
- [27] Petigny L, Périno S, Minuti M, Visinoni F, Wajsman J, Chemat F. Simultaneous microwave extraction and separation of volatile and non-volatile organic compounds of boldo leaves. from lab to industrial scale. *Int. J. Mol. Sci.* 2014, 15, 7183–7198.
- [28] Bayramoglu B, Sahin S, Sumnu G Extraction of essential oil from laurel leaves by using microwaves. *Sep. Sci. Technol.* 2009, 44, 722–733.
- [29] Grigoras CG, Destandau E, Fougère L, Elfakir C Evaluation of apple pomace extracts as a source of bioactive compounds. *Ind. Crops Prod.* 2013, 49, 794–804.
- [30] Ferhat MA, Meklati BY, Chemat F Comparison of different isolation methods of essential oil from Citrus fruits: Cold pressing, hydrodistillation and microwave ‘dry’ distillation. *Flavour Frag. J* 2007, 22, 494–504.
- [31] Fidalgo A, Ciriminna R, Carnaroglio D, et al. Eco-friendly extraction of pectin and essential oils from orange and lemon peels. *ACS Sustain Chem Eng* 2016, 4, 2243–2251.
- [32] Kratchanova M, Pavlova E, Panchev I The effect of microwave heating of fresh orange peels on the fruit tissue and quality of extracted pectin. *Carbohydr. Polym.* 2004, 56, 181–185.
- [33] Sahraoui N, Vian MA, Bornard I, Boutekedjiret C, Chemat F Improved microwave steam distillation apparatus for isolation of essential oils Comparison with conventional steam distillation. *J. Chromatogr. A* 2008, 1210, 229–233.
- [34] Boukroufa M, Boutekedjiret C, Petigny L, Rakotomanomana N, Chemat F. Bio-refinery of orange peels waste: A new concept based on integrated green and solvent free extraction processes using ultrasound and microwave techniques to obtain essential oil, polyphenols and pectin. *Ultrason. Sonochem.* 2015, 24, 72–79.
- [35] Sahraoui N, Vian MA, El Maataoui M, Boutekedjiret C, Chemat F Valorization of citrus by-products using Microwave Steam Distillation (MSD). *Innov Food Sci Emerg* 2011, 12, 163–170.
- [36] Virot M, Tomao V, Ginies C, Visinoni F, Chemat F Green procedure with a green solvent for fats and oils’ determination. Microwave-integrated Soxhlet using limonene followed by microwave Clevenger distillation. *J. Chromatogr. A* 2008, 1196–1197, 147–152.
- [37] Paré JR, Sigouin M, Lapointe J Microwave-Assisted Natural Products Extraction. 1991, Patent US 5,002,784,
- [38] Rodriguez-Jasso RM, Mussatto SI, Pastrana L, Aguilar CN, Teixeira JA. Microwave-assisted extraction of sulfated polysaccharides (fucoïdan) from brown seaweed. *Carbohydr. Polym.* 2011, 86, 1137–1144.
- [39] Vian MA, Fernandez X, Visinoni F, Chemat F Microwave hydrodiffusion and gravity, a new technique for extraction of essential oils. *J. Chromatogr. A* 2008, 1190, 14–17.
- [40] Jacotet-Navarro M, Rombaut N, Deslis S, et al. Towards a “dry” bio-refinery without solvents or added water using microwaves and ultrasound for total valorization of fruit and vegetable by-products. *Green Chem.* 2016, 18, 3106–3115.
- [41] Xiao XH, Song W, Wang JY, Li GK. Microwave-assisted extraction performed in low temperature and in vacuo for the extraction of labile compounds in food samples. *Anal. Chim. Acta* 2012, 712, 85–93.
- [42] Mengal P, Mompon B Method and apparatus for solvent free microwave extraction of natural products. 1996, Eur. Pat. P. EP 698 076 B1.
- [43] Mengal P, Mompon B Method and plant for solvent-free microwave extraction of natural products. 1994, WO Pat. 94/26853.
- [44] Farhat A, Ginies C, Romdhane M, Chemat F Eco-friendly and cleaner process for isolation of essential oil using microwave energy Experimental and theoretical study. *J. Chromatogr. A* 2009, 1216, 5077–5085.



- [45] Virota M, Tomao V, Colnagui G, Visinoni F, Chemat F New microwave-integrated Soxhlet extraction. An advantageous tool for the extraction of lipids from food products. *J. Chromatogr. A* 2007, 1174, 138–144.
- [46] Zill-e-Huma, H, Abert Vian M, Maingonnat JF, Chemat F Clean recovery of antioxidant flavonoids from onions: Optimising solvent free microwave extraction method. *J. Chromatogr. A* 2009, 1216, 7700–7707.
- [47] Périno-Issartier S, Zill-e-Huma, H, Abert-Vian M, Chemat F Solvent free microwave-assisted extraction of antioxidants from sea buckthorn (*Hippophae rhamnoides*) food by-products. *Food Bioprocess Technol.* 2011, 4, 1020–1028.
- [48] Barba AA, D'Amore M, Rispoli M, Marra F, Lamberti G Microwave assisted drying of banana: effects on reducing sugars and polyphenols contents. *Czech J Food Sci* 2014, 32, 369–375.
- [49] Chang TS, Siddiq M, Sinha NK, Cash JN. Plum juice quality affected by enzyme treatment and fining. *J. Food Sci.* 1994, 59, 1065–1069.
- [50] Ahmad J, Langrish TAG. Optimisation of total phenolic acids extraction from mandarin peels using microwave energy: The importance of the Maillard reaction. *J. Food Eng.* 2012, 109, 162–174.
- [51] Tsubaki S, Nakauchi M, Ozaki Y, Azuma JI. Microwave heating for solubilization of polysaccharide and polyphenol from soybean residue (Okara). *Food Sci. Technol. Res.* 2009, 15, 307–314.
- [52] Tsubaki S, Iida H, Sakamoto M, Azuma JI. Microwave heating of tea residue yields polysaccharides, polyphenols, and plant biopolyester. *J. Agr. Food. Chem.* 2008, 56, 11293–11299.
- [53] Paredes-López O, Cervantes-Ceja ML, Vigna-Pérez M, Hernández-Pérez T. Berries: Improving human health and healthy aging, and promoting quality life-A Review. 2010, 65, 299–308.
- [54] Rice-Evans CA, Miller NJ, Paganga G Structure-antioxidant activity relationships of flavonoids and phenolic acids. *Free Radic. Biol. Med.* 1996, 20, 933–956.
- [55] Hayat K, Zhang X, Farooq U, et al. Effect of microwave treatment on phenolic content and antioxidant activity of citrus mandarin pomace. *Food Chem.* 2010, 123, 423–429.
- [56] Wang L, Wang ZM, Li TC, Zhou X, Ding L, Mang HQ. Rapid extraction and analysis of essential oil from *Cinnamomum cassia* Presl. *Chem. Res. Chin. Univ.* 2008, 24, 275–280.
- [57] Fernandez-Agullo A, Freire MS, Gonzalez-Alvarez J Effect of the extraction technique on the recovery of bioactive compounds from eucalyptus (*Eucalyptus globulus*) wood industrial wastes. *Ind. Crops Prod.* 2015, 64, 105–113.
- [58] Liazid A, Guerrero RF, Cantos E, Palma M, Barroso CG. Microwave assisted extraction of anthocyanins from grape skins. *Food Chem.* 2011, 124, 1238–1243.
- [59] Hofmann T, Nebehaj E, Stefanovits-Bányai É, Albert L Antioxidant capacity and total phenol content of beech (*Fagus sylvatica* L.) bark extracts. *Ind. Crops Prod.* 2015, 77, 375–381.
- [60] Chen Y, Yu QJ, Li X, Luo Y, Liu H Extraction and HPLC characterization of chlorogenic acid from tobacco residuals. *Sep. Sci. Technol.* 2007, 42, 3481–3492.
- [61] Bai XL, Yue TL, Yuan YH, Zhang HW. Optimization of microwave-assisted extraction of polyphenols from apple pomace using response surface methodology and HPLC analysis. *J. Sep. Sci.* 2010, 33, 3751–3758.
- [62] Dahmoune F, Boulekbache L, Moussi K, Aoun O, Spigno G, Madani K Valorization of *Citrus limon* residues for the recovery of antioxidants: Evaluation and optimization of microwave and ultrasound application to solvent extraction. *Ind. Crops Prod.* 2013, 50, 77–87.
- [63] Yeoh S, Shi J, Langrish TAG. Comparisons between different techniques for water-based extraction of pectin from orange peels. *Desalination* 2008, 218, 229–237.
- [64] Drosou C, Kyriakopoulou K, Bimpilas A, Tsimogiannis D, Krokida M A comparative study on different extraction techniques to recover red grape pomace polyphenols from vinification byproducts. *Ind. Crops Prod.* 2015, 75, 141–149.

- [65] Bittar SA, Perino-Issartier S, Dangles O, Chemat F An innovative grape juice enriched in polyphenols by microwave-assisted extraction. *Food Chem.* 2013, 141, 3268–3272.
- [66] Li YP, Skouroumounis GK, Eley GM, Taylor DK. Microwave-assistance provides very rapid and efficient extraction of grape seed polyphenols. *Food Chem.* 2011, 129, 570–576.
- [67] Yu HB, Ding LF, Wang Z, Shi LX. Study on extraction of polyphenol from grape Peel microwave-assisted activity. 2014, 864–867, 520–525.
- [68] Delgado-Torre MP, Ferreiro-Vera C, Priego-Capote F, Pérez-Juan PM, Luque de Castro MD. Comparison of accelerated methods for the extraction of phenolic compounds from different vine-shoot cultivars. *J. Agr. Food. Chem.* 2012, 60, 3051–3060.
- [69] Hua L, Guoqin H, Dan L Application of the microwave-assisted process to the fast extraction of isoflavone from the waste residue of the soybeans. *Bull. Korean Chem. Soc.* 2009, 30, 2687–2690.
- [70] Passos CP, Sério A, Kukurová K, Ciesarová Z, Nunes FM, Coimbra MA. Microwave assisted extraction of carbohydrate-rich fractions from spent coffee grounds: formulation of biscuits enriched in dietary fibre. *Trends in Carbohydr. Res.* 2015, 1, 12–17.
- [71] Srivastava R, Kulshreshtha DK. Bioactive polysaccharides from plants *Phytochemistry* 1989, 28, 2877–2883.
- [72] Ferreira SS, Passos CP, Madureira P, Vilanova M, Coimbra MA. Structure-function relationships of immunostimulatory polysaccharides: A review. *Carbohydr. Polym.* 2015, 132, 378–396.
- [73] Ando H, Sakaki T, Kokusho T, Shibata M, Uemura Y, Hatate Y Decomposition behavior of plant biomass in hot-compressed water. *Ind. & Eng. Chem. Res.* 2000, 39, 3688–3693.
- [74] Yu Y, Lou X, Wu H Some recent advances in hydrolysis of biomass in hot-compressed water and its comparisons with other hydrolysis methods. *Energy Fuels* 2008, 22, 46–60.
- [75] Benko Z, Andersson A, Szengyel Z, Gaspar M, Reczey K, Stalbrand H Heat extraction of corn fiber hemicellulose. *Appl Biochem Biotech* 2007, 137, 253–265.
- [76] Passos CP, Coimbra MA. Microwave superheated water extraction of polysaccharides from spent coffee grounds. *Carbohydr. Polym.* 2013, 94, 626–633.
- [77] Passos CP, Moreira ASP, Domingues MRM, Evtuguin DV, Coimbra MA. Sequential microwave superheated water extraction of mannans from spent coffee grounds. *Carbohydr. Polym.* 2014, 103, 333–338.
- [78] Coelho E, Rocha MAM, Saraiva JA, Coimbra MA. Microwave superheated water and dilute alkali extraction of brewers' spent grain arabinoxylans and arabinoxylo-oligosaccharides. *Carbohydr. Polym.* 2014, 99, 415–422.
- [79] Warrant J, Janssen HG. Controlled production of oligosaccharides from amylose by acid-hydrolysis under microwave treatment: Comparison with conventional heating. *Carbohydr. Polym.* 2007, 69, 353–362.
- [80] Fischer K, Bipp HP. Generation of organic acids and monosaccharides by hydrolytic and oxidative transformation of food processing residues. *Bioresour. Technol.* 2005, 96, 831–842.
- [81] Singh V, Tiwari A Hydrolytic fragmentation of seed gums under microwave irradiation. *Int. J. Biol. Macromol.* 2009, 44, 186–189.
- [82] Fan SP, Jiang LQ, Chia CH, Fang Z, Zakaria S, Chee KL. High yield production of sugars from de-proteinated palm kernel cake under microwave irradiation via dilute sulfuric acid hydrolysis. *Bioresour. Technol.* 2014, 153, 69–78.
- [83] Hernoux-Villière A, Lassi U, Hu T, et al. Simultaneous microwave/ultrasound-assisted hydrolysis of starch-based industrial waste into reducing sugars. *Acs Sustain Chem Eng* 2013, 1, 995–1002.

- [84] Azuma JI, Higashino J, Isaka M, Koshijima T Microwave irradiation of lignocellulosic materials. iv. Enhancement of enzymatic susceptibility of microwave-irradiated softwoods. *Wood Res.* 1984, 71, 13–24.
- [85] Du B, Zhu FM, Xu BJ. beta-Glucan extraction from bran of hull-less barley by accelerated solvent extraction combined with response surface methodology. *J. Cereal Sci.* 2014, 59, 95–100.
- [86] Navarrete A, Herrero M, Martín A, Cocero MJ, Ibáñez E Valorization of solid wastes from essential oil industry. *J. Food Eng.* 2011, 104, 196–201.
- [87] Yapo BM. Pectic substances: From simple pectic polysaccharides to complex pectins – A new hypothetical model. *Carbohydr. Polym.* 2011, 86, 373–385.
- [88] Paulsen BS, Barsett H Bioactive pectic polysaccharides, Book chapter in *Polysaccharides I*, Book series *Advances in Polymer Science* Edited by Thomas Heinze, Springer. 2005, 186, 69–101.
- [89] Guo X, Han D, Xi H, et al. Extraction of pectin from navel orange peel assisted by ultra-high pressure, microwave or traditional heating: A comparison. *Carbohydr. Polym.* 2012, 88, 441–448.
- [90] Fishman ML, Chau HK, Coffin DR, et al. Physico-chemical characterization of a cellulosic fraction from sugar beet pulp. *Cellulose* 2011, 18, 787–801.
- [91] Fishman ML, Chau HK, Cooke PH, Hotchkiss Jr AT. Global structure of microwave-assisted flash-extracted sugar beet pectin. *J. Agr. Food. Chem.* 2008, 56, 1471–1478.
- [92] Fishman ML, Chau HK, Cooke PH, Yadav MP, Hotchkiss AT. Physico-chemical characterization of alkaline soluble polysaccharides from sugar beet pulp. *Food Hydrocolloids* 2009, 23, 1554–1562.
- [93] Hiranvarachat B, Devahastin S Enhancement of microwave-assisted extraction via intermittent radiation: Extraction of carotenoids from carrot peels. *J. Food Eng.* 2014, 126, 17–26.
- [94] Strati IF, Oreopoulou V Recovery of carotenoids from tomato processing by-products – a review. *Food Res Int.* 2014, 65, 311–321.
- [95] Grosso C, Valentão P, Ferreres F, Andrade PB. Alternative and efficient extraction methods for marine-derived compounds. *Mar. Drugs* 2015, 13, 3182–3230.
- [96] Pasquet V, Chérouvrier JR, Farhat F, et al. Study on the microalgal pigments extraction process: Performance of microwave assisted extraction. *Process Biochem.* 2011, 46, 59–67.
- [97] Heleno SA, Prieto MA, Barros L, Rodrigues A, Barreiro MF, Ferreira ICFR. Optimization of microwave-assisted extraction of ergosterol from *Agaricus bisporus* L. by-products using response surface methodology. *Food Bioprod. Process.* 2016, 100, 25–35.
- [98] Terigar BG, Balasubramanian S, Sabliov CM, Lima M, Boldor D Soybean and rice bran oil extraction in a continuous microwave system: From laboratory to pilot scale. *J. Food Eng.* 2011, 104, 208–217.
- [99] Glasnov TN, Kappe CO. Microwave-assisted synthesis under continuous-flow conditions. *Macromol. Rapid Commun.* 2007, 28, 395–410.
- [100] Bergamelli F, Iannelli M, Marafie JA, Moseley JD. A commercial continuous flow microwave reactor evaluated for scale-up. *Org. Process Res. Dev.* 2010, 14, 926–930.
- [101] Ciriminna R, Carnaroglio D, Delisi R, Arvati S, Tamburino A, Pagliaro M. Industrial feasibility of natural products extraction with microwave technology. *ChemistrySelect* 2016, 1, 549–555.
- [102] Wang S, Chen F, Wu J, Wang Z, Liao X, Hu X Optimization of pectin extraction assisted by microwave from apple pomace using response surface methodology. *J. Food Eng.* 2007, 78, 693–700.
- [103] Li XL, He XL, Lv YP, He Q Extraction and functional properties of water-soluble dietary fiber from apple pomace. *J Food Process Eng* 2014, 37, 293–298.

- [104] Fishman ML, Chau HK, Hoagland PD, Hotchkiss AT. Microwave-assisted extraction of lime pectin. *Food Hydrocolloids* 2006, 20, 1170–1177.
- [105] Khodaei N, Karboune S, Orsat V Microwave-assisted alkaline extraction of galactan-rich rhamnogalacturonan I from potato cell wall by-product. *Food Chem.* 2016, 190, 495–505.
- [106] Yoshida T, Tsubaki S, Teramoto Y, Azuma JI. Optimization of microwave-assisted extraction of carbohydrates from industrial waste of corn starch production using response surface methodology. *Bioresour. Technol.* 2010, 101, 7820–7826.
- [107] Deng A, Ren J, Wang W, et al. Production of xylo-sugars from corncob by oxalic acid-assisted ball milling and microwave-induced hydrothermal treatments. *Ind. Crops Prod.* 2016, 79, 137–145.
- [108] Li J, Zu YG, Fu YJ, et al. Optimization of microwave-assisted extraction of triterpene saponins from defatted residue of yellow horn (*Xanthoceras sorbifolia* Bunge.) kernel and evaluation of its antioxidant activity. *Innov Food Sci Emerg* 2010, 11, 637–643.
- [109] Mellouk H, Meullemiestre A, Maache-Rezzoug Z, Bejjani B, Dani A, Rezzoug SA. Valorization of industrial wastes from French maritime pine bark by solvent free microwave extraction of volatiles. *J Clean Prod* 2016, 112, 4398–4405.
- [110] Belafi-Bako K, Cserjesi P, Beszedes S, Csanadi Z, Hodur C Berry Pectins: microwave-assisted extraction and rheological properties. *Food Bioprocess Tech* 2012, 5, 1100–1105.
- [111] Chanioti S, Siamandoura P, Tzia C Evaluation of extracts prepared from olive oil by-products using microwave-assisted enzymatic extraction: effect of encapsulation on the stability of final products. *Waste Biomass Valor.* 2016, 7, 831–842.

Simona Collina and Serena Della Volpe

## 18 The Use of microwaves in drug discovery

### 18.1 Introduction

During the last 30 years, the impact of new advances in genomics and proteomics has caused several unexpected changes in the process of drug discovery (DD) due to a huge rise in the number of pharmacological targets, which translated into an increased demand for new molecules in a very short period of time. The identification of new chemical entities (NCEs) that can be used as a starting point (or lead compound) for a new drug requires the preparation of a great amount of compounds to submit to biological assays. Developing NCEs with the desired biological properties is time consuming and expensive, and traditional organic synthesis methods are orders of magnitude too slow to meet the demand for novel compounds to test as potential drug candidates for newly discovered targets [1, 2].

In the scenario of DD, microwave-assisted organic synthesis (MAOS) plays an important role, both for lead generation and lead optimization, because of its numerous benefits, including faster chemistry (it reduces reaction times from days or hours to minutes), greater versatility, and the formation of cleaner products compared to conventional synthetic methods [2], ultimately potentially speeding the entire process. MAOS can be applied not only to the conventional so-called one-molecule-at-a-time synthetic chemistry but also to combinatorial chemistry, an approach that emerged at the end of the 1980s. Combinatorial chemistry allows us to discover new bioactive compounds more quickly and inexpensively than was formerly possible. It makes it possible to synthesize and purify a great number of molecules (from tens to hundreds) at the same time, thus revealing new leads or drawing structure-activity relationships (SAR) in much shorter timeframes compared to the past [1]. This approach exploits two main methodologies. The first method consists of a series of so-called pool and split phases on the starting compounds previously attached to polymer beads [3]. The second, and nowadays most common, modus is parallel synthesis; different chemical structure combinations are obtained separately, in parallel, using a number of reaction vessels and by mechanically adding the appropriate reagents to each one. This method is very useful for the development of small focused libraries based on a specific scaffold [4]. Combinatorial and parallel synthesis can greatly benefit from the unique features offered by modern microwave reactor technology. These include the possibility of high-speed parallel processing of chemical transformations in the context of library production and the rapid optimization of reaction conditions for library preparation using automated sequential synthesis [5]. In view of these considerations,

<https://doi.org/10.1515/9783110479935-018>

it is clear that MAOS has a high potential in the process of and in the early phase of drug development.

Even though synthetic compounds are the classic active substances and still represent around 90% of drugs currently marketed, we cannot forget that nature is an important source of compounds with therapeutic potential. So-called nature-aided DD consists in the isolation, purification, and full characterization of new bioactive molecules from natural matrices. This process has some limitations, requiring long extraction times and large solvent volumes and causing degradation of thermolabile components, and in this context, the application of microwave-assisted extraction (MAE, also known as microwave-assisted solvent extraction, MASE) for the isolation and extraction of compounds from plant materials has taken on increasing importance. This technique entails less solvent consumption, gives high and fast extraction performance, and offers protection to thermolabile constituents. Finally, microwave-enhanced technologies can be used for biotechnological applications and in the discovery of new targets [6].

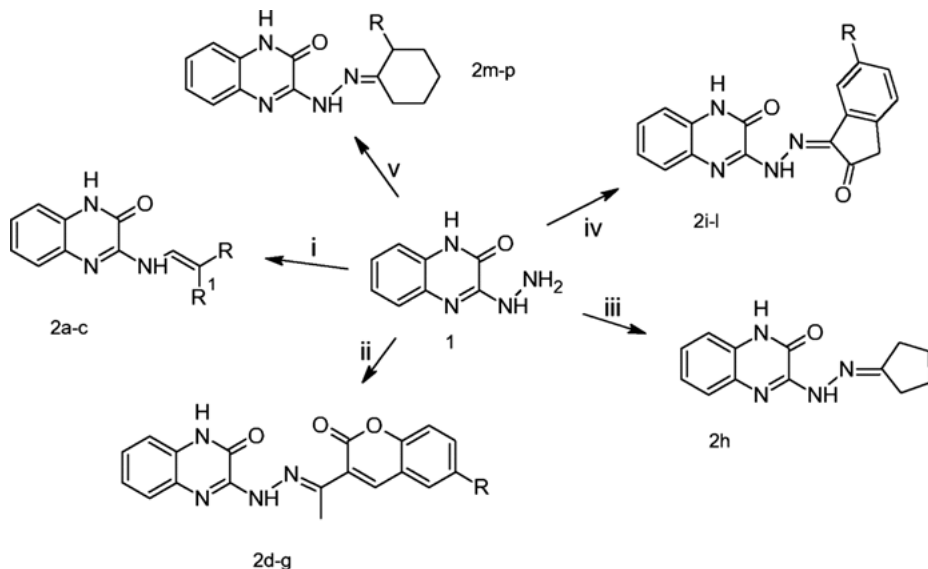
In this chapter, we will focus on the main applications of microwaves in the process of DD, including both MAOS, for the discovery of new potential drugs and for the preparation of radio-ligands, and MAE, for the extraction of natural compounds. We will also briefly present the high potential of microwave-enhanced methodologies in biotechnological DD.

Some successful examples presented here will introduce students to the field of microwave-assisted DD.

## 18.2 MAOS in drug discovery: synthesis of small molecules

As previously stated, the process of DD is time consuming and expensive. Accordingly, there is considerable interest in technologies that allow for faster synthesis and screening of new compounds. One such high-speed method is represented by MAOS [7]. During reaction optimizations, several parameters must be taken into consideration: temperature, time, solvent, presence of additives and catalysts, and molar ratios of substrates. In MAOS, all these parameters can be assessed in a few hours, and, as a consequence, compound libraries can be rapidly synthesized either in a parallel or a sequential (automated) format. Furthermore, MAOS often facilitates the discovery of novel reaction pathways because the extreme reaction conditions attainable by microwave heating sometimes lead to unusual reactivity that cannot always be obtained through conventional heating methods. This eventually causes the expansion of the chemical space in general, and *biologically relevant, medicinal chemistry space* in particular, producing significant advantages in the process of DD [7]. For both phases of lead discovery and optimization, MAOS techniques can often be exploited, affording the chance to prepare compound libraries [7].

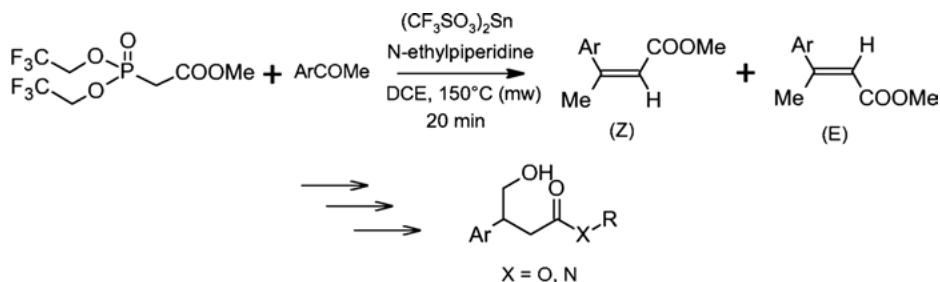
Microwave heating can be applied to so-called classical solution-phase synthesis, as reported by Ajani et al., to discover new compounds with an antimicrobial profile. A series of 2-quinoxalinone-3-hydrazone derivatives was obtained by condensation of key-intermediate 3-hydrazinoquinoxalin-2(1*H*)-one **1** with various ketones, by microwave irradiation. All the synthesized hydrazone derivatives **2a-p** were obtained in very short times (1–3 min) and excellent yields (55–99%) (Scheme 18.1) and were found to be active against streptomycin-resistant *Escherichia coli* and *Klebsiella pneumoniae* [8, 9].



**Scheme 18.1:** Synthesis of derivatives **2a-p**. (i) acyclic ketone, (ii) 3-substituted 3-acethylcoumarine, (iii) cyclopentanone, (iv) 5-substituted isatin, (v) 2-substituted cyclohexanone obtained using MAOS (140 °C).

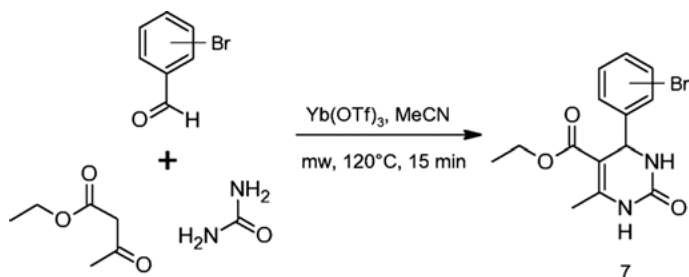
Another successful example of the application of MAOS in classical solution-phase synthesis is the preparation of a DD library, based on a 3-aryl-4-hydroxybutyrate scaffold, in order to inspect the molecular features characterizing the binding to protein kinase C (PKC) [10]. The authors chose (*Z*)-3,3-trisubstituted  $\alpha,\beta$ -unsaturated methyl ester synthetic intermediates and subjected them to simple synthetic steps to obtain the desired chemical diversity (Scheme 18.2). Upon optimization of the experimental conditions, the key step involving a Horner–Wadsworth–Emmons (HWE) reaction under microwave irradiation was carried out on seven different aryl methyl ketones and yielded the desired intermediates with a conversion higher than 50% and a satisfactory (*Z*)-selectivity on six out of seven compounds. Compared to the conventional heating method [11], which entailed two steps and long timeframes along with

low yields and low reproducibility, this synthetic route proved to be short, selective, and versatile.



**Scheme 18.2:** HWE olefination of aryl methyl ketones to develop a 3-aryl-4-hydroxybutyrate-based library.

Interestingly, microwave-assisted heating can be applied to multicomponent reactions. It is well known that building multiple bonds in a one-pot, multicomponent reaction promotes a sustainable synthetic approach to the discovery of new potential drugs [12]. This technique works to create molecular diversity in contrast to the commonly costly and time-consuming DD process, which is often further aggravated by attrition rates in reaching the marketplace and could benefit from coupling with microwaves [12]. The most interesting applications of MMS include Hantzsch, Biginelli, and Ugi reactions, and many examples of these can be found in the literature. In the context of DD, a noteworthy MMS example is that proposed by Larhed et al. to develop a series of dihydropyrimidone (DHPM) derivatives [13]. DHPMs show extensive pharmacological activities, and they are classified as one of the most important groups of druglike scaffolds. Bromophenyl-substituted DHPMs were obtained in close analogy to a previously described microwave-assisted Biginelli multicomponent condensation (Scheme 18.3) [14]. Further microwave-assisted metal-catalyzed functionalizations on *o*, *m*, and *p* positions afforded a series of DHPMs used to generate a large array of



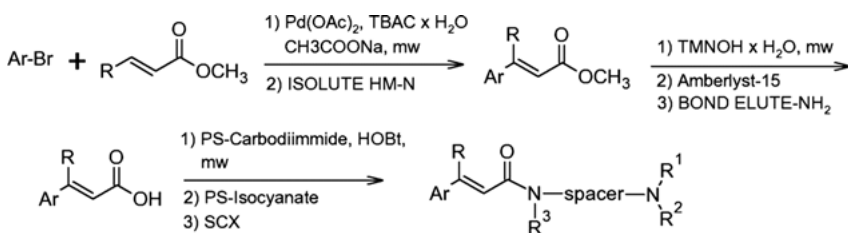
**Scheme 18.3:** Synthesis of 4-(Bromophenyl)-DHPMs via microwave-assisted Biginelli reaction.



novel structures; given the interest in privileged DHPM-based compound selections, this combination strategy was proposed for further applications in different areas of DD [13]. Similarly to structurally related dihydropyridines (DHPs), DHPMs can be active as calcium channel modulators [15], although they show interesting profiles as  $\alpha_{1a}$  adrenoceptor-selective antagonists, kinesin motor protein inhibitors, and anti-HIV agents [16].

Since the early 2000s, the use of MAOS combined with the use of polymer-supported reagents (PSRs) has gained increasing attention in the DD field [17]. These reagents allow the simplification of reaction work-up and product isolation, reduced to simple filtration through silica gel to remove the soluble PSR and evaporation of solvent [5]. PSRs are used for the preparation of libraries constructed both in solution and on solid supports. For small focused libraries, solution-phase chemistry (polymer-assisted solution-phase synthesis, PASPS) is generally preferred, whereas for the construction of very large libraries on resins solid-phase organic synthesis (SPOS) is more convenient.

Several applications of microwave heating combined with PASPS have been reported in the literature. An example is the preparation of a discovery library based on an (*N*-alkylaminoalkyl-substituted)arylalkenylamidic scaffold to discover ligands targeting sigma receptors [18]. Combining 4 different arylbromides, 2 methyl acrylates, and 8 amines in a 3-step synthesis, a library of 64 members was obtained with an overall high purity, equal to or greater than 80%, suitable for biological screening. Each reaction step was microwave enhanced, and the last one involved the use of a PSR (Scheme 18.4). The use of solid-phase extraction (SPE) further simplified the reaction work-up [18].

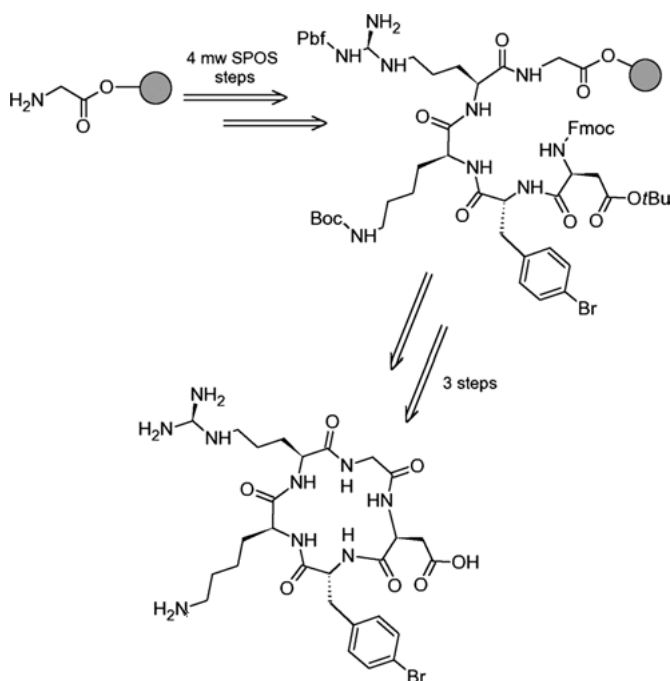


**Scheme 18.4:** Synthesis pathway of a series of (*N*-alkylaminoalkyl-substituted)arylalkenylamides).

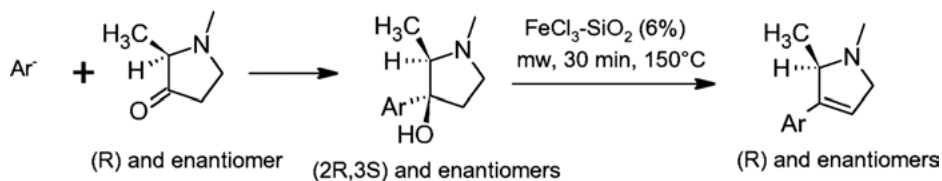
Regarding SPOS, it must be underlined that, throughout the previous decade, this strategy has dominated combinatorial chemistry, and microwave-assisted solid-phase organic techniques have been the subject of several studies [19]. Because of the relatively long reaction times usually associated with solid-phase synthesis, the decision to study its combination with microwave irradiation is not surprising. A variety of polymer supports have been employed, ranging from standard polystyrene resins to polypropylene membranes. In most of the reported experiments, significant rate

enhancements were observed compared to the standard thermal protocols, with reactions being carried out in either sealed or open vessels. Similar to solution-phase combinatorial synthesis, microwave-assisted SPOS produces compounds in a soluble form immediately available for biological screening [2]. Many examples of MAOS being used to achieve single transformations, using either solid-supported reagents or solid-supported substrates, are reported in the literature [20–22]. Moreover, several reports suggesting the concept of carrying out microwave-enhanced SPOS in parallel have been published in the past few years [35].

An interesting example is the microwaved-enhanced solid-phase synthesis of cyclic Arginyglycylaspartic acid (RGD) peptides. Such peptides are known to be potent antagonists for the  $\alpha_v\beta_3$  integrin receptor and they are sometimes used for positron emission tomography (PET) imaging (both as tracers, after conjugation to a radioactive tracer or a fluorophore, and standards). Yamada et al. performed the synthesis of linear pentapeptides, *H*-Asp(OtBu)-Xxx-Yyy-Arg(Pbf)-Gly-OH (Xxx = *D*-Phe(*p*-Br) or *D*-Tyr, Yyy = Lys(Boc) or MeVal), through SPOS under microwave heating to 50 °C (Scheme 18.5). The synthesis was accelerated compared to traditional methods and the reaction conditions used avoided the formation of unwanted byproducts. Cyclization of the linear peptides followed by deprotection afforded the desired cyclic RGD peptides with high purity [23].



**Scheme 18.5:** Microwave-assisted SPOS of RGD peptides.



**Scheme 18.6:** Synthetic procedure for 1,2-dimethyl-3-[2-(6-substituted naphthyl)]-2H,5H-pyrrolines via solvent-free MAOS.

It is important not to forget that MAOS has emerged as a new lead in organic synthesis to make this chemistry green thanks to the lower solvent consumption in comparison with conventional synthesis. In particular, organic reactions operated with green solvents or without solvents have attracted the attention of medicinal chemists because of their lower environmental impact and the potential damaging effects of organic solvents on biological systems. In this context, solvent-free reaction conditions and, in particular, microwave-assisted solvent-free methods, are of great interest [24–27]. Briefly, a solid support capable of absorbing microwave radiations (e.g., clay), is first imbued with a solution of reagents in a volatile solvent. The solvent is then evaporated, and the solid support with adsorbed reagents is irradiated by microwaves. In some cases a small amount of *N,N'*-dimethylformamide is added as an energy-transfer medium. The reaction takes place in the solid phase, and the products are then removed from the support using a suitable solvent. Solvent-free strategies must not be confused with the application of solid-phase chemistry, where the reactant is covalently linked to a polymer resin [28].

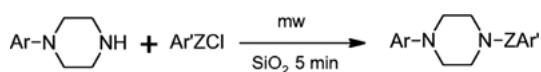
A solvent-free strategy was utilized by Collina et al. to improve yields of a traditional heating procedure for a small series of enantiomeric 1,2-dimethyl-3-[2-(6-substituted naphthyl)]-2H,5H-pyrrolines as antinociceptive agents [29]. The reaction was carried out on a solid support in dry medium in a borosil closed vessel (Scheme 18.6). Upon purification, the reaction showed retained regioselectivity and afforded all compounds in substantially higher yields (range 50% up to 90%) and reduced reaction times (from 15 h to 30 min).

Another interesting application of microwave-assisted solvent-free reaction was reported by Williams. A procedure to prepare *N*-substituted arylpiperazines was set up combining synthesis, purification, analysis, and screening of combinatorial libraries, all on a single thin-layer chromatography (TLC) plate. After the reagents were spotted on the baseline, the plate was irradiated with microwaves for 5 min (585 W) and cooled [30]. The products were then eluted and isolated from the silica. A library of 40 *N*-substituted arylpiperazines was synthesized and purified for biological screening in 30 min (Scheme 18.7). This methodology has been extended to incorporate screening by bio-autographical agar overlay [30]. Such arylpiperazines are currently being studied as neuroprotective agents given their affinity for dopamine and serotonin receptors [31].

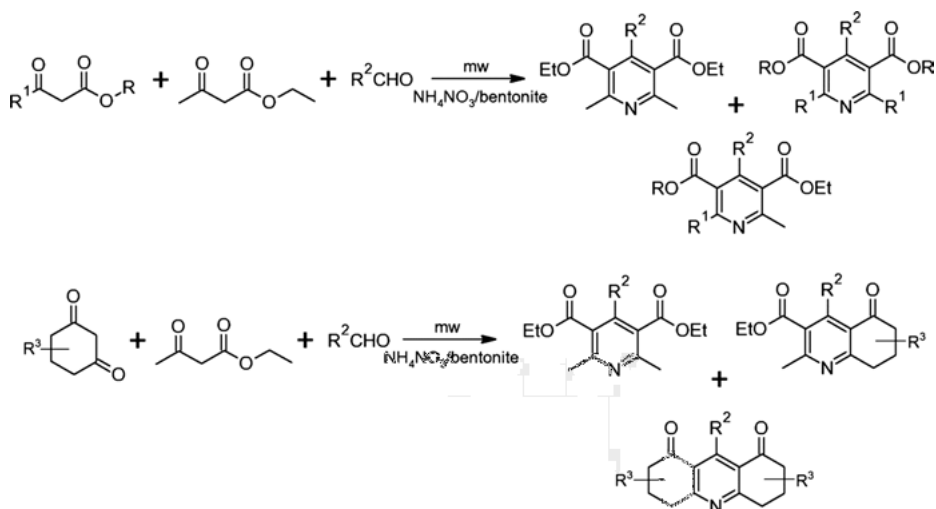
An interesting example of parallel MMS in solvent-free conditions is represented by the optimization of the 3-component Hantzsch reaction in a 96-well microtiter plate. This approach allows for libraries of diverse pyridines to be produced with a high-throughput, automated single step (Scheme 18.8) [28, 32]. Several 1,3-dicarbonyl compounds and aldehydes were used as building blocks. Analysis on the final products showed that the reactions were uniformly successful across the 96-well reactor plate, thereby demonstrating that the outcome of parallel reactions in a multiple-reactor array is not negatively affected by the presence of microwave-absorbing material in adjacent wells or a potentially uneven distribution of microwave energy inside the oven. No unreacted starting material was found in any of the reactions, and the high-performance liquid chromatography (HPLC) purity of the products was over 70%. All of the expected 96 nonsymmetrical pyridines were synthesized. Additionally, 70 out of 108 symmetrical pyridines were formed, suggesting that some bulky 1,3-dicarbonyl compounds react slower [32]. Such variously decorated pyridines show a wide range of pharmacologically suitable activities, including antiviral, anticancer, antioxidant, antibacterial, antifungal, and antidiabetic potential [33].

To be honest, although the use of previously mentioned solvent-free techniques might be a green solution, this approach can only work for a few reactions, and the lack of reaction medium might in some cases lead to overheating of the reaction mixture. Therefore, to avoid the presence of interfering solvents in final compounds and to reduce and prevent pollution caused by chemical activities, water might be used as a nontoxic reaction medium [34]. In fact, water is nontoxic, noncorrosive, and nonflammable. Furthermore, it can be easily contained because of its relatively high vapor pressure compared to organic solvents; finally, thanks to its chemical-physical characteristics, water is an ideal solvent for use in microwave-assisted strategies [34]. Nonetheless, its use does carry with it a few limitations, the main difficulty being that most organic substrates are insoluble in it, which makes the reaction mixture heterogeneous; this inconvenience can be overcome through the use of phase transfer catalysts, though this ultimately raises the costs of synthetic procedures. Moreover, in general, the isolation of products from an aqueous medium may represent another issue, but in most cases, this can be resolved through coupling with microwaves [34].

The applications of MAOS in aqueous media are numerous and include coupling reactions, oxidative deaminations, *N*-arylation of amino acids, amino-carbonylations, and so on [34–43]. Many reported studies concern heterocyclic compounds, characterizing several classes of pharmaceutically exploitable natural and synthetic compounds [44, 45]. Among various examples, diverse nitrogen-containing heterocycles, including substituted azetidines, pyrrolidines, piperidines, azepanes, *N*-substituted

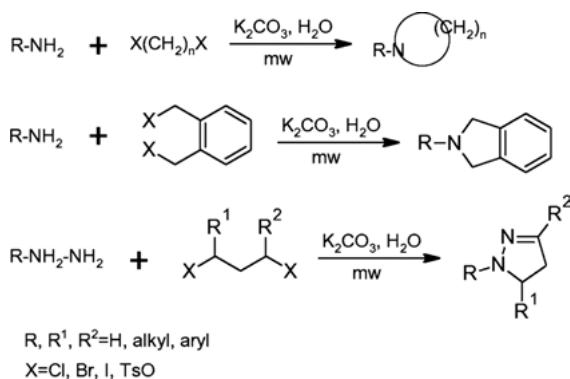


**Scheme 18.7:** Arylpiperazine derivatives formed via parallel spot synthesis on a single TLC plate.



**Scheme 18.8:** Microwave-assisted combinatorial/parallel Hantzsch synthesis of diverse pyridines.

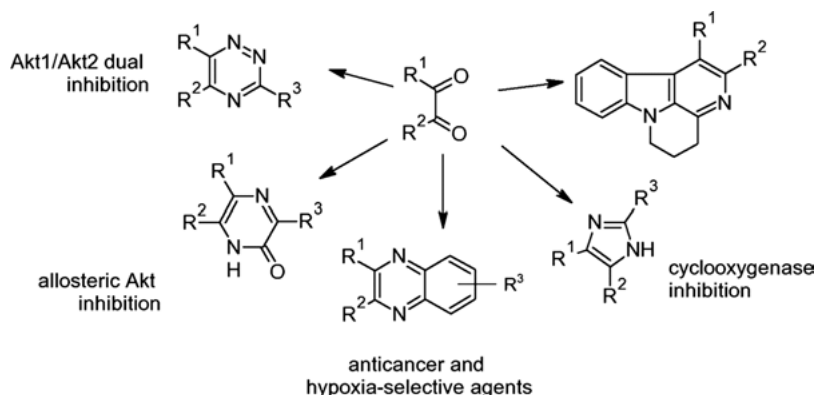
2,3-dihydro-1*H*-isoindoles, 4,5-dihydropyrazoles, pyrazolidines, and 1,2-dihydrophthalazines [34], which represent important building blocks for potentially biologically active compounds [46–48], can be easily obtained starting with a series of double *N*-alkylation of primary amines and hydrazine derivatives (Scheme 18.9). Some of the potential applications of such synthesized compounds include their use as pesticides, anticonvulsants, and potent vasorelaxing agents [46–48].



**Scheme 18.9:** MAOS of various nitrogen-containing heterocycles in aqueous media.

Finally, we also need to direct our attention to the potential of MAOS applications in the concept of diversity-oriented synthesis (DOS), which emerged during the last 10 years and is of great relevance in the DD process [49]. The DOS approach, in contrast

to classical library design in which the same scaffold is decorated, as it were, with different substituents, is directed at creating collections of compounds which might be used to find ligands targeting different receptors rather than being directed toward a single biological entity [50]. Since many pharmaceutical leads obtained from high-throughput screenings are small organic compounds, efficient strategies to generate diverse libraries of such molecules are of particular significance [7]. The usefulness of this approach is confirmed by its many applications; particularly interesting is a series of microwave-assisted protocols developed to generate diverse libraries of heterocyclic scaffolds from common 1,2-diketone intermediates [51–56] (Scheme 18.10), including variously decorated 1,2,4-triazines [51], pyrazine-2(1*H*)-ones [52], fused pyrazines (e.g., quinoxalines [53]), imidazoles [54], and canthine derivatives [55]. In most cases, microwave-enhanced procedures had short timeframes (5–10 min) and afforded the corresponding nitrogen heterocycle in high yields compared to conventional methods (8–24 h, 30–65% yields) [7]. Among the different activities of synthesized compounds are cytotoxicity and cyclooxygenase inhibition (imidazoles) [54], allosteric Akt inhibition (pyrazine-2(1*H*)-ones) [52], and Akt1 and Akt2 dual inhibition (1,2,4-triazines) [51]. Quinoxalines have been studied as anticancer and hypoxia-selective agents [57].



**Scheme 18.10:** Microwave-enhanced generation of heterocyclic scaffolds with potential biological activity starting from various 1,2-diketones.

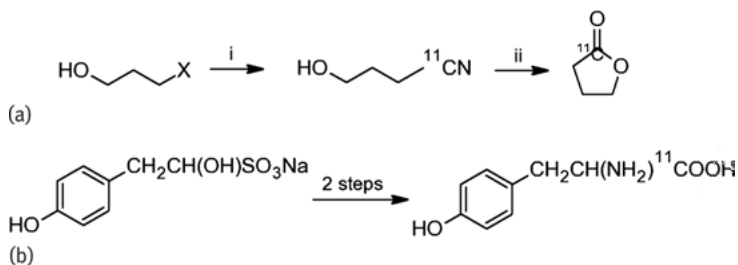
## 18.3 MAOS in drug development: synthesis of radioligands for PET

A particular case of MAOS application is the preparation of tracers labeled with isotopes with short half-lives, like <sup>11</sup>C ( $t_{1/2}$  = 20.4 min) and <sup>18</sup>F ( $t_{1/2}$  = 109.8 min) [58]. Conventional chemical syntheses of these short-half-life radionuclides show numer-

ous drawbacks. By utilizing microwave-assisted synthesis methods, many of these limitations can be overcome, thus allowing the preparation of diverse families of agents with defined cellular targets. MAOS has been successful in reducing reaction times by up to 50% and, in some cases, significantly increases the yield of the final radiochemical product. One of the first applications of microwave-enhanced radiochemistry was in the synthesis of PET pharmaceuticals. Radio-labeled compounds can be used to evaluate first-pass pharmacokinetics/pharmacodynamics in early-stage DD, in *in vivo* imaging studies and in human PET for the diagnosis of several pathologies. The first use of microwaves in PET was reported in 1987 [58], and since then several microwave-assisted radiolabeling procedures have been reported [59]. The synthesis of PET radiopharmaceuticals has been achieved using monomodal instruments, which are optimized to heat small volumes efficiently. In addition to usual timeframe- and yield-related advantages, these systems achieve high levels of reproducibility; this aspect is most important for PET radiopharmaceuticals that are required for human studies, for which the use of validated reproducible procedures is a requirement of good manufacturing practice (GMP) regulations [20]. Finally, legal/environmental issues, such as the amount of radioactivity released to the atmosphere, together with the cost associated with the storage of radioactive waste, are additional factors that contribute to the development of this more environmentally acceptable approach to radiosynthesis [59]. Hereinafter, a few practical advantages in the applications of microwave heating to labeling with  $^{11}\text{C}$  and  $^{18}\text{F}$  are described.

In radiolabeling with carbon-11, most schemes begin with  $^{11}\text{CO}_2$  and usually require, first, the conversion of  $^{11}\text{CO}_2$  into the necessary small reactive molecules to couple with the compound to label. For every 10 min that a procedure takes with  $^{11}\text{C}$ , the amount of radioactive material and the product's specific activity will decrease by 29% due to the decay of the radionuclide. This eventually entails that, although a radiotracer may be produced in higher chemical yield with longer reaction times, the actual radiochemical yield and specific activity may be reduced by that time to a point where the product cannot be used for its purpose. In this field, the use of fast-performing functionalization reactions to label target molecules is highly necessary [59]. Methods for introducing a  $^{11}\text{C}$  label into an organic molecule include reactions of organometallics with  $^{11}\text{CO}_2$  to give carboxylic acids (or, subsequently, alcohols); N-, O-, S-alkylations using  $^{11}\text{RX}$  ( $\text{R} = \text{CH}_3, \text{Et}, n\text{-Pr}, \text{iso-Pr}$ ;  $\text{X} = \text{I}, \text{OTf}$ ); substitutions/condensations using  $^{11}\text{CN}_2$  to give labeled nitriles (convertible to amines, amides, acids, aldehydes, and alcohols); the formation of C–C bonds with labeled organometallics (e.g.,  $^{11}\text{RLi}$ ,  $^{11}\text{RCuLi}$ , and  $^{11}\text{RMgX}$ ); condensations/substitutions using  $^{11}\text{C}$ -nitroalkanes; C–C bonds via  $^{11}\text{C}$ -ylides or Pd-coupling reactions using  $^{11}\text{RX}$ ; insertions with  $^{11}\text{C}$ -diazomethane; condensations with  $\text{R}^{11}\text{C}(\text{O})\text{X}$  and  $^{11}\text{C}(\text{O})\text{X}_2$ ; and, finally, condensations/reactions with multifunctional precursors. Microwave-assisted techniques have achieved dramatic accelerations in some of these reactions, which under conventional heating require relatively long times and stringent conditions [59].

Elander et al. investigated the use of a microwave resonance cavity to shorten reaction times in two typical radiolabeling reactions with  $^{11}\text{C}$  (Scheme 18.11) [58]; (a) a cyano-dehalogenation reaction and the following hydrolysis of the nitrile and (b) the Bucher–Strecker synthesis of an amino acid from two previous studies chosen for their relative difficulty under thermal conditions (steps from the syntheses of anticancer [ $^{11}\text{C}$ ]busulfan [60] and of DL-[ $^{11}\text{C}$ ]tyrosine [61]).

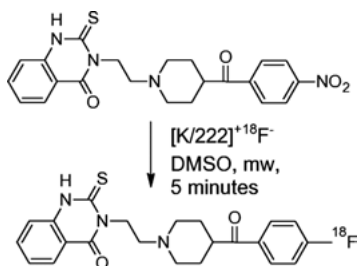


**Scheme 18.11:** Two microwave-assisted radiolabeling reactions performed using [ $^{11}\text{C}$ ]cyanide; X=Br, Cl.

The study, designed to define the time requirements to afford the same yields with microwave and thermal treatment approaches, demonstrated a reduction in all reaction times by using microwave-assisted labeling, leading to end-of-synthesis radioactivity gain (owing to the prevention of decay-caused loss of radioactivity).

Concerning  $^{18}\text{F}$ , its introduction for labeling lead compounds in industrial and medicinal chemistry is widely practiced. Organofluorine chemistry has, however, always been complicated by the necessity to manage the highly reactive electrophilic reagents or to strictly eliminate hydrating agents from fluoride so that its nucleophilic properties can be utilized. The same issues unfortunately come up in PET radiochemistry. Although there are relatively few general methods for labeling molecules with  $^{18}\text{F}$ , this isotope is frequently used mainly because the half-life of nearly 2 h allows not only longer synthetic pathways but also the use of the final product for longer time spans [59]. Strategies for incorporating  $^{18}\text{F}$  into specific positions in organic compounds include electrophilic additions to alkenes and regioselective aromatic substitutions via fluorodemetalation reactions using reagents such as  $^{18}\text{F}_2$  and  $\text{CH}_3\text{COO}^{18}\text{F}$ ; nucleophilic aromatic substitutions using activated substrates and  $^{18}\text{F}_2$  solubilized with aminopolyethers or tetraalkylammonium salts; nucleophilic aliphatic substitutions of halides or sulfonates using  $^{18}\text{F}_2$  solubilized with aminopolyethers or tetraalkylammonium salts; and N-, O-, S-alkylations using  $^{18}\text{F}-(\text{CH}_2)_n\text{X}$  ( $n=2$  or  $3$ , X = halides, sulfonate esters) [59]. All of the listed reactions benefit from microwave irradiation, although some require optimization of the parameters involved. Lemaire et al. reported a microwave-assisted radiosynthesis of [ $^{11}\text{F}$ ]altanserin by nucleophilic





**Scheme 18.12:** Microwave-enhanced radiolabeling of  $[^{18}F]$ altanserin starting from its nitroprecursor.

substitution of the nitro group of precursor nitroaltanserin, previously synthesized from *p*-nitrobenzoyl-4-piperidine (Scheme 18.12) [62].

Altanserin is a fluorobenzoyl derivative structurally related to ketanserin [63]. Based on its *in vitro* binding affinity toward 5 HT<sub>2</sub> receptors (high preference compared to D<sub>2</sub> and α<sub>1</sub>),  $[^{18}F]$ altanserin was considered as a potentially interesting radiotracer for *in vivo* serotonin receptor binding in the CNS; the presented synthesis and HPLC afforded the radiotracer in 40% yield.

Results from the following *in vivo* investigation in rats were consistent with *in vitro* studies and led the way to the use of  $[^{18}F]$ altanserin as a radioligand for PET studies of 5 HT<sub>2</sub> receptors in the living brain [62].

## 18.4 MAE: drug discovery based on natural products

As stated earlier, DD based on organic synthesis is not the only area that has benefited from the introduction of microwave-assisted technologies; a very important application involves the discovery of biologically active compounds found in nature, especially among plants. Extraction constitutes the first crucial step for research and development (R&D) of plant secondary metabolites; the extracts obtained need to undergo further purification and analysis, and the isolated metabolites must be identified and fully characterized. Traditional extraction techniques (i.e., soaking, maceration, water percolation, Soxhlet extraction) often entail long extraction times, which are linked to risks of the degradation of thermolabile active compounds [64, 65]. Over the past two decades, various extraction techniques have been proposed, most of which gave better results in terms of efficiency, extraction time, and amount of solvent used [64, 66–68]. In particular, MAE attracted much interest because of its moderate cost, good performance under atmospheric conditions, high and fast extraction performance ability, low solvent consumption, and protection offered to thermolabile constituents [69–71]. The reason for its high extraction efficiency is linked to its mechanism, which is very different from that, for example, of heat-reflux extraction. The efficiency of MAE strongly relies on the selection of operating conditions and parameters affecting the

extraction mechanisms and yield: the main factors affecting MAE performance are solvent nature and volume, extraction time, microwave power, temperature, sample characteristics, and stirring parameters.

The process of DD greatly benefits from screening of plant-derived compounds due to the structural diversity already present in nature, which took millennia of random mutations and selective evolution for nature to achieve. In this context, MAE is of great importance because it is suitable for the extraction of wide chemical classes of secondary metabolites, such as flavonoids, quinones, phenylpropanoids, terpenoids, and alkaloids, in very short times. To date, MAE must be considered a robust alternative to traditional extraction techniques, especially for analytical purposes and in the early stages of DD. Hereinafter, just two representative examples of MAE applications will be briefly discussed.

In a study aimed at assessing the plant productivity of *Crataegus monogyna* Jacq. (Hawthorn), the influence of the extraction method on the yield of metabolites was evaluated [72]. Hawthorn is among the oldest medicinal plants of the Western world, and the extract from leaves and flowering tops displays numerous pharmacological activities, including sedative, hypotensive, vasodilator, and cardiotonic properties, and they are able to effectively decrease the total amount of cholesterol in plasma [73, 74]. Hawthorn extracts are characterized by the presence of different secondary active metabolites, including procyanidins, flavonoids, and amines. Among the flavonoids, flavonol-O-glycosides (hyperoside, quercetin, rutin), and flavone-C-glycosides (vitexin, vitexin-2''-O-rhamnoside, acetylvitexin-2''-O-rhamnoside) are especially important [75]. Among the tested extraction methods, MAE gave rise to the highest extraction efficiency as well as high reproducibility, and therefore it was proposed as a valid strategy for quick screening of plant materials gathered in various environments to assess Hawthorn productivity and to determine the best ecological conditions for cultivation.

An example of MAE application in the discovery of bioactive compounds regards the discovery of new anti-inflammatory drugs, acting via a TNF $\alpha$  blocking mechanism. Briefly, TNF $\alpha$  is a cytokine involved in different pathophysiological pathways, and blockers for this factor are used in cases of chronic inflammatory diseases (rheumatoid arthritis, bowel diseases, and psoriasis) [76]. Since to date such compounds come mostly from biotech and have not yet been fully evaluated for long-term safety [77], the need for small organic molecules targeting and inhibiting TNF $\alpha$  for the treatment of inflammation-related pathologies is still strongly felt [78, 79]. Studying *Amygdalus lycioides* Spach and combining MAE with a bioassay-guided fractionation approach, (S)-naringenin (Figure 18.1) was identified as the compound responsible for the anti-inflammatory effect, based on a tumor necrosis factor  $\alpha$  (TNF $\alpha$ )-blocking mechanism [80, 81]. This compound could represent the starting point for the development of new treatments of middle-stage psoriasis [82].

To conclude, it is important to underline how advancements in extraction approaches can not only make the extraction step itself more efficient but also help speed

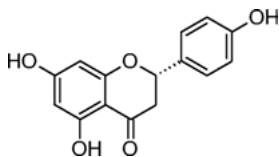


Fig. 18.1: Structure of (S)-naringenin.

up the screening process for new scaffolds with promising activities to then optimize through synthetic and semisynthetic strategies.

## 18.5 MAOS and biotechnology

A great opportunity for the identification of potential new drugs for the treatment of disease comes from the study of human genes and proteins. Information gathered from genome and proteome research have already led to identifying a number of proteins as targets for new drugs. Interestingly, as genetic differences among individuals are found, researchers can study proteins to develop personalized drugs that are more effective for the individual. Biotechnological DD falls into this context, and it exploits a number of experiments including studies of protein–protein interactions [83, 84], processing events [85, 86], and posttranslational modifications [87, 88]. These analyses, aimed at finding either the proteins or the posttranslational modifications with a crucial role in definite cellular pathways, entail the characterization of very complex material, usually in low amounts, and require long timeframes, often imposing limitations on the use of these procedures. Therefore, studies are currently being carried out that combine microwave irradiation and proteomics protocols to reduce sample preparation time and to devise novel work flows to characterize recombinant proteins [89]. Microwave-assisted methods also have great potential in other biotechnological applications; among these, we can mention selective transformations and generation of small collections of molecules, separation of enantiomeric compounds [6], and biopolymer synthesis. Although some of these methods do not yet represent the standard, further advancements in both technology and instrumentation will involve the incorporation of these procedures in day-to-day laboratory life. Hereinafter, examples of microwave-enhanced biotechnological applications will be briefly discussed.

Microwave-assisted enzyme catalysis had its first application with enzymatic hydrolysis reactions for protein digestion in proteomic analysis. Chen and coworkers [90] successfully enhanced the rate of hydrolysis of peptides and proteins in a 6 M HCl solution in a closed system, and Pramanik et al. [91] achieved the complete digestion of several known biologically active proteins within a few minutes, in comparison with the several hours needed under normal methods. In all cases, microwave-assisted protein digestion afforded complete digestion even for tightly folded proteins such as ubiquitin, which entails longer timeframes for enzymatic digestion when using conventional methods; in general, this approach improved the digestion efficiency com-

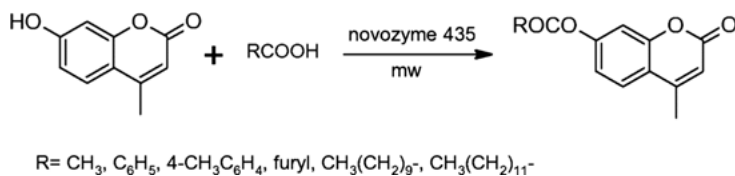
pared to traditional conditions and achieved complete digestion within 10 min [92]. Moreover, in the context of DD where the aim is to characterize definite proteins, researchers are often dealing with low (subfemtomole) amounts. Microwave-enhanced tryptic digestions achieve higher peptide retrieval along with better sensitivity in a significantly shorter incubation time compared to conventional protocols, and it has been suggested that shorter incubation times also significantly decrease adhesion of peptides derived from proteolysis to vial walls, affording in the end higher amounts of peptides. In addition, microwave-assisted enzymatic digestion permits identification of proteins or posttranslational modifications even in low quantities, which would not be feasible using traditional methods [89].

In addition to enzyme-mediated procedures enhanced by microwave irradiation, several microwave-assisted protocols for proteomics exist for protein quantitation [93, 94] and sequencing [95], as for specific molecular weight (MW), including sample preparation, purity, and monoclonality analysis of monoclonal antibodies (MAB) used as biotherapeutics [96, 97]. Most of the protocols for protein processing exploit microwave-assisted acid hydrolysis (MAAH) [98]; this method involves the hydrolysis of the protein of interest in acid for a brief time period (2 min) under microwave irradiation, and, though not universally applicable, it shows great versatility. Moreover, MAAH has shown results consistent with those obtained with much more time-consuming conventional hydrolysis procedures, and nowadays MAAH kits are commercially available for a number of applications, rendering this technology more widely available [89].

It is thus clear, as previously stated, that advances in the field of proteomics not only have been and still are among the main factors that oblige and allow for the development of new and improved techniques for, among other disciplines, DD, but efforts are continuously being made to push for the progress of proteomics itself. In this context, we cannot forget that nucleic acids are of high importance for both therapeutic [99–102] and chemical applications [103]. The need to produce large amounts of nucleic acids prompted the development of microfluidic microwave heating devices for small volumes of solution. An interesting application of such devices is the polymerase chain reaction (PCR), an enzyme-mediated technique used for the amplification of DNA sequences. PCR produces amplifications of orders of magnitude starting from a few copies of DNA strands through thermal cycles by employing a heat-stable DNA polymerase. Despite its great qualities, which include versatility and a need for very small amounts of starting materials (1 pg–1 µg depending on the DNA source [104]), PCR can still have some limitations, in connection with timeframes (particularly related to heating cycles) and scaling up, especially when compared to the demands of pharmaceutical research and industry (these factors often limit the reaction volume to 0.2 mL); from this perspective, microwave-enhanced approaches may once again come to the rescue. In 2004, Gullberg et al. performed a proof-of-principle study on the suitability of microwaves for PCR on the milliliter scale [105]; upon the variation of parameters such as process thermal cycle temperatures and intervals and reaction vol-

ume (starting from 2.5 mL up to 15 mL), the group achieved a 92 to 100% amplification efficiency and temperature profiles currently not achievable on this scale through conventional heating techniques. Thermal cycles were controlled through two detectors, an infrared pyrometer detecting the temperature of the surface layer and a fluoroptic probe located inside the vessel. Moreover, the enzyme used, Taq polymerase, proved to resist 33 microwave pulses while maintaining equivalent efficiency regardless of the heating method used [105]. To sum up, a controlled microwave methodology for rapid milliliter-scale PCR is available and can be successfully employed for the amplification of DNA using heating rates and quantities an order of magnitude faster and larger than currently marketed instruments.

Biocatalysis is also used in the synthesis of NCEs and related intermediates and is often employed for its qualities regarding chemo-, regio-, stereo-, enantio-, and diastereoselectivity. Microwave irradiation can increase the rate of enzymatic reactions, leaving the structure of enzyme molecules unchanged; accordingly, this methodology may be used for obtaining chiral molecules on large scales and at relatively low costs [6]. Indeed, enzyme-catalyzed resolution of racemic compounds has shown to be a valid alternative to other procedures. However, while biocatalyzed reactions have attracted great attention for the synthesis of enantiomerically pure compounds, they are slow and involve long timeframes. Aside from its use in single transformations in synthetic pathways for biologically interesting compounds, enzyme catalysis may also be used to produce small collections of molecules to screen for activity. On this note, while studying the synergism between biocatalysis and microwave heating for the acylation of 7-hydroxy-4-methyl-2*H*-chromene-2-one with different fatty acids, Kidwai et al. [106] developed a small series of 7-hydroxy-4-methyl-2*H*-chromene-2-one derivatives (Scheme 18.13); this molecule is one of the members of the benzopyrone family and is already used for various pharmaceutical applications. Derivatization has led to diverse molecules with distinctive biological properties.



**Scheme 18.13:** Microwave-assisted acylation of 7-hydroxy-4-methyl-2*H*chromene-2-one catalyzed by novozyme 435.

Among other applications, microwave-assisted enzymatic polymerizations are attracting growing attention due to the relatively newfound synergism of lipase (and biocatalysis in general) and microwave irradiation [107, 108]. In addition, given the rising interest surrounding the use of biopolymers in medicine and pharmaceuticals [109]

(for delivery, implants, and sutures, for example) and the design and development of functionalized biopolymers with innate antimicrobial activity [110, 111], it is becoming fairly obvious that fast and efficient synthetic methods for identification, optimization, and, eventually, production of these polymers are needed; further research in this area is still required, and it holds great promise.

Microwave-enhanced enzyme catalysis is still rather new, and so far studies have mainly focused on hydrolytic enzymes; it is evident that deeper research on microwave coupling to other classes of enzymes is still required. Furthermore, the exact mechanism behind the interaction between microwave irradiation and proteins is still a subject of debate (it has been proposed that either the increased, more controlled, and quickly reached temperatures or the enhanced agitation derived from the dipolar rotation of molecules accounts for the improved procedure efficiency [112]); when clarified, the acquired knowledge will allow for further utilization of related technologies [89].

## 18.6 Conclusions

Owing to the rise of the number of drug targets in the last 30 years, pharmaceutical researchers, in both industry and academia, are evidently under a growing amount of pressure to increase R&D productivity [113]. The development of technologies and related instrumentation deeply influences the pace of the DD process, with a great impact on the subsequent phases concerning both drug development and clinical stages. The advent of microwave-assisted technologies, among others, in the fields of synthesis (MAOS), extraction (MAE), and, more recently, biotechnology, has opened the way to newer, faster approaches to the discovery of new potential drugs. The best results so far obtained come mainly from coupling with other high-performing approaches and technologies. The advantages of combining microwave heating technology with combinatorial chemistry, or better with synthetic processes in general, and with extraction from natural matrices mainly include reduced reaction times, an increase in the purity of resulting products, and an enhancement of chemical yields, thus speeding up the entire process. To date, microwave heating is undoubtedly a milestone for medicinal chemistry researchers and must be considered the first choice for carrying out synthetic transformations requiring heat. For this reason we believe that in the near future microwave synthesizers will be a standard technology present in most laboratories.

To conclude, DD remains a challenging and demanding interdisciplinary process. A full combination of strategies and techniques is required to achieve results. Strength in this field is gained through the combination of various techniques and the collaboration of researchers working in different disciplines. It is clear that interdisciplinarity is key, and an open dialogue between different scientific professions is the only way to allow for an increase in the knowledge of the human body, the mechanisms in-

volved in pathogenesis, and the ways we can interact with these pathways to improve our lives. Microwave chemistry has already been successfully coupled with other technologies and strategies, as discussed earlier. Considering the success thus far obtained from combining multidisciplinary approaches with microwave heating, we strongly encourage scientists, and students in particular, to explore new areas of application in the wide world of pharmaceutical research.

## Bibliography

- [1] Tapas AR, Magar DD, Kawtikwar PS, Sakarkar DM, Kakde RB. Microwaves in drug discovery and development: A review. *Int J PharmTech Res.* 2009, 1, 1039–1050.
- [2] Santagada V, Frecentese F, Perissutti E, Favretto L, Caliendo G. The application of microwaves in combinatorial and high-throughput synthesis as new synthetic procedure in drug discovery. *QSAR Comb Sci.* 2004, 23, 919–944.
- [3] Pandeya SN, Thakkare D. Combinatorial chemistry: a novel method in drug discovery and its application. *Indian Journal of Chemistry.* 2005, 44B, 335–348.
- [4] Combinatorial Chemistry, 2012 (Accessed July 8, 2016, at [www.screening-compounds.com](http://www.screening-compounds.com))
- [5] Kappe CO. High-speed combinatorial synthesis utilizing microwave irradiation. *Curr Opin Chem Biol.* 2002, 6, 314–320.
- [6] Yadav GD, Devendran S. Microwave Assisted Enzyme Catalysis: Practice and Perspective. In: Coelho MAZ, Ribeiro BD. *White Biotechnology for Sustainable Chemistry.* Cambridge, UK, The Royal Society of Chemistry. 2016, 52–103.
- [7] Kappe CO, Dallinger D. The impact of microwave synthesis on drug discovery. *Nature Reviews Drug Discovery,* 2006, 5, 51–63.
- [8] Nascimento-Júnior NM, Kummerle AE, Barreiro EJ, Fraga CAM. MAOS and Medicinal Chemistry: Some Important Examples from the Last Years. *Molecules.* 2011, 16, 9274–9297.
- [9] Ajani OO, Obafemi CA, Nwinyi OC, Akinpelu DA. Microwave assisted synthesis and antimicrobial activity of 2-quinoxalinone-3-hydrazone derivatives. *Bioorg Med Chem.* 2010, 18, 214–221.
- [10] Rossi D, Carnevale Baraglia A, Serra M, Azzolina O, Collina S. An Efficient Procedure Based on a MW-Assisted Horner–Wadsworth–Emmons Reaction for the Synthesis of (Z)-3,3-Trisubstituted-unsaturated Esters. *Molecules.* 2010, 15, 5928–5942.
- [11] Sano S, Takehisa T, Ogawa S, Yokoyama K, Nagao Y. Stereoselective synthesis of tetrasubstituted (Z)-alkenes from aryl alkyl ketones utilizing the Horner–Wadsworth–Emmons reaction. *Chem Pharm Bull.* 2002, 50, 1300–1302.
- [12] Hugel HM. Microwave multicomponent synthesis. *Molecules.* 2009, 14, 4936–4972.
- [13] Wannberg J, Dallinger D, Kappe CO, Larhed M. Microwave-Enhanced and Metal-Catalyzed Functionalizations of the 4-Aryl-Dihydropyrimidone Template. *J Comb Chem.* 2005, 7, 574–583.
- [14] Stadler A, Kappe CO. Automated Library Generation Using Sequential Microwave-Assisted Chemistry. Application toward the Biginelli Multicomponent Condensation. *J Comb Chem.* 2001, 3, 624–630.
- [15] Kappe CO. Biologically active dihydropyrimidones of the Biginelli-type – a literature survey. *Eur J Med Chem.* 2000, 35, 1043–1052.
- [16] Heys L, Moore CG, Murphy PJ. The guanidine metabolites of *Ptilocaulis spiculifer* and related compounds; isolation and synthesis. *Chem Soc Rev.* 2000, 29, 57–67.

- [17] Kirschning A, Monenschein H, Wittenberg R. Functionalized polymers – emerging versatile tools for solution-phase chemistry and automated parallel synthesis. *Angew Chem Int Ed Engl.* 2001, 40, 650–679.
- [18] Urbano M, Collina S, Rossi D, Carnevale Baraglia A, Alcaro S, Artese A, Azzolina O. Design and Synthesis of a (N-Alkylaminoalkyl-Substituted)Arylalkenylamide. *Drug Discovery Library Letters in Drug Design & Discovery.* 2007, 4, 605–610.
- [19] Kappe CO. Speeding up solid-phase chemistry by microwave irradiation. A tool for high-throughput synthesis. *Am Lab.* 2001, 33, 13–19.
- [20] Wathey B, Tierney J, Lidström P, Westman J. The impact of microwave-assisted organic chemistry on drug discovery. *DDT.* 2006, 7, 373–380.
- [21] Lidström P, Tierney J, Wathey B, Westman J. Microwave-assisted organic synthesis – a review. *Tetrahedron.* 2001, 57, 9225–9283.
- [22] Habermann J, Ley SV, Scott JS. Synthesis of the potent analgesic compound (+/-)-epibatidine using an orchestrated multi-step sequence of polymer supported reagents. *J Chem Soc. Perkin Trans.* 1999, 1, 1253–1255.
- [23] Yamada K, Nagashima I, Hachisu M, Matsuo I, Shimizu H. Efficient solid-phase synthesis of cyclic RGD peptides under controlled microwave heating. *Tetrahedron Letters.* 2012, 53, 1066–1070.
- [24] Kappe CO, Kumar D, Varma RS. Microwave-assisted high-speed parallel synthesis of 4-aryl-3,4 dihydropyrimidin-2(1H)-ones using a solventless Biginelli condensation protocol. *Synthesis.* 1999, 10, 1799–1803.
- [25] Varma RS, Kumar D. Microwave-accelerated three-component condensation reaction on clay: solvent-free synthesis of imidazo[1,2-a] annulated pyridines, pyrazines and pyrimidines. *Tetrahedron Lett.* 1999, 40, 7665–7669.
- [26] Usyatinsky AY, Khmel'nitsky YL. Microwave-assisted synthesis of substituted imidazoles on a solid support under solvent-free conditions. *Tetrahedron Lett.* 2000, 41, 5031–5034.
- [27] Olsson R, Hansen HC, Andersson CM. Microwave-assisted solvent-free parallel synthesis of thioamides. *Tetrahedron Lett.* 2000, 41, 7947–7950.
- [28] Larhed M, Hallberg A. Microwave-assisted high-speed chemistry: a new technique in drug discovery. *DDT.* 2001, 6, 406–416.
- [29] Collina S, Loddo G, Barbieri A, Linati L, Alcaro S, Chimenti P, Azzolina O. Microwave assisted synthesis of chiral pyrrolines with biological activity. *Tetrahedron: Asymmetry.* 2004, 15, 3601–3608.
- [30] Williams L. Thin layer chromatography as a tool for reaction optimization in microwave-assisted synthesis. *Chem Commun.* 2000, 6, 435–436.
- [31] Popovic M, Stanojevic Z, Tosic J, Isakovic A, Paunovic V, Petricevic A, Martinovic T, Ciric D, Kravic-Stevovic T, Soskic V, Kostic-Rajacic S, Shakib K, Bumbasirevic V, Trjkovic V. Neuroprotective arylpiperazine dopaminergic/serotonergic ligands suppress experimental autoimmune encephalomyelitis in rats. *J Neurochem.* 2015, 135, 125–138.
- [32] Cotterill IC, Usyatinsky AY, Arnold JM, Clark DS, Dordick JS, Michels PC, Khmel'nitsky YL. Microwave-assisted combinatorial chemistry, synthesis of substituted pyridines. *Tetrahedron Lett.* 1998, 39, 1117–1120.
- [33] Chaubey A, Pandeya SN. Pyridine a versatile nucleuse in pharmaceutical field. *Asian J Pharm Clin Res.* 2011, 4, 5–8.
- [34] Polshettiwar V, Varma RS. Aqueous microwave chemistry: a clean and green synthetic tool for rapid drug discovery. *Chem Soc Rev.* 2008, 37, 1546–1557.
- [35] Plechkova NV, Seddon KR. Applications of ionic liquids in the chemical industry. *Chem Soc Rev.* 2008, 37, 123–150.



- [36] Leadbeater NE, Marco M. Rapid and Amenable Suzuki Coupling Reaction in Water Using Microwave and Conventional Heating. *J Org Chem.* 2003, 68, 888–892.
- [37] Crozet MD, Castera-Ducros C, Vanelle P. An efficient microwave-assisted Suzuki cross-coupling reaction of imidazo[1,2-a]pyridines in aqueous medium. *Tetrahedron Lett.* 2006, 47, 7061–7065.
- [38] Miyaura N, Yamada K, Suzuki A. A new stereospecific cross-coupling by the palladium-catalyzed reaction of 1-alkenylboranes with 1-alkenyl or 1-alkynyl halides. *Tetrahedron Lett.* 1979, 36, 3437–3440.
- [39] Arvela RK, Leadbeater NE. Microwave-Promoted Heck Coupling Using Ultralow Metal Catalyst Concentrations. *J Org Chem.* 2005, 70, 1786–1790.
- [40] Arvela RK, Pasquini S, Larhed M. Highly Regioselective Internal Heck Arylation of Hydroxyalkyl Vinyl Ethers by Aryl Halides in Water. *J Org Chem.* 2007, 72, 6390–6396.
- [41] Arfan M, Khan R, Anjum S, Ahmad S, Choudhary MI. Water promoted, microwave assisted oxidative novel deamination of N-amino quinazolinones. *Chin Chem Lett.* 2008, 19, 161–165.
- [42] Rottger S, Sjöberg PJR, Larhed M. Microwave-Enhanced Copper-Catalyzed N-Arylation of Free and Protected Amino Acids in Water. *J Comb Chem.* 2007, 9, 204–209.
- [43] Wu X, Larhed M. Microwave-Enhanced Aminocarbonylations in Water. *Org. Lett.* 2005, 7, 3327–3329.
- [44] Garuti L, Roberti M, Pizzirani D. Nitrogen-containing heterocyclic quinones: a class of potential selective antitumor agents. *Mini-Rev Med Chem.* 2007, 7, 481–489.
- [45] Sperry JB, Wright DL. Furans, thiophenes and related heterocycles in drug discovery. *Curr Opin Drug Discovery Dev.* 2005, 8, 723–740.
- [46] Ju Y, Varma RS. Microwave-assisted cyclocondensation of hydrazine derivatives with alkyl dihalides or ditosylates in aqueous media: syntheses of pyrazole, pyrazolidine and phthalazine derivatives. *Tetrahedron Lett.* 2005, 46, 6011–6014.
- [47] Ju Y, Varma RS. An Efficient and Simple Aqueous N-Heterocyclization of Aniline Derivatives: Microwave-Assisted Synthesis of N-Aryl Azacycloalkanes. *Org Lett.* 2005, 7, 2409–2411.
- [48] Ju Y, Varma RS. Aqueous N-Heterocyclization of Primary Amines and Hydrazines with Dihalides: Microwave-Assisted Syntheses of N-Azacycloalkanes, Isoindole, Pyrazole, Pyrazolidine, and Phthalazine Derivatives. *J Org Chem.* 2006, 71, 135–141.
- [49] Tan, DS. Diversity-oriented synthesis: exploring the intersections between chemistry and biology. *Nature Chem Biol.* 2005, 1, 74–84.
- [50] Fergus S. Assessment of structural diversity in combinatorial synthesis. *Curr Opin Chem Biol.* 2005, 9, 304–309.
- [51] Zhao Z, Leister WH, Strauss KA, Wisnoski DD, Lindsley CW. Broadening the scope of 1,2,4-triazine synthesis by the application of microwave technology. *Tetrahedron Lett.* 2003, 44, 1123–1127.
- [52] Lindsley CW, Zhao Z, Leister WH, Robinson RG, Barnett SF, Defeo-Jones D, Jones RE, Hartman GD, Huff JR, Huber HE, Duggan ME. Allosteric Akt (PKB) inhibitors: discovery and SAR of isozyme selective inhibitors. *Bioorg Med Chem Lett.* 2005, 15, 761–764.
- [53] Zhao Z, Wisnoski DD, Wolkenberg SE, Leister WH, Wang Y, Lindsley CW. General microwave-assisted protocols for the expedient synthesis of quinoxalines and heterocyclic pyrazines. *Tetrahedron Lett.* 2004, 45, 4873–4876.
- [54] Wolkenberg SE, Wisnoski DD, Leister WH, Wang Y, Zhao Z, Lindsley CW. Efficient synthesis of imidazoles from aldehydes and 1,2-diketones using microwave irradiation. *Org Lett.* 2004, 6, 1453–1456.
- [55] Lindsley CW, Wisnoski DD, Wang Y, Leister WH, Zhao Z. A one pot microwave-mediated synthesis of the basic canthine skeleton: expedient access to unnatural  $\beta$ -carboline alkaloids. *Tetrahedron Lett.* 2003, 44, 4495–4498.

- [56] Zhao Z, Leister WH, Robinson RG, Barnett SF, Defeo-Jones D, Jones RE, Hartman GD, Huff JR, Huber HE, Duggan ME, Lindsley CW. Discovery of 2, 3, 5-trisubstituted pyridine derivatives as potent Akt1 and Akt2 dual inhibitors. *Bioorg Med Chem Lett*. 2005, 15, 905–909.
- [57] Gali-Muhtasib HU, Haddadin MJ, Rahhal DN, Younes IH. Quinoxaline 1,4-dioxides as anti-cancer and hypoxia-selective drugs. *Oncol Rep*. 2001, 8, 679–684.
- [58] Thorell JO, Stone-Elander S, Elander N. Use of a microwave cavity to reduce reaction times in radiolabeling with  $[11\text{C}]$ cyanide. *J Label Compd Radiopharm*. 1992, 31, 207–217.
- [59] Elander N, Jones JR, Lub SY, Stone-Elander S. Microwave enhanced radiochemistry. *Chem Soc Rev*. 2000, 29, 239–249.
- [60] Hassan M, Thorell JO, Warne N, Stone-Elander S.  $11\text{C}$ -labeling of busulphan. *Appl. Radiat. Isot*. 1991, 42, 1055.
- [61] Halldin C, Schoeps KO, Stone-Elander S, Wiesel FA. The Bücherer-Strecker synthesis of d- and l-(1– $11\text{C}$ )tyrosine and the in vivo study of l-(1– $11\text{C}$ )tyrosine in human brain using positron emission tomography. *Eur J Nucl Med*. 1987, 12, 288.
- [62] Lemaire C, Cantineau R, Guillaume M, Plenevaux A, Christiaens L. fluorine- 18-Altanserin: A Radioligand for the Study of Serotonin Receptors with PET: Radiolabeling and In Vivo Biologic Behavior in Rats. *The Journal of Nuclear Medicine*. 1991, 32, 2266–2272.
- [63] Lemaire C, Cantineau R, Christiaens L, Guillaume M. NCA adiofluorination of altanserin as a potential serotonin receptor-binding radiopharmaceutical for positron emission tomography. *J Labelled Compd Radiopharm*. 1988, 26, 336–337.
- [64] Chan CH, Yusoff R, Ngoh GC, Kung FW. J. *Chromatogr. A*. 2011, 1218, 6213–6225.
- [65] Luque de Castro MD, Garcia-Ayuso LE. Anal. Soxhlet extraction of solid materials: an outdated technique with a promising innovative future. *Chim Acta*. 1998, 369, 1–10.
- [66] Ondruschka B, Asghari J. Microwave-Assisted Extraction – A State-of-the-Art Overview of Varieties. *Chimia*. 2006, 60, 321–325.
- [67] Herrero M, Mendiola JA, Cifuentes A, Ibáñez EJ. Supercritical fluid extraction: Recent advances and applications. *Chromatogr A*. 2010, 1217, 2495–2511.
- [68] Wang L, Weller CL. Recent advances in extraction of nutraceuticals from plants. *Trends Food Sci Technol*. 2006, 17, 300–312.
- [69] Sparr Eskilsson C, Björklund E. Analytical-scale microwave-assisted extraction. *J Chromatogr A*. 2000, 902, 227–250.
- [70] Li H, Li G, Zhang Z. Chin. Development of Microwave Assisted Extraction. *J Anal Chem*. 2003, 31, 1261–1268.
- [71] Mandal V, Mohan Y, Hemalatha S. Microwave assisted extraction – an innovative and promising extraction tool for medicinal plant research. *Pharmacognosy Reviews*. 2007, 1, 7–18.
- [72] Martino E, Collina S, Rossi D, Bazzoni D, Gaggeri R, Bracco F, Azzolina O. Influence of the Extraction Mode on the Yield of Hyperoside, Vitexin and Vitexin-2'' -O Rhamnoside from *Crataegus monogyna* Jacq. (Hawthorn). *Phytochem Anal*. 2008, 19, 534–540.
- [73] Prabhakar MC, Bano H, Kumar I, Shamsi MA, Khan SY. Pharmacological investigations on vitexin. *Planta Med*. 1981, 43, 396–403.
- [74] Weihmayr T, Ernst E. Therapeutic effectiveness of *Crataegus*. *Fortschr Med*. 1996, 114, 27–29.
- [75] Rehwald A, Meier B, Sticher O. Qualitative and quantitative reversed-phase high-performance liquid chromatography of flavonoids in *Crataegus* leaves and flowers. *J Chromatogr A*. 1994, 677, 25–33.
- [76] Ornetti P, Chevillote H, Zerrak A, Maillerfert JF. Anti-tumor necrosis factor-alpha therapy for rheumatoid and other inflammatory arthropathies: Update on safety in older patients. *Drug Aging*. 2006, 23, 855–860.
- [77] Bachamm F, Nast A, Sterry W, Philipp S. Safety and efficacy of the tumor necrosis factor antagonists. *Semin Cutan Med Surg*. 2010, 29, 35–47.

- [78] Mossner R, Schon MP, Reich K. Tumor necrosis factor antagonists in the therapy of psoriasis. *Clin Dermatol*. 2008, 26, 486–502.
- [79] Reimold AM. TNF $\alpha$  as therapeutic target: New drugs, more applications. *Curr Drug Targets Inflamm Allergy*. 2002, 1, 377–392.
- [80] Gaggeri R, Rossi D, Christodoulou MS, Passarella D, Leoni F, Azzolina O, Collina S. Chiral Flavanones from *Amygdalus lycioides* Spach: Structural Elucidation and Identification of TNF $\alpha$  Inhibitors by Bioactivity-guided Fractionation. *Molecules*. 2012, 17, 1665–1674.
- [81] Gaggeri R, Rossi D, Hajikarimian N, Martino E, Bracco F, Grisoli P, Dacarro C, Leoni F, Mascheroni G, Collina S. Preliminary study on TNF $\alpha$ -blocker activity of *Amygdalus lycioides* Spach extracts. *Open Nat Prod J*. 2010, 3, 20–25.
- [82] Chlapanidas T, Perteghella S, Leoni F, Faragò S, Marazzi M, Rossi D, Martino E, Gaggeri R, Collina S. TNF- $\alpha$  Blocker Effect of Naringenin-Loaded Sericin Microparticles that Are Potentially Useful in the Treatment of Psoriasis. *Int J Mol Sci*. 2014, 15, 13624–13636.
- [83] Kayagaki N, Phung Q, Chan S, Chaudhari R, Quan C, O'Rourke KM, Eby M, Pietras E, Cheng G, Bazan JF, Zhang Z, Arnott D, Dixit VM. A deubiquitinase that regulates type I interferon production. *Science*. 2007, 318, 1628–1632.
- [84] Dornan D, Wertz I, Shimizu H, Arnott D, Frantz GD, Dowd P, O'Rourke K, Koeppen H, Dixit VM. The ubiquitin ligase COP1 is a critical negative regulator of p53. *Nature*. 2004, 429, 86–92.
- [85] Kirchhofer D, Lipari MT, Santell L, Billeci KL, Maun HR, Sandoval WN, Moran P, Ridgway J, Eigenbrot C, Lazarus RA. Utilizing the activation mechanism of serine proteases to engineer hepatocyte growth factor into a Met antagonist. *Proc Natl Acad Sci. USA*. 2007, 104, 5306–5311.
- [86] Edosada CY, Quan C, Tran T, Pham V, Wiesmann C, Fairbrother W, Wolf BB. Peptide substrate profiling defines fibroblast activation protein as an endopeptidase of strict Gly(2)-Pro(1)-cleaving specificity. *FEBS Lett*. 2006, 580, 1581–1586.
- [87] Mollah S, Wertz IE, Phung Q, Arnott D, Dixit VM, Lill JR. Targeted mass spectrometric strategy for global mapping of ubiquitination on proteins. *Rapid Commun Mass Spectrom*. 2007, 21, 3357–3364.
- [88] Olsen JV, Blagoev B, Gnäd F, Macek B, Kumar C, Mortensen P, Mann M. Global, in vivo, and site-specific phosphorylation dynamics in signaling networks. *Cell*. 2006, 127, 635–648.
- [89] Sandoval WN, Pham VC, Lill JR. Recent developments in microwave-assisted protein chemistries – can this be integrated into the drug discovery and validation process? *Drug Discovery Today*. 2008, 13, 1075–1081.
- [90] Chen ST, Chiou SH, Wang KT. Enhancement of Chemical Reactions by Microwave Irradiation. *J Chin Chem Soc*. 1991, 38, 85–91.
- [91] Pramanik BN, Mirza UA, Ing YH, Liu YH, Bartner PL, Weber PC, Bose AK. Microwave-enhanced enzyme reaction for protein mapping by mass spectrometry: a new approach to protein digestion in minutes. *Protein Sci*. 2002, 11, 2676–2687.
- [92] Lin SS, Wu CH, Sun MC, Sun CM, Ho YP. Microwave-assisted enzyme-catalyzed reactions in various solvent systems. *J Am Soc Mass Spectrom*. 2005, 16, 581–588.
- [93] Chiou SH, Wang KT. A rapid and novel means of protein hydrolysis by microwave irradiation using Teflon–Pyrex tubes. In: Villafranca JJ. *Current Research in Protein Chemistry: Techniques, Structure, and Function*. San Diego, CA, USA, Academic Press, 1990, 3–10.
- [94] Davidson I. Hydrolysis of samples for amino acid analysis. In: Smith BJ. *Methods in Molecular Biology*. Totowa, NJ, Humana Press, 1996, 119–129.
- [95] Zhong H, hang Y, Wen Z, Li L. Protein sequencing by mass analysis of polypeptide ladders after controlled protein hydrolysis. *Nat. Biotechnol*. 2004, 22, 1291–1296.
- [96] Sandoval W, Pham V, Ingle ES, Liu PS, Lill JR. Applications of microwave-assisted proteomics in biotechnology. *Comb Chem. High Throughput Screen*. 2007, 10, 751–765.

- [97] Lee BS, Krishnanchettiar S, Lateef SS, Lateef NS, Gupta S. Characterization of oligosaccharide moieties of intact glycoproteins by microwave-assisted partial acid hydrolysis and mass spectrometry. *Rapid Commun Mass Spectrom*. 2005, 19, 2629–2635.
- [98] Lill JR, Ingle ES, Liu PS, Pham V, Sandoval WN. Microwave-assisted proteomics. *Mass Spectrom Rev*. 2007, 26, 657–671.
- [99] Bock LC, Griffin LC, Latham JA, Vermaas EH, Toole JJ. Selection of single-stranded DNA molecules that bind and inhibit human thrombin. *Nature*. 1992, 355, 564–566.
- [100] Lorsch JR, Szostak JW. Chance and necessity in the selection of nucleic acid catalysts. *Acc Chem Res*. 1996, 29, 103–110.
- [101] King DJ, Ventura DA, Brasier AR, Gorenstein DG. Novel combinatorial selection of phosphorothioate oligonucleotide aptamers. *Biochemistry*. 1998, 37, 16489–16493.
- [102] Green LS, Jellinek D, Jenison R, Ostman A, Heldin CH, Janjic N. Inhibitory DNA ligands to platelet-derived growth factor B-chain. *Biochemistry*. 1996, 35, 14413–14424.
- [103] Stuhlmann F, Jaschke A. Characterization of an RNA Active Site: Interactions between a Diels-Alderase Ribozyme and Its Substrates and Products. *J Am Chem Soc*. 2002, 124, 3238–3244.
- [104] Guidelines for PCR Optimization with Taq DNA Polymerase, New England BioLabs Inc., 2016. (Accessed October 10, 2016, at [www.neb.com/](http://www.neb.com/))
- [105] Orling K, Nilsson P, Gullberg M, Larhed M. An Efficient Method to Perform Milliliter-Scale PCR Utilizing Highly Controlled Microwave Thermocycling. *Chem Commun*. 2004, 790–791.
- [106] Kidwai M, Mothra P, Podder R. Enzyme catalyzed acylation of 7-hydroxy-4-methyl-2H-chromene-2-one using microwave. *Ind J Chem*. 2009, 48, 1307–1310.
- [107] Mahapatro A, Matos Negrón TD. Biodegradable poly-pentadecalactone (PDL) synthesis via synergistic lipase and microwave catalysis. *Am J Biomed Eng*. 2013, 3, 9–13.
- [108] Matos TD, King N, Simmons L, Walker C, McClain AR, Mahapatro A, Rispoli FJ, McDonnell KT, Shah V. Microwave assisted lipase catalyzed solvent-free polycaprolactone synthesis. *Green Chem Lett Rev*. 2011, 4, 73–79.
- [109] Ulery BD, Nair LS, Laurencin CT. Biomedical applications of biodegradable polymers. *J Polym Sci B Polym Phys*. 2011, 12, 832–864.
- [110] Iqbal HM, Kyazze G, Locke IC, Tron T, Keshavarz T. Development of bio-composites with novel characteristics: Evaluation of phenol-induced antibacterial, biocompatible and biodegradable behaviours. *Carbohydrate Polymers*. 2015, 131, 197–207.
- [111] Iqbal HM, Kyazze G, Locke IC, Tron T, Keshavarz T. Development of novel antibacterial active, HaCaT biocompatible and biodegradable CA-g-P(3HB)-EC biocomposites with caffeic acid as a functional entity. *eXPRESS Polymer Letters*. 2015, 9, 764–772.
- [112] Collins JM, Leadbeater NE. Microwave energy: a versatile tool for the biosciences. *Org Biomol Chem* 2007, 5, 1141–1150.
- [113] Wagner R. Microwave-assisted synthesis in the pharmaceutical industry a current perspective and future prospects. *Drug Discovery World Summer* 2006, 59–66.

Karin Engen, Jonas Sävmarker, Luke R. Odell, and Mats Larhed

## 19 Microwave heating in medicinal chemistry

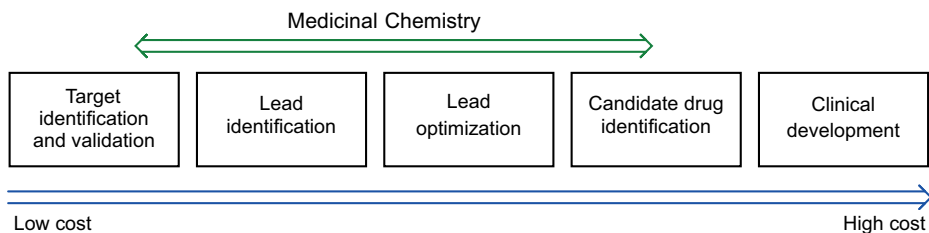
### 19.1 Introduction

All major scientific disciplines constantly redefine their purposes and goals. This is true also of medicinal chemistry, a field that, according to Burger [1], ‘tries to be based on the ever-increasing hope that biochemical rationales for drug discovery may be found.’ Medicinal chemistry is a hybrid discipline and its definition and progress have evolved over time; in 1998 the International Union of Pure and Applied Chemistry (IUPAC) defined medicinal chemistry as

‘a chemistry-based discipline, also involving aspects of biological, medical and pharmaceutical sciences. It is concerned with the invention, discovery, design, identification and preparation of biologically active compounds, the study of their metabolism, the interpretation of their mode of action at the molecular level and the construction of structure-activity relationships’.

A drug discovery program often starts with the identification of a medical need and an idea of how to address it by interacting with an identified key protein (the target). A series of activities follows that are both iterative and parallel with the goal of launching a new drug on the market at the end of the program (Figure 19.1). The role of medicinal chemistry in this process is chiefly concerned with three main stages: lead identification, lead optimization, and candidate drug identification.

The identification of a so-called hit molecule (a substance that modulates the target of interest) is crucial for an early project to move forward. A number of different hit identification strategies make use of different chemical substance screening approaches. One of the most common techniques is known as high-throughput screening (HTS), which relies on the rapid evaluation of large collections of compounds (chemical libraries). After identifying a biologically active hit molecule, for example via HTS, the goal of an early preclinical drug discovery project is most often to identify one or more compounds (leads) that have appropriate chemical and



**Fig. 19.1:** Principal stages of drug discovery and development.

<https://doi.org/10.1515/9783110479935-019>

biological properties to serve as starting points for further optimization. Thus, a lead compound has biological activity that is likely to be of therapeutic value; however, the structure is still suboptimal and requires further modification to, for example, increase binding to the target protein or selectivity toward other proteins and improve pharmacokinetic properties (e.g., metabolism, cell permeability, solubility). This is achieved by altering the lead compound structure through the chemical synthesis of new analogs and subsequent *in vitro* evaluation in an iterative manner. This process is time consuming and seldom trivial, and there is a constant demand for new, fast, efficient, and reliable synthetic methods for the rapid synthesis of new and improved analogs. The most promising molecules are then selected for further development and *in vivo* evaluation. These advanced, optimized compounds are called *candidate drugs*. The most promising molecules are then selected for further development and *in vivo* evaluation. Medicinal chemistry concerns mainly the principal stages: lead identification, lead optimization, and candidate drug identification (Figure 19.1).

Today, the modern molecular biology revolution has had a major impact on drug discovery, and this has provided both new challenges and opportunities for the medicinal chemist. Despite the development of modern biology and computer-based methods for drug design, the art of organic synthesis is still a significant key component of medicinal chemistry owing to the constant need to prepare improved test molecules for biological evaluation. There is little doubt that in the future new processes for *rational drug design* or *computer-based virtual screening* will become increasingly important, but at the present time the preparation of organic molecules for HTS and active-molecule development (lead identification and lead optimization) still constitute important and widely employed methods for early drug discovery (Figure 19.1). In this area, tools that allow selective and fast synthesis and convenient purifications of test compounds (analogs) are highly desirable. Thus, the expectations placed on the preparative medicinal chemist today are not only to synthesize and purify desired target compounds, but also to do it quickly. The need for rapid compound production is especially important for lead identification and lead optimization. To meet these high expectations, a set of emerging technologies has emerged, including the use of controlled microwave (MW) irradiation as a convenient high-density energy source for fast compound production.

The MW chemistry story in the drug discovery area began in the late 1990s, although a number of pioneers had started using MW irradiation for organic synthesis much earlier [2]. Today, dedicated instruments for MW heating are ubiquitous in organic and medicinal chemistry laboratories, and this technique is among the standard arsenal of tools available to facilitate compound production. The number of publications in this field is now exceedingly large, and the focus of this chapter is limited to a few selected examples, describing the MW synthesis of small molecules of value for medicinal chemistry projects.

## 19.2 Lead identification

The identification of high-quality lead molecules is a critical phase in the discovery of drug candidates since decisions made at this stage in the process are likely to have a significant impact on the outcome of the project. The initial aim at the lead identification stage is to identify so-called hits. These hit molecules then undergo further optimization and exploration through the chemical synthesis of related compounds (known as chemical libraries) and subsequent biological evaluation. This information is then used to design and synthesize new compounds with improved properties that are again tested in various assays, and the cycle is continued until the optimal compound properties are obtained. Here the importance of high-speed chemical transformations to enable rapid compound turnaround is crucial. By employing MW heating and especially superheating (i.e., pressurized reactions heated to well above the solvent boiling point), it has been demonstrated that the chemical reaction rates can be significantly enhanced, which enables the synthesis of a wide range of compounds in a short time. The advantages of using MW processing over traditional heating include shorter reaction times, higher reaction control, and the possibility to quickly change factors such as temperature, reaction time, solvent, and others, resulting in increased productivity. This provides opportunities for fast hypothesis testing and exploration of structure-activity-relationship (SAR) studies of various biologically active compounds. (Figure 19.2) A number of selected examples are presented below.

To investigate cyclic sulfamides as a novel scaffold as HIV-1 protease inhibitors, a set of compounds were prepared utilizing palladium-catalyzed cross couplings as a key diversity-generating step (Scheme 19.1) [3]. These reactions often have a significant thermal barrier, and the use of MW superheating allowed a large library of compounds exploring various aryl-substituents to be synthesized in only 20 min or 10 min for Heck and Suzuki–Miyaura (10 min) couplings. The resulting SAR investigation yielded compounds with an increase in potency from  $K_i > 20 \mu\text{M}$  to  $0.53 \mu\text{M}$ .

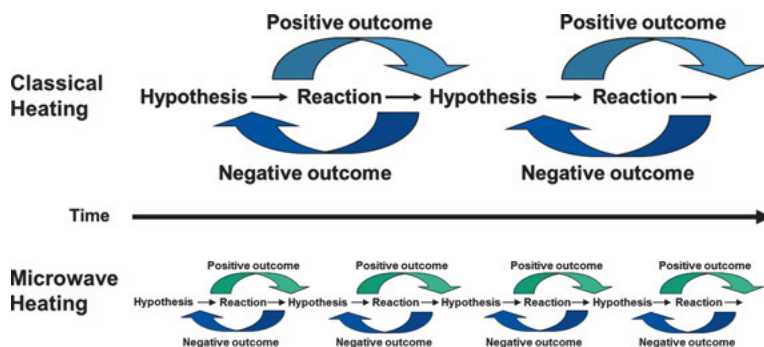
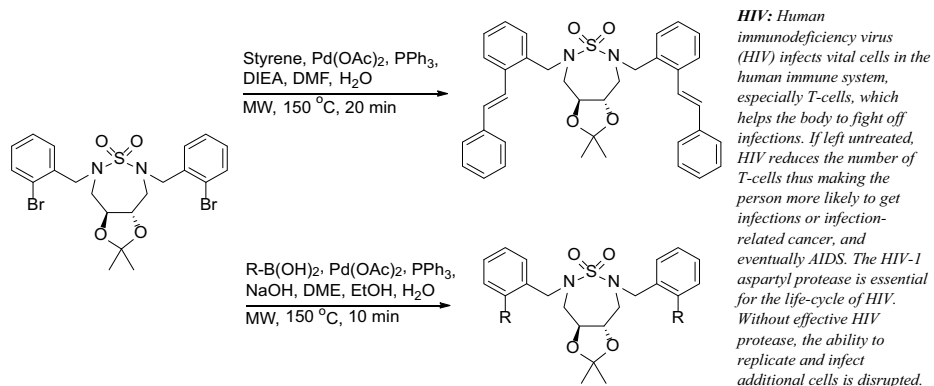


Fig. 19.2: Enhanced medicinal chemistry productivity through high-density MW heating.



**Scheme 19.1:** Various MW-promoted Pd-mediated coupling reactions to synthesize HIV-1 protease inhibitors.

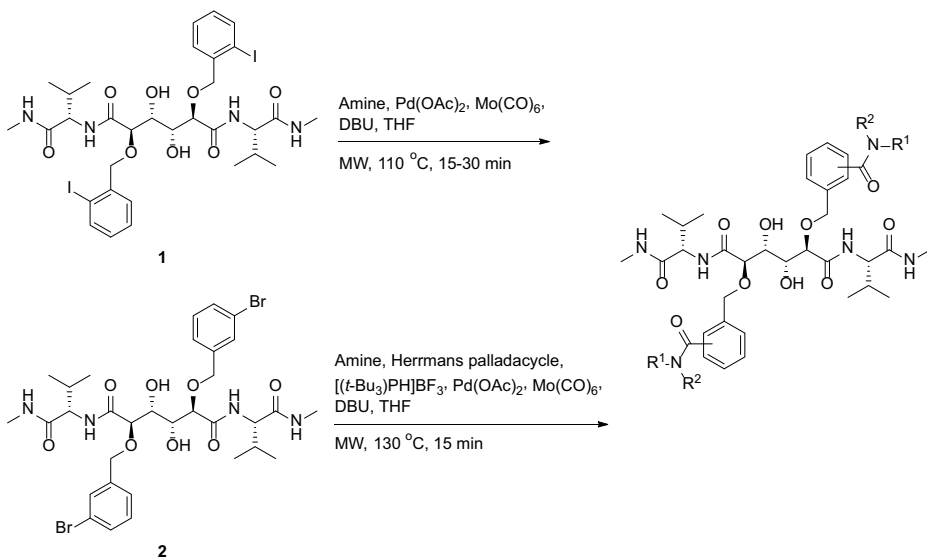
In another medicinal chemistry project, various  $C_2$ -symmetric 1,2-dihydroxyethylene-based HIV-1 protease inhibitors could be achieved by Pd-catalyzed carbonylative couplings [4]. By starting from an aryl iodide (**1**, Scheme 19.2) or aryl bromide (**2**, Scheme 19.2) precursor, various amide substituents could be introduced into the P1/P1' side chain by MW-assisted aminocarbonylations using primary and secondary amine nucleophiles and *in situ* release of CO.

The use of MW heating was crucial to the rapid SAR exploration around modulators of the angiotensin II receptor ( $AT_2R$ ) [5]. MW-assisted superheating facilitated the synthesis of a large library of functionalized thiophene derivatives in as little as 2 min (Scheme 19.3). These studies led to the identification of C21, the first nonpeptide agonist of this receptor system, which is currently in clinical trials for the treatment of pulmonary fibrosis.

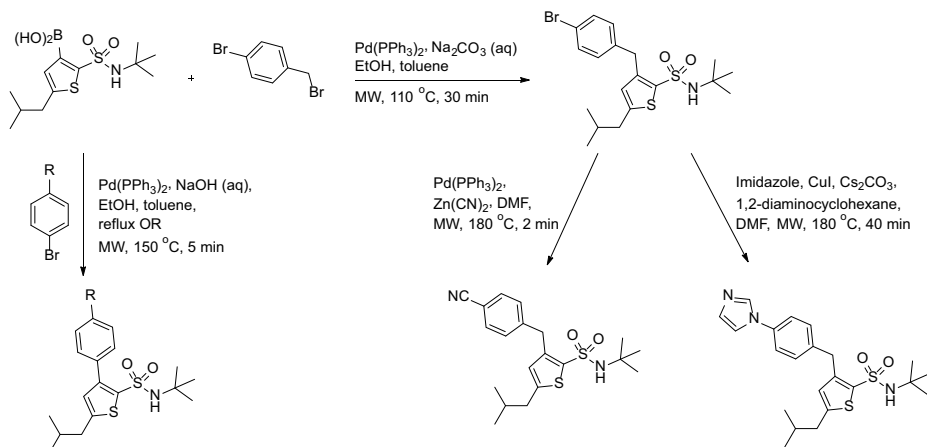
Similarly, shorter reaction times were also achieved through the use of MW-assisted superheating in the search for safer and more selective opioid agonists. In this study, an impressive 192 compounds were rapidly produced in parallel using MW-promoted reductive aminations as well as Suzuki–Miyaura couplings (Scheme 19.4) [6]. The scaffold optimization strategy proved successful, delivering a series of opioid agonists with  $K_i$  values of less than 10 nM for either the  $\mu$ - or the  $\delta$ -opioid receptors.

In a high-throughput screening campaign aimed at identifying compounds active against protein kinase B, the quinoxaline derivative **3** was identified as a promising hit candidate (Figure 19.3). To rapidly investigate the SAR, over 200 compounds were synthesized from *p*-bromomethyl benzyl starting with an  $S_N2$  reaction with various primary and secondary amines, followed by an MW-assisted annulation with 1,2-diaminobenzene (Scheme 19.5) [7]. One of the obtained compounds displayed a tenfold increase in potency; however, it had poor aqueous solubility and no *in vitro* cellular activity. The latter was most likely due to cell permeability. To further address these issues, the key diketone intermediate was treated with either 24 differ-



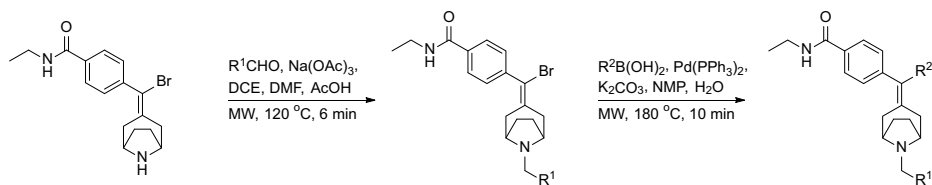


**Scheme 19.2:** Previously unexplored amide expansion of P1/P1' side chains of HIV-1 protease inhibitors could be achieved by MW-promoted aminocarbonylations generating more potent inhibitors.



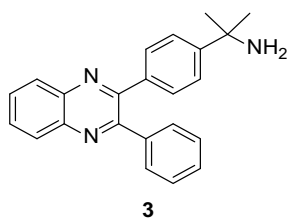
**AT<sub>2</sub> receptor modulators:** The renin-angiotensin system (RAS) plays an important role in blood-pressure regulation and electrolyte balance. The most well-known component of RAS is the octapeptide angiotensin II (Ang II), which binds to AT<sub>1</sub> and AT<sub>2</sub> receptors. The function of the AT<sub>1</sub> receptor has been extensively studied and several antagonists exist in clinic (e.g. losartan). The role of the AT<sub>2</sub> receptor has in recent years attracted considerable interest due to its role in organ development and differentiation, restoration of heart function after myocardial infarction, and its anti-inflammatory as well as neuroprotective and neuroregenerative properties.

**Scheme 19.3:** MW-promoted synthesis of AT<sub>2</sub> receptor modulators.



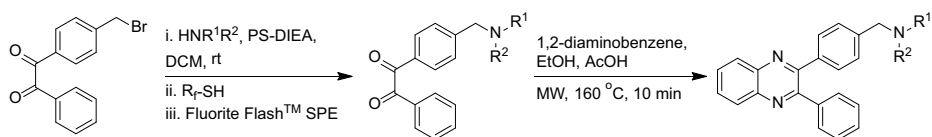
**Pain:** Morphine is one of the most frequently used opioid agonists used to treat severe pain, despite its serious side effects like respiratory depression and high liability for addiction and abuse. The adverse effects are derived from morphine binding to both the  $\mu$ - and  $\delta$ -subtypes of the opioid receptors.

**Scheme 19.4:** MW-assisted reactions were used to synthesize novel opioid agonists to treat pain.



**Akt inhibitors:** Akt, also known as protein kinase B, is a serine/threonine kinase proposed to be a promising target for cancer treatment due to its role in regulation of apoptosis.

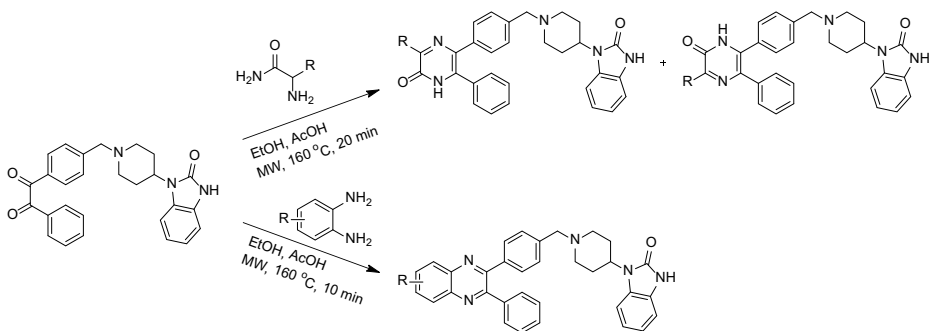
**Fig. 19.3:** Hit compound from a screen for novel Akt (protein kinase B) inhibitors.



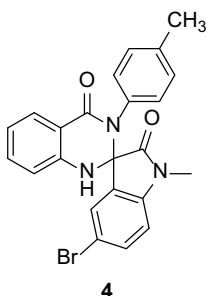
**Scheme 19.5:** To explore the SAR of identified hit compound **3**, 200 compounds were easily obtained using an MW-assisted ring closure reaction.

ent  $\alpha$ -aminocarboxamides to deliver 48 regioisomeric pyrazinones or with 50 different aryl-1,2-diamines to afford a second-generation library of quinoxaline based Akt inhibitors (Scheme 19.6). The most promising compound showed increased potency for both Akt1 and Akt2 as well as improved solubility and cell permeability. Importantly, it was also shown to sensitize tumor cells to induce apoptosis and to inhibit phosphorylation of Akt1 and Akt 2 *in vivo*, providing an excellent lead compound for further optimization studies.

In an attempt to identify novel inhibitors able to be used as cognitive enhancers, a screening campaign was performed that revealed spiro-oxindole dihydroquinazolinone **4** (Figure 19.4) as a promising starting point. The hit compound and derivatives thereof could be synthesized via an MW-promoted continuous-flow three-component reaction in an MW-absorbing silicon carbide reactor (SiC) (Scheme 19.7) [8]. The spiro compounds could also be further modified by MW-assisted Suzuki–Miyaura cross couplings, this time using a MW-transparent borosilicate reactor.

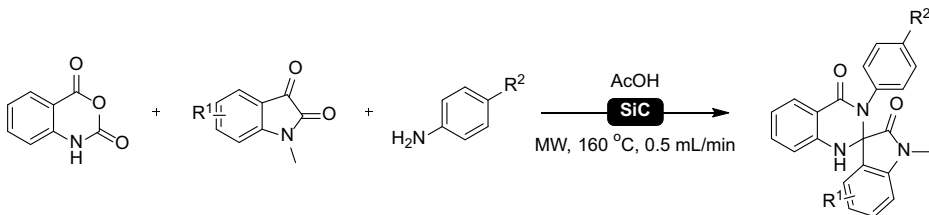


**Scheme 19.6:** Synthesis of second generation of Akt inhibitors obtained by MW-promoted ring closure reactions.



**Cognitive enhancers:** *Insulin-regulated aminopeptidase (IRAP)* is an *MI* aminopeptidase present in high densities in the brain. It has been demonstrated that inhibition of IRAP is beneficial for memory and learning. Thus, IRAP is considered a potential new target for treatment of cognitive disorders.

**Fig. 19.4:** Hit compound from a screen performed in an attempt to identify novel small-molecule-based IRAP inhibitors.



**Scheme 19.7:** MW-promoted continuous-flow multicomponent synthesis of various spiro-oxindole dihydroquinazolinone inhibitors.

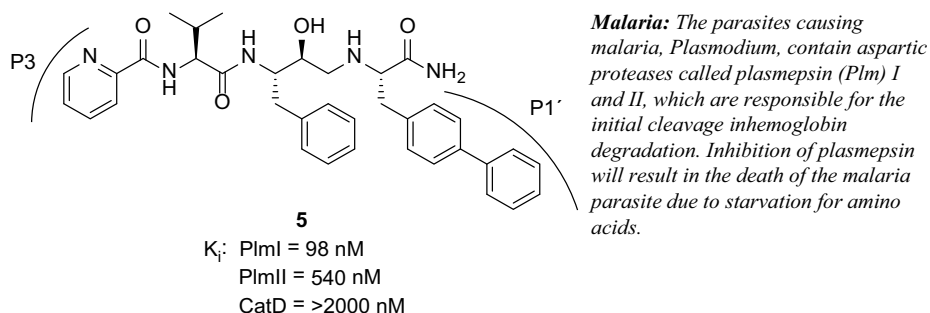
### 19.3 Lead optimization

Following the identification of a promising lead compound, the next stage of the drug discovery process involves the extensive optimization of the compound (lead optimization) with the ultimate aim of identifying a compound that possesses the required properties of the targeted preclinical development candidate. In addition to fulfilling potency and selectivity (the primary goals of a hit compound), a potential develop-

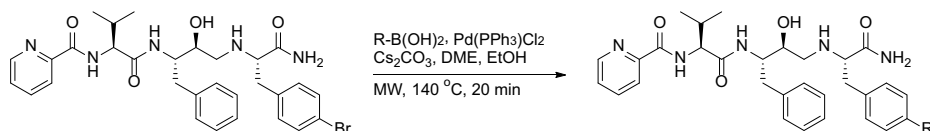
ment candidate should possess appropriate ADME properties to deliver acceptable exposure of the compound at the target site by the preferred route of administration. This allows data obtained from subsequent *in vivo* profiling in preclinical disease models to be interpreted with confidence and facilitate predictions for future clinical efficacy. At this stage chemical modifications are often limited to certain parts of the lead structure, making MW-promoted transformations, in parallel or sequence, particularly useful. Following in this section will be a few selected examples to further demonstrate the power and convenience derived from innovate instrument design utilizing MW technology.

In this first example, the starting point was a known plasmepsin (Plm) I and II inhibitor (**5** Figure 19.5) with reasonable selectivity over the very similar human protease cathepsin D (CatD) and with good Caco-2 cell penetration. An automated MW-based synthesizer instrument was then used to perform Suzuki–Miyaura cross-coupling reactions to rapidly explore the P1' side chain (Scheme 19.8) [9]. Investigations using different boronic acids revealed that larger bicyclic substituents increased potency (**6**, Figure 19.6). In addition, various carboxylic acids in the P3 position were investigated, and subsequently a combination of the most active side chains were prepared (**7**, Figure 19.6), displaying high potency and moderate selectivity for PlmI and PlmII (Figure 19.6).

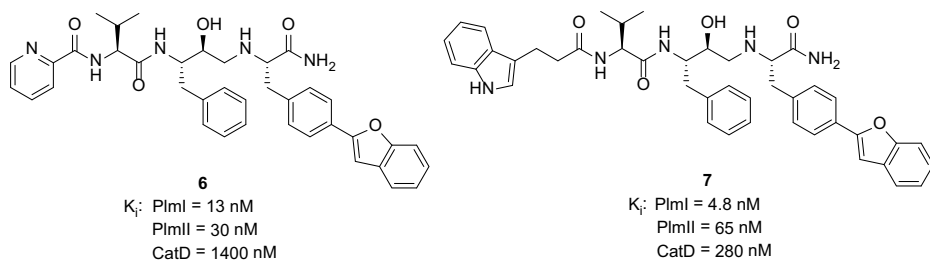
In an attempt to explore the metabolic stability of a series of AT2 receptor antagonists, various alcohols were rapidly introduced via transesterification using both MW-promoted batch [10] and continuous-flow [11] procedures (Scheme 19.9).



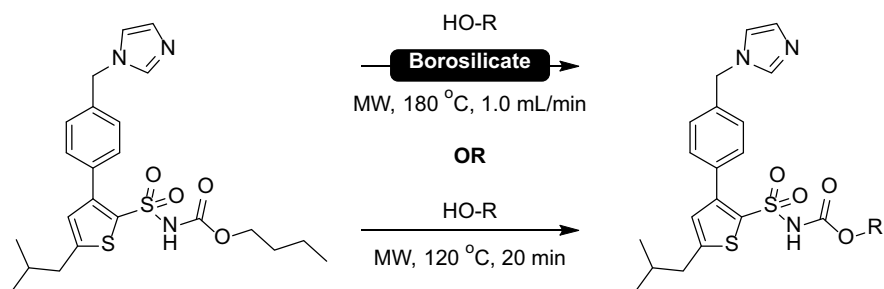
**Fig. 19.5:** Known malarial protease inhibitor.



**Scheme 19.8:** Suzuki–Miyaura couplings to explore the P1' side chain of novel malarial protease inhibitors.



**Fig. 19.6:** Optimized malarial protease inhibitors.



**Scheme 19.9:** MW-promoted transesterifications of sulfonamide carbamates as a cheap and fast way of synthesizing AT2 receptor ligands. The reaction can be performed in both a batch and a continuous-flow manner.

## 19.4 MW-assisted synthesis of active pharmaceutical ingredients

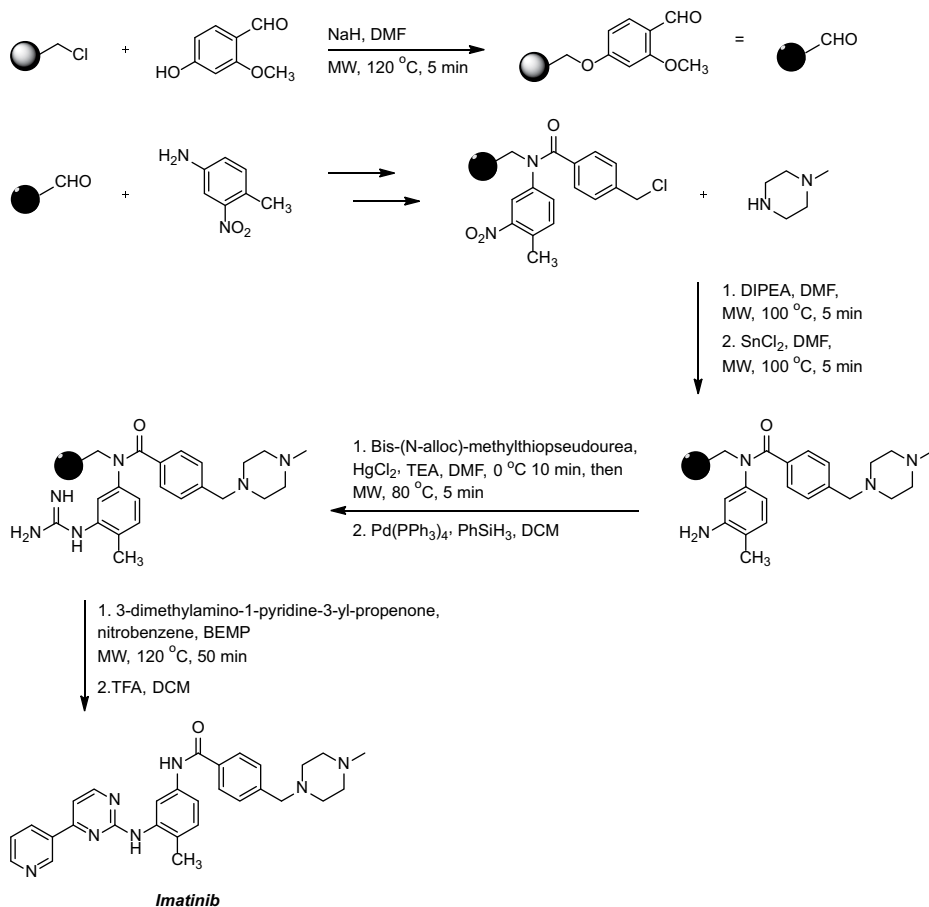
MW heating has not only been utilized as an enabling tool in early drug discovery projects; there are also a number of examples of this technique being employed in the preparation of already marketed drug substances. Although there are, to the best of our knowledge, no reported examples of MW heating in the production-scale synthesis of active pharmaceutical ingredients (APIs), the application of this technique in the small-scale synthesis of APIs showcases its powerful usefulness for the preparation of biologically active substances.

### 19.4.1 Imatinib

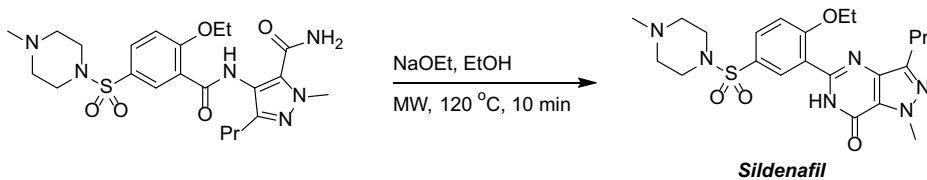
In the synthesis of imatinib (Gleevec<sup>®</sup>), an inhibitor of BCR-ABL and c-kit oncogenic tyrosine kinases used for the treatment of chronic myeloid leukemia and gastrointestinal tumor, MW heating was used to promote difficult reactions and reduce reaction times (Scheme 19.10). Furthermore, the presented synthetic route also allowed the introduction of various substituents onto the core structure to obtain a library of diverse compounds [12].

## 19.4.2 Sildenafil

Sildenafil, also known as Viagra<sup>®</sup>, is one of the best-known treatment options for male erectile dysfunction. It acts as a potent and selective inhibitor of phosphodiesterase type 5 (PDE-5) to prevent degradation of cyclic guanosine monophosphate (cGMP). Increased levels of cGMP leads to smooth muscle relaxation of the intimal cushions allowing inflow of blood. In one example of the synthesis of sildenafil, MW heating was used in the final base-mediated cyclization step to obtain the target molecule in quantitative yield (Scheme 19.11) [13].



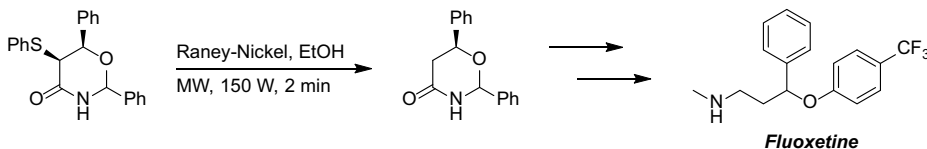
**Scheme 19.10:** The cancer drug imatinib (Gleevec<sup>®</sup>) can be synthesized using solid support and MW irradiation in several of the key steps to obtain the final compound in a short amount of time.



**Scheme 19.11:** The final cyclization step in the synthesis of sildenafil (Viagra<sup>®</sup>) can be performed in a high-yielding MW-assisted reaction.

### 19.4.3 Fluoxetine

Fluoxetine (Prozac<sup>®</sup>) is one of the most well documented drugs in popular culture and is mainly used to treat depression. It exerts its effect by inhibiting the reuptake of the monoamine neurotransmitter serotonin. In one of the reported synthetic routes, an MW-assisted desulfurization reaction was used as a key step in the synthesis of the target compound (Scheme 19.12) [14].



**Scheme 19.12:** A novel MW-promoted desulfurization reaction used in the synthesis of fluoxetine (Prozac<sup>®</sup>), a common drug for the treatment of depression.

## Conclusion

Controlled MW heating is one constituent of the collection of novel techniques that provide medicinal chemists with new possibilities for rapid lead identification and optimization. Clearly, today's medicinal chemists are increasingly incorporating MW technologies into both industrial and academic drug discovery laboratories. This is not only due to the large number of successful examples in the literature, some of which are presented herein, but also due to innovative instrument design making MW synthesizers safe and extremely convenient to use. With these advances, the age of high-speed MW chemistry continues to evolve, and MW chemistry's use will continue to be of importance for the future development of medicinal chemistry.

## Bibliography

- [1] Burger A. *A Guide to the Chemical Basis of Drug Design*; John Wiley & Sons: New York, 1983.
- [2] Strauss C, Trainor R. Developments in Microwave-Assisted Organic Chemistry. *Aust. J. Chem.* 1995, 48, 1665–1692.

- [3] Ax A, Schaal W, Vrang L, Samuelsson B, Hallberg A, Karlén A. Cyclic Sulfamide HIV-1 Protease Inhibitors, with Sidechains Spanning from P2/P2' to P1/P1'. *Bioorg. Med. Chem.* 2005, 13, 755–764.
- [4] Wannberg J, Kaiser N-F. K., Vrang L, Samuelsson B, Mats Larhed A, Hallberg A. High-Speed Synthesis of Potent C2-Symmetric HIV-1 Protease Inhibitors by In-Situ Aminocarbonylations. *J. Comb. Chem.* 2005, 7, 611–617.
- [5] Wan Y, Wallinder C, Plouffe B, Beaudry H, Mahalingam AK, Wu X, Johansson B, Holm M, Botoros M, Karlén A, et al. Design, Synthesis, and Biological Evaluation of the First Selective Nonpeptide AT2 Receptor Agonist. *J. Med. Chem.* 2004, 47, 5995–6008.
- [6] Coats SJ, Schulz MJ, Carson JR, Codd EE, Hlasta DJ, Pitis PM, Stone DJ, Zhang S-P., Colburn RW, Dax SL. Parallel Methods for the Preparation and SAR Exploration of N-Ethyl-4-[(8-Alkyl-8-Aza-bicyclo[3.2.1]oct-3-ylidene)-Aryl-Methyl]-Benzamides, Powerful Mu and Delta Opioid Agonists. *Bioorg. Med. Chem. Lett.* 2004, 14, 5493–5498.
- [7] Lindsley CW, Zhao Z, Leister WH, Robinson RG, Barnett SF, Defeo-Jones D, Jones RE, Hartman GD, Huff JR, Huber HE, et al. Allosteric Akt (PKB) Inhibitors: Discovery and SAR of Isozyme Selective Inhibitors. *Bioorg. Med. Chem. Lett.* 2005, 15, 761–764.
- [8] Engen K, Sävmarker J, Rosenström U, Wannberg J, Lundbäck T, Jenmalm-Jensen A, Larhed M. Microwave Heated Flow Synthesis of Spiro-Oxindole Dihydroquinazolinone Based IRAP Inhibitors. *Org. Process Res. Dev.* 2014, 18, 1582–1588.
- [9] Nöteberg D, Schaal W, Hamelink E, Vrang L, Larhed M. High-Speed Optimization of Inhibitors of the Malarial Proteases Plasmeprin I and II. *J. Comb. Chem.* 2003, 5, 456–464.
- [10] Isaksson R, Kumpiö I, Larhed M, Wannberg J. Rapid and Straightforward Transesterification of Sulfonyl Carbamates. *Tetrahedron Lett.* 2016, 57, 1476–1478.
- [11] Kumpiö I, Isaksson R, Sävmarker J, Wannberg J, Larhed M. Microwave Promoted Transcarbamylation Reaction of Sulfonylcarbamates under Continuous-Flow Conditions. *Org. Process Res. Dev.* 2016, 20, 440–445.
- [12] Leonetti F, Capaldi C, Carotti A. Microwave-Assisted Solid Phase Synthesis of Imatinib, a Blockbuster Anticancer Drug. *Tetrahedron Lett.* 2007, 48, 3455–3458.
- [13] Baxendale IR, Ley SV. Polymer-Supported Reagents for Multi-Step Organic Synthesis: Application to the Synthesis of Sildenafil. *Bioorg. Med. Chem. Lett.* 2000, 10, 1983–1986.
- [14] Panunzio M, Tamanini E, Bandini E, Campana E, D'Aurizio A, Vicennati P. 5-Phenylthio-1,3-Oxazinan-4-Ones via Hetero Diels–Alder Reactions: Synthesis of (R)- and (S)-Duloxetine and Fluoxetine. *Tetrahedron* 2006, 62, 12270–12280.



Silvia Tabasso

## 20 Microwave-assisted biomass conversion

### 20.1 Introduction

Recent decades have seen increasing demands for renewable sources of energy to replace the depleting fossil-based ones. The emerging concept of *biorefinery* deals with the use of biomass instead of oil to produce energy and chemicals. Biomass is biological material derived from living, or recently living, organisms, referring to both animal- and vegetable-derived feedstocks. Specifically, first-generation biomass refers to materials that compete with food production, such as dedicated crops (e.g., maize and edible oil seeds). The use of these sources for the production of fuels and chemicals faces some ethical issues, which is why second-generation bio-based products have been widely studied in recent years. They involve the utilization of lignocellulosic (LC) biomass as feedstocks in integrated biorefineries [1]. LCs represent the most abundant and biorenewable biomass on Earth, referring to the nonedible portion of plants. These features make the use of LC feedstocks more advantageous than other biomass supplies as they do not compete with food production and animal feed. These raw materials could be either fast-growing, nonedible crops or, better yet, forestry, agricultural, and agro-industrial LC wastes. In addition, the need to avoid waste and find new renewable resources for fuels and chemicals has focused attention on a new and promising feedstock for biorefineries: food supply chain waste (FSCW) [2]. In the past, algae were part of second-generation biomass. However, their widespread use and potentiality make them deserving of their own category, the so-called third generation of biomass. Even if their utilization, for example in the production of biofuels, comes with several major advantages, it must contend with one essential drawback that is important enough to constitute a deal breaker. The main disadvantage lies in the water-based waste production of algal biofuel, which requires non-scalable amounts of water and fertilizers (specifically nitrogen and phosphorus). The levels of greenhouse gas emissions involved in producing the needed amount of fertilizer would offset all the advantages of using biofuels. It is this weak point that needs to be overcome before algal biodiesel is declared a runaway success on a global scale. For this reason, in this chapter, we will focus on the microwave (MW)-assisted conversion of LC and FSCW. Residual second-generation biomass is accumulated in large quantities and represents a negative-cost feedstock for a number of value-added products because its disposal causes severe economic and environmental issues. On the other hand, the conversion of LC and FSCW material is not easily accomplished because of their structural complexity; thus, the crucial challenge is to produce added-value chemicals, energy, and fuels at high selectivity and yields with sustainable processes.

<https://doi.org/10.1515/9783110479935-020>

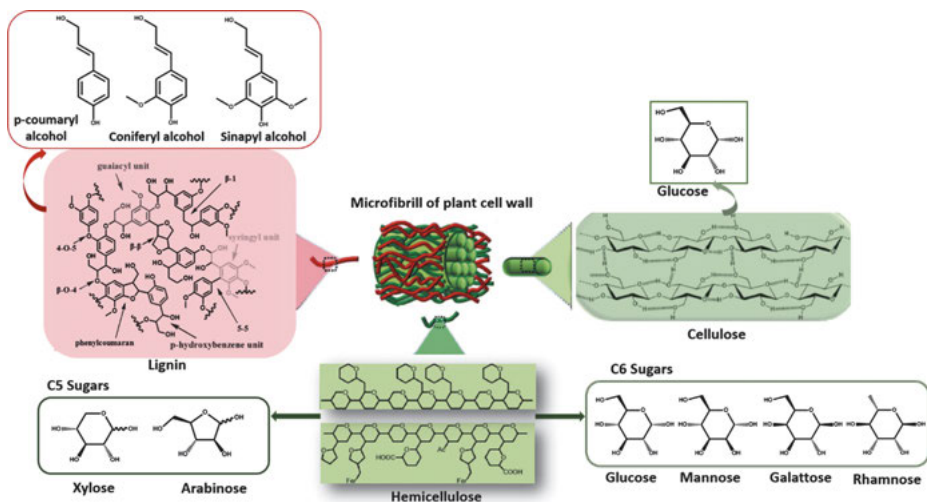
With this aim, the application of MWs to biomass conversion have attracted growing interest. Indeed, the advantages of MWs rely on the enhancement of reaction rates and yields, combined with improved selectivity.

In addition, under MW irradiation, the production of chemicals from biomass proceeds at markedly lower temperatures compared to conventional heating. Therefore, the obtained molecules have a high degree of functionality compared to conventional heating. Furthermore, MW-assisted processes do not require a high degree of feedstock grinding, which reduces pretreatment steps and, consequently, energy consumption. For these reasons, generally speaking, the energy consumption related to MW-assisted biomass conversion is significantly reduced compared to conventional processing because of the much shorter operating time, the lower temperatures, and the reduced number of pretreatment steps. Therefore, the energy cost is lower than with other protocols. However, large-scale processing of biomass face certain economic issues, such as overall energy balance and capital costs. Nevertheless, when moving from laboratory scale to kilogram scale and from single-mode to multimode reactors, MW heating processes can be more efficient than conventional heating experiments under the same conditions [3]. Following these considerations and the many examples of energy-efficient MW processes, it is worth noting the importance of promoting large-/industrial-scale MWs under continuous processing for biomass valorization. This could lead to highly energy-efficient protocols, especially if the equipment and instrumentation are optimized for a particular process or application [4].

In this chapter, the effects of MWs on LC biomass will be presented, followed by some case studies showing the efficiency of MW dielectric heating in synthesizing valuable molecules.

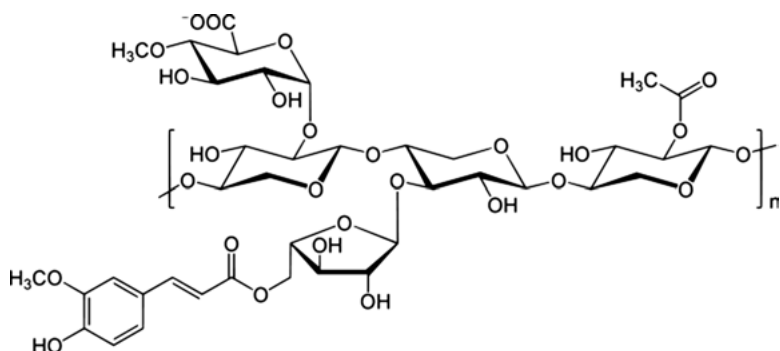
## 20.2 Composition of biomass

Residual biomass commonly used for the production of energy and chemicals comes from food, forestry, and agricultural waste. The main components of biomass are carbohydrates and lignin, with minor compounds comprising triglycerides (fats and oils), proteins, and terpenes [5]. Carbohydrates can be divided into storage carbohydrates – starch, inulin, and sucrose – and structural polysaccharides. In particular, forestry and agricultural residues belong to the class of LC biomass, which constitutes the cell wall of plants and are mainly composed of cellulose, hemicellulose, and lignin, together with small amounts of other components like acetyl groups, minerals, and phenolic substituents (Figure 20.1). The proportions of the three major components varies from one species to another, depending on the botanical origin. Lignocellulose has evolved to resist degradation, and this robustness, responsible for its recalcitrance to chemical and enzymatic degradation, comes from the crystallinity of cellulose, hydrophobicity of lignin, and encapsulation of cellulose by the lignin–hemicellulose matrix [6].



**Fig. 20.1:** Main components and structure of lignocellulose. Adapted with permission from Ref. [6]. Copyright 2015 The Royal Society of Chemistry.

Cellulose is the most abundant component of LC biomass, constituted by glucose units linked by  $\beta$ -1,4-glycosidic bonds. Furthermore, many intramolecular and intermolecular hydrogen bonds are responsible for the stiffness of the structure (Figure 20.1). The conversion of cellulose into fuels and valuable chemicals is of prime importance because it represents about half of the organic carbon in the biosphere. Conversely, hemicellulose has an amorphous structure composed of several heteropolymers randomly disposed, including xylans, galactomannans, and glucomannans. The composition of hemicelluloses differs from one species to another; for example, xylans are present in grasses and hardwood (from dicot angiosperm trees), while glucomannans are the main components of softwood (gymnosperm trees, like resinous species). Furthermore, the term xylans refers to a large spectrum of structures (Figure 20.2).



**Fig. 20.2:** Example of one possible xylan unit.

Because of their structural variety, hemicelluloses yields after hydrolysis different C5 and C6 monosaccharides, such as xylose, arabinose, mannose, glucose, galactose, and acetylated sugars. Hemicelluloses are cross-linked with lignin in the plant cell walls [7]. Lignin is composed entirely of aromatic units, namely polyphenolics. Its nonuniform structure imparts stiffness and resistance to plant cell walls.

## 20.3 Microwave interactions with biomass

For conversion into fuels and platform chemicals, biomass must undergo the separation of the main components or their depolymerization. There are essentially two ways to achieve this: thermochemical and hydrolytic processes (Figure 20.3). Thermochemical processes involve pyrolysis (usually high temperatures, with inert atmosphere or in a vacuum), while hydrothermal processes occur in an excess of water and often require the presence of strong acids or high pressures.

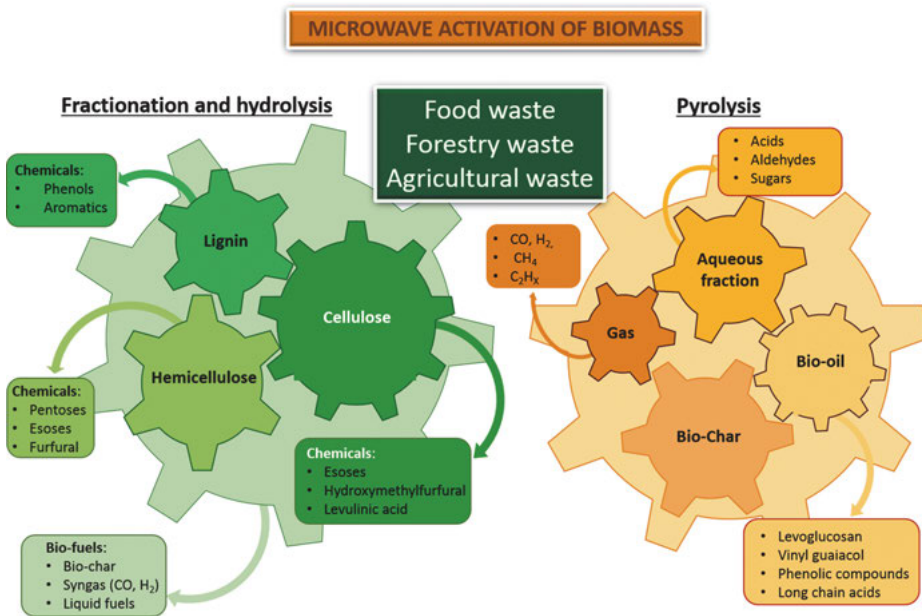


Fig. 20.3: Microwave-assisted processes for biomass valorization

### 20.3.1 Hydrothermal conversion of cellulose

Hydrothermal processing allows the hydrolysis of LC biomass into simple sugars using elevated pressures and temperatures. The synergy between microwaves and hydrothermal processes provides a potentially faster and more efficient way to convert biomass into sugars without additives, making it more sustainable. Comparison of the hydrolysis of cellulose under MW and conventional heating reveals that at temperatures above 190 °C, MWs markedly influence the cellulose mass loss. On the other hand, analysis of hydrolysis products shows much higher glucose yields at 220 °C under MW irradiation than under conventional heating [8]. In addition, among the products, levoglucosan is present only after MW-assisted hydrolysis. This difference in products could suggest the hypothesis that the MW active center might not be accessible to hydrolyzing media under conventional heating, which would support the possible existence of nonthermal specific events. Analysis of the behavior of cellulose with modulated differential scanning calorimetry (MDSC) revealed that depolymerization is related to a glass transition starting at 180 °C [9]. This thermal event occurs within the amorphous region, as the crystalline part undergoes major structural changes well above 220 °C.

Because cellulose depolymerization strongly depends on the hydrogen bond network (Figure 20.4), a proton/deuterium exchange experiment was performed at 220 °C under both MW and conventional heating, to understand which bonds were the most accessible. Such information was extrapolated by the ratios between the area of the O–D and O–H bands in the corresponding 2500 and 3400  $\text{cm}^{-1}$  regions of the ATR-FTIR spectra (Figure 20.5).

As indicated by the higher ratio values, microwaves made the hydrogen bonds more accessible than after conventional heating. In particular, in the remaining cellulose, after microwave treatment the CH<sub>2</sub>O(6)-related hydrogen bonds (intra-chain O(2)–H···O(6) and interchain O(3')···H–O(6)), were more prone to proton/deuterium exchange than the intrachain O(3)–H···O(5) hydrogen bond.

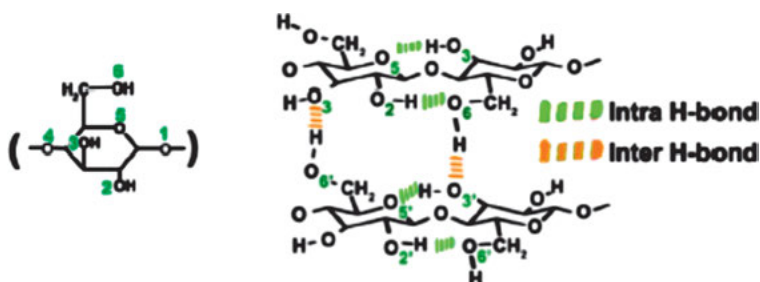


Fig. 20.4: Hydrogen bond network of cellulose. Reprinted with permission from [8]. Copyright 2013 American Chemical Society

$$\frac{A_{(6)}^0 \text{D-O}(3')}{A_{(6)}^0 \text{H-O}(3')} = 1 \quad \frac{A_{(6)}^0 \text{D-O}(3')}{A_{(6)}^0 \text{H-O}(3')} = 0,17$$

$$\frac{A_{(6)}^0 \text{D-O}(2)}{A_{(6)}^0 \text{H-O}(2)} = 1,48 \quad \frac{A_{(6)}^0 \text{D-O}(2)}{A_{(6)}^0 \text{H-O}(2)} = 0,31$$

$$\frac{A_{(3)}^0 \text{D-O}(5)}{A_{(3)}^0 \text{H-O}(5)} = 0,82 \quad \frac{A_{(3)}^0 \text{D-O}(5)}{A_{(3)}^0 \text{H-O}(5)} = 0,25$$

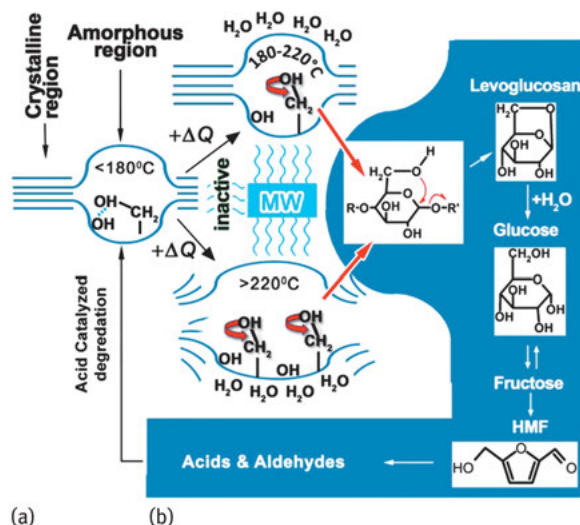
(a) (b)

**Fig. 20.5:** Ratios of either microwave (a) or conventional (b) O–D to O–H deconvoluted peak areas. Adapted with permission from [8]. Copyright 2013 American Chemical Society

In contrast, interchain  $\text{O}(3') \cdots \text{H}-\text{O}(6)$  was not very involved in the proton/deuterium exchange after conventional heating. It can thus be assumed the MW activation of  $\text{CH}_2\text{OH}$  pendant groups, which became more accessible after heating.

The interaction of microwaves with cellulose as a function of temperature is summarized in Figure 20.6.

As stated earlier, at temperatures drop below  $180^\circ\text{C}$ , the  $\text{CH}_2\text{OH}$  groups are not accessible to MW irradiation in both the amorphous and crystalline regions because hydrogen bonds are very strongly cross-linked (Figure 20.6a). Above the glass transition temperature of the amorphous region ( $180^\circ\text{C}$ ) the weakening of the hydrogen-bonding network allows the hydroxymethyl groups to rotate and vibrate freely, thereby al-



**Fig. 20.6:** Schematic representation of cellulose–MW interaction as a function of temperature: (a) mechanism of  $\text{CH}_2\text{OH}$  group activation; (b) scheme of cellulose degradation toward acids and aldehydes. Reprinted with permission from [8]. Copyright 2013 American Chemical Society

lowing for their alignment with the MW field. These groups then behave as so-called molecular radiators that transfer the MW energy to the surrounding environment. Owing to these motions, CH<sub>2</sub>OH groups can collide with the anomeric carbon atom of the same molecule, leading to the formation of levoglucosan, which can undergo hydrolysis, affording glucose (Figure 20.6b). Levoglucosan is thus produced only after MW-assisted activation of the hydroxymethyl groups. This is why it was not detected after conventional heating treatment. Furthermore, above 220 °C, rotational motions induced by MWs involve the crystalline portion of cellulose. Interestingly, it was recently observed that glucose monomers were not able to undergo this MW-assisted activation mechanism because the surrounding water molecules absorbed the energy very efficiently.

### 20.3.2 Microwave-assisted pyrolysis of biomass

Pyrolysis is a technique for biopolymer deconstruction, yielding gas, bio-oil, and bio-char products. The use of MWs for biomass pyrolysis is relatively new, dating back to the 1980s, and is generally performed at temperatures similar to those in conventional pyrolysis (> 350 °C), resulting in gasification or liquefaction of the starting material to produce fuels [10]. Nevertheless, high temperatures and heating rates in former MW pyrolysis studies may be masking important lower-temperature processes. It has been demonstrated that the interaction of MWs with various types of biomass involve different pyrolytic mechanisms, enabling operation at much lower temperatures than previously reported [9], owing to the specific MW effects. Indeed, as for the hydrothermal processes described earlier, the temperature at which pyrolysis occurs depends on biomass thermal properties, which are related to the glass transition temperature of the biomass components (i.e., 180–190 °C for lignin, 180–200 °C for amorphous cellulose, 230–250 °C for crystalline cellulose). Low-temperature MW-assisted pyrolysis has therefore attracted increased interest in terms of energy savings and product formation. Actually, mild pyrolysis conditions can substantially change the composition obtained (Table 20.1). For example, lower temperatures afford lower yields

**Tab. 20.1:** Comparison of products obtained under conventional and microwave-assisted pyrolysis of wheat straw

Product	Conventional pyrolysis (600 °C)	MW-Pyrolysis (180 °C)
Total bio-oil	34%	37%
Bio-char	23%	38%
Gas	43%	25%
Guaiacol (g/l)	3	23
Phenols (g/l)	8	20

of gaseous fractions compared to bio-char and bio-oil. Meanwhile, the gas fraction presents higher yields of syngas ( $\text{CO} + \text{H}_2$ ), along with a mixture of alkanes/alkenes.

Low-temperature MW bio-oil is much more similar in composition to crude oil than other pyrolysis oils and generally shows a smaller number of compounds that are strictly dependent on the starting biomass. For example, the main constituents of the bio-oil obtained from the pyrolysis of wheat straw are levoglucosan and vinyl guaiacol, while barley dust leads to a bio-oil enriched in phenolic compounds emerging from the lignin breakdown. In addition, the mild pyrolysis of wheat straw afforded an aqueous fraction containing almost low-molecular-weight acids and aldehydes. As shown in Table 20.2, MW bio-oil contains more phenolic compounds than a conventional one, whose main products are acetic acid and furfural. Furthermore, under MW conditions, long-chain acids such as hexadecanoic acid are obtained [11].

Under MW irradiation, bio-char is produced at temperatures 100 °C lower and is endowed with a calorific value 30% greater, so valuable fuels can be obtained, replacing coal. In addition, the calorific value of char dramatically increases at 180 °C, owing to the interaction with MWs of the amorphous region, while no increase in rate is observed in conventional conditions [9].

**Tab. 20.2:** Composition of bio-oil obtained under conventional and MW-assisted pyrolysis of wheat straw.

Conventional pyrolysis (600 °C)	MW-assisted pyrolysis (180 °C) <sup>a</sup>
Acetic acid	Acetic acid
–	N-hexadecanoic acid <sup>a</sup>
Furfural	Furfural
2-furanmethanol	2-furanmethanol
Furan-2(5H)-one	
2-methylcyclopent-2-enone	
3-methylcyclopent-2-enone	
3-methylcyclopentane-1,2-dione	
Vinyl guaiacol	Vinyl guaiacol
–	Syringol <sup>a</sup>
Methoxyeugenol	Methoxyeugenol
–	<i>trans</i> -isoeugenol <sup>a</sup>
–	Guaiacol <sup>a</sup>
Creosol	Creosol
2,4-diethylphenol	Phenol
<i>o</i> -, <i>m</i> -, <i>p</i> -cresol	<i>o</i> -, <i>m</i> -, <i>p</i> -cresol
–	Vanillin <sup>a</sup>
–	Levoglucosan <sup>a</sup>
–	1,4:3,6-dianhydro- $\alpha$ -D-glucopyranose <sup>a</sup>

<sup>a</sup> These products are produced only after MW-assisted treatment.



Solid char may also act as a catalyst in a pyrolysis process, thanks to the carbonaceous or metallic active sites. Such heterogeneous reactions as, for example, methane decomposition are particularly favored by MW heating because the material is at higher temperatures than the surrounding area.

## 20.4 Case studies

### 20.4.1 Application of microwave heating in lignocellulosic biomass pretreatment for bioethanol production

Biofuels such as bioethanol are produced by the fermentation of sugars, which can be obtained after the breakdown of the LC structure of plant materials. So-called second-generation bioethanol is more advantageous than the first-generation one because LC biomass does not compete with crops grown for food and is very abundant.

Owing to lignocellulose recalcitrance, a biomass pretreatment is usually necessary to improve the yields of monosaccharides after enzymatic hydrolysis and represents the key step of the whole process (Figure 20.7).

A pretreatment should prompt the degradation or reduction of lignin content and reduce cellulose crystallinity, increasing its porosity and surface area, in order to make the biomass more susceptible to enzymes during the subsequent saccharification steps. Microwave pretreatment has been shown to be more effective than other pretreatment methods. Indeed, compared to conventional processes, MW-assisted pretreatment involves a more uniform temperature distribution, with lower temperatures, thereby avoiding or limiting the formation of inhibitory byproducts, such as furfurals. In addition, it has been demonstrated that the MW pretreatment technique is very effective at reducing the lignin ratio in biomass, leading to an increase in the proportion of cellulose and hemicellulose. Both thermal and nonthermal effects are involved in the mechanism of MW-based pretreatment. Indeed, this is more effective if the temperature is about 200 °C. As an example, Table 20.3 shows a comparison between MW-assisted and conventional pretreatment of switchgrass under the same

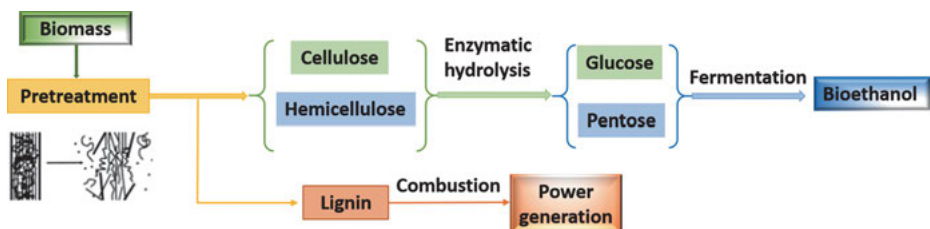


Fig. 20.7: Schematic representation of bioethanol production from LC biomass

**Tab. 20.3:** Sugar yields after MW-assisted and conventional pretreatment (both performed at 190 °C for 30 min) and enzymatic hydrolysis

	Microwave			Conventional-heating		
	Pretreatment	Hydrolysis	Combined	Pretreatment	Hydrolysis	Combined
Xylose	11.8	1.50	13.3	8.10	3.7	11.8
Glucose	1.80	19.4	21.2	1.70	9.1	10.8
Total sugar	13.6	20.9	34.5	9.7	12.8	22.6

conditions based on the yields of the sugars obtained from both the pretreatment and enzymatic hydrolysis [12].

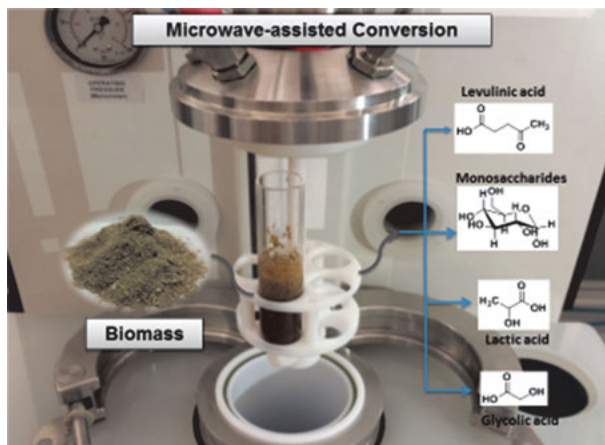
The xylose yield after the MW pretreatment stage was higher than under conventional heating, while the increase in the glucose yield occurred after the hydrolysis step. To summarize, the results show that MW heating enhances the solubilization and depolymerization of hemicellulose in the pretreatment stage and the enzymatic digestibility of cellulose in the enzymatic saccharification step. However, MWs cannot totally break the lignocellulose framework, as the total sugar yield after MW irradiation was much higher than after conventional processing, but remain relatively low. The synergistic effect of alkali and MWs is more efficient in enhancing the total sugar yield, owing to the effective removal of the lignin barrier. For example, when switchgrass was presoaked in alkali solution and treated by MW heating, a sugar yield of 99% of maximum potential sugars was achieved.

However, because the pretreatment stage is the rate-limiting step in an economically feasible process for enzymatic hydrolysis of cellulose, for the large-scale pretreatment processes, the optimal pretreatment conditions need to be a compromise with energy input and cost savings.

#### 20.4.2 MW-assisted valorization of postharvest tomato plant wastes (PHTP)

The versatility of MWs enables the conversion of agricultural residues into different valuable products with high yields and selectivity by simply varying the reaction conditions (Figure 20.8). Indeed, a flash process afforded either pure levulinic acid (LevA) or a mixture of monosaccharides (Ms) depending on the temperature, using hydrochloric acid as a catalyst, in only 2 min (Table 20.4). LevA is a valuable platform chemical used for the production of fine chemicals (such as pharmaceutical agents, herbicides, food fragrances) and biofuels.

On the other hand, divalent cations proved very efficient at catalyzing the conversion of PHTP into lactic (LA) and glycolic acid (GA). Good conversions and yields were achieved during the same MW flash process by simply varying the catalytic system and the temperature.



**Fig. 20.8:** MW-assisted biomass conversion of PHTP. Adapted with permission of The Royal Society of Chemistry from [13]. Copyright 2013 The Royal Society of Chemistry

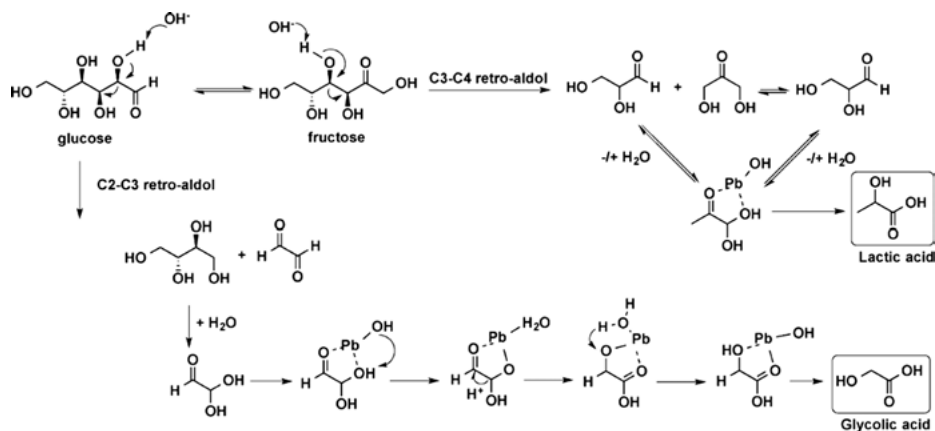
**Tab. 20.4:** Valuable products from MW-assisted biomass conversion under different conditions

Catalyst	Temperature (°C)	Biomass conversion (%)	Yield (%)			
			LevA	Ms	LA	GA
HCl (1 M)	150 °C	62	–	52	–	–
HCl (1 M)	225 °C	78	63	–	–	–
Pb(NO <sub>3</sub> ) <sub>2</sub> (35 mM)	220 °C	50	–	–	34	21

Reaction conditions: 2 min, N<sub>2</sub> (3 MPa).

It is well known that Pb(II) generates Pb(II)-OH in water, and it is this species that stabilizes the intermediates (Scheme 20.1). Owing to the equilibrium between fructose and glucose, both LA and GA are produced under these conditions. Indeed, LA is formed through a C3-C4 retro-aldol reaction from fructose, while a C2-C3 retro-aldol reaction on glucose affords GA.

However, this process is highly selective in terms of these two platform chemicals, which can then be used for the synthesis of bio-based polymers and oligomers. In particular, copolymers of LA and GA (PLGA) have been used for medical applications, owing to their degradation into nontoxic monomers. Low-molecular-weight PLGA suitable for short-term drug release can be obtained through direct poly-condensation of LA and GA. This process is slow and suffers from low yields due to the need for water removal in the condensation of carboxylic and hydroxyl groups. Furthermore, toxic catalysts such as Sn, Zn, and Sb salts are often used. Microwaves can help overcome these problems; for example, an innovative catalyst and solvent-free protocol was performed in only 3 h affording co-oligomers. A dedicated MW reactor working under vacuum allowed for efficient water elimination, leading to quantitative yields.



**Scheme 20.1:** Reaction mechanism for the conversion of biomass into LA and GA. Reprinted with permission from [14]. Copyright 2015 Wiley-VCH Verlag GmbH & Co.

## 20.5 Conclusion

The purpose of this chapter was to provide some insight into biomass valorization, underlining the benefits of MW-assisted biomass processing. After a short description of the structure and composition of LC biomass, the interactions of MWs occurring in the different conversion processes were described. The existence of specific nonthermal effects was thus demonstrated, explaining the formation of different products compared to conventional heating, at lower temperatures. Finally, through a series of case studies, the power of MWs in the conversion of several LC feedstocks into valuable molecules was demonstrated.

## Questions

1. How can different biomass components be separated from each other?
2. Which processes can be used for biomass valorization?
3. What temperature is the most conducive to interactions of biomass components with MWs?
4. Which parts and groups of biomass constituents are more prone to interacting with MWs?
5. What platform chemicals can be obtained through MW-assisted acid catalyzed processes?

## Further readings

1. Tabasso S, Cravotto G. Platform Chemicals from Biomass Using Microwave Irradiation. In: Production of Biofuels and Chemicals with Microwave, Springer Book Series – Biofuels and Biorefineries, Springer, Berlin, Germany, 2014, 128–144.
2. Fan J, Budarin V, Gronnow, M. J, Clark, J H. Low-Temperature Microwave Pyrolysis and Large Scale Microwave Applications, In: Alternative Energy Sources for Green Chemistry, the Royal Society of Chemistry, Cambridge, UK, 2016, 64–90.

## Bibliography

- [1] Clark J H. Green chemistry for the second generation biorefinery – sustainable chemical manufacturing based on biomass. *J. Chem. Technol. Biotechnol.*, 2007, 82, 603–609.
- [2] Pfaltzgraff L A, De Bruyn M, Cooper, E C, Budarin V L, Clark J H. Food waste biomass: A resource for high-value chemicals. *Green Chem.*, 2013, 15, 307–314.
- [3] Moseley J D, Kappe C O. A critical assessment of the greenness and energy efficiency of microwave-assisted organic synthesis. *Green Chem.*, 2011, 13, 794–806.
- [4] Darryl R, Godwin D R, Lawton S J, Moseley J D, Welham M J, Weston N P. Efficiency of Conventionally-Heated Pilot Plant Reactors Compared with Microwave Reactors *Energy Environ. Sci.*, 2012, 5, 5481–5488.
- [5] Sheldon R A. Green and sustainable manufacture of chemicals from biomass: state of the art. *Green Chem.*, 2014, 16, 950–963.
- [6] Isikgora F H, Becer R. Lignocellulosic biomass: a sustainable platform for the production of bio-based chemicals and polymers. *Polym. Chem.*, 2015, 6, 4497–4559.
- [7] Agbor V B, Cicek N, Sparling R, Berlin A, Levin D B. Biomass pretreatment: fundamentals toward application. *Biotechnol. Adv.*, 2011, 29, 675–685.
- [8] Fan J, De Bruyn M, Budarin V L, Gronnow M J, Shuttleworth P S, Breeden S, Macquarrie D J, Clark J H. Direct Microwave-Assisted Hydrothermal Depolymerization of Cellulose. *J. Am. Chem. Soc.* 2013, 135, 11728–11731.
- [9] Budarin V L, Clark J H; Lanigan B A, Shuttleworth P S, Macquarrie D J. Microwave assisted decomposition of cellulose: A new thermochemical route for biomass exploitation. *Bioresour. Technol.* 2010, 101, 3776–3779.
- [10] Fernández Y, Arenillas A, Menéndez J A. Microwave Heating Applied to Pyrolysis, In: Advances in Induction and Microwave Heating of Mineral and Organic Materials, Edn. Collegium. Vienna, Austria, 2011, 723–752.
- [11] Budarin V L, Clark J H, Lanigan B A, Shuttleworth P, Breeden S W, Wilson A J, Macquarrie D J, Milkowski K, Jones J, Bridgeman T, Ross A. The preparation of high-grade bio-oils through the controlled, low temperature microwave activation of wheat straw. *Bioresour. Technol.* 2009, 100, 6064–6068.
- [12] Hu Z, Zhiyou W Z. Enhancing enzymatic digestibility of switchgrass by microwave-assisted alkali pretreatment. *Biochem. Engin. Journ.* 2008, 38, 369–378.
- [13] Tabasso S, Montoneri E, Carnaroglio D, Caporaso M, Cravotto G. Microwave-assisted flash conversion of non-edible polysaccharides and post-harvest tomato plant waste to levulinic acid. *Green Chem.* 2014, 16, 73–76.
- [14] Carnaroglio D, Tabasso S, Kwasek B, Bogdal D, Calcio Gaudino E, Cravotto G. From Biomass to Bio-based Lactic – Glycolic Acid oligomers: a gram-scale microwave-assisted protocol. *ChemSusChem* 2015, 8, 1342–1349.

Zhilin Wu and Giancarlo Cravotto

## 21 Microwave technology for environmental remediation

A number of new and advanced technologies, which are based on incineration, catalytic conversion, adsorption, regeneration, etc. and which aim to meet the increasingly stringent requirements of environmental protection, have been developed and commercialized for gaseous pollution control and wastewater treatment, as well as solid and liquid waste disposal [1]. Thermal treatment is an important process for environmental remediation and is used in thermal desorption, evaporation and steam distillation, decomposition and the creaking of pollutants. The development of thermal technologies that have high treatment and energy efficiency, low costs, small space volume as well as being low maintenance and contaminant free has become a trending topic [1, 2]. Microwaves (MWs) are electromagnetic radiation in the 1–10 GHz frequency range [3]. MW heating (MWH) is induced by the direct absorption of electromagnetic waves [4], termed MW dielectric heating [5] or MW dielectric-loss heating [6]. MWH can offer unique advantages, including selective heating and the potential for the recovery of value-added products, to improve processing time, remote operation to limit personnel exposure to hazardous waste and *in situ* reactant addition to reduce contamination risk during material transfer [7]. These factors lead to a reduction in energy consumption and process duration [4].

MWH has been widely used in the decontamination of waste gas, wastewater and sludge, soil, liquid and solid wastes and has proven itself to be superior to conventional heating (CH) in accelerating reaction rates and improving yields, as well as selectively activating and suppressing reaction pathways [8–10]. Typical MW processes, such as MW-induced plasma, MW-assisted desorption, MW-driven pyrolysis and MW-enhanced decomposition will be critically reviewed in this chapter, while the principles of the processes involved and the reaction technologies are outlined. Special attention will be paid to gaseous pollution control, evaporation, drying and desorption, pyrolysis and the decomposition of organic pollutants.

### 21.1 Microwave-induced plasmas

Plasma is generally created by applying electrical energy or electromagnetic radiation to gas in order to reorganize the electronic structure of the species (atoms, molecules) and to produce excited species such as electrons and ions [3]. Plasma technologies of

---

**Note:** This chapter is dedicated to Prof. Bernd Ondruschka on the occasion of his 70<sup>th</sup> birthday.

<https://doi.org/10.1515/9783110479935-021>

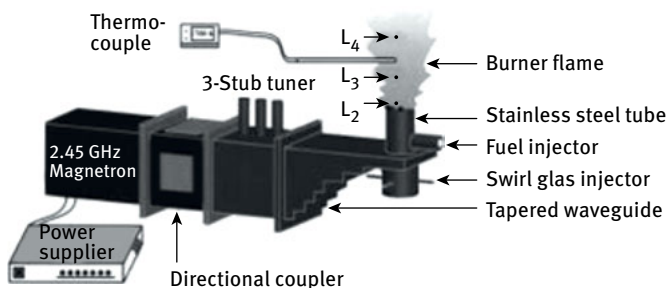


Fig. 21.1: Schematic diagram of a MIP system and plasma torch [12]

gaseous pollution control for acid gases ( $\text{NO}_x$  and  $\text{SO}_2$ ), volatile organic compounds (VOCs), greenhouse gases, ozone layer depleting substances, etc. have been developed and become significant due to advantages such as lower cost, higher removal efficiency, smaller space volume, etc. [11].

Only electrons follow the oscillations of electric fields under MW irradiation. MWs transmit energy to the plasma gas electrons in a microwave-induced plasma (MIPs) system where elastic collisions between electrons and heavy particles occur. The large mass of the heavy particles means that the collided electrons rebound, whereas the heavy particles remain static. The electrons are thus accelerated and the heavy particles are slightly heated. The electrons obtain enough energy to produce inelastic excitation or even ionizing collisions after several elastic collisions. The gas is partially ionized and becomes plasma, which supports MW propagation. MIPs are thus chemically active media [3], which also act as a source of a radical pool and high temperature [12]. Such a high-density plasma environment can be used to dissociate and ionize waste molecules and decompose and burn out gaseous, liquid and solid chemicals. Figure 21.1 shows a schematic diagram of a MIP system and plasma torch. The plasma generated inside the discharge tube is stabilized by injecting a swirl gas, which keeps the torch flame at about 5000 K [13].

Plasmas are referred to as thermal or nonthermal plasmas depending on the temperatures involved. Thermal plasma (especially arc plasma) has been extensively industrialized, whereas the use of nonthermal plasma is limited by the vacuum equipment required. Thermal plasmas have high electron density ( $n_e$ ,  $10^{21}$ – $10^{26}/\text{m}^3$ ), similar electron temperature ( $T_e$ ) and heavy particle temperature ( $T_h$ ) (10,000 K) as compared to nonthermal plasmas (glow discharges), which have relatively lower electron density ( $< 10^{19}/\text{m}^3$ ), high  $T_e$  (10,000–100,000 K) and low  $T_h$  (300–1000 K). As far as the huge mass difference between electrons and heavy particles is concerned, the plasma temperature (or gas temperature) is fixed by  $T_h$  [3].

MW plasma structures are highly dependent on carrier gas type, gas flow rate and MW power. MIPs were obtained at atmospheric pressure by MW propagation under an argon flow of 0.2–17 L/min in the 1970s. The plasma produced within a quartz tube is restricted to a diameter of approximately 1 or 2 mm, but its length can reach some tens

of centimeters at 100 W of MW power. This plasma is quite uniform along the axis, with a typical  $n_e$  of  $3\text{--}8 \times 10^{17}/\text{m}^3$  and gas temperatures of below 6000 K (nonthermal plasma) [13, 14]. In general, MW discharges are classified as atmospheric plasma sources. The  $n_e$  of MIPs can range from  $10^{17}$  to  $10^{22}/\text{m}^3$  with  $T_e$  values of 13,000–90,000 K and  $T_h$  values of 500–10,000 K in various MIP devices. High gas temperatures can only be obtained at high working powers [3].

The generation of large-volume, high-pressure and nonthermal plasma has been continuously pursued [15]. The nature of the plasma gas is important since it influences plasma temperature. The temperature does not change if the working gas is Ar, Ar/H<sub>2</sub>, N<sub>2</sub>, air, O<sub>2</sub>, or Ar/He because the ionization energies are very close (between 13.5 and 16 eV). However, the ionization energy is much higher in a helium plasma (24 eV), resulting in gas temperatures of 4000 to 5000 K [3]. General MIP torch characteristics ( $n_e$ ,  $T_e$ ) are in between those of arc plasmas and glow discharge plasma generators. By injecting fuel gases into the MIP torch [16], the flame volume of the MIP burner is more than 50 times that of the torch plasma; meanwhile the temperature of the MIP burner flame, with kerosene (25 mL/min) and oxygen (20 L/min), drastically increases from 550 to about 1850 K [12]. This behavior enables a wide range of applications to be performed with those plasma sources, especially in environmental remediation.

The decontamination mechanism of MW-induced plasma can be explained as follows: first there is the dissociation of gaseous molecules forming active species under nonthermal plasmas, [13, 17] then the thermal decomposition of gaseous molecules at high temperatures [18] and, finally, radical reactions [13]. MWs of 2.45 GHz are typically fed into the cavity or jet, resulting in a sufficiently high electric field to ignite the gas and maintain stable ionization. A number of MIPs with gas control systems have been fabricated to destroy or break down polluting emissions, including the dissociation of H<sub>2</sub>S<sup>1</sup>, desulfurization and denitrification of flue gas, the abatement of perfluorocompounds (PFCs) and the destruction of VOCs.

### 21.1.1 Dissociation of hydrogen sulfide

The conventional treatment for H<sub>2</sub>S<sup>1</sup> is the Claus process, which produces sulfur and water, resulting in a loss of the valuable hydrogen. H<sub>2</sub>S treatment would be more economically valuable if H<sub>2</sub> and S products could be recovered [18]. The MIP process saves a substantial amount of energy since it requires less energy to dissociate H<sub>2</sub>S. An analysis of standard heats of formation led to the theoretical energy required to produce H<sub>2</sub> from H<sub>2</sub>S dissociation being calculated as only 20.6 kJ/mol, as compared to 63.2 kJ/mol in steam methane reforming and 285.8 kJ/mol in the water electrolysis

<sup>1</sup> <http://www.osti.gov/scitech/biblio/5015768>



method [18]. The almost complete conversion of  $\text{H}_2\text{S}$  into  $\text{H}_2$  and  $\text{S}$  was thus achieved in the MIP reactor at about 2400 K under atmospheric pressure [18]. Furthermore, the plasma process can dissociate  $\text{H}_2\text{S}$  in the presence of  $\text{CO}_2$ ,  $\text{H}_2\text{O}$ , and  $\text{CH}_4$  [19]. Despite the large number of thermal decomposition methods available, MIP dissociation of  $\text{H}_2\text{S}$  prevails as the method of choice as it provides the best conversion and energy efficiency [17, 18].

### 21.1.2 Desulfurization and denitrification of flue gas

Electron beam (EB) irradiation, MW and a combination of EB/MW have been used to remove  $\text{NO}_x$  and  $\text{SO}_2$  from simulated flue gases [20, 21]. The MW applicators consisted of a power-controlled generator and a 2.45 GHz magnetron of 850 W. Simultaneous desulfurization and denitrification were performed at 65–70 °C in a gaseous mixture (7% Ar, 25%  $\text{H}_2\text{O}$ , 10%  $\text{CO}_2$ , 2000 ppm  $\text{SO}_2$ , 1000 ppm  $\text{NO}_x$ ) with  $\text{NH}_3$  added in stoichiometric amounts.  $\text{NO}_x$  removal efficiency reached 63% for EB and 70% for EB/MW.  $\text{SO}_2$  removal efficiency was 80% under MW, 85% under EB and 90% under EB/MW. Removal efficiency strongly depended on MW applicator structure type, residence time and MW power level. The presence of a lower concentration of Ar in the gaseous mixture increased  $\text{SO}_2$  removal efficiency. The combined EB/MW method granted a significant decrease in average EB power at the same removal efficiency. In another study, NO was almost completely converted to  $\text{N}_2$  by MIP under He. NO conversion was nearly 80% in the NO,  $\text{O}_2$  and He system, while the selectivity to  $\text{N}_2$  was 80%.  $\text{N}_2$  yield was not affected when 5%  $\text{H}_2\text{O}$  was added to the system. NO conversion increased and the selectivity to  $\text{N}_2$  increased even further as MW power was increased [22].

### 21.1.3 Abatement of greenhouse gas: PFCs

PFCs have long lifetimes and serious global warming implications. Several electrodeless atmospheric MIP torch devices have been developed in order to destroy all similar global warming gases emitted during the manufacture of semiconductors. An earlier study saw the destruction of ppt concentrations of  $\text{C}_2\text{F}_6$  in  $\text{O}_2$  and natural gas mixtures performed in a low-pressure (11.3 Torr) plasma reactor. A destruction and removal efficiency (DRE) of 99.6% was achieved for  $\text{C}_2\text{F}_6$  in only milliseconds at 500–2000 W MW power [23]. The abatement of PFCs has more recently been carried out using additive gases, such as  $\text{O}_2$ ,  $\text{N}_2$  and air, giving nearly 100% DRE for all PFCs investigated [24, 25]. DRE increased with increasing MW power and decreased with increasing gas flow rate and discharge tube radius [26]. In practice, the DRE of  $\text{CCl}_3\text{F}$  in  $\text{N}_2$  was up to 100% with the removal rate of several hundred g/h and energy efficiency of about 1 kg/kWh. This impressive performance, superior to that of other methods, was achieved without

**Tab. 21.1:** Abatement of PFCs by MIP at atmospheric pressure

PFC	Additive gases flow (L/min)	Power (W)	DRE	Generating gas	Ref.
C <sub>2</sub> F <sub>6</sub> CF <sub>4</sub> SF <sub>6</sub> CHF <sub>3</sub>	O <sub>2</sub>		Near 100%	CO <sub>2</sub> , COF <sub>2</sub> , F <sub>2</sub> CO <sub>2</sub> , COF <sub>2</sub> , F <sub>2</sub> SO <sub>2</sub> F <sub>2</sub> , SO <sub>2</sub> , F <sub>2</sub> CO <sub>2</sub> , COF <sub>2</sub> , F <sub>2</sub> , HF	[25]
SF <sub>6</sub> , 0.1–2.4%	O <sub>2</sub> , N <sub>2</sub> (30)	6000	Higher than 95%		[26]
CCl <sub>3</sub> F, 50%	N <sub>2</sub> (1–3)	200–400	Up to 100%		[27]
CF <sub>4</sub>	O <sub>2</sub>			F <sub>2</sub>	[28]
CF <sub>4</sub>	O <sub>2</sub> , air		> 99%		[29]
SF <sub>6</sub>	O <sub>2</sub> , N <sub>2</sub> , air	1100	98.4–99.1%		[30]

DRE: Destruction and removal efficiency

generating any significant unwanted byproducts [27]. More results on the abatement of PFCs using MIPs are listed in Table 21.1<sup>2</sup>.

#### 21.1.4 Destruction of VOCs

Besides PFCs, chlorinated and nonchlorinated VOCs can also be cracked using MIP at atmospheric pressure [31, 32]. Nearly 100% decomposition of dimethyl and diisopropyl methylphosphonates was achieved in only 0.13–2.4 s by MIPs in He and air, while phosphoric acid or its precursors, dealkylated phosphonic acids, were the main products in this work [33]. The safe and complete elimination of dimethyl methylphosphonate with added O<sub>2</sub> was also demonstrated at a destruction rate of 1.14 L/h at 1.2 kW MW power [34]. More recently, however, ethanol was reformed under MIP to produce H<sub>2</sub>, CO and solid carbon. The average yield of H<sub>2</sub> reached 98.4% [35]. Cyclopentane hydrate was decomposed by MIP to generate gases with 65% H<sub>2</sub>, 12% CO and 8% CO<sub>2</sub> [36].

The complete destruction of trichloroethene and toluene under Ar, O<sub>2</sub> and steam has been achieved by MIP at 500–600 W MW power. No hazardous byproducts were observed in the presence of sufficient O<sub>2</sub> [37]. CCl<sub>4</sub> concentration was achieved, via complete decomposition, on the ppb scale with Ar in a He atmosphere at the MIP reactor outlet. Under high Ar flow rates and CCl<sub>4</sub> concentrations, the energy efficiency of this decomposition reached about 3 kg/kWh. The main gaseous byproducts were CO<sub>2</sub>, NO and N<sub>2</sub>O in addition to small amounts of Cl<sub>2</sub>. In another demonstration the full decomposition of highly concentrated VOCs (several to several tens of percent) was achieved under nonthermal MIP at 100–400 W MW power at a gas flow rate of

<sup>2</sup> <http://iopscience.iop.org/article/10.1143/APEX.4.066201/meta>

1–3 L/min. The energy efficiency of decomposition was generally around 1 kg/kWh, indicating a relatively low energy cost [38]. The use of MIP not only efficiently destroyed VOCs here, but also produced the valuable fuel gases  $H_2$  and  $CO$ .

## 21.2 MW-assisted evaporation and desorption

### 21.2.1 Ammonia evaporation from wastewater

Ammonia nitrogen ( $NH_3-N$ ) contaminated wastewater has threatened the safety of water resources for some time, especially since it induces water body eutrophication. MWH evaporation has been developed for the efficient removal of  $NH_3-N$  from water. MWH time and pH value are the critical factors for removal efficiency [39, 40]. The highest  $NH_3-N$  removal was obtained at pH 11 in 3 min. The formation of molecular ammonia ( $NH_3$ ) was thus the dominant step and the subsequent evaporation of  $NH_3$  occurred under MWH. MWH led to higher  $NH_3-N$  removal than CH. In coke plant wastewater, 5000 mg/L of the initial  $NH_3-N$  concentration was reduced to 350 mg/L (93% removal) in 10 min at pH 11 and 750 W MWH [39, 40]. The highest  $NH_3-N$  removal efficiency of municipal wastewater has been set at 90.5% in 4 min at a pH of 11 [40].

### 21.2.2 Desorption of organic pollutants on granulated activated carbon

Granulated activated carbon (GAC) is a common adsorber used to remove organic contaminants from wastewater and can be thermally treated to perform the desorption and decomposition of organics. GAC effectively absorbs MW energy meaning that its temperature rose to over 1100 °C in a few minutes under MWH. At such high temperatures, adsorbed organics are desorbed and decomposed [41].

In an experiment, 13–30 mg/L benzene, toluene, xylene and a mixture of them, as well as 5–400 mg/L phenol were adsorbed on a GAC packed bed. The maximum adsorption capacity for 400 mg/L phenol was 220 mg/g GAC. The adsorbed organics were completely removed from the saturated GAC by MWH. ‘Arcing’ was created among the GAC particles during MWH, while the GAC temperature reached 1200–1800 °C [42, 43]. During the process, 1000 mg/L pentachlorophenol (PCP) was adsorbed onto 1 g GAC in a 0.5 mL solution, and then the exhausted GAC was treated for 100 s at 600 W MW power. More than 99% PCP was destroyed [44]. GAC was also modified by Cu and elemental Cu was distributed uniformly over the GAC surface. The adsorption capacity of GAC decreased after loading Cu because Cu occupied the adsorption sites. Most of the PCP adsorbed onto virgin GAC decomposed or was bound irreversibly to GAC after 10 min of MW at 850 W, while less than 2% was transformed into intermediates. The more rapid decomposition of PCP was observed on Cu-loaded GAC with larger amounts of intermediates formed [41].

### 21.2.3 Dehydration of sludge, solid waste and biomass

Thermal treatment methods require the energy-consuming drying of organic wastes, which typically contain 70–80% moisture [45]. The benefits of MW drying include instant energy transfer and selective heating to water by direct MW absorption, thus minimizing conductive and convective losses of heat, while reducing drying times, energy consumption and costs [46].

#### 21.2.3.1 Dehydration of sewage sludge

The sludge drying rate is directly proportional to MW power, but inversely proportional to sample mass. The desired temperature has been achieved in short times at higher power [47]. The kinetics of sludge drying showed three distinct phases; the short adaptation period, the long constant drying rate period and the falling drying rate period [48]. MWH thus enhances sludge dehydration in short contact times, and a drying time of 1 min at 900 W was found to be the ideal condition, yielding maximum sludge dehydration characteristics as well as optimal disintegration (1.5–2%), extracellular polymeric substance concentration (1500–2000 mg/L), and particle size distribution (120–140  $\mu\text{m}$ ) [49]. MW drying induces a significant increase in the calorific value of sewage sludge from 5.65 to 18.75 MJ/kg, due to substantial volume reduction [47, 48].

#### 21.2.3.2 Dehydration of solid waste

Gypsum<sup>3</sup> is the byproduct of flue gas desulfurization and can be dried at 12 kW at 2.45 GHz in a continuous-feed MW system. Drying efficiencies of 49–73% have been achieved, resulting in moisture reduction from 7 to less than 1% [50]. In another study, an all-in-one MW thermochemical process (drying, pyrolysis and gasification) was developed to improve the efficiency of biorefineries. MWH was able to eliminate the need for the predrying of municipal solid waste to produce a high quantity of synthesis gas (syngas). Syngas compositions differed over the first 20 min and remained constant thereafter depending on initial moisture content and pyrolysis time. Furthermore, moisture content improved volumetric gas production by almost 50% [51].

#### 21.2.3.3 Drying biomass

Pine<sup>4</sup> wood sawdust, peanut shells and maize stalks have been dried at 200–800 W in a bench-scale fluidized bed MW reactor and compared to drying in an electrical oven at 105 °C. Dehydration was finished within 6 min at 600 W MW power, but took about 40 min in an electrical oven. The yields of solid char and liquid oil were increased by pyrolysis at 500 °C after MW drying, while the yield of gaseous products decreased.

<sup>3</sup> <http://papers.sae.org/2007-01-3266/>

<sup>4</sup> <http://pubs.acs.org/doi/pdf/10.1021/ef700300m>

Meanwhile, the viscosity and heating value of the bio-oil increased because the water content decreased and the average molecular weight increased. MW drying obviously suppressed the further reaction of volatiles during biomass pyrolysis, leading to higher quantities and better quality bio-oil being produced during the fast pyrolysis process [46]. In a large-scale study for drying tobacco stems, underused tobacco industry waste was transformed into a viable product via the preparation of biomass material from stem granules. The optimal MW drying time for stem granules with 30% moisture content and 30 mm of material thickness was 150 s at 35 kW MW power, giving a stem granule yield of 64% [52].

#### 21.2.4 Desorption of organics from contaminated soil

The MWH steam distillation process for the removal of VOCs from contaminated soil has been widely investigated. Temperature, humidity, residual contaminant concentration and permittivity are critical factors for efficient removal, but the dielectric properties of the soil matrix play the most important role in electromagnetic field propagation [53]. The addition of carbon particles enhanced MW absorption [54]. Desorbed contaminants were collected on an activated carbon (AC) absorption tower before AC was moved offsite for regeneration. Nearly 100% DRE was achieved with phenanthrene in sludge and 60% with pentachlorophenol in contaminated soil [53]. The overall efficiency of polychlorinated biphenyl (PCB) removal from contaminated soil was higher than 98% at a steam-to-soil mass ratio of 3 : 1. The rapid expansion and evaporation of pore water accelerated PCB evaporation rates. Increased PCB solubility in the heated aqueous phase was also hypothesized [55]. Soils that were heavily contaminated with polycyclic aromatic hydrocarbons (PAHs) behaved very differently in a MW field to lightly contaminated versions, with bulk soil temperatures limited to 100 °C for the lightly contaminated soils. A PAH removal rate of more than 95% was achieved under moderate processing conditions. Complete remediation of the soils was shown to be possible at high MW powers and/or long residence times. Moreover, PAH removal occurred at bulk temperatures that were well below the boiling points of the compounds, because thermal desorption, selective heating and entrainment mechanisms were all exploited [56].

Diesel fuel in soil has been removed at 100–1000 W MWH for 5–60 min. MW power significantly influenced removal kinetics, while the peak temperature depended on moisture in the soil. The minimal contaminant concentrations were achievable at higher than 600 W MW power for over 60 min. Soil temperature reached about 100 °C in less than 10 min MWH and the effect of the distillation process improved removal yield. Soil temperature dominated the remedial treatment at longer times [57]. A small amount of carbon fiber was added to the crude oil-contaminated soil in order to enhance thermal remediation. The carbon fiber efficiently improved the conversion of MW energy into thermal energy. The soil was heated to approximately 700 °C in 4 min

at 800 W MW power with the addition of 0.1 wt.% carbon fiber. The oil contaminant was removed from the soil matrix and recovered using an ice-salt bath condensation system [58].

### 21.2.5 Stripping of oil from drill cuttings

The oil levels of oil contaminated drill cuttings<sup>5</sup> (OCDC) have been reduced to below the current environmental discharge limit in short MW-assisted stripping times (e.g. 20 s). Increasing water content in the samples efficiently improved the stripping of oil [59, 60]. Water molecules absorbed the bulk of the applied MW energy, which was subsequently transferred to the oil in the form of heat, and caused thermal desorption. The boiling point of oil was reduced when it was mixed with water, since free water was beneficial to uniform heating, whilst bound water significantly affected the latter stages of oil removal [61]. The pore structures in the drilling waste enabled the water inside to be superheated. The oil was thus heated to higher temperatures and then removed by sweep gas [62]. Although water has high dielectric properties, it is not efficient in removing heavy oils due to its volatility. Additional dielectric material (salt water) with a high loss factor contributed to oil removal at low concentrations, whereas high concentrations were less effective. The addition of AC was found to be more efficient for both light and heavy petroleum oils [63]. MWH did not cause the chemical conversion of the recovered organic phase, at least not in significant amounts [59]. However, higher MW power and electric field strength promoted the pyrolysis of the oil. The potential effects of bound water are, most likely, one reason behind pyrolysis being induced [64].

Cutting mixtures containing rounder and larger particles experienced greater removal of drilling fluid than mixtures consisting of less-round and finer particles. An increase in bed height led to higher efficiency in terms of *n*-paraffin removal. The use of a sweep gas increased *n*-paraffin removal from 75 to 90% [59]. A combination of MWH and the nitrogen and steam stripping process obviously provided a steep improvement in performance. Enhancements in MWH process time, of some orders of magnitude, were shown as well as greatly improved levels of remediation [65]. Furthermore, the cost of using MWH for the remediation of oily waste was up to 20 times lower than for CH [61].

### 21.2.6 Regeneration of adsorbents

The sorption process is a common method for removing inorganic and organic contaminants. Adsorbents must therefore be regenerated if the process is to be efficient,

---

<sup>5</sup> <http://www.sciencedirect.com/science/article/pii/S0301479707000904>

economical and environmentally friendly. Conductive, convective and radiative losses are minimized as MW energy is absorbed directly by the absorbers and/or absorbates. Extremely rapid heating is also possible, i.e. 1400 °C in less than 1 min. The regeneration process is thus shortened considerably and is more efficient under MWH [66, 67]. Regeneration systems also create a highly concentrated effluent, which is recovered via condensation at near-ambient temperatures [68]. The thermal absorption processes of AC, zeolite and polymeric resins using MWH have been extensively studied since the 1980s.

#### **21.2.6.1 For flue gases: SO<sub>2</sub>, NO<sub>x</sub> and CO<sub>2</sub>**

The pollutants in the flue gas emitted from power plants have been removed to meet the requirements of environmental protection by applying adsorption on AC, MW desorption and MW-induced decomposition. The adsorption capacity and removal efficiency of NO decreased with increasing SO<sub>2</sub> concentrations in flue gas during desulfurization and denitrification. The adsorption capacity of NO increased slightly at first, and then dropped to 12.8 mg/g, while desulfurization efficiency decreased with increasing SO<sub>2</sub> concentration. The adsorption capacity of SO<sub>2</sub> declined with increasing O<sub>2</sub> content in flue gas, while the adsorption capacity of NO increased. Overall NO and SO<sub>2</sub> removal efficiencies reached more than 99%. The adsorption capacity of NO decreased with an increase of moisture in the flue gas, but the adsorption capacity of SO<sub>2</sub> increased, giving NO and SO<sub>2</sub> removal efficiencies that were relatively stable. The adsorption capacities of both NO and SO<sub>2</sub> decreased with increasing CO<sub>2</sub> content. The efficiencies of desulfurization and denitrification increased initially, then started to fall when the CO<sub>2</sub> content exceeded 12.4% [69].

Boiler flue gas contains up to 10% (v/v) CO<sub>2</sub> in air, but can be readily enriched to a stream containing >70% CO<sub>2</sub> which may be ideal for use in acidification, precipitation, stripping, etc. In order to rapidly produce high purity CO<sub>2</sub>, the adsorbent surface has been treated with MW-assisted vacuum to liberate water and CO<sub>2</sub>. The adsorption was conducted in a column of 13X zeolite with 12% CO<sub>2</sub> in a N<sub>2</sub> gas mixture. MWH improved the rapid desorption of CO<sub>2</sub> and water and improved integrated CO<sub>2</sub> purity in the blowdown stream from 60 to 80%. The brief exposure of an adsorbent to MW radiation raised the required vacuum level for the regeneration of high humidity flue gas streams [70].

#### **21.2.6.2 Organic solvents**

Organic solvents, such as methyl ethyl ketone, acetone, tetrachloroethylene, trichloroethylene and methanol vapors, have been removed via adsorption onto GAC, carbon based molecular sieves, ZSM-5 synthetic zeolite, silicalite zeolite, etc. The saturated adsorbents were then regenerated in a MW field where the solvent was quickly desorbed and recovered from the inner pores [67]. The MW-induced regeneration restored the original adsorption capacity and surface area [71]. The higher MW power may re-

sult in self-burning of AC, caused by the presence of traces of O<sub>2</sub>, which might slightly deteriorate the pore structures of AC. However, the lower MW power cannot start desorption. The introduction of N<sub>2</sub> flow during regeneration was necessary to release the desorbed solvent from AC, but might cool the adsorption system at a higher N<sub>2</sub> flow rate [72]. MWH was also used in the regeneration of AC fibers saturated with ethanol at atmospheric pressure and under vacuum conditions. The adsorption of AC fibers after MW regeneration for some time was larger than for fresh AC fibers, and the rate of total mass loss was 3.54–4.74% [73, 74]. The efficiencies of several MW desorption solvents on AC conditions are listed in Table 21.2.

Polymeric adsorbents can also be regenerated by MWH, while MW regenerated adsorption favors the use of low dielectric loss-factor polymeric adsorbents and operation under low pressure conditions (about 5 torr absolute pressure) [68]. The adsorption and MW-assisted desorption behavior of highly porous hypercrosslinked polystyrene adsorbents toward benzene was investigated under humidified conditions. Compared to the as-synthesized adsorbents, sulfonated adsorbents showed reduced adsorption capacities, but improved desorption efficiencies in a semicontinuous mode at 600 W. The increased desorption efficiency was mainly attributed to a larger amount of adsorbed water, which indirectly allowed the heating of polymer adsorbents to reach higher temperatures upon MW irradiation [75]. The MW systems were similar in terms of capital and operating costs to conventional steam regeneration systems and therefore may be an attractive alternative for recovering solvents [76].

### 21.2.6.3 For other organic contaminants

Organic contaminants such as phenol, PCP, pyridine, indole and quinoline in water have been adsorbed and removed using GAC and then decomposed, while GAC was regenerated under MWH [77]. MWH preserved the porous structure of regenerated AC more efficiently than CH. CH shifted the micropore size distribution towards pores of narrower sizes and significantly reduced the apparent BET surface areas during regeneration cycles. The adsorptive capacity of the carbon material was reduced after six adsorption-desorption cycles in both MWH and CH systems, but the phenol adsorption capacities decreased to a greater extent in the samples regenerated by CH (electric

**Tab. 21.2:** Desorption efficiency of solvents on AC using MWH

Solvents	AC amount (g)	MW power (W)	Carrier gas flow (L/min)	Heating time (min)	Desorption rate (%)	Outlet concentration (%)
Toluene	5	500	N <sub>2</sub> , 0.06	3	77.2	[72]
Ethanol	3.5	680	Vacuum, 0.05 MPa	3	95.3	97.5 [73]
Ethanol	3	528	N <sub>2</sub> , 23	3	90.2	95.6 [74]



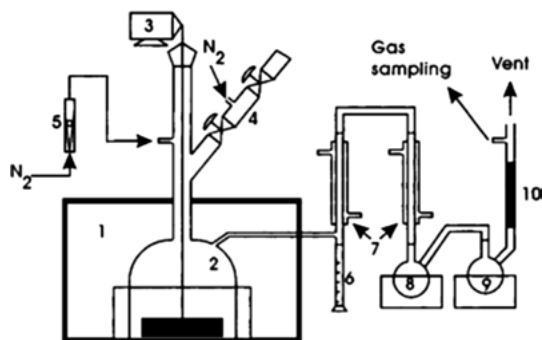
furnace) [66]. Most of the PCP adsorbed onto GAC, and the byproducts formed, were decomposed into CO<sub>2</sub>, H<sub>2</sub>O and HCl or tightly bound to GAC under MWH for 10 min at 850 W. Less than 2% PCP was transformed into intermediates in the distillate [77]. Likewise, pyridine, indole and quinoline-adsorbed bamboo charcoals have been effectively regenerated by MWH [78].

Salicylic acid, a metabolite of a common analgesic frequently found in wastewater from the pharmaceutical industry, has been adsorbed by AC. Regeneration efficiencies under MWH were around 99% after six cycles. Stripping efficiency was higher than 95% at high temperatures and decreased at 450 °C, but the blocked micropores reduced the loading capacities in successive cycles [79]. A 2,4,5-trichlorobiphenyl (PCB29) adsorption process has been carried out in a continuous flow GAC adsorption column. After adsorption, the PCB29-loaded GAC was dried at 103 °C and regenerated by MWH at 700 W for 5 min [80]. After the regeneration of the dye-loaded carbons using MWH for 2–5 min at 2.45 GHz, the carbon yield and monolayer adsorption capacities for methylene blue (MB) were maintained at 68.4–82.8% and 154.7–195.2 mg/g, even after five adsorption-regeneration cycles [81]. In comparison, 100 mg/L Reactive Black 5 (RB5) was adsorbed onto 100 g/L GAC giving an 82% removal rate within 4 h. However, RB5-loaded GAC was not effectively regenerated under MWH for 30 s at 800 W. Electrocoagulation showed high decolorization, but 61% COD residue and toxicity remained after treatment. COD and toxicity in the electrocoagulation-treated solutions were effectively removed on 20 g/L GAC in 4 h and the intermediate-loaded GAC was effectively regenerated by MWH for 30 s at 800 W [82].

In short, MWH preserved the pore structure, original active sites and adsorption capacity of the regenerated AC [81], which was reused after five to seven adsorption/MW regeneration cycles. Its adsorption capacity was maintained at a relatively high level, even higher than that of virgin GAC [77, 80, 82].

### 21.3 Microwave-driven pyrolysis

Feedstock recycling (tertiary recycling) is the processing of waste into fuels or basic chemicals. Pyrolysis (thermolysis) is a well-known process of thermal and chemical decomposition in an oxygen depleted environment, generally leading to smaller molecules. It can be operated at a wide range of temperatures in order to target specific products (typically between 400–700 °C for a predominantly liquid yield; over 700 °C for predominantly C<sub>1</sub>–C<sub>3</sub> light hydrocarbons). More attention has been given to MW-driven pyrolysis (MWP) since 2000 [83]. MWP is generally an environmentally friendly technology, which converts organic waste into commercially valuable gas, liquid and solid products. The intense localized, molecular heating caused by MW power enables it to dispose of all types of waste, including organic waste and biomass, sewage sludge, municipal solid waste, polymeric materials (plastics and rubbers), as well as



**Fig. 21.2:** Schematic drawing of MWP apparatus: (1) MW oven, (2) reactor, (3) motor, (4) feeder, (5) gas flow meter, (6) main collection flask, (7) water-cooled condensers, (8,9) cold traps, (10) cotton wool filter [83]

waste oils in a safe and reliable manner [84]. A typical MWP experimental apparatus is shown in Figure 21.2 [83].

### 21.3.1 Organic waste and biomass

The ability to valorize a wide range of renewable, abundant and cheap feedstocks, such as waste paper, wood sawdust, straw and corn stover and other organic wastes, is highly attractive and beneficial [85]. Extensive research into biomass valorization has led to an increasing diversity of methods, including the pyrolysis of biomass for production of syngas, bio-oil and char/carbonaceous residue [86, 87]. The reactions of solid and liquid carbonaceous materials occurs *in situ* with CO<sub>2</sub> and high temperatures inducing self-gasification, which takes place at about 800 °C under CH, but occurs at lower temperatures with MWH [88, 89]. A great deal of effort has been made to improve pyrolysis processes, to provide higher yields, better liquid biofuel quality and better energy efficiency. The carbonaceous residue is the primary solid product alongside the superior char, which can be used as absorber AC for decontamination [90, 91]. Since the late 1970s, MWP has been considered one of the most promising attempts at achieving organic waste and biomass valorization, mainly due to the efficient heating of feedstock under MW dielectric heating effects [6, 92]. The MWP of biomass and tar cracking in biomass gasifiers has therefore been termed a MW-assisted biorefinery<sup>6</sup> [93]. Figure 21.3 shows the process and product components of a MW-assisted biorefinery<sup>6</sup>.

The distribution of pyrolysis products is generated by increasing the temperature, while requiring less time and energy consumption than conventional heating

<sup>6</sup> <http://enerzi.co/wp-content/uploads/2015/12/Article4.pdf>

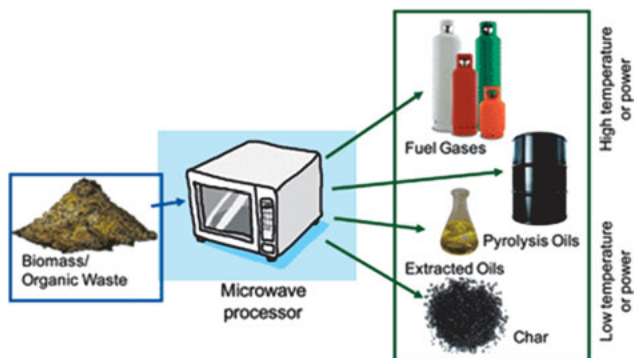


Fig. 21.3: The process and product components of a MW-assisted biorefinery [85]

pyrolysis (CHP) and increasing the quality of value-added products [87, 94]. MWP produces greater gas yields with elevated syngas content at significantly reduced temperatures than CHP. Higher  $H_2$  and  $CO$  contents and lower  $CH_4$  and  $CO_2$  contents have been achieved under MWP than under CHP at the same temperature [95, 96]. Bio-oils produced by CHP contained a greater number of phenolic, pyrrole and alkane compounds, whereas benzene and pyridine were more predominant in MWP-produced oils [97]. Less char material was furnished by MWP as higher volatile gas transfer from the core region led to clean micropores with more open structures and larger specific areas of char than produced by CHP [98, 100]. As the temperature increased from 400 to 600 °C, the yields of gas products increased from 17.7 to 22.3 wt.% and the ratio of syngas to total gas products increased from 67.2 to 77.1 vol.% [101].

Wood is a relatively good MW absorber compared to water at room temperature. However, as temperature increases, wood starts to become MW transparent as the inherent moisture evaporates. Selective heating of the bound water before evaporation may heat the remaining bulk to pyrolysis temperatures. Furthermore, a high volatiles content of 70% in oil palm empty fruit bunch provides the advantage of high reactivity. A moderate potassium content of 12.8% was also shown to positively affect MW absorption and increase temperature [102]. Potassium can inhibit volatile release and promote secondary cracking reactions in heavy hydrocarbons (oil) to form noncondensable gases. However, low dielectric constant and loss of dried material values would require the addition of MW absorbers for the pyrolysis reaction to occur [102]. With char, AC or silicon carbide (SiC), biomass can be rapidly heated to pyrolytic temperatures (500 °C) within seconds. The advantages of adding a MW absorber include a substantial reduction in the consumption of energy, time and costs for the production of bio-oil [103, 104].

Metal oxides and salts, such as  $KAc$ ,  $Al_2O_3$ ,  $MgCl_2$ ,  $H_3BO_3$  and  $Na_2HPO_4$ , can increase bio-oil yield by suppressing charcoal or gas yield in the MWP of corn stover and aspen wood pellets. The catalysts may work as a MW absorber to accelerate heating or

participate in so-called ‘in situ upgrading’ of pyrolytic vapors [105]. More liquid products and fewer gas products have been generated using metal-oxide catalysts, possibly due to the existence of Fischer–Tropsch synthesis. The lowest concentration of CO<sub>2</sub> was obtained when adding CaO. The yields of H<sub>2</sub> and CO increased with the promotion of gasification reactions between carbon and CO<sub>2</sub> and the dry reforming and cracking reaction of CH<sub>4</sub> under high temperature using K<sub>2</sub>CO<sub>3</sub> [106]. Due to the increasing temperature, the metal-oxide catalysts have been shown to effectively increase the mass reduction ratio but lower the calorific values of solid residues. Meanwhile, the catalyst lowered the formation of PAHs and thus made liquid products less toxic [107]. A large number of volatiles were released resulting in an increase in the number of pores, the specific surface area and the pore volume. This produced a uniform pore structure of chars, while the average pore size decreased from 282 (400 °C) to 47 nm (600 °C) [101].

The degradation of biomass increases with increasing MW power. Higher power input also favors syngas production. H<sub>2</sub> concentration has been shown to increase by approximately 20 vol.% with the increase in MW power, leading to a high heating rate. At constant temperature (500 °C), the yield of solid products decreased with increasing MW power during the heating stage [106]. At 500 W MW power, the pyrolysis performance of a stover under N<sub>2</sub> atmosphere was generally better than under CO<sub>2</sub> atmosphere. This may be due to the better heat absorbability of CO<sub>2</sub> molecules, which reduced the heat. The major product was CO under N<sub>2</sub> atmosphere, but CO<sub>2</sub> was the major product under CO<sub>2</sub> atmosphere [107]. The MWP of rice straw produced H<sub>2</sub>-rich fuel gas. Gas components included 50.7% H<sub>2</sub>, 16.1% CO, 22.6% CO<sub>2</sub> and 7.4% CH<sub>4</sub> [108]. Additionally, a large biomass particle size can be used directly in MWP. The MW penetration depth of 35 mm was found to be highest at 20% moisture, indicating the significant reduction of energy consumption and costs that it provides over grinding smaller particle sizes and moisture removal [102, 104]. The bio-oil and syngas yields provided by the MWP<sup>7</sup> of solid waste and biomass under various conditions are listed in Table 21.3<sup>7</sup>.

### 21.3.2 Sewage sludge

Sludge<sup>8</sup> weight loss of 85% has been achieved, as the majority of volatile matter is released before 600 °C [109]. In general, the sample was simply dried when raw wet sludge was treated by MWH without an additional MW absorber. When the sludge was mixed with a small amount of char or graphite, temperatures of up to 900–1000 °C were achieved in a few minutes, so that pyrolysis took place rather than drying [110, 112]. MWP took a much shorter time than CHP [111, 113], and the multimode MW oven

<sup>7</sup> <http://iopscience.iop.org/article/10.1143/APEX.4.066201/meta>

<sup>8</sup> <http://www.sciencedirect.com/science/article/pii/S0043135402000179>

Tab. 21.3: Bio-oil and syngas yield from the MWP of solid waste and biomass

Raw materials	Tem- pera- ture (°C)	MW power (W)	Bio-oil yields (%)	Syngas yield (%)	Solid yield (%)	Main components in oil or gas	Caloric value	Ref.
Bio-oil as main product								
tea waste	500		30.4		43.3	<i>n</i> -alkanes and alkenes, and branched hydrocarbons		[114]
waste office paper	400		19 organic, 23 aqueous phase			carbohydrates, aromatics and carbonyl- containing moieties		[115]
rice husk,		300/75%	22.4			22% D-allose, 71% dodecanoic acid and 75% octasiloxane		[116]
sawdust,		MW	33.6					
bagasse		absorber	19.1					
residues								
oil palm shell		800/25%	28			85% phenol	29.5 MJ/kg char	[117]
		AC						
engine oil	650		74 C <sub>5</sub> -C <sub>10</sub> hydrocarbons, 65-85 C <sub>5</sub> -C <sub>20</sub>			42% H <sub>2</sub> and CO and 33% aliphatic hydrocarbon (78% C <sub>1</sub> -C <sub>6</sub> ) gas	4.7 to 5.5 MJ/m <sup>3</sup>	[118]

Tab. 21.3 (cont.)

Raw materials	Tem- pera- ture (°C)	MW power (W)	Bio-oil yields (%)	Syngas yield (%)	Solid yield (%)	Main components in oil or gas	Caloric value	Ref.
Syngas as main product								
sewage, sludge, coffee hulls		MWP		lowest con- centration		highest H <sub>2</sub> /CO molar ratio		[94]
glycerol				highest con- centration		lowest H <sub>2</sub> /CO ratio		
waste papers		800		59, 2.10 m <sup>3</sup> /kg		31–43% H <sub>2</sub> and CO		[119]
coffee hulls	500			a larger yield of the gas		40% H <sub>2</sub>		[95]
	800					72% syngas (H <sub>2</sub> + CO) in MWP		
	1000					30% H <sub>2</sub>		
rice straw		400–500	alkanes, polar, and low-ringed PAHs			53% syngas (H <sub>2</sub> + CO) in CHP		[120]
						55% H <sub>2</sub>		
						13% CO		
						17% CO <sub>2</sub>		
						10% CH <sub>4</sub>		
rice straw		300	50	more gaseous product	less solid residues	21% H <sub>2</sub> 57% CO		[121]
						8% CH <sub>4</sub> 14% CO <sub>2</sub>		
rice straw		800		67.5, 40.5 mg/g		34–48% H <sub>2</sub>		[122]
		900				40–53% H <sub>2</sub>		
		1000				45–56% H <sub>2</sub>		

also favored cracking and dehydrogenation reactions to a greater extent than the single mode MW oven [111].

The pyrolysis process produced a considerable amount of valuable gases, which could be used as fuels due to their high calorific values. MWP increased syngas content of CO and H<sub>2</sub> (62–66 vol.%), while CHP generated gases with an elevated proportion of hydrocarbons (around 25%) [113, 123, 124]. The presence of moisture increased the H<sub>2</sub> and CO<sub>2</sub> content and decreased that of CO. A low concentration of CO<sub>2</sub> and a high concentration of CO was produced in MWP because of the self-gasification of the residue, and the gasification reaction was more highly favored by MWP than CHP [123]. Pyrolysis oils were trapped in a series of condensers. The oils from the MW oven contained *n*-alkanes and 1-alkenes, aromatic compounds, nitrogenated compounds, long chain aliphatic carboxylic acids, ketones and esters and also monoterpenes and steroids. The oil from CHP (electric oven) was basically composed of PAHs, which have significant environmental and toxicological impact. By contrast, these compounds were not produced by MWP [111, 112, 123], however, MWP produced similar quantities of polychlorinated dibenzo-*p*-dioxins and dibenzofurans (PCDD/Fs) as CHP [109].

MW absorbers play an important role in the MWP of sewage sludge in view of their significant influence on the yield and property of biofuel products. The highest temperature achieved was 1130 °C with SiC, resulting in the highest gas fraction yield (up to 63.2 wt.%). The addition of residue char promoted condensation reactions and resulted in an increase in solid yield. The use of graphite instead of char produced more cracking in the large aliphatic chains, leading to a higher proportion of 1-alkenes than alkanes and an increase in the proportion of monoaromatics [111], since the relatively low temperatures with graphite favored the cyclization of the alkenes in the pyrolysis oils. AC was able to prolong the residence time of volatiles in the hot zone, thanks to its porous structure, generating the maximum concentration of H<sub>2</sub> and CO (60%) in the pyrolysis gas [125].

Moreover, the addition of catalysts, such as CaO, CaCO<sub>3</sub>, NiO, Ni<sub>2</sub>O<sub>3</sub>,  $\gamma$ -Al<sub>2</sub>O<sub>3</sub> and TiO<sub>2</sub>, not only affected the temperature evolution of sewage sludge but also changed the pyrolytic product distribution and gas composition under MWH. The addition of the catalysts, except CaO, increased heating rates, which were ordered as follows: Ni<sub>2</sub>O<sub>3</sub>  $\approx$   $\gamma$ -Al<sub>2</sub>O<sub>3</sub> > TiO<sub>2</sub> > NiO > CaCO<sub>3</sub>. Ni-based catalysts, especially Ni<sub>2</sub>O<sub>3</sub>, gave the highest decomposition of organic matter in sewage sludge activity, while also remarkably increasing the yields of bio-oil and pyrolytic gas. CaO favored the production of H<sub>2</sub>-rich syngas, while CO-rich syngas was generated over Ni-based catalysts.  $\gamma$ -Al<sub>2</sub>O<sub>3</sub> and TiO<sub>2</sub> also promoted the decomposition of organic matter and produced higher organic volatiles, but they showed almost no impact on the percentages of combustible gas and the H<sub>2</sub>/CO ratio [126].

### 21.3.3 Municipal solid waste

The MWP of municipal solid waste (MSW) can occur at low MW powers (over 150 W) [127]. MSW was quickly heated to 600 °C under MWH using MW absorbers, including aluminum, AC, garnet, iron, silica beads, cement, SiC, TiO<sub>2</sub>, fly ash and graphite. Besides greatly affecting the yields of bio-oil, gases and char, MW absorbers played a catalytic role in altering selectivity to various components in bio-oil. The highest bio-oil yield of 53 wt.% was achieved using graphite, while the bio-oil itself mostly contained oxygenated compounds (furans, phenolics, cyclo-oxygenates), and aliphatic and aromatic hydrocarbons (mono and polycyclics), of which aromatic hydrocarbons were the main products. This corresponded to nearly 95% energy recovery and 85% deoxygenation in bio-oil. High selectivity to monoaromatics, such as benzene, toluene, xylene, styrene, and C<sub>8</sub>–C<sub>20</sub> aliphatic hydrocarbons, as well as low selectivity to polycyclic aromatics, were obtained with a majority of the MW absorber-MSW combinations. Methane, ethylene, propylene, isobutylene and hydrogen were the major gaseous products [128]. The composition of the pyrolysis gaseous products included CO<sub>2</sub>, CO, CH<sub>4</sub>, etc. when graphite, charcoal or iron were used [129]. A rich-syngas fraction with a high H<sub>2</sub> content (50–55 vol.%) was obtained using a char/waste weight ratio range of 0.2/1 to 1/1. Moreover, moisture content had a positive effect on gas production because gasification of the char occurred [127]. The appropriate pyrolytic temperature was controlled up to 600 °C in a large MWP system (20 kW). The total combustible gas (CH<sub>4</sub>, C<sub>2</sub>H<sub>2</sub>, C<sub>2</sub>H<sub>4</sub>, C<sub>2</sub>H<sub>6</sub>, etc.) content was 74.9% with an average calorific value of 36.02 MJ/m<sup>3</sup>, while the tar calorific value was 54.7 MJ/m<sup>3</sup>. Energy consumption for MWP ranged from 0.58 to 0.7 kWh/kg [130].

### 21.3.4 Polymeric materials

#### 21.3.4.1 Plastics

As waste plastics are predominately thermoplastics, they serve as a good feedstock for the pyrolysis process. However, thermoplastics like polyethylene (PE) and polyethylene terephthalate (PET) have poor dielectric properties meaning that they are not particularly useful for MWH, unless exposed together with MW absorber materials. When pulverized carbon is mixed with shredded or pelletized plastics, the added carbon absorbs the electromagnetic radiation and transports the energy to the plastics via conduction [131]. However, polyvinyl chloride (PVC) is a polar plastic, which absorbs MW power more efficiently. Dielectric loss increases with material temperature and an abrupt rise in dielectric loss occurs at a given temperature, after which the temperature of the irradiated materials starts to rise quickly. As a result, a dehydrochlorination yield of more than 90% has been achieved and 15% of volatilized organic materials were released by the decomposition of PVC with MWP [132].



AC and ferrite can enhance the decomposition of plastics. In experiment, 100 g polystyrene (PS) and 47.3 g of carbon were heated at 3 kW MW power, producing 86.5% liquid containing higher amounts of single ring aromatic compounds (93.9% aromatics C<sub>6</sub>–C<sub>10</sub>, of which 66.0% styrene), 9.8% char and 3.7% gas [133, 134]. The MW-metal interaction may enhance pyrolysis and affect the nature of products. The iron mesh generated heat in the 1100–1200 °C range, which converted PS into 80% liquid, 15% gas and 5% char residue. The liquid product contained styrene in addition to polycyclic aromatics and condensed ring aromatic compounds [135]. High temperature was attained by the interaction between MW and aluminum, which was in the form of a tightly coiled wire, strips and a cylinder. The pyrolytic rate of PS was faster with the coil, slower with the strips and negligible with the cylinder [136]. H<sub>2</sub> and metallic iron were generated from plastics and iron ore powder mixtures by MWH. About 57–88% H<sub>2</sub>, contained in the samples, was recovered in the form of H<sub>2</sub> and CH<sub>4</sub>. The concentration of the gases generated could be controlled by changing the blending composition of the plastic and iron ore powder mixtures. About 88% of the hydrogen in the sample was recovered in the form of H<sub>2</sub> and CH<sub>4</sub> under C/O (2/1) conditions while H<sub>2</sub> did not contribute to the reduction of iron ore [137].

The liquid yield of PS was higher under reduced pressure than at ambient pressure. This liquid was clear and displayed low viscosity and density. Additionally, a dark brown liquid was formed when pyrolysis was carried out in a stream of nitrogen, but the yield was 94.3 wt.%. The maximum concentration of styrene in the liquid was obtained (71.9 wt.%) under 21.3 kPa of residual pressure. The substitution of carbon with SiC gave almost the same amount of liquid, but the rate of pyrolysis was strongly reduced leading to the formation of large amounts of valuable chemicals, such as styrene,  $\alpha$ -methylstyrene and toluene, while gas and char formed in low amounts was used as fuel [138].

Low density polyethylene (LDPE) gave significant amounts of gasoline-range hydrocarbons via MWP over ZSM-5. A temperature of 450 °C and a reactant to catalyst ratio of 2/1 were the optimized conditions that maximized the yield of upgraded oil (32.6 wt.%). Single ring aromatic hydrocarbons were enriched and became the most abundant compounds (74.7–88.5%) in the upgraded pyrolysis oils. Low temperatures and high reactant to catalyst ratios both gave rise to the formation of less desirable PAHs, whereas high temperatures and high ratios contributed to the formation of single ring aromatic hydrocarbons [139]. High density polyethylene (HDPE) was converted into waxy products by CHP, but a low viscosity fraction was produced at very low MW power with tires or char. The liquid fraction from HDPE contained linear alkanes and 1-alkenes, but only negligible amounts of branched, cyclic and aromatic hydrocarbons were formed [140]. The oil from pyrolysis consisted mainly of various aromatic compounds and had an energy content of about 36 MJ/kg. The main component of the gaseous product was methane [141].

#### 21.3.4.2 Rubber and tires

Large amounts of rubber are used as tires for airplanes, trucks, cars, two-wheelers, etc. However, after use, almost the entire amount of rubber from the worn out tires must be discarded, which again takes a very long time to degrade naturally because of the crosslinked structure of the rubber and the presence of stabilizers and other additives. This poses two major problems: the wastage of valuable rubber and the disposal of waste tires leading to environmental pollution [142]. MWP is one of the most promising means of recycling rubber and tires because they absorb MW, while the process can recover energy and materials to generate value-added products [143].

Tires containing a large amount of aromatics (styrene copolymers) were pyrolyzed faster than tires rich in natural rubber [144]. Tires were cracked in a shorter time by MWP than by CHP. Typical products were a solid residue (char), containing up to 92.0% carbon and appreciable quantities of mineral matter, a low viscosity oil with a large amount of single ring aromatic hydrocarbons and a gas containing light hydrocarbons, hydrogen and traces of N<sub>2</sub>. The three products collected had high calorific values, amounting to 34, 45 and 46 MJ/kg for solid, liquid and gas fractions respectively [143]. The liquid fraction is the most desirable because its hydrocarbon composition means that it can be used as fuel and a source of chemicals. The presence of a fractionating system allows a liquid to be obtained that contains mostly aromatic and olefinic compounds with low density (0.92–0.88 g/mL) and viscosity (3.92–1.25 cP) [144].

#### 21.3.4.3 Electronic waste: waste printed circuit boards

The development of the electronics industry has led to significant amounts of waste electrical and electronic equipment (WEEE) or 'electronic waste' being generated. Much of it has high bromine content (5–15%), which poses challenges for disposal techniques. MWP has been proposed as a novel means of disposing of WEEE. Rapid heating by MW irradiation means that dioxins and furans can be effectively avoided. Gas and liquid products are recovered as fuel gas and chemical feedstock after pyrolysis and the abundant metals Fe and Cu are easily separated and recovered from the solid products [145].

The thermal degradation of waste printed circuit boards (WPCBs) in a controlled conventional thermogravimetric analyzer (TGA) has been carried out at 300–600 °C, at which temperature pyrolysis of organic matter took place along with an expulsion of volumetric volatiles. The corresponding activation energy was decreased from 267 to 168 kJ/mol, while heating rates increased from 20 to 50 °C/min. Similarly, the MWP processing of WPCB material was carried out in only a single stage at a MW power of 700 W. Here, the activation energy was calculated to be only 49 kJ/mol, much lower than that found in a conventional TGA subjected to a similar heating rate, indicating that the adoption of MW technology for the disposal of WPCBs and even for WEEE could well be an attractive option [146].

Processing at 270–350 °C in a TGA under a N<sub>2</sub> or CO<sub>2</sub> atmosphere led to only one significant reaction occurring: the decomposition of epoxy resin. However, the WPCB decomposition process involved simultaneous thermal cracking and oxidative decomposition reactions in an air atmosphere. Most of the Br contained in WPCBs was released into noncondensable gas as HBr during the MWP of WPCBs [147]. Adding AC can efficiently increase heating rate and improve the pyrolytic temperature. The high temperatures and rapid pyrolysis promote gaseous product yields and the decomposition of brominated compounds into hydrogen bromide. MWP also benefited the capture of Br and the debromination of byproducts. The use of a calcium carbonate (CaCO<sub>3</sub>) layer overhead led to over 95% debromination of the liquid products and over 50% capture of total Br [148]. The MWP of WPCBs yielded an average of 78.6 wt.% solid residue, 15.7 wt.% oil and 5.7 wt.% gas. Solid residues were rich in metals, while the oils were abundant in phenolic compounds, bisphenol A (BPA) and other aromatic compounds, which could then be reclaimed as chemicals or fuels [147]. The gas product is combustible with a caloric value of 18.8 MJ/m<sup>3</sup> [149].

### 21.3.5 Waste oil

Waste automotive engine oil (WAE0) can also be cracked by MWP. Process temperature significantly influences the overall yield and the formation of recovered oils. The recovered liquid and gaseous products contained various light hydrocarbons, which could act as valuable fuels or industrial feedstock [150]. The cost of recovery is relatively low compared to production from crude oil, as the number of purification stages is reduced. The operating temperature (200–1000 °C) was controlled by MW power in a continuous stirred bed reactor with AC [151]. The recovered gases (41 wt.% yield) contained substantial concentrations of light aliphatic hydrocarbons (up to 86 vol.%) at higher temperatures. Both H<sub>2</sub> and CO can be used as a valuable syngas. The high yield of gaseous hydrocarbons can be attributed to the unique heating mode and chemical environment present during MWP [152, 153]. Alternatively, 88 wt.% of condensable oil could be generated at lower temperatures. This oil showed fuel properties comparable to traditional fossil fuel derived liquid transportation fuels. The oil product showed significantly high recovery (90%) of the energy present in the waste oil and was also relatively contaminant free, with low levels of sulfur, oxygen and toxic PAHs [154]. MWP of WAE0 gave the greatest yields of recovered liquid oil at 600 °C. The product contained light paraffin and aromatic hydrocarbons, such as benzene, toluene, xylene and benzene derivatives [152, 155].

Metallic char with a porous structure and high surface area showed high thermal stability in a N<sub>2</sub> atmosphere. Metal and metal oxide phases were attached or adsorbed onto the char, making it a potentially suitable catalyst for use in pyrolysis cracking processes. The metallic char initially acted as an adsorptive support for the adsorption of metals, metal oxides and waste oil. The char then became a MW absorber and allowed

heating to occur up to a high temperature in a short time. The arcing and sparks during MWP of waste oil indicated that hot spots (up to 650 °C) were being formed. The metallic states in the metallic char functioned as a catalyst, which enhanced cracking and heterogeneous reactions and converted waste oil to produce higher yields of light hydrocarbons [118].

Furthermore, WAEO contains a variety of contaminants, including Pb, Mg, Cu, Zn, Cr, As, Cd, chlorides and chlorinated compounds. The recovered liquid oils showed a significant reduction in the metal contaminants accumulated throughout their use cycle: a 93–97% reduction in Cu, Ni, Pb, Zn, Fe, a 46% reduction in Cd and a 32% reduction in Cr [152]. MWP can be conveniently performed under continuous operation and the apparatus was fitted with magnetrons capable of delivering 5 kW MW power and treating waste oil at a feed rate of 5 kg/h with a positive energy ratio of eight (energy content of hydrocarbon products/electrical energy supplied for MWH) and a net energy output of 179.4 MJ/h [154].

## 21.4 Microwave-enhanced decomposition

### 21.4.1 Decomposition of gaseous pollutants

The use of MW dielectric heating in the heterogeneous catalytic decomposition of gaseous pollutants has been widely studied [5, 156]. Desulfurization and denitrification on carbon and zeolite-supported catalysts as well as the catalytic decomposition of VOCs are attractive protocols.

#### 21.4.1.1 Desulfurization and denitrification on carbon

MW-carbon reduction without other catalysts has been used in the desulfurization and denitrification of flue gas [157]. First, SO<sub>2</sub> and NO<sub>x</sub> were adsorbed on a char or anthracite bed and then decomposed by MW-enhanced reduction to elemental S and N. The removal rates of SO<sub>2</sub> and NO<sub>x</sub> were 95–100%. During the 21-cycle adsorption and decomposition, the surface area of the bed carbon was increased from seven to 700 m<sup>2</sup>/g [158]. MW power, reactor type and temperature-raising rate are the critical factors for removal efficiency [157].

The presence of up to 10% O<sub>2</sub> can maintain or enhance the efficiency of desulfurization and denitrification, while additional CO<sub>2</sub> can improve removal efficiency [159, 160]. However, high concentrations of O<sub>2</sub> and CO<sub>2</sub> caused a loss of AC, thereby inhibiting desulfurization and denitrification [160]. The additional catalyst was thus used to reduce the reaction temperature at the lower MW power. After adding a Cu-based catalyst, the reaction temperature decreased by about 200 °C and removal efficiency increased by 25% [161]. The presence of SO<sub>2</sub> inhibited the denitrification reaction to some extent. Water vapor in the flue gas also had an inhibitory effect on desulfur-

ization, while accelerating denitrification. When the moisture content was more than 9%, the efficiency of desulfurization and denitrification decreased [160].

#### 21.4.1.2 Catalytic decomposition of SO<sub>2</sub> and NO<sub>x</sub> on zeolite

Desulfurization and denitrification have also been performed via catalytic reduction or oxidation on zeolite under MWH. NO<sub>x</sub> can be reduced to elemental N with ammonium bicarbonate on Ga-A, Fe, FeCoCu, FeCu and Cu/5A zeolites in the presence of excess O<sub>2</sub> (14–19%). This is attributed to the formation of NH<sub>3</sub> by thermal decomposition of ammonium bicarbonate. At a lower temperature of 80–120 °C at 259–280 W MW power, NO<sub>x</sub> removal efficiency over Ga-A zeolites was 81.8–95.8% and the NO removal rate was about 70.6–89 mg/h [162]. Simultaneous desulfurization and denitrification with ammonium bicarbonate on zeolite<sup>9</sup> were<sup>10</sup> carried out under MWH. SO<sub>2</sub> was reduced to elemental S at a desulfurization efficiency of 76.1–99.5%. NO<sub>x</sub> concentration had little effect on denitrification, and had no influence on desulfurization, while SO<sub>2</sub> concentration had no effect on denitrification [163].

Moreover, simultaneous desulfurization and denitrification can also occur via a catalytic oxidative process without ammonium bicarbonate over Fe/Ca-5A zeolite [164]. Oxidative desulfurization and denitrification with KMnO<sub>4</sub> on zeolite<sup>9</sup> was performed via the oxidation of SO<sub>2</sub> to sulfate and NO<sub>x</sub> to nitrates. The oxidative method exhibited higher removal efficiency than the reductive methods [165]. The removal efficiencies of the various catalysts and methods are compared in Table 21.4.

#### 21.4.1.3 Catalytic decomposition of VOCs

The continuous decomposition of 2000 ppm VOCs, such as acetone, *n*-hexane and dichloromethane (DCM), has been conducted on a magnetite (Fe<sub>3</sub>O<sub>4</sub>) fixed bed with MWH. The bulk temperature of the fixed bed rose violently to 600 °C from room temperature in only 6.5 min, even though the inlet gas was at a high flow and relative humidity was high at 75%. The complete decomposition of VOCs in the inlet stream was achieved at 645 W MW power in 10 min, while the conversion of VOCs was stable when the fixed bed had been heated for 10 min. Furthermore, the effect of the addition of water to the inlet stream on decomposition was insignificant [169].

Toluene was oxidized and efficiently degraded on a fixed bed containing a zeolite supported copper oxide (CuO/zeolite) catalyst mixed with SiC. Under optimal conditions, 92% toluene was removed, which corresponds to a 80%–90% total organic carbon (TOC) removal rate. Furthermore, the catalyst was highly stable even after eight consecutive 6-h runs [170]. Gaseous toluene was also degraded over the carbon nanodot (CND, 2–7 nm) modified Cu-Mn-Ce/ZSM (CND-CMCZ) catalyst under MWH. CND-

<sup>9</sup> <http://www.sciencedirect.com/science/article/pii/S0304389408008030>

<sup>10</sup> [https://scholar.google.de/scholar?cites=8885827753601662780&as\\_sdt=2005&scioldt=0,5&hl=de](https://scholar.google.de/scholar?cites=8885827753601662780&as_sdt=2005&scioldt=0,5&hl=de)

**Tab. 21.4:** Comparison of desulfurization and denitrification efficiencies of various catalysts and methods

Pollutants	MW power (W)	Zeolite catalysts	Reluctant or oxidant	Residence time (s)	Desulfurization efficiency (%)	Denitrification efficiency (%)	Ref.
NO	259–280	Ga-A	ammonium bicarbonate	0.259		95.0	[162]
SO <sub>2</sub> /NO <sub>x</sub>	211–280	Ga-A	ammonium bicarbonate	0.315	99.1	86.5	[163]
SO <sub>2</sub> /NO <sub>x</sub>	280	Fe/Ca-5A	ammonium bicarbonate	0.358	95.6	97.3	[164]
SO <sub>2</sub> /NO <sub>x</sub>	280	Fe/Ca-5A		0.358	69.5	79.3	[164]
SO <sub>2</sub> /NO <sub>x</sub>	280	FeCoCu-5A	ammonium bicarbonate	0.358	99.5	86.1	[166]
SO <sub>2</sub> /NO <sub>x</sub>		FeCu	ammonium bicarbonate		93.4	95.8	[167]
SO <sub>2</sub> /NO <sub>x</sub>		FeCu			79.6	91.7	[167]
SO <sub>2</sub> /NO <sub>x</sub>		Cu	ammonium bicarbonate		76.1	81.8	[168]
SO <sub>2</sub> /NO <sub>x</sub>	259		KMnO <sub>4</sub>	0.357	96.8	98.4	[165]

CMCZ has a higher adsorptive capacity and heating rate under MWH than the unmodified Cu-Mn-Ce/ZSM catalyst due to the similar features it shares with the analogous humic acids. As a result, 75% gaseous toluene was degraded over the CND-CMCZ catalyst in a period of 80 min at a lower reaction bed temperature (150 °C). Although the degradation efficiency of gaseous toluene was further improved by increasing the reaction bed temperature (200–250 °C), the role of CND modification for improving catalytic performance was obviously reduced. This could be ascribed to the structure and surface functional group damage of carbon nanodots at higher catalytic temperatures [171].

#### 21.4.2 Organic wastewater treatment

MW chemistry has been studied widely in the field of organic wastewater treatment due to its rapid heating at the molecular level and its ‘hot spot’ effect on the surface of a MW absorber [172]. Various combinations of MWH with GAC, H<sub>2</sub>O<sub>2</sub>, Fenton oxidation, photocatalytic oxidation, etc. have gained a great deal of attention [173, 174].

### 21.4.2.1 Decomposition on GAC

When the uneven surfaces of AC particles are heated under MW irradiation, numerous hot spots form synchronically, as shown in Figure 21.4. The temperature of these hot spots can ordinarily reach over 1200 °C. Both thermal and nonthermal effects lead to organic compounds being destroyed rapidly and completely. According to the decay of TOC, decomposition over GAC is almost equal to the oxidation combustion of organic pollutants. CO<sub>2</sub>, H<sub>2</sub>O and various inorganic ions are produced [2].

An 87.8% removal rate for 1.25 mg Congo red in a 25 mL solution was typically achieved with 50 mg AC in 1.5 min MWH. Complete decomposition was achieved with more AC (90 mg) after the same MWH time. The advantages of the GAC/MW process thus include high degradation efficiency, short reaction time, low cost and a lack of secondary pollution [2].

Catalytic wet air oxidation (CWAO) is an effective method for the treatment of heavily contaminated wastewater. However, its application has been limited by its working conditions of very high pressure and high temperature. A combination of CWAO and MWH (CWAO/MW) is a promising method with which to treat heavily contaminated wastewater under milder conditions [175]. Significant arcing in the bed can be obtained with partial wetting under MWH. Arcing leads to hot spot formation and thermal runaway [176]. Optimal removal of H-acid (1-amino-8-naphthol-3, 6-disulfonic acid, 3000 mg/L) over AC with air reached 92.6% in 20 min using CWAO/MW and the removal of TOC was 84.2% in 60 min. After treatment, the amino group in H acid was converted into nitrate, and the sulfonic group into sulfate, and the ratio of BOD<sub>5</sub>/COD increased from 0.008 to 0.467, indicating a significant improvement in the biodegradability of wastewater [175]. At lower temperature (150 °C) and pressure (0.8 MPa) and using O<sub>2</sub> and GAC (5 wt.%), more than 90% COD was removed from the heavily contaminated petroleum wastewater using CWAO/MW and the BOD<sub>5</sub>/COD ratio was increased from 0.04 to 0.47 in 30 min. The reactive activation energy for COD conversion was calculated to be 25.11 kJ/mol [177].

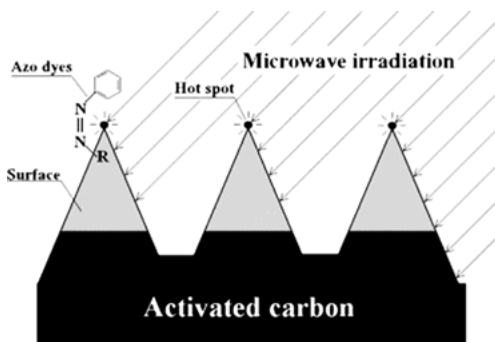
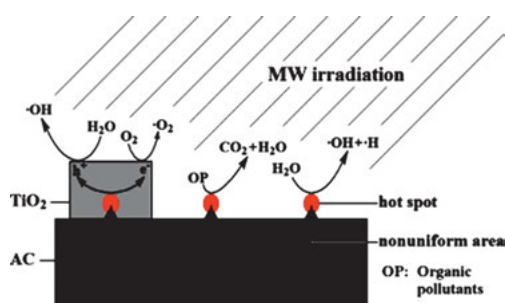


Fig. 21.4: Formation of hot spots on the uneven surfaces of AC particles under MW irradiation [2]

The removal of *p*-nitrophenol (PNP, 1330 mg/L) was 90%, which corresponds to 80% TOC removal, on a GAC fixed bed in a continuous flow reactor with 6.4 mL/min influent flow and 100 mL/min air flow at 500 W MW power. After processing, the PNP nitro group was converted to nitrite and nitrate. The biodegradability of the wastewater was clearly improved [178]. Moreover, the oxidation of PNP was further enhanced on a carbon supported copper (Cu/GAC) catalyst under MWH. The removal rate of PNP reached 91.8%, corresponding to 88% TOC removal, in the Cu/GAC fixed bed reactor in continuous flow mode under ambient pressure. The Cu/GAC catalyst exhibited higher TOC decomposition efficiency than GAC and maintained good stability on a long run. The reaction reached a steady state after 80 min of running with the surface temperature of the Cu/GAC or GAC fixed bed usually varying in the 250–320 °C range, meaning that organic compounds could be completely transformed [179]. In another study, *p*-chlorophenol was rapidly degraded over CuO/GAC in 5 min at 70 °C and 0.3 MPa and then mineralized and more than 90% of TOC was removed in 15 min using CWAO/MW. The reaction activation energy ( $E_a$ ) of decomposition with  $H_2O_2$  decreased from 47.7 to 43.1 kJ/mol under MW irradiation [180].

AC was modified by the addition of a nanoscale semiconductor material,  $TiO_2$  or ZnO, to obtain the carbon supported catalysts  $TiO_2/AC$  or ZnO/AC. The degradation of sodium dodecyl benzene sulfonate (SDBS) was carried out under MW irradiation. The  $TiO_2/AC$  system exhibited superior catalytic activity [181]. Furthermore, the degradation of methyl orange (azo dye) was significantly enhanced over  $TiO_2/AC$  under MW irradiation, which was attributed to the production of the hydroxyl radical ( $OH^\bullet$ ), as shown in Figure 21.5.  $OH^\bullet$  formation over  $TiO_2/AC$  under MW irradiation has been demonstrated as occurring via the oxidation of 1,5-diphenyl carbazide to 1,5-diphenyl carbazone and the effect of radical scavengers, such as 2,6-di-*tert*-butyl-4-methylphenol, mannitol and vitamin C. In addition, anatase  $TiO_2/AC$  generated more OH radicals than rutile  $TiO_2/AC$  under MW irradiation [182].

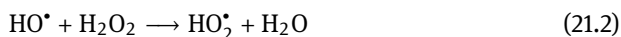


**Fig. 21.5:** The mechanism of catalytic decomposition of organics over  $TiO_2/AC$  under MW irradiation [183]



#### 21.4.2.2 Oxidation with H<sub>2</sub>O<sub>2</sub>

H<sub>2</sub>O<sub>2</sub> is a common oxidant with which to oxidize organic pollutants because of its easy use and high oxidizing power, but the oxidation rate is quite low. Fenton oxidation (H<sub>2</sub>O<sub>2</sub> + Fe<sup>2+</sup>) is a popular AOP, but this process is dependent on the pH of solutions, while the large amounts of ferrous ions remaining have to be removed from the effluent before the oxidation process. MWH, however, can enhance the oxidative decomposition efficiency of organic pollutants by H<sub>2</sub>O<sub>2</sub> without pH limitations or an additional catalyst, avoiding the removal and regeneration of catalysts after processing [184, 185]. MW-enhanced oxidation was induced by OH radicals and radical reactions originating from H<sub>2</sub>O<sub>2</sub> under MW irradiation, as shown in the following reactions [186]:



The discoloration rates of malachite green (MG) were much higher under MWH than CH, implying MW was more beneficial for the generation of OH radicals [186]. In addition, the degradation of rhodamine B (RhB) and MB in the MW-H<sub>2</sub>O<sub>2</sub> system was very competitive at extreme alkaline pH, which was mainly attributed to oxidation by the O<sub>2</sub> formed *in situ* and the MW thermal effect [187]. Furthermore, the oxidation of phenol with H<sub>2</sub>O<sub>2</sub> can be rapidly accomplished under MWH and 82.4% of phenol (300 mg/L) was removed after only 1 min at 668 W MW power [188].

#### 21.4.2.3 Fenton and Fenton-like oxidation

MW has emerged as a powerful and efficient technique for the elimination of persistent organic pollutants (POPs) with Fenton's reagent via their complete mineralization to CO<sub>2</sub>, H<sub>2</sub>O and lower molecular weight acids. The rapid degradation of aromatic halides, halogenated phenols and PCBs in polluted waters was achieved under MWH and a moderate excess (5–30 eq) of Fenton's reagent at neutral pH. Acidification with acetic acid (pH 2.0–2.3) did not affect the process, but sulfuric acid (pH 1.7–2.0) facilitated complete degradation [189]. The Fenton/MW process not only enhanced degradation efficiency, but also reduced the yield of Fe-containing sludge, as well as improving the biodegradability of the effluent [190]. The Fenton/MW process removed 95.8% dimethyl sulfoxide (DMSO) from treated wastewater in 5 min across a wide pH value range (2–7). The highest mineralization level (51.3% TOC removal) was achieved in a shorter time (10 min) than the 28.4% TOC removal achieved by Fenton oxidation under stirring at an ambient temperature, which took 240 min. This fact is attributed to MW absorption by polar molecules and ions, such as Fe<sup>2+</sup>, DMSO and H<sub>2</sub>O<sub>2</sub> [191].

MG was not degraded under MWH alone, whereas 23.5% MG was degraded under Fenton oxidation in 5 min. Under Fenton/MW, 95.4% MG was degraded at pH 3.4 after 5 min in the presence of 0.08 mM Fe<sup>2+</sup> and 12.5 mM H<sub>2</sub>O<sub>2</sub>, while the COD removal rate was 82.0% after 5 min [192]. Furthermore, 93% oxidative degradation of MB was

achieved with the Fenton/MW process in only 1 min and the removal rate was even higher than when using Fenton oxidation alone for 65 min. Degradation efficiency increased with the concentration of Fenton's reagent, but was slightly affected by pH values in the range of 2–7 [193].  $\text{Cu}^{2+}$  was used in a Fenton-like/MW process to treat olive mill wastewater, which contains high organic matter levels of polyphenols (PP) as well as COD and BOD. Discoloration and PP removal rate reached 98.0% and 81.8% respectively, with 12 M  $\text{H}_2\text{O}_2$  in 12 min at 680 W [194]. Pharmaceutical wastewater with a high COD concentration (49.9 g/L) has been treated for 6 min with 1.3 g/L  $\text{Fe}_2(\text{SO}_4)_3$  and 4.9 g/L  $\text{H}_2\text{O}_2$  at pH 4.4 and 300 W MW power. During the process, 57.5% COD and 55.1% UV254 were removed, while the  $\text{BOD}_5/\text{COD}$  ratio increased from 0.165 to 0.470 after processing [190].

MW irradiation has also been used to enhance the mineralization of azo dye wastewater via the electro-Fenton oxidation process. Both cathode and anode surfaces were activated efficiently under MW irradiation. MW irradiation accelerated the  $\text{Fe}^{3+}/\text{Fe}^{2+}$  redox cycles on cathodes, leading to relatively steady  $\text{Fe}^{2+}$  recovery. The transduction of electrons was promoted and the electrosynthesis of  $\text{H}_2\text{O}_2$  from  $\text{O}_2$  was greatly accelerated on the cathode. Additionally, the blocking of the electrode surface by intermediates was enormously alleviated and more active sites producing OH radicals were formed on the surface of the anode. Consequently, the concentration of the formed OH radicals was significantly promoted in the electro-Fenton/MW process, which was 2.3 times higher than that from the traditional electro-Fenton process. The removal rates of TOC and methyl orange and mineralization current efficiency were around 3.1, 1.1 and 3.2 times higher respectively than without MW irradiation [195].

#### 21.4.2.4 Other catalytic oxidations

The activation of persulfate by MWH has been confirmed as effective in the destruction of organic pollutants. As compared with CH, MWH has an enhanced effect on the degradation reaction rate and process time. The oxidative degradation of an azo dye, acid orange 7 (AO7), with persulfate was enhanced by MW irradiation, both in the presence and absence of AC. The oxidative role of  $\text{SO}_4^{\bullet-}$  and  $\text{OH}^{\bullet}$  on the degradation of AO7 was demonstrated by quenching tests using specific alcohols leading to the observation that  $\text{SO}_4^{\bullet-}$  played the dominant role [196]. Complete decolorization was still achieved in the presence of chloride ions (up to 0.50 mol/L), but it needs longer reactions times (8–9 min) [197]. The oxidative degradation of sulfamethoxazole (SMX) by persulfate under MWH was enhanced by higher reaction temperatures, persulfate amounts and pH values, while higher initial concentrations of SMX and the presence of phosphates reduced degradation rates. High concentrations of chloride also inhibited degradation, while low concentrations of chloride and carbonate were favorable to degradation. It was proposed that the decomposition mechanisms include the hydroxylation of the benzene ring, the oxidation of the amine group at the benzene ring and S-N cleavage. The significant reduction of acute toxicity in SMX solutions after

treatment was demonstrated by tests with *Photobacterium phosphoreum*, *Vibrio fischeri* and *Vibrio qinghaiensis* [196].

The catalytic oxidation of 100 mg/L phenol with chlorine dioxide (ClO<sub>2</sub>) in synthetic wastewater has been effectively enhanced by MW irradiation in the presence of CuO<sub>x</sub>/γ-Al<sub>2</sub>O<sub>3</sub> [198]. Improved γ-Al<sub>2</sub>O<sub>3</sub> thermal ability and high Cu loading in the catalyst were achieved by adding La<sub>2</sub>O<sub>3</sub> to CuO<sub>x</sub>/γ-Al<sub>2</sub>O<sub>3</sub> [199]. More OH radicals were formed in the MW catalytic oxidation system with CuO<sub>x</sub>-La<sub>2</sub>O<sub>3</sub>/γ-Al<sub>2</sub>O<sub>3</sub> as demonstrated by the observation of fluorescence intensity [200]. Furthermore, a nickel oxide catalyst has been proven to be a *nano*-NiO<sub>2</sub> with OH groups and active oxygen. The catalytic activity of the NiO<sub>2</sub> catalyst was attributed to its MW absorbing property and the role of active oxygen and OH groups under MW irradiation [201]. A rice hull/MnFe<sub>2</sub>O<sub>4</sub> composite (RHM) has been prepared via calcination under a nitrogen atmosphere in which a rice hull was pyrolyzed to form a porous substrate that consisted of silica and AC, while monodisperse spinel MnFe<sub>2</sub>O<sub>4</sub> nanoparticles (around 59 nm) were distributed on the substrate. MnFe<sub>2</sub>O<sub>4</sub> displayed high catalytic activity under MW irradiation [202]. The removal efficiencies of various organic pollutants under catalytic oxidation are summarized in Table 21.5.

#### 21.4.2.5 Oxidation: photodegradation?

MW-assisted UV photocatalytic oxidation (UV/MW) is a potential method with which to treat organic pollutants with nonbiological degradability and high toxicity [203]. A series of photocatalytic decompositions of organic pollutants in an aqueous TiO<sub>2</sub> dispersion using an integrated MW/UV-illumination (PD/MW) method has been reported. The device consisted of a double quartz cylindrical plasma photoreactor (DQCPP) equipped with a MW powered electrodeless Hg/Ne irradiation source. The latter is only activated by MW irradiation [204, 205]. The experimental output ultraviolet (UV) energy was in the 210–300 and 310–400 nm wavelength ranges at applied MW powers of 74–621 W. The DQCPP and a water-cooled DQCPP reactor absorbed more than 50% MW irradiation. The smallest loss occurred at 178.9 W, at which power setting the degradation of RhB was subsequently examined. Highly intense mercury lines were seen at 365, 404, 435, 546 and 579 nm [206]. About 80% of the RhB was photomineralized in an aqueous TiO<sub>2</sub> dispersion after 60 min irradiation under the DQCPP lamp [206].

In the integrated PD/MW method there is enhanced formation of reactive oxygen species (OH radicals), and the activity of bulk water and the TiO<sub>2</sub> particle surface are somehow affected by MW irradiation. The greater efficacy of the PD/MW degradation method has been obtained at low concentrations of molecular oxygen and at low radiant exitance of the light source [207]. Based on the assessment of TOC, the efficiency of complete mineralization of the dye is as follows: PD/MW > PD/CH > PD > MW. In all cases, MW radiation alone had no effect on the removal of TOC. Degradation with MW irradiation was especially efficient when coupled to UV irradiation. MW irradiation

Tab. 21.5: The removal efficiencies of various organic pollutants with catalytic oxidation

Pollutant concentration (mg/L)	Oxidant concentration (mg/L)	Catalyst amount (g/L)	MW power (W)	pH value	Time (min)	Removal rate (%)	COD removal rate (%)	Ref.
azo dye – acid orange 7 (1000)	persulfate		800	higher	5–7	100		[197]
azo dye – acid orange 7 (500)	persulfate	AC (1)		higher	3	100	> 95.0	[197]
phenol (100)	ClO <sub>2</sub> (80)	CuO <sub>x</sub> /γ-Al <sub>2</sub> O <sub>3</sub> (50)	50	9	5	92.2	79.1	[198]
phenol (100)	ClO <sub>2</sub>	CuO <sub>x</sub> -La <sub>2</sub> O <sub>3</sub> /γ-Al <sub>2</sub> O <sub>3</sub>				91.7	50.4	[199]
remazol golden yellow dye	ClO <sub>2</sub> (80)	CuO <sub>x</sub> -La <sub>2</sub> O <sub>3</sub> /γ-Al <sub>2</sub> O <sub>3</sub> (70)	400	7	1.5	94.0	67.9 (TOC)	[200]
triphenylmethane dye crystal violet (100)		nano-NiO <sub>2</sub>			5	97.0	81.0 (TOC)	[201]
COD (150,00)		rice hull/MnFe <sub>2</sub> O <sub>4</sub> composite (15)			6		> 70.0	[202]

tion caused an increase in the hydrophobic character of the TiO<sub>2</sub> surface, with consequences for the adsorption mode of the dye substrate and thus on the overall mechanism of degradation. Such nonthermal effects provided by MW irradiation led to more efficient dye substrate photodegradation and mineralization [208].

The photocatalyzed degradation of 2,4-dichlorophenoxyacetic acid (2,4-D) in an aqueous TiO<sub>2</sub> dispersion has been conducted using PD/MW. The greater efficiency of the MW-assisted process is ascribed to a nonthermal MW radiation effect on the breakup of the aromatic ring of 2,4-D (oxidation), but evidently not on the dechlorination process (reduction) [209]. The degradation rates of 2,4-D were  $2 \times 10^{-3}$  mM/min with PD/MW and  $1.1 \times 10^{-3}$  mM/min with PD, even though the light irradiance was sixtimes greater in the latter method. The coupled PD/MW method was thus about ten times more efficient than the PD method alone [210]. Near-quantitative mineralization of BPA occurred after only 90 min of irradiation with the PD/MW and PD/CH routes. Additionally, the PD route only gave 67% mineralization under identical conditions [211]. A number of organics, such as benzoic acid, phthalic acid, *o*-formylbenzoic acid, phthalaldehyde, succinic acid, dimethyl phthalate, diethyl phthalate, phenol and 4-chlorophenol, were initially adsorbed onto the surface of the TiO<sub>2</sub> particles, after which degradation occurred under PD/MW. Thus the polar model substrates (dipole moment) underwent oxidative degradation under MW radiation [212, 213].

Moreover, a novel MW discharge electrodeless lamp (MDEL) has been developed for wastewater treatment with AOPs using environmentally risk-free gases (e.g. Xe, N<sub>2</sub>, He, O<sub>2</sub>, H<sub>2</sub> and Ar alone or a mixture thereof) that provide the needed light plasma source. The most efficient in the degradation of 2,4-D and BPA was the MDEL/TiO<sub>2</sub> system, followed closely by MDEL alone (without TiO<sub>2</sub>) [214]. This novel lamp provides an additional light source in the photooxidation of environmental contaminants without the need for a metal-oxide photocatalyst. Process dynamics using W-MDEL were greater than for many conventional photochemical methods that employ low-pressure Hg arc electrode lamps [215].

Furthermore, various photocatalysts and oxidants were used in the UV/MW process. MW irradiation was able to considerably enhance the photocatalytic degradation of phenol, 4-chlorophenol, AO7 and TOC in the UV/H<sub>2</sub>O<sub>2</sub> and UV/TiO<sub>2</sub> systems. The synergistic effects between MW irradiation and TiO<sub>2</sub> photocatalysis have been demonstrated [174, 216]. The indirect reaction between phenol and an OH radical might be dominant under UV/H<sub>2</sub>O<sub>2</sub>, while the direct reaction of phenol and H<sub>2</sub>O<sub>2</sub> was dominant in the UV/H<sub>2</sub>O<sub>2</sub>/MW process [217]. RhB (30 mg/L) was almost completely decolorized in 10 min under UV/TiO<sub>2</sub>-AC/MW, while mineralization efficiency was 96.0% after 20 min. The reaction rate constant of pseudofirst-order kinetics for RhB using TiO<sub>2</sub>-AC was 4.16 times more than when using TiO<sub>2</sub> [218].

The TOC removal efficiency for an endocrine disruptor dimethyl phthalate (DMP, 50 mg/L) over 0.1 g ZrO<sub>x</sub>/ZnO in a 100 mL solution was 88% after 30 min using UV/MW, which was about 15% higher than when using TiO<sub>2</sub>. The ZrO<sub>x</sub>/ZnO catalyst was reused six times without obvious decreases in catalytic activity [219]. The removal efficiency

of 1000 mg/L TOC in synthetic wastewater containing aniline and nitrophenol reached 78% using UV/H<sub>2</sub>O<sub>2</sub>/MW with 5 g/L Fe<sub>2</sub>O<sub>3</sub>/CuO (4 : 1) [203]. The removal rate of reactive red 195 using the combined Fe/AC-MDEL/NaClO method was near 100%, which corresponds to 82% COD removal [220].

### 21.4.3 Soil remediation

A MW-assisted, solvent-free method for soil decontamination marks a considerable advance in the search for more efficient, environmentally friendly procedures for the degradative oxidation of organic pollutants [221]. Most PCBs, Aroclors and PAHs in soil decomposed with Cu<sub>2</sub>O or Al powder and 10 N NaOH, graphite fibers (pencil lead) or iron wire under MW irradiation. None of the decomposition products could be extracted from the soil following remediation, and most were probably either mineralized or very tightly bound to the soil [222–224].

Catalytic decontamination methods with various MW absorbers and reagents have been extensively and efficiently explored [225]. GAC has been added to soil to rapidly increase the temperature of a reaction system. About 80% of PCBs in soil were effectively removed using GAC, sodium hypophosphite and iron powder (as reductants) in 10 min under MW irradiation, and the further addition of iron powder was able to increase the average removal efficiency to more than 95%. An appropriate amount of water proved to be helpful in promoting the removal of PCBs from soil via steam distillation and in acting as a cosolvent for sodium hypophosphite and an H donor for iron powder [226]. The removal rates of PCBs were thus highly dependent on MW power, soil moisture content and the amount of GAC added [227]. For the removal of chloramphenicol (CAP) in soil, high MW power and GAC amount were beneficial for completed decomposition, while the initial CAP concentration was a minute factor [228].

Over 95% removal of PCBs from soil has been achieved using MnO<sub>2</sub> and MW irradiation. Removal efficiency is higher in acidic soil than in neutral soil. The removal efficiency increased considerably with increasing amounts of MnO<sub>2</sub>, soil mass and MW power [229]. When MnO<sub>2</sub> powder was used as a MW absorber, a complete removal of hexachlorobenzene (HCB) was obtained with the addition of 50% H<sub>2</sub>SO<sub>4</sub> in 10 min, but no significant decomposition was observed after the addition of 10 M NaOH or H<sub>2</sub>O under the same conditions. By contrast, when Fe powder was used, the effects of adding H<sub>2</sub>SO<sub>4</sub> and NaOH on HCB removal were very similar. More than 95% removal was achieved in any case when H<sub>2</sub>SO<sub>4</sub>, NaOH, H<sub>2</sub>O or Na<sub>2</sub>SO<sub>4</sub> were added, without MnO<sub>2</sub> or Fe. The water contained in the damp soil may act as a MW absorber and remediate the contaminated soil without additional MW absorbers. No intermediates were detected in the processes, indicating that the products degraded from HCB were tightly bound to the soil. HCB content decreased from 55.8 to 0.91 mg/kg after treatment [230]. The halogenated aromatics in the solid were efficiently decom-

posed using nontoxic oxidants, such as sodium percarbonate and the urea/hydrogen peroxide complex (Fenton-like reagents), under MW irradiation. 4-chloronaphthol, 2,4-dichlorophenoxyacetic acid and *p*-nonylphenol were degraded completely, while 2,4-dibromophenol was degraded to a large extent [221].

In conclusion, MW-induced plasmas, MW-assisted desorption, MW-driven pyrolysis and MW-enhanced decomposition have become established methods for the decontamination of waste gases, wastewater, solid wastes and soil. Furthermore, MW irradiation has been extensively applied in a number of other environmental remediation processes, including the microbial inactivation of medical waste, wastewater and sludge [231, 232], sludge digestion [233, 234], vitrification and immobilization of nuclear waste and heavy metals in soils [235, 236], pretreatment for bioconversion of biomass and sludge [237], biodiesel synthesis [238], material preparation for environmental remediation [239, 240], and the digestion and extraction of samples for environmental analyses [241], among others.

## Bibliography

- [1] Chang JS. Recent development of plasma pollution control technology: a critical review. *Sci. Technol. Adv. Mater.* 2001, 2, 571–576.
- [2] Zhang Z, Shan Y, Wang J, Ling H, Zang S, Gao W, Zhao Z, Zhang H. Investigation on the rapid degradation of congo red catalyzed by activated carbon powder under microwave irradiation. *J. Hazard. Mater.* 2007, 147, 325–333.
- [3] Tendero C, Tixier C, Tristant P, Desmaison J, Leprince P. Atmospheric pressure plasmas: A review. *Spectrochim. Acta, Part B* 2006, 61, 2–30.
- [4] Bykov YV, Rybakov K, Semenov V. High-temperature microwave processing of materials. *J. Phys. D: Appl. Phys.* 2001, 34, R55.
- [5] Zhang X, Hayward DO. Applications of microwave dielectric heating in environment-related heterogeneous gas-phase catalytic systems. *Inorg. Chim. Acta* 2006, 359, 3421–3433.
- [6] Krieger-Brockett B. Microwave pyrolysis of biomass. *Res. Chem. Intermed.* 1994, 20, 39–49.
- [7] Tabasso S, Carnaroglio D, Gaudino EC, Cravotto G. Microwave, ultrasound and ball mill procedures for bio-waste valorisation. *Green Chem.* 2015, 17, 684–693.
- [8] Appleton T, Colder R, Kingman S, Lowndes I, Read A. Microwave technology for energy-efficient processing of waste. *Appl. Energy* 2005, 81, 85–113.
- [9] Jones D, Lelyveld T, Mavroidis S, Kingman S, Miles N. Microwave heating applications in environmental engineering – a review. *Resour. Conserv. Recycl.* 2002, 34, 75–90.
- [10] Lam SS, Chase HA. A review on waste to energy processes using microwave pyrolysis. *Energies* 2012, 5, 4209–4232.
- [11] Urashima K, Chang JS. Removal of volatile organic compounds from air streams and industrial flue gases by non-thermal plasma technology. *IEEE Trans. Dielectr. Electr. Insul.* 2000, 7, 602–614.
- [12] Hong YC, Cho SC, Bang CU, Shin DH, Kim JH, Uhm HS, Yi WJ. Microwave plasma burner and temperature measurements in its flames. *Appl. Phys. Lett.* 2006, 88, 201502.
- [13] Uhm HS, Hong YC, Shin DH. A microwave plasma torch and its applications. *Plasma Sources Sci. Technol.* 2006, 15, S26.

- [14] Hubert J, Moisan M, Ricard A. A new microwave plasma at atmospheric pressure. *Spectrochim. Acta, Part B* 1979, 34, 1–10.
- [15] Kunhardt EE. Generation of large-volume, atmospheric-pressure, nonequilibrium plasmas. *IEEE Trans. Plasma Sci.* 2000, 28, 189–200.
- [16] Bang CU, Hong YC, Cho SC, Uhm HS, Yi WJ. Methane-augmented microwave plasma burner. *IEEE Trans. Plasma Sci.* 2006, 34, 1751–1756.
- [17] Zhao GB, John S, Zhang JJ, Hamann JC, Muknahallipatna SS, Legowski S, Ackerman JF, Argyle MD. Production of hydrogen and sulfur from hydrogen sulfide in a nonthermal-plasma pulsed corona discharge reactor. *Chem. Eng. Sci.* 2007, 62, 2216–2227.
- [18] Sassi M, Amira N. Chemical reactor network modeling of a microwave plasma thermal decomposition of  $\text{H}_2\text{S}$  into hydrogen and sulfur. *Int. J. Hydrogen Energ.* 2012, 37, 10010–10019.
- [19] Harkness JB, Gorski AJ, Daniels EJ. Hydrogen sulfide waste treatment microwave plasma dissociation. 25. Intersociety energy conversion engineering conference, Reno, NV, USA, 12–17 Aug 1990.
- [20] Martin D, Radoiu M, Calinescu I, Indreias I, Oproiu C, Marghitu S, Toma M, Bestea V, Cramariuc R, Margaritescu A. Combined electron beam and microwave treatment for flue gas purification. *Mater. Manuf. Processes* 1999, 14, 365–382.
- [21] Radoiu M, Martin D, Georgescu I, Calinescu I, Bestea V, Indreias I, Matei C. A laboratory test unit for exhausted gas cleaning by electron beam and combined electron beam-microwave irradiation. *Nucl. Instrum. Methods Phys. Res., Sect. B* 1998, 139, 506–510.
- [22] Tang JW, Yang HH, Ren LL, Wang A, Ma L, Zhang T, Lin L, others. The decomposition of NO in microwave discharge. *Chem. J. Chinese U.* 2002, 23, 632–635.
- [23] Hartz CL, Bevan JW, Jackson MW, Wofford BA. Innovative surface wave plasma reactor technique for PFC abatement. *Environ. Sci. Technol.* 1998, 32, 682–687.
- [24] Hong YC, Kim HS, Uhm HS. Reduction of perfluorocompound emissions by microwave plasma torch. *Thin Solid Films* 2003, 435, 329–334.
- [25] Mohindra V, Chae H, Sawin HH, Mocella MT. Abatement of perfluorocompounds (PFCs) in a microwave tubular reactor using  $\text{O}_2$  as an additive gas. *IEEE Trans. Semicond. Manuf.* 1997, 10, 399–411.
- [26] Kabouzi Y, Moisan M, Rostaing J, Trassy C, Guérin D, Keroack D, Zakrzewski Z. Abatement of perfluorinated compounds using microwave plasmas at atmospheric pressure. *J. Appl. Phys.* 2003, 93, 9483–9496.
- [27] Jasiski M, Mizeraczyk J, Zakrzewski Z, Ohkubo T, Chang JS. CFC-11 destruction by microwave torch generated atmospheric-pressure nitrogen discharge. *J. Phys. D: Appl. Phys.* 2002, 35, 2274.
- [28] Windarto HF, Matsumoto T, Akatsuka H, Suzuki M. Decontamination process using  $\text{CF}_4 - \text{O}_2$  microwave discharge plasma at atmospheric pressure. *J. Nucl. Sci. Technol.* 2000, 37, 787–792.
- [29] Hong YC, Uhm HS. Abatement of  $\text{CF}_4$  by atmospheric-pressure microwave plasma torch. *Phys. Plasmas* 2003, 10, 3410–3414.
- [30] Ahmadi Z, Khani MR, Kooshki S, Mirzajani F, Shokri B. Investigation of variation power and additive gas effect on the destruction using atmospheric microwave plasma torch. *IEEE Trans. Plasma Sci.* 2011, 39, 1834–1841.
- [31] Cha CY, Carlisle CT. Microwave process for removal and destruction of volatile organic compounds. *Environ. Prog.* 2001, 20, 145–150.
- [32] Rubio S, Quintero M, Rodero A, Rodriguez JF. Assessment of a new carbon tetrachloride destruction system based on a microwave plasma torch operating at atmospheric pressure. *J. Hazard. Mater.* 2007, 148, 419–427.



- [33] Bailin LJ, Sibert ME, Jonas LA, Bell AT. Microwave decomposition of toxic vapor simulants. *Environ. Sci. Technol.* 1975, 9, 254–258.
- [34] Uhm HS, Cho SC, Hong YC, Park YG, Park JS. Destruction of dimethyl methylphosphonate using a microwave plasma torch. *Appl. Phys. Lett.* 2008, 92, 071503.
- [35] Tsyganov D, Bundaleska N, Tatarova E, Ferreira C. Ethanol reforming into hydrogen-rich gas applying microwave 'tornado'-type plasma. *Int. J. Hydrogen Energ.* 2013, 38, 14512–14530.
- [36] Nomura S, Putra AEE, Mukasa S, Yamashita H, Toyota H. Plasma decomposition of clathrate hydrates by 2.45 GHz microwave irradiation at atmospheric pressure. *Appl. Phys Express* 2011, 4, 066201.
- [37] Ko Y, Yang G, Chang DP, Kennedy IM. Microwave plasma conversion of volatile organic compounds. *J. Air Waste Manage. Assoc.* 2003, 53, 580–585.
- [38] Mizeraczyk J, Jasiski M, Zakrzewski Z. Hazardous gas treatment using atmospheric pressure microwave discharges. *Plasma Phys. Contr. F.* 2005, 47, B589.
- [39] Lin L, Yuan S, Chen J, Xu Z, Lu X. Removal of ammonia nitrogen in wastewater by microwave radiation. *J. Hazard. Mater.* 2009, 161, 1063–1068.
- [40] Rabah FK, Darwish MS. Characterization of ammonia removal from municipal wastewater using microwave energy: Batch experiment. *Environ. Nat. Resour. Res.* 2013, 3, 42.
- [41] Liu X, Quan X, Bo L, Chen S, Zhao Y, Chang M. Temperature measurement of GAC and decomposition of PCP loaded on GAC and GAC-supported copper catalyst in microwave irradiation. *Appl. Catal., A* 2004, 264, 53–58.
- [42] Jon CJG, Tai H. Application of granulated activated carbon packed-bed reactor in microwave radiation field to treat BTX. *Chemosphere* 1998, 37, 685–698.
- [43] Tai HS, Jou CJG. Application of granular activated carbon packed-bed reactor in microwave radiation field to treat phenol. *Chemosphere* 1999, 38, 2667–2680.
- [44] Jou CJ, Wu CR. Granular activated carbon coupled with microwave energy for treating pentachlorophenol-containing wastewater. *Environ. Prog.* 2008, 27, 111–116.
- [45] Bohlmann JT, Lorth CM, Drews A, Buchholz R. Microwave high-pressure thermochemical conversion of sewage sludge as an alternative to incineration. *Chem. Eng. Technol.* 1999, 22, 404–409.
- [46] Wang X, Chen H, Luo K, Shao J, Yang H. The influence of microwave drying on biomass pyrolysis. *Energy Fuels* 2007, 22, 67–74.
- [47] Chen Z, Afzal MT, Salema AA. Microwave drying wastewater sewage sludge. *JOCET* 2014, 2, 282–286.
- [48] Menendez J, Dominguez A, Inguanzo M, Pis J. Microwave-induced drying, pyrolysis and gasification (MWDPG) of sewage sludge: Vitrification of the solid residue. *J. Anal. Appl. Pyrol.* 2005, 74, 406–412.
- [49] Yu Q, Lei H, Yu G, Feng X, Li Z, Wu Z. Influence of microwave irradiation on sludge dewaterability. *Chem. Eng. J.* 2009, 155, 88–93.
- [50] Lindroth DP, Berglund WR. Microwave drying of flue gas desulfurized (by-product) gypsum. *Int. J. Surf. Min. Reclamat. Environ.* 1995, 9, 169–177.
- [51] Beneroso D, Bermúdez J, Arenillas A, Menéndez J. Integrated microwave drying, pyrolysis and gasification for valorisation of organic wastes to syngas. *Fuel* 2014, 132, 20–26.
- [52] Zi W, Zhang X, Peng J, Zhang L, Long M, Zuo J. Optimization of microwave drying biomass material of stem granules from waste tobacco using response surface methodology. *Drying Technol.* 2013, 31, 1234–1244.
- [53] Acierno D, Barba AA, d Amore M, others. Microwaves in soil remediation from VOCs. 1: Heat and mass transfer aspects. *AIChE J.* 2003, 49, 1909–1921.
- [54] George CE, Lightsey GR, Jun I, Fan J. Soil decontamination via microwave and radio frequency co-volatilization. *Environ. Prog.* 1992, 11, 216–219.

- [55] Di P, Chang DP. Investigation of polychlorinated biphenyl removal from contaminated soil using microwave-generated steam. *J. Air Waste Manage. Assoc.* 2001, 51, 482–488.
- [56] Robinson J, Kingman S, Snape C, Shang H, Barranco R, Saeid A. Separation of polyaromatic hydrocarbons from contaminated soils using microwave heating. *Sep. Purif. Technol.* 2009, 69, 249–254.
- [57] Falciglia PP, Urso G, Vagliasindi FGA. Microwave heating remediation of soils contaminated with diesel fuel. *J. Soils Sediments* 2013, 13, 1396.
- [58] Li D, Zhang Y, Xie Q, Zhao Y. Microwave thermal remediation of crude oil contaminated soil enhanced by carbon fiber. *J. Environ. Sci.* 2009, 21, 1290–1295.
- [59] Santos JM, Pereira MS, Júnior IP, Pena MMR, Ataíde CH. Microwave drying of drilled cuttings in the context of waste disposal and drilling fluid recovery. *Energy Technol.* 2014, 2, 832–838.
- [60] Shang H, Snape C, Kingman S, Robinson J. Microwave treatment of oil-contaminated North Sea drill cuttings in a high power multimode cavity. *Sep. Purif. Technol.* 2006, 49, 84–90.
- [61] Shang H, Robinson J, Kingman S, Snape C, Wu Q. Theoretical study of microwave enhanced thermal decontamination of oil contaminated waste. *Chem. Eng. Technol.* 2007, 30, 121–130.
- [62] Shang H, Kingman S, Snape C, Robinson J. A new technology of microwave treatment of oil contaminated drilling waste in a single mode cavity. *Acta Petrol. Sin.* 2009, 3, 012.
- [63] Shang H, Guo Y, Yang X, Zhang W. Influence of materials dielectric properties on the petroleum oil removal from waste under microwave irradiation. *Can. J. Chem. Eng.* 2012, 90, 1465–1471.
- [64] Robinson J, Snape C, Kingman S, Shang H. Thermal desorption and pyrolysis of oil contaminated drill cuttings by microwave heating. *J. Anal. Appl. Pyrol.* 2008, 81, 27–32.
- [65] Robinson J, Kingman S, Onobrakpeya O. Microwave-assisted stripping of oil contaminated drill cuttings. *J. Environ. Manage.* 2008, 88, 211–218.
- [66] Ania C, Parra J, Menendez J, Pis J. Effect of microwave and conventional regeneration on the microporous and mesoporous network and on the adsorptive capacity of activated carbons. *Microporous Mesoporous Mater.* 2005, 85, 7–15.
- [67] Meier M, Turner M, Vallee S, Conner WC, Lee KH, Yngvesson KS. Microwave regeneration of zeolites in a 1 meter column. *AIChE J.* 2009, 55, 1906–1913.
- [68] Price DW, Schmidt PS. VOC recovery through microwave regeneration of adsorbents: process design studies. *J. Air Waste Manage. Assoc.* 1998, 48, 1135–1145.
- [69] Ma S, Yao J, Gao L, Ma X, Zhao Y. Experimental study on removals of SO<sub>2</sub> and NO<sub>x</sub> using adsorption of activated carbon/microwave desorption. *J. Air Waste Manage. Assoc.* 2012, 62, 1012–1021.
- [70] Webley PA, Zhang J. Microwave assisted vacuum regeneration for CO<sub>2</sub> capture from wet flue gas. *Adsorption* 2014, 20, 201–210.
- [71] Coss PM, Cha CY. Microwave regeneration of activated carbon used for removal of solvents from vented air. *J. Air Waste Manage. Assoc.* 2000, 50, 529–535.
- [72] Chen M, Huang J, Wang J, Ning P, Jiang Y, Xu Y. Thermal behaviors and regeneration of activated carbon saturated with toluene induced by microwave irradiation. *J. Chem. Eng. Jpn.* 2009, 42, 325–329.
- [73] Feng QL, Wang CX, Wang XQ, Ning P. Regeneration of activated carbon fiber using microwave under vacuum condition. *Appl. Mech. Mater.* 2013, 373, 2019–2023.
- [74] Wang CX, Wang XQ, Ning P, Feng QL. Regeneration of activated carbon fiber by microwave under nitrogen condition. *Appl. Mech. Mater.* 2013, 373, 2024–2029.
- [75] Meng QB, Yang GS, Lee YS. Preparation of highly porous hypercrosslinked polystyrene adsorbents: Effects of hydrophilicity on the adsorption and microwave-assisted desorption behavior toward benzene. *Micropor. Mesopor. Mat.* 2013, 181, 222–227.

- [76] Price DW, Schmidt PS. VOC recovery through microwave regeneration of adsorbents: Comparative economic feasibility studies. *J. Air Waste Manage. Assoc.* 1998, 48, 1146–1155.
- [77] Liu X, Quan X, Bo L, Chen S, Zhao Y. Simultaneous pentachlorophenol decomposition and granular activated carbon regeneration assisted by microwave irradiation. *Carbon* 2004, 42, 415–422.
- [78] Liao P, Yuan S, Xie W, Zhang W, Tong M, Wang K. Adsorption of nitrogen-heterocyclic compounds on bamboo charcoal: kinetics, thermodynamics, and microwave regeneration. *J. Colloid Interface Sci.* 2013, 390, 189–195.
- [79] Ania C, Parra J, Menendez J, Pis J. Microwave-assisted regeneration of activated carbons loaded with pharmaceuticals. *Water Res.* 2007, 41, 3299–3306.
- [80] Liu X, Yu G, Han W. Granular activated carbon adsorption and microwave regeneration for the treatment of 2, 4, 5-trichlorobiphenyl in simulated soil-washing solution. *J. Hazard. Mater.* 2007, 147, 746–751.
- [81] Foo K, Hameed B. Microwave-assisted regeneration of activated carbon. *Bioresour. Technol.* 2012, 119, 234–240.
- [82] Chang SH, Wang KS, Liang HH, Chen HY, Li HC, Peng TH, Su YC, Chang CY. Treatment of Reactive Black 5 by combined electrocoagulation-granular activated carbon adsorption-microwave regeneration process. *J. Hazard. Mater.* 2010, 175, 850–857.
- [83] Ludlow-Palafox C, Chase HA. Microwave-induced pyrolysis of plastic wastes. *Ind. Eng. Chem. Res.* 2001, 40, 4749–4756.
- [84] Nema S, Ganeshprasad K. Plasma pyrolysis of medical waste. *Curr. Sci.* 2002, 83, 271–278.
- [85] Luque R, Menéndez JA, Arenillas A, Cot J. Microwave-assisted pyrolysis of biomass feedstocks: the way forward? *Energy Environ. Sci.* 2012, 5, 5481–5488.
- [86] Bridgwater AV. Review of fast pyrolysis of biomass and product upgrading. *Biomass Bioenerg.* 2012, 38, 68–94.
- [87] Motasemi F, Afzal MT. A review on the microwave-assisted pyrolysis technique. *Renew. Sust. Energ. Rev.* 2013, 28, 317–330.
- [88] Ismail N, Ani F. Syngas production from microwave gasification of oil palm biochars. *Carbon* 2014, 64, 79–40.
- [89] Menéndez J, Domínguez A, Fernández Y, Pis J. Evidence of self-gasification during the microwave-induced pyrolysis of coffee hulls. *Energy Fuels* 2007, 21, 373–378.
- [90] Ferrera-Lorenzo N, Fuente E, Suárez-Ruiz I, Ruiz B. KOH activated carbon from conventional and microwave heating system of a macroalgae waste from the Agar-Agar industry. *Fuel Process. Technol.* 2014, 121, 25–31.
- [91] Foo K, Hameed B. Adsorption characteristics of industrial solid waste derived activated carbon prepared by microwave heating for methylene blue. *Fuel Process. Technol.* 2012, 99, 103–109.
- [92] Yin C. Microwave-assisted pyrolysis of biomass for liquid biofuels production. *Bioresour. Technol.* 2012, 120, 273–284.
- [93] Sobhy A, Chaouki J. Microwave-assisted biorefinery. *Chem. Eng. Trans.* 2010, 19, 25–30.
- [94] Fernández Y, Menéndez J. Influence of feed characteristics on the microwave-assisted pyrolysis used to produce syngas from biomass wastes. *J. Anal. Appl. Pyrol.* 2011, 91, 316–322.
- [95] Domínguez A, Menéndez J, Fernandez Y, Pis J, Nabais JV, Carrott P, Carrott MR. Conventional and microwave induced pyrolysis of coffee hulls for the production of a hydrogen rich fuel gas. *J. Anal. Appl. Pyrol.* 2007, 79, 128–135.
- [96] Shuttleworth P, Budarin V, Gronnow M, Clark JH, Luque R. Low temperature microwave-assisted vs conventional pyrolysis of various biomass feedstocks. *J. Nat. Gas Chem.* 2012, 21, 270–274.

- [97] Ferrera-Lorenzo N, Fuente E, Bermúdez J, Suárez-Ruiz I, Ruiz B. Conventional and microwave pyrolysis of a macroalgae waste from the Agar-Agar industry. Prospects for bio-fuel production. *Bioresour. Technol.* 2014, 151, 199–206.
- [98] Maldhure AV, Ekhe JD. Microwave treated activated carbon from industrial waste lignin for endosulfan adsorption. *J. Chem. Technol. Biotechnol.* 2011, 86, 1074–1080.
- [99] Njoku V, Foo K, Asif M, Hameed B. Preparation of activated carbons from rambutan (*Nephelium lappaceum*) peel by microwave-induced KOH activation for acid yellow 17 dye adsorption. *Chem. Eng. J.* 2014, 250, 198–204.
- [100] Wang XH, Chen HP, Ding XJ, Yang HP, Zhang SH, Shen YQ. Properties of gas and char from microwave pyrolysis of pine sawdust. *BioResources* 2009, 4, 946–959.
- [101] Zhao X, Wang M, Liu H, Li L, Ma C, Song Z. A microwave reactor for characterization of pyrolyzed biomass. *Bioresour. Technol.* 2012, 104, 673–678.
- [102] Omar R, Idris A, Yunus R, Khalid K, Isma MA. Characterization of empty fruit bunch for microwave-assisted pyrolysis. *Fuel* 2011, 90, 1536–1544.
- [103] Mushtaq F, Abdullah TAT, Mat R, Ani FN. Optimization and characterization of bio-oil produced by microwave assisted pyrolysis of oil palm shell waste biomass with microwave absorber. *Bioresour. Technol.* 2015, 190, 442–450.
- [104] Salema AA, Ani FN. Microwave induced pyrolysis of oil palm biomass. *Bioresour. Technol.* 2011, 102, 3388–3395.
- [105] Wan Y, Chen P, Zhang B, Yang C, Liu Y, Lin X, Ruan R. Microwave-assisted pyrolysis of biomass: Catalysts to improve product selectivity. *J. Anal. Appl. Pyrol.* 2009, 86, 161–167.
- [106] Zhao X, Wang M, Liu H, Zhao C, Ma C, Song Z. Effect of temperature and additives on the yields of products and microwave pyrolysis behaviors of wheat straw. *J. Anal. Appl. Pyrol.* 2013, 100, 49–55.
- [107] Huang YF, Kuan WH, Chang CC, Tzou YM. Catalytic and atmospheric effects on microwave pyrolysis of corn stover. *Bioresour. Technol.* 2013, 131, 274–280.
- [108] Huang YF, Kuan WH, Lo SL, Lin CF. Hydrogen-rich fuel gas from rice straw via microwave-induced pyrolysis. *Bioresour. Technol.* 2010, 101, 1968–1973.
- [109] Dai Q, Jiang X, Wang F, Chi Y, Yan J. PCDD/Fs in wet sewage sludge pyrolysis using conventional and microwave heating. *J. Anal. Appl. Pyrol.* 2013, 104, 280–286.
- [110] Domínguez A, Menéndez JA, Inguanzo M, Bernad PL, Pis JJ. Gas chromatographic-mass spectrometric study of the oil fractions produced by microwave-assisted pyrolysis of different sewage sludges. *J. Chromatogr. A* 2003, 1012, 193–206.
- [111] Domínguez A, Menéndez J, Inguanzo M, Pis J. Investigations into the characteristics of oils produced from microwave pyrolysis of sewage sludge. *Fuel Process. Technol.* 2005, 86, 1007–1020.
- [112] Menéndez JA, Inguanzo M, Pis JJ. Microwave-induced pyrolysis of sewage sludge. *Water Res.* 2002, 36, 3261–3264.
- [113] Menéndez J, Domínguez A, Inguanzo M, Pis J. Microwave pyrolysis of sewage sludge: analysis of the gas fraction. *J. Anal. Appl. Pyrol.* 2004, 71, 657–667.
- [114] Uzun BB, Apaydin-Varol E, Ates F, Özbay N, Pütün AE. Synthetic fuel production from tea waste: characterisation of bio-oil and bio-char. *Fuel* 2010, 89, 176–184.
- [115] Zhang Z, Macquarrie DJ, Budarin VL, Hunt AJ, Gronnow MJ, Fan J, Shuttleworth PS, Clark JH, Matharu AS, others. Low-temperature microwave-assisted pyrolysis of waste office paper and the application of bio-oil as an AI adhesive. *Green Chem.* 2015, 17, 260–270.
- [116] Mushtaq F, Sami Channa A, Mat R, Ani FN. Microwave assisted pyrolysis of waste biomass resources for bio-oil production. *Appl. Mech. Mater.* 2014.
- [117] Abubakar Z, Salema AA, Ani FN. A new technique to pyrolyse biomass in a microwave system: effect of stirrer speed. *Bioresour. Technol.* 2013, 128, 578–585.

- [118] Lam SS, Liew RK, Cheng CK, Chase HA. Catalytic microwave pyrolysis of waste engine oil using metallic pyrolysis char. *Appl. Catal., B* 2015, 176, 601–617.
- [119] Khongkrapan P, Tippayawong N, Kiatsiriroat T. Thermochemical conversion of waste papers to fuel gas in a microwave plasma reactor. *JOCET* 2013, 1, 80–83.
- [120] Huang YF, Kuan WH, Lo SL, Lin CF. Total recovery of resources and energy from rice straw using microwave-induced pyrolysis. *Bioresour. Technol.* 2008, 99, 8252–8258.
- [121] Huang YF, Chiueh PT, Kuan WH, Lo SL. Microwave pyrolysis of rice straw: products, mechanism, and kinetics. *Bioresour. Technol.* 2013, 142, 620–624.
- [122] Lin YC, Wu TY, Liu WY, Hsiao YH. Production of hydrogen from rice straw using microwave-induced pyrolysis. *Fuel* 2014, 119, 21–26.
- [123] Domínguez A, Fernández Y, Fidalgo B, Pis JJ, Menéndez JA. Bio-syngas production with low concentrations of CO<sub>2</sub> and CH<sub>4</sub> from microwave-induced pyrolysis of wet and dried sewage sludge. *Chemosphere* 2008, 70, 397–403.
- [124] Domínguez A, Menéndez JA, Inguanzo M, Pis JJ. Production of bio-fuels by high temperature pyrolysis of sewage sludge using conventional and microwave heating. *Bioresour. Technol.* 2006, 97, 1185–1193.
- [125] Zuo W, Tian Y, Ren N. The important role of microwave receptors in bio-fuel production by microwave-induced pyrolysis of sewage sludge. *Waste Manag.* 2011, 31, 1321–1326.
- [126] Yu Y, Yu J, Sun B, Yan Z. Influence of catalyst types on the microwave-induced pyrolysis of sewage sludge. *J. Anal. Appl. Pyrol.* 2014, 106, 86–91.
- [127] Beneroso D, Bermúdez J, Arenillas A, Menéndez J. Influence of the microwave absorbent and moisture content on the microwave pyrolysis of an organic municipal solid waste. *J. Anal. Appl. Pyrol.* 2014, 105, 234–240.
- [128] Suriapparao DV, Vinu R. Bio-oil production via catalytic microwave pyrolysis of model municipal solid waste component mixtures. *RSC Adv.* 2015, 5, 57619–57631.
- [129] Gedam VV, Regupathi I. Pyrolysis of municipal solid waste for syngas production by microwave irradiation. *Nat. Resour. Res.* 2012, 21, 75–82.
- [130] Li X, Yan J, Yang H, Peng T, Yang Q. Study on processing technology for microwave pyrolysis of municipal solid waste. In: 2011 International Conference on Materials for Renewable Energy & Environment (ICMREE), Volume 1. IEEE; 2011, 336–340. DOI: 10.1109/ICMREE.2011.5930825
- [131] Sharobem TT. Tertiary Recycling of Waste Plastics: An Assessment of Pyrolysis by Microwave Radiation. Master Thesis, Department of Earth and Environmental Engineering Fu Foundation of Engineering and Applied Science, Columbia University May 2010.
- [132] Moriwaki S, Machida M, Tatsumoto H, Kuga M, Ogura T. A study on thermal runaway of poly (vinyl chloride) by microwave irradiation. *J. Anal. Appl. Pyrol.* 2006, 76, 238–242.
- [133] Moriwaki S, Machida M, Tatsumoto H, Otsubo Y, Aikawa M, Ogura T. Dehydrochlorination of poly (vinyl chloride) by microwave irradiation. *Appl. Therm. Eng.* 2006, 26, 745–750.
- [134] Undri A, Frediani M, Rosi L, Frediani P. Reverse polymerization of waste polystyrene through microwave assisted pyrolysis. *J. Anal. Appl. Pyrol.* 2014, 105, 35–42.
- [135] Hussain Z, Khan KM, Hussain K. Microwave-metal interaction pyrolysis of polystyrene. *J. Anal. Appl. Pyrol.* 2010, 89, 39–43.
- [136] Hussain Z, Khan KM, Perveen S, Hussain K, Voelter W. The conversion of waste polystyrene into useful hydrocarbons by microwave-metal interaction pyrolysis. *Fuel Process. Technol.* 2012, 94, 145–150.
- [137] Nishioka K, Taniguchi T, Ueki Y, Ohno K, Maeda T, Shimizu M. Gasification and reduction behavior of plastics and iron ore mixtures by microwave heating. *ISIJ Int.* 2007, 47, 602–607.
- [138] Bartoli M, Rosi L, Frediani M, Undri A, Frediani P. Depolymerization of polystyrene at reduced pressure through a microwave assisted pyrolysis. *J. Anal. Appl. Pyrol.* 2015, 113, 281–287.

- [139] Zhang X, Lei H, Yadavalli G, Zhu L, Wei Y, Liu Y. Gasoline-range hydrocarbons produced from microwave-induced pyrolysis of low-density polyethylene over ZSM-5. *Fuel* 2015, 144, 33–42.
- [140] Undri A, Rosi L, Frediani M, Frediani P. Efficient disposal of waste polyolefins through microwave assisted pyrolysis. *Fuel* 2014, 116, 662–671.
- [141] Åkesson D, Foltynowicz Z, Christeen J, Skrifvars M. Products obtained from decomposition of glass fiber-reinforced composites using microwave pyrolysis. *Polimery* 2013, 58, 582–586.
- [142] Adhikari B, De D, Maiti S. Reclamation and recycling of waste rubber. *Prog. Polym. Sci.* 2000, 25, 909–948.
- [143] Undri A, Meini S, Rosi L, Frediani M, Frediani P. Microwave pyrolysis of polymeric materials: waste tires treatment and characterization of the value-added products. *J. Anal. Appl. Pyrol.* 2013, 103, 149–158.
- [144] Undri A, Rosi L, Frediani M, Frediani P. Upgraded fuel from microwave assisted pyrolysis of waste tire. *Fuel* 2014, 115, 600–608.
- [145] Andersson M, Wedel MK, Forsgren C, Christéen J. Microwave assisted pyrolysis of residual fractions of waste electrical and electronics equipment. *Miner. Eng.* 2012, 29, 105–111.
- [146] Sun J, Wang W, Liu Z, Ma Q, Zhao C, Ma C. Kinetic study of the pyrolysis of waste printed circuit boards subject to conventional and microwave heating. *Energies* 2012, 5, 3295–3306.
- [147] Zhang Z, Zhao X, Kwon E, Castaldi MJ. Experimental research on microwave induced thermal decomposition of printed circuit board wastes. In 18th Annual North American Waste-to-Energy Conference. American Society of Mechanical Engineers; 2010, 15–21. doi:10.1115/NAWTEC18-3536.
- [148] Sun J, Wang W, Liu Z, Ma C. Study of the transference rules for bromine in waste printed circuit boards during microwave-induced pyrolysis. *J Air Waste Manag Assoc* 2011, 61, 535–542.
- [149] Sun J, Wang W, Liu Z, Ma C. Recycling of waste printed circuit boards by microwave-induced pyrolysis and featured mechanical processing. *Ind. Eng. Chem. Res.* 2011, 50, 11763–11769.
- [150] Lam SS, Russell AD, Chase HA. Microwave pyrolysis, a novel process for recycling waste automotive engine oil. *Energy* 2010, 35, 2985–2991.
- [151] Abo-Dief HM, Altalhi AA, Mohamed AT. Waste oil recycling using microwave pyrolysis reactors. *Journal of Industrial and Intelligent Information* 2014, 2, 314–319. doi: 10.12720/jiii.2.4.314–319.
- [152] Lam SS, Russell AD, Chase HA. Pyrolysis using microwave heating: a sustainable process for recycling used car engine oil. *Ind. Eng. Chem. Res.* 2010, 49, 10845–10851.
- [153] Lam SS, Russell AD, Lee CL, Lam SK, Chase HA. Production of hydrogen and light hydrocarbons as a potential gaseous fuel from microwave-heated pyrolysis of waste automotive engine oil. *Int. J. Hydrogen Energy.* 2012, 37, 5011–5021.
- [154] Lam SS, Russell AD, Lee CL, Chase HA. Microwave-heated pyrolysis of waste automotive engine oil: Influence of operation parameters on the yield, composition, and fuel properties of pyrolysis oil. *Fuel* 2012, 92, 327–339.
- [155] Lam SS, Russell AD, Chase HA. From waste to valuable fuel: How microwave-heated pyrolysis can recycle waste automotive engine oil. *Prep. Pap.-Am. Chem. Soc., Div. Fuel Chem* 2011, 56, 19–21.
- [156] Will H, Scholz P, Ondruschka B. Heterogeneous gas-phase catalysis under microwave irradiation – a new multi-mode microwave applicator. *Top. Catal.* 2004, 29, 175.
- [157] Zhang DX, Yu AM, Jin QH. Studies on microwave-carbon reduction method for the treatment of nitric oxide. *Chem. J. Chinese U.* 1997, 18, 1271–1274.
- [158] Cha CY. Microwave induced reactions of SO<sub>2</sub> and NO<sub>x</sub> decomposition in the char-bed. *Res. Chem. Intermed.* 1994, 20, 13–28.
- [159] Cha CY, Kim DS. Microwave induced reactions of sulfur dioxide and nitrogen oxides in char and anthracite bed. *Carbon* 2001, 39, 1159–1166.

- [160] Jin Y, Xin J, YAO J, Zhang B, Song D, Shi R. Influences of co-existing components in flue gas on simultaneous desulfurization and denitrification using microwave irradiation over activated carbon. *J. Fuel Chem. Technol.* 2011, 39, 460–464.
- [161] Ma S, Jin X, Wang M, Jin Y, Yao J, Liu W. Experimental study on removing NO from flue gas using microwave irradiation over activated carbon carried catalyst. *Sci. China Technol. SC* 2011, 54, 3431–3436.
- [162] Wei Z, Du Z, Lin Z, He H, Qiu R. Removal of NO<sub>x</sub> by microwave reactor with ammonium bicarbonate and Ga-A zeolites at low temperature. *Energy* 2007, 32, 1455–1459.
- [163] Wei Z, Lin Z, Niu H, He H, Ji Y. Simultaneous desulfurization and denitrification by microwave reactor with ammonium bicarbonate and zeolite. *J. Hazard. Mater.* 2009, 162, 837–841.
- [164] Wei Z, Zeng G, Xie Z. Microwave catalytic desulfurization and denitrification simultaneously on Fe/Ca-5A zeolite catalyst. *Energy Fuels* 2009, 23, 2947–2951.
- [165] Wei Z, Niu H, Ji Y. Simultaneous removal of SO<sub>2</sub> and NO<sub>x</sub> by microwave with potassium permanganate over zeolite. *Fuel Process. Technol.* 2009, 90, 324–329.
- [166] Wei Z, Zeng G, Xie Z, Sun J. Simultaneous desulfurization and denitrification by microwave catalytic over FeCoCu/Zeolite 5A catalyst. *J. Environ. Eng.* 2010, 136, 1403–1408.
- [167] Wei Z, Zeng G, Xie Z, Ma C, Liu X, Sun J, Liu L. Microwave catalytic NO<sub>x</sub> and SO<sub>2</sub> removal using FeCu/zeolite as catalyst. *Fuel* 2011, 90, 1599–1603.
- [168] Hu F, Zeng G, Li H, Wei Z, Sun J, Ye Q, Xie Z. Microwave Catalytic Conversion of SO<sub>2</sub> and NO<sub>x</sub> over Cu/zeolite. *Energ. Sci. Technol.* 2011, 1, 21–28.
- [169] Lee BN, Ying WT, Shen YT. Microwave-induced combustion of volatile organic compounds in an industrial flue gas over the magnetite fixed-bed. *Chemosphere* 2007, 69, 1821–1826.
- [170] Bo L, Liao J, Zhang Y, Wang X, Yang Q. CuO/zeolite catalyzed oxidation of gaseous toluene under microwave heating. *Front Environ. Sci. En.* 2013, 7, 395–402.
- [171] Sun J, Bo L, Yang L, Liang X, Hu X. A carbon nanodot modified Cu-Mn-Ce/ZSM catalyst for the enhanced microwave-assisted degradation of gaseous toluene. *RSC Adv.* 2014, 4, 14385–14391.
- [172] Wang N, Wang P. Study and application status of microwave in organic wastewater treatment—a review. *Chem. Eng. J.* 2016, 283, 193–214.
- [173] Remya N, Lin JG. Current status of microwave application in wastewater treatment – a review. *Chem. Eng. J.* 2011, 166, 797–813.
- [174] Ai Z, Yang P, Lu X. Degradation of 4-chlorophenol by a microwave assisted photocatalysis method. *J. Hazard. Mater.* 2005, 124, 147–152.
- [175] Zhang Y, Quan X, Chen S, Zhao Y, Yang F. Microwave assisted catalytic wet air oxidation of H-acid in aqueous solution under the atmospheric pressure using activated carbon as catalyst. *J. Hazard. Mater.* 2006, 137, 534–540.
- [176] Polaert I, Estel L, Ledoux A. Microwave-assisted remediation of phenol wastewater on activated charcoal. *Chem. Eng. Sci.* 2005, 60, 6354–6359.
- [177] Sun Y, Zhang Y, Quan X. Treatment of petroleum refinery wastewater by microwave-assisted catalytic wet air oxidation under low temperature and low pressure. *Sep. Purif. Technol.* 2008, 62, 565–570.
- [178] Bo L, Quan X, Chen S, Zhao H, Zhao Y. Degradation of p-nitrophenol in aqueous solution by microwave assisted oxidation process through a granular activated carbon fixed bed. *Water Res.* 2006, 40, 3061–3068.
- [179] Bo LL, Zhang YB, Quan X, Zhao B. Microwave assisted catalytic oxidation of p-nitrophenol in aqueous solution using carbon-supported copper catalyst. *J. Hazard. Mater.* 2008, 153, 1201–1206.
- [180] Zhao G, Lv B, Jin Y, Li D. P-chlorophenol wastewater treatment by microwave-enhanced catalytic wet peroxide oxidation. *Water Environ. Res.* 2010, 82, 120–127.

- [181] Zhang Z, Xu D, Shen M, Wu D, Chen Z, Ji X, Li F, Xu Y. Degradation of surfactant wastewater under microwave irradiation in the presence of activated carbon assisted with nano-sized TiO<sub>2</sub> or nano-sized ZnO. *Water Sci. Technol.* 2011, 63, 424–431.
- [182] Zhang Z, Yu F, Huang L, Jiatieli J, Li Y, Song L, Yu N, Dionysiou DD. Confirmation of hydroxyl radicals (OH) generated in the presence of TiO<sub>2</sub> supported on AC under microwave irradiation. *J. Hazard. Mater.* 2014, 278, 152–157.
- [183] Zhang Z, Xu Y, Ma X, Li F, Liu D, Chen Z, Zhang F, Dionysiou DD. Microwave degradation of methyl orange dye in aqueous solution in the presence of *nano*-TiO<sub>2</sub>-supported activated carbon (supported-TiO<sub>2</sub>/AC/MW). *J. Hazard. Mater.* 2012, 209–210, 271–277.
- [184] Sanz J, Lombrana J, De Luis A, Ortueta M, Varona F. Microwave and Fenton's reagent oxidation of wastewater. *Environ. Chem. Lett.* 2003, 1, 45–50.
- [185] Wu ZL, Ondruschka B, Cravotto G. Degradation of phenol under combined irradiation of microwaves and ultrasound. *Environ. Sci. Technol.* 2008, 42, 8083–8087.
- [186] Ju Y, Yang S, Ding Y, Sun C, Gu C, He Z, Qin C, He H, Xu B. Microwave-enhanced H<sub>2</sub>O<sub>2</sub>-based process for treating aqueous malachite green solutions: intermediates and degradation mechanism. *J. Hazard. Mater.* 2009, 171, 123–132.
- [187] Hong J, Yuan N, Wang Y, Qi S. Efficient degradation of Rhodamine B in microwave-H<sub>2</sub>O<sub>2</sub> system at alkaline pH. *Chem. Eng. J.* 2012, 191, 364–368.
- [188] Prasannakumar BR, Regupathi I, Murugesan T. An optimization study on microwave irradiated decomposition of phenol in the presence of H<sub>2</sub>O<sub>2</sub>. *J. Chem. Technol. Biotechnol.* 2009, 84, 83–91.
- [189] Cravotto G, Di Carlo S, Tumiatti V, Roggero C, Bremner HD. Degradation of persistent organic pollutants by Fenton's reagent facilitated by microwave or high-intensity ultrasound. *Environ. Technol.* 2005, 26, 721–724.
- [190] Yang Y, Wang P, Shi S, Liu Y. Microwave enhanced Fenton-like process for the treatment of high concentration pharmaceutical wastewater. *J. Hazard. Mater.* 2009, 168, 238–245.
- [191] Li N, Wang P, Zuo C, Cao H, Liu Q. Microwave-enhanced Fenton process for DMSO-containing wastewater. *Environ. Eng. Sci.* 2010, 27, 271–280.
- [192] Zheng H, Zhang H, Sun X, Zhang P, Tshukudu T, Zhu G. The catalytic oxidation of malachite green by the microwave-Fenton processes. *Water Sci. Technol.* 2010, 62, 1304–1311.
- [193] Liu ST, Huang J, Ye Y, Zhang AB, Pan L, Chen XG. Microwave enhanced Fenton process for the removal of methylene blue from aqueous solution. *Chem. Eng. J.* 2013, 215, 586–590.
- [194] Iboukhoulef H, Amrane A, Kadi H. Microwave-enhanced Fenton-like system, Cu(II)/H<sub>2</sub>O<sub>2</sub>, for olive mill wastewater treatment. *Environ. Technol.* 2013, 34, 853–860.
- [195] Wang Y, Zhao H, Gao J, Zhao G, Zhang Y, Zhang Y. Rapid mineralization of azo-dye wastewater by microwave synergistic electro-Fenton oxidation process. *J. Phys.Chem. C* 2012, 116, 7457–7463.
- [196] Qi C, Liu X, Lin C, Zhang X, Ma J, Tan H, Ye W. Degradation of sulfamethoxazole by microwave-activated persulfate: kinetics, mechanism and acute toxicity. *Chem. Eng. J.* 2014, 249, 6–14.
- [197] Yang S, Wang P, Yang X, Wei G, Zhang W, Shan L. A novel advanced oxidation process to degrade organic pollutants in wastewater: microwave-activated persulfate oxidation. *J Environ Sci (China)* 2009, 21, 1175–1180.
- [198] Bi X, Wang P, Jiang H, Xu H, Shi SJ, Huang J. Treatment of phenol wastewater by microwave-induced ClO<sub>2</sub> – CuO<sub>x</sub>/Al<sub>2</sub>O<sub>3</sub> catalytic oxidation process. *J Environ Sci (China)* 2007, 19, 1510–1515.
- [199] Bi X, Wang P, Jiang H. Catalytic activity of CuO<sub>n</sub>–La<sub>2</sub>O<sub>3</sub>/*gamma*-Al<sub>2</sub>O<sub>3</sub> for microwave assisted ClO<sub>2</sub> catalytic oxidation of phenol wastewater. *J. Hazard. Mater.* 2008, 154, 543–549.
- [200] Bi X, Wang P, Jiao C, Cao H. Degradation of remazol golden yellow dye wastewater in microwave enhanced ClO<sub>2</sub> catalytic oxidation process. *J. Hazard. Mater.* 2009, 168, 895–900.



- [201] He H, Yang S, Yu K, Ju Y, Sun C, Wang L. Microwave induced catalytic degradation of crystal violet in nano-nickel dioxide suspensions. *J. Hazard. Mater.* 2010, 173, 393–400.
- [202] Lv S, Chen X, Ye Y, Yin S, Cheng J, Xia M. Rice hull/MnFe<sub>2</sub>O<sub>4</sub> composite: preparation, characterization and its rapid microwave-assisted COD removal for organic wastewater. *J. Hazard. Mater.* 2009, 171, 634–639.
- [203] Li X, Xu F, Wang J, Zhang C, Chen Y, Zhu S, Shen S. Preparation of Fe-Cu catalysts and treatment of a wastewater mixture by microwave-assisted UV catalytic oxidation processes. *Environ. Technol.* 2010, 31, 433–443.
- [204] Horikoshi S, Hidaka H, Serpone N. Environmental remediation by an integrated microwave/UV-illumination method II.: Characteristics of a novel UV-VIS-microwave integrated irradiation device in photodegradation processes. *J. Photochem. Photobiol., A* 2002, 153, 185–189.
- [205] Horikoshi S, Kajitani M, Hidaka H, Serpone N. Investigation of factors that influence TiO<sub>2</sub> photoassisted degradations under simultaneous illumination by UV and microwave radiation fields. *J. Photochem. Photobiol., A* 2008, 196, 159–164.
- [206] Horikoshi S, Hidaka H, Serpone N. Environmental remediation by an integrated microwave/UV illumination technique. 3. A microwave-powered plasma light source and photoreactor to degrade pollutants in aqueous dispersions of TiO<sub>2</sub> illuminated by the emitted UV/visible radiation. *Environ. Sci. Technol.* 2002, 36, 5229–5237.
- [207] Horikoshi S, Hidaka H, Serpone N. Environmental remediation by an integrated microwave/UV-illumination method. 1. Microwave-assisted degradation of rhodamine-B dye in aqueous TiO<sub>2</sub> dispersions. *Environ. Sci. Technol.* 2002, 36, 1357–1366.
- [208] Horikoshi S, Saitou A, Hidaka H, Serpone N. Environmental remediation by an integrated microwave/UV illumination method. V. Thermal and nonthermal effects of microwave radiation on the photocatalyst and on the photodegradation of rhodamine-B under UV/Vis radiation. *Environ. Sci. Technol.* 2003, 37, 5813–5822.
- [209] Horikoshi S, Hidaka H, Serpone N. Environmental remediation by an integrated microwave/UV-illumination technique: IV. Non-thermal effects in the microwave-assisted degradation of 2, 4-dichlorophenoxyacetic acid in UV-irradiated TiO<sub>2</sub>/H<sub>2</sub>O dispersions. *J. Photochem. Photobiol., A* 2003, 159, 289–300.
- [210] Horikoshi S, Hidaka H, Serpone N. Environmental remediation by an integrated microwave/UV illumination technique: VI. A simple modified domestic microwave oven integrating an electrodeless UV-Vis lamp to photodegrade environmental pollutants in aqueous media. *J. Photochem. Photobiol., A* 2004, 161, 221–225.
- [211] Horikoshi S, Tokunaga A, Hidaka H, Serpone N. Environmental remediation by an integrated microwave/UV illumination method: VII. Thermal/non-thermal effects in the microwave-assisted photocatalyzed mineralization of bisphenol-A. *J. Photochem. Photobiol., A* 2004, 162, 33–40.
- [212] Horikoshi S, Hojo F, Hidaka H, Serpone N. Environmental remediation by an integrated microwave/UV illumination technique. 8. Fate of carboxylic acids, aldehydes, alkoxy carbonyl and phenolic substrates in a microwave radiation field in the presence of TiO<sub>2</sub> particles under UV irradiation. *Environ. Sci. Technol.* 2004, 38, 2198–2208.
- [213] Horikoshi S, Tokunaga A, Watanabe N, Hidaka H, Serpone N. Environmental remediation by an integrated microwave/UV illumination technique: IX. Peculiar hydrolytic and co-catalytic effects of platinum on the TiO<sub>2</sub> photocatalyzed degradation of the 4-chlorophenol toxin in a microwave radiation field. *J. Photochem. Photobiol., A* 2006, 177, 129–143.
- [214] Horikoshi S, Kajitani M, Sato S, Serpone N. A novel environmental risk-free microwave discharge electrodeless lamp (MDEL) in advanced oxidation processes: Degradation of the 2, 4-D herbicide. *J. Photochem. Photobiol., A* 2007, 189, 355–363.

- [215] Horikoshi S, Miura T, Kajitani M, Serpone N. Microwave discharge electrodeless lamps (MDEL). III. A novel tungsten-triggered MDEL device emitting VUV and UVC radiation for use in wastewater treatment. *Photochem. Photobiol. Sci.* 2008, 7, 303–310.
- [216] Ferrari C, Longo I, Tombari E, Gasperini L. A new integrated photoreactor for microwave assisted decolorization of Acid Orange 7 (AO7) in aqueous solutions. *Int. J. Chem. Reactor Eng.* 2010, 8.
- [217] Han DH, Cha SY, Yang HY. Improvement of oxidative decomposition of aqueous phenol by microwave irradiation in UV/H<sub>2</sub>O<sub>2</sub> process and kinetic study. *Water Res.* 2004, 38, 2782–2790.
- [218] Zhong H, Shaogui Y, Yongming J, Cheng S. Microwave photocatalytic degradation of rhodamine B using TiO<sub>2</sub> supported on activated carbon: mechanism implication. *J. Environ. Sci.* 2009, 21, 268–272.
- [219] Liao W, Zheng T, Wang P, Tu S, Pan W. Efficient microwave-assisted photocatalytic degradation of endocrine disruptor dimethyl phthalate over composite catalyst ZrOx/ZnO. *J. Environ. Sci.* 2010, 22, 1800–1806.
- [220] Fu J, Xu Z, Li QS, Chen S, An SQ, Zeng QF, Zhu HL. Treatment of simulated wastewater containing Reactive Red 195 by zero-valent iron/activated carbon combined with microwave discharge electrodeless lamp/sodium hypochlorite. *J. Environ. Sci.* 2010, 22, 512–518.
- [221] Cravotto G, Di Carlo S, Ondruschka B, Tumiatti V, Roggero CM. Decontamination of soil containing POPs by the combined action of solid Fenton-like reagents and microwaves. *Chemosphere* 2007, 69, 1326–1329.
- [222] Abramovitch RA, Bangzhou H, Abramovitch DA, Jiangao S. In situ decomposition of PCBs in soil using microwave energy. *Chemosphere* 1999, 38, 2227–2236.
- [223] Abramovitch RA, Bangzhou H, Abramovitch DA, Jiangao S. In situ decomposition of PAHs in soil and desorption of organic solvents using microwave energy. *Chemosphere* 1999, 39, 81–87.
- [224] Abramovitch RA, Bangzhou H, Davis M, Peters L. Decomposition of PCB's and other polychlorinated aromatics in soil using microwave energy. *Chemosphere* 1998, 37, 1427–1436.
- [225] Menéndez J, Arenillas A, Fidalgo B, Fernández Y, Zubizarreta L, Calvo EG, Bermúdez JM. Microwave heating processes involving carbon materials. *Fuel Process. Technol.* 2010, 91, 1–8.
- [226] Liu X, Zhang Q, Zhang G, Wang R. Application of microwave irradiation in the removal of polychlorinated biphenyls from soil contaminated by capacitor oil. *Chemosphere* 2008, 72, 1655–1658.
- [227] Liu X, Yu G. Combined effect of microwave and activated carbon on the remediation of polychlorinated biphenyl-contaminated soil. *Chemosphere* 2006, 63, 228–235.
- [228] Lin L, Yuan S, Chen J, Wang L, Wan J, Lu X. Treatment of chloramphenicol-contaminated soil by microwave radiation. *Chemosphere* 2010, 78, 66–71.
- [229] Huang G, Zhao L, Dong Y, Zhang Q. Remediation of soils contaminated with polychlorinated biphenyls by microwave-irradiated manganese dioxide. *J. Hazard. Mater.* 2011, 186, 128–132.
- [230] Yuan S, Tian M, Lu X. Microwave remediation of soil contaminated with hexachlorobenzene. *J. Hazard. Mater.* 2006, 137, 878–885.
- [231] Park DK, Bitton G, Melker R. Microbial inactivation by microwave radiation in the home environment. *J. Environ. Health* 2006, 69, 17–24; quiz 39–40.
- [232] Pino-Jelcic SA, Hong SM, Park JK. Enhanced anaerobic biodegradability and inactivation of fecal coliforms and *Salmonella* spp. in wastewater sludge by using microwaves. *Water Environ. Res.* 2006, 78, 209–216.
- [233] Eskicioglu C, Terzian N, Kennedy KJ, Droste RL, Hamoda M. Athermal microwave effects for enhancing digestibility of waste activated sludge. *Water Res.* 2007, 41, 2457–2466.

- [234] Park B, Ahn JH, Kim J, Hwang S. Use of microwave pretreatment for enhanced anaerobiosis of secondary sludge. *Water Sci. Technol.* 2004, 50, 17–23.
- [235] Abramovitch RA, ChangQing L, Hicks E, Sinard J. In situ remediation of soils contaminated with toxic metal ions using microwave energy. *Chemosphere* 2003, 53, 1077–1085.
- [236] Morrell M, Hardwick W, Murphy V, Wace P. A pilot plant demonstration of the vitrification of radioactive solutions using microwave power. *Nucl. Chem. Waste Manage.* 1986, 6, 193–195.
- [237] Li A, Antizar-Ladislao B, Khraisheh M. Bioconversion of municipal solid waste to glucose for bio-ethanol production. *Bioprocess. Biosyst. Eng.* 2007, 30, 189–196.
- [238] Saifuddin N, Chua K. Production of ethyl ester (biodiesel) from used frying oil: optimization of transesterification process using microwave irradiation. *Malaysian J. Chem.* 2004, 6, 77–82.
- [239] Hirata M, Kawasaki N, Nakamura T, Matsumoto K, Kabayama M, Tamura T, Tanada S. Adsorption of dyes onto carbonaceous materials produced from coffee grounds by microwave treatment. *J. Colloid Interface Sci.* 2002, 254, 17–22.
- [240] Lei L, Li X, Zhang X. Ammonium removal from aqueous solutions using microwave-treated natural Chinese zeolite. *Sep. Purif. Technol.* 2008, 58, 359–366.
- [241] Barnabas IJ, Dean JR, Fowles IA, Owen SP. Extraction of polycyclic aromatic hydrocarbons from highly contaminated soils using microwave energy. *Analyst* 1995, 120, 1897–1904.

## 22 Microwaves in the omics field

### Abbreviations list:

**ELISA**, enzyme-linked immunosorbent assay  
**emPCR**, emulsion polymerase chain reaction  
**ESI-MS/MS**, electrospray ionization-tandem mass spectrometry  
**FISH**, fluorescence *in situ* hybridization  
**FF-PET**, formalin-fixed, paraffin-embedded tissue  
**GLP**, good laboratory practice  
**ICATt**, isotope-coded affinity tags  
**ICP**, inductively coupled plasma  
**imFASP**, filter-aided sample preparation  
**iTRAQ<sub>t</sub>**, isobaric tags for relative and absolute quantitation  
**LC**, liquid chromatography  
**LLE**, liquid–liquid extraction  
**MAAH**, microwave-assisted acid hydrolysis  
**MAE**, microwave-assisted extraction  
**MALDI**, matrix-assisted laser desorption ionization  
**MAMEF**, microwave-accelerated metal-enhanced fluorescence  
**MT-MEC**, microwave-triggered metal-enhanced chemiluminescence  
**MW**, microwave(s)  
**NGS**, next-generation sequencing  
**PCR**, polymerase chain reaction  
**QTOF**, quadrupole time of flight  
**RCA**, rolling circle amplification  
**TFA**, trifluoroacetic acid

### 22.1 Introduction

*Omics* is at present a magic suffix from the Latin *ome*, which means mass or massive and refers to the enormous number of analytical data produced and required to obtain the information pursued by the so-called omics disciplines. Thus, an analytical process must be used to obtain the data required in an omics study. One or several steps of the analytical process can be assisted by microwave (MW) energy to accelerate, improve, or allow the acquisition of target analytical data.

<https://doi.org/10.1515/9783110479935-022>

### 22.1.1 Steps in the analytical process

An analytical process consists of a variable number of steps that mediate between the system under study and the acquisition of the analytical information in the required form. The steps can be divided into three groups:

(1) From sampling to acquisition of the so-called analytical sample, that is, the sample or that part of it that holds analytical interest and is ready to be inserted into a detector or high-resolution equipment connected to the detector. These steps can in turn be divided into sample pretreatment (SP) or preliminary operations that only involve physical changes (that is, sampling, homogenization, grinding, drilling, milling, or sieving) and sample preparation. The latter involves steps that typically can be assisted by MW, namely, digestion, leaching (also known as solid–liquid extraction or leaching), hydrolysis, and derivatization as the commonest sample preparation steps. Nevertheless, others are also occasionally assisted by MWs.

(2) Acquisition of signals from analytical sample. In most cases, the required analytical platform consists of high-resolution equipment (liquid or gas chromatographs for proper separation of target analytes) connected online to a multidetector, usually a mass spectrometer. Note that this detector does not require complete separation of the analytes, only of those that in fragmentation provide similar fragments.

(3) Treatment of raw data, a complex and usually time-consuming process that requires in-depth training of the user in the mining of relevant information from the data.

Errors in any step of the analytical process influences the final results. Figure 22.1 shows the main steps that can be accelerated, improved, or made possible by MW assistance.

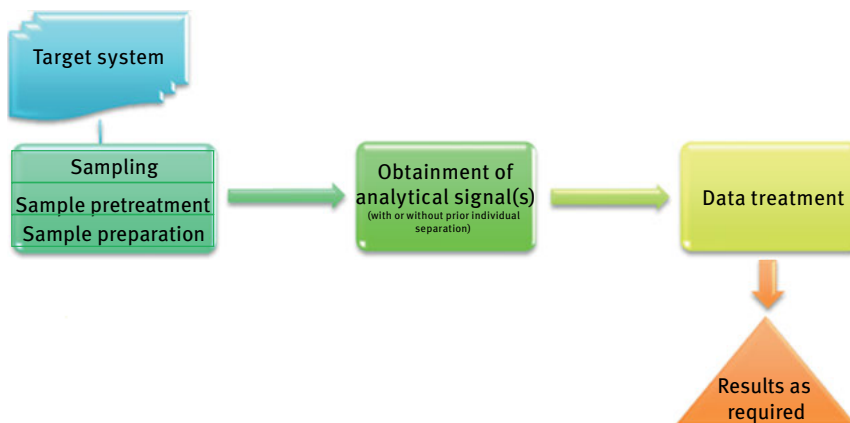


Fig. 22.1: The analytical process.

### 22.1.2 Omics definitions

Although omics disciplines emerged at the end of the twentieth century, their explosive growth so far in the twenty-first century has led some to refer to the present time as the omics era. The diversity of each of the omics fields has required subdivision into subdisciplines to simplify the content of each; nevertheless, only the four great omics (those directly connected to genes and their expression constituting the so-called omics cascade) are defined here in the chronological order in which they appeared in the scientific world. Figure 22.2 presents a scheme of them, the subject matter of each omics discipline, and the relationships among them. Note that there is not only a downstream relationship between adjacent or separated omics, as considered by classical or reductionist dogma of molecular biology [1], but also down- and up-stream relations with feedback loops that make it possible for one discipline to acquire key information from the others almost independently of their position.

*Genomics* is the discipline that addresses the study of all genes and their relationships to identify their combined influence on the growth and development of an organism. It applies recombinant DNA, DNA sequencing, and bioinformatics to sequence, assemble, and analyze the function and structure of genomes (the complete set of DNA within a single cell of an organism) [2]. The complexity of this omics is shown by the subdiscipline (or parallel discipline, depending on the authors) known as *epigenetics* [3].

*Transcriptomics* is a discipline concerned with the study of the transcriptome – the complete set of RNA transcripts that are produced from a particular genome, under specific circumstances or in a specific cell using high-throughput methods such as microarray analysis. A comparison of transcriptomes allows for the identification of genes that are differentially expressed in distinct cell populations in response to different cell treatments. DNA microarrays or chips<sup>1</sup> are the most useful tools for studying transcriptomes [4].

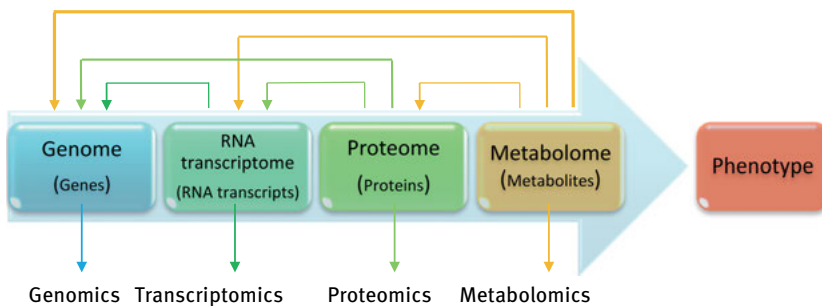


Fig. 22.2: General scheme of omics disciplines.

<sup>1</sup> <http://medical-dictionary.thefreedictionary.com/DNA>

*Proteomics* is the discipline involving the large-scale study of proteins, particularly their structures and functions. Therefore, its object of research is the proteome, the entire set of proteins produced or modified by an organism or system, which varies with time and distinct requirements, or stresses, that a cell or organism undergoes [5].

*Metabolomics*, the youngest of the great omics, is the discipline that studies the metabolome, which is composed by primary and secondary metabolites: in general, the low-molecular-weight compounds (sugars, amino acids, organic acids, fatty acids, among others) in the cells of an organism at a specified time under specific environmental–biological conditions [6].

The close relationship among the great omics shown in Figure 22.2 gave place to systems biology or the joint use of data from two or more of these omics for a wider and accurate information on a given system [7].

### 22.1.3 Common aspects of MW-assisted steps in omics

Two aspects characterize the application of MW in steps belonging to omics disciplines:

- The device used to apply this type of energy, which in turn involves decisions on two aspects: MW mode and continuous or batch performance of the target step subjected to MW.
- The medium or solvent with which the sample (or, following separation, the part of it to be subjected to analysis) is in contact when MW is applied. Note that the crucial influence of the medium on the MW effect experienced by the target components of the sample is discussed in Chapters 2 and 3.

#### 22.1.3.1 MW modes and equipment for assisting omics

The two general formats of MW performance (multimode and monomode) have been described in the literature for carrying out analytical MW-assisted steps in the great omics and their subdisciplines – particularly in sample preparation. Both MW modes have been used in commercial devices and laboratory designs. Household MW ovens have been, and are at present, very frequently used for accelerating characteristic omics steps, despite their multimode performance without efficient control of temperature dispersion. This performance may be very susceptible to hot spots and uneven temperature distribution, which can be a source of irreproducibility in the final analysis [8]. In the omics area, it is imperative for samples to be treated in a homogeneous manner and that temperatures be accurately controlled, especially when dealing with potentially heat-labile compounds. To minimize the effects of uneven temperature distribution, adding beakers of cold water to household MW ovens to absorb excess thermal energy or placing samples in pretested fixed locations within the MW cavity, after mapping, to improve reproducibility has been reported. Dedicated equipment is,

therefore, the preferred option. Many systems are currently available with specific biological and biochemical applications from different companies that market systems for performing high-throughput digestions, including temperature stabilization and control.

### 22.1.3.2 Continuous/batch performance and high-throughput formats

Though most MW devices work in a batch, discontinuous way, some continuous systems have also been designed to work in omics. Thus, Comer and Organ described in 2005 a system composed of a continuous-flow, MW-assisted, parallel capillary that showed the potential for flow-based systems that could be used for omics experiments [9].

In 2008 Hauser and Basile described an online MW system designed specifically for the cleavage of aspartic acid from proteins, with the option of also performing online reduction by the introduction of dithiothreitol [10]. Resultant proteolysis products from cleavage could either be directly spotted onto a matrix-assisted laser desorption-ionization (MALDI) plate for MALDI–quadrupole time-of-flight (QTOF) analysis or coupled to a reverse phase liquid chromatography (LC) column for further separation and analysis by electrospray ionization-tandem mass spectrometry (ESI-MS/MS).

High-throughput batch formats for working simultaneously with a number of samples is the most desirable *modus operandi* in omics research. Many commercial MW systems designed for laboratory applications can be purchased with an autosampler, which allows samples to be sequentially exposed to MW-induced reactions. However, in omics, it is sometimes advantageous to prepare samples in a 96-well microtiter plate format, particularly for immunohistochemical techniques or proteolysis experiments that are typically performed in batch. Zhu-Shimoni et al. used this system for the development and comparison of two enzyme-linked immunosorbent assay (ELISA) formats for the analysis of protein A leached from an immunoaffinity resin [11].

### 22.1.3.3 Solvents used in MW-assisted steps in different omics

As discussed in Chapter 2, MW heating can cause a sudden increase in the internal temperature of a solution, which may result in an explosion; therefore, solvent properties must be very well verified beforehand.

In dealing with the acceleration of proteolytic digestion, it has become increasingly popular to include a small amount of organic solvent in digestion buffers to partially denature the substrate protein and, thereby, allow easier accessibility to the proteolytic enzyme. In addition, the presence and nature of surfactants in the working medium can affect positively or negatively the MW-assisted sample preparation step [12]. On the other hand, enzymes that can perform catalysis in nonaqueous media are often highly compatible with MW assistance, in which they tend to be extremely thermally stable without noticeable inactivation [13].



Selection of an appropriate solvent is more difficult in metabolomics because of the wide range of metabolite polarities. In dealing with extraction, no single, ideal solvent exists.

In planning the overall analytical process, it is interesting to contemplate the possibility of direct introduction of the digested extract, eluate, and so forth (i.e., the analytical sample) into the analytical equipment. This involves selecting a solvent that meets the specific requirements of the analytical tool being used.

## 22.2 MW assistance in genomics and transcriptomics

MW is an omnipresent energy in the improvement of genomics analysis as all the steps of the overall analytical process can be successfully assisted by MW: those involved in sample preparation and in detection, in most cases with dramatic shortening of the time or dramatic improvement of sensitivity. The importance of the polymerase chain reaction (PCR) allows for the division of MW-assisted sample preparation steps into those preceding PCR and PCR itself. In dealing with detection, MW energy has been used to improve mainly the fluorescent emission of reagents for labelling to the target analytes.

Less frequent, but also of interest, is the use of MWs to preserve DNA integrity during storage by dehydration and supra-zero temperature, thereby avoiding the shortcomings associated with either cryopreservation or freeze drying [14].

### 22.2.1 MW assistance in sample preparation in genomics and transcriptomics

#### 22.2.1.1 MW-assisted steps previous to PCR

There are two main steps prior to PCR that can be assisted by MW: cell fixation and cell lysis.

*Cell fixation* is performed with two main aims: to reduce alterations to DNA (and proteins) by preserving samples and facilitate storage and transport. Archived formalin-fixed, paraffin-embedded tissue (FF-PET), the typical source of DNA available for procurement, involves three phases: (1) tissue deparaffinization, (2) tissue digestion, and (3) DNA purification. Bödör et al. demonstrated that RNA isolated with the help of MW energy is suitable for quantitative expression analysis [15]. In addition, histoprocessing MW-based sample preparation reduces processing time compared to conventional methods and results in an approximately tenfold decrease in the cost of chemicals and perfect preservation of tissue and cellular structures.

It is worth noting that most MW devices that have been used so far for cell fixation have been household ovens. A recent contribution from Engelberg et al. using an MW processor programmable to deliver continuous power at any output from 100 to 750 W has shown that 1 h of optimized MW-assisted formalin fixation is better than conven-

tional fixation for 24 h, while preserving tissue structure by assessing and validating antigenicity [16].

*Cell lysis* is a common step in liberating DNA prior to genomics. Conventional protocols for cell lysis are tedious, time consuming, costly, or limited to a small number of samples per run as they include the growth of mycelium in a liquid culture, followed by freeze drying or maceration in liquid N<sub>2</sub> and grinding of the frozen material to break the cell walls [17]. Methods based on the use of a household MW oven have been reported to help in the alteration of cell walls and membranes for subsequent action of lysis buffers to break open cell and organelle membranes. The methods, which can be applied on mycelium or on spores, are cheap because expensive reagents or equipment are not required [18, 19]. The DNA extracts are pure enough to amplify fragments of about 0.5–1.0 Kb. It was shown that MW irradiation of samples can denature tissue DNA in *in situ* hybridization [20] and in the pretreatment step for DNA extraction from fungi, plants, and animals [19, 21]. In addition, MW irradiation destroyed cell structures and exposed DNA [19].

A number of sample preparation methods reported so far support the usefulness of MW assistance to accelerate or improve this step in genomics and transcriptomics studies. Thus, enzymatic reactions of nucleic acids such as site-specific cleavage, ligation, dephosphorylation, and phosphorylation, generally requiring long incubation times, are carried out in dramatically shorter times (within 20–50 s) when assisted by MW [22]. Nevertheless, MW assistance is not always the best option. Thus, different DNA fragmentation approaches (assisted by MW, heating at high temperature, or assisted by ultrasound) were compared by measuring the subsequent PCR efficiency. Taken as 100% efficiency obtained after ultrasound application, the efficiencies of the first two were 2.86 and 3.78%, respectively [23]. The wine industry has recently taken advantage of MW-assisted lysis of yeast lees to create new wine styles [24].

### **22.2.1.2 MW assistance with key tools in genomics and transcriptomics: PCR and rolling circle amplification (RCA)**

Two key tools in molecular biology have revolutionized the field of diagnostics, forensics and biomedical discovery by amplifying the nucleotide material by several orders of magnitude: the PCR and a variation of this technique, RCA.

*PCR* usually involves the use of a heat-stable DNA polymerase to assemble new strands of DNA from free nucleotides, which are aligned along a single-stranded DNA template (primer). Thermocyclers are the devices typically used to provide the high temperatures needed to separate DNA double-helix strands. Heating and cooling steps are alternated to allow DNA synthesis. The slow dissipation of heat transfer of a thermocycler typically limits reaction volumes to 0.2 mL or so to allow adequate heat penetration in a reasonable time period.

A focused MW device was used in 2003 as a source of heat for the first MW-assisted PCR [25]. Improvements by the same group led to an efficient milliliter-scale PCR uti-

lizing highly controlled MW thermocycling [26], thus demonstrating that high-density MW *in situ* heating was in many ways superior to traditional heating-block heating. By refining the method, the authors achieved, after 33 s, a concentration of PCR product between 10 and 30 nmol/L and an amplification efficiency of 92–96% in 1 h and 34 min [13]. These experiments showed that both Taq polymerase and the nucleotide sequences employed were not destroyed by prolonged MW irradiation and that PCRs can benefit from MW assistance.

More recent contributions for the temperature control of MW irradiation have been reported at the milliliter-scale PCR [27]. Even an MW device working at several frequencies and with accurate temperature control has been reported [28].

RCA is the process of nucleic acid replication that can rapidly synthesize multiple copies of circular molecules of DNA or RNA, such as plasmids, the genomes of bacteriophages, and the circular RNA genome of viroids [27]. It is an isothermal nucleic acid amplification technique that uses two primers, a circularized template and a DNA polymerase with strand displacement activity. In addition to synthesizing many copies of repeated sequences from circular DNA and RNA templates, it detects single-nucleotide polymorphisms using a circularized DNA probe [29].

In 2006, Yoshimura et al. published an article on MW-assisted RCA in which the reaction was developed in a volume of 25 mL with 1 mL of primer template mixture and continuous MW irradiation between 120 and 160 W keeping the reaction mixtures at 65 °C. The results suggested that an MW irradiation RCA was more effective than an analogous traditional heating-block reaction [30]. The improvements in MW devices optimized for enzymatic-scale reactions have recently led to mining in the differential heating mechanisms of MW, which strongly depend on the reaction components, although the overall reaction temperatures are the same. The optimized protocol showed that MW-assisted RCA was accelerated over fourfold compared with conventional RCA [31].

Since the first introduction of massively parallel DNA sequencing in 2003, so-called next-generation sequencing (NGS) has become a robust tool, dominating genomic discovery research [32]. DNA fragmentation with NGS goals has recently been assisted by MW as a simple, unbiased, and easy-to-multiplex way to fragment genomic DNA randomly. The procedure was compared with heating DNA at high temperatures for the same purpose and using adaptive ultrasound application as the control. Both treatments caused severe reduction in PCR amplification efficiency, which led to low production in emulsion PCR (emPCR). The result was improved by amplification prior to emPCR. Further improvements, such as DNA strand repair, are needed for the method to be applied practically in NGS [23].

## 22.2.2 MW-assisted detection in genomics and transcriptomics

In addition, MW assistance can dramatically increase the rapidity and sensitivity of fluorescence detection in genomics and transcriptomics in two main ways: by facilitating hybridization (MW-assisted fluorescence in situ hybridization – MW-FISH) or by accelerating the fluorescence emission by a metal support (MW-accelerated metal-enhanced fluorescence – MAMEF).

### 22.2.2.1 MW-FISH

MW assistance was introduced into the FISH procedure a decade ago to facilitate detection in poorly preserved FF-PET. After increased efficiency and validity of signal detection with MW irradiation were demonstrated in lymphocyte cytosmear preparations and cancer cell stamp preparations [33, 34], the appearance of variations in MW-FISH protocols needed standardization for adaptation to the requirements of each laboratory [35]. The MW-FISH protocol is especially powerful for arrays consisting of specimens that have been fixed in various ways, stored, and sometimes even neglected for a long time. In fact, the signal efficiency is increased from 40% by a conventional protocol to 95% by the MW-FISH protocol, and it can be implemented in several ways: (1) FISH with intermittent MW irradiation [36]; (2) repeated FISH application; and (3) double staining with immunohistochemistry [37].

Taking advantage of MW assistance in both PCR (completed in 26 min) and instant quality (IQ) FISH (hybridization for 1 h) in addition to morphological examination of blood smears, a method was recently developed to diagnose patients having acute promyelocytic leukemia within 4 h based on molecular–cytogenetic results [38]. The rapid diagnosis can allow effective therapies to be applied promptly.

### 22.2.2.2 MAMEF

The change in fluorescence intensity in MAMEF allows one to track the hybridization of a complementary target on a solid surface. In the first published study [39], an approximately 12-fold increase in fluorescence intensity from a DNA hybridization assay on silver island films was obtained as compared to the fluorescence intensity from the same assay but in free solution. After overcoming some problems, the key points that make MAMEF attractive, particularly for the detection of pathogens in blood, include: (1) rapidity and sensitivity; (2) capacity for multiplexation – three DNA or protein targets can presently be identified within 20–40 s in one sample well; (3) variety of standard inexpensive sample well-reader technologies, which facilitates detection; (4) no washing steps required to remove excess fluorescent probe or labeled DNA antibody; (5) disposable chambers to minimize cross contamination; (6) no centrifugation steps; and (7) quantitation by comparing fluorescence with a standard curve. These achievements make possible the development of the assay into a point-of-care device that can be used by minimally trained people.

## 22.3 MW assistance in proteomics

The complexity and number of proteins make proteomics analysis a difficult task that involves a large number of steps. The duration and characteristics of these steps can be improved by MW assistance. Two stages should be distinguished in sample preparation in proteomics: one involving physical and chemical steps aimed at sample clean-up, and a second sample preparation stage consisting of chemical steps that precede either detection or introduction into high-resolution equipment.

The first step of either the top-down or bottom-up procedure is aimed at freeing all protein components present (essentially lipids, fatty nucleic components of organic and inorganic nature of low molecular mass and cofactors such as vitamins, salts, and inorganic ions). Therefore, this step involves substeps such as the extraction or solubilization of proteins, removal of lipids by extraction with organic solvents, and removal of nucleic acids by nuclease digestion, coprecipitation with basic compounds, or ultracentrifugation. The use of a minimum number of substeps and not altering the protein profile or loss of any protein are the aims pursued in this first SP step that has not been assisted by MW or any type of auxiliary energy, although extraction, precipitation, or digestion are assisted by ultrasound in other omics [40].

The key steps of proteomics analysis that benefit from MW assistance are protein separation and subsequent operations. Protein separation is achieved by electrophoretic mobility on a gel, after which the electrophoretic development is fixed with a reagent to immobilize the gel and to stop migration or dispersion; then enzymatic hydrolysis and detection are steps that can be favored by MW energy.

### 22.3.1 MW assistance in sample preparation in proteomics

The steps and substeps involved in proteomics sample preparation benefit greatly from MW irradiation. The most significant among these are as follows:

#### 22.3.1.1 MW-assisted staining–destaining

Although MW irradiation had been successfully employed to speed up the analytical substeps of sample preparation, such as fixation, staining, and destaining since the early 1990s, the first citation was provided by Nestayy et al., who studied the effect of MW energy on the staining of proteins in gels or membranes by common stains and using a household MW oven, with a drastic reduction in the time required for staining and destaining gels [41]. Increased proteolytic cleavage was observed after MW-assisted staining compared to conventional methods (i.e., room-temperature incubation), which was attributed to increased denaturation of proteins embedded in the matrices after MW exposure – note that the digestion itself was not performed in the presence of MW radiation, only the staining and destaining of the gel or mem-

brane. This denaturation resulted in greater accessibility of the substrate proteolytic sites to the enzyme.

Overall, it was concluded that MW irradiation of proteins separated in gel or membranes often significantly improved proteolytic coverage compared to traditional gel-staining techniques. In addition, they did not appear to cause any detrimental effects such as loss of posttranslational modifications or increased deamidation or oxidation. The total time for a dye-based blue-black ink staining method to quantitatively visualize proteins spotted onto a nitrocellulose membrane was reduced from more than 30 min to less than 3 min by employing MW assistance; this also provided a 500-fold dynamic range for quantification from low nanogram to mid-microgram total protein amounts [42].

### 22.3.1.2 MW-assisted protein hydrolysis

Despite major advances in so-called top-down MS methods for characterizing proteins, the traditional bottom-up approach involving the digestion of a protein into smaller peptides and subsequent peptide mass fingerprinting or reversed-phase separation and QTOF identification remains the most widely used analytical methodology for protein characterization. The traditional rate-limiting hydrolysis step in protein sample preparation has been overcome by MW assistance in the in-solution approach, mainly by enzyme-catalyzed reactions, but also by chemical reactions.

*MW-assisted enzymatic hydrolysis* has been catalyzed mainly by trypsin that cleaves to the carboxyl termini of arginine (Arg) and lysine (Lys) – except when sterically hindered by a neighboring proline residue. The lengthy digestion periods (8 h to overnight) required to ensure complete hydrolysis promoted the acceleration of proteolytic cleavage of proteins under controlled MW conditions (i.e., at preset temperature, pressure, and power) in a monomode MW system, with complete digestion of several nonreduced, tightly folded proteins within 12 min, by contrast with no proteolysis when using a water bath for the same time [43]. The authors also showed successful application to in-gel tryptic digestion since MW irradiation facilitates digestion of proteins embedded in a semi-immobile matrix. MW accelerated proteolysis within the first few minutes, but the effect dropped after 30 min, suggesting that the enzyme was rapidly denatured and inactivated upon MW exposure [43].

MW-assisted tryptic digestion on immobilized surfaces such as magnetite beads provided the optimum material among 150 substances examined for MW absorption [44]. Chen and Chen expanded on this concept by using magnetite beads to accelerate other MW-assisted enzymatic digestions [45].

Studies aimed at clarifying whether the faster reaction rate is due to the MW quantum effect or the thermal effect were conducted using conventional heating and MW-assisted tryptic digestion of several proteins and quantitative analysis by MS. Overall, similar results were provided by both methods when working at the same temperature (50 °C) for the same time, demonstrating that no nonthermal effect exists in MW-

assisted tryptic digestion [46]. Nevertheless, the use of a household MW oven for the experiments – and the difficulty of temperature control in it – makes necessary the assessment of the results using a commercial MW device in which the working conditions can be better established.

Recent advances in MW-assisted tryptic digestion combine this step with in situ filter-aided SP (termed imFASP) for the preparation of microgram and even nanogram amounts of complex proteins with high efficiency in 1 h. Compared with the traditional in-solution sample preparation method, the imFASP method generates more protein and peptide, and identifications were improved by at least 30 and 44%, respectively [47].

Other enzymes that produce peptide fragments larger than trypsin does are Lys C, Glu-C, and endoproteinase Asp-N, among others [48], thus giving place to middle-down proteomics, with fragments of 15–50 amino acids. The MW assistance in this case is controversial as the mild catalytic effect of the Glu-C enzyme is attributed to denaturation owing to high temperature rather than autolysis [49] and to increased dipole movements of the  $\alpha$  helices of proteins that may boost catalysis in the presence of MW radiation [50].

*Chemical proteolysis by acids or other reagents* has also been assisted by MW to increase yields and decrease reaction times, mainly using trifluoroacetic acid (TFA). The main advantages of controlled MW-assisted acid hydrolysis (MAAH) of proteins versus its catalyzed counterparts are as follows: (1) proteins can be dissolved in any solvent, including acids; (2) special buffers are unnecessary [51]; (3) cleavages result in longer peptides than the average tryptic peptide [52].

The controversy over the results obtained for MAAH by household MW devices as compared with commercial devices designed with analytical purposes in mind has recently been clarified using both types of devices to degrade a standard protein into many peptides with overlapping sequences identified by LC–ESI MS/MS. No differences were found in the hydrolysis carried out by the two MW devices [53]. However, to meet the regulatory or good laboratory practice (GLP) requirements in clinical or pharmaceutical laboratories, the use of a commercial MW device is often required.

*MW-assisted hydrolysis in the absence of either enzymes or acids* provides interesting results, with hydrolysis times as shorter as 4 min when working at high temperatures and pressures, and avoiding the risk of explosion using custom-made vials made of Teflon or Pyrex [54]. Similar amino acid recoveries were obtained for proteins hydrolyzed under MW irradiation at 175 °C for 10 min or with two common protocols (viz., non-MW-mediated incubation at 110 °C for 24 h or 150 °C for 1 h [55]). This MW-assisted approach has been validated with the quantitation of thousands of recombinant proteins and proved an invaluable tool for the rapid quantitation of proteins in the biotechnology industry.

### 22.3.1.3 Other MW-assisted sample preparation steps in proteomics analysis

Other steps in proteomics analysis successfully assisted by MW are the N- and C-terminal sequencing [56], and the identification and characterization of posttranslational modifications [57].

## 22.3.2 MW assistance in identification/quantitation in proteomics

Among the most used techniques for the identification or quantitation in proteomics successfully assisted by MW are isotope-coded affinity tags (ICATt) [58], isobaric tags for relative and absolute quantitation (iTRAQt), and those based on fluorescence or chemiluminescence emission.

The experiments by Rutherford et al. showed that the time required for biotin cleavage in ICATt was reduced from more than 10 h to 30 min; and the time for reaction between peptides and the iTRAQt reagents decreased from 2 h to 10 min in the presence of MW without degradation caused by high temperatures, possibly because of the short incubation time [59].

Fluorescence and chemiluminescence for protein quantitation have also benefited from the accelerating effect of MW. Derivatization to yield emissive products in this case uses the immunoassay antigen–antibody binding format for analyte recognition and, most often, fluorescence-based readouts [60]. The two rate-limiting factors of a typical immunoassay (the slow antigen–antibody binding kinetics and the quantum yield of the tagged fluorophore) to generate a fluorescence signal readout can be accelerated by low-power MW radiation, as demonstrated by Geddes et al. [61, 62]. The authors showed silver nanostructures dramatically increasing the quantum yield of proximity fluorophores and also that using low-power MW facilitated rapid, uniform heating without disturbing either the silver nanostructures or the proteins being assayed, but boosting mass transport of proteins to the silvered surface [60].

Another achievement of Geddes et al. was *MW-triggered metal-enhanced chemiluminescence* (MT-MEC), also based on low-power MW, in this case in combination with enzymes and chemiluminescent species to afford significantly faster total quantitative protein detection than conventional methods. The authors combined the principles of MW circuitry and antenna design with their work by using MT-MEC to demonstrate the potential of triggering chemically and enzyme-catalyzed chemiluminescence reactions and the utility of MW-triggered chemiluminescence assays to dramatically improve signal-to-noise ratios in surface assays [62].

## 22.4 MW assistance in metabolomics

Contrary to the other omics, metabolomics has benefited from MW assistance only in sample preparation, but with the greatest number of uses for this step. They include



drying, digestion, solid–liquid extraction, liquid–liquid extraction, steam distillation (for volatile metabolites), and derivatization.

#### **22.4.1 MW-assisted drying in metabolomics**

Freeze drying allows for the removal of water from biological tissues in plant and food samples by freezing cellular components immediately and sublimating ice under conditions of high vacuum and low temperatures. Although freeze drying restricts biological activity, some cellular metabolites are altered owing to the increase in cell volume during freezing, the effect being different depending on the plant–metabolite binomial [63]. There is no increase in the cell volume with MW treatments, and they destroy enzyme activities; therefore metabolomic changes due to enzymes such as peroxidases and glycosidases are avoided [64]. MW-assisted drying warrants in-depth study with a view to expanding its use for sample preparation in plant metabolomic analyses.

#### **22.4.2 MW-assisted solid–liquid extraction in metabolomics**

MW-assisted metabolomics in solid–liquid extraction or leaching has been widely implemented, more frequently with plants than with animal samples as the latter (especially those for clinical metabolomics) are usually liquid, for example, blood, urine, saliva, or tears, or, less commonly, gaseous (e.g., exhaled air). Metabolites in leaves, branches, roots, and fruits are usually dissolved by solid–liquid extraction of the sample. The greatest shortcoming of leaching metabolites from plants is the presence of a wide variety of compounds at very different levels and spanning a broad range of polarity. As no single extractant can remove the whole range of metabolites potentially present in a solid sample, the choice of extractant strongly limits the study of the metabolome, which usually requires different extractants of different polarity – in turn, this behavior involves a degree of selectivity. In fact, the dissolution rate is governed by physical and chemical forces and by the rate of diffusion from the sample particles into the extractant, with the latter being a phenomenon favored by using external energy (conventional heating or MW) to raise the temperature as well as ultrasonication to increase mass transfer favored by the cavitation phenomenon [40], which in some cases affects the stability of the metabolites. MW-assisted extraction (MAE) has proved an advantageous choice in this context, particularly when extraction of a given family of metabolites is the aim.

Because of the large variety of metabolite families in both the vegetable and animal kingdoms, one of the most typical families – phenols – is used to illustrate both the effect of MW on the extraction process and the importance of the extractant. Phenols constitute a large group of widely studied secondary plant metabolites with

multiple biological effects [65]. The two major classes of phenols (phenolic acids and flavonoids) are conventionally extracted at a refluxing temperature of 90 °C for at least 2 h and use relatively high amounts of extractants. The research on MAE – which in all cases increases yields, shortens times, and reduces the required volume of extractant – has evolved over time with the MW equipment used, the method of monitoring the process, and the final information provided.

Research by Proestos and Komaitis [66] involved the use of a household MW oven to accelerate the extraction of phenols from aromatic plants and monitoring the process by the Folin–Ciocalteu (F–C) assay, which was compared with the conventional reflux method (90 °C for 2 h). The authors assayed four extractants of different polarity (acetone, methanol, water, and ethyl acetate–water) to check their influence on the different polarity of the target phenols. The overall phenol content provided by the F–C method showed that MAE assistance decreased yield significantly ( $p < 0.05$ ) in the following solvent sequence: acetone > methanol > water > ethyl acetate–water; by the conventional method phenolic levels decreased significantly ( $p < 0.05$ ) by a decrease in the polarity of the solvent: water > methanol > acetone > ethyl acetate–water. LC–molecular absorption detection of the extracts revealed that MAE provided significantly higher concentrations of phenols ( $p < 0.05$ ) than did conventional extraction, with a similar composition of both extracts and a significant reduction of the time for MAE (from 2 h to 4 min).

The study of whole metabolic patterns in both wild and genetically modified organisms is a matter of growing interest in understanding the biological function of a genome. The mechanisms through which plants regulate the metabolism of a key, low-concentration anion such as phosphate were investigated using boiling water to extract phosphorus compounds from crushed *Arabidopsis* samples, then irradiated with MW (600 W for 15 s), and finally analyzed by ion chromatography–MS/MS. The potential dirt extract did not interfere with high-resolution detectors [67].

The greatest concern with green chemistry recently led to the use of green solvents for MAE in closed vessel systems under controlled temperature and pressure conditions. Selective extractants and strict control of the extraction temperature and time are required for subsequent target analyses for the different compound classes or families when sensitive determination is needed; alternatively, a compromise in the working conditions can be made to accomplish partial extraction of the different metabolite classes or families for coverage metabolomics analysis [68].

Simultaneous emulsification–extraction of polar and nonpolar compounds from solid plant material with two immiscible extractants can be achieved by taking advantage of the emulsion formed with an immiscible system of two extractants under MW irradiation [69]. Boiling of the extractant with the lower boiling point promoted the formation of an emulsion that facilitated mass transfer of the analytes from the solid matrix to the extractants to an extent dependent on their nature combined with the high contact surface for exchange and the temperature created in the whole system. The leaching of polar and nonpolar compounds (phenols and lipids) from alpe-

rujo with ethanol–water and hexane as extractants required 14 min for quantitative extraction, which was implemented in a commercial digester, followed by analysis of the polar and nonpolar fractions by LC–MS/MS and gas chromatography (GC)–ion-trap MS, respectively.

### 22.4.3 MW-assisted digestion in metabolomics

Digestion is not a common step in metabolomic analysis since the drastic conditions usually alter metabolic profiles, but this treatment is used for elemental determination.

The ionome, defined as the elemental composition of an organism, includes both essential and nonessential elements and represents the inorganic fraction of cellular and organic systems; therefore, the ionome can be regarded as the inorganic subset of the metabolome [70]. The omics discipline to study the ionome is ionomics, which involves the quantitative simultaneous determination of the elemental composition of living organisms and the changes in such composition in response to physiological stimuli, developmental state, and genetic modifications [71].

The best tool for ionomics analysis is the inductively coupled plasma (ICP)-MS approach, following sample digestion in open or closed systems and with or without MW assistance. Hermetically closed vessels of the appropriate material were used to introduce the samples into either a household MW oven or a commercial MW digester prior to multielemental analysis of melon or fish tissue, respectively [72], in both cases with drastic shortening of the preparation step as compared with conventional digestion without auxiliary energy.

An example of a more complex MW-assisted digestion is that consisting of four programmed steps by temperature rising from 8 to 200 °C in 20 min (followed by size-exclusion chromatography coupled online with ultraviolet detection and off-line with graphite furnace atomic absorption spectrometry detection and MALDI–QTOF) allowed for the estimation of molecular weight distribution in water-soluble Cu, Fe, Mn, and Zn species in Brazil nuts, cupuaçu seeds, and coconut pulp [73].

A recent comprehensive metabolomics study of selenium in fish muscle was carried out in which ultrasound-assisted extraction was used to obtain an analytical sample to be used for identification of selenosugar and Se-methylselenoneine by LC–ESI–Orbitrap MS, while total selenium levels in the sample were determined after MW-assisted digestion by LC–ICP–MS and quantitation by external calibration with standard solutions of selenosugar. The study opens up a new perspective on the role of these compounds both as excretory products of Se metabolism in humans and other mammals and in Se supplementation studies [74].

#### 22.4.4 MW-assisted liquid–liquid extraction in metabolomics

Liquid–liquid extraction (LLE) has not been extensively used with MW assistance, either in general or in metabolomics in particular. The sample type most often subjected to MW-assisted LLE has been urine, prior to the determination of the metabolic profile of infant urine by comprehensive two-dimensional GC for subsequent application to the diagnosis of organic acidurias and for biomarker discovery [75]. Only 90 s in an MW commercial device working at 450 W was enough, following dilution of the sample, addition of internal standard, saturation with solid sodium chloride 6 mol/L hydrochloric acid, and ethyl acetate. Although the overall method is described by the authors as LLE assisted by MW, the LLE step was in fact performed in the absence of MW radiation.

#### 22.4.5 MW-assisted steam distillation in metabolomics

One infrequent, but interesting, MW-assisted sample preparation step is steam distillation, also known as *solvent-free microwave extraction*. This treatment is specially indicated for the removal of essential oils from aromatic plants; therefore, it is discussed at length in Chapter 4. The use of MW radiation has led to a dramatic shortening of extraction times relative to conventional steam distillation.

#### 22.4.6 MW-assisted derivatization in metabolomics

Derivatization is a common step in analytical chemistry in general and metabolomics in particular and is implemented for very different purposes, the most common use being to increase the volatility or thermal stability of metabolites for gas chromatographic separation, as well as to facilitate the detection of metabolites and improve chromatographic separation when compared. As compared with conventional derivatization methods – where heat is transferred from the vessel wall to the solution – in MW-assisted derivatization the energy is directly distributed evenly and directly to the solution, a more effective way of heating that dramatically shortens the required time and makes metabolomics and MW-assisted derivatization an excellent association. The approach is used in both targeted and untargeted metabolomics analysis.

A very common application of MW-assisted derivatization in targeted metabolomics is the silylation of organic acids, alcohols, carbohydrates, steroids, and amino acids [76]. This affords the fast determination of amino acids in blood and urine – a frequent need in metabolomics since their abnormal accumulation in the body is a symptom of a deficiency of enzymes associated with an amino acid metabolic pathway. Other derivatization reactions benefiting from MW assistance prior to GC separation and MS determination are acylation and alkylation [76].

An example of MW-assisted derivatization as a nonprivative step prior to GC is a method based on liquid–liquid microextraction for concentration/clean-up prior to MW-assisted derivatization of lipoic acid in urine to improve both molecular absorption and MALDI-QTOF detection after capillary LC. Three major metabolites of lipoic acid were also identified in the study and then structurally confirmed by Orbitrap [77].

A study compared the effect of MW irradiation, ultrasonication, ultracentrifugation, and conventional heating on the derivatization to dinitrophenyl derivatives of nine amino alcohols for their subsequent enantioseparation on  $\alpha$ 1-acid glycoprotein and  $\beta$ -cyclodextrin columns. MW-assisted derivatization proved the best choice, with shorter derivatization times and higher efficiency than the others [78].

Miniaturization is a highly desirable goal and a growing trend in MW-assisted sample preparation in metabolomics. MW-assisted derivatization protocols have been reported for use prior to GC–MS that use a silicon-carbide-based microtiter plate platform fitted with screw-capped GC vials. The researchers selected three standard derivatization protocols (acetylation for morphine, pentafluoropropionylation for 6-monoacetylphorphine, and trimethylsilylation for  $\Delta$ 9-tetrahydrocannabinol) and achieved complete derivatization within 5 min at 100 °C in a dedicated multimode MW device equipped with online temperature monitoring. The platform allowed the simultaneous derivatization of 80 reaction mixtures under strictly controlled temperature conditions [79].

One typical derivatization reaction for improving detection is the formation of fluorescent compounds from nonfluorescent or poorly fluorescent analytes. Metabolites such as histidine, and 1- and 3-methylhistidine in human serum, were individually separated by capillary electrophoresis after MW-assisted derivatization using fluorescein isothiocyanate and a household MW oven for 150 s. The use of an MW system not specifically designed for research purposes introduced irreproducibility problems that were easily resolved using a commercial dedicated device [80].

## 22.5 Trends in MW assistance in omics

Despite its fast growth, the analytical assistance by MW in omics is still in its infancy. Questions such as the exact mechanisms of action of MW compared to conventional heating and the actual uses and potential of this field remain unanswered. So far, the kinetics and specificity of MW-assisted incubations and reactions in genomics, transcriptomics, and proteomics have only been examined in a very small number of areas and on a limited number of systems. By contrast, MW-assisted steps involving metabolites have been developed almost since the inception of MW devices in the analytical laboratory.

Past research and present needs suggest some foreseeable trends in the use of MW to assist omics, namely:

- (a) Magnetite beads for accelerated MW-assisted enzymatic digestion and other SP steps;
- (b) Quantum dots, extensively used as fluorescence reporters in biomedical research, and at present inserted in the omics arena [81], will foreseeably require technical modifications based on MW assistance;
- (c) Nanostructured materials, widely introduced in the clinical field [82, 83], and in the omics area as a result, will take advantage of MWs to improve the target processes, particularly in integrative omics studies [84];
- (d) Microfluidic technologies, of growing presence in omics [85] and in nanomedicine in general [86] and nanoscale platforms [87], can be expected to benefit from MW assistance, thereby improving and accelerating their performance;
- (e) Bioinformatic methods [88], including nanoparticle ontology [89] and nanoinformatics [90], can be expected to facilitate the interpretation of interactions of micro- and nano-omics systems with MW.

The question of what type of MW device to use for MW-assisted omic reactions at the micro- and nanoscale can be answered by new commercially available miniaturized MW devices.

## Bibliography

- [1] Van Regenmorte MHV. Reductionism and complexity in molecular biology. *EMBO Rep* 2004, 5, 1016–1020.
- [2] A brief guide to genomics. National Human Genome Research Institute, 2016. (Accessed August 18, 2016, at <https://www.genome.gov/18016863/a-brief-guide-to-genomics/>)
- [3] He C, Cole P. Introduction: epigenetics. *Chem Rev* 2015, 115, 2223–2224.
- [4] Burgess DJ. Putting transcriptomics in its place. *Nat Rev Genet* 2015, 16, 319.
- [5] Chandrasekhar K, Dileep A, Lebonah DE, Kumari JP. A short review on proteomics and its applications. *ILNS* 2014, 17, 77–84.
- [6] Lämmerhofer M, Weckwerth W. *Metabolomics in practice: successful strategies to generate and analyze metabolic data*. Wiley-VHC, Weinheim, Germany, Wiley-VHC, 2013.
- [7] Chuang HY, Hofree M, Ideker T. A decade of systems biology. *Annu Rev Cell Dev Biol* 2010, 26, 721–744.
- [8] Dalpé Y, Séguin SM. Microwave-assisted technology for the clearing and staining of arbuscular mycorrhizal fungi in roots. *Mycorrhiza* 2013, 23, 333–340.
- [9] Jadaon MM, Dashti AA, Lewis HL, Habeeb FM. Whole-blood polymerase chain reaction and restriction fragment length polymorphism: a simplified method by microwave irradiation. *Med Princ Pract* 2009, 18, 280–283.
- [10] Comer E, Organ MG. A microreactor for microwave-assisted capillary (continuous flow) organic synthesis. *J Am Chem Soc* 2005, 127, 8160–8167.
- [11] Hauser NJ, Basile F. Online microwave D-cleavage LC–ESI-MS/MS of intact proteins: site-specific cleavages at aspartic acid residues and disulfide bonds. *J Proteome Res* 2008, 7, 1012–1026.

- [12] Lin SS, Wu CH, Sun MC, Sun CM, Ho YP. Microwave-assisted enzyme-catalyzed reactions in various solvent systems. *J Am. Soc Mass Spectrom* 2005, 16, 581–588.
- [13] Sandoval WN, Arellano F, Arnott D, Raab H, Vandlen R, Lill JR. Rapid removal of N-linked oligosaccharides using microwave assisted enzyme catalyzed deglycosylation. *Int J Mass Spectrom* 2007, 259, 117–123.
- [14] Lee PC, Paramore E, Van Vorst M et al. Optimal preservation of DNA integrity in cat germinal vesicles after microwave-assisted dehydration and supra-zero temperature storage. *Cryobiology* 2013, 67, 422.
- [15] Hayat MA. Factors affecting the quality of fixation, in fixation for electron microscopy. Ed. Hayat MA. NY, USA, Academic Press, 1981, 11–63.
- [16] Engelberg JA, Giberson RT, Young LJT, Hubbard NE, Cardiff RD. The use of mouse models of breast cancer and quantitative image analysis to evaluate hormone receptor antigenicity after microwave-assisted formalin fixation. *J Histochem Cytochem* 2014, 62, 319–334.
- [17] Podar M, Abulencia CB, Walcher M et al. Targeted access to the genomes of low-abundance organisms in complex microbial communities. *Appl Environ Microb* 2007, 73, 3205–3214.
- [18] Leach J, Finkelstein DB, Rambosek JA. Rapid miniprep of DNA from filamentous fungi. *Fung Gen Newsl* 1986, 33, 32–33.
- [19] Goodwin DC, Lee SB. Microwave mini-prep of total genomic DNA from fungi, plants, protists and animals for PCR. *Biotechniques* 1993, 15, 438–444.
- [20] Ferreira AVB, Glass NL. PCR from fungal spores after microwave treatment. *Fung Genet Newsl* 1996, 43, 25–26.
- [21] Coates PJ, Hall PA, Butler MG, D'Ardenne MG. Rapid technique of DNA-DNA in situ hybridisation on formalin fixed tissue sections using microwave irradiation. *J Clin Pathol* 1987, 40, 865–869.
- [22] Das RH, Ahirwar R, Kumar S, Nahar P. Microwave-mediated enzymatic modifications of DNA. *Anal Biochem* 2015, 471, 26–28.
- [23] Yang Y, Hang J. Fragmentation of genomic DNA using microwave irradiation. *J Biomol Tech* 2013, 24, 98–103.
- [24] Characterisation of lees and novel uses for yeast lees to create new wine styles. Adelaide. Adelaide Research & Scholarship, 2014 (Accessed August 18, 2016, at <http://hdl.handle.net/2440/84695>).
- [25] Hanson KR. Chlorogenic acid biosynthesis. Chemical synthesis and properties of the mono-O-cinnamoylquinic acids. *Biochem* 1965, 4, 2719–2735.
- [26] Fermer C, Nilsson P, Larhed M. Microwave-assisted high-speed PCR. *Eur J Pharm Sci* 2003, 18, 129–132.
- [27] Orrling K, Nilsson P, Gullberg M, Larhed M. An efficient method to perform milliliter-scale PCR utilizing highly controlled microwave thermocycling. *Chem Commun* 2004, 790–791.
- [28] Shaw KJ, Docker PT, Yelland JV et al. Rapid PCR amplification using a microfluidic device with integrated microwave heating and air impingement cooling. *Lab Chip* 2010, 10, 1725–1728.
- [29] Cheng Y, Li Z, Zhang X, Du B, Fan Y. Homogeneous and label-free fluorescence detection of singlenucleotide polymorphism using target-primed branched rolling circle amplification. *Anal Biochem* 2008, 378, 123–126.
- [30] Demidov VV. Rolling-circle amplification in DNA diagnostics: the power of simplicity. *Expert Rev Mol Diagn* 2002, 2, 542–548.
- [31] Yoshimura T, Suzuki T, Mineki S, Ohuchi S. Controlled microwave heating accelerates rolling circle amplification. *PLoS ONE* 2015, 10(9):e0136532. doi:10.1371/journal.pone.0136532
- [32] Loman NJ, Misra RV, Dallman TJ et al. Performance comparison of benchtop high-throughput sequencing platforms. *Nat Biotechnol* 2012, 30, 434–439.
- [33] Van de Rijn M, Fletcher JA. Genetics of soft tissue tumors. *Annu Rev Pathol* 2006, 1, 435–466.

- [34] Kitayama Y, Igarashi H, Sugimura H. Amplification of FISH signals using intermittent microwave irradiation for analysis of chromosomal instability in gastric cancer, *Mol Pathol* 1999, 52, 357–359.
- [35] Kitayama Y, Igarashi H, Sugimura H. Different vulnerability among chromosomes to numerical instability in gastric carcinogenesis: stage-dependent analysis by FISH with the use of microwave irradiation. *Clin Cancer Res* 2000, 6, 3139–3146.
- [36] Wilkens L, Gerr H, Gadzicki D, Kreipe H, Schlegelberger B. Standardised fluorescence in situ hybridisation in cytological and histological specimens. *Virchows Arch* 2005, 447, 586–592.
- [37] Ridderstrale KK, Grushko TA, Kim HJ, Olopade IO. Single-day FISH procedure for paraffin-embedded tissue sections using a microwave oven. *Biotechniques* 2005, 39, 316–320.
- [38] Shigeto S, Matsuda K, Yamaguchi A et al. Rapid diagnosis of acute promyelocytic leukemia with the *PML-RARA* fusion gene using a combination of droplet-reverse transcription-polymerase chain reaction and instant-quality fluorescence in situ hybridization. *Clin Chim Acta* 2016, 453, 38–41.
- [39] Igarashi H, Yamashita K, Suzuki M et al. Simultaneous imaging of membrane antigen and the corresponding chromosomal locus in pathology archives. *Pathol Int* 2005, 55, 753–756.
- [40] Luque de Castro MD, Priego-Capote F. Analytical applications of ultrasound. Elsevier Science, Amsterdam, Netherlands, Elsevier Science 2006.
- [41] Aslan K. Rapid whole blood bioassays using microwave-accelerated metal-enhanced fluorescence. *Nano Biomed Eng* 2010, 2, 1–9.
- [42] Nestayy VJ, Dacanay A, Kelly JF, Ross NW. Microwave-assisted protein staining: mass spectrometry compatible methods for rapid protein visualisation. *Rapid Commun Mass Spectrom* 2002, 16, 272–280.
- [43] Pramanik BN, Mirza UA, Ing YH et al. Microwave-enhanced enzyme reaction for protein mapping by mass spectrometry: a new approach to protein digestion in minutes. *Protein Sci* 2002, 11, 2676–2687.
- [44] Walkeiwicz JW, Clark AE, McGill SL. *Miner Metall Proc* 1988, 124, 247–252.
- [45] Chen WY, Chen YC. Acceleration of microwave-assisted enzymatic digestion reactions by magnetite beads. *Anal Chem* 2007, 79, 2394–2401.
- [46] Muralidhar Reddy P, Huang YS, Chen CT, Chang PC, Ho YP. Evaluating the potential nonthermal microwave effects of microwave-assisted proteolytic reactions, *J Proteomics* 2013, 80, 160–170.
- [47] Zhao Q, Fang F, Wu C et al. ImFASP: an integrated approach combining in-situ filter-aided sample pretreatment with microwave-assisted protein digestion for fast and efficient proteome sample preparation. *Anal Chim Acta* 2016, 912, 58–64.
- [48] Login GR, Schnitt SJ, Dvorak AM. Microwave fixation provides rapid, primary fixation for light and electron microscopy and for immunohistochemistry and immunocytochemistry. *Eur J Morphol* 1991, 29, 206–210.
- [49] Vesper HW, Mi L, Enada A, Myers GL. Assessment of microwave-assisted enzymatic digestion by measuring glycosylated hemoglobin A1c by mass spectrometry. *Rapid Commun Mass Spectrom* 2005, 19, 2865–2870.
- [50] Collins JM, Leadbeater NE. Microwave energy: a versatile tool for the biosciences. *Org Biomol Chem* 2007, 5, 1141–1150.
- [51] Zhong H, Marcus SL, Li L. Microwave-assisted acid hydrolysis of proteins combined with liquid chromatography MALDI MS/MS for protein identification. *J Am Soc Mass Spectrom*, 2005, 16, 471–481.
- [52] Swatkoski S, Gutierrez P, Wynne C et al. Evaluation of microwave-accelerated residue-specific acid cleavage for proteomic applications. *J Proteome Res* 2008, 7, 579–586.



- [53] Chen L, Wang N, Li L. Development of microwave-assisted acid hydrolysis of proteins using a commercial microwave reactor and its combination with LC–MS for protein full-sequence analysis. *Talanta* 2014, 129, 290–295.
- [54] Chiou SH, Wan KT. *Current research in protein chemistry: techniques, structure, and function*. Academic Press, San Diego, CA, USA, 1990.
- [55] Sandoval WN, Pham V, Ingle ES, Liu PS, Lill JR. Applications of microwave-assisted proteomics in biotechnology. *Comb Chem High Throughput Screen* 2007, 10, 751–765.
- [56] Zhong H, Zhang Y, Wen Z, Li L. Protein sequencing by mass analysis of polypeptide ladders after controlled protein hydrolysis. *Nat Biotechnol* 2004, 22, 1291–1296.
- [57] Tzeng YK, Chang CC, Huang CN, Wu CC, Han CC, Chang HC. Facile MALDI-MS analysis of neutral glycans in NaOH-doped matrixes: microwave-assisted deglycosylation and one-step purification with diamond nanoparticles. *Anal Chem* 2008, 80, 6809–6814.
- [58] Gygi SP, Rist B, Gerber SA, Turecek F, Gelb MH, Aebersold R. Quantitative analysis of complex protein mixtures using isotope-coded affinity tags. *Nat Biotechnol* 1999, 17, 994–999.
- [59] Rutherford JL, Bonapace J, Nguyen M, Pekar T, Innamorati D, Pirro J. Higher-throughput cleavable ICAT analysis using microwave technology. *Proceedings of the CHI Beyond Genome conference*. San Francisco, CA, 2004.
- [60] Aslan K, Geddes CD. Microwave-accelerated metal-enhanced fluorescence: platform technology for ultrafast and ultrabright assays. *Anal Chem* 2005, 77, 8057–8067.
- [61] Previte MJ, Aslan K, Malyn SN, Geddes CD. Microwave triggered metal enhanced chemiluminescence: quantitative protein determination. *Anal Chem* 2006, 78, 8020–8027.
- [62] Kyong Kim H, Verpoorte R. Sample preparation for plant metabolomics. *Phytochem Anal* 2010, 21, 4–13.
- [63] Oikawa A, Otsuka T, Jikumaru Y et al. Effects of freeze-drying of samples on metabolite levels in metabolome analyses. *J Sep Sci* 2011, 34, 3561–3567.
- [64] Verpoorte R, Choi YH, Mustafa NR, Kim HK. Metabolomics: back to basics. *Phytochem Rev* 2008, 7, 525–537.
- [65] Hurtado E, Gómez M, Carrasco A, Fernández A. Application and potential of capillary electroseparation methods to determine antioxidant phenolic compounds from plant food material. *J Pharm Biomed Anal* 2010, 53, 1130–1160.
- [66] Proestos C, Komaitis M. Application of microwave-assisted extraction to the fast extraction of plant phenolic compounds. *LWT* 2008, 41, 652–659.
- [67] Sekiguchi Y, Mitsuhashi N, Inoue Y, Yagisawa H, Mimura T. Analysis of sugar phosphates in plants by ion chromatography on a titanium dioxide column with pulsed amperometric detection. *J Chromatogr A* 2004, 1039, 71–76.
- [68] Tan SN, Yong JW, Teo CC, Ge L, Chan YW, Hew CS. Determination of metabolites in *Uncaria sinensis* by HPLC and GC–MS after green solvent microwave-assisted extraction. *Talanta* 2011, 83, 891–898.
- [69] Pérez-Serradilla JA, Japón-Luján R, Luque de Castro MD. Simultaneous microwave-assisted solid–liquid extraction of polar and nonpolar compounds from alperujo. *Anal Chim Acta* 2007, 602, 82–88.
- [70] Salt DE. Update on plant ionomics, *Plant Physiol* 2004, 136, 2451–2456.
- [71] Lahner B, Gong J, Mahmoudian M et al. Genomic scale profiling of nutrient and trace elements in *Arabidopsis thaliana*. *Nat Biotechnol* 2003, 21, 1215–1221.
- [72] Moing A, Aharoni A, Biais B et al. Extensive metabolic cross-talk in melon fruit revealed by spatial and developmental combinatorial metabolomics. *New Phytol* 2011, 190, 683–696.
- [73] Naozuka J, Marana SR, Oliveira PV, Water-soluble Cu, Fe, Mn and Zn species in nuts and seeds. *J Food Comp Anal* 2010, 23, 78–85.

- [74] Kroepfl N, Jensen KB, Francesconi KA, Kuehnelt D. Human excretory products of selenium are natural constituents of marine fish muscle. *Anal Bioanal Chem* 2015, 407, 7713–7719.
- [75] Kouremenos KA, Pitt J, Marriott PJ. Metabolic profiling of infant urine using comprehensive two-dimensional gas chromatography: application to the diagnosis of organic acidurias and biomarker discovery. *J Chromatogr A* 2010, 1217, 104–111.
- [76] Söderholm SL, Damm M, Kappe CO. Microwave-assisted derivatization procedures for gas chromatography–mass spectrometry analysis. *Mol Divers* 2010, 14, 869–888.
- [77] Tsai CJ, Chen YL, Feng CH. Dispersive liquid–liquid microextraction combined with microwave-assisted derivatization for determining lipoic acid and its metabolites in human urine. *J Chromatogr A* 2013, 1310, 31–36.
- [78] Bhushan R, Kumar R. Comparative application of microwave, ultrasonication, ultracentrifugation and conventional heating for preparation of sample as dinitrophenyl derivative for direct enantioseparation of certain amino alcohols and 1-amino-2-propanol from vitamin B12 hydrolysate on alpha1-acid glycoprotein and beta-cyclodextrin columns. *J Chromatogr A* 2009, 1216, 7941–7945.
- [79] Damm M, Rechberger G, Kollroser M, Kappe CO. Microwave-assisted high-throughput derivatization techniques utilizing silicon carbide microtiter platforms. *J Chromatogr A* 2010, 1217, 167–170.
- [80] Zhou L, Yan N, Zhang H, Zhou X, Pu Q, Hu Z, Microwave-accelerated derivatization for capillary electrophoresis with laser-induced fluorescence detection: a case study for determination of histidine, 1- and 3-methylhistidine in human urine. *Talanta* 2010, 82, 72–77.
- [81] Dua P, Jeong SH, Lee SE, Hong SW, Kim SY, Lee D. Evaluation of toxicity and gene expression changes triggered by quantum dots. *Bull Korean Chem Soc* 31, 1555–1560.
- [82] Phan JH, Moffitt RA, Stokes TH et al. Convergence of biomarkers, bioinformatics and nanotechnology for individualized cancer treatment. *Trends Biotechnol* 2009, 27, 350–358.
- [83] Feliu N, Fadeel B. Nanotoxicology: no small matter. *Nanoscale* 2010, 2, 2514–2520.
- [84] Gibb EA, Enfield KSS, Tsui IFL et al. Deciphering squamous cell carcinoma using multidimensional genomic approaches. *J Skin Cancer* 2011, 2011, 16 pages.
- [85] Brouzes E, Medkova M, Savenelli N et al. Droplet microfluidic technology for single-cell high-throughput screening. *Proc Natl Acad Sci USA* 2009, 106, 14195–14200.
- [86] Sakamoto JH, van de Ven AL, Godin B et al. Enabling individualized therapy through nanotechnology. *Pharmacological Res* 2010, 62, 57–89.
- [87] Soundararajan V, Warnock K, Sasisekharan R. Multifunctional nanoscale platforms for targeting of the cancer cell immortality spectrum. *Macromol Rapid Commun* 2010, 31, 202–216.
- [88] Cho SJ, Maysinger D, Jain M, Röder B, Hackbarth S, Winnik FM. Long-term exposure to CdTe quantum dots causes functional impairments in live cells. *Langmuir* 2007, 23, 1974–1980.
- [89] Thomas DG, Pappu RV, Baker NA. Nanoparticle ontology for cancer nanotechnology research. *J Biomedical Informatics* 2011, 44, 59–74.
- [90] De la Iglesia D, Chiesa S, Kern J et al. Nanoinformatics: new challenges for biomedical informatics at the nano level. Eds. Adlassning KP, Blobel B, Mantas J, Masic I. Amsterdam, Netherlands, IOS Press, 2009, 987–991.

Cezar Augusto Bizzi, Erico Marlon de Moraes Flores, and Marcia Foster Mesko

## 23 Microwaves in sample preparation for elemental determination

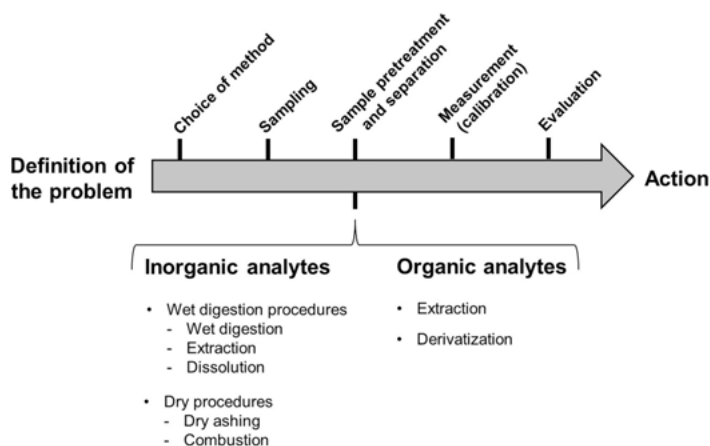
Since the first use of microwave (MW) heating in analytical laboratories, conducted in 1975 using a homemade MW oven [1], chemists have gradually paid increased attention to this versatile source of energy. Beyond providing a simple alternative to conventional heating, the advent of MW heating allowed for many improvements in analytical procedures and started a rapid evolution of instrumentation, mainly devoted to sample preparation for further analysis. Powerful instrumentation that is able to operate under high pressure and high temperature has been developed, allowing suitable digestion for most analytical techniques. This improvement has made it possible to obtain information at concentration levels as low as  $\text{pg g}^{-1}$ . To better elucidate how MW has been used in analytical procedures, in this chapter the main aspects related to the use of MW energy for sample preparation aiming at elemental determination will be discussed.

### 23.1 Introduction to microwave-assisted sample preparation

In a simple way, analytical chemistry protocols deal with the development and proposition of fit-for-intended-purpose methods, which aims to determine one or more elements or chemical species in several matrices. Chemical analysis, by definition, comprises a multistage investigation, normally organized as a series of subtasks (steps, operations) or sequence of analyses, as summarized in Figure 23.1 [2]. Not all tasks are mandatory, but they can be used as a guide for obtaining accurate and traceable information [3].

Chemical analysis with a focus on elemental determination has been governed by powerful instrumentation. The fast evolution observed for instrumental techniques came as a result of sensitive methods able to provide information at very low levels (e.g.,  $\text{pg g}^{-1}$ ). Better limits of detection (LODs) using analytical methods can be achieved using sensitivity analytical techniques combined with an appropriate sample preparation procedure. When complex samples must be analyzed beyond their inorganic or organic constitution, the most common approach is to use spectrometric techniques. Among these techniques, it is possible to emphasize those based on inductively coupled plasma (ICP-based techniques) for providing multielemental information with relatively good LOD, such as inductively coupled plasma optical emission spectrometry (ICP-OES) and inductively coupled plasma mass spectrometry (ICP-MS).

<https://doi.org/10.1515/9783110479935-023>



**Fig. 23.1:** Summarized subtasks of analytical sequence. In detail are shown the most common approaches used for sample preparation aimed at inorganic and organic analytes.

In addition, elemental determination has also been performed by atomic absorption spectrometry (AAS). AAS is still the most common technique for elemental determination and it involves flame atomization (F-AAS), graphite furnace atomization (GF-AAS), or chemical vapor generation (CVG-AAS). Essentially, each analytical method includes some kind of sample preparation (e.g., extraction, digestion or decomposition, matrix separation). Even when analytical instrumentation that allows solid sampling is used for elemental determination, some pretreatment is required (e.g., grinding).

For techniques using samples in solid state, as well as those requiring solubilized samples, sample preparation is generally the most time-consuming step in the analytical sequence, and the largest fraction of analytical costs are also spent in this step. Additionally, it might be considered one of the main aspects influencing the precision and accuracy of the final result, both of which are closely linked to systematic errors, elemental contaminations, and analyte losses. Despite the possible problems linked to sample preparation, the chemist must choose the most appropriate method by considering LOD, throughput, and costs as key factors [3, 4].

In the most used frequency of MW in analytical laboratories (2.45 GHz), the electromagnetic field changes  $4.9 \times 10^9$  times per second [5], and this becomes the most significant aspect when looking for MW applications for sample pretreatment. Because a heating rate can be obtained alongside aspects related to accurate temperature and pressure control, a fast dissemination of MW energy is adopted in analytical routines.

Several alternatives are already available for sample preparation looking for elemental determination, which are normally based on the so-called wet or dry ash methods. Wet procedures can generally be performed in two different ways: (1) wet digestion or dissolution, which comprises relatively high temperature conditions combined

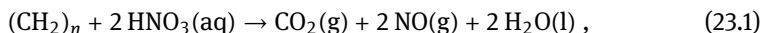
with oxidizing agents for complete oxidation/dissolution of sample matrix, and (2) extraction or leaching, where milder reaction conditions are used for a simple analyte extraction, without complete destruction of the sample matrix. On the other hand, dry ash methods are mainly applied to organic matrices and are based on the oxidation of organic matter due to the action of oxygen gas when the sample is exposed to high temperatures or even ignited in an oxygen-rich atmosphere. Both wet and dry ash methods can be performed in open or closed systems using MW as a heating source.

## 23.2 Microwave-assisted wet digestion/dissolution

Wet digestion is the most common sample preparation strategy for elemental determination. Acids are normally used once the sample is converted into an appropriate form for further instrumental analysis. When working with samples containing a large quantity of organic compounds (e.g., biological tissues), wet-digestion-based or organic matter oxidation is the conventional approach [3]. For samples whose constitution is inorganic (e.g., geological and metallurgical samples), a dissolution step is generally used [6]. Both procedures are based on the use of oxidizing and nonoxidizing reagents as described in Table 23.1.

### 23.2.1 Microwave-assisted wet digestion of organic matrices

Wet digestion with oxidizing acids is the most common sample preparation strategy for further elemental determination of organic matrices [8]. It is based on the oxidation reaction of compounds in the organic matrix due to the action of an oxidizing agent (normally  $\text{HNO}_3$ ,  $\text{H}_2\text{O}_2$ , or their mixtures), of which  $\text{HNO}_3$  is the most common. When the oxidizing agent comes in contact with organic matter, a spontaneous and exothermic reaction begins. Under ideal conditions, organic matter is fully oxidized to  $\text{CO}_2$  and water, as presented in Equation (23.1). The aim of this reaction is that inorganic analytes will ideally be present in final solutions free of any organic compound, ready to be determined by analytical techniques:



where “ $(\text{CH}_2)_n$ ” is a general representation of organic material.

Although the oxidation of organic matter is thermodynamically spontaneous, depending on the organic matrix and operational conditions, this reaction normally takes a long time to complete. Nevertheless, it can be sped up by increasing the sample surface area (e.g., sample milling), applying high temperatures, or increasing the acid concentration.

Although some approaches can be taken to speed up digestion, the analyst is normally dependent on the instrumentation facilities as well as the source of heat-

**Tab. 23.1:** Characteristics of common reagents used for wet digestion [7–9].

Reagent	Characteristics
HNO <sub>3</sub>	Nitric acid is the most common reagent for the oxidation of organic matrices. Its oxidation potential is strongly dependent on the reaction temperature. Since the boiling temperature of an azeotropic mixture with water is 121 °C at atmospheric pressure, the use of closed reactors is normally recommended to increase its oxidizing power. An important feature is related to the ability of HNO <sub>3</sub> to dissolve most metals to form soluble nitrates. Such oxidizing action can be further enhanced by the addition of other acids or H <sub>2</sub> O <sub>2</sub> .
H <sub>2</sub> SO <sub>4</sub>	Concentrated sulfuric acid (98%) can carbonize organic substances. Its boiling temperature is 338 °C, being higher than the working range of all polytetrafluorethylene (PTFE) materials normally used in MW-assisted reactions. It is a strong dehydrating agent and commonly used in combination with HNO <sub>3</sub> or H <sub>2</sub> O <sub>2</sub> .
HClO <sub>4</sub>	Perchloric acid presents an oxidizing power directly related to its concentration and reaction temperature. It has a strong tendency to react violently with organic matter under heating, but its mixture with HNO <sub>3</sub> decreases the reaction rate. HClO <sub>4</sub> is not recommended for MW digestion due to its thermal decomposition at 245 °C, which releases higher amounts of gaseous by-products, leading to high excess of pressure, so its use should be avoided.
H <sub>2</sub> O <sub>2</sub>	Hydrogen peroxide is normally used in concentrations ranging from 30 to 50%. At higher concentrations it can react explosively with some organic compounds. It is frequently used in combination with HNO <sub>3</sub> and H <sub>2</sub> SO <sub>4</sub> in wet digestions.
HCl	Hydrochloric acid is a nonoxidizing agent that exhibits weak reducing properties. HCl readily dissolves many metal carbonates, peroxides, and alkali hydroxides. Although a major part of metals form soluble chlorides, some elements can form insoluble compounds as AgCl, HgCl, TiCl, and PbCl <sub>2</sub> . While HCl reacts with most metals, it is normally combined with HNO <sub>3</sub> to form <i>Aqua regia</i> , which is able to dissolve even noble metals.
HF	Hydrofluoric acid has a strong complexing nature. It is most commonly used for inorganic matrices because it is one of the few acids that can dissolve silicates. Glass or quartz reactors cannot be used for sample digestion. In some cases its removal before analysis is mandatory to prevent equipment damage. In this case, usually boric acid is added to neutralize active HF, and, usually, it is necessary to filter the sample solution at the end of the digestion.  Its use prevents the formation of sparingly soluble products of groups 4, 5, 13, and 14 of the periodic table, increasing the solubility and stability of, for example, Si, Sn, Ti, Zr, Hf, Nb, Ta, and Pa.

ing (conventional or MW). In this sense, several systems are available for closed and open vessels, including batch and flow procedures using MW in multimode systems (MW cavity), monomode systems (MW applicators), and directed monomode systems (focused MW) [3, 10].

When looking for MW heating, it is important to consider the material of the vessels/reactors, which must be MW transparent, such as quartz, glass, PTFE, perfluoroalkoxy (PFA), or chemically modified PTFE (e.g., TFM<sup>®</sup>). MW-transparent materials

have the main advantage of having practically no interaction with the MW field, which means the material does not absorb any energy [10, 11]. Because of this characteristic, if the action of MW is expected to heat the system, the reaction mixture, which contains the oxidizing agent or its diluted solution (normally with water), must be MW absorbent and capable of dissipating the absorbed energy as heat [10, 11]. This provides one of the main advantages of using MW heating for sample preparation: selective heating, which saves energy and time. Additionally, according to the reactor design, volumetric heating can be expected, without a temperature gradient in the solution, ensuring the reaction happens to the same extent everywhere. If the reaction mixture is not MW absorbent (e.g., nonpolar solvents), the vessel/reactor can interact with the MW field (e.g., SiC), dissipate the energy as heat, and conductively heat the nonpolar solvent [12]. However, this approach is not often used for wet digestion, and this aspect will not be covered in this chapter.

Because the MW energy related to 2.45 GHz is not able to break chemical bonds, in this chapter the discussion will be focused on how MW energy can facilitate wet digestion procedures when it is performed under ambient pressure or not and how it can drive the oxidation of organic matter when oxidizing agents are used.

### Digestion efficiency

Digestion efficiency is the most important aspect of sample preparation, as the majority of analytical techniques present poor tolerance to solids present in final digests as well as to the amount of carbon compounds that remain dissolved after organic matter oxidation and to the final acidity. In routine analysis, analysts normally use residual carbon to evaluate the digestion efficiency and its influence on the determination step. It can sometimes be qualitatively performed by visual evaluation of the digest's aspect. If the final solution is completely clear, without solids as suspended particles, the oxidation of organic matter can be assumed to have been successful. Although it can quickly provide enough information for routine analysis, many organic compounds can be just partially oxidized and remain dissolved without necessarily being completely digested. Dissolved carbon can impair the determination step by causing interference in several techniques, introducing a source of error and leading to equipment damage in some instances [13, 14]. In this sense, more accurate information can be obtained by residual carbon determination in the final digests. This allows for a better choice of analytical technique as the residual carbon can indicate that a dilution must be applied prior to analysis.

Many possibilities can be used to express residual carbon and, in turn, digestion efficiency. Two of them will be covered in this section: (1) *residual carbon content* (RCC) is the relation between the carbon mass that is still dissolved in solution after a digestion procedure and the total organic carbon (TOC) present in the original sample, expressed as a percentage of carbon remaining in the final digest; and (2) *dissolved organic carbon* (DOC, or simply residual carbon) is the final concentration of dissolved

carbon that remains after digestion, expressed as the concentration of C (e.g., in milligrams per liter,  $\text{mg L}^{-1}$ ). Basically, DOC just makes reference to the dissolved carbon present in the final digest, without any correlation to the TOC originally present in the sample. Although DOC does not provide enough information about the efficiency of organic matter oxidation (as can be evaluated by means of RCC value), it provides very important information for the determination step. Conventional RCC values in solution after wet digestion in closed systems falls below 30% (depending on the matrix complexity and digestion conditions). Considering the analytical instrumentation that is widely used for elemental determination, it is well known that severe interference can be observed. As an example, when dealing with ICP-MS determination of elements that present high ionization potential, such as As, Hg, Se, and I, modifications in the ionized population may be observed when carbon concentration higher than  $5 \text{ g L}^{-1}$  is present in the final digest. Under such conditions, the accuracy and precision of the final result are impaired [14]. Both RCC and DOC are important parameters that help chemists evaluate digestion efficiency, as well as select the most appropriate detection technique to be used for elemental determination.

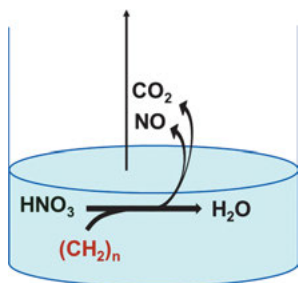
### Open systems

Wet digestion using open vessels is one of the oldest and most common methods for sample preparation for organic and inorganic samples used in chemical laboratories. Although it can be easily performed using a simple hot plate or long-neck vessels in a heating block, it is not often performed under MW heating. One of the main limitations is the MW applicator, which must be specially designed for avoiding MW leakage while the reaction mixture is irradiated. As the system is open, the vapor atmosphere can corrode even the metallic cavity used for MW irradiation, which requires careful consideration of operational costs and safety. Although few alternatives to open digestion systems are commercially available for MW heating, they can satisfy the minimum requirements for safety reactions [15, 16].

The main advantages of open systems include easy handling, low operational costs, relatively fast reactions (when compared with, for example, dry ashing), high sample throughput (relative to the number of samples per run), and ambient-pressure reaction, which represent safer operational conditions [17]. Since there is a low risk of explosion, sample masses as high as 10 g can be digested [8]. However, the ambient-pressure conditions of operations also represent a main disadvantage of open systems. The reactional mixture used cannot exceed the ambient-pressure boiling temperature of the corresponding acid or acid mixture. Consequently, reactions are limited by the relatively low maximum temperature that can be achieved.

During the heating program it is possible to use different kinds of condensers [9], and this approach can improve the reflux of solvent and minimize analyte losses. However, it must be considered that digestion efficiency is still the same and is limited by the temperature of the digestion medium [8, 9]. A schematic representation of wet digestion using open systems is shown in Figure 23.2.





**Fig. 23.2:** Sample digestion representation based on use of open systems. An organic matrix is represented by  $(\text{CH}_2)_n$ , which is ideally converted into water and  $\text{CO}_2$ .

Since the reaction is dependent on the boiling temperature of the reaction mixture, this aspect results in some limitations on the efficiency of digestion. Although there is a superheating phenomenon, which is promoted by MW and can increase the solvent boiling temperature [18], it is only observed when there is no more suspended solid material from the sample or in homogeneous reactions. Considering these aspects, to ensure an efficient digestion, it is necessary to carefully evaluate the composition of the sample matrix. Each main component of an organic matrix presents a different reactivity for oxidation (e.g., carbohydrates, proteins, and fat). With the use of  $\text{HNO}_3$ , the most common acid used for wet digestion, which has a relatively low boiling temperature ( $121^\circ\text{C}$ , azeotropic mixture with water), complete oxidation of many kinds of organic matter is almost impossible [19].

To increase the digestion efficiency, higher temperatures can be obtained when two or more acids are mixed. For this purpose, the most common mixture is  $\text{HNO}_3$  and  $\text{H}_2\text{SO}_4$ , which allows digestion at temperatures as high as  $338^\circ\text{C}$  (atmospheric-pressure boiling temperature of 98%  $\text{H}_2\text{SO}_4$ ) [9]. In addition, since the system is open, acid consumption while the sample is oxidized, or even acid loss by evaporation, results in the need for sequential acid addition. However, this means a huge amount of acid consumption for a single operation, increasing costs, the residual acidity of the solution to be analyzed, and blank values, in addition to opposing the principles of green chemistry by demanding a higher amount of reagents and generating higher volumes of residues.

Despite the disadvantages already mentioned, some possibilities in sample preparation can be highlighted when using open systems, which makes this approach a versatile tool for the preparation of organic samples, as follows:

#### *Small-vessel wet digestion:*

Similar to a so-called one-pot reaction, this approach aims to use just one vessel for the entire analytical sequence. Basically, up to a few milligrams of sample mass are digested with microliters of acid mixture (normally  $\text{HNO}_3$  and  $\text{H}_2\text{SO}_4$ ) in a small vessel (in general up to 5 mL capacity). In this case, a relatively high number of vessels can be used compared to larger-scale conventional digestion. One of the main advantages is that the same vessel used for digestion can also be used for other steps in an analyt-

ical sequence (e.g., weighing, dilution) in agreement with the single-vessel principle. Special care must be taken about the vessel material, which must support at least the acid boiling temperature before melting [20–22].

#### *Sample gradual addition of preheated acid:*

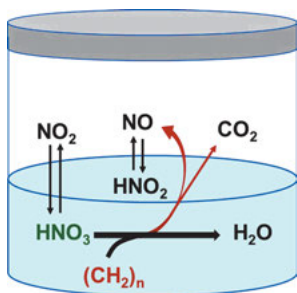
Although the conventional procedure for wet digestion is based on the addition of room-temperature reagents over the sample, open systems allow for preheating the oxidant mixture before sample addition. Because every subsample is completely digested before the next addition, it is possible to achieve better digestion efficiency. Thus, the acid remains during the entire digestion time in excess, which reduces the overall reaction time. It also contributes to reducing the amount of acid required for sample digestion, decreasing the risk of contamination, and leading to better limits of detection [16].

#### **Closed systems**

Closed systems offer the advantage of essentially isolating the digestion step from the laboratory atmosphere, which minimizes contamination and significantly reduces the losses of volatile species [8]. Despite presenting the possibility of working with temperatures higher than that observed for reactions at ambient pressure, the limited internal volume of digestion vessels normally represents the main inconvenience of closed vessel wet digestion: the risk of leakage or even explosions. This aspect comprises the main challenge of working with closed vessels, which must tolerate the highest pressure possible in order to allow the digestion of high sample mass while providing safe operational conditions. In addition, given the advantages of MW heating, this reactor must be MW transparent, which restricts even more the number of possibilities and often represents physical limitations on the system design.

Fluorinated polymers, such as PTFE, PFA, and TFM, are the most common vessel materials. However, they do not possess proper mechanical characteristics for supporting the high temperatures and pressures required in sample preparation of difficult matrices. Modified PTFE can tolerate working temperatures close to 300 °C, and considering that digestion requires relatively high temperatures (180 °C or more), the mechanical resistance of fluorinated polymers, in turn, normally requires special jackets made of polyether-ether-ketone (PEEK), alumina, or Kevlar® tape (DuPont). Depending on the vessel design, it allows one to work under pressures of up to 100 bar [3]. Alternatively, there are digestion vessels made of quartz that are able to work up to 300 °C and 80 bar and do not require any kind of jacket to increase mechanical resistance. It is worth noting that in this system the maximum temperature is related to the PTFE parts present in the quartz vessel (e.g., cover) [3].

In closed systems, organic matter oxidation is assured by a synergistic effect of elevated temperature and pressure; reactions occur at a relatively high temperature due to the increase in boiling temperature of acid [8]. At the same time that the reaction



**Fig. 23.3:** Sample digestion scheme based on the use of closed systems. Reactions occur in high pressure conditions due to the confinement of vapour and gases produced during digestion.

rate is increased due to a high reaction temperature, it also increases the acid oxidizing power, resulting in high digestion efficiency and fast procedures. In a manner similar to that of other closed systems, the evaporated acid remains inside the reactor, and a lower amount of reagent is required (Figure 23.3) [23, 24].

In MW heating systems, the cooler vessel walls increase the condensation rate, resulting in lower pressure and the possibility of temperature increase. This means that less acid can be enough for achieving the same digestion efficiency [25]. In a first approximation, the total pressure ( $P_{\text{tot}}$ ) in a closed system is the sum of the partial pressures ( $p$ ) of the main constituents present in the gas phase. The main contribution is related to solvent evaporation (e.g., acid, water) and gaseous reaction products ( $\text{CO}_2$ ), as presented in Equation (23.2) (considering the reaction using just  $\text{HNO}_3$  as oxidizing agent) [26]. It is important to mention that even the sample mass becomes a practical limitation due to the high pressure and risk of explosions. Depending on the volume of the vessel, sample mass is normally limited to 0.5 g per vessel (dry basis).

$$P_{\text{tot}} = p_{\text{HNO}_3} + p_{\text{CO}_2} + p_{\text{H}_2\text{O}} + \dots \quad (23.2)$$

Several advantages can be pointed out for closed vessel wet digestion compared to that performed in open vessels. Some of these advantages can be seen in Table 23.2. Despite the improved digestion efficiency, which increases the compatibility of final digests with the analytical technique, the main feature of closed systems is the reduced amount of reagents required for sample digestion.

**Tab. 23.2:** Main and general features of closed and open vessels used for sample wet digestion.

Parameter	Open vessel	Closed vessel
Sample mass	+++	++
Reagent consumption	+++	++
Digestion efficiency	+	+++
Risk of loss/contamination	+++	+
Digestion time	+++	+
Safety	++	++
Cost	+	++

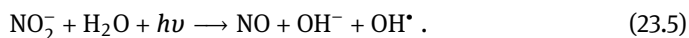
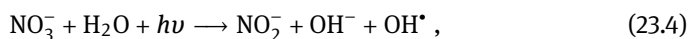
To further reduce the amount of reagents used for digestion, some recent developments have been made regarding closed vessel systems. Among them, special attention must be paid to MW-assisted ultraviolet (UV) digestion, O<sub>2</sub>-pressurized wet digestion with diluted reagents, and the use of single reaction chamber (SRC) systems, as briefly described in what follows.

### *MW-assisted ultraviolet digestion*

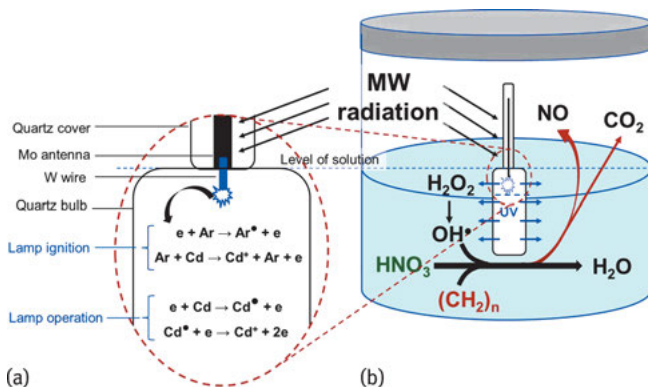
UV radiation comprises an electromagnetic spectrum range between visible light and X-ray, with wavelengths ( $\lambda$ ) from 40 up to 400 nm ( $1 \text{ nm} = 1 \times 10^{-9} \text{ m}$ ). It can be divided into near-UV (200–400 nm) and far or vacuum UV ( $\lambda < 200 \text{ nm}$ ). Conventionally, UV radiation can be artificially produced by means of deuterium or xenon lamps, fluorescent lamps, mercury vapor lamps, and certain kinds of lasers (nitrogen and Nd:YAG) or light emitting diode (LEDs) [27]. UV radiation has been used for derivatization procedures prior to elemental determination, where a mercury vapor lamp was directly adapted in a nebulization chamber prior to an inductively coupled plasma mass spectrometer. Such an approach is not covered in the present text, and related references can be found in the literature [28–30].

To allow the use of UV energy simultaneously with MW, an electrodeless discharge lamp ignited by MW (MWL) was developed [31]. MWL has a molybdenum antenna for coupling MW radiation, which ends with a tungsten filament responsible for focusing the energy stored in the antenna and releasing it inside a low-pressure quartz bulb filled with argon or helium (0.001 to 0.004 bar). Commercial MWL models have cadmium vapor inside their bulbs (1 mg), and the main emission line is 228 nm. A brief mechanism of MWL ignition and operation is presented in Figure 23.4a.

When UV radiation acts over dissolved organic material several intermediates are produced, such as singlet oxygen and hydroxyl radicals, which present high reactivity. Moreover, to break organic bonds, a small number of reagents for the oxidation process, normally H<sub>2</sub>O<sub>2</sub>, O<sub>3</sub>, K<sub>2</sub>S<sub>2</sub>O<sub>8</sub>, K<sub>2</sub>Cr<sub>2</sub>O<sub>7</sub>, or HNO<sub>3</sub>, must be added [27]. Very briefly, the main reactions that contribute to organic matter oxidations are based on the number of hydroxyl radicals formed according to Equations (23.3) to (23.5):



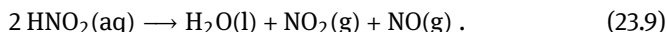
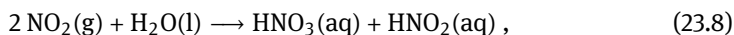
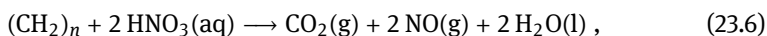
Since MWL started to be used for sample digestion, much more complex matrices have been digested with a relatively lower amount of reagents compared to the same procedure without MWL. Samples such as skimmed milk powder [31], algae [32], chocolate [33], crude oil [34], and petroleum coke [35] have been efficiently digested for further determination of several elements by atomic spectrometric techniques. A general overview of the MWL for helping organic matter oxidation can be seen in Figure 23.4b.



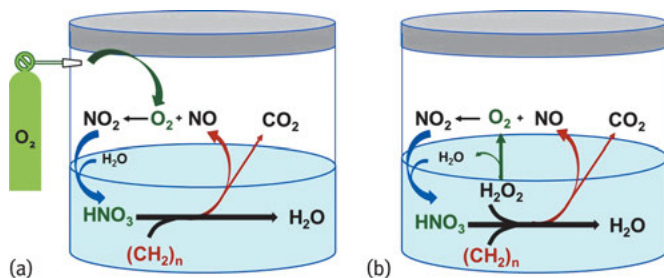
**Fig. 23.4:** Schematic representation of MW-assisted UV digestion: (a) MWL workup and (b) MWL for helping digestion efficiency.

#### *O<sub>2</sub>-pressurized wet digestion with diluted reagents*

While the majority of wet digestion procedures are based on the use of concentrated reagents (mainly  $14 \text{ mol L}^{-1} \text{ HNO}_3$ ), when using closed systems assisted by MW there is a possibility of employing diluted reagents. In this sense, two basic requirements must be followed in order to make possible an efficient digestion procedure using diluted  $\text{HNO}_3$ : (1) the presence of enough oxygen in the gas phase inside the closed digestion vessel and (2) a temperature gradient along the reaction vessel (between gas and liquid phases) at the beginning of the MW heating program [36]. These requirements are easily understood by considering the reactions involved for organic matter oxidation with  $\text{HNO}_3$ , as presented in Equations (23.6)–(23.9):

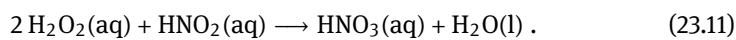
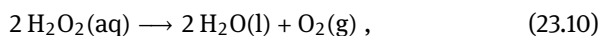


The very first requirement, and perhaps the easiest to control and explore, is the one responsible for the oxidation of  $\text{NO}(\text{g})$  (from organic matter digestion) in the gas phase to  $\text{NO}_2(\text{g})$ . The second one, which depends on the reactor design or capability of simultaneous cool-down of the external vessel walls, contributes to a less pronounced increment in the pressure once it is associated with the absorption of the oxidized species in the gas phase. Consequently, while the organic matter is oxidized (Equation (23.6)), producing  $\text{NO}(\text{g})$ , this product is further oxidized to  $\text{NO}_2(\text{g})$  if enough  $\text{O}_2$  is still present in the gas phase (Equation (23.7)). After that, a disproportionation reaction occurs and  $\text{NO}_2(\text{l})$  is converted to  $\text{NO}_3^-$  and  $\text{NO}_2^-$  (Equation (23.8)). The  $\text{HNO}_3$  formed in situ will restart the oxidation cycle, which remains active while there is  $\text{O}_2$  still present in the gas phase of the closed vessel [25]. Several approaches can be used



**Fig. 23.5:** Schematic representation of  $O_2$ -pressurized MW-assisted wet digestion: (a) nitric acid regeneration using oxygen gas and (b) nitric acid regeneration using hydrogen peroxide.

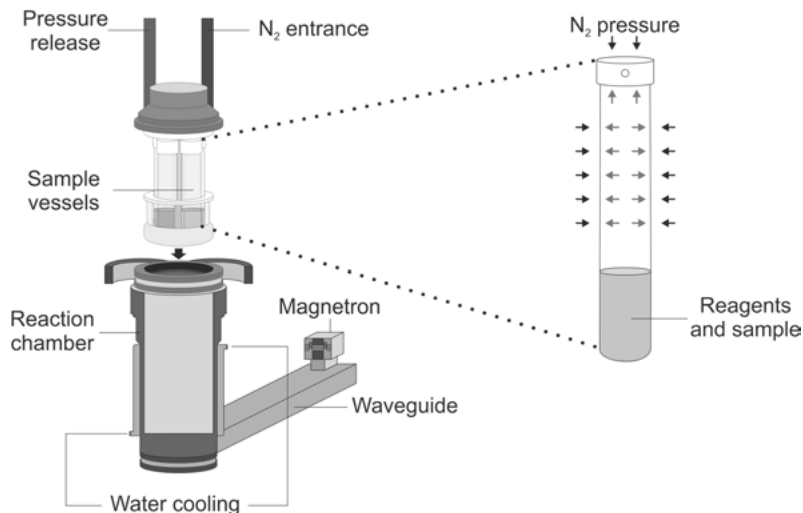
for this kind of wet digestion procedure. One is based on pressurizing the reactor with  $O_2$  gas, which requires a reactor with valves properly designed for this purpose, as presented in Figure 23.5a. Another approach is based on the use of  $H_2O_2$  as an oxygen source. This reagent presents further contributions to organic matter oxidation using diluted reagents. Despite  $H_2O_2$  being a source of  $O_2$ , due to its thermal decomposition (Equation (23.10)), it naturally acts as an oxidant over organic matter, and it may oxidize  $HNO_2$  present in the medium to  $HNO_3$  (Equation (23.11)):



Using  $O_2$ -pressurized wet digestion with diluted reagents, several organic matrices can be efficiently digested using diluted acid solutions ( $2 \text{ mol L}^{-1}$  or less). The action of an excess of oxygen was proven to be required, regardless of its chemical form, because it can be used as a gaseous oxygen [37–39] or from a hydrogen peroxide solution [40]. In addition, the positive effect of intensified temperature gradient promoted by MW heating [41] and simultaneous cooling of external vessel walls [42] have also been reported in the literature. Both features help chemists to better understand the oxidation of organic matter, saving costs and generating less residue. These aspects are graphically represented in Figure 23.5b.

### Single reaction chamber system

This system was recently proposed and comprises a closed SRC heated by MWs. The main feature is related to the possibility of working in extreme conditions, such as high pressure (up to 199 bar) and high temperature (up to  $300^\circ\text{C}$ ). The SRC system is heated by MWs by the bottom part of the chamber, where an antenna is positioned for MW irradiation, assuring a suitable distribution of MW energy (up to 1.5 kW). The chamber, which is metallic (except for the PTFE bottom), is internally covered by a TFM<sup>®</sup> vessel (1 L internal volume), and a sample is placed within it using small digestion vessels (normally quartz, glass, or TFM, although it is even possible to use disposable



**Fig. 23.6:** SRC system with MW-assisted heating. *Top:* digestion vessels placed in the holder; *bottom:* metallic chamber with internal PTFE cover; *detail:* digestion vessel with pressure equilibrium indicated by arrows.

vessels). Digestion vessels are immersed in an MW absorber solution present in the bottom part of the SRC system. The cap of digestion vessels has a small hole for pressure equilibrium. In this case, due to the pressure in the whole chamber (40 to 50 bar of Ar or N<sub>2</sub>, before the heating program) evaporation of the solution is avoided, and gaseous products are kept dissolved in the liquid phase. This is a very important aspect because it makes it possible to use several kinds of MW-transparent materials for performing wet digestion. In this case, there is no restriction if the vessels are mechanically resistant, as they are in a condition of pressure equilibrium inside and outside, so they will not be strained if the thermal resistance of the material is respected. Since the SRC system begins reacting at a high pressure, the pressure itself acts as a seal for avoiding any kind of sample projection and solvent evaporation. Figure 23.6 shows a simplified scheme of the SRC system.

Owing to the benefits of the SRC system, it is possible to highlight the high working pressure compared to any other closed system used for MW-assisted wet digestion, as well as the maximum sample mass that can be digested. As this system can support a high pressure, it allows operation temperatures close to 300 °C, providing very high digestion efficiency for organic matter oxidation, even using diluted acid solutions [43]. As the chamber has 1 L internal volume, the generated CO<sub>2</sub> is diffused throughout the whole volume of the chamber, avoiding a sudden increase of pressure, and then allowing simultaneous digestion of sample masses as high as 20 g (considering the sum of sample mass present in each digestion vessel) [9].

The SRC system has been used on samples that are difficult to oxidize in other systems under milder reaction conditions, for example, drugs [44], polymers [45], crude oil [46], and food [47, 48], with high digestion efficiency enabling a determination step with no observable interferences due to matrix effects.

### 23.2.2 Microwave-assisted wet decomposition/dissolution of inorganic matrices

Inorganic samples generally present low solubility in water, meaning they require appropriate solvents and, sometimes, extreme operational conditions. Unlike the procedure for organic samples, the dissolution of geological, metallurgical, and environmental samples is strongly dependent on the solvent and its interaction with the sample. Since the reaction is not only related to the oxidizing action of the reagents used, acid mixtures may be employed for improving sample dissolution (e.g., mixture of complexing and oxidizing agents). For example, if a sample contains a large proportion of silicates, HF is strongly recommended [7].

The mechanism of dissolution usually involves a simple reaction between an acid (diluted or concentrated) and the sample (for elements less electronegative than hydrogen) to form a water-soluble salt of the metal and some other products. Examples of this class of matrices include metal oxides, carbonates, and sulfides, which are soluble even in diluted acid medium. Some exceptions can be observed when this mechanism is considered. For instance, Al and Cr become passive in the presence of certain concentrated acids due to the formation of an insoluble film of oxide on the metal surface that prevents further acid attack [49].

Closed systems can be used for sample dissolution. Since few gaseous products are released to the gas phase (with exception of metals), the pressure is not a critical point and relatively high sample masses can be used. Additionally, dissolution should work at ambient temperature, but a rough increase in the temperature may be performed if necessary [49].

However, in some instances when working with samples that are not soluble in either diluted or concentrated mixtures of acids, fusion methods can be employed prior to sample dissolution. This method is based on the use of a finely ground sample with acidic or basic electrolytes (in solid state) at a ratio of 1 : 2 to 1 : 50 (sample: electrolyte mixture, called flux). The mixture is then placed in nickel or platinum crucible and heated until the flux melts. The mixture is heated until the dissolution of the inorganic sample and then cooled. The success of this procedure is dependent on the electrolyte used, which acts as a Lewis acid or base when fused and reacts with the sample, resulting in a new solid material that is soluble in diluted acids or even water [6].

To perform MW heating, MW furnaces equipped with heating elements (SiC plates positioned on the top or side of the MW cavity, or SiC crucibles) have been used, which speed up the fusion procedure even for sample presenting refractory materials. The most common electrolytes used for fusion procedures are detailed in Table 23.3.



**Tab. 23.3:** Characteristics of common electrolytes used for fusion procedures [49, 50].

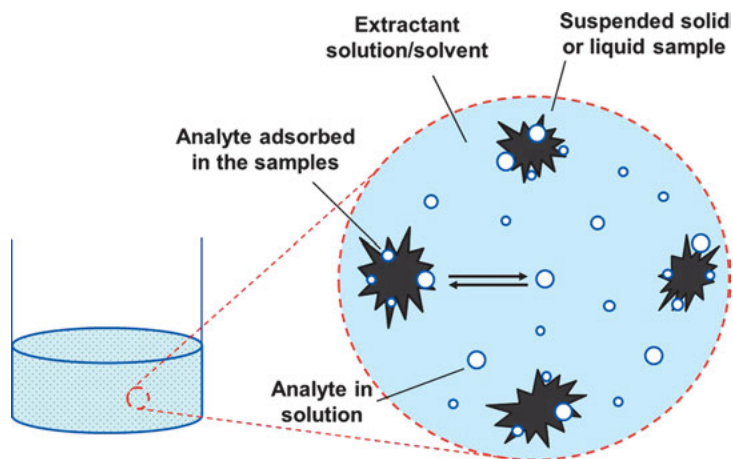
<b>Lewis Basic flux</b>	
Sodium carbonate	Melting temperature (m.t.) 851 °C. Powerful flux for silicates and other refractory compounds.
Sodium and potassium peroxide	m.t. 318 and 360 °C, respectively. Powerful flux for silicates, aluminosilicates, silicon carbides.
Sodium (dissodium) peroxide	m.t. 460 °C. Basic oxidizing flux for sulfides and acid insoluble alloys of Fe, Ni, Cr, Mo, W, and La.
<b>Lewis acid flux</b>	
Potassium hydrogen sulfate (KHSO <sub>4</sub> ) and potassium pyrosulfate (K <sub>2</sub> S <sub>2</sub> O <sub>7</sub> )	m.t. 197 and 325 °C, respectively. They are normally used at 500 °C and present a wide range of applications due to the following reactions: $2\text{KHSO}_4 \longrightarrow \text{K}_2\text{S}_2\text{O}_7 + \text{H}_2\text{O} \uparrow$ $\text{K}_2\text{S}_2\text{O}_7 \longrightarrow \text{K}_2\text{SO}_4 + \text{SO}_3$ SO <sub>3</sub> act as Lewis acid, used for Al <sub>2</sub> O <sub>3</sub> , BeO, Fe <sub>2</sub> O <sub>3</sub> , Cr <sub>2</sub> O <sub>3</sub> , and MoO <sub>3</sub> , for example. All these oxides are converted to soluble sulfates.
Boric oxide	m.t. 450 °C. acidic flux for silicates, used as an alternative to basic flux when alkaline metals must be determined.
Disodium tetraborate decahydrate (Borax, Na <sub>2</sub> B <sub>4</sub> O <sub>7</sub> · 10 H <sub>2</sub> O)	Fusion temperatures vary from 1000 to 1200 °C. Very useful for Al <sub>2</sub> O <sub>3</sub> , ZrO <sub>2</sub> , Zr ores, minerals containing rare earth elements, Ti, Nb, or Ta
Lithium metaborate (LiBO <sub>2</sub> ) and lithium tetraborate (Li <sub>2</sub> B <sub>4</sub> O <sub>7</sub> )	m.t. 845 and 920 °C, respectively. Recommended for reactions with basic compounds.

### 23.3 Microwave-assisted extraction

This approach can be applied to samples considered inert to oxidation even at conditions of higher temperature and pressure. Samples like aluminates, carbides, silicates, or mixtures of several refractory materials make sample preparation one of the most challenging tasks [51, 52]. An extraction or leaching step is a suitable option.

The fundamental basis of the extraction step includes the separation of components of sample in either solid or liquid state. Extraction efficiency is a result of the extension of desorption/partitioning mechanisms, which may happen according to the affinity of analyte to the extracting solvent [6]. Analytical approaches that employ an extraction process are dependent on the migration of inorganic or organic analytes by a desorption, diffusion, or solubilization process to a suitable solvent. The basic requirement is dependent on the interaction between solvent and analyte, which must be stronger than that observed for the analyte and sample matrix [53]. A general approach to extraction processes is presented in Figure 23.7.

As the analyte extraction is strongly dependent on the equilibrium between free analyte (in solution) and its association with sample matrix (or dissolved, in cases



**Fig. 23.7:** Schematic representation of sample preparation based on extraction approach. In detail is shown analyte migration to extracting solution and its equilibrium dependency.

of liquid samples), it is necessary to consider how physical and chemical properties might influence the extraction process. Two factors may be considered since they are the most influential: (1) the solubility of the analyte in the extracting solvent and (2) chemical equilibrium driving the migration of analyte from sample to extracting solvent [6]. Both aspects are dependent on thermodynamic parameters, and temperature is the most significant because it can be directly controlled by chemists to speed up the overall process.

### 23.3.1 Microwave-assisted extraction for speciation studies

The main motivation for choosing extraction as a sample preparation method is the search for mild conditions, as it uses fewer reagents, lower temperature, and less time, so total oxidation of organic matter does not seem to be required [54]. In this sense, a feasible alternative to conventional leaching of elements is procedures based on MW-assisted extraction (MAE). MAE has been successfully performed in efforts to improve the efficiency of element extraction and for reducing the overall time of the analytical process. MW energy can be used, and MAE can be performed practically in the same instrumentation available for wet digestion. In addition, household ovens could be used in some laboratories considering that mild heating and a short time are usually enough. However, it is necessary to take into account the conditions to perform a safe procedure. The extracting solution must be carefully chosen according to the chemical and physical properties of the element to be determined. Normally, polar solvents are chosen when working with MW heating. Weak acid solutions, or even diluted acids (10%  $m\ m^{-1}$  or less), are the most common choice when extracting metal, metalloids,

and nonmetals because they are soluble in this medium. On the other hand, halogens normally require an alkaline solution suitable for extraction and analyte stabilization of extracts. In some cases, chelating agents (e.g., ethylenediaminetetraacetic acid) are needed to ensure quantitative recoveries, or only ultrapure water can be used [54, 55].

Perhaps one of the most important applications of extraction procedures to speciation analysis. When performing speciation studies, it is not the total concentration of an element that is of concern but the concentration of one or more species of an element (e.g., As(III), As(V) or even organic As compounds) [54, 56, 57]. These studies provide very rich information about the toxicity, stability, or bioavailability of any chemical species in the environment or in living organisms [56]. In this particular case, sample preparation conditions must be milder than those observed for wet digestion. In this sense, chemical information (e.g., oxidation state, chemical structure) is kept practically invariable since analytes just migrate from sample to solvent. In this way, MAE arises as a promising alternative, and some aspects must be taken into consideration when chemical speciation is desired. Some species are unstable at higher temperatures, which requires a careful temperature control, as well as for volatiles species that require a closed system to avoid losses. Another issue that needs attention is that separation and detection techniques normally require compatible solvents, which must be suitable for quantitative analyte extraction and analytical instrumentation (e.g., mercaptoethanol damage C8 and C18 chromatographic columns; some species should be interconverted according to selected solvent) [54, 56].

The use of MAE for total element extraction or for extraction of species requires a careful evaluation of sample mass-to-solvent ratio, temperature and time of heating to ensure quantitative extraction. Once conditions are milder, extraction may be incomplete if suitable conditions are not chosen, which are mainly dependent on the sample matrix and analyte(s). In cases where extraction is assured, MAE provides the advantage of saving time, energy, and reagents, in agreement with the principles of green analytical chemistry [58].

### 23.4 Microwave-assisted sample combustion

In spite of the high performance of wet digestion, especially in closed vessels, this method is not suitable for some types of matrices (e.g., petroleum and its products, polymers, and carbon nanotubes), as well as for the subsequent determination of elements such as halogens [3, 59]. In this sense, combustion methods may be an excellent alternative because they allow the conversion of organic matter to its oxidation products (mainly CO<sub>2</sub> and H<sub>2</sub>O). Considering the high temperature achieved during the combustion process, practically all organic matrices may be digested using these methods. In addition, it is important to mention that oxygen is the main reagent used and, consequently, the risk of contamination is lower when compared to wet digestion methods, in which concentrated inorganic acids are generally used. In many cases,

combustion may be considered as more suitable for further trace element determination than other methods. During the combustion, nonvolatile elements can remain in the ash portion and be further dissolved, while volatile elements are released to the gas phase and absorbed in a suitable solution when using a closed system [3].

### 23.4.1 Dry ashing

This section presents a brief description of dry ashing and MW-induced combustion (MIC) and discusses the main features and drawbacks of these methods, especially those related to the use of open and closed vessels. Moreover, it is important to mention that dry ashing is one of the most commonly used methods for sample digestion, while the MIC method is a new concept in combustion. It is initiated by MW radiation that may be performed in open or closed vessels.

Dry ashing has been widely used for sample digestion [60–65], especially because of its simple procedure, instrumentation, and materials. Moreover, its use is recommended in some official methods described by pharmacopeias, the American Society for Testing and Materials (ASTM), and the Association of Official Analytical Chemists International (AOAC International) [66]. Dry ashing involves the combustion or pyrolysis of organic material using the oxygen present in air as an oxidizing agent. In this way, organic compounds are mainly converted to  $\text{CO}_2$  and  $\text{H}_2\text{O}$ , and the resulting inorganic fraction (ash) is generally solubilized for subsequent analysis. In this method, the sample is placed in a crucible and heated (in general from 400 to 800 °C) using a laboratory flame, a muffle furnace, or other heating source until all the organic material is completely oxidized. The inorganic residue consists mostly of metal oxides as well as nonvolatile sulfates, phosphates, and silicates [3, 6].

High sample masses (> 10 g) may be digested using the dry ashing method, because it is performed in an open system and because of the high temperatures achieved during this process. However, it is important to mention that this method presents some limitations, considering that some elements (e.g., As, Br, Cl, F, Ge, Hg, I, P, S, Sb, Se, and Tl) can be converted into volatile species and can be totally or partially lost during the sample preparation step. These losses can be more severe when higher decomposition temperatures are used or species that contribute to the loss of some elements are present in the sample matrix [3, 6].

In this sense, in view of the fact that most nonmetals are oxidized to volatile species during dry ashing, this method has been widely applied for subsequent determination of metals. Despite this, the use of ashing aids such as alkali metal oxides, hydroxides, or carbonates, which are able to form nonvolatile compounds with nonmetals, can contribute to the reduction of losses of elements by volatilization [6]. However, it is important to mention that the use of ashing aids can result in contamination or interference during the determination step.

Other disadvantages related to the use of the dry ashing method are the possibility of losses by projection of sample outside the crucible during heating [3] and the high amount of time commonly required for sample preparation (from 2 to 16 h) [59, 63–65, 67, 68]. In this context, analytical instruments based on MW heating have been developed that can contribute to overcoming these drawbacks. In these systems, the MW furnace chamber is heated by the interaction of MW radiation with MW-absorbing elements (e.g., SiC) [3, 12]. The furnace chamber is insulated with an MW-transparent ceramic housing, which minimizes heat loss and transfer to the surrounding area [3, 69].

MW instruments greatly reduce the time required to perform the digestion of samples by dry ashing. The time involved in the digestion step using this approach is generally less than 1 h.

Currently, some systems based on MW heating are commercially available. A commercial MW furnace system is available in two configurations: high temperature and high capacity [15]. The high-temperature furnace reaches 1200 °C and allows processing of up to eight crucibles (25 mL) per run. On the other hand, some furnaces can reach 1000 °C and process up to 15 crucibles (25 mL) per run. In these systems, any type of crucible normally used in conventional muffle furnaces may also be used, including platinum crucibles. Moreover, this system has programmable temperature control, auto-start/auto-shutdown software, a built-in exhaust system, entry and storage of up to 20 methods, and a built-in diagnostics system [15].

Another MW muffle furnace system allows a fast heating rate, and thus it can reach a temperature of 800 °C in less than 30 min (Pyro, Milestone Inc.). Furthermore, this system has a large cavity, which makes it possible to use up to 12 crucibles (40 mm wide) at a time. The characteristics of the MW-absorbing silicon carbide elements allow the use of many types of crucibles (e.g., metal, porcelain, quartz) within the MW furnace, as in the recently introduced system [15]. Additionally, a dedicated system for sulfate ashing was recently introduced in the market. It enables analysts to add H<sub>2</sub>SO<sub>4</sub> to samples and place crucibles directly into the MW muffle furnace, when a sulfate ashing procedure needs to be performed [69]. Although these systems have contributed to overcoming the disadvantages of the dry ashing method using conventional muffle furnaces, drawbacks such as the possibility of losses of some elements by volatilization can still occur, leading to inaccurate results. In this sense, MIC can be an alternative, especially because it involves the use of a closed system for sample preparation.

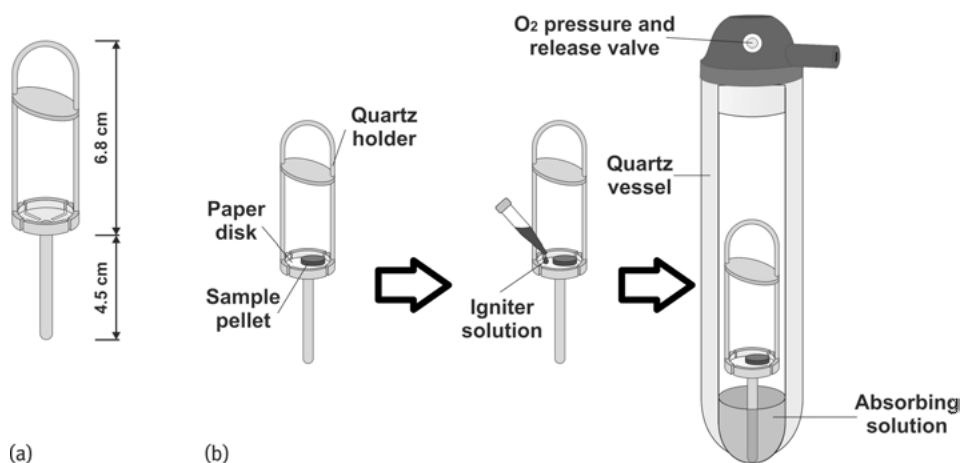
#### **23.4.2 Microwave-induced combustion**

MIC involves the oxidation of organic matter in a closed vessel pressurized with oxygen, and ignition is assisted by MW radiation. This system is commercially available (Anton Paar GmbH) and combines the advantages of both combustion and MW-as-

sisted wet digestion methods in closed systems [70]. The main advantages of this method are the possibility to decompose several kinds of samples, achieving lower RCC in digests; the reduced sample preparation time; the possibility to choose the most suitable absorbing solution; and the possibility of further determination of metals and nonmetals. Moreover, the MIC method is performed in the same quartz vessel used for the conventional wet digestion method, minimizing contamination by metals that could be released from the digestion vessel as occurs in a combustion bomb. However, for sample preparation by MIC, a small quartz holder should be inserted into the vessel [3].

The quartz holder used in the MIC method is shown in Figure 23.8a. This holder is made of quartz because quartz is a material that resists the higher temperatures reached during combustion (higher than 1000 °C) and avoids the interaction of analytes with the holder surface. The holder has some slits, which are important to assure that an effective interaction occurs between oxygen and the sample during combustion. Furthermore, the upper part of the holder contains a quartz disk that protects the PTFE cap of the quartz vessel from the flame generated during combustion [3].

In the MIC method, a sample in the form of a pellet or wrapped in a special material (e.g., paper or polyethylene film) is placed on a quartz holder containing a disk of filter paper moistened with ammonium nitrate solution (50  $\mu\text{L}$ , 6  $\text{mol L}^{-1}$ ), which is used as an igniter together with MW radiation [3, 71]. After, the quartz holder is inserted into the quartz vessel containing the absorbing solution, the vessels are closed and pressurized with oxygen (typically 20 bar) before MW heating. After combustion, a reflux step can be used to improve the absorption of the analyte(s) in a suitable solution, which is compatible with the analyte and determination technique. The general procedure for the MIC method is shown in Figure 23.8b [3].



**Fig. 23.8:** (a) Commercial quartz holder with dimensions and (b) general procedure for MIC method.

A  $\text{NH}_4\text{NO}_3$  solution ( $6 \text{ mol L}^{-1}$ ) is commonly used for ignition in MIC, although other oxidizing substances can also be used, such as  $\text{Ca}(\text{NO}_3)_2$ ,  $\text{KNO}_3$ ,  $\text{Mg}(\text{NO}_3)_2$ , and  $\text{NaNO}_3$  [71]. Ignition using these substances occurs because the MW radiation heating the solution added on the filter paper disk promotes an exothermic reaction between the reagent and organic matter, leading to ignition in an oxygen-rich atmosphere [3].

Although the initial applications of the MIC method were devoted to the digestion of biological samples [72, 73], this method is suitable for the digestion of matrices considered hard to digest, such as active pharmaceutical ingredients [74], elastomers [75], carbon nanotubes [76], coal [77], crude oil [78], and petroleum coke [79]. Moreover, the MIC method has been suitable for the subsequent determination of nonmetals in several types of matrices [77–86]. In this context, currently, MIC was selected as the reference method by the National Institute of Standards and Technology (NIST) for the certification of S concentration in sub-bituminous coal, indicating its widespread acceptance and suitability for further certification processes [77].

The MIC method has also been applied to promote the volatilization of some elements from matrices with high inorganic content. An important advantage is that the analyte can be separated from a sample matrix, minimizing inferences in the determination step [3]. Applications of the MIC for sample preparation of matrices with high inorganic content include the further determination of inorganic pollutants (As, Cd, Hg, and Pb) in soil [87, 88], halogens in soil [89], and Cl and F determination in cement [90]. In these studies, a combustible substance (microcrystalline cellulose) was blended with the sample to increase the combustion temperature and make analyte volatilization easier.

For most applications using MIC, especially when biological samples are digested, the use of concentrated reagents is not necessary because it is possible to use dilute acids, alkaline solutions, or even water. In addition, a reflux step from 5 to 10 min is recommended to ensure quantitative results and suitable precision.

Additionally, it is important to emphasize that the maximum sample mass that can be digested by MIC is dependent on the sample composition and the pressure generated in the system during the combustion process. The sample mass commonly used in procedures by MIC is 0.5 g [59, 72–74, 80, 81, 83–86, 91–103]. However, a method was recently proposed that allows the digestion of up to 1 g of honey using microcrystalline cellulose as a combustion aid for further Br and I determination by inductively coupled plasma mass spectrometry (ICP-MS) [82].

Another system based on combustion induced by MW radiation is focused microwave-induced combustion (FMIC) [104]. This system was proposed to overcome the limitation of wet digestion in open vessels that was discussed previously in this chapter. The FMIC method was developed in a commercial focused MW oven, commonly used for wet digestion in open vessels, which allows for temperature control in each cavity and works at atmospheric pressure (Figure 23.9) [3, 104].

The way samples are introduced into a system as well as the ignition process are similar to those used in the MIC method. However, the sample holder is slightly differ-

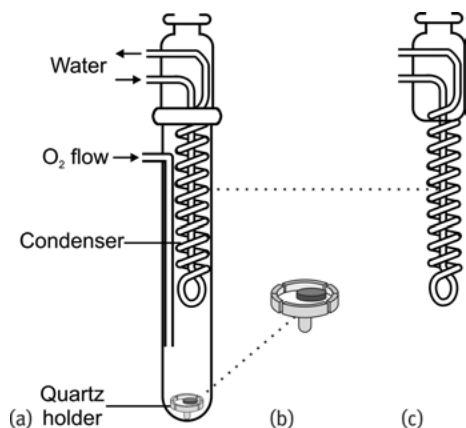


Fig. 23.9: (a) FMIC system, (b) quartz holder, and (c) water-cooled condenser.

ent. The sample holder is also constructed in quartz, and it is positioned about 7 mm from the bottom part of the glass vessel, because in this position better ignition and combustion were observed [104].

For sample preparation by FMIC, the glass vessels originally used in the wet digestion system should be modified to allow the entrance of oxygen flow. This change is carried out to supply oxygen for starting and sustaining the combustion process. Moreover, the ignition step is performed without any solution inside the vessel. Thus, the absorbing solution is added after finishing the combustion process using the reagent addition module, when a reflux step could be performed. This procedure is performed because quickly heating the solution could cause it to evaporate and, consequently, wetting the paper and sample before ignition [3, 104].

In the FMIC system, a lab-made water-cooled condenser is used to assure that the absorbing solution is retained inside the vessel even after 5 min of reflux. Despite the use of a partially open vessel, blank values for FMIC are generally low, probably due to the use of diluted reagents. In addition, as observed for the MIC method, low RCCs (below 1%) have been obtained after digestion of biological samples [3].

Because FMIC was recently proposed, there are still few applications using this sample preparation. However, this method has been applied for the digestion of botanical and biological samples, allowing the digestion of high sample masses (1.5 to 3 g) using only diluted nitric acid solution for analyte absorption [104–106]. The high sample mass digested by FMIC is possible because it is performed in open vessels and oxygen can be supplied during the reaction, which is another advantage compared to MIC.



## 23.5 Safety aspects, quality control, and quality assurance

### 23.5.1 General aspects of safety

The use of MW radiation in sample preparation requires extreme attention of the analyst, especially because concentrated reagents as well as high temperatures are commonly used in this step. In addition, in closed systems the high pressures that can be achieved increase the operational risks. Although several types of equipment include security devices that minimize the possibility of accidents (e.g., pressure release during the digestion process), careful operation and extensive knowledge on the analyst side are of high importance.

In MW systems conventionally used for wet or dry procedures, MWs are distributed inside in a cavity shielded against leakage, unless a particular waveguide is used. During the digestion, security devices limit the emission of MWs in extreme reaction conditions. Thus, it is important to think about the adequacy of domestic MW ovens for sample preparation, especially to assure safe conditions for the analyst.

In this sense, knowledge of the operation of safety devices for each type of equipment is of the utmost importance to ensure the security of the analyst. Moreover, when planning and performing the sample preparation step using MW heating, it is essential to choose safe manipulation practices according to the operational limits [107]. In this section, the main features of security devices in several open and closed MW systems will be discussed.

#### 23.5.1.1 Characteristics of samples, reagents and decomposition system

The type of system (open or closed vessel) and operating conditions (e.g., maximum pressure and temperature, reagents) must be selected according to sample characteristics [108]. In general, security aspects are more critical when samples with high organic content are digested, especially in closed vessels. This occurs in view of the conversion of organic compounds to carbon dioxide and water, which increases the internal pressure of the vessels.

The reagents used for sample digestion methods have a direct impact on safety because most of them are generally toxic, corrosive, and highly reactive. In this context, the analyst should know the safety aspects, toxicity of reagents, and how to prevent accidents that may occur [4, 39]. A general standard safety precaution procedure when handling hazardous chemicals, such as acids, is to use protective eyeglasses and wear gloves, as well as working under a fume hood. The main characteristics of the reagents commonly used in wet digestion are present in Table 23.1. Considering the main characteristics of the reagents, special attention must be given to certain cases, such as the following [112]:

1. Nitric acid should be used with special care when highly aromatic compounds are to be digested. Toluol and other substances containing aromatic structures can

be nitrated to explosive derivatives. Moreover, substances containing glyceride or cellulose bear a high risk of forming highly explosive compounds during reaction with  $\text{HNO}_3$ .

2. The use of  $\text{H}_2\text{SO}_4$  is not recommended in MW-assisted decomposition in view of its low vapor pressure and high boiling temperature, which result in high temperatures that will exceed the limits of polyfluorovessels and can cause irreversible damage. For safe operation, it is recommended to use quartz vessels and measure the temperature directly in the solution.
3. Perchloric acid, with its extremely high inherent chemical energy, is dangerous when in direct contact with organic material, and immediate explosions may happen. In view of its unpredictable behavior in pressurized systems, its use is strongly discouraged, even in mixture with  $\text{HNO}_3$ . Perchloric acid must be handled under specially constructed fume cabinets, with attention to the potential for immediate explosive reactions when in contact with organic materials. Moreover, the walls and tubing of these cabinets must be washed regularly from perchloric acids and salts. Dry perchlorates may explode very rigorously and unpredictably, and thus they are able to damage large parts of laboratories and buildings.
4. Hydrofluoric acid (HF) is a dangerous acid. It is nonodorous, and body contact with the acid is not necessarily realized immediately. It is absorbed by the skin and penetrates easily. When inhaled, it enters the organism rapidly too. Because of its incontrovertible dangers, specific actions of precaution are mandatory before HF is used in practice. Even small amounts of HF or diluted solutions have to be handled according to strict regulations defined on safety data sheets. The user has to be aware of the regulations and follow the advice and specific precautions required for handling this acid in the laboratory. Acid-resistant gloves made of thicker plastics prevent penetration of the acid, even during extended contact. Skin protection – not only from protective goggles but also by a whole-face shield – should be used when working with HF. In case of accidents caused by HF, first-aid equipment must be available in the laboratory, consisting of, for example, calcium gluconate gel, ampoules, or spray.

Combined with the risks of the reagents, the higher heating rates of MW can result in risks to safety, especially when using closed vessels. Thus, MW systems require safety devices and sensors that interrupt MW emission when an unsafe situation is detected [109].

#### *Digestion systems in open vessels*

Concerning digestion systems, it is important to mention that in general open vessel systems are easier to handle when compared to closed vessels. The main security recommendation for this type of system is to use fume exhaust in case of gas release into the laboratory atmosphere. For open vessels, the temperature is generally equal to

or lower than the boiling temperature of reagents involved in the process performed in this system. The safety as well as the quality of digestion is directly related to the reagents and the ramp of temperature used.

When MW radiation is used, the temperature of the solutions inside the reaction vessels should be monitored in real time because the heating is performed directly in the solution. Furthermore, the heating program and sample mass must be optimized carefully to avoid overheating and projections of liquids.

To achieve efficient digestion in open vessels, a large amount of concentrated acids is usually required. The use of concentrated acids in addition to a high temperature is generally suitable for the digestion of several types of materials [110]. However, the high residual acidity in digests can lead to interference during the analysis and damage to equipment components. In this sense, complete (or partial) removal of the original acid used for digestion, and subsequent dissolution in a less concentrated solvent, is a common alternative used to overcome this problem, although overheating and projections of the reaction medium may occur, exposing the analyst to risks.

#### *Digestion systems in closed vessels*

The use of a closed system allows an increase of the boiling temperature of reagents, thereby improving the digestion rate of organic matter. On the other hand, the high pressure reached in these systems requires vessels with suitable mechanical, chemical, and thermal resistance. In this context, the use of closed systems has been considered a trend in analytical chemistry. Currently marketed instruments present different types of vessels (for medium and high pressure) [111–113]. The rotors are equipped with individual control systems or reference vessels for measuring the pressure and temperature during the digestion process. However, the systems for cooling and vessels pressure relief depend on the equipment. Many systems are equipped with a combined exhaust unit, which minimizes the release of acid vapors to the laboratory when the vessels are opened or the security seal fails.

Instantaneous measurement of temperature and pressure in vessels is still considered a challenge. Sensors commonly used on the outside of reaction vessels are not considered accurate and routinely require calibration procedures. On the other hand, sensors containing materials such as PTFE or mixtures containing this polymer (such as PTFE-TFM) – transparent to infrared (IR) when a suitable wavelength is used – are more accurate. Generally, there is a sensor installed in each MW oven and the temperature is measured sequentially in the vessels. In addition, it is possible to limit the maximum temperature and optimize heating ramps. Although IR sensors are widely used in MW systems, the temperature measured outside of the reaction vessels is lower than that inside of the vessels. To overcome this disadvantage, some manufacturers have systems that allow sensors to measure the temperature inside the digestion vessels [111, 113]. However, the sensor is applied to only one reaction vessel, so it is necessary to assure identical conditions in other vessels.

In general, some MW ovens are equipped with cooling systems, which are based on airflows into the cavity [42, 113] or around the digestion vessels [111]. External cooling of vessels is important to achieve higher temperatures while preventing excessive increases of pressure [111, 112].

Pressure sensors can be based on the expansion of gases inside vessels, and pressure measurement is performed through moving parts detected by an optical sensor [114]. Alternatively, the pressure inside vessels may be measured using an internal sensor.

Some instruments are equipped with safety devices that allow gases to be released when the maximum system pressure is exceeded [112, 113]. In case of an explosion, some types of equipment are programmed not to open the door in order to ensure safer conditions for the analyst [113].

In view of the risks during the digestion process when using high-pressure vessels, some manufacturers have developed semiclosed systems [113]. In these systems it is possible to control the release of the generated gases through the opening of a valve at a preselected pressure. It is important to mention that in these systems the vessels are not completely depressurized during digestion in order to avoid losses of analytes and projections.

In this sense, a protocol for the temperature, pressure, and power measurements is common when digestion is performed on modern instruments, as these operational requirements are important to the safety of a method. The analyst must choose the parameters of the method while taking the type of sample into account.

## 23.5.2 Analytical quality assurance

### 23.5.2.1 Method development

Several guidelines in the literature aim to make method development a simpler task. However, several parameters must be considered in order to assure safe conditions as well as accurate results.

First, it is necessary to select a suitable digestion method from those often available in cookbooks for MW ovens. This choice should be carried out by taking into account the literature, the conditions recommended by the instrument manufacturer, and the characteristics of the sample.

In this sense, it is always recommended to start with a small sample mass and to know the behavior of the reagents to be used. In addition, the use of a method with a low heating ramp is preferable when the sample reactivity is unknown. Another consideration that should be highlighted is the importance of choosing an appropriate sample mass for digestion with the aim of achieving the maximal analyte concentration in the solution for measurement as well as full digestion or extraction without overloading the instrument. For open systems, for example, although they allow digestion of larger sample masses without increasing the vessel pressure, they may be

susceptible to losses of volatile analytes and contamination, which can cause problems in the reproducibility, accuracy, and precision of results [115]. In this way, it is also important to mention that knowledge about the stability of the analytes during the process of digestion or extraction and of the chemicals used is a required precondition [116].

During method development, some parameters should be evaluated to prevent the occurrence of interference and assure the efficiency of the method and quality of the results. Determination techniques such as those based on electrochemical phenomena require a full conversion of the analyte element into the ionic state as well as a complete digestion with very low levels of residual carbon to assure the precision and accuracy of the results [116]. Another important parameter is the final concentration of acids in digests, which should be as similar as possible to the calibration solutions. In addition to the parameters cited earlier, the reagent-to-sample ratio should also be considered. Moreover, the reagents used in the sample preparation method must be suitable for the determination techniques and, in this case, the use of HF is usually avoided considering that most equipment devices are made of glass or quartz. The interaction of reagents with analytes must also be considered because in some cases the analytes could form insoluble compounds (e.g., BaSO<sub>4</sub> when H<sub>2</sub>SO<sub>4</sub> is used for sample digestion) or compounds that can cause spectral interference in the determination step, such as the very well-known interference of <sup>40</sup>Ar<sup>35</sup>Cl<sup>+</sup> when determining <sup>75</sup>As<sup>+</sup> by CP-MS analysis (if HCl is used in sample digestion) [7]. These examples demonstrate the importance of a careful evaluation of all the factors that may directly or indirectly affect the analytical quality assurance [9, 116].

To validate the method, parameters such as linearity, linear range, repeatability and reproducibility, LOD and limit of quantification, robustness, and accuracy must be carefully evaluated. In this process, the use of a sample with the same or a similar matrix and with a known element or species concentration is highly recommended to ensure the accuracy of the results. The most common strategies are digestion of a certified reference material (CRM) or a well-analyzed laboratory standard and recovery tests with a standard solution. This is performed by spiking the sample prior to sample preparation, and it will only provide accurate information when the analyte is added on a sample of the same chemical species that is present in the sample. In this sense, it is possible to highlight the importance of using appropriate strategies for the evaluation of accuracy or method validation.

### 23.5.2.2 Instrumental and operative quality control

The proper functioning of the MW unit for sample preparation is as important as careful method development. For this reason, periodic verification of the instrument should be performed, paying attention to the temperature, pressure, power, and cooling sensor/control, especially in closed systems. The power of MWs, for example, is not a constant parameter of the equipment, and for this reason the manufacturer

should supply instructions and tools for calibration of the effective MW power to assure reproducible program conditions. Temperature is another parameter that is very important for the quality of digestion, and it should also be properly measured, especially in extraction methods, which require an accurate control [117].

Final digests with color and remaining solids generally indicate an inefficient sample digestion, which may occur for several reasons. Moreover, sometimes a colorless solution may still contain significant amounts of carbon, which may interfere in the determination step, and so the concentration of the element should always be verified [8]. The main problems are related to the use of unsuitable MW irradiation programs, such as the use of a very short digestion time, as well as a low temperature reached during digestion. In these cases, it is necessary to change the MW program to improve the digestion efficiency. In some cases it is also necessary to conduct a careful evaluation of the chemicals used in the digestion process. Samples containing silica or titanium dioxide, for example, usually need HF or HCl to dissolve these components and provide suitable solutions for analysis. Hydrofluoric acid and hydrochloric acid are often used to dissolve silicates arising from a matrix and metallic precipitates formed during digestion, respectively.

### 23.5.2.3 Analytical quality control

One of the main sources of error in analytical chemistry is sample contamination, which can be the result of the chemicals, materials, and procedures used during sample preparation and determination. In this way, especially for the determination of elements at low concentration, it is recommended to use only suprapure or sub-boiling distilled chemicals. Moreover, all materials coming in contact with the sample, sample solution, and calibration solutions should be washed and decontaminated in advance, generally with diluted nitric acid followed by ultrapure water, including new equipment and accessories before the first use [118].

Digestion vessels must always be cleaned after each use in order to avoid carry-over to the next digest. Scratches should be avoided during mechanical cleaning, regardless of the type of material the vessels are made of. This is important because scratches inside vessels contribute to the risk of explosion, particularly in quartz vessels, and increase the adsorption of elements or molecules on the corroded surface, which can result in analyte losses or increased memory effects.

Samples with low levels of an element should be digested prior to samples with high concentrations of that element in aims of avoiding cross-contamination. In addition, storage vessels of digests as well as the storage conditions should always be evaluated with respect to analyte stability in solution.

To control all of these probable sources of error, it is strongly recommended to carry out at least one blank decomposition per batch. This is very important for analytical quality assurance and must contain the same chemicals as used for the samples. In addition, it is worth noting that the experiments should always be performed at

least in triplicate. Independent repetition analysis of one sample is also recommended and may provide information about homogeneity as well as analyte losses or sample contamination. Nevertheless, it is not usually performed due to the resulting increase in analysis time [116].

After all, as previously mentioned, an appropriate method of validation or accuracy evaluation must be done. With regard to recovery tests using standard solutions, a rate between 90 and 110% is usually accepted as a tolerable level. If the analyte recovery is less than the set limits, the method has to be optimized. Moreover, recovery alone does not guarantee full availability of the analytes. A more appropriate way to check accuracy is to use a known standard reference material with a composition close to that of the sample of interest.

Despite this, the use of a CRM or, alternatively, a well-known sample, which should present the same or a similar sample matrix, is certainly the most appropriate method of analytical quality control [119, 120]. The analyte concentration in these materials shall also be similar to that of the sample. Recommendations described in the certificates of these materials with respect to their use (drying, homogeneity, among others) should be followed in order to obtain reliable results. Additionally, the use of reference methods as well as those described in the literature and other determination techniques is also useful to ensure the quality of results and the accuracy of the method.

## 23.6 Conclusions

Taking into account the use of MWs as a source of heating for sample preparation, some advantages can be highlighted. They provide localized heating, allowing higher heating rates and shorter processing times. Because the vessel walls are MW transparent, they do not heat directly through MW interaction, allowing a selective heating of solution with low losses of heat. Modern instrumentation is relatively compact, with pressure and temperature sensors that offer safe operational conditions. The possibility of monitoring several parameters during the chemical process allows better understanding of chemical reactions and, for instance, a rational use of reagents in order to save costs and prevent residue generation. These aspects, although dependent not only on MW heating, can be considered consequences of MW technology and will certainly change the routine of every analytical laboratory.

## Bibliography

- [1] Abusamra A, Morris JS, Koirtyohann SR. Wet ashing of some biological samples in a microwave oven, *Analytical Chemistry* 1975, 47(8), 1475–1477.

- [2] CE(2002). "Guide to Quality in Analytical Chemistry. An Aid to Accreditation." CITAC/ EURACHEM, Teddington.
- [3] Flores EMM. Microwave-assisted sample preparation for trace element determination, Elsevier, Amsterdam, 2014.
- [4] Arruda MAZ. Trends in sample preparation. New York: Nova Science Publishers, 2007. 304 p.
- [5] Kingston HM, Jassie LB. Introduction to Microwave Sample Preparation: Theory and Practice, American Chemical Society 1988.
- [6] Anderson R. Sample pretreatment and separation. Analytical chemistry by open learning, John Wiley & Sons, London, 1987.
- [7] Montaser A. Inductively Coupled Plasma Mass Spectrometry, Wiley 1998.
- [8] Matusiewicz H. Wet digestion methods, in: Mester Z, Sturgeon R(Eds.), Sample Preparation for Trace Element Analysis, Elsevier, Amsterdam, 2003, pp. 193–234.
- [9] Muller EI, Mesko MF, Moraes DP, Korn MGA, .Flores EMM. Wet digestion using microwave heating, in: Flores EMM ed., Microwave-assisted sample preparation for trace element determination, Elsevier, Amsterdam, 2014, p. 400.
- [10] Kingston HM, Haswell SJ, Microwave-enhanced Chemistry: Fundamentals, Sample Preparation, and Applications, American Chemical Society 1997.
- [11] Zlotorzynski A. The application of microwave-radiation to analytical and environmental chemistry, Critical Reviews in Analytical Chemistry 1995, 25(1), 43–76.
- [12] Kremsner JM, Kappe CO. Silicon Carbide Passive Heating Elements in Microwave-Assisted Organic Synthesis, The Journal of Organic Chemistry 2006, 71(12), 4651–4658.
- [13] Grindlay G, Gras L, Mora J, de Loos-Vollebregt MTC. Carbon-related matrix effects in inductively coupled plasma atomic emission spectrometry, Spectrochimica Acta Part B-Atomic Spectroscopy 2008, 63(2), 234–243.
- [14] Grindlay G, Mora J, de Loos-Vollebregt M, Vanhaecke F. A systematic study on the influence of carbon on the behavior of hard-to-ionize elements in inductively coupled plasma-mass spectrometry, Spectrochimica Acta Part B-Atomic Spectroscopy 2013, 86, 42–49.
- [15] Corporation C, CEM Corporation, Phoenix. <http://cem.com/phoenix/>, (accessed October 05.2016).
- [16] Santos DM, Pedroso MM, Costa LM, Nogueira ARA, Nobrega JA. A new procedure for bovine milk digestion in a focused microwave oven: gradual sample addition to pre-heated acid, Talanta 2005, 65(2), 505–510.
- [17] Matusiewicz H. Systems for microwave-assisted wet digestion, in: Flores EMM ed., Microwave-assisted sample preparation for trace element determination, Elsevier, Amsterdam, 2014, pp. 77–96.
- [18] Baghurst DR, Mingos DMP. Superheating effects associated with microwave dielectrical heating, Journal of the Chemical Society-Chemical Communications 1992, 9, 674–677.
- [19] Daniel MM, Batchelor JD, Rhoades CB, Jones BT. The effect of digestion temperature on matrix decomposition using a high pressure asher, Atomic Spectroscopy 1998, 19(6), 198–203.
- [20] Flores EMM, Saidelles APF, Barin JS, Mortari SR, Martins AF. Hair sample decomposition using polypropylene vials for determination of arsenic by hydride generation atomic absorption spectrometry, Journal of Analytical Atomic Spectrometry 2001, 16(12), 1419–1423.
- [21] Brancalion ML, Arruda MAZ. Evaluation of medicinal plant decomposition efficiency using microwave ovens and mini-vials for Cd determination by TS-FF-AAS, Microchimica Acta 2005, 150(3–4), 283–290.
- [22] Sussulini A, Garcia JS, Arruda MAZ. Microwave-assisted decomposition of polyacrylamide gels containing metalloproteins using mini-vials: An auxiliary strategy for metallomics studies, Analytical Biochemistry 2007, 361(1), 146–148.



- [23] Kingston HM, Jassie LB. Microwave-energy for acid decomposition at elevated-temperatures and pressure using biological and botanical samples, *Analytical Chemistry* 1986, 58(12), 2534–2541.
- [24] Richter RC, Link D, Kingston HM. Microwave-enhanced chemistry, *Analytical Chemistry* 2001, 73(1), 30A-37A.
- [25] Bizzi CA, Nobrega JA, Barin JS. Diluted acids in microwave-assisted wet digestion, in: Flores EMM ed., *Microwave-assisted sample preparation for trace element determination*, Elsevier, Amsterdam, 2014, pp. 179–204.
- [26] Zischka M, Kettisch P, Schalk A, Knapp G. Closed vessel microwave-assisted wet digestion with simultaneous control of pressure and temperature in all vessels, *Fresenius Journal of Analytical Chemistry* 1998, 361(2), 90–95.
- [27] Pereira JSF, Wiltische H, Knapp G. Microwave-assisted ultraviolet digestion, in: Flores EMM ed., *Microwave-assisted sample preparation for trace element determination*, Elsevier, Amsterdam, 2014, pp. 205–229.
- [28] Grinberg P, Sturgeon RE. Photochemical vapor generation of iodine for detection by ICP-MS, *Journal of Analytical Atomic Spectrometry* 2009, 24(4), 508–514.
- [29] Sturgeon RE, Willie SN, Mester Z, UV/spray chamber for generation of volatile photo-induced products having enhanced sample introduction efficiency, *Journal of Analytical Atomic Spectrometry* 2006, 21(3), 263–265.
- [30] Grinberg P, Sturgeon RE. Ultra-trace determination of iodine in sediments and biological material using UV photochemical generation-inductively coupled plasma mass spectrometry, *Spectrochimica Acta Part B-Atomic Spectroscopy* 2009, 64(3), 235–241.
- [31] Florian D, Knapp G. High-temperature, microwave-assisted UV digestion: A promising sample preparation technique for trace element analysis, *Analytical Chemistry* 2001, 73(7), 1515–1520.
- [32] Mesko MF, Picoloto RS, Ferreira LR, Costa VC, Pereira CMP, Colepicolo P, Muller EI, Flores EMM. Ultraviolet radiation combined with microwave-assisted wet digestion of Antarctic seaweeds for further determination of toxic elements by ICP-MS, *Journal of Analytical Atomic Spectrometry* 2015, 30(1), 260–266.
- [33] Hartwig CA, Pereira RM, Rondan FS, Cruz SM, Duarte FA, Flores EMM, Mesko MF. The synergic effect of microwave and ultraviolet radiation for chocolate digestion and further determination of As, Cd, Ni and Pb by ICP-MS, *Journal of Analytical Atomic Spectrometry* 2016, 31(2), 523–530.
- [34] Pereira JSF, Picoloto RS, Pereira LSF, Guimaraes RCL, Guarnieri AR, Flores EMM. High-Efficiency Microwave-Assisted Digestion Combined to in Situ Ultraviolet Radiation for the Determination of Rare Earth Elements by Ultrasonic Nebulization ICPMS in Crude Oils, *Analytical Chemistry* 2013, 85(22), 11034–11040.
- [35] Oliveira JSS, Picoloto RS, Bizzi CA, Mello PA, Barin JS, Flores EMM. Microwave-assisted ultraviolet digestion of petroleum coke for the simultaneous determination of nickel, vanadium and sulfur by ICP-OES, *Talanta* 2015, 144, 1052–1058.
- [36] Bizzi CA, Flores EMM, Picoloto RS, Barin JS, Nobrega JA. Microwave-assisted digestion in closed vessels: effect of pressurization with oxygen on digestion process with diluted nitric acid, *Analytical Methods* 2010, 2(6), 734–738.
- [37] Bizzi CA, Barin JS, Garcia EE, Nobrega JA, Dressler VL, Flores EMM. Improvement of microwave-assisted digestion of milk powder with diluted nitric acid using oxygen as auxiliary reagent, *Spectrochimica Acta Part B-Atomic Spectroscopy* 2011, 66(5), 394–398.
- [38] Bizzi CA, Barin JS, Muller EI, Schmidt L, Nobrega JA, Flores EMM. Evaluation of oxygen pressurized microwave-assisted digestion of botanical materials using diluted nitric acid, *Talanta* 2011, 83(5), 1324–1328.

- [39] Bizzi CA, Flores EMM, Barin JS, Garcia EE, Nobrega JA. Understanding the process of microwave-assisted digestion combining diluted nitric acid and oxygen as auxiliary reagent, *Microchemical Journal* 2011, 99(2), 193–196.
- [40] Bizzi CA, Flores ELM, Nobrega JA, Oliveira JSS, Schmidt L, Mortari SR. Evaluation of a digestion procedure based on the use of diluted nitric acid solutions and H<sub>2</sub>O<sub>2</sub> for the multielement determination of whole milk powder and bovine liver by ICP-based techniques, *Journal of Analytical Atomic Spectrometry* 2014, 29(2), 332–338.
- [41] Castro JT, Santos EC, Santos WPC, Costa LM, Korn M, Nobrega JA, Korn MGA. A critical evaluation of digestion procedures for coffee samples using diluted nitric acid in closed vessels for inductively coupled plasma optical emission spectrometry, *Talanta* 2009, 78(4–5), 1378–1382.
- [42] Bizzi CA, Nobrega JA, Barin JS, Oliveira JSS, Schmidt L, Mello PA, Flores EMM. Effect of simultaneous cooling on microwave-assisted wet digestion of biological samples with diluted nitric acid and O<sub>2</sub> pressure, *Analytica Chimica Acta* 2014, 837, 16–22.
- [43] Nobrega JA, Pirola C, Fialho LL, Rota G, Jordao C, Pollo F. Microwave-assisted digestion of organic samples: How simple can it become?, *Talanta* 2012, 98, 272–276.
- [44] Muller ALH, Oliveira JSS, Mello PA, Muller EI, Flores EMM. Study and determination of elemental impurities by ICP-MS in active pharmaceutical ingredients using single reaction chamber digestion in compliance with USP requirements, *Talanta* 2015, 136, 161–169.
- [45] Pereira LSF, Pedrotti MF, Miceli TM, Pereira JSF, Flores EMM. Determination of elemental impurities in poly(vinyl chloride) by inductively coupled plasma optical emission spectrometry, *Talanta* 2016, 152, 371–377.
- [46] Druzian GT, Pereira LSF, Mello PA, Mesko MF, Duarte FA, Flores EMM. Rare earth element determination in heavy crude oil by USN-ICP-MS after digestion using a microwave-assisted single reaction chamber, *Journal of Analytical Atomic Spectrometry* 2016, 31(6), 1185–1191.
- [47] Muller CC, Muller ALH, Pirola C, Duarte FA, Flores EMM, Muller EI. Feasibility of nut digestion using single reaction chamber for further trace element determination by ICP-OES, *Microchemical Journal* 2014, 116, 255–260.
- [48] Muller EI, Souza JP, Muller CC, Muller ALH, Mello PA, Bizzi CA. Microwave-assisted wet digestion with H<sub>2</sub>O<sub>2</sub> at high temperature and pressure using single reaction chamber for elemental determination in milk powder by ICP-OES and ICP-MS, *Talanta* 2016, 156, 232–238.
- [49] Anderson R. Sample pretreatment and separation, Wiley India Pvt. Limited 2008.
- [50] Claisse F. Fusion and fluxes, in: n Mester Z, Sturgeon R(Eds.), *Sample preparation for trace element analysis*, Elsevier, Amsterdam, 2003, pp. 301–311.
- [51] King EE, Barclay D. Microwave-based extraction, in: Z.n. Mester, Sturgeon R(Eds.), *Sample preparation for trace element analysis*, Elsevier, Amsterdam, 2003, pp. 257–300.
- [52] Dean JR. *Extraction Techniques in Analytical Sciences*, Wiley 2010.
- [53] Letellier M, Budzinski H. Microwave assisted extraction of organic compounds, *Analisis* 1999, 27(3), 259–271.
- [54] Duarte FA, Oliveira PV, Nogueira ARA. Microwave-assisted extraction, in: Flores EMM ed., *Microwave-assisted sample preparation for trace element determination*, Elsevier, Amsterdam, 2014, pp. 231–251.
- [55] Borkowska-Burnecka J. Microwave assisted extraction for trace element analysis of plant materials by ICP-AES, *Fresenius Journal of Analytical Chemistry* 2000, 368(6), 633–637.
- [56] Mesko MF, Hartwig CA, Bizzi CA, Muller EI, Duarte FA, Mello PA. Separation techniques for elemental speciation in soil, sediments, and environmental samples, in: s. Speciation studies in soil, and environmental samples, Bakirdere S ed., CRC Press, Boca Raton, 2014, pp. 202–241.

- [57] Duarte FA, Pereira JSF, Mesko MF, Goldschmidt F, Flores EMM, Dressier VL. Evaluation of liquid chromatography inductively coupled plasma mass spectrometry for arsenic speciation in water from industrial treatment of shale, *Spectrochimica Acta Part B-Atomic Spectroscopy* 2007, 62(9), 978–984.
- [58] Chemat F, Cravotto G. *Microwave-assisted Extraction for Bioactive Compounds: Theory and Practice*, Springer US2012.
- [59] Pereira LSF, Iop GD, Flores EMM, Burrow RA, Mello PA, Duarte FA. Strategies for the determination of trace and toxic elements in pitch: Evaluation of combustion and wet digestion methods for sample preparation, *Fuel* 2016, 163, 175–179.
- [60] Adeli A, Dabney SM, Tewolde H, Jenkins JN. Effects of tillage and broiler litter on crop productions in an eroded soil, *Soil and Tillage Research* 2017, 165, 198–209.
- [61] Bakirdere S, Bölücek C, Yaman M. Determination of contamination levels of Pb, Cd, Cu, Ni, and Mn caused by former lead mining gallery, *Environmental Monitoring and Assessment* 2016, 188(3), 1–7.
- [62] Enders MSP, de Souza JP, Balestrin P, Mello PA, Duarte FA, Muller EI. Microwave-induced combustion of high purity nuclear flexible graphite for the determination of potentially embrittling elements using atomic spectrometric techniques, *Microchemical Journal* 2016, 124, 321–325.
- [63] Judprasong K, Jongjaithe N, Chavasit V. Comparison of methods for iodine analysis in foods, *Food Chemistry* 2016, 193, 12–17.
- [64] Zornoza R, Moreno-Barriga F, Acosta JA, Muñoz MA, Faz A, Stability, nutrient availability and hydrophobicity of biochars derived from manure, crop residues, and municipal solid waste for their use as soil amendments, *Chemosphere* 2016, 144, 122–130.
- [65] Zubakina EA, Solovyev ND, Savinkova ES, Slesar NI. Sample preparation for cadmium quantification in sunflower (*Helianthus annuus*) seeds using anodic stripping voltammetry, *Analytical Methods* 2016, 8(2), 326–332.
- [66] Chemists OA, Horwitz W. *Official Methods of Analysis of the AOAC International*, The Association.
- [67] Guo X, Meng H, Tang Q, Pan R, Zhu S, Yu S. Effects of the precipitation pH on the ethanolic precipitation of sugar beet pectins, *Food Hydrocolloids* 2016, 52, 431–437.
- [68] Ploegaerts G, Desmet C, Van kriecken M, Assay of sodium in food: Comparison of different preparation methods and assay techniques, *Journal of Food Composition and Analysis* 2016, 45, 66–72.
- [69] Inc M. PYRO and PYRO SA. <http://www.milestonesci.com/pyro-and-pyro-sa>, (accessed October 05, 2016.2016).
- [70] Flores EMM, Barin JS, Mesko MF, Knapp G. Sample preparation techniques based on combustion reactions in closed vessels – A brief overview and recent applications, *Spectrochimica Acta Part B: Atomic Spectroscopy* 2007, 62(9), 1051–1064.
- [71] Pereira LSF, Bizzi CA, Schmidt L, Mesko MF, Barin JS, Flores EMM. Evaluation of nitrates as igniters for microwave-induced combustion: understanding the mechanism of ignition, *RSC Advances* 2015, 5(13), 9532–9538.
- [72] Mesko MF, de Moraes DP, Barin JS, Dressler VL, Knapp G, de Moraes Flores EMM. Digestion of biological materials using the microwave-assisted sample combustion technique, *Microchemical Journal* 2006, 82(2), 183–188.
- [73] Flores EMM, Barin JS, Paniz JNG, Medeiros JA, Knapp G. Microwave-Assisted Sample Combustion: A Technique for Sample Preparation in Trace Element Determination, *Analytical Chemistry* 2004, 76(13), 3525–3529.

- [74] Barin JS, Tischer B, Picoloto RS, Antes FG, da Silva FEB, Paula FR, Flores EMM. Determination of toxic elements in tricyclic active pharmaceutical ingredients by ICP-MS: a critical study of digestion methods, *Journal of Analytical Atomic Spectrometry* 2014, 29(2), 352–358.
- [75] Moraes DP, Mesko MF, Mello PA, Paniz JNG, Dressler VL, Knapp G, Flores EMM. Application of microwave induced combustion in closed vessels for carbon black-containing elastomers decomposition, *Spectrochimica Acta Part B: Atomic Spectroscopy* 2007, 62(9), 1065–1071.
- [76] Antes FG, dos Santos MFP, Guimarães RCL, Paniz JNG, Flores EMM, Dressler VL. Heavy crude oil sample preparation by pyrohydrolysis for further chlorine determination, *Analytical Methods* 2011, 3(2), 288–293.
- [77] Christopher SJ, Vetter TW. Application of Microwave-Induced Combustion and Isotope Dilution Strategies for Quantification of Sulfur in Coals via Sector-Field Inductively Coupled Plasma Mass Spectrometry, *Analytical Chemistry* 2016, 88(9), 4635–4643.
- [78] Pereira JSF, Moraes DP, Muller EI, Barin JS, Diehl LO, Mesko MF, Dressler VL, Flores EMM. Chlorine determination in crude oil fractions after digestion using microwave-induced combustion, *Brazilian Journal of Analytical Chemistry* 2011, 3, 119–123.
- [79] Pereira JSF, Diehl LO, Duarte FA, Santos MFP, Guimarães RCL, Dressler VL, Flores EMM. Chloride determination by ion chromatography in petroleum coke after digestion by microwave-induced combustion, *Journal of Chromatography A* 2008, 1213(2), 249–252.
- [80] Pereira JSF, Moreira CM, Albers CN, Jacobsen OS, Flores EMM. Determination of total organic halogen (TOX) in humic acids after microwave-induced combustion, *Chemosphere* 2011, 83(3), 281–286.
- [81] Crizel MG, Hartwig CA, Novo DLR, Toralles IG, Schmidt L, Muller EI, Mesko MF. A new method for chlorine determination in commercial pet food after decomposition by microwave-induced combustion, *Analytical Methods* 2015, 7(10), 4315–4320.
- [82] Costa VC, Picoloto RS, Hartwig CA, Mello PA, Flores EMM, Mesko MF. Feasibility of ultra-trace determination of bromine and iodine in honey by ICP-MS using high sample mass in microwave-induced combustion, *Analytical and Bioanalytical Chemistry* 2015, 407(26), 7957–7964.
- [83] Mesko MF, Mello PA, Bizzi CA, Dressler VL, Knapp G, Flores EMM. Iodine determination in food by inductively coupled plasma mass spectrometry after digestion by microwave-induced combustion, *Analytical and Bioanalytical Chemistry* 2010, 398(2), 1125–1131.
- [84] Mello PA, Giesbrecht CK, Alencar MS, Moreira EM, Paniz JNG, Dressler VL, Flores MM. Determination of Sulfur in Petroleum Coke Combining Closed Vessel Microwave-Induced Combustion and Inductively Coupled Plasma-Optical Emission Spectrometry, *Analytical Letters* 2008, 41(9), 1623–1632.
- [85] Muller ALH, Mello PA, Mesko MF, Duarte FA, Dressler VL, Muller EI, Flores EMM. Bromine and iodine determination in active pharmaceutical ingredients by ICP-MS, *Journal of Analytical Atomic Spectrometry* 2012, 27(11), 1889–1894.
- [86] Antes FG, Pereira JSF, Spadoa LC, Muller EI, Flores EMM, Dressler VL. Fluoride determination in carbon nanotubes by ion selective electrode, *Journal of the Brazilian Chemical Society* 2012, 23, 1193–1198.
- [87] Picoloto RS, Wiltsche H, Knapp G, Barin JS, Flores EMM. Mercury determination in soil by CVG-ICP-MS after volatilization using microwave-induced combustion, *Analytical Methods* 2012, 4(3), 630–636.
- [88] Picoloto RS, Wiltsche H, Knapp G, Mello PA, Barin JS, Flores EMM. Determination of inorganic pollutants in soil after volatilization using microwave-induced combustion, *Spectrochimica Acta Part B: Atomic Spectroscopy* 2013, 86, 123–130.

- [89] Pereira LSF, Pedrotti MF, Enders MSP, Albers CN, Pereira JSF, Flores EMM. Multitechnique Determination of Halogens in Soil after Selective Volatilization Using Microwave-Induced Combustion, *Analytical Chemistry* 2017, 89(1), 980–987.
- [90] Pereira RM, Costa VC, Hartwig CA, Picoloto RS, Flores EMM, Duarte FA, Mesko MF. Feasibility of halogen determination in noncombustible inorganic matrices by ion chromatography after a novel volatilization method using microwave-induced combustion, *Talanta* 2016, 147, 76–81.
- [91] Hartwig CA, Toralles IG, Crizel MG, Hermes Muller AL, Picoloto RS, Moraes Flores EM, Mesko MF. Determination of bromine and iodine in shrimp and its parts by ICP-MS after decomposition using microwave-induced combustion, *Analytical Methods* 2014, 6(18), 7540–7546.
- [92] Mesko MF, Toralles IG, Crizel MG, Costa VC, Pires NRX, Pereira CMP, Picoloto RS, Mello PA. Determinação de bromo e iodo em alga marinha comestível por ICP-MS após decomposição por combustão iniciada por micro-ondas, *Química Nova* 2014, 37, 964–968.
- [93] Mesko MF, Toralles IG, Hartwig CA, Coelho GS, Muller ALH, Bizzi CA, Mello PA. Bromine and Iodine Contents in Raw and Cooked Shrimp and Its Parts, *Journal of Agricultural and Food Chemistry* 2016, 64(8), 1817–1822.
- [94] Antes FG, Duarte FA, Mesko MF, Nunes MAG, Pereira VA, Müller EI, Dressler VL, Flores EMM. Determination of toxic elements in coal by ICP-MS after digestion using microwave-induced combustion, *Talanta* 2010, 83(2), 364–369.
- [95] Bizzi CA, Paniz JNG, Rodrigues LF, Dressler VL, Flores EMM. Solid sampling coupled to flame furnace atomic absorption spectrometry for Mn and Ni determination in petroleum coke, *Microchemical Journal* 2010, 96(1), 64–70.
- [96] Maciel JV, Knorr CL, Flores EMM, Müller EI, Mesko MF, Primel EG, Duarte FA. Feasibility of microwave-induced combustion for trace element determination in *Engraulis anchoita* by ICP-MS, *Food Chemistry* 2014, 145, 927–931.
- [97] Cruz SM, Schmidt L, Dalla Nora FM, Pedrotti MF, Bizzi CA, Barin JS, Flores EMM. Microwave-induced combustion method for the determination of trace and ultratrace element impurities in graphite samples by ICP-OES and ICP-MS, *Microchemical Journal* 2015, 123, 28–32.
- [98] Muller ALH, Muller CC, Lyra F, Mello PA, Mesko MF, Muller EI, Flores EMM. Determination of Toxic Elements in Nuts by Inductively Coupled Plasma Mass Spectrometry after Microwave-Induced Combustion, *Food Analytical Methods* 2013, 6(1), 258–264.
- [99] Pereira JSF, Pereira LSF, Mello PA, Guimaraes RCL, Guarnieri RA, Fonseca TCO, Flores EMM. Microwave-induced combustion of crude oil for further rare earth elements determination by USN-ICP-MS, *Analytica Chimica Acta* 2014, 844, 8–14.
- [100] Moraes DP, Pereira JSF, Diehl LO, Mesko MF, Dressler VL, Paniz JNG, Knapp G, Flores MM. Evaluation of sample preparation methods for elastomer digestion for further halogens determination, *Analytical and Bioanalytical Chemistry* 2010, 397(2), 563–570.
- [101] Barbosa JTP, Santos CMM, dos Santos Bispo L, Lyra FH, David JM, d M. Korn GA, Flores EMM. Bromine, Chlorine, and Iodine Determination in Soybean and its Products by ICP-MS After Digestion Using Microwave-Induced Combustion, *Food Analytical Methods* 2013, 6(4), 1065–1070.
- [102] Müller ALH, Bizzi CA, Pereira JSF, Mesko MF, Moraes DP, Flores EMM, Muller EI. Bromine and chlorine determination in cigarette tobacco using microwave-induced combustion and inductively coupled plasma optical emission spectrometry, *Journal of the Brazilian Chemical Society* 2011, 22, 1649–1655.
- [103] Duarte FA, Pereira JSF, Barin JS, Mesko MF, Dressler VL, Flores EMM, Knapp G. Seafood digestion by microwave-induced combustion for total arsenic determination by atomic spectrometry techniques with hydride generation, *Journal of Analytical Atomic Spectrometry* 2009, 24(2), 224–227.

- [104] Mesko MF, Pereira JSF, Moraes DP, Barin JS, Mello PA, Paniz JNG, Nóbrega JA, Korn MGA, Flores EMM. Focused Microwave-Induced Combustion: A New Technique for Sample Digestion, *Analytical Chemistry* 2010, 82(5), 2155–2160.
- [105] Barin JS, Pereira JSF, Mello PA, Knorr CL, Moraes DP, Mesko MF, Nóbrega JA, Korn MGA, Flores EMM. Focused microwave-induced combustion for digestion of botanical samples and metals determination by ICP OES and ICP-MS, *Talanta* 2012, 94, 308–314.
- [106] Pereira JSF, Pereira LSF, Schmidt L, Moreira CM, Barin JS, Flores EMM. Metals determination in milk powder samples for adult and infant nutrition after focused-microwave induced combustion, *Microchemical Journal* 2013, 109, 29–35.
- [107] Leadbeater N E; Mcgowan CB Laboratory experiments using microwave heating. Boca Raton: CRC Press, 2013, 232 p.
- [108] Flores ÉMM, Barin JS, Mesko MF, Knapp G. Sample preparation techniques based on combustion reactions in closed vessels – A brief overview and recent applications, *Spectrochimica Acta Part B: Atomic Spectroscopy* 2007, 62(9), 1051–1064.
- [109] Mello PA, Barin JS, Guarnieri RA, É.M.d.M. Flores, *Microwave Heating, Microwave-Assisted Sample Preparation for Trace Element Analysis*, Elsevier, Amsterdam, 2014, pp. 59–75.
- [110] Mello PA, Pereira JSF, Mesko MF, Barin JS, Flores EMM. Sample preparation methods for subsequent determination of metals and non-metals in crude oil – A review, *Analytica Chimica Acta* 2012, 746, 15–36.
- [111] Anton Paar – Sample Preparation.; available in <http://www.anton-paar.com/corp-en/products/group/sample-preparation/> accessed in october, 2016.
- [112] Berghof – Digestion Technology. Available in <http://www.berghof.com/en/products/laboratory-equipment/digestion-technology/microwave-digestion/overview/>. Accessed in October, 2016.
- [113] Milestone – Microwave Digestion. Available in <http://www.milestonesrl.com/en/microwavedigestion.html>. Accessed in october, 2016.
- [114] Fecher PA, Schlemmer GC, Schoeberl KS. Safety aspects, quality control, and quality assurance using microwave-assisted sample preparation systems, in: Flores ÉMM ed., *Microwave-Assisted sample preparation for trace element determination*, Elsevier, Amsterdam, 2014, pp. 345–384.
- [115] Mello PA, Barin JS, Duarte FA, Bizzi CA, Diehl LO, Muller EI, Flores EMM. Analytical methods for the determination of halogens in bioanalytical sciences: a review, *Analytical and Bioanalytical Chemistry* 2013, 405(24), 7615–7642.
- [116] Fecher PA, Schlemmer GC, Schoeberl KS, Flores ÉMM, Chapter 12 – Safety Aspects, Quality Control, and Quality Assurance using Microwave-Assisted Sample Preparation Systems, *Microwave-Assisted Sample Preparation for Trace Element Analysis*, Elsevier, Amsterdam, 2014, pp. 345–384.
- [117] Ottenender H. Rückstände und Kontaminanten in Getreide und Getreideerzeugnissen, *Agri-media*, Clenze, 2010.
- [118] DIN EN 13805. Foodstuffs – Determination of trace elements – Pressure digestion. Beuth Verlag. Publication date 2002-06. Updated version expected in 2014.
- [119] DIN EN 13804. Determination of elements and their chemical species – General considerations and specific requirements. Beuth Verlag. Publication date 2013-06.
- [120] ISO/IEC Guide 98-3 (2008). Uncertainty of measurement – part 3: guide of the expression of uncertainty in measurement. ISO, Geneva.

Juliano Smanioto Barin, Fábio Andrei Duarte, Paola de Azevedo Mello, and Éder Lisandro de Moraes Flores

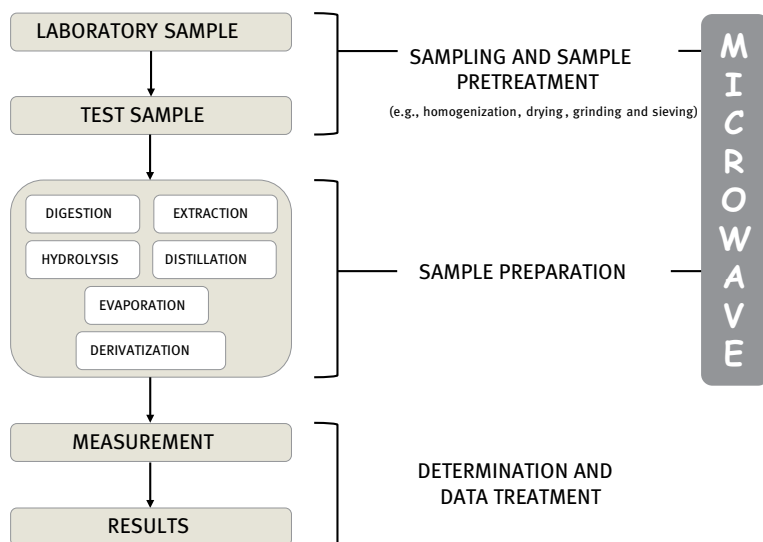
## 24 Microwave-assisted sample preparation for organic analysis

### 24.1 Introduction

Although many instrumental techniques for the determination of analytes have matured and automation is commonplace, sample preparation is still considered slow, labor-intensive, and a bottleneck in laboratory processes [1]. Even though many new solutions/products are available to improve such methodologies, users are still faced with the same dated problems regarding sample preparation. Taking into account that the analytical steps are much faster (e.g., chromatographic analysis is now performed in a few minutes), the slowness of sample preparation methods remains a limitation. In this regard, microwave-based systems have been used as an important tool to speed up analyses, and there is a trend toward expanding their use even more. For example, from three surveys performed with chromatography users, the data indicated that microwave-assisted extraction (MAE), which was used by only 2.6% of the 2002 respondents, jumped to 8% in 2013 and 10% in 2016 [1, 2]. When respondents were asked about which techniques they planned to use in the future, MAE came out on top, indicating that there may be an increasing demand for it in the near future [1]. This trend can be explained by the significant reduction in sample preparation time allowed by MAE methods (usually less than 0.5 h for several samples treated simultaneously), which enhances the productivity and reduces the workload in routine analysis.

Extractions are a rich field for microwave application. However, its use has been not restricted to this purpose. Microwave-assisted methods could be used combined with other analytical operations performed in chemical analyses, such as drying, solvent evaporation, and derivatization steps, as shown in Figure 24.1. The analytical sequence involves the steps of sampling and preliminary treatments in the laboratory, which are often performed to assure the homogenization and suitable storage of the sample. Afterward, the sample is weighed and prepared for analysis using several approaches, depending on the sample matrix as well as the analytes and their concentration. The main objective of such steps is the conversion of the sample and analytes into a suitable medium for further analysis. As a consequence, a reduction of interference from the sample matrix during analyte determination and often a separation or elimination of such compounds are performed using digestion, distillation, hydrolysis, or extraction. Considering that solvents are used as a liquid medium for major applications, they can be removed totally or partially by evaporation, with consequent

<https://doi.org/10.1515/9783110479935-024>



**Fig. 24.1:** Analytical sequence often used during analyses and the application of microwave in specific steps.

concentration of analytes. This last procedure is important to improve the detectability of analytes found at low concentration in the samples.

As expected and recently described in the literature, microwave radiation could be used in several steps involved in the analytical sequence. In sample pretreatment, microwave radiation could be used for drying, making it a suitable approach to drying plant materials because it can remove water, reducing the degradation of pigments or microbiological contamination, in comparison to conventional oven drying [3]. Digestion or hydrolysis could also be performed using microwave radiation in combination with chemicals or enzymes. Distillation or evaporation of solvents is also feasible, and commercial devices for such tasks are available [4–6]. When required, derivatization could also be performed using microwave radiation with a significant reduction of heating time [7, 8]. Despite the increasing use of microwave radiation in these fields, solvent extraction is by far the most common use of microwaves in organic analysis. In this way, the main aspects of MAE are detailed as follows.

## 24.2 General aspects of microwave-assisted extraction

Microwave-assisted extraction is a leaching process that occurs by the dissolution of sample components from a solid with a liquid in which the solid phase is not wholly soluble [9, 10]. Extraction (also defined as partition or distribution according to the International Union of Pure and Applied Chemistry) refers to the distribution of a spe-



cific chemical species between two phases [10]. This process can be improved by microwave radiation, which is known as MAE. In this particular case, the extraction solvent (when the extraction phase is a solvent) seems to be *fit for purpose*. Using this approach, the process of transferring a compound from any matrix to an appropriate liquid phase can be performed with advantages over the process using conventional heating. It is possible to assist a liquid-liquid extraction process (when the compound is initially present as a solute in an immiscible liquid phase) or a leaching (when the extractable material is present in a solid). In MAE, the microwave energy is used to heat the solvent in contact with the sample or even the sample directly. The heating by microwaves is more efficient and faster than convection and conduction heating, enhancing the migration rate of compounds into the extraction solvent [9].

Regarding the instrumentation, MAE may be performed in closed vessels with controlled temperature and pressure or in open vessels at atmospheric pressure. To this end, several approaches are used for irradiation using monomode (focused) [11], multimode (cavity) [12, 13], or directed multimode cavity [14] systems. However, despite the application mode, the absorption of microwave radiation is the most important aspect in MAE and is dependent on the properties of the extraction solvent and samples. This means that depending on the solvent chosen for extraction, different heating profiles can be observed. In general, solvents with a high dipole moment are good microwave absorbers, while others are microwave transparent or poorly absorbing solvents (Table 24.1). In general, the values of  $\tan \delta$  could be related to microwave heating patterns, in which higher values indicate a good microwave absorber.

For extractions using microwave-transparent or poorly absorbing solvents (e.g., hexane, carbon tetrachloride, tetrahydrofuran), the use of a passive heating element (PHE) could be an alternative. In this case, a strong microwave absorber (e.g., cylinders of sintered silicon carbide) is inserted into the solvent and, subsequently, transfers the generated thermal energy via the conduction phenomena to the liquid medium [18]. The PHEs are inert, stable, and virtually reusable. Figure 24.2 shows the effect of heating using a PHE in toluene as well as a comparison with the heating of pure water. Heating profiles were obtained during irradiation of 10 mL of each solvent (water or toluene) and also 9.4 mL of toluene containing a PHE (silicon carbide) for 250 s at 600 W. It is possible to observe that when pure toluene is slightly heated during irradiation, PHE can make the same solvent heat up to about 55 °C after 250 s. In contrast, pure water reached almost 90 °C when the same microwave irradiation program was used.

Despite the important role of the solvent in MAE (and that most analytical chemistry applications are reported using solvents), solvent-free microwave extraction (SFME) is also possible. Some devices have been used for the extraction of natural compounds from plants. In such systems, fresh or rehydrated plant material is placed in a microwave reactor, without any addition of solvent or water. The internal heating of the *in situ* water within the cells of the plant material leads to their rupture, releasing the target compounds. This process releases volatile compounds (e.g., es-

**Tab. 24.1:** Properties of some common solvents [15–17].

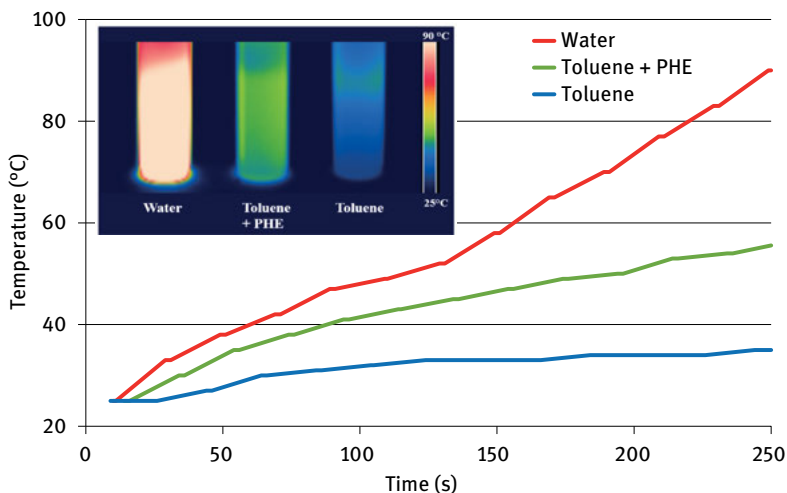
Solvent	Molecular weight (g mol <sup>-1</sup> )	Boiling point (°C) <sup>a</sup>	Density (g mL <sup>-1</sup> )	Solubility in water (%)	tan $\delta$	Dielectric constant <sup>b</sup>
<i>Organic solvents</i>						
Acetic acid	60.05	118	1.051	Miscible	0.174	6.2
Acetone	58.08	56	0.790	Miscible	0.055	20.6
Acetonitrile	41.05	81.6	0.782	Miscible	–	37.5
Chloroform	119.38	61	1.480	0.82	–	4.8
Cyclohexane	84.16	81	0.778	0.0055	–	2.01
Diethyl ether	74.12	34.5	0.715	6.9	–	4.3
Dimethyl-formamide	73.09	153	0.945	Miscible	–	36.7
Dimethylsulfoxide	78.14	189	1.101	Miscible	–	46.6
Ethanol	46.07	78	0.789	Miscible	0.25	22.4
Ethyl acetate	88.11	77	0.895	7.7	0.53	6.02
Ethylene glycol	62.07	198	1.115	Miscible	1	37.7
Glycerin	92.09	290	1.261	Miscible	–	46.53
Hexane	86.18	69	0.659	0.00095	–	1.9
Methanol	32.04	64	0.792	Miscible	0.64	32.6
Tetrahydrofuran	72.11	66	0.888	Miscible	–	7.6
Toluene	92.14	110.6	0.867	0.052	0.040	2.38
<i>Inorganic solvents</i>						
Water	18.02	100	0.998	–	0.157	79.7
Hydrochloric acid, 37%	36.46	110	1.19	Miscible	–	4.60
Nitric acid, 65%	63.01	122	1.42	Miscible	–	50.0 ±10.0 <sup>d</sup>
Phosphoric acid, 85%	98.00	213	1.71	Miscible	–	–
Sulfuric acid, 98%	98.08	338	1.84	Miscible	–	84.0

<sup>a</sup> atmospheric pressure boiling point; <sup>b</sup> obtained at 20 °C unless specified otherwise;

<sup>c</sup> obtained at 0 °C; <sup>d</sup> obtained at 14 °C

sential oil), which are evaporated by azeotropic distillation with the *in situ* water of the plant material. A cooling system outside the microwave oven condenses the distillate continuously, which is then collected in a flask, in a similar way to that of the conventional Clevenger apparatus for the extraction of essential oil. The excess water is refluxed to the extraction vessel to restore the *in situ* water to the plant material and to provide uniform conditions for the temperature and humidity for extraction. More information about these systems can be obtained in other chapters of this book as well as in specific literature [19, 20].

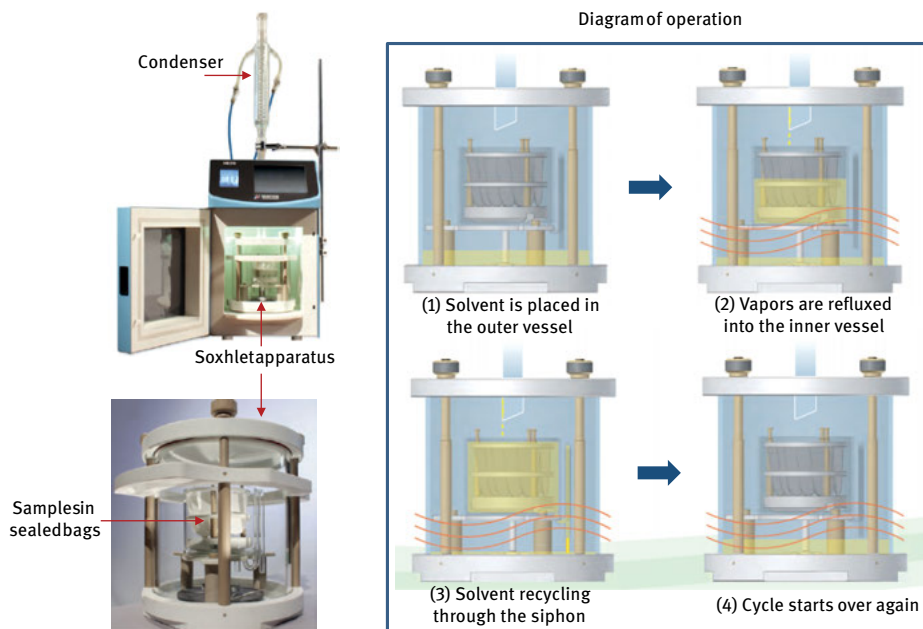
Although certain high-throughput laboratories use the latest automation equipment and process hundreds or sometimes thousands of samples a day, many laboratories are still using methods based on classical protocols for sample preparation with some degree of miniaturization or low levels of automation taking place [1]. Classical protocols, like conventional Soxhlet extraction, which has been a standard method



**Fig. 24.2:** Heating behavior of water and toluene under microwave irradiation and the use of PHE. Experiments performed in quartz vessels in a microwave cavity. Temperatures were measured using an infrared thermal imaging camera.

for over a century, are still widely used. They have been used as the starting point for the development of a variety of modifications intended to bring conventional extraction closer to that of the more recent sample preparation methods. Thus, microwave-assisted methods have reached many advantages, shortening extraction times with the use of auxiliary forms of energy and automating the extraction system [21]. In this way, conventional Soxhlet extraction has been improved by the use of microwave heating. Devices have been used in monomode (focused) or multimode (cavity) equipment with inherent advantages and shortcomings. In Figure 24.3 a microwave-assisted Soxhlet (multimode) device is shown with the description of the main steps involved. More information about microwave-assisted Soxhlet systems and their combination with other auxiliary energies (e.g., ultrasound) can be obtained in the literature [21, 22].

The main aspects related to the heating using microwaves are discussed in previous chapters or can be found in specific literature [23–28]. Taking into account sample preparation for organic analytes, microwaves can improve some aspects in the interaction between phases, improving or facilitating extraction. Extraction involving liquid phases (liquid samples, for example, water, liquid waste, beverages, liquid pharmaceuticals) can be improved mainly as a result of heating, which can facilitate the partition of analyte between its original liquid phase and the extractant. In particular, extraction involving the solid sample and the extraction solution can occur as a result of some mechanisms [26]: (1) the sample can be immersed in a solvent or a mixture of solvents that are good microwave absorbers; (2) analytes in the sample can be extracted in a mixture of solvents with both high and low dielectric losses mixed



**Fig. 24.3:** Microwave-assisted Soxhlet device used in multimode equipment [4]. Courtesy from Milestone Srl.

in varying proportions; or (3) samples with high capacity to absorb microwaves (e.g., samples with high water content) can be extracted with a transparent solvent [29].

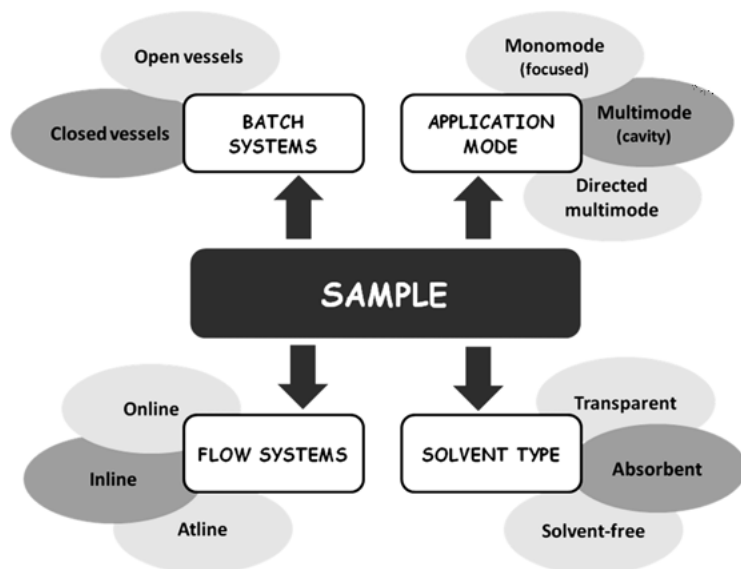
In general, MAE can be performed using a lower amount of solvent and can be completed in less time than under conventional extraction. A careful optimization of methods must be carried out to propose an MAE method that combines accuracy and benefits, such as less time, savings in costs, energy, and reagents, and minimization of residues. The type of solvent must be selected with a view toward maximizing microwave absorption by the total mixture (sample and solvent). In addition, the selection of solvent must also consider analyte solubility (preferably compared to other compounds) and that solvent must be compatible with the determination technique. The amount of sample and solvent must be selected in such a way as to assure that the sample is completely immersed in the solvent and that the amount of sample is enough to allow a solution that is not more diluted than the limit of quantification (LOQ) of the determination technique. Finally, a microwave heating program comprises the selection of microwave irradiation power, time of irradiation, final temperature, and limit pressure. In addition, the microwave heating program must be proposed in such a way that extraction efficiency is optimal, maintaining the integrity of the analyte and using a method that is as simple as possible. In Table 24.2, the main parameters affecting MAE are summarized.

Tab. 24.2: Summary of contributing parameters for MAE.

Parameter	Effects
Solvent type	<ul style="list-style-type: none"> <li>– Polar organic solvents are suitable for the extraction of general organic compounds; mixtures of solvents can also be used to assure extraction and absorption of microwave radiation [29, 30].</li> <li>– Diluted HNO<sub>3</sub> and HCl are common acids for most applications devoted to further metal and metalloid determination [25, 31].</li> <li>– Solutions containing buffers and organic solvents, such as methanol, or complexant agents, such as EDTA, are common extractants for organometallic analytes [32].</li> </ul>
Sample mass and amount of solvent	<ul style="list-style-type: none"> <li>– Suitable proportions of sample and extraction medium must be optimized to assure quantitative extraction; usually an excess of solvent is used [31].</li> <li>– Instrumentation possibilities (e.g., vessel/system size and limit pressure) also influences the definition of those amounts.</li> </ul>
Particle size (for solid samples)	<ul style="list-style-type: none"> <li>– Lower particle sizes generally allow for higher extraction efficiency [33].</li> </ul>
Microwave heating program	<ul style="list-style-type: none"> <li>– Maximum temperature is a crucial parameter to avoid degradation of compounds [34].</li> <li>– Extraction time can last from a few minutes up to hours, but it is typically less than that under conventional heating.</li> <li>– A careful optimization of the heating program (power, time, and temperature) must assure complete extraction without degradation of target compounds [31].</li> </ul>

An advantage of microwave heating is usually a reduced susceptibility to thermal degradation and the formation of artifacts, because shorter reaction times are required in comparison to conventional heating. The temperature is a key parameter to avoid degradation, and its value is closely related to the physical properties of the solvent as well as the kind of microwave system used. The use of closed vessels for extraction using microwaves prevents the risk of loss or contamination, but the boiling point of the solvent is increased in such devices. Therefore, the control of the solvent temperature is critical to assure the reproducibility of extractions, and an evaluation of the temperature for extractions is recommended to avoid thermal degradation of analytes and the formation of artifacts. Alternatively, microwaves may be absorbed only by the matrix, resulting in the heating of samples and release of solutes into the cold solvent (not heated by microwaves) [35].

Once the solvent has been chosen, the instrumentation (type of system and vessels) must be selected. Figure 24.4 shows an overview of the possible choices according to the requirements of a certain analytical protocol as well as the instrumentation available. Equipment used for sample preparation prior to the determination of or-



**Fig. 24.4:** Aspects to be considered for selection of a microwave-assisted sample preparation method.

organic compounds are commonly based on a multimode, monomode, or directed multimode setup. Multimode equipment (the same principle behind household ovens) is by far the most common system in laboratories. The higher analytical frequency (related to the number of samples per run), the availability of sensors for controlling temperature and pressure, and facilities for safe operation by several manufacturers lead to a widespread use of such system in laboratories. Despite the more focused energy under monomode or a directed multimode apparatus, this is not the most important parameter in the extraction of organic compounds. This aspect requires careful attention because even a small amount of excess energy can result in conversion or degradation of some compounds.

In general, MAE systems can be operated using open or closed vessels, although closed systems have been more extensively used. Open systems are operated at atmospheric pressure, and this characteristic is more prone to solvent evaporation and consequent analyte loss (depending on its volatility). To overcome this drawback, a condenser can be coupled to the upper part of the extraction vessel, like a microwave-assisted Soxhlet system (as discussed previously). The outstanding feature of closed systems is that pressure and temperature can be monitored and regulated efficiently (optional pressurization with alternative gases is available in specific equipment), providing benefits such as fast extraction, lower solvent consumption, and lower analyte loss, but with relatively high cost for acquisition and maintenance. For new instruments (from the last 10–15 years), safety is the main concern, and different systems

have been developed [29, 30, 36, 37]. Independent of the system (open or closed), the extraction time using microwave is reduced, and the high heating rate generally provides efficient extraction in a few minutes. However, the high temperature achieved mainly in closed systems (higher than the boiling point of the solvent) may affect the stability of some organic compounds.

From the development of MAE methods, some improvements, such as simplification, miniaturization, and automation, always have been considered as trends. In general, when a MAE procedure is finished, the vessels must be cooled to room temperature, and the extract should be filtered/centrifuged, making the whole procedure longer and more complex. Alternative possibilities for conducting MAE in closed vessels involve online approaches. For online systems, after extraction an aliquot of extract is pumped for subsequent treatment in the extraction vessel. The main advantages of online protocols are the reduced sample contamination and analyte loss and the lower manipulation of toxic organic solvents by the analyst [30, 38–40]. Dynamic MAE (DMAE) is a variant of an online system, where a fresh extraction solvent is continuously supplied and the analytes are transferred out of the extraction vessel as soon as they are extracted [41, 42]. The main advantages of DMAE are the lower incidence of degradation of compounds and the low risk of contamination. Moreover, the extract could be filtered online and DMAE can be combined with other sample treatment methods. In online DMAE, the extraction, separation, and determination of analytes are integrated and the process can be automated. A typical extraction mode of online DMAE is continuous sampling. In this sampling mode, a representative mixture of the sample and the extraction solvent is continuously introduced into the extraction vessel [43]. DMAE can be carried out for processing single or multiple samples. In single-mode DMAE, an extraction solvent is introduced with a high-pressure pump or peristaltic pump. The solvent is pumped through the sample and the extracted analyte is transferred to the next step (clean-up or detection). The main advantage of the multi-sample approach is the improvement of the sample throughput and the better use of microwave energy [41, 44]. At-line coupling is also a useful approach that makes automation easier. It is based on the injection of pretreated sample solutions using an autosampler combined with a transport unit for liquid handling. In at-line mode, the automated transfer of the sample solution is performed using commercially available robotic systems equipped with transport units (e.g., a robotic programmable arm). However, automated systems require costly equipment, and the sample loss accompanied by decreased sensitivity can be caused by the sample collection and injection processes. Unlike the online approaches, at-line extraction is performed in open systems prone to analyte degradation or evaporation by air or light exposure [40].

## 24.3 Applications of MAE to the analysis of organic compounds

An important field for the application of MAE is in the extraction of organic pollutants (contaminants) from several matrices, with a special focus on food and environmental samples. Among the classes of contaminants, flame retardants, pharmaceutical compounds, personal care products, agrochemicals, polycyclic aromatic hydrocarbons, and surfactants can be highlighted [29, 30]. The general characteristics of MAE methods available in the literature are shown in Table 24.3.

Compared to other extraction approaches, the optimization of the experimental conditions of MAE has relatively few parameters that influence extraction efficiency (e.g., matrix composition, type of solvent, time and power/temperature) as previously discussed [29]. This is an advantage for routine analysis, and special attention should be given to the temperature applied during extraction, to avoid analyte degradation or volatilization (mainly for open systems). An important characteristic of MAE is the use of a relatively high sample mass (up to 10 g in some cases). However, this high sample amount sometimes requires the use of a higher volume of solvents (quite often from 20 up to 30 mL). The type of solvent is another aspect of MAE that should be considered, as the use of toxic solvents (such as organochlorides) is a common (poor) choice. As an alternative to these solvents, ionic liquids or deep eutectic solvents can be used taking into account their greener characteristics. These alternative solvents present a negligible volatile nature despite the relatively low boiling temperature (in general lower than 100 °C), which represents an advancement in terms of the reduction of the environmental footprint [45]. Nevertheless, this low volatility afforded by ionic liquids also makes more complex the isolation and recovery of the extracted compounds [45], especially when these solvents are not compatible with the technique used for analyte determination.

Among the main advantages of MAE for the extraction of organic pollutants is the feasibility for the multiclass extraction of organic analytes, combining lower extraction time, lower reagent consumption, suitable reproducibility, control of pressure and temperature available in most systems, and a higher sample throughput compared to some classical liquid-liquid or liquid-solid methods. It is important to highlight that specific effects of microwaves on some samples have been found, because they interact selectively with the free water molecules present in samples, leading to rapid heating and temperature increase, followed by rupture or destruction of the matrix macrostructure. Therefore, the localized heating allowed in microwave extraction could improve the release of analytes from sample to solvent and reduce the time needed for extraction [35].

Although several MAE methods have been developed, some trends can be highlighted: (1) improvements in online monitoring or online coupling regarding detection techniques, (2) use of small extraction flasks and lower volumes of solvents as a consequence, (3) use of monomode systems for the reduction of time and increase of extraction efficiency, and (4) investigations for the replacement of commonly used solvents to more friendly ones (e.g., deep eutectic solvents or ionic liquids).



Tab. 24.3: Selected applications of MAE.

Extracted compounds	Material	Extraction conditions	Key references
Flame retardants*: BDE, PBDE, PBB, PCB, PCN, TBEP, TBP, TCEP, TCPP, TDCP, TEHP, TiBP, TPP, TPPO, TPpP, TPrP, HBCD, TMP, TEP, THP, among others	Biological and plant tissues, environmental samples, and polymers	Type of solvent or mixture: dichloromethane, dichloromethane + pentane, dichloromethane + hexane, dichloromethane + methanol, hexane + acetone, and tetrahydrofuran. Volume of solvent: 8 to 48 mL. Temperature: 75 to 150 °C. Extraction time: 2 to 30 min.	[46–54]
Surfactants**: LAS, NP, NPEO, OP, among others.	Most applications for environmental samples and a few for biological tissues	Type of solvent or mixture: methanol, methanol + dichloromethane, hexane, and acetone. Volume of solvent: 5 to 45 mL. Temperature: 100 to 120 °C. Extraction time: 10 to 35 min.	[55–59]
Agrochemicals: pesticides, insecticides, fungicides, and herbicides	Food, biological tissues, plant tissues, and environmental samples	Type of solvent or mixture: water, ethyl acetate, acetonitrile, hexane, methanol, ionic liquid, acetone + hexane, acetonitrile + water, and tetrahydrofuran + hexane. Volume of solvent: 5 to 40 mL. Temperature: 50 to 160 °C. Extraction time: 2.5 to 20 min.	[60–71]
Polycyclic aromatic hydrocarbons: several compounds	Food, biological tissues, and environmental samples	Type of solvent or mixture: acetonitrile, ethanol, dimethyl sulfoxide, ionic liquid, water, and hexane + acetone. Volume of solvent: 5 to 30 mL. Temperature: 60 to 110 °C. Extraction time: 2 to 20 min.	[72–79]
Pharmaceutical compounds: antibiotics, anti-inflammatory drugs, estrogens, among others.	Most applications for environmental samples and a few for biological tissues	Type of solvent or mixture: water, methanol, dichloromethane, methanol + water, acetonitrile + water, methanol + dichloromethane, phosphate buffer + ethyl acetate, and hexane + acetone. Volume of solvent: 5 to 40 mL. Temperature: 65 to 170 °C. Extraction time: 4 to 22 min.	[57, 66, 80–87]
Personal care products: polycyclic musks, musk ketone, musk moskene, musk xylene, nitromusks, triclosan, among others.	Environmental samples	Type of solvent: acetone, dichloromethane, hexane, and methanol. Volume of solvent: 8 to 30 mL. Temperature: 80 to 130 °C. Extraction time: 3 to 35 min.	[80, 88–90]

&lt;

\* BDE – brominated diphenylether; PBDE – polybrominated diphenylether; PBB – polybrominated biphenyl; PCB – polychlorinated biphenyl; PCN – polychlorinated naphthalene; TBEP – tris(2-butoxyethyl)phosphate; TBP – tributylphosphate; TCEP – tris(2-chloroethyl)phosphate; TCPP – tri(2-chloroisopropyl)phosphate; TDCP – tris(1,3-dichloroisopropyl)phosphate; TEHP – tris(2-ethylhexyl)phosphate; TiBP – triisobutylphosphate; TPP – triphenylphosphate; TPPO – triphenylphosphine oxide; TPrP – tri-propyl phosphate; HBCD – hexabromocyclododecane, TMP – trimethyl phosphate, TEP – triethyl phosphate; THP – trihexyl phosphate

\*\* LAS – linear alkylbenzene sulfonate; NP – nonylphenol; NPEO – nonylphenol ethoxylate; OP – octylphenol

## Bibliography

- [1] Majors RE. Trends in sample preparation, LCGC North America 2013, 31, 190–202.
- [2] Raynie DE. Trends in sample preparation, LCGC North America 2016, 34, 174–188.
- [3] Vadivambal R, Jayas DS. Changes in quality of microwave-treated agricultural products—a review, Biosystems Engineering 2007, 98, 1–16.
- [4] ETHOS X Advanced Microwave Extraction System for GC and HPLC Analysis, Milestone Srl, Sorisole, Italy. Available at: <http://www.milestonesrl.com/en/microwaveextraction/ethos-x.html>, 19/12/2016.
- [5] Microwave Evaporation: Rotor 8EVAP, Anton Paar GmbH, Austria. Available at: <http://www.anton-paar.com/us-en/products/details/microwave-evaporation-rotor-8evap/>, 19/12/2016.
- [6] CEM Corporation. MARS 6 Accessories, CEM Corporation, Matthews, USA. Available at: <http://fr.cem.com/e107/content666.html>, 19/12/2016.
- [7] Söderholm SL, Damm M, Kappe CO. Microwave-assisted derivatization procedures for gas chromatography/mass spectrometry analysis, Molecular Diversity 2010, 14, 869–888.
- [8] Lavilla I, Romero V, Costas I, Bendicho C. Greener derivatization in analytical chemistry, TrAC Trends in Analytical Chemistry 2014, 61, 1–10.
- [9] Poole C, Mester Z, Miró M, Pedersen-Bjergaard S, Pawliszyn J. in *Pure and Applied Chemistry*, Vol. 88, 2016, p. 517.
- [10] IUPAC, Compendium of Chemical Terminology, 2nd ed. (the “Gold Book”). Compiled by A.D. McNaught and A. Wilkinson. Blackwell Scientific Publications, Oxford 1997.
- [11] CEM Corporation. STAR – Open Vessel Microwave Digestion Technology, CEM Corporation, Matthews, USA. Available at: <http://cem.com/e107/star-technology.html>, 19/12/2016.
- [12] Microwave Sample Preparation for Instrumentation – ETHOS UP, Milestone Srl, Sorisole, Italy. Available at: <http://www.milestonesrl.com/ethos-up>, 19/12/2016.
- [13] Microwave Reaction System: Multiwave PRO, Anton Paar GmbH, Graz, Austria. Available at: <http://www.anton-paar.com/us-en/products/details/microwave-reaction-system-multiwave-pro/>, 19/12/2016.
- [14] Microwave Digestion System: Multiwave GO, Anton Paar GmbH, Graz, Austria. Available at: <http://www.anton-paar.com/us-en/products/details/microwave-digestion-system-multiwave-go/>, 19/12/2016.
- [15] Lide DR. *CRC Handbook of Chemistry and Physics*, CRC Press, Boca Raton, 2003.
- [16] Mester Z, Sturgeon R ed. Sample preparation for trace element analysis, Vol. XLI, edn. Elsevier, Amsterdam, 2003.
- [17] Smallwood IM. *Handbook of organic solvent properties*, John Wiley & Sons, New York, 1996.
- [18] Kremsner JM, Kappe CO. Silicon carbide passive heating elements in microwave-assisted organic synthesis, The Journal of Organic Chemistry 2006, 71, 4651–4658.

- [19] Rostagno MA, Prado JM. *Natural product extraction: principles and applications* RSC, 2013.
- [20] Chemat F, Cravotto G. *Microwave-assisted extraction for bioactive compounds. Theory and practice*, Springer, New York, 2013.
- [21] Luque de Castro MD, Priego-Capote F. Soxhlet extraction: past and present panacea, *Journal of Chromatography A* 2010, 1217, 2383–2389.
- [22] Cravotto G, Bicchi C, Mantegna S, Binello A, Tomao V, Chemat F. Extraction of kiwi seed oil: Soxhlet versus four different non-conventional techniques, *Natural Product Research* 2011, 25, 974–981.
- [23] Zlotorzynski A. The application of microwave-radiation to analytical and environmental chemistry, *Critical Reviews in Analytical Chemistry* 1995, 25, 43–76.
- [24] Kubrakova IV, Toropchenova ES. Microwave heating for enhancing efficiency of analytical operations (Review), *Inorganic Materials* 2008, 44, 1509–1519.
- [25] Agazzi A, Pirola C. Fundamentals, methods and future trends of environmental microwave sample preparation, *Microchemical Journal* 2000, 67, 337–341.
- [26] H. M. (Skip)Kingston, Haswell SJ. *Microwave-enhanced chemistry – fundamentals, sample preparation and applications*, American Chemical Society, Washington, 1997.
- [27] Nobrega JA, Donati GL. “Microwave-assisted sample preparation for spectrochemistry” In *Encyclopedia of Analytical Chemistry*, Vol. Online (ed.: Meyers RA), John Wiley & Sons, Ltd., Chichester, 2011, a9185.
- [28] Flores EMM ed. *Microwave-assisted sample preparation for trace element determination*, Vol. edn. Elsevier, Amsterdam, 2014.
- [29] Sanchez-Prado L, Garcia-Jares C, Llompart M. Microwave-assisted extraction: Application to the determination of emerging pollutants in solid samples, *Journal of Chromatography A* 2010, 1217, 2390–2414.
- [30] Wang H, Ding J, Ren N. Recent advances in microwave-assisted extraction of trace organic pollutants from food and environmental samples, *TrAC Trends in Analytical Chemistry* 2016, 75, 197–208.
- [31] Krishna MVB, Chandrasekaran K, Venkateswarlu G, Karunasagar D. A cost-effective and rapid microwave-assisted acid extraction method for the multi-elemental analysis of sediments by ICP-AES and ICP-MS, *Analytical Methods* 2012, 4, 3290–3299.
- [32] Dressler VL, Antes FG, Moreira CM, Pozebon D, Duarte FA. As, Hg, I, Sb, Se and Sn speciation in body fluids and biological tissues using hyphenated-ICP-MS Techniques: A Review, *International Journal of Mass Spectrometry* 2011, 307, 149–162.
- [33] Wickstrom T, Ogner G, Remedios G. Effects of Different pretreatments (sieving, milling, and grinding) on quality of determination of Kjeldahl nitrogen, ph, and extractable elements in forest soils, *Communications in Soil Science and Plant Analysis* 2004, 35, 369–384.
- [34] Araujo GCL, Nogueira ARA, Nobrega JA. Microwave single vessel acid-vapor extraction: effect of experimental parameters on Co and Fe determination in biological samples, *Microchimica Acta* 2004, 144, 81–85.
- [35] Camel V. Recent extraction techniques for solid matrices-supercritical fluid extraction, pressurized fluid extraction and microwave-assisted extraction: their potential and pitfalls, *Analyst* 2001, 126, 1182–1193.
- [36] Luque-Garcia JL, Luque de Castro MD. Where is microwave-based analytical equipment for solid sample pre-treatment going?, *TrAC Trends in Analytical Chemistry* 2003, 22, 90–98.
- [37] Zhang HF, Yang XH, Wang Y. Microwave assisted extraction of secondary metabolites from plants: Current status and future directions, *Trends in Food Science & Technology* 2011, 22, 672–688.

- [38] Aguilera-Herrador E, Lucena R, Cárdenas S, Valcárcel M. Continuous flow configuration for total hydrocarbons index determination in soils by evaporative light scattering detection, *Journal of Chromatography A* 2007, 1141, 302–307.
- [39] Deng X, Xie P, Qi M, Liang G, Chen J, Ma Z, Jiang Y. Microwave-assisted purge-and-trap extraction device coupled with gas chromatography and mass spectrometry for the determination of five predominant odors in sediment, fish tissues, and algal cells, *Journal of Chromatography A* 2012, 1219, 75–82.
- [40] Pan J, Zhang C, Zhang Z, Li G. Review of online coupling of sample preparation techniques with liquid chromatography, *Analytica Chimica Acta* 2014, 815, 1–15.
- [41] Chen L, Jin H, Ding L, Zhang H, Wang X, Wang Z, Li J, Qu C, Wang Y, Zhang H. On-line coupling of dynamic microwave-assisted extraction with high-performance liquid chromatography for determination of andrographolide and dehydroandrographolide in *Andrographis paniculata* Nees, *Journal of Chromatography A* 2007, 1140, 71–77.
- [42] Chan CH, Yusoff R, Ngoh GC, Kung FWL. Microwave-assisted extractions of active ingredients from plants, *Journal of Chromatography A* 2011, 1218, 6213–6225.
- [43] Gao S, You J, Wang Y, Zhang R, Zhang H. On-line continuous sampling dynamic microwave-assisted extraction coupled with high performance liquid chromatographic separation for the determination of lignans in Wuweizi and naphthoquinones in Zicao, *Journal of Chromatography B*, 2012, 887–888, 35–42.
- [44] Wang H, Chen L, Xu Y, Zeng Q, Zhang X, Zhao Q, Ding L. Dynamic microwave-assisted extraction coupled on-line with clean-up for determination of caffeine in tea, *LWT – Food Science and Technology* 2011, 44, 1490–1495.
- [45] Passos H, Freire MG, Coutinho JAP. Ionic liquid solutions as extractive solvents for value-added compounds from biomass, *Green Chemistry* 2014, 16, 4786–4815.
- [46] Shin M, Svoboda ML, Falletta P. Microwave-assisted extraction (MAE) for the determination of polybrominated diphenylethers (PBDEs) in sewage sludge, *Analytical and Bioanalytical Chemistry* 2007, 387, 2923–2929.
- [47] García M, Rodríguez I, Cela R. Microwave-assisted extraction of organophosphate flame retardants and plasticizers from indoor dust samples, *Journal of Chromatography A* 2007, 1152, 280–286.
- [48] García-López M, Rodríguez I, Cela R, Kroening KK, Caruso JA. Determination of organophosphate flame retardants and plasticizers in sediment samples using microwave-assisted extraction and gas chromatography with inductively coupled plasma mass spectrometry, *Talanta* 2009, 79, 824–829.
- [49] Carro AM, Lorenzo RA, Fernández F, Phan-Tan-Luu R, Cela R. Microwave-assisted extraction followed by headspace solid-phase microextraction and gas chromatography with mass spectrometry detection (MAE-HSSPME-GC-MS/MS) for determination of polybrominated compounds in aquaculture samples, *Analytical and Bioanalytical Chemistry* 2007, 388, 1021–1029.
- [50] Yusà V, Pardo O, Pastor A, de la Guardia M. Optimization of a microwave-assisted extraction large-volume injection and gas chromatography–ion trap mass spectrometry procedure for the determination of polybrominated diphenyl ethers, polybrominated biphenyls and polychlorinated naphthalenes in sediments, *Analytica Chimica Acta* 2006, 557, 304–313.
- [51] Otake T, Itoh N, Ohata M, Hanari N. Optimization of microwave-assisted extraction for the determination of organic flame retardants in acrylonitrile butadiene styrene, *Analytical Letters* 2015, 48, 2319–2328.
- [52] Beser MI, Beltrán J, Yusà V. Design of experiment approach for the optimization of polybrominated diphenyl ethers determination in fine airborne particulate matter by microwave-as-

- sisted extraction and gas chromatography coupled to tandem mass spectrometry, *Journal of Chromatography A* 2014, 1323, 1–10.
- [53] Ma Y, Cui K, Zeng F, Wen J, Liu H, Zhu F, Ouyang G, Luan T, Zeng Z, Microwave-assisted extraction combined with gel permeation chromatography and silica gel cleanup followed by gas chromatography–mass spectrometry for the determination of organophosphorus flame retardants and plasticizers in biological samples, *Analytica Chimica Acta* 2013, 786, 47–53.
- [54] Song S, Shao M, Tang H, He Y, Wang W, Liu L, Wu J, Development, comparison and application of sorbent-assisted accelerated solvent extraction, microwave-assisted extraction and ultrasonic-assisted extraction for the determination of polybrominated diphenyl ethers in sediments, *Journal of Chromatography A* 2016, 1475, 1–7.
- [55] Pedersen SN, Lindholm C. Quantification of the xenoestrogens 4-tert.-octylphenol and bisphenol A in water and in fish tissue based on microwave assisted extraction, solid-phase extraction and liquid chromatography–mass spectrometry, *Journal of Chromatography A* 1999, 864, 17–24.
- [56] Liu R, Zhou JL, Wilding A, Microwave-assisted extraction followed by gas chromatography–mass spectrometry for the determination of endocrine disrupting chemicals in river sediments, *Journal of Chromatography A* 2004, 1038, 19–26.
- [57] Morales-Muñoz S, Luque-García JL, Ramos MJ, Martínez-Bueno MJ, d MDL. Castro, Sequential automated focused microwave-assisted soxhlet extraction of compounds with different polarity from marine sediments prior to gas chromatography mass spectrometry detection, *Chromatographia* 2005, 62, 69–74.
- [58] Stuart JD, Capulong CP, Launer KD, Pan X. Analyses of phenolic endocrine disrupting chemicals in marine samples by both gas and liquid chromatography–mass spectrometry, *Journal of Chromatography A* 2005, 1079, 136–145.
- [59] Villar M, Callejón M, Jiménez JC, Alonso E, Guiráum A. Optimization and validation of a new method for analysis of linear alkylbenzene sulfonates in sewage sludge by liquid chromatography after microwave-assisted extraction, *Analytica Chimica Acta* 2007, 599, 92–97.
- [60] Merdassa Y, f J. Liu, Megersa N. Development of a one-step microwave-assisted extraction procedure for highly efficient extraction of multiclass fungicides in soils, *Analytical Methods* 2014, 6, 3025–3033.
- [61] Su YS, Yan CT, Ponnusamy VK, Jen JF. Novel solvent-free microwave-assisted extraction coupled with low-density solvent-based in-tube ultrasound-assisted emulsification microextraction for the fast analysis of organophosphorus pesticides in soils, *Journal of Separation Science* 2013, 36, 2339–2347.
- [62] Coscollà C, Castillo M, Pastor A, Yusà V. Determination of 40 currently used pesticides in airborne particulate matter (PM 10) by microwave-assisted extraction and gas chromatography coupled to triple quadrupole mass spectrometry, *Analytica Chimica Acta* 2011, 693, 72–81.
- [63] Moreno DV, Ferrera ZS, Rodríguez JJS. SPME and SPE comparative study for coupling with microwave-assisted micellar extraction in the analysis of organochlorine pesticides residues in seaweed samples, *Microchemical Journal* 2007, 87, 139–146.
- [64] Li H, Wei Y, You J, Lydy MJ. Analysis of sediment-associated insecticides using ultrasound assisted microwave extraction and gas chromatography–mass spectrometry, *Talanta* 2010, 83, 171–177.
- [65] Á. Sánchez-Rodríguez, Sosa-Ferrera Z, Santana-Rodríguez JJ. Applicability of microwave-assisted extraction combined with LC–MS/MS in the evaluation of booster biocide levels in harbour sediments, *Chemosphere* 2011, 82, 96–102.
- [66] Förster M, Laabs V, Lamshöft M, Pütz T, Amelung W. Analysis of aged sulfadiazine residues in soils using microwave extraction and liquid chromatography tandem mass spectrometry, *Analytical and Bioanalytical Chemistry* 2008, 391, 1029–1038.

- [67] Merdassa Y, Liu JF, Megersa N, Tessema M. An efficient and fast microwave-assisted extraction method developed for the simultaneous determination of 18 organochlorine pesticides in sediment, *International Journal of Environmental Analytical Chemistry* 2015, 95, 225–239.
- [68] Zhang Y, Lin N, Su S, Shen G, Chen Y, Yang C, Li W, Shen H, Huang Y, Chen H, Wang X, Liu W, Tao S. Freeze drying reduces the extractability of organochlorine pesticides in fish muscle tissue by microwave-assisted method, *Environmental Pollution* 2014, 191, 250–252.
- [69] Wang R, Su P, Zhong Q, Zhang Y, Yang Y. Ionic liquid-based microwave-assisted extraction of organochlorine pesticides from soil, *Journal of Liquid Chromatography & Related Technologies* 2013, 36, 687–699.
- [70] Papadakis EN, Kyrgidou A, Vryzas Z, Papadopoulou-Mourkidou E. Development of a microwave-assisted extraction method for the determination of organochlorine pesticides in mussel tissue, *Food Analytical Methods* 2014, 7, 1271–1277.
- [71] Merdassa Y, J. Liu, Megersa N. Development of a one-step microwave-assisted extraction method for simultaneous determination of organophosphorus pesticides and fungicides in soils by gas chromatography–mass spectrometry, *Talanta* 2013, 114, 227–234.
- [72] Germán-Hernández M, Pino V, Anderson JL, Afonso AM. Use of ionic liquid aggregates of 1-hexadecyl-3-butyl imidazolium bromide in a focused-microwave assisted extraction method followed by high-performance liquid chromatography with ultraviolet and fluorescence detection to determine the 15 + 1 EU priority PAHs in toasted cereals (“gofios”), *Talanta* 2011, 85, 1199–1206.
- [73] Lv J, Shi R, Cai Y, Liu Y. Assessment of polycyclic aromatic hydrocarbons (PAHs) pollution in soil of suburban areas in Tianjin, China, *Bulletin of Environmental Contamination and Toxicology* 2010, 85, 5–9.
- [74] Ghasemzadeh-Mohammadi V, Mohammadi A, Hashemi M, Khaksar R, Haratian P. Microwave-assisted extraction and dispersive liquid–liquid microextraction followed by gas chromatography–mass spectrometry for isolation and determination of polycyclic aromatic hydrocarbons in smoked fish, *Journal of Chromatography A* 2012, 1237, 30–36.
- [75] Li XY, Li N, Luo HD, Lin LR, Zou ZX, Jia YZ, Li YQ. A novel synchronous fluorescence spectroscopic approach for the rapid determination of three polycyclic aromatic hydrocarbons in tea with simple microwave-assisted pretreatment of sample, *Journal of Agricultural and Food Chemistry* 2011, 59, 5899–5905.
- [76] Guo L, Lee HK. Microwave assisted extraction combined with solvent bar microextraction for one-step solvent-minimized extraction, cleanup and preconcentration of polycyclic aromatic hydrocarbons in soil samples, *Journal of Chromatography A* 2013, 1286, 9–15.
- [77] Pino V, Anderson JL, Ayala JH, González V, Afonso AM. The ionic liquid 1-hexadecyl-3-methylimidazolium bromide as novel extracting system for polycyclic aromatic hydrocarbons contained in sediments using focused microwave-assisted extraction, *Journal of Chromatography A* 2008, 1182, 145–152.
- [78] Mekonnen KN, Chandravanshi BS, Redi-Abshiro M, Ambushe AA, McCrindle RI, Moyo S. Distribution of polycyclic aromatic hydrocarbons in sediments of Akaki River, Lake Awassa, and Lake Ziway, Ethiopia, *Environmental Monitoring and Assessment* 2015, 187, 474.
- [79] Sibiyi P, Chimuka L, Cukrowska E, Tutu H. Development and application of microwave assisted extraction (MAE) for the extraction of five polycyclic aromatic hydrocarbons in sediment samples in Johannesburg area, South Africa, *Environmental Monitoring and Assessment* 2013, 185, 5537–5550.
- [80] Rice SL, Mitra S. Microwave-assisted solvent extraction of solid matrices and subsequent detection of pharmaceuticals and personal care products (PPCPs) using gas chromatography–mass spectrometry, *Analytica Chimica Acta* 2007, 589, 125–132.

- [81] Cueva-Mestanza R, Torres-Padrón ME, Sosa-Ferrera Z, Santana-Rodríguez JJ. Microwave-assisted micellar extraction coupled with solid-phase extraction for preconcentration of pharmaceuticals in molluscs prior to determination by HPLC, *Biomedical Chromatography* 2008, 22, 1115–1122.
- [82] Prat MD, Ramil D, Compañó R, Hernández-Arteseros JA, Granados M. Determination of flumequine and oxolinic acid in sediments and soils by microwave-assisted extraction and liquid chromatography-fluorescence, *Analytica Chimica Acta* 2006, 567, 229–235.
- [83] Förster M, Laabs V, Lamshöft M, Groeneweg J, Zühlke S, Spitteller M, Krauss M, Kaupenjohann M, Amelung W. Sequestration of manure-applied sulfadiazine residues in soils, *Environmental Science & Technology* 2009, 43, 1824–1830.
- [84] Labadie P, Budzinski H. Determination of steroidal hormone profiles along the jalle d'eyssines river (near Bordeaux, France), *Environmental Science & Technology* 2005, 39, 5113–5120.
- [85] Kumirska J, Migowska N, Caban M, Łukaszewicz P, Stepnowski P. Simultaneous determination of non-steroidal anti-inflammatory drugs and oestrogenic hormones in environmental solid samples, *Science of The Total Environment* 2015, 508, 498–505.
- [86] Fernández P, Fernández AM, Bermejo AM, Lorenzo RA, Carro AM. Optimization of microwave-assisted extraction of analgesic and anti-inflammatory drugs from human plasma and urine using response surface experimental designst, *Journal of Separation Science* 2013, 36, 1446–1454.
- [87] Guedes-Alonso R, Santana-Viera S, Montesdeoca-Esponda S, Afonso-Olivares C, Sosa-Ferrera Z, Santana-Rodríguez JJ. Application of microwave-assisted extraction and ultra-high performance liquid chromatography–tandem mass spectrometry for the analysis of sex hormones and corticosteroids in sewage sludge samples, *Analytical and Bioanalytical Chemistry* 2016, 408, 6833–6844.
- [88] Regueiro J, Llompart M, Garcia-Jares C, Cela R. Development of a high-throughput method for the determination of organochlorinated compounds, nitromusks and pyrethroid insecticides in indoor dust, *Journal of Chromatography A* 2007, 1174, 112–124.
- [89] Morales S, Canosa P, Rodríguez I, Rubí E, Cela R. Microwave assisted extraction followed by gas chromatography with tandem mass spectrometry for the determination of triclosan and two related chlorophenols in sludge and sediments, *Journal of Chromatography A* 2005, 1082, 128–135.
- [90] Azzouz A, Ballesteros E. Determination of 13 endocrine disrupting chemicals in environmental solid samples using microwave-assisted solvent extraction and continuous solid-phase extraction followed by gas chromatography–mass spectrometry, *Analytical and Bioanalytical Chemistry* 2016, 408, 231–241.

Richard Morrison

## 25 Microwave chemistry in the organic instructional laboratory

The instructional laboratory curriculum is greatly enhanced and broadened through the incorporation of microwave promotion. A comprehensive overview of potential applications for organic chemistry is beyond the scope of this chapter. However, the advantages gained through the use of microwave heating in the instructional laboratory are substantial and allow students to study reactions and synthetic strategies previously beyond the reach of undergraduate researchers. This chapter initially presents the general advantages achieved through microwave irradiation. Thereafter, three instructional laboratory experiments are presented to demonstrate specific advantages achieved through microwave promotion.

### 25.1 Introduction

The instructional laboratory is necessarily an introductory experience. The objective of the instructional laboratory curriculum is to provide a safe and supervised setting wherein students obtain hands-on experience with experimental procedures and analytical techniques. In the process, students come to understand and appreciate the importance of scientific investigation and the value of the results they obtain through well-planned and careful experimentation.

There are several constraints within which the instructional laboratory curriculum must operate. First and foremost, laboratory experiments must be safe for students. This means that experimental procedures are limited to chemicals and reagents that do not present any significant danger to inexperienced users. This imperative presents perhaps the most substantial challenge to the development and implementation of laboratory experiments.

Second, laboratory experiments must be designed to have a high success rate. Although in a research setting the apparent failure of an experiment can be extremely instructive in planning and modifying future experiments, the failure to achieve a positive result from an experiment in the instructional laboratory is problematic due to the difficulty and time involved in trouble shooting the problem, identifying the cause, and subsequently modifying the experimental procedure to achieve the desired result. Such an effort can lead a student investigator far astray from the desired objective of the experimental exercise and consequently from the intended exposure to procedures and techniques associated with the experiment.

<https://doi.org/10.1515/9783110479935-025>



A third constraint that shapes the development of instructional experimentation is the time within which an experiment must be performed. For example, a given synthetic transformation that requires a 6 h reflux can be fairly easily accommodated in a research laboratory setting. However, instructional laboratory periods typically cannot incorporate a 6 h reflux followed by 1 to 2 h of work-up and product analysis. As a result, experimental procedures in the instructional laboratory that utilize traditional heating methods are most commonly limited to transformations that can be completed within 2 h. The time constraint associated with traditional heating eliminates from consideration a wide array of reactions and transformations that otherwise would be interesting and instructive for students to perform and analyze.

A fourth constraint that limits the efficacy of the instructional laboratory results from the generalization of a given experiment. A typical laboratory exercise requires all students to follow the same procedure and obtain the same product or result. In this scenario, for example, if all students in the laboratory section obtain the same organic solid, the success of the experiment is determined for each student by the calculated percent yield of the product and its purity, most commonly measured by melting point determination. As described, the traditional instructional laboratory exercise is woefully lacking in exposure to and use of modern analytical instrumentation. However, an experiment is greatly improved by individually varying the experimental results obtained from a procedure or synthetic transformation. This is achieved through the use of *unknowns*. Unknowns allow all students in a class to explore the same transformation or methodology but obtain individualized results. If, for example, the experimental procedure is modified to include an array of possible reactants and the identity of the reactant is unknown to the student researcher, the experimental result will be unique for each student and dependent upon the unknown reactant. Thus, the incorporation of unknowns individualizes the experimental results for students without significantly changing the experimental procedure. Furthermore, analysis of individualized experimental results necessarily entails the use of modern analytical instrumentation.

## 25.2 Advantages of microwave promotion

Incorporation of microwave promotion into the instructional laboratory curriculum has several advantages that address the limitations previously discussed.

### 25.2.1 Safety

Modern microwave research instrumentation is designed with redundant safety features. A standard reflux in the traditional organic laboratory entailed multiple student setups where reactions were carried out on a benchtop in close proximity to other reac-

tions. The use of portable shields to surround the reaction partially isolated each student's setup but did not completely protect other students from mishaps, spills and accidents. In contrast, microwave-promoted reactions are performed in explosion-proof chambers. Each student reaction is performed in a self-contained reaction vessel mounted on a carousel. Reaction parameters for heat, reaction time, and microwave power can be tailored to the experiment with respective maxima programmed into the reaction protocol. Unsafe departures from the programmed protocols are immediately detected, and microwave irradiation is terminated automatically.

### 25.2.2 Yields and product purity

Microwave promotion often leads to increased reaction yields with greater product purity. These benefits are extremely useful in the instructional laboratory because they obviate the need for repeated extractions and recrystallizations or column chromatography. When the desired product is obtained in high yield and purity, the balance of the laboratory time is used for product analysis and structure elucidation. As a result, students have more time to use analytical instrumentation such as Fourier transform infrared spectroscopy (FTIR), gas chromatography–mass spectrometry, and Nuclear magnetic resonance (NMR) spectroscopy.

### 25.2.3 Reduced heating times

One of the most important advantages of microwave promotion is the abbreviated heating time required to accomplish a desired transformation. Prior to the advent of microwave promotion, instructional laboratory experiments were limited to a small subset of procedures that could be accomplished by traditional heating methods within approximately 2 h. Consequently, for some experiments the number of potential laboratory exercises was limited to only one or two candidates. This limitation did not allow professors much latitude in the selection of exercises and severely constrained students' exposure to the wide array of transformations that make organic chemistry engaging to explore and study. Reduced reaction times realized by microwave promotion of organic reactions allow instructors to consider and incorporate a wide array of transformations previously beyond consideration. Reactions that require as much as 24 h to complete using traditional heating methods can be completed in 20 to 30 min in the microwave. Thus, the potential transformations that can now be accomplished within a standard laboratory period via microwave promotion that increases the number of candidate experiments several fold.

### 25.2.4 Reactant and reagent unknowns

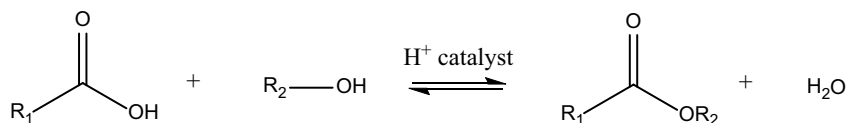
Microwave promotion facilitates the use of unknowns. The use of unknowns is a powerful and effective tool that encourages students to work independently and attentively. For example, if the transformation being explored in a laboratory exercise is the Williamson Ether Synthesis, the unknown may be the primary organohalide, such as benzyl bromide or 1-bromo-3-methylbutane. Alternatively, the unknown may be the alkoxide nucleophile, such as sodium methoxide or sodium ethoxide. Students introduce their reaction mixture containing one or two unknown components into a glass or Teflon reaction vessel and place it in a numbered position on the carousel of the microwave reactor. Because these reactants possess similar reactivities, the reaction conditions can be standardized. Once all vessels are loaded, the standardized reaction protocol is begun. Within 15 min the reaction is completed and the vessels are allowed to cool. There are four possible products from this modest assortment of reactants: benzyl ethyl ether, benzyl methyl ether, 1-ethoxy-3-methylbutane, and 1-methoxy-3-methylbutane. Each product exhibits characteristic C–O bond, stretching vibrations in the IR spectrum between 1050 and 1200  $\text{cm}^{-1}$ , which confirms the formation of an ether product. Identification of each unique product is accomplished by  $^1\text{H}$  NMR and  $^{13}\text{C}$  NMR. The time saved in the laboratory period due to the abbreviated heating time realized through microwave promotion allows students to use the balance of the allotted time for structure elucidation and identification of their unknown reactant(s). In summary, owing to the reduced heating time associated with microwave promotion, the instructional laboratory period focuses on structure elucidation and the utility of modern analytical instrumentation. Thus, the instructional laboratory models more closely resembles the research laboratory experience.

## 25.3 Examples of instructional laboratory experiments that utilize microwave promotion

### 1: Fischer esterification [1]

Carboxylic acid esters are derivatives of carboxylic acids that contain a carbon group in place of the acidic proton of the carboxyl group. They are produced on the industrial scale via a process known as Fischer esterification. The reaction is an equilibrium reaction between a carboxylic acid and an alcohol in the presence of sulfuric acid catalyst. Scheme 25.1 shows a general reaction scheme for the Fischer esterification reaction.

Because the reaction is an equilibrium, Le Chatlier's principle must be applied to drive the reaction to completion. In this reaction, the addition of excess acetic acid, which can be easily removed by acid-base extraction, is used to drive the reaction to completion. The product esters obtained in this experiment are fragrant and are sold commercially.  $^1\text{H}$  NMR and  $^{13}\text{C}$  NMR will be used to characterize the product esters.

**Scheme 25.1:** General reaction scheme for Fischer esterification.

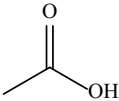
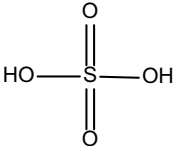
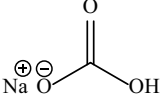
### Techniques

Microwave heating; liquid/liquid extraction; decantation; FTIR,  $^1\text{H}$  NMR, and  $^{13}\text{C}$  NMR spectroscopy

### Reactants and reagents

Gather and record all of the indicated physical data for the known reactants and reagents. Once you have identified your product ester, gather and record the indicated physical data for your unknown alcohol. Information can be found on material data safety sheets (MSDSs) for each compound.

**Tab. 25.1**

Compound	Structure	MW	BP	Density
Glacial acetic acid		60.052 g/mol	117.9 °C	1.045 g/mL
Sulfuric acid		98.072 g/mol	337.0 °C	1.830 g/mL
Unknown Alcohol	ROH	—	—	—
Sodium Bicarbonate		84.006 g/mol	solid	2.16 g/mL

### Safety

Alcohols and esters are flammable. Acetic acid and sulfuric acid cause severe burns and should be handled with care. Pressure may build up when neutralizing sodium bicarbonate due to the release of carbon dioxide gas. Never open microwave vessels

outside of a hood or before the temperature has decreased below the boiling point of any chemical contained inside.

### Experimental procedure

Obtain 5 mL of glacial acetic acid and 4 mL of an unknown alcohol from your graduate teaching assistant and add these to a microwave vessel. In the hood, carefully add 1 mL of concentrated sulfuric acid and a small round stir bar. Seal the microwave vessel, write the vessel number in your laboratory notebook, and place vessel in the microwave carousel. The reaction will be heated for 10 min in the microwave (compared to 1 h by standard reflux). Once the vessel is cool, pour the contents into a separatory funnel, add 10 mL of water, and shake gently. The ester will separate from the water layer. Remove the aqueous layer and wash with an additional 10 mL of water. Wash the ester again with 10 mL portions of 5% sodium bicarbonate until the resulting aqueous wash is basic according to pH paper. This removes excess acetic acid from the organic layer. (Note: Carbon dioxide is formed during the sodium bicarbonate wash steps, so be careful to vent the separatory funnel to relieve any pressure buildup.) Finally, wash the ester with 5 mL of brine solution to remove residual water from the organic layer. Transfer the organic layer to a weighing vial and determine the mass of your product ester.

### Product analysis

Place approximately 0.5 mL of your product ester on the diamond attenuated total reflection (ATR) crystal of the infrared spectrometer and obtain an FTIR spectrum of your product. Identify characteristic absorptions for your ester.

Transfer a sufficient amount of neat solution to an NMR tube to fill the tube to approximately one-third its total volume. Obtain  $^1\text{H}$  NMR and  $^{13}\text{C}$  NMR spectra. Alternatively for benchtop  $^1\text{H}$  NMR analysis, add two drops of tetramethylsilane (TMS) to the neat ester and introduce 0.10 mL of the ester/TMS solution to the capillary inlet. Determine the product ester formed in your esterification reaction using your spectra and associated signals from the  $^1\text{H}$  NMR spectra with your product. Example FTIR and  $^1\text{H}$  NMR spectra (Figure 25.1 and Figure 25.2, respectively) of propyl acetate are shown in what follows.

## 2: Week 1: Multistep synthesis: Arbuzov reaction [2–5]

Phosphonate esters are formed from the reaction of organohalides with phosphoric acid esters by the Arbuzov reaction (also known as the Michaelis–Arbuzov reaction). Phosphonates are important in organic synthesis and agriculture. They also have applications in chemical warfare in nerve gases such as Sarin because they are potent inhibitors of the enzyme acetyl cholinesterase and are therefore extremely toxic to the

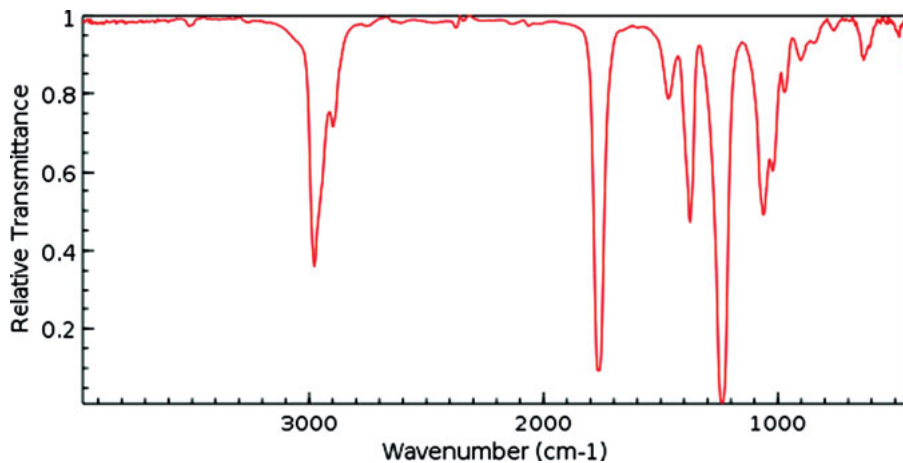
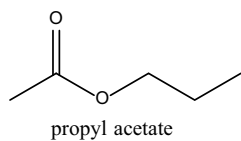


Fig. 25.1: FTIR spectrum of propyl acetate.

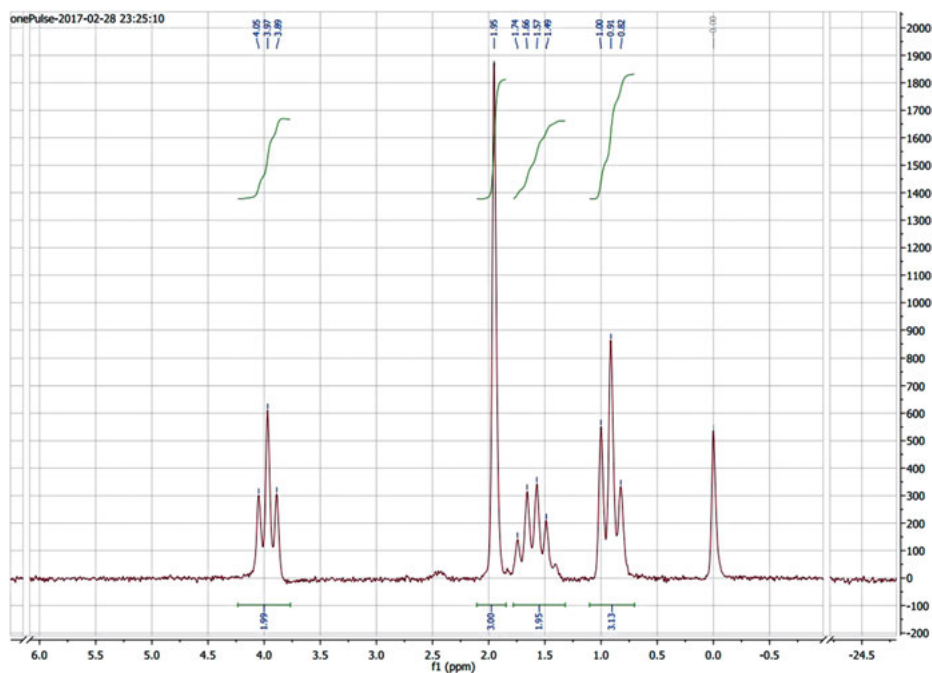
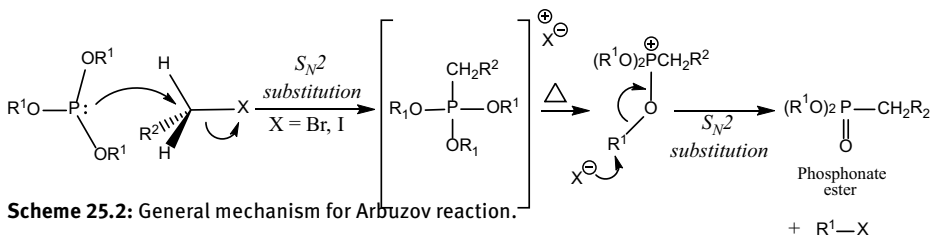


Fig. 25.2: Benchtop 82 MHz  $^1\text{H}$  NMR spectrum of propyl acetate.

parasympathetic nervous system. Phosphonates formed by the Arbuzov reaction yield alkenes from carbonyl compounds in the Horner–Emmons–Wadsworth modification of the Wittig reaction [6–9].

The first step of the mechanism involves an  $S_N2$  nucleophilic attack of the organo-halide by the phosphorus to form a phosphonium salt. Microwave heating promotes a C–O bond cleavage of the phosphonium salt affected by an  $S_N2$  nucleophilic attack of the halide ion ( $X^-$ ) to afford the phosphonate ester. Scheme 25.2 shows a general reaction scheme for the Arbuzov reaction.



### Reactants and reagents

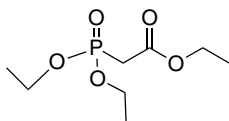
Gather and record all of the indicated physical data for the known reactants and reagents. Information can be found on MSDSs for each compound.

Tab. 25.2

Compound	Structure	MW	BP	Density
Triethylphosphite		166.16 g/mol	156 °C	0.969 g/mL
Ethyl bromoacetate		167.01 g/mol	158 °C	1.51 g/mL

### Safety

It is imperative that you proceed with caution, especially when opening the microwave vessel upon cooling. Bromoethane is a low boiling liquid. Components of the reaction are irritants to the skin and eyes and can be toxic with prolonged exposure. Read their MSDSs carefully!



**Fig. 25.3:** Structure of Arbuzov phosphonate ester product derived from triethyl phosphite and ethyl bromoacetate.

### Experimental procedure

Obtain and mix 13.6 g of triethylphosphite and 13.6 g of ethyl bromoacetate. These are precise molar equivalents, and it is essential to be accurate in your measurements to ensure the greatest purity of product. Introduce the mixture into a microwave vessel containing a stir bar. Seal the microwave vessel and place it in your assigned position of the microwave rotor. Your graduate teaching assistant will execute a microwave reflux program that will raise the temperature of the vessels from room temperature to 200 °C within 10 min, reflux at 200 °C for 30 min, and then cool for 10 min. Upon completion, allow the vessels to cool until they can be comfortably held, then open the vessels in the hood. Obtain a gas chromatogram of the reaction mixture to verify full conversion of the starting materials into product.

### Product analysis

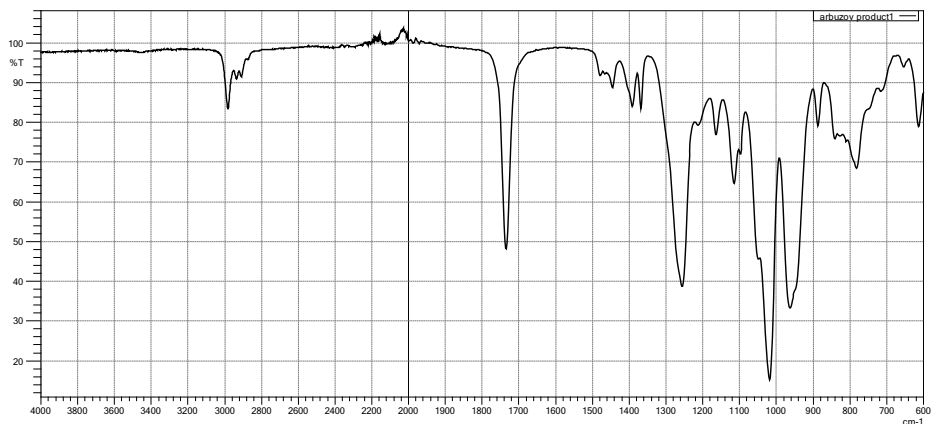
Place a small amount of your product phosphonate ester on the diamond ATR of the infrared spectrometer and obtain an FTIR spectrum. Identify characteristic absorptions.

Transfer approximately 15 mg of your product to an NMR tube. Using a pipette, add a sufficient volume of  $\text{CDCl}_3$  to the NMR tube such that the total volume of product and NMR solvent constitutes approximate one-third of the total volume of the NMR tube. Obtain  $^1\text{H}$  NMR and  $^{13}\text{C}$  NMR spectra for your product. Once you have confirmed your product, seal in a glass vial with Parafilm and place it in a small beaker in your laboratory drawer. Your phosphonate ester is a reactant in the second step of the multistep synthesis: the Horner–Emmons–Wadsworth reaction with an unknown ketone. Example FTIR and  $^1\text{H}$  NMR spectra (Figures 25.4 and 25.5, respectively) of the Arbuzov phosphonate ester product derived from triethylphosphite and ethyl bromoacetate are shown in what follows.

## 3: Decarboxylation of amino acids

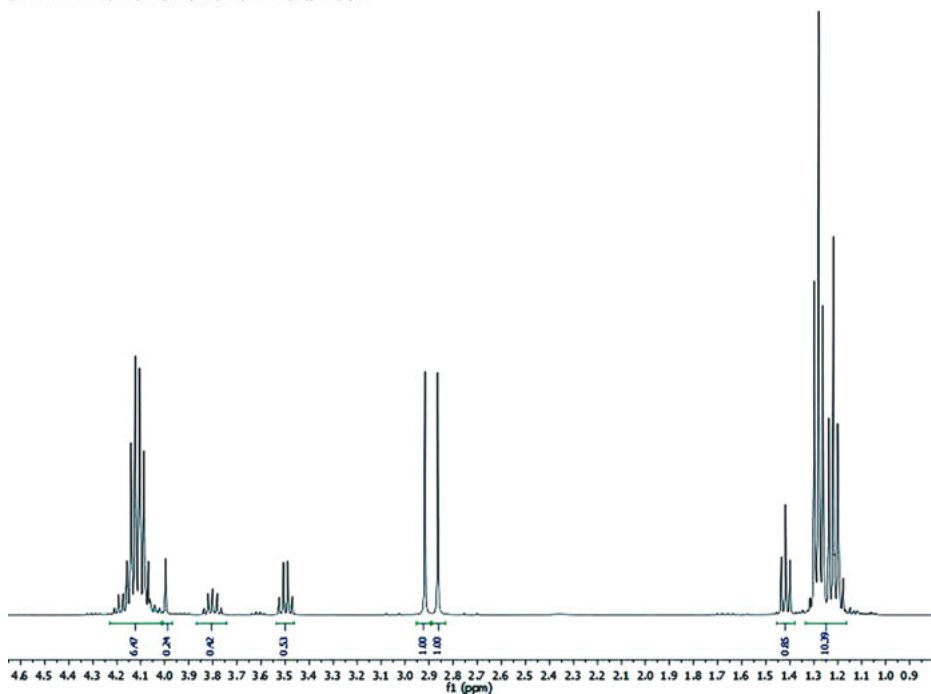
Amino acids are the building blocks of proteins and as such are essential to life. In addition, some amino acids are the progenitors of neurotransmitters and hormones that regulate an array of biological functions and processes. For example, epinephrine, also known as adrenaline, plays an essential role in the fight-or-flight response by increasing blood flow to muscles, output of the heart, pupil dilation, and blood sugar. A complementary neurotransmitter to epinephrine is norepinephrine. It is the main





**Fig. 25.4:** FTIR spectrum of Arbusov phosphonate ester product derived from triethylphosphite and ethyl bromoacetate.

//C:\CHEMPC374-01\Data\data\maysnard\rmr\arbu20V\10\data\1\1r



**Fig. 25.5:** 400 MHz  $^1\text{H}$  NMR spectrum of Arbusov phosphonate ester product derived from triethylphosphite and ethyl bromoacetate

neurotransmitter of the sympathetic nerves in the cardiovascular system and plays a major role in the tonic and reflexive changes in cardiovascular tone. Both of these essential neurotransmitters are structurally identified as catecholamines and are synthesized in the body from the amino acid tyrosine. Dopamine is another neurotransmitter that is synthesized in the body from tyrosine. Dopamine functions in the so-called reward system of neural structures that comprise any stimulus, object, event, or activity that induces us to approach and consume. Similarly, serotonin, a neurotransmitter synthesized from the amino acid tryptophan, is thought to be responsible for overall happiness and sense of wellbeing. All of these neurotransmitters have one thing in common: they are all biologically synthesized by decarboxylation of amino acid precursors.

In this reaction you will decarboxylate an unknown amino acid using a newly discovered and patented technique involving microwave promotion developed in the research laboratory of Dr. Richard Morrison at the University of Georgia. Reflux in a sealed vessel under microwave irradiation allows the reaction to proceed at a temperature much higher than the normal boiling point of the solvent. As you recall, the Arrhenius equation relates reaction rate to temperature. A general rule of thumb is that the reaction rate doubles for every 10 °C incremental increase in temperature.

### Reactants and reagents

Gather and record all of the indicated physical data for the following reactants and reagents. Information can be found on the MSDS for each compound.

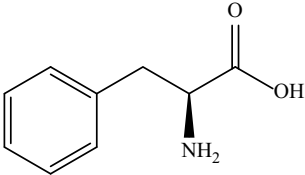
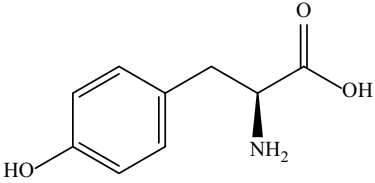
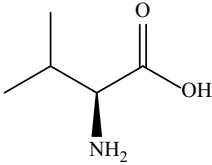
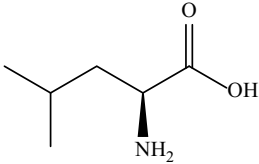
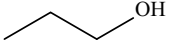
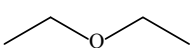
### Safety

Proceed with caution, especially when opening the microwave vessel upon cooling.

### Experimental procedure

Measure 0.905 g of your assigned unknown amino acid into a microwave vessel. Record the letter of your unknown. Add 2.75 g of the organocatalyst to the vessel along with 5.5 mL of 1-propanol and a magnetic stir bar. Seal the microwave vessel and place it in your assigned position on the microwave carousel. When the carousel is fully loaded, your graduate laboratory assistant will execute a microwave reflux program that will raise the temperature of the vessels from room temperature to 190 °C over 5 min and heat at 190 °C for an additional 5 min with continuous stirring. Following heating, allow time for the vessel to cool to room temperature then *open the vessel slowly and carefully* as gas is evolved (refer to your reaction mechanism). Note any physical changes to the reaction mixture. *Slowly* add 10 mL of 2M HCl to the mixture. Seal the vessel again and place it in your slot on the microwave carousel. Your graduate laboratory assistant will execute another 5 min heating regimen at 190 °C with stirring. Allow to cool and open carefully. Wash the aqueous reaction mixture twice

Tab. 25.3

Compound	Structure	MW	MP or BP
L-phenylalanine		165.19 g/mol	283.0 °C melting point
L-tyrosine		181.19 g/mol	344.0 °C melting point
L-valine		117.15 g/mol	315.0 °C melting point
L-leucine		131.17 g/mol	293.0 °C melting point
1-propanol		60.09 g/mol	97.2 °C boiling point
Diethyl ether		74.12 g/mol	34.6 °C boiling point

with two 25 mL portions of diethyl ether. Do not discard any layers until the product has been confirmed. Heat the aqueous solution to dryness with a heat gun.

### Product analysis

Neutralize the ammonium hydrochloride salt with aqueous sodium bicarbonate and extract the free amine base in ether. Dry the ether extract with anhydrous sodium sulfate, decant the dried ether solution into a round-bottom flask, and remove ether using a rotovap. Weigh your product and obtain an IR spectrum. Add a few drops of  $\text{CDCl}_3$  to your product amine. Obtain a  $^1\text{H}$  NMR spectrum using the benchtop NMR instrument.

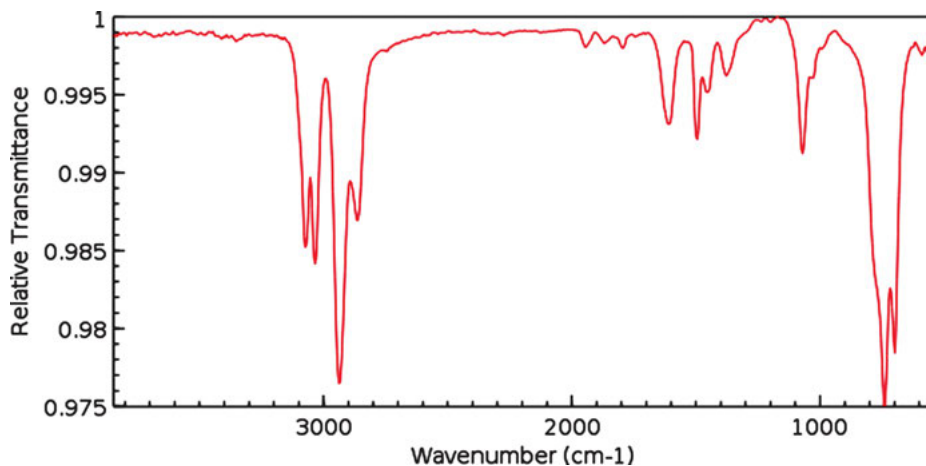


Fig. 25.6: FTIR spectrum of phenylethyl amine.

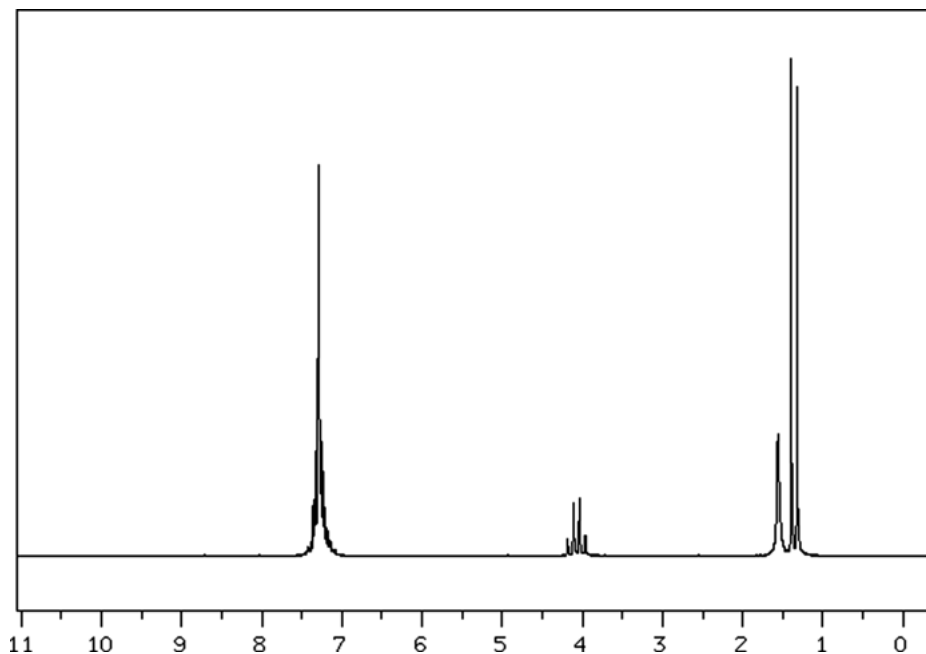
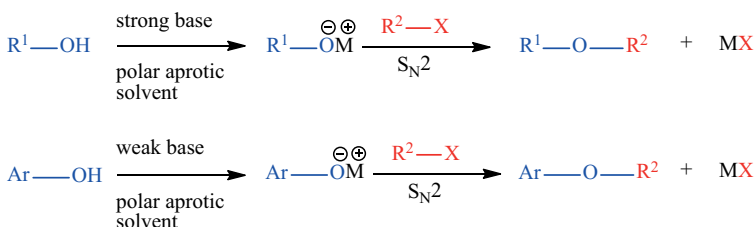


Fig. 25.7: <sup>1</sup>H NMR spectrum of phenylethyl amine.

Assign the <sup>1</sup>H NMR signals of your amine produced by decarboxylation. Then compare your results to the amino acid unknowns and identify the amino acid that correlates structurally to your product amine. Example FTIR and <sup>1</sup>H NMR spectra (Figure 25.6 and Figure 25.7, respectively) for the decarboxylation of phenylalanine are shown in what follows.

#### 4: Williamson ether synthesis

W. Williamson was the first to establish the correct formula for diethyl ether in 1851 [10–12]. Diethyl ether was first prepared by V. Cordus in 1544 by heating ethanol with sulfuric acid. Williamson synthesized diethyl ether from sodium ethoxide and ethyl chloride. The reaction of alkyl, allyl, or benzyl halides with aromatic or aliphatic alkoxides to afford the corresponding ethers is known as the Williamson ether synthesis. The reaction of metal alkoxides and phenoxides is usually carried out in polar aprotic solvents such as dimethylformamide or dimethyl sulfoxide to minimize side products resulting from E2 dehydrohalogenation. Primary alkyl, methyl, allylic, and benzylic halides give the highest yields, because these undergo S<sub>N</sub>2-type halide displacement by the nucleophile.



**Scheme 25.3:** General reaction scheme for Williamson ether synthesis.

#### Techniques

Microwave heating, column chromatography, FTIR, and <sup>1</sup>H NMR spectroscopy

#### Reactants and reagents

Gather and record all of the indicated data for the known reactants and reagents. Information can be found on the MSDS for each compound.

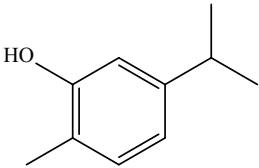
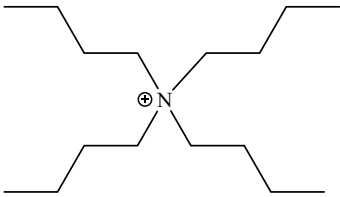
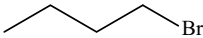
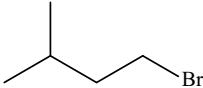
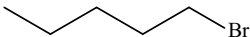
#### Safety

KOH is a strong base. If you get any on your skin, wash the affected area immediately with copious amounts of water. Avoid inhaling silica gel. It is a severe respiratory irritant. Never open microwave vessels outside of a hood or before the temperature has lowered below the boiling point of any chemical contained inside.

#### Experimental procedure

Add 1.50 g of carvacrol, 3.56 g of 25% KOH, and a spin bar to the microwave vessel. Add 1.45 g of tetrabutylammonium bromide (TBAB) to the vessel and allow it to dissolve. To this mixture add 1.51 g of the alkyl halide. Place your microwave vessel in

Tab. 25.4

Compound	Structure	MW
Carvacrol		150.22 g/mol
Potassium Hydroxide	$\text{K}^{\oplus} \text{OH}^{\ominus}$	56.11 g/mol
Tetrabutylammonium bromide		322.37 g/mol
1-bromobutane		137.02 g/mol
1-bromo-3-methylbutane		151.05 g/mol
1-bromopentane		151.05 g/mol

your numbered slot in the carousel. Once the carousel is loaded with all of the vessels, the heating protocol is implemented: 5 min ramp to 100 °C; hold at 100 °C for 25 min; discontinue heating and allow vessel to cool to room temperature.

Remove the spin bar and rinse with 10 mL of diethyl ether, collecting the wash solution in the vessel. Empty the vessel into a small separatory funnel. Add 10 mL of distilled water to the separatory funnel, stopper, and gently invert the funnel, then separate the resulting aqueous layer into a 250 mL flask. Collect the remaining ether layer in a separate 250 mL flask. Reintroduce the aqueous layer back into the separatory funnel and extract with 20 mL of diethyl ether. Combine the ether extracts and wash three times with 5% KOH, discarding the aqueous layers after each wash. Dry the ether extract with anhydrous sodium sulfate.

Use a small glass column to purify your ether product. To prepare your column, push a small amount of cotton or glass wool down the column toward the stopcock with copper wire. Fill about 75% of the column with silica gel and secure with a small clamp. Before adding your product mixture, the column must be *packed*. To pack the column, add a steady amount of dichloromethane (DCM) to the top of the column.

NOTE: It is *crucial* that the DCM be continuously added until you are ready to use thus preventing the column from drying. First, place a 250 mL round-bottom flask under your column to collect your DCM/ether solution containing your product, and then add your product mixture to the column using a pipette. Once all of your product mixture is added to the column, add an additional 20 mL of DCM to the column to elute all of your product from the silica gel. Upon completion, the used silica gel should be placed in the container labeled “used silica gel.”

Carefully remove the DCM/ether solvent from the 250 mL round-bottom flask using a rotovap.

### Product analysis

Place approximately 0.5 g of your product ether on the diamond ATR of the infrared spectrometer, and obtain an FTIR spectrum of your product. Identify the characteristic C–O bond stretching vibrations in the IR spectrum between  $1050$  and  $1200\text{ cm}^{-1}$ , which confirms the formation of an ether product.

Transfer a small amount of your product to an NMR tube, dilute with  $\text{CDCl}_3$  to fill the tube to approximately one-third its total volume, and obtain the  $^1\text{H}$  NMR spectrum. Correlate signals from the  $^1\text{H}$  NMR spectrum to one of the unknown alkyl halides, and draw a structure for the product ether you formed. Example FTIR and  $^1\text{H}$  NMR spectra (Figure 25.9 and Figure 25.10, respectively) of the product ether formed from carvacrol and 1-bromopentane are shown in what follows.

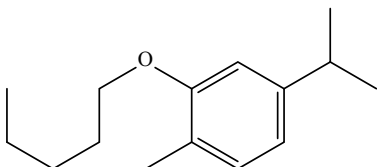


Fig. 25.8: Williamson ether product of carvacrol and 1-bromopentane.

## 25.4 Conclusions

Microwave promotion of organic reactions is a valuable synthetic and instructional tool. Reduced heating times combined with numerous safety features available with modern microwave instruments allow many previously inaccessible transformations to be performed in the instructional laboratory. Moreover, students can perform individualized reactions with a variety of unknown reactants using general reaction protocols, thereby encouraging each student to become more fully invested in the success of the reaction and subsequent product analysis and structure elucidation. The range

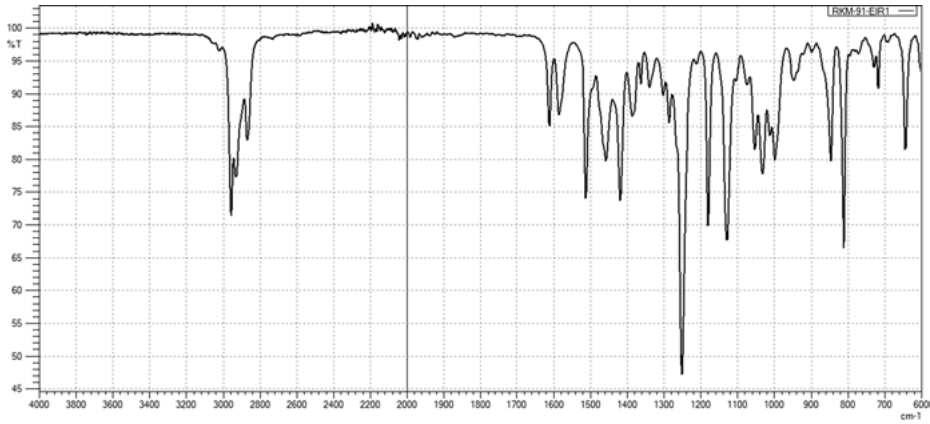


Fig. 25.9: FTIR spectrum of Williamson ether product derived from carvacrol and 1-bromopentane

C:\Data\data\rmaynard\nmr\Jan09-2017\10\data\1\1.r

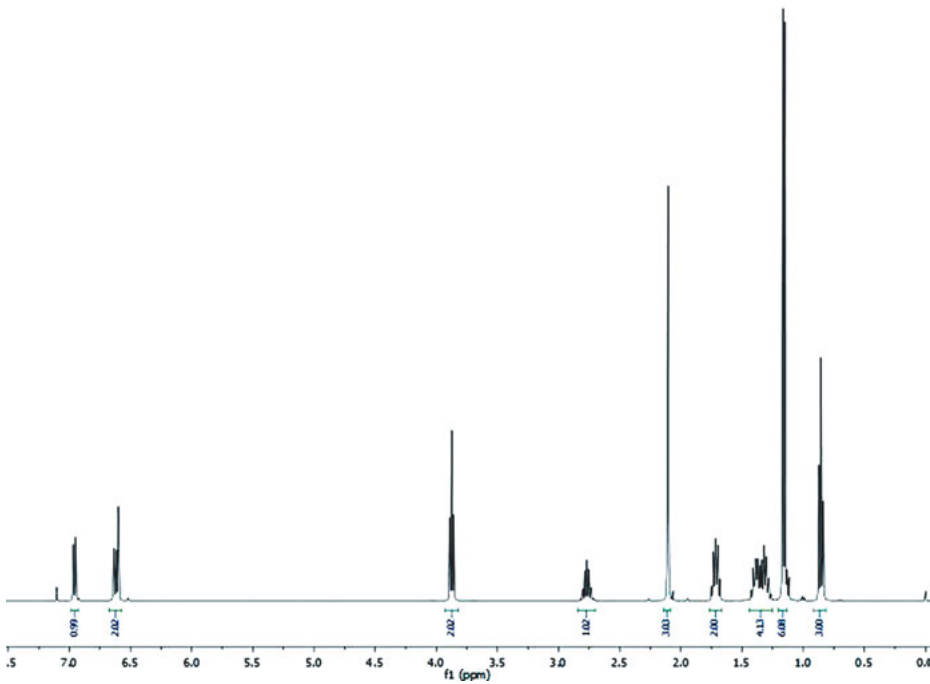


Fig. 25.10: <sup>1</sup>H NMR spectrum of Williamson ether product derived from carvacrol and 1-bromopentane.



of methods and reactions now made possible through microwave promotion has the potential to revolutionize instructional laboratories. Previous instructional laboratory experiment development was constrained by considerations surrounding what can be done on the benchtop within a 3 to 4 h time period. With the incorporation of microwave promotion, the paradigm that directs experiment development has become significantly broader and more inclusive. As a result, professors have greater latitude in choosing what they want their students to study and explore, thereby creating a more engaging and expansive intellectual environment for training future scientists.

## Bibliography

- [1] Fischer E, Speier A. Darstellung der Ester. *Chem. Ber.* 1895, 28, 3252–3258.
- [2] Michaelis A, Kaehne R. The reaction of alkyl iodides with phosphites. *Chem. Ber.* 1898, 31, 1048–1055.
- [3] Arbuzov A. *J. Russ. Phys. Chem. Soc.* 1906, 38, 687.
- [4] Arbuzov A. *J. Russ. Phys. Chem. Soc.* 1910, 42, 395.
- [5] Bhattacharya AK, Thyagarajan G. Michaelis-Arbuzov rearrangement. *Chem. Rev.* 1981, 81, 415–430.
- [6] Horner L, Hoffman H, Wippel HG. Phosphorus organic compounds. XII. Phosphine oxides as reagents for olefin formation. *Chem. Ber.* 1958, 91, 61–63.
- [7] Horner L, Hoffman H, Wippel HG, Klahre G. Phosphorus organic compounds. XX. Phosphine oxides as reagents for olefin formation. *Chem. Ber.* 1959, 92, 2499–2505.
- [8] Wadsworth WS Jr, Emmons WD. The utility of phosphonate carbanions in olefin synthesis. *J. Am. Chem. Soc.* 1961, 83, 1733–1738.
- [9] Boutagy J, Thomas R. Olefin synthesis with organic phosphonate carbanions. *Chem. Rev.* (Washington, DC) 1974, 74, 87–99.
- [10] Williamson W. About the theory of the ether bond. *Liebigs Ann. Chem.* 1851, 77, 37–49.
- [11] Williamson W. *J. Chem. Soc.* 1852, 106, 229.
- [12] Dermer OC. Metallic salts of alcohols and alcohol analogs. *Chem. Rev.* 1934, 14, 385–430.

# **A snapshot of more common commercial microwave reactors**

by the Editors

A great deal of progress has been made in the field of microwave (MW) technology, in both science and manufacture, since the early 1980s. Scientific interest and demand have driven the development of innovation in the manufacture of MW ovens and, later, of dedicated MW reactors.

The growing interest in the synthetic chemistry applications of this intriguing energy source in the 1990s stimulated the development of safer and more reliable equipment. Within a decade, a number of creative companies, including Prolabo, CEM, MLS Milestone, Anton Paar, Biotage, and Sairem, had decided to take on this challenging task.

This appendix aims to provide an overview of the laboratory MW chemical reactors available on the market, as of May 2017. Other well-established companies, including Püschner, MKS, MEAM, and others, offer batch and flow systems for pilot and industrial applications.

## **MLS Milestone**

MLS Milestone is a European company that has been active in the field of advanced MW applications since 1988. It has more than 20,000 instruments installed in large and small research institutions, universities, and industrial laboratories worldwide. MLS Milestone is the pioneer in MW-assisted laboratory processes, having become the world's leading manufacturer by offering a wide range of application possibilities and, at the same time, high-quality products protected by patent rights.



FlexiWAVE

The flexiWAVE overcomes the limitations of conventional MW synthesis devices with its single MW platform that, in combination with specific accessories, allows chemists to perform classic glassware and high-pressure (up to 100 bar) synthesis, as well as solid-phase reactions.

<https://www.milestonesrl.com/en/microwavesynthesis/flexiwave.html?view=featured>



FlexiWAVE – High temperature

The flexiWAVE with high-temperature muffle setup has an extremely fast heating rate. The incredibly fast heating rate (5 min to 800 °C and 10 min to 1000 °C) is the revolutionary feature of flexiWAVE MW platform, making this configuration the best choice for high-temperature applications. Today flexiWAVE has become the first MW reactor for chemical synthesis able to work up to 1200 °C.

<https://www.milestonesrl.com/en/microwavesynthesis/flexiwave.html?view=featured>



SynthWAVE

MLS Milestone has created a new concept in MW instrumentation, the revolutionary SynthWAVE. It matches the growing demand for scale-up of chemical reactions in the gram to kilogram range. It handles single or multiple reactions at temperatures of up to 300 °C and pressures of up to 199 bar. Small-scale synthesis methods are easily transferred to SynthWAVE. Incredibly easy to use, SynthWAVE allows chemists to run large-scale batch and parallel reactions working with a modified atmosphere like never before.

<https://www.milestonesrl.com/en/microwavesynthesis/synthwave.html?view=featured>

---

## CEM

CEM Corporation, a private company based in Matthews, North Carolina, was founded in 1978. CEM Corporation is global provider of MW solutions for laboratory applications.

---



Discover SP

The Discover SP is able to perform virtually any type of chemical transformation, from organic to inorganic, materials, and more. Small scales and large scales, high temperatures and low temperatures, and gaseous reagents can all be used on a single simple system.

<http://cem.com/en/discover-sp/#adv>

---



The MARS 6 multimode reactor is suitable for running a single vessel or up to 40 in parallel. Fully customizable, the MARS 6 benchtop system can be dedicated for synthesis or serve as an all-in-one MW reactor for a variety of applications.

Mars 6

<http://www.cem.com/mars6-synthesis-vessels>

---



The Phoenix Microwave Muffle Furnace System is available with your choice of either a high-temperature or high-capacity furnace. The high-temperature furnaces reach 1200 °C and can process up to eight 25 mL crucibles. For laboratories needing greater throughput, the high-capacity furnaces reach 1000 °C and hold up to fifteen 25 mL crucibles.

Phoenix

<http://cem.com/phoenix>

---

## Anton Paar

Anton Paar, an Austrian company, started in 1922 as a one-man machine repair workshop. It is the world's leader in the measurement of density, concentration, and CO<sub>2</sub> and in the field of rheometry. Most recently, Anton Paar has moved into the business of MW solutions.



MultiwavePRO

The Multiwave PRO MW reaction system provides neat reaction products from a broad variety of substrates in varying scales. Multiwave PRO can work at high temperatures and provides comprehensive safety features. Its wide range of accessories allows digestion, parallel development, multigram synthesis, leaching, oxygen combustion, solvent extraction, drying, evaporation, and UV digestion with a single system.

<http://www.anton-paar.com/sg-en/products/details/microwave-reaction-system-multiwave-pro/>



Masterwave BTR

Based on a revolutionary new technique, the all-new Masterwave BTR benchtop reactor is the first to enable MW synthesis in the kilolab. Productivity in the lab is considerably increased up to kilogram amounts per day. The benchtop reactor's magnetically driven paddle stirrer provides independent stirring regimes for individual content. Owing its rising-sensor temperature measurement technique, Masterwave BTR features the high-temperature accuracy required for direct method transfer from any smaller MW device.

<http://www.anton-paar.com/sg-en/products/details/microwave-synthesis-in-the-kilolab-masterwave-btr/>



Monowave 400/200

Monowave 400 and Monowave 200 are high-performance MW reactors specially designed for small-scale MW synthesis applications in research and development laboratories. Autosampler MAS 24 can still be operated with the Software-guided Loading Strategy and additionally in Open Access Mode. The MAS 24 Autosampler option allows for unattended sequential processing of 24 experiments.

<http://www.anton-paar.com/sg-en/products/details/microwave-synthesis-monowave-400200/>

## Biotage

Biotage, a Swedish company, offers solutions, knowledge, and experience in the areas of analytical chemistry, medicinal chemistry, peptide synthesis, separation, and purification.



Initiator+

Biotage® Initiator+ represents the latest in MW synthesis performance. This instrument's high-end specifications enable the chemist to explore new areas and perform the latest innovations in chemistry. It has a reliable and upgradeable platform that allows chemists to make great discoveries in less time than was possible previously.

<http://www.biotage.com/product-page/biotage-initiator>

## Sairem

Sairem, a French company, was founded in 1978. Sairem's experience covers specific electronic design, MW and radio frequency (RF) engineering, MW and RF application development, standard RF and MW generator supplier, and MW and RF process installers.



SAIREM offers a series of MW reactors that can be easily integrated into applications for the development of, for example, new molecules, synthetic chemistry, the synthesis of nanoparticles, vegetal extraction, biotechnology, and environmental applications.

Minilabotron 2000

<http://www.sairem.com/chimie-16.html>



